DETERMINANTS OF ATRIAL REPOLARIZATION AND ARRHYTHMIAS

by

Zhiguo Wang

Department of Pharmacology and Therapeutics

A thesis submitted to the Faculty of Graduate Studies and Research

McGill University, Montreal

June, 1994 in partial fulfilment of the requirements

for the degree of Doctor of Philosophy

ISBN 0-612-05812-3

Canada

This thesis is dedicated to:

my wife, Xiaofan Yang, for her love, encouragement, understanding, and patience

my baby boy, Ritchie Wang, for his bringing me new hope, and for his happiness and future

ABSTRACT

A key to improved treatment of cardiac arrhythmias is an understanding of their ionic determinants. Refractoriness has long been known to be a major determinant of arrhythmias, particularly the reentrant ones. Membrane repolarization, being a major determinant of refractoriness, is controlled by ion currents, particularly the repolarizing K^+ currents. Many drugs are believed to exert their beneficial actions on arrhythmias by delaying repolarization and thereby prolonging refractoriness. The determinants of repolarization in human atrium are poorly understood, and many discrepancies between basic research and clinical observations remain unexplained. This thesis presents a series of studies aimed: (1) to understand factors determining the occurrence of atrial arrhythmias; (2) to evaluate cellular mechanisms of drug actions on arrhythmias; (3) to determine ionic mechanisms controlling atrial repolarization. To achieve these goals we used approaches at three different levels: the whole animal level (with a mapping system), the cellular level (with microelectrode techniques), and the ionic level (with whole-cell patch-clamp techniques). Several antiarrhythmic agents have been used as pharmacological probes to study the mechanisms of drug action in arrhythmias, to assess the properties of desirable drug actions, and to explore the characteristics of drug-channel interactions.

We found that class Ic agents produce use-dependent prolongation of refractoriness by delaying atrial repolarization in vitro at rapid activation rates, potentially explaining the efficacy of these drugs in clinical AF. To evaluate this possibility, we developed an animal model of atrial fibrillation (AF) to study mechanisms of arrhythmia and drug actions. These results emphasize the importance of refractoriness in determining drug actions on the occurrence of arrhythmias.

We discovered that the transient outward K^+ current (I_{to1}) in human atrial myocytes, unlike in many animal species, is frequency independent at physiologic rates, hence may still contribute importantly to repolarization even at rapid heart rates characteristic of tachyarrhythmias. We have characterized the delayed rectifier K^+ current (I_K), which had been believed to be absent in human atrium, as a composite of two components: the rapid one (I_{Kr}) and the slow one (I_{Ks}). Variability in the magnitude of I_K and I_{to1} provides an explanation for the long-recognized variation in atrial action potential morphology and duration. This finding improves our understanding of actions of many antiarrhythmic drugs, which are known to block I_K in animal species and to be effective antiarrhythmic drugs in patients. We have identified a novel depolarization-induced ultra-rapidly activating delay rectifier K^+ current (I_{Kur}), which closely resembles the expressed currents from Kv1.5 subfamily of *Shaker* K^+ channel genes. This finding reveals the possible physiological function of these cloned channels in the human heart, which was previously unknown. We have obtained data against the presence in human atria of Ca^{++}-activated transient outward Cl^- current (I_{to2}) and other Cl^- currents found in animal species. Our studies therefore indicate that the three voltage-dependent K^+ currents - I_{to1}, I_K, and I_{Kur}, are the major repolarizing currents governing the occurrence of arrhythmias and antiarrhythmic drug actions in human atrium.

We have studied the state-dependent actions of antiarrhythmic drugs on I_{to1}, and proposed a hypothesis that drug blockade of K^+ channels is actually a consequence of drug mimicking the endogenous inactivation 'ball' of the channel protein. We have also provided evidence suggesting a role of Na/K pump current in rate-dependent acceleration of repolarization, and that indirect inhibition of Na/K pump current may be the mechanism by which class Ic agents cause use-dependent delaying of repolarization.

FRENCH ABSTRACT

La compréhension des déterminantes ioniques est essentielle pour améliorer les traitements des arythmies cardiaques. L'aspect réfractaire fut, pour longtemps, une déterminante majeure d'arythmies en particulier de réentrée. La repolarisation membranaire, une déterminante majeure de l'aspect réfractaire, est contrôlée par des courants ioniques particulièrement, les courants potassiques sortants. Plusieurs drogues sont supposées d'exercer leur effet bénéfique sur les arythmies en retardant la repolarisation et par conséquent prolonger l'aspect humaine sont peu comprises, et beaucoup de contradictions entre la recherche fondamentale et les observations cliniques restent non-expliquées. Cette thèse présente une série d'études visant (1) à comprendre les facteurs déterminants la production d'arhythmies auriculaires; (2) à évaluer les mécanismes cellulaires sous-jacents l'action des médicaments sur les arythmies; (3) à déterminer les mécanismes ioniques controllants la repolarisation auriculaire. Pour arriver à nos buts on a adopté trois approches à trois niveaux différents: au niveau de l'animal entier (en utilisant un système de cartographie), au niveau cellulaire (en utilisant la technique de voltage impose). Plusieurs agents antiarythmiques ont été utilisés comme sondages pharmacologiques pour étudier les mécanismes d'action des médicaments en présence d'arythmies, pour évaluer les propriétés de leurs actions désirables, et pour sonder les caractéristiques des interactions drogues-canal.

On a trouvé que les agents appartenants à la classe Ic produisent une prolongation occupation-dépendante de l'aspect réfractaire en retardant la repolarisation auriculaire in vitro à hautes fréquences d'activation, potentiellement expliquant l'efficacité de ces agents contre la fibrillation auriculaire clinique (FA). Pour évaluer cette possibilité, on a développé un modèle animal de FA pour étudier les mécanismes d'arythmies et ;'action des médicaments. es résultatsmettent l'accent sur l'importance de l'aspect réfractaire sur la détermination de l'influence des médicaments sur la production d'arythmies.

On a découvert que le courant potassique transitoire sortant (I_{to1}) dans les myosites auriculaires chez l'humain, est fréquence-indépendant à des fréquences physiologiques, d'ou la possibilité d'une importante contribution de ce courant à la repolarisation en présence de tachyarythmies. n a caractérisé le courant potassique tardif-rectificatrue (I_K), qu'on croyait absent chez l'humain, comme mixte de deux composantes: l'une rapide (I_{Kr}) et l'autre lente (I_{Ks}). La variabilité dans la magnitude de I_K et I_{to1} nous fournit une explication à la *variabilité* longtemps connue de la morphologie et durée du potentiel d'action auriculaire. Cette découvert améliore notre compréhension de l'action de plusieurs agents antiarhythmiques qui bloquent I_K dans les espèces *animales* et étant efficaces chez les patients. On a identifié un nouveau courant potassique tardif-rectificateur induit par dépolarisation et s'activant ultrarapidemment qu'on a surnommé (I_{Kur}), qui montre beaucoup de ressemblance aux courants exprimés de la sous-famille Kv1.5 de la famille *Shaker* des gènes de canaux potassiques. Cette découverte révèle la fonction physiologique possible de ces canaux clonés du coeur humain, qui avant ça était inconnue. On a obtenue des données contre la présence, dans l'oreillette humaine, du curant transitoire Cl^- sortant activé par le $Ça^{2+}$ (I_{to2}) et d'autres courants Cl^- trouvés chez d'autres espèces animales. Nos études indiquent que les trois courants potassiques voltage-dépentant-I_{to1}, I_{Kr} et I_{Kur} sont les majeurs courants repolarisants gouvernant la production d'arythmies et l'action des agents antiarhythmiques sur l'oeillette humaine.

On a étudié l'état-dépendant de l'action des médicaments antiarhythmiques sur I_{to1}, et on a proposé l'hypothèse que le blocage des canaux potassiques par ces médicament est actuellement une conséquence de la drogue imitant la balle d'inactivation endogène de la protéine du canal. n a aussi fournit l'évidence suggérant un rôle du curant généré par la pompe Na^+/K^+ dans l'accélération fréquence-dépendante de la repolarisation, et qu'une inhibition indirecte de la pompe Na^+/K^+ pourrait être le mécanisme par lequel les agents Ic causent un délaie fréquence-dépendant de la repolarisation.

ACKNOWLEDGMENTS

I am heartily indebted to my supervisor, Dr. Stanley Nattel, for his close supervision, pertinent guidance, enthusiastic inspiration, and suggestions over the whole period of my graduate studies; for the impact he has been giving me with his scientific attitude; for his never-failing support, and father-like concern in all aspects; for his creative discussion, constructive criticism and careful proof-reading and correction of this thesis; were it not for all he has done for me, this thesis would have never been possible.

I am sincerely indebted to Dr. Bernard Fermini, for his excellent teaching and supervision on my patch-clamp studies, for his frequent input of fresh ideas and helpful suggestions, for his friendship, for his bringing in lots of pleasure and fun with his great sense of humour and extensive knowledge, and also for his wonderful recommendation for me to achieve studentship.

I am deeply grateful to Dr. Mario Talajic, for his active participation in experimental design, data analysis, and discussion for parts of my works, and for his wonderful recommendation for me to achieve studentship.

I would like to give my deep thanks to Dr. AC Cuello, Chairman of the Department of Pharmacology and Therapeutics for giving me the opportunity to pursue my graduate studies in this wonderful department.

I would like to extend my thanks to Guylaine Nicole, for her expert preparation of cells for my patch-clamp studies; Carol Matthews, for her expert analysis of drug concentrations in blood samples for my in vivo studies; Christine Villemaire, for her help in mapping techniques and computer application; Nancy Turmel, for her excellent assistance in my mapping studies; to Dr. Conrad Pelletier and Dr. Michel Carrier for providing me with human tissues for my microelectrode and patch-clamp studies; to Lise de Repentigny and Mary Morello for typing all the manuscripts included in this thesis. I also wish to express my attachment to all my friends with whom I have spent my time in the lab, including Mohsen Nayebpour, Suzanne Ranger, Guirong Li, Jianlin Feng, and Jinjun Wang for their friendship, wonderful collaboration, and invaluable help in different aspects of my life.

Special thanks to the Heart and Stroke Foundation of Canada for its continuous financial support from 1991-1994.

PREFACE

Note on the Format of this Thesis

In accordance with the Faculty of Graduate Studies and Research the candidate has the option of including as part of his thesis the text of original papers already published by learned journals, and original papers submitted or suitable for submission to learned journals. The exact wording relating to this option is as follows:

> The Candidate has the option, subject to the approval of the Department, of including as part of the thesis the text of an original paper, or papers, suitable for submission to learned journals for publication. In this case the thesis must still conform to all requirements explained in this document, and additional material (e.g. experimental data, details of equipment and experimental design) may need to be provided. In any case, abstract, full introduction and conclusion must be included, and where more than one manuscript appears, connecting texts and common abstract, introduction and conclusion are required. A mere collection of manuscripts is not acceptable; nor can reprints of published paper be accepted. While the inclusion of manuscripts co-authored by the Candidate and others is not prohibited for a test period, the Candidate is warned to make an explicit statement on who contributed to such work and to what extent. Copyright clearance from the co-author or co-authors must be included when the thesis is submitted. Supervisors and others will have to bear witness to the accuracy of such claims before the Oral Committee. It should be noted that the task of the External Examiner is much more difficult in such cases.

This thesis is composed of the following published and submitted papers co-authored by myself and others:

1. Wang Z, Pelletier LC, Talajic M, Nattel S: Effects of flecainide and quinidine on human atrial action potentials: role of rate-dependence and comparison with guinea pig, rabbit, and dog tissues. **Circulation** 82:274-283, 1990.
2. Wang Z, Page P, Nattel S: The mechanism of flecainide's antiarrhythmic action in experimental atrial fibrillation. **Circ Res** 71:271-287, 1992.

3. Wang J, Bourne GW, Wang Z, Villemaire C, Talajic M, Nattel S: Comparative mechanisms of antiarrhythmic drug action in experimental atrial fibrillation - The importance of use-dependent effects on refractoriness. **Circulation** 1993;88:1030-1044.

4. Wang Z, Feng J, Nattel S. Sustained Atrial Fibrillation in Dogs-Underlying Electrophysiologic determinants and Mechanism of Antiarrhythmic Action of Flecainide. (submitted to **Circulation**, in revision)

5. Fermini B, Wang Z, Duan DY, Nattel S: Differences in the rate dependence of the transient outward current in rabbit atrium. **Am J Physiol** 263:H1747-H1754, 1992.

6. Wang Z, Fermini B, Nattel S: The Delayed Outward Potassium Current (I_x) in Human Atrial Myocytes. **Circ Res** 73:276-285, 1993.

7. Wang Z, Fermini B, Nattel S: Rapid and Slow Components of Delayed Rectifier Outward Current in Human Atrial Myocytes. (**Cardiovasc Res**, in revision)

8. Wang Z, Fermini B, Nattel S: Sustained Depolarization-Induced Outward Current in Human Atrial Myocytes: Evidence for a Novel Delayed Rectifier Potassium Current Similar to Kv1.5 Cloned Channel Currents. **Circ Res** 1993;73:1061-1076.

9. Fedida D, Wible B, Wang Z, Fermini B, Faust F, Nattel S, Brown AM: Identity of a Novel Delayed Rectifier Current from Human Heart with a Cloned K^+ Channel Current. **Circ Res** 73:210-216, 1993.

10. Li G, Feng J, Wang Z, Fermini B, Nattel S. Comparative mechanisms of 4-aminopyridine resistant transient outward current in human and rabbit atrial myocytes. **Am J Physiol** (in press).

11. Absence of Cl^- currents in human atrial cells.

12. Wang Z, Fermini B, Nattel S: Effects of Flecainide, Quinidine, and 4-aminopyridine on Transient and Sustained Outward Currents in Human Atrial Myocytes. **J Pharmacol Exp Ther** (in press).

13. Wang Z, Fermini B, Nattel S: Mechanism of Flecainide's Rate-Dependent Actions on Action Potential Duration in Canine Atrial Tissue. **J Pharmacol Exp Ther** 1993;267:575-581

STATEMENT OF AUTHORSHIP

The following is a statement regarding the contributions of myself and co-authors to the papers listed in PREFACE.

Paper 1. I designed and performed the experiments, analyzed the data, and wrote the manuscript. Dr. Nattel provided close supervision in all aspects, generating the initial idea, clarifying the thoughts, reorganizing the data, and producing the final version. Dr. LC Pelletier provided the human atrial tissues for my study. Dr. M Talajic participated in discussing the data, giving suggestions, and reading the manuscripts.

Paper 2. The hypothesis was proposed based on the findings in paper 1. I designed and performed the experiments, analyzed the data, and wrote the manuscript. Dr. Nattel provided close supervision in all aspects, clarifying the ideas, reorganizing the data, and producing the final version. Dr. Pagé helped me analyzing the data, and reading the manuscript.

Paper 3. The initial idea was derived from paper 1 and 2. Jinjun Wang performed most parts of the experiments, analyzed the data, and wrote the manuscript. Dr. Bourne conducted parts of experiments and analyzed the data. I carried out the first few experiments, provided the technical supervision for Jinjun Wang and Dr. Bourne, helped them analyzing the data, and participating in discussing the results. Christine Villemaire participated in doing some experiments and provided technical assistance. Dr. Talajic participated in discussing the data and reading the manuscript. Dr. Nattel served in a supervisory capacity in all aspects and produced the final version of the paper.

Paper 4. The initial idea, experimental design, data analysis, and paper writing were generated by myself. Dr. Nattel served in a supervisory capacity in all aspects, clarifying the ideas, reorganizing the data, and producing the final version.

Paper 5. Dr. Fermini made the initial findings and performed parts of the experiments and wrote the paper. I performed most parts of the experiments and provided about 80% of the data presented in the paper. Dayue Duan provided a part of data. Dr. Nattel gave overall supervision, clarifying the ideas and improving the writing.

Paper 6. I made the initial finding, proposed the ideas and design, conducted all the experimental work and data analysis, and wrote the manuscript. Dr. Fermini helped me in designing the protocols, participated in discussing ideas and reading the manuscript. Dr. Nattel provided close supervision in all aspects, including sorting out thoughts, improving the experimental design, producing the final version of the paper.

Paper 7. Same as Paper 6.

Paper 8. I made the findings, proposed the ideas, designed the studies, performed the experiments, analyzed the data, and wrote the manuscript. Dr. Fermini helped me in designing the protocols, participated in discussing ideas and reading the manuscript. Dr. Nattel provided overall supervision, establishing the hypothesis, clarifying the ideas, modifying the designs, improving data analysis, and producing the final version of the paper.

Paper 9. Dr. Fedida performed the electrophysiological part of the studies on expressed currents from cloned K^+ channel. Dr. Wible completed the molecular cloning of the K^+ channel cDNA. I conducted the electrophysiological part of the studies on native current in human atrial myocytes. Dr. Fermini helped me in my part of the studies. Dr. Faust was involved in the molecular cloning of the K^+ channel cDNA. Dr. Nattel served in a supervisory capacity in the electrophysiological part of the studies. Dr. Brown served in a supervisory capacity in both molecular cloning and electrophysiological characterization of the cloned K^+ channel.

Paper 10. I proposed the original idea and performed parts of the experimental work and data analysis. Dr. Li conducted most parts of the studies, analyzed the data, and wrote the manuscript. Jianlin Feng completed parts of the experiments and data analysis. Dr. Fermini participated in discussing the data, giving suggestions, and reading the manuscript. Dr. Nattel provided overall supervision and produced the final version of the paper.

Paper 12. I made the findings and proposed the ideas. I completed most parts of the experimental work and data analysis, and wrote the manuscript. Jianlin Feng performed parts of the experiments and data analysis. Dr. Fermini participated in discussing data and reading the manuscript. Dr. Nattel provided overall supervision, clarifying ideas, generating hypothesis, analyzing data, and producing the final version of the paper.

Paper 13. I proposed the initial idea and performed all experimental work and data analysis, and wrote the manuscript. Dr. Fermini participated in discussing data, giving suggestions, and reading the manuscript. Dr. Nattel provided overall supervision, clarifying ideas, analyzing data, and producing the final version of the paper.

LIST OF ABBREVIATION

CV	Conduction Velocity (m/s)
ERP	Effective Refractory Period (ms)
WL	Wavelength (cm)
BCL	Basic Cycle Length (ms)
AF	Atrial Fibrillation
VNS	Vagal Nerve Stimulation
EAD	Early Afterdepolarization
DAD	Delayed Afterdepolarization
AP(s)	Action potential(s)
APD	Action Potential Duration (ms)
APD_{20}	Action Potential Duration to 20% Repolarization (ms)
APD_{50}	Action Potential Duration to 50% Repolarization (ms)
APD_{90}	Action Potential Duration to 90% Repolarization (ms)
APD_{95}	Action Potential Duration to 95% Repolarization (ms)
V_{max}	Maximum Rate of Voltage Rise During Phase 0 (V/s)
RP	Resting Potential (mV)
APA	Action Potential Amplitude (mV)
OS	Action Potential Overshoot (mV)
I_{Na}	Inward Na^+ Current
I_{Ca}	Inward Ca^{2+} Current
I_{K1}	Inward Rectifier K^+ Current
I_K	Delayed Rectifier K^+ Current
I_{Kr}	Fast Component of Delayed Rectifier K^+ Current
I_{Ks}	Slow Component of Delayed Rectifier K^+ Current
I_{Kstep}	I_K Amplitude at the End of the Depolarizing Step
I_{Ktail}	Amplitude of I_K tail Current
I_{to}	Transient Outward Current
I_{to1}	4AP-sensitive Transient Outward K^+ Current
I_{to2}	Ca^{2+}-activated Transient Outward Current
I_{sus}	Sustained Depolarization-induced Outward K^+ Current
I_{Kp}	Plateau K^+ Current
I_{Kur}	Ultra-rapidly Activating Delayed Rectifier Outward K^+ Current

I_{KAch}	Ach-induced K^+ Current
I_{KATP}	ATP-sensitive K^+ Current
I_{ClcAMP}	cAMP-activated Cl^- Current
I_{ClCa}	Ca^{++}-activated Cl^- Current
I_{ClATP}	ATP-activated Purinergic Cl^- Current
I_{ClPKC}	Protein Kinase C-induced Cl^- Current
$I_{Clswell}$	Swelling-induced Cl^- Current
HK1	Cloned Human Cardiac K^+ Channel (Kv1.4)
HK2	Cloned Human Cardiac K^+ Channel (Kv1.5)
fHK	Cloned Human Fetal Cardiac K^+ Channel
I_{sK}	Cloned Cardiac K^+ Channel, the Minimal K^+ Channel or the Slow K^+ Channel
I-V relation	Current-voltage Relation
R_s	Series Resistance
R_i	Internal Resistance
R_m	Specific Membrane Resistance
R_{in}	Input Resistance
r	Cell Radius (μm)
l	Cell Length (μm)
SC	Space Constant
τ	Time Constant
τ_c	Capacitance Time Constant
τ_{act}	Activation Time Constant
τ_{inact}	Inactivation Time Constant
τ_{deact}	Deactivation Time Constant
$V_{1/2}$	Voltage for Half-maximal Activation or Inactivation
Flec (F)	Flecainide
Quin (Q)	Quinidine
4AP	4-Aminopyridine
TEA	Tetraethylammonium Chloride
Caf	Caffeine
DIDS	4,4'-Diisothiocyanatostilbene-2,2'-disulfonic Acid
α-DTX	α-Dendrotoxin
Ach	Acetylcholine
Iso	Isoproterenol

CONTENTS

TITLE	i
DEDICATION	ii
ABSTRACT	iii
ACKNOWLEDGMENTS	v
PREPACE	vi
STATEMENT OF AUTHORSHIP	viii
LIST OF ABBREVIATIONS	x
CONTENTS	xii
CHAPTER 1. INTRODUCTION	
1. REPOLARIZATION AND ARRHYTHMIAS	1
1-1. Repolarization and refractoriness	1
1-2. Repolarization and arrhythmias	3
1-2-1. Refractoriness and reentry	3
1-2-2. Repolarization and early afterdepolarization	6
1-2-3. Effects of altering repolarization on clinical arrhythmias	7
1-3. Drug actions on repolarization and refractoriness	7
2. FACTORS AFFECTING ACTION POTENTIALS	8
2-1. Basic characteristics and species differences	8
2-2. Developmental differences	9
2-3. Regional differences	10
2-4. Frequency dependence	11
2-5. Electrophysiology of diseased atria	12
2-6. Drug actions on repolarization	12
3. PROPERTIES OF KNOWN REPOLARIZING CURRENTS	13
3-1. Potassium currents	13
3-1-1. Voltage-dependent potassium currents	13
3-1-1-1. The 4-AP-sensitive transient outward K^+ current (I_{to1})	13
3-1-1-2. The delayed rectifier outward K^+ current (I_K)	15
3-1-1-3. The inward rectifying background K^+ current (I_{K1})	16
3-1-1-4. K^+ currents activated at plateau voltages	17
3-1-2. G protein-gated K^+ current	18
3-1-2-1. Acetylcholine-activated K^+ current (I_{KAch})	18
3-1-3. Ligand-regulated K^+ currents	19
3-1-3-1. ATP-sensitive K^+ current (I_{KATP})	19

3-2. Na/K pump current ($I_{Na/K}$) 19
3-3. Na/Ca exchange current ($I_{Na/Ca}$) 20
3-4. Cardiac Chloride currents 21
3-4-1. cAMP-regulated Cl^- current (I_{ClcAMP}) 21
3-4-2. Ca^{++}-activated Cl^- current (I_{ClCa} or I_{to2}) 21
3-4-3. Other Cl^- currents 21
3-5. Currents expressed by cloned K^+ channels 22
3-6. Repolarizing currents in human atrial myocytes 22
3-6-1. 4AP-sensitive transient outward K^+ current (I_{to1}) 23
3-6-2. Ca^{++}-activated transient outward current (I_{to2}) 23
3-6-3. Inward rectifier K^+ current (I_{K1}) 23
3-6-4. Ach-induced K^+ current (I_{KAch}) 24
3-6-5. ATP-sensitive K^+ current (I_{KATP}) 24
3-6-6. Na/K pump current ($I_{Na/K}$) 24
3-6-7. Expressed currents by cloned K^+ channels 24
3-6-7-1. Current expressed by Kv1.4 24
3-6-7-2. Current expressed by Kv1.5 25
3-6-7-3. Current expressed by I_{sK} or minK 26
3-6. Summary 26
4. QUESTIONS RAISED FROM THE ABOVE OVERVIEW 27
5. APPROACHES TO ADDRESS THE ABOVE QUESTIONS 28
5-1. Atrial epicardial activation mapping-whole dog experiments 28
5-2. Standard microelectrode techniques-cellular approaches 28
5-3. Whole-cell patch-clamp techniques-studies of ion currents 28
6. REFERENCES 29
CHAPTER 2. FACTORS AFFECTING REPOLARIZATION AND ARRHYTHMIA 47
1. Effects of drugs on human atrial action potentials: Role of rate-dependent changes in repolarization 48
2. The mechanism of flecainide's antiarrhythmic action in experimental atrial fibrillation 60
3. Comparative mechanisms of antiarrhythmic drug action: The importance of use-dependent effects on refractoriness 78
4. Sustained atrial fibrillation-underlying electrophysiologic determinants 94

CHAPTER 3. REPOLARIZING CURRENTS IN HUMAN ATRIUM 163

1. The rate dependence of the 4-aminopyridine sensitive transient outward current (I_{to}) 121
2. The delayed outward potassium current (I_k) 130
3. Rapid and slow components of delayed rectifier outward potassium current (I_{Kr} and I_{Ks}) 140
4. Sustained depolarization-induced outward current (I_{Kur}) and its role in repolarizing human atrial myocytes 148
5. Identity of a novel delayed rectifier current from human heart (I_{Kur}) with a Kv1.5 cloned K^+ channel current 164
6. Comparative mechanisms of 4-AP resistant I_{to} in human and rabbit atrial myocytes 172
7. Absence of Cl^- currents in human atrial cells under physiologic conditions 198

CHAPTER 4. DRUG EFFECTS ON REPOLARIZING CURRENTS AND REPOLARIZATION

1. Effects of drugs on the transient and the sustained outward currents in human atrial myocytes 208
2. Mechanism of flecainide's rate-dependent actions on action potential duration in canine atrial tissue 248

CHAPTER 5. GENERAL DISCUSSION

1. Summary of novel findings in this thesis 255
2. Direction of future research 261
3. References 265

CHAPTER 1

INTRODUCTION

1. Repolarization and Arrhythmias

Upon receiving stimuli or impulses, cardiac cells, like other excitable cells such as neurons and skeletal muscles, will generate a pattern of changes in transmembrane potentials, i.e. action potentials (APs). The unique characteristic of the cardiac action potential which distinguishes it from those in other tissues is that the cardiac AP has a long plateau phase and total duration due to a slow rate of membrane repolarization. Membrane potential is governed by ion currents flowing through channels or carried by exchangers[1-1,2]. Figure 1 is a schematic representation of a typical cardiac AP, summarizing the relationships between various ion currents and resultant changes of membrane potential.

The large K^+ conductance produced by I_{K1} determines the level of membrane polarization-the resting membrane potential[1-1,2,3]. Na^+ entering into the cell generates the initial fast depolarization (phase 0 upstroke of the AP), changing the membrane potential from a negative to a positive value[1-3]. K^+ flowing out leads to membrane repolarization, bringing the membrane back to its original negative value. I_{to1}, a transient outward K^+ current, is responsible for phase 1 rapid repolarization[1-1,2,4,5]. Slow inward current (I_{Ca}) accounts for the maintained phase 2 plateau or 'dome' (the secondary depolarization)[1-6], and I_{to2} may counteract I_{Ca}[1-7,8,9]. Activation of I_{Kr} and I_{Ks}, the delayed rectifiers, results in termination of phase 2 plateau/dome and initiation of phase 3 repolarization[1-2,4 10,11,12,13]. I_{K1} may contribute importantly to the final phase of repolarization[1-3,14]. Na/K pump is crucial in maintaining the ionic balance between both sides of the membrane by extruding Na^+ back to the outside and importing K^+ back to the inside, and in doing so it generates an outward current[1-15,16,17]. Therefore, the Na/K pump may also play a significant role in repolarizing the membrane[1-15,16,17]. A possible involvement of I_{Cl} in regulating resting potential and repolarization has also been suggested[1-18]. In atrial cells and Purkinje fibers, I_{KAch} can contribute importantly to membrane repolarization[1-2]. Under pathological conditions, the role of I_{KATP} becomes significant[1-2,19]. The plateau phase, the major determinant of the cardiac action potential duration (APD), is determined by a delicate balance between inward and outward current[1-2,4]. Any net change in plateau current can lead to a substantial alteration of membrane potential due to the high input resistance, resulting in an acceleration or a deceleration of repolarization[1-2,4]. Different species and tissues may have different AP characteristics because of different underlying ionic mechanisms, as will be discussed in later sections.

1-1. Repolarization and refractoriness

Normal cardiac function depends on normal electrophysiological activity of the heart. Disorders of cardiac rhythm are a consequence of abnormal electrophysiological activity. Normally, once a cell fires, it loses its excitability until repolarization proceeds to the point that

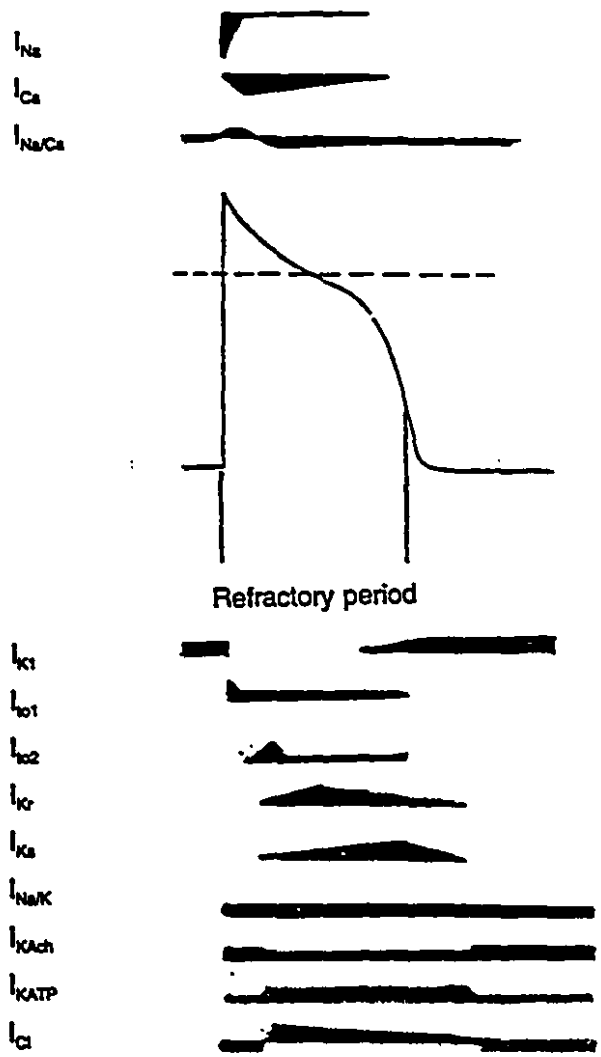

Figure 1. Diagram illustrating ion currents contributing to membrane resting and action potentials of cardiac cells. Solid bars indicate the relative size and duration of each individual current. Adapted from figure 1 of reference 1-2 with modification.

the voltage- and time-dependent recovery of excitability occurs. This duration is the refractory period, as shown in Figure 1. Any stimuli or impulses falling into this period will not elicit a propagated AP. This implies that the refractory period prevents cells from responding to excessively rapid activation or premature excitation. Thus, the long action potential duration (APD) of cardiac myocytes has a major physiologic significance in preventing cardiac arrhythmias.

In the normal atrial or ventricular myocardium, the recovery of excitability is strictly proportional to the duration of repolarization[1-20,21]. This is indicated by several facts: (1) Longer ERP is always associated with longer APD, and vice versa. For example, APD varies among different species. Action potentials from atrial tissues of various species have increasing duration in the order: guinea pig[1-22], rabbit[1-23], dog[1-24,25], and man[1-26-49]. The ERP also has the same relative order among the same species[1-23,25,49]. In the same species, APD is the longest in Purkinje fibres, then in ventricular muscle, and the shortest in atrial cells. Correspondingly, ERP follows the same gradient from Purkinje fibres to ventricle, and then to atrium. (2) Changes in ERP parallel changes in repolarization. Any interventions that abbreviate or lengthen APD will simultaneously abbreviate or lengthen ERP[1-50-53]. For instance, acceleration of heart rate shortens APD[1-49]. The same correlation between heart rate and ERP also holds true[1-49]. Drugs that prolong APD also increase ERP (see below). (3) In the normal myocardium, the dispersion of refractoriness parallels the dispersion of repolarization. For example, as described by Spach and colleagues[1-24,25], both APD and ERP are longer in the area of the sinus node and gradually decrease with increasing distance from the sinus node.

1-2. Repolarization and arrhythmias

The timing of repolarization controls the duration of the AP, which determines the length of refractory period, which in turn is a crucial determinant of arrhythmias[1-52,54,55]. The consequences of APD prolongation are two-fold. On one hand, slowing repolarization or lengthening APD is beneficial for reentrant arrhythmias, and other types of arrhythmias including DAD-induced triggered activity (delayed afterdepolarization). On the other hand, APD prolongation, particularly at slow heart rates, may also be proarrhythmic in the ventricle by inducing early afterdepolarizations, torsade de pointes arrhythmias, and the long QT syndrome[1-52,56].

1-2-1. Refractoriness and reentry

Reentry refers to a situation in which an area of the myocardium is reexcited by a circulating impulse[1-1,57]. The concept that a circulating impulse could reexcite the same tissue over and over again was first proposed by McWilliam as early as 1897 in an article entitled "Fibrillar Contraction of the Heart"[1-58] This concept, later known as reentry, was experimentally confirmed in independent studies more than 10 years later by Mayer[1-59], Mines[1-60], and Garrey[1-61]. From their studies on rings of excitable tissue, the roles of refractoriness, slow conduction, and unidirectional block in causing reentry were defined. Lewis[1-62] further applied concepts about reentry developed in studies of rings of tissue in which there was an anatomically defined reentrant pathway around an obstacle to the anatomical properties of the heart, and

further applied concepts about reentry developed in studies of rings of tissue in which there was an anatomically defined reentrant pathway around an obstacle to the anatomical properties of the heart, and established the concept of anatomical reentry. It was shown that anatomical reentry may occur in the peripheral Purkinje system[1-63] and bundle branches in the ventricles[1-64], the A-V conducting system and a bypass track in the preexcitation syndrome[1-65], and atrial vessels such as the inferior vena cava[1-66]. Schmitt and Erlanger in 1928 proposed the idea of functional reentry[1-67]. Reentry that occurs because of functional heterogeneities in the electrophysiological properties of cardiac fibers, such as heterogeneities of refractory period, has subsequently been shown to be an important cause of arrhythmias such as atrial flutter and fibrillation. The theory of functional reentry was further developed by Allessie et al. [1-68] in their paper on the "leading circle" mechanism. Reentry caused by this mechanism can be initiated in the atrial free wall by a premature impulse that blocks in a region with relatively longer ERP but conducts slowly through adjacent regions with shorter ERP. The slowly conducting impulse eventually returns to the area of block after it has recovered excitability, and then conducts through this region to reexcite areas on the proximal side of the block.

Figure 2 is a diagram for functional reentry. The arrow indicates the direction of impulse propagation. The darkened area represents the absolute refractory period and dotted area the effective refractory period. There is no excitable gap in this type of reentry. The total circuit time, or the cycle length of reentry, is determined by the ERP. Atrial fibrillation has been shown to be a typical example of functional reentry[1-69,70,71,72]. The persistence of AF depends on the co-existence of multiple reentrant wavelets[1-61,69,70,73,74,75].

Reentry underlies many clinical and experimental arrhythmias, including ventricular tachycardia[1-76], ventricular fibrillation[1-77], atrial repetitive activity[1-76], atrial flutter[1-76], atrial fibrillation[1-69-72,76], W-P-W syndrome[1-65], atrioventricular reentry[1-65], etc. The two pre-conditions for reentry are (1) unidirectional block as a consequence of non-uniformity of refractory period; (2) slow conduction[1-1,57].

The ability to initiate reentrant tachycardia is related to the local ERP at the site of stimulation. When the local ERP is short, premature beats with a short coupling interval can be induced. The shorter the coupling interval of a premature beat, the greater the chance that this impulse will result in unidirectional block and, thus, initiate tachycardia. Prolongation of ERP will increase the shortest possible coupling interval of a premature beat. If this increase is large enough, the coupling interval will be too long to initiate a propagating impulse able to induce unidirectional block and reentrant tachycardia. In addition, lengthening of ERP is also likely to constitute an antifibrillatory mechanism. The tachycardia cycle length will be prolonged and will prevent the arrhythmia from deteriorating into fibrillation. In addition, the long ERP will delay the onset of the next action potential, and therefore the tachycardia will be slowed and will be hemodynamically more stable[1-50,52].

CIRCUS MOVEMENT WITHOUT ANATOMIC OBSTACLE (LEADING CIRCLE MODEL)

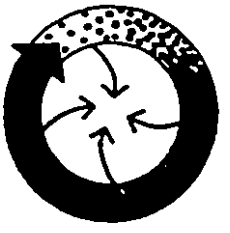

1. Length of circuit determined by conduction velocity, stimulating efficacy, and refractory period.
2. Length of the circuit can change with alterations in electrophysiologic properties.
3. No gap of full excitability.
4. Shortcut of the circuit possible.
5. Revolution time proportional to refractory period.

Figure 2. Diagram illustrating the properties of reentry circuit without the involvement of a central anatomical obstacle (functional reentry). Arrows indicate directions of wavefront propagation. Solid and dotted bars represent the absolute and the effective refractory period, respectively. Adapted from figure 8 of reference 1-68 with modification.

It is known that wavelength of excitation (WL), defined as the minimal length of an excitation

It is known that wavelength of excitation (WL), defined as the minimal length of an excitation pathway which can support a reentrant circuit (formulated as the product of conduction velocity (CV) and refractory period (ERP)[1-78-82]), is an important determinant of reentry and a powerful predictor of different types of atrial arrhythmias[1-70,78,82]. When WL is long because of an increased ERP, a large area of conduction block is required, while when WL is short (because of depressed conduction, shortened ERP or both) small areas of conduction block may set up reentrant circuits. Because conduction block is more likely to occur in small areas than in a large portion of the myocardium, it is to be expected that the inducibility of reentrant arrhythmias also depends on the WL. Since for perpetuation of AF a critical number of wandering wavelets is required, the WL is also important for the degree of stability of fibrillation. If the WL during fibrillation is relatively long, the reentry circuits will be larger, fewer waves can circulate through the atria, and fibrillation will be short-lasting. If, however, the WL during fibrillation is short, a greater number of wavelets will be present, and fibrillation will tend to be stable and long-lasting[1-70]. In this sense repolarization (ERP), as one of the determinants of WL, has its crucial role in determining reentry.

Spatial heterogeneity of repolarization in cardiac tissue has been a long-recognized phenomenon. The elegant studies performed by Spach and colleagues[1-24,25] demonstrated that in canine right atrium regional differences in repolarization follow an overall simple pattern: the longest action potentials were recorded in cells located in the area of the sinus node, and APD decreased gradually with increasing distance from the sinus node area. Under physiologic situations this pattern of dispersion of repolarization ensures the safety of propagation of impulses that conduct from the sinus node area to the A-V node. Hence, it provides a fundamental protective mechanism to ensure synchronous atrial contractions by preventing reentrant repetitive activity following the most commonly occurring "premature" impulses. On the other hand, spatial dispersion of refractoriness as a consequence of inhomogeneity of cellular repolarization is also an important factor in arrhythmias. The most likely mechanism of arrhythmia to be facilitated by dispersion of repolarization is reentry. The premature beats initiating tachycardia are most effective when propagating across a border between two areas of sharply different ERPs in the direction of the shorter ERP while being blocked in the direction of the longer ERP. Thus, the site with the longer APD forms the focus of unidirectional block and serves as a barrier around which the impulse is spreading. An example of an experimental model in which dispersion of repolarization is considered to play a crucial role in the maintenance of arrhythmia is the circus-movement tachycardia induced in a segment of rabbit atrial tissue[1-23,82]. Increased inhomogeneity of ERP has also been confirmed in patients with atrial flutter or/and atrial fibrillation[1-49,83-86].

1-2-2. Repolarization and early afterdepolarization

Delaying of repolarization is not always beneficial, but could also be proarrhythmic under certain circumstances. Early afterdepolarizations (EADs) in the ventricles are now thought to be important in the genesis of torsade de pointes in the setting of prolonged cardiac repolarization[1-1,52,56,57,87]. EADs refer to

oscillations in the membrane potential that occur during the plateau or phase 3 repolarization[1-57]. Once EADs cause surrounding repolarized tissue to reach threshold and fire, single or multiple APs (so-called triggered activity) can be induced. EAD amplitude increases and the likelihood of initiating a triggered arrhythmia is enhanced as drive rate decreases[1-56,57]. Any factors which cause excessive lengthening of APD, particularly at slow activation rates and promote inward Na^+ or/and Ca^{++} current, may induce EADs[1-1,52,56,57]. Thus, drugs that increase APD not only have the ability to prevent both atrial and ventricular fibrillation but, given the appropriate clinical setting, they also have the proclivity to induce torsade de pointes ventricular arrhythmias[1-58].

1-2-3. Effects of altering repolarization on clinical arrhythmias

In clinical settings where the cardiac action potential is shortened, there is an increased probability of fibrillation; likewise, there is a decreased probability of fibrillation in the setting of prolonged refractoriness. For example, in the case of hypothyroidism, a situation in which there is uniform prolongation of repolarization[1-89,90], arrhythmias of all kinds are uncommon. In contrast, in thyrotoxicosis, in which atrial APD is markedly abbreviated[1-91], a high incidence of atrial fibrillation (AF) is well documented. Vagal stimulation in experimental animals markedly shortens APD in the atria and increases inhomogeneity of excitability due to non-uniform vagal inervation, a setting in which AF can be induced readily by a single atrial extrastimulus[1-92]. It is also known that patients with AF tend to have a shorter APD and effective refractory period (ERP)[1-49,83,93-96]. Similarly, patients cardioverted to sinus rhythm relapse more frequently to AF if they have a shorter APD than if they have a longer APD[1-93]. Dilated atria have shorter ERP, and patients with enlarged atria are more susceptible to atrial arrhythmias[1-97]. Drugs which produce lengthening of APD negate the tendency for the development of the arrhythmia. Studies by Olsson et al.[1-98] and Gavrilescu et al.[1-93-95] indicate that a correlation exists between atrial monophasic action potential duration and the tendency for AF and flutter.

1-3. Drug actions on repolarization and refractoriness

Since ERP is a major determinant of the likelihood of arrhythmias, and since repolarization is the major determinant of the ERP, interventions that alter repolarization can critically affect arrhythmias. In fact, many antiarrhythmic drugs in clinical use are believed to exert their beneficial actions by delaying repolarization or prolonging ERP[1-50-55]. On the other hand, as mentioned above, proarrhythmic effects may also arise with APD-prolonging drugs.

Based on the current classification system[1-99-101], antiarrhythmic drugs are divided into six categories: Class I drugs, local anesthetics, are Na^+ channel blockers. Based on their kinetics of blocking action, they are further divided into three subgroups: 1) Class Ia agents, e.g., quinidine and procainamide, have moderate potency at delaying conduction, and also increase APD; 2) Class Ib drugs such as lidocaine and mexilitine slow conduction with the lowest potency, have rapid recovery kinetics, and produce little if any change in APD; 3) Class Ic drugs such as flecainide and propafenone are the most potent Na^+

on repolarization. 4) Class II drugs are β-receptor antagonists. 5) Class III drugs such as d-sotalol prolong repolarization with minimal action on conduction. 6) Class IV agents are Ca^{++} channel blockers.

Drugs that increase APD have been used to treat cardiac arrhythmias for a long time. Quinidine was introduced in 1918 for controlling cardiac arrhythmias, especially atrial fibrillation. Lewis[1-102] recognized the significance of changes in ERP as a major determinant of the salutary effect of drugs in this arrhythmia.

The major action of class III drugs is delaying repolarization[1-30-54,99-101]. They demonstrate greater efficacy than class I agents in preventing ventricular arrhythmias occurring during acute ischemia or evoked by programmed electrical stimulation, while producing less cardiac depression[1-52]. However, these agents produce reverse use-dependent APD prolongation, an effect which may limit their effectiveness in arrhythmias[1-103], because of: (1) a diminished ability to prolong repolarization at fast heart rates corresponding to tachycardias; (2) an excessive APD lengthening at slow heart rates, which may result in EAD-induced triggered activity.

Interestingly, class Ic agents, flecainide and propafenone, have been found highly effective in converting AF to sinus rhythm and preventing its recurrence[1-68-70] despite the fact that they are believed to have no effects on repolarization according to the current classification system of antiarrhythmic drugs[1-99-101]. Theoretically, conduction slowing produced by class Ic drugs should favour reentry, and this might be one of the mechanisms by which this class of agents is proarrhythmic as shown by the CAST studies[1-117,118]. This apparent discrepancy between the efficacy of class Ic drugs in AF and their typical electrophysiologic actions presents a challenge to our understanding of AF and/or antiarrhythmic drug action. Resolving it was one of the goals of this thesis.

2. Factors Affecting Action Potential Duration and Morphology

Microelectrode techniques were first used to record transmembrane potentials from human atria by Trautwein and his co-workers (1962)[1-34] after extracorporeal techniques for open heart surgery had been developed. Although this work represented a milestone, the first systematic study of clinically normal human atrium by Gelband et al. (1972)[1-37] did not appear until 10 years later.

The properties of action potentials are species specific, age-related, regionally variable within a given tissue, and frequency dependent. These differences can modify the tissue response to interventions, and thus they must be considered in understanding the relationship between the electrophysiological activity of cardiac cells and arrhythmias, the relationship between basic research and clinical observations, and the mechanisms of arrhythmias and antiarrhythmic actions.

2-1. Basic characteristics of atrial action potentials and species differences

Characteristics of human atrial action potentials have been extensively studied[1-26-49]. In most cases, isolated specimens from right atrial appendages were employed. Action potentials at 35-37°C at a physiological heart rate (about 1 Hz) have a rapid phase 1 repolarization forming an initial sharp spike,

followed by a phase 2 secondary depolarization or long plateau with a notch between phase 1 and phase 2. The rate of phase 3 and the final phase of repolarization is relatively slow. Overall action potential morphology has been referred to as a 'spike and dome'. In some cells, action potentials display triangular configurations with clear phase 1 repolarization and no phase 2 plateau[1-27,29]. In some other cells, a more or less rectangular shape of the action potential has been observed, with a small phase 1 followed by a high level plateau and relatively rapid phase 3 repolarization[1-33,40].

Cells with a typical 'spike and dome' waveform have resting potentials around -70 to -86 mV, and action potential amplitudes of 85-110 mV[1-26-49]. The rate of rise of phase 0 upstroke (V_{max}) ranges from 180-300 V/sec. Action potential duration to 50% and 90% of repolarization (APD_{50} and APD_{90}) average 150-220 msec and 300-480 msec, respectively[1-26-49]. There are major differences in action potential characteristics among species. Rat atrial action potentials have typical triangular shape without separation of different phases of repolarization[1-119]. The APD is very brief compared to other species. Action potentials recorded in rabbit atrium have similar morphology but a phase 1 is distinct from later phases of repolarization[1-23]. A prominent transient outward current has been recorded in the above species[1-120]. In contrast, action potentials of guinea pig atrium show a high level of the plateau and relatively steep phase 3 repolarization without phase 1 rapid repolarization[1-22]. In the dog, it has been demonstrated that action potential morphology and duration vary in a spatial pattern[1-24,25]. In some areas, 'spike and dome' action potentials with longer duration like those found in man are seen, and in other regions, triangular shaped action potentials are recorded with shorter duration. By comparison, the APD of various species decreases in the order man > dog > rabbit > guinea pig > rat, whereas resting potential and V_{max} are in the same range among different species.

2-2. Developmental differences

Variations in action potential properties are seen even in the same species and the same type of tissue. Escande et al.[1-29] correlated changes of action potential plateau shape in human atrial fibres to the age of the patients. They found that in adult tissues (30-67 years) there was only one type of action potential, the 'spike and dome' configuration, whereas in young atria (2-22 months) only 'triangular' shaped action potentials were seen. APD_{90} of cells from young patients was significantly briefer than that of adults (266±11 vs. 448±19 ms). 4-aminopyridine (4-AP), a transient outward K^+ current blocker, transformed the 'spike and dome' adult type of action potential to a triangular action potential like that seen in young patients. In addition, the use-dependence of APs from adults and young patients were found to be different (see ***Frequency dependence***). Differences in repolarization between adult and young atria have also been found in in vivo studies of normal subjects[1-121-123]. Atrial ERP in children was significantly shorter than the value in adults, and similarly, dispersion of refractoriness is less in young patients relative to adults.

Other observations suggest that age-related differences may not be so absolute. Spach et al.[1-27]

found 'spike and dome' action potentials in atrial pectinate muscle bundles from 49 patients over a broad range of ages from 1 to 70 years. Studies performed by Tuganowski and Cekanski[1-33] in atrial tissues from human embryonic hearts demonstrated, in the same preparations, three different types of APs. The 'spike and dome' type similar to the 'adult type', as defined by Escande et al.[1-29], was the most frequently observed configuration. The second type of AP, which was less frequently seen, had a triangular shape resembling the 'young type' action potentials in Escande's description. Finally, there was a third type of action potential, less commonly observed, with short duration and a more or less rectangular waveform. In fact, many earlier and later studies also reported several types of action potentials, regardless of the age of patients. Both 'spike and dome' and triangular shapes of action potentials have been recorded in the same atrial preparations from patients at ages ranging from 1 to 70 years[1-34-39,41]. Action potentials with rectangular configuration was also found in studies by Mary-Rabine et al[1-40].

In summary, it appears clear that atrial action potentials undergo certain developmental changes. However, the definition of 'adult type' and 'young type' action potentials may be an oversimplification. Variations exist among subjects of similar age, the same patient, or even the same preparation. There are three possible explanations: (1) The aforementioned three different types of action potentials may exist in different proportions in adults compared to younger individuals; (2) There is a different spatial distribution of the three different types of action potentials in different ages of patients, so that preparations obtained from different parts of atria would have different combinations of the types; and (3) both (1) and (2). The ionic mechanisms underlying the different shapes of action potentials are poorly understood. Escande et al.[1-27] have proposed that there is a larger I_{to1} in cells with a 'spike and dome' compared to cells with a triangular shape[1-27].

2-3. Regional differences

Spatial variation of repolarization is a well-recognized phenomenon in cardiac tissue. Action potentials recorded at different regions, such as the sinus node, atrium, AV node, ventricle and ventricular conducting (His-Purkinje) system, have substantial differences in morphology. Even in the same type of tissue under the same conditions, action potentials may vary from site to site (or cell to cell). The shape and duration of the action potential vary markedly throughout the right atrium[1-124-128]. Spach et al. (1989)[1-24,25] performed a thorough analysis of the spatial pattern and the dimension of the inhomogeneities of repolarization in canine right atrium. Their results demonstrate that although there are multiple regional differences in AP configuration, duration, and response to activity, the overall distribution produced a rather simple spatial pattern in which the longest APs occurred in the region of the sinus node, and the AP duration decreased with increasing distance from the sinus node. Action potentials recorded within the upper crista terminalis had 'spike and dome' configuration. When the recording site was moved to the lower crista, the plateau phase was no longer seen, and APs were generally triangular but with the initial rapid repolarization, the 'spike'. In the pectinate muscle, APs showed a triangular shape without the spike.

Whether similar regional differences of repolarization are also present in human atrium is still unclear. An early study performed by Gelband et al.[1-37] described two types of action potentials recorded from cells that they designated specialized fibers and contractile fibers. Although there is no solid evidence for the existence of specialized fibres in human atria, their work did demonstrate spatial variations of action potentials: action potentials recorded in the bundle connecting the pectinate muscles had a prominent phase 1 spike and phase 2 plateau with longer APDs, whereas action potentials recorded in the pectinate muscles showed a triangular shape and briefer duration. This pattern is similar to what has been seen in the canine right atrium. Studies in human embryonic heart by Tuganowski and Cekanski (1971)[1-33] also provided evidence for regional differences of repolarization. They found that 'spike and dome' action potentials were very widespread over the atria. Triangular action potentials were recorded in appendages, whereas action potentials with brief duration were mostly observed in the region near the septum. Boutjdir et al.[1-49] discovered about 70 msec dispersion of ERP measured at five sites around (0.8 mm) the simulating electrode. In vivo investigations support the concept of spatial variation of repolarization. Hayward and Taggart[1-46] reported that the duration of monophasic action potentials in the high right atrium are approximately 20-30 msec longer than the values obtained in the low right atrium. Luck[1-64] has also reported approximately 40 msec dispersion of refractoriness in human atrium paced at an interval of 500 msec.

2-4. Frequency dependence

Heart rate is a critical modulator of action potential characteristics, particularly the duration of action potential and refractoriness. Frequency-dependent changes in the electrical activity of the heart have been extensively studied at the cellular level in a variety of species, including guinea pig[1-127,128], dog[1-129,130], rabbit[1-131,132] and man[1-26-28,128].

Studies on human atrial fibers by several groups[1-26-28] reported similar findings on the frequency-dependent properties of action potentials: (1) The typical "spike and dome" morphology of human atrial action potentials were seen at a physiological heart rate (1 Hz). Little change in the shape occurred until the stimulus rate was increased beyond 2 Hz. Further increases in the frequency resulted in the disappearance of the secondary depolarization ("dome") with development of a distinct plateau at about 2.5 Hz. At higher rates, the plateau was abolished, although the initial repolarization phase was not noticeably modified, and phases 2 and 3 merged to produced a triangular morphology. (2) The rate of repolarization was substantially accelerated at faster rates, resulting in rate-dependent shortening of the APD. APD measured at the shortest pacing interval (approximately 210 msec) which produces 1:1 capture was less than 50% of the value determined at 1 Hz[1-28]. At even higher rates (corresponding to atrial flutter), there was an alternation in plateau duration[1-28].

Application of Ca^{++} channel blockers such as Co^{++} and diltiazem aggravated APD shortening at rapid rates, indicating that Ca^{++} current contributes to maintaining APD[1-28]. Low concentrations of TTX

further shortened APD, suggesting a possible role of TTX-sensitive plateau Na^+ channels[1-28]. The effects of 4-aminopyridine (4-AP), a K^+ channel blocker, on human atrial fibers depends on atrial activation rate. 4-AP shortens APD at physiologic and slower rates[1-28-30], whereas it slows repolarization at high frequencies[1-28], supposedly by blocking the transient outward current (I_{to1}). This suggests that I_{to1} might modulate the action potential at high frequencies. Similarly, ouabain also shortens APD at slow rates[1-28,31] but lengthens APD during fast pacing[1-28], suggesting that the Na/K ATPase contributes to the control of APD at rapid rates.

Frequency-dependent APD shortening seems to be a common property for most species and tissues. In rabbit ventricular preparations, however, an opposite frequency-dependence has been consistently observed at frequencies ranging from 0.1 to 2 Hz: APD is prolonged and the plateau elevated with increasing heart rate. Application of 4-AP or verapamil both eliminate this pattern of rate-dependent change[1-132].

2-5. Electrophysiology of diseased atria

The major cellular electrophysiological characteristics of human atrium as determined in normal tissues have been summarized above. Although this information is of great value for assessing the possible relation between cellular repolarization and rhythm disorders, direct relevance to the electrophysiological activities of arrhythmic atria is still unclear. So far, only one study has focused on the alterations of repolarization occurring in arrhythmic atria. Boutjdir et al.[1-49] identified several important changes in cellular electrophysiologic properties in atria of patients with AF (52±13 years old) relative to non-AF atria (35±17 years old). Action potentials from non-AF hearts typically showed 'spike and dome' waveforms, whereas AF atria had only triangular-shaped action potentials. Atrial APDs from AF hearts were consistently shorter than those of non-AF hearts. Similarly, ERP of AF atria was also shorter relative to non-AF atria. In the AF group, the dispersion of ERP (determined as the longest minus the shortest ERP measured at five different sites around the stimulation electrode at a given basic cycle length) was significantly higher than in the non-AF group. Increased dispersion of atrial refractoriness and shortened ERP in patients with documented episodes of AF have also been reported in clinical studies[1-83-86]. It is likely, based on the above observations, that altered repolarization is an important factor in determining AF, because nonuniform abbreviation of refractoriness may predispose to reentrant arrhythmias like atrial fibrillation.

2-6. Drug actions on repolarization

Drug modulation of atrial repolarization has been studied in a variety of animal species. Class I drugs, such as quinidine[1-22,133], flecainide[1-134,135] and encainide[1-136], have been shown to increase APD in guinea pig, rabbit, and canine atrial tissues. APD-lengthening effects of class III agents (sotalol, amiodorane, tedisamil, etc) in atrial tissues have also been reported[1-48,50-55].

Pharmacological responses of human atrial tissues to several antiarrhythmic agents have also been

assessed[1-30,41,43,45,46]. Hordof and co-workers[1-39] observed APD-prolonging effects of procainamide in human atrial preparations. Prolongation of APD and ERP by flecainide was reported[1-41,135], but the effects were found to depend on the morphology and duration of APs. In cells with triangular configuration, no significant changes in APD and ERP were observed. In cells with 'spike and dome' shape, flecainide increased APD and ERP. Penticainide (CM 7857), a new class ' antiarrhythmic agent, has also been reported to have a preferential action on 'spike and dome' action potentials, relative to triangular ones[1-43]. Studies with in vivo monophasic atrial action potentials showed that sotalol increased APD with stronger actions in low right atrium than in high right atrium at various pacing cycle lengths[1-46]. The action of verapamil was more complicated: it produced a decrease in the duration of the plateau but a prolongation of the time to full repolarization. Ouabain was found to abbreviate APD at slow pacing rates but to prolong APD at high frequencies[1-28,31], causing rate-dependent APD prolongation.

Variations in action potential morphology and duration among different species bring up some questions: Do drug actions in different species differ? Can results obtained in other animal species be extrapolated to human atrium? What are the ionic bases of differences in action potential morphology and drug response across species?

3. Properties of Known Repolarizing Currents

Repolarizing currents refer to all outward currents that serve to repolarize the membrane back towards its initial resting potential after depolarization. Several classes of repolarizing currents have been defined, including potassium currents, Na pump current, Na/Ca exchange current, and chloride currents. K^+ currents are believed to constitute the major repolarizing currents in the heart. K^+ channels are the most structurally and functionally diverse set of channel proteins[1-2,139-141]. Based on the gating mechanisms of K^+ channels, they are classified into several subclasses: voltage-dependent K^+ channels (A-type channels, delayed rectifiers, inward rectifiers, plateau K^+ channels), G protein-gated K^+ channels (Ach-activated K^+ channels), and ligand-regulated K^+ channels (Na^+-activated, ATP-sensitive K^+ channels).

3-1. Potassium currents

3-1-1. Voltage-dependent potassium currents

Gating (activation, inactivation, deactivation or reactivation, etc) of this subclass of K^+ channels is voltage-dependent, although it may be regulated by G proteins[1-137,138], and it may be modulated by endogenous neurotransmitters or hormones. K^+ channels are believed to be the most fundamental and important repolarizing currents under physiological conditions and are the major target for many antiarrhythmic drugs[1-139-141].

3-1-1-1. The 4-AP-sensitive transient outward K^+ current (I_{to1})

An outward K^+ current with rapidly activating and inactivating properties was originally found in neurons, and named A type current[1-142]. This current is important in modulating the firing properties in

"encoding" nerve cells[1-142]. The cardiac equivalent to A type current was firstly described by Dudel and colleagues in 1967 with two-microelectrode voltage-clamp techniques in shortened Purkinje fiber strands[1-143], and later by Fozzard et al[1-144]. They denoted this current "positive dynamic current", and attributed it to an influx of chloride ions. This current was renamed, however, early outward current (I_{eo}) by Kenyon and Gibbons in 1979[1-145,146], and the ionic selectivity of this current was also re-identified as K^+ ions based on the 4-aminopyridine (4-AP) sensitivity of the channels. They also noted a small, 4-AP insensitive current (about 20% of the total), probably carried by Cl^- ions. Siegelbaum and Tsien[1-147] provided evidence that I_{to} was partially a $[Ca]_i$-activated current in Purkinje fibers. Their argument was based on simultaneous measurements of membrane current and contractile activity in microelectrode-clamped shortened Purkinje fibres. I_{to} was well correlated with contraction and, in addition, removal of $[Ca]_o$, replacement of $[Ca]_o$ by other permeant divalent ions, and buffering $[Ca]_i$ by injection of EGTA all inhibited I_{to}. They therefore ascribed this component of I_{to} to Ca^{++}-activated K^+ channels. More recently, Zygmunt and Gibbons[1-148,149] have presented data suggesting a role for Ca^{++}-activated Cl^- channels in rabbit atrial and ventricular myocytes, rather than Ca^{++}-activated K^+ channels as previously believed. Clearly, the total I_{to} may reflect the sum of several types of underlying ion channels. In fact, two components of cardiac I_{to}, a 4-AP sensitive Ca^{++} independent current (I_{to1}) and a 4-AP resistant current (I_{to2}), have been identified in a variety of species, including sheep Purkinje fibres[1-150], calf Purkinje fibres[1-151], rat[1-152], mouse[1-153] and canine[1-154] ventricular myocytes, rabbit atrial[1-155] and ventricular[1-156] cells, and adult human atrial cells[1-157]. While I_{to2} in rabbit heart appears to be a Cl^- current, the nature of this current in other species has not yet been clarified.

Voltage-dependence I_{to1} is elicited upon membrane depolarization. The half-activation voltage ($V_{1/2}$) ranges from -10 to +10 mV in different studies[1-120,155,159]. I_{to1} is fully activated at about +30 mV. Voltage-dependent steady-state inactivation of I_{to1} develops between -60 and -10 mV. $V_{1/2}$ for inactivation of I_{to1} lies between -40 mV and -15 mV[1-120,155,159]. Most studies show that I_{to1} activation occurs at voltages much more positive than inactivation, indicating that very little steady-state (window) current flows through I_{to1} channels. In addition, activation and recovery kinetics are also voltage-dependent (see below).

Time-dependence The major feature that distinguishes I_{to1} from other K^+ currents is its rapidly activating and inactivating properties. I_{to1} decay can be fitted by a single exponential or double exponential[1-120,155,158,159]. The inactivation time constant (τ) for test pulses to +20 mV, obtained at room temperature (22-24°C), is about 35 msec. The activation kinetics have not been quantitatively determined, but the activation τ could be estimated to be within 10 msec at plateau voltage range[1-120,155,158,159]. Activation is obviously more rapid at more positive potentials.

Frequency-dependence In most animal species such as rabbit atrial and ventricular cells[1-156], sheep Purkinje fibers[1-160,161], dog Purkinje fibers and ventricular muscles[1-154], I_{to1} was found to be strongly

frequency-dependent: the size of the current decreases as stimulation frequency increases. This frequency dependence of I_{to1} has been attributed to the relatively slow time course of recovery. For example, at room temperature, the reactivation time course of I_{to1} in rabbit heart was found to be a bi-exponential process with a time constant for the slow component in the range of 5 sec[1-120].

Pharmacological sensitivity 4-AP has been shown to be a fairly selective I_{to1} blocker in some species, and has been used as a pharmacologic probe for studying I_{to1}[1-120,155,158,159,160,161]. I_{to1} has been found to be inhibited by many antiarrhythmic drugs, such as quinidine[1-162], disopyramide[1-163], propafenone[1-164], tedisamil[1-165], and sotalol[1-166]. Blockade of I_{to1} by these agents could account for at least part of their ability to prolong the action potential.

Physiological roles The notch between phase 1 rapid repolarization and phase 2 plateau (spike and dome morphology) of an action potential has been attributed to the rapid activation and inactivation of I_{to1}[1-155,158,160,161]. The ability of 4-AP to lengthen the plateau duration of action potentials[1-29,30] also indicates the importance of I_{to1} in controlling action potential repolarization. The slow reactivation of I_{to1} is probably the mechanism for the rate-dependent APD lengthening seen in rabbit heart[1-131,132,155]. Furthermore, regional differences in I_{to1} channel density in the canine heart have been demonstrated to be responsible for differences in action potential morphology, action potential duration, and sensitivity to drugs, heart rate and ischemia noted between canine epicardium and endocardium[1-167-169].

3-1-1-2. The delayed rectifier outward K^+ current (I_K)

Delayed rectification has been used to denote K^+ channel activity that shows time-dependent activation and little or no inactivation upon depolarization. Channels open when the cell is depolarized, and the number of channels that open is a function of both the time spent at a given depolarized potential and the potential itself. The time-dependent opening of delayed rectifier channels is thought to be largely responsible for controlling the duration of the plateau phase of the action potential in many tissues. Since Noble and Tsien[1-170,171] provided the first quantitative description of I_K in the heart, I_K has been well characterized in vertebrate cardiac cells, such as Purkinje fibres from calf[1-172], sheep[1-171], and rabbit[1-166]; ventricular cells from guinea pig[1-11,173], rat[1-174], and cat[1-175]; atrial myocytes from frog[1-176], guinea pig[1-12], rabbit[1-120,155,162,177], and chick[1-178]; and nodal cells from rabbit[1-179]. Prior to work described in this thesis, I_K had been identified in neither human ventricle nor in atrium, and I_K was believed to be either absent or minimal in human atrial cells[1-30,157].

Noble and Tsien originally showed that I_K in sheep Purkinje fibres fail to satisfy the envelope-of-tails test and related this observation to two kinetically distinct current components that they designated I_{x1} and I_{x2}[1-171]. Shrier and Clay[1-178] also reported detailed characterization of two I_K components, I_{x1} and I_{x2} in chick atrial cells. Sanguinetti and Jurkiewicz have provided further evidence to suggest that I_K in guinea pig cardiac myocytes consist of two components, a rapid component I_{Kr} and a slow one I_{Ks}, which can be

separated on the basis of the response to a novel class III drug, E-4031, and their different voltage-dependence and kinetics[1-11,12].

Voltage-dependence The activation threshold of I_{Kr} is -40 mV, more negative than the value of -20 mV for I_{Ks}[1-12]. The I-V relation of I_{Kr} shows substantial inward rectification at potentials positive to 0 mV, whereas I_{Ks} has a linear I-V relation. The $V_{1/2}$ and k of I_{Kr}[1-12] are -19 mV and 5.2 mV, respectively, while corresponding values for I_{Ks} were +24 mV and 15.7 mV, more positive than those for I_{Kr}. The aggregate current of these two components had values in between those for I_{Kr} and I_{Ks}.

Time-dependence Activation and deactivation kinetics of I_{Kr} are rapid compared to those of I_{Ks}. The activation τ of I_{Kr} ranges from 160 msec to 30 msec at potentials between -30 mV and +30 mV, while values for I_{Ks} are about one order of magnitude slower[1-12].

Frequency-dependence Studies have demonstrated that I_{Ks} activation accumulates at rapid depolarization rates due to its slow deactivation kinetics[1-180]. This frequency-dependent increase in the current amplitude of I_{Ks} can contribute to rate-dependent APD abbreviation. Although I_{Kr} is relatively frequency independent, its contribution to net repolarizing current is believed to be reduced at rapid activation rates because of the increase in I_{Ks}[1-180].

Pharmacological sensitivity I_{Kr} is sensitive to Co^{2+} and La^{3+} [1-162], and to many antiarrhythmic agents including the class Ia drugs quinidine[1-181,183] and disopyramide[1-163], the class Ic agents flecainide[1-184] and encainide[1-148], and the class III antiarrhythmics E-4031[1-11,12], sotalol[1-166], dofetilide[1-180], amiodarone[1-185], clofilium[1-186], risotilide[1-187], UK 68,798[1-188], and tedisamil[1-189]. I_{Ks} is insensitive to Co^{2+} and La^{3+}, but is sensitive to adrenergic modulation. β-adrenergic agonists, cAMP and its analogues, and phosphodiesterase inhibitors considerably enhance I_{Ks} in cardiac cells[1-190-192], and lead to acceleration of repolarization or APD shortening. Clofilium and amiodarone have been shown to block both I_{Kr} and I_{Ks}[1-181,193].

Physiological role I_K is considered the major repolarizing current in controlling the plateau phase of action potential in many tissues. Many antiarrhythmic drugs exert their beneficial actions against arrhythmias by blocking I_K channels. Recent advances in drug development have, in fact, focused on drugs that specifically target these K^+ channels[1-54,194]. However, it has also recently been recognized that specific I_{Kr} blockers produce reverse use-dependent prolongation of APD, which limits the therapeutic potential of these drugs due to the diminished effectiveness in terminating tachycardias and a tendency to produce EAD at slow heart rates[1-103]. It has been speculated that specific I_{Ks} blockers might produce use-dependent APD prolongation which would be a clinically favourable drug action[1-180].

3-1-1-3. The inward rectifying K^+ current (I_{K1})

Weidmann (1951)[1-195] showed that the plateau of the cardiac action potential is characterized by high cellular input resistance, by demonstrating that injection of small currents during this period of the action potential caused marked changes in the action potential configuration. One of the principal

mechanisms underlying the low-conductance action potential plateau is the strongly nonlinear voltage dependence of the major background K^+ channel-I_{K1}. McAllister and Noble (1966)[1-196] first measured the I-V relationship of I_{K1} in calf Purkinje fibres. This channel preferentially passes current in the inward direction, but provides high resistance to flow in the outward direction, ie, inward I_{K1} is large whereas outward I_{K1} is very small for equal and opposite driving forces, a phenomenon attributed to channel closure on depolarization and voltage-dependent fast block by internal magnesium[1-2,140]. I_{K1} has been identified in different type of tissues from various species, and its size varies among the tissues in the order Purkinje fibres > ventricular cells > atrial cells > and sinus nodal cells[1-2].

There are several common properties of I_{K1} from various species: (1) The current shows strong inward rectification[1-196-199]; (2) Over the physiological range of voltages, I_{K1} is time independent; (3) The reversal potential of this current is about -90 mV[1-197], close to the K^+ equilibrium potential; (4) I_{K1} is sensitive to Ba^{+1-197}, and it is also inhibited by antiarrhythmic drugs such as quinidine[1-200], disopyramide[1-163], sotalol[1-166], amiodarone[1-201], and clofilium[1-202]. I_{K1} is known to be responsible for maintenance of the cell resting potential[1-14]. At voltages near the action potential plateau, -10 to +20 mV, there is no I_{K1} under normal physiologic conditions, thus it provides a minimal contribution to the plateau phase of repolarization. It has been thought that during the final phases of repolarization, there is a large outward I_{K1} current because of its negative slope conductance. This seems to be the case in the ventricle but not in the atrium. Hume et al.[1-173] has demonstrated that the density of I_{K1} is much higher in ventricle than in atrium, and this difference accounts for the faster rate of final repolarization in the ventricle.

3-1-1-4. K^+ currents activated at plateau voltages

Recently, another class of novel K^+ channels has been recognized in a few cardiac preparations including adult rat atrial myocytes[1-203], guinea pig ventricular myocytes[1-204], and neonatal dog ventricular cells[1-205]. They all activate much faster than classical I_K and show little or no inactivation.

Upon depolarization of rat atrial myocytes to potentials positive to +30 mV, the current rises rapidly to a maximal level with little or no inactivation during a 100-ms pulses, followed by tail currents upon repolarization to the holding potential[1-203]. The activation τ varies from 5.3 to 1.4 ms over the range of -10 to +50 mV, similar to values for I_{to1} in rat ventricular cells, but approximately 10-fold faster than those of classical I_K[1-203]. The mean percentage of time-dependent inactivation of the current measured during a 100 ms depolarization to +50 mV was about 20%. The half voltage for activation ($V_{1/2}$) was found to be -1.5 mV, whereas $V_{1/2}$ for steady-state voltage-dependent inactivation was -41 mV. This current is highly K^+ selective with a mean reversal potential of -75.5 mV. It is strongly suppressed by millimolar concentrations of 4-AP, but unaffected by 50 mM TEA.

In guinea pig ventricular myocytes, an outward K^+ current (I_{Kp}) with high activity at plateau potentials has been recorded at the single channel level[1-204]. The channel demonstrates a 14 pS conductance at physiological potassium concentrations and does not rectify over the voltage range of the action potential.

The ensemble-averaged current during depolarizing steps from -60 to +80 mV has a time-dependent, rapid activation (τ=5.2 ms) without inactivation.

Recently, Jeck and Boyden[1-205] reported a novel rapidly activating and slowly decaying outward current in neonatal canine ventricular cells. The form of this current is similar to the depolarization-activated K^+ current in rat atrial cells[1-203] and I_{Kp} in guinea pig ventricular cells[1-204]. The current is insensitive to 4-AP. There is little or no change in the current amplitude when the frequency of clamp steps is increased. The ion selectivity of this channel is undefined, although it is believed to be carried by K^+ ions[1-204].

3-1-2. G protein-gated K^+ currents

3-1-2-1. Acetylcholine-activated K^+ current (I_{KAch})

Acetylcholine (Ach) decreases heart rate, slows AV conduction and shortens atrial APD[1-23,140], by increasing membrane permeability to K^+ ions[1-23,140]. The K^+ current induced by Ach was originally considered to be I_{K1}, but subsequent studies provided strong evidence that Ach-induced current is distinct from I_{K1}. I_{KAch} has been identified in a number of cardiac preparations: atrial tissues from bullfrog[1-206], chick[1-207], guinea pig[1-208], and man[1-196,209,210]; SA and AV nodal cells from rabbit[1-211], and guinea pig[1-212]; and Purkinje fibres from rabbit[1-213].

Electrophysiologic characteristics One of the major characteristics of I_{KAch} is, like I_{K1}, the strong inward rectification of its I-V relationship[1-206-213]. Another typical feature of I_{KAch} is "relaxation", i.e. the current decreases with time after voltage steps, although Ach remains present[1-206-213]. Single channel recordings show that the Ach-sensitive K^+ channel has a kinetic behaviour characterized by short openings, grouped in bursts, and separated by longer periods without activity[1-196,212]. The slope conductance is approximately 45 pS for negative membrane potentials under symmetrical K^+ concentrations ($[K^+]$=140)[1-196,212].

Mechanisms of activation Ach induces I_{KAch} by activating M2 muscarinic receptors[1-214]. Patch-clamp studies argue against the involvement of cytoplasmic second messengers and suggest a crucial role for a membrane delimited G-protein in the activation of I_{KAch} channels after binding of Ach to M2-receptors[1-214]. The direct application of exogenous G proteins (GTP or GTPγs) to cell-free membrane patches opens I_{KAch} channels[1-196,214,215].

Pharmacological sensitivity Atropine inhibits activation of I_{KAch} by Ach, and the G-protein inactivator pertussis toxin prevents I_{KAch} channel activity[1-196,214,215]. Some antiarrhythmic agents, including flecainide, can also inhibit I_{KAch}[1-216]. This is potentially important because the activation of I_{KAch} accelerates repolarization, which shortens ERP and favours reentry, resulting in atrial fibrillation in some patients. The blockade of I_{KAch} by drugs may reverse the ERP shortening, reducing the likelihood of AF.

Physiologic role Although the contribution of I_{KAch} to basal K^+ conductance is small[1-196], I_{KAch} could produce substantial membrane hyperpolarization and APD shortening when vagal tone is enhanced. In the absence of any agonist, spontaneous openings of I_{KAch} channels have also been observed at a low

frequency[1-217]. The mechanism responsible for the basal activity of I_{KAch} may involve direct phosphorylation of G proteins by a membrane-associated kinase[1-218]. In the absence of vagal stimulation, I_{KAch} may thus act as a background outward current that contributes to the resting potential[1-219]. In mammals, its role is restricted to the sinoatrial and atrioventricular nodes, the atrium and the Purkinje system[1-2].

3-1-3. Ligand-regulated K^+ currents

3-1-3-1. ATP-sensitive K^+ current (I_{KATP})

Since Noma (1983)[1-220] first discovered K^+ channels that are regulated by cytoplasmic ATP in heart cell membranes, this type of channel has been identified in many other types of cells including pancreatic β cells[1-221], skeletal muscle cells[1-222], and arterial smooth muscle cells[1-223]. Two studies have confirmed the existence of I_{KATP} in human atrium[1-196,224].

Electrophysiologic properties I_{KATP} is activated when intracellular ATP concentration is reduced to levels below 100 μM. The I-V relation of I_{KATP} shows less inward rectification than I_{K1} and I_{KAch}. The single channel conductance at negative potentials is about 75 pS[1-196] and at positive potentials is only 30 pS.

Physiologic role When cellular ATP falls below a critical value, such as during ischemia or metabolic inhibition, the resultant increase in I_{KATP} enhances repolarizing currents, shortens APD, and perhaps even suppresses electrical excitability by maintaining or increasing resting membrane potential. In this sense, I_{KATP} has been thought of as cardioprotective because of the possibility of suppression of arrhythmogenic electrical activity in ischemic zones[1-225].

Pharmacological sensitivity I_{KATP} is sensitive to inhibition by glibenclamide[1-225]. 2 μM glibenclamide suppresses I_{KATP} by about 70%. Recently, Wu et al. reported that a number of antiarrhythmic drugs significantly blocked I_{KATP}[1-226], indicating potential role of I_{KATP} in mediating efficacy of these drugs. Even in the presence of millimolar concentrations of cytoplasmic ATP, I_{KATP} can be activated by a class of drugs referred to as potassium channel openers, including pinacidil, diazoxide, nicorandil, cromakalim, and RP 49356[1-227-230]. These compounds are promising in the treatment of hypertension because of the higher sensitivity of I_{KATP} in smooth muscle to these drugs than in heart muscle. However, their use at sufficiently high concentrations will activate I_{KATP} in the heart, resulting in APD shortening, and promoting reentry.

3-2. Na^+/K^+ pump current ($I_{Na/K}$)

The Na^+/K^+ pump is crucial in maintaining ionic equilibrium by extruding intracellular Na^+, which enters during cell excitation, to the outside, while returning extracellular K^+, which leaves the cell during repolarization, back to the inside. The first clear-cut demonstration that the cardiac Na/K pump is electrogenic was made by Vassalle (1970)[1-231], who subjected spontaneously beating Purkinje fibres to periods of rapid drive (2 Hz) and noted a gradual hyperpolarization during the drive. Each Na^+/K^+ pump cycle exports three Na^+ and imports two K^+ ions, with a resulting extrusion of net positive charge constituting outward current[1-15,16]. The Na^+/K^+ transport stoichiometry appears to be independent of $[K^+]_o$ and

membrane potential[1-15,16].

The Na^+/K^+ pump exerts both direct and indirect influences on the electrical activity of cardiac cells. It exerts a direct influence via its electrogenic activity and an indirect influence through its control of the intracellular concentrations of Na^+ and K^+ ions. Studies have suggested that the hyperpolarization and reduction in the duration of the action potential plateau caused by rapid activation of Purkinje fibers are due to an increment in Na^+/K^+ pump current[1-132,133]. The temporary suppression of automaticity in Purkinje fibres after overdrive is caused by an increase in Na^+/K^+ pump current[1-131]. Under certain circumstances, the hyperpolarization caused by pump current can have an antiarrhythmic effect. The suppression of bursts of triggered activity following overdrive in canine atrium has been attributed to a transient stimulation of Na^+/K^+ pump, because the effect is abolished by acetylstrophanthidin[1-234].

3-3. Na^+/Ca^{++} exchange current ($I_{Na/Ca}$)

The long-lasting plateau in cardiac cells is the consequence of both the slow inward I_{Ca}[1-236] and Na^+/Ca^{++} exchanger-generated inward current $I_{Na/Ca}$[1-236,237]. The Na^+/Ca^{++} exchanger moves Ca^{++} either into or out of the cytosol across the plasma membrane, depending on the transmembrane potential and the concentrations of Na^+ and Ca^{++} on either side of the membrane. The stoichiometry of Na^+/Ca^{++} exchange of the sarcolemma is three Na^+ to one Ca^{++}; thus it is electrogenic. Voltage-clamp experiments have shown that the exchange is voltage-sensitive, and that it may contribute significantly to the current carried during the cardiac action potential[1-238]. Studies in human ventricular preparations indicate that the early part of the action potential plateau is dominated by I_{Ca}, whereas $I_{Na/Ca}$ is relatively more important during the later part, and tends to lengthen APD[1-237].

3-4. Cardiac Chloride currents

Since Harvey and Hume[1-239] discovered isoproterenol-activated Cl^- current in rabbit ventricular myocytes in 1989, there has been increasing activity in this field. So far, at least five distinct Cl^- conductance pathways have been electrophysiologically defined in cardiac cells[1-240].

3-4-1. cAMP-regulated Cl^- current (I_{ClcAMP})

Following ß-adrenergic stimulation or direct activation of adenylyl cyclase a time-independent, outwardly rectifying Cl^- current is elicited. Intracellular dialysis with cAMP or the catalytic subunit of PKA induces the same current sensitive to DIDS or 9-AC, potent blockers of anion fluxes. This Cl^- current has been recorded in ventricular cells of rabbit[1-241,242,243,244] and guinea pig[1-245]. I_{ClcAMP} has not been found in atrial myocytes of any species. Experimental data suggests that I_{ClcAMP} may be involved in regulating resting membrane potential[1-241] and rate of repolarization[1-242]. It was shown that activation of I_{ClcAMP} decreased APD by 50% when I_{Ca} and I_K were both minimized[1-243]. On the other hand, APD was significantly prolonged following the addition of DIDS. Activation of this current may participate in the mechanism of *histamine*-induced ventricular tachyarrhythmias[1-244]. Yamawake et al.[1-245] also reported that under conditions of symmetrical Cl^- concentration 1 µM isoproterenol depolarized resting membrane potential, slowed

repolarization, and induced early afterdepolarizations (EADs). This indicates that during hypokalemia or decreased K^+ conductance, I_{ClcAMP} may contribute to the genesis of arrhythmias through facilitation of membrane depolarization and abnormal automaticity.

3-4-2. Ca^{++}-activated Cl^- current (I_{ClCa})

A 4-AP resistant component of transient outward current (I_{to2}) has been described in diverse animal species, including Purkinje fibres from calf, dog, and sheep[1-147,150,151], ventricular cells from dog, rabbit, rat and mouse[1-148,153,154,156], and atrial myocytes from elephant seal, rabbit, and man[1-149,157,246], respectively. I_{to2} is an outward current that may be triggered by an increase in the intracellular calcium concentration[1-147,246,247] due to sarcoplasmic reticulum Ca^{++} release[1-147] in response to Ca^{++} entry into the cell through Ca^{++} channels. This current has been considered to be a Ca^{++}-activated K^+ current. Recent findings of Zygmunt and Gibbons[1-148,149], however, indicate that I_{to2} is actually carried by Cl^- ions in the rabbit heart, in which it has been designated I_{ClCa}.

The I-V relationship of I_{ClCa} is bell-shaped, showing a voltage-dependent increase in amplitude to a maximum value and then a progressive reduction at voltages positive to +40 mV approaching the Ca^{++} reversal potential. I_{to2} in rabbit is the only cardiac Cl^- current that is known to be time-dependent[1-149]. The time-dependent activation of I_{to2} lags behind that of I_{to1}. In rabbit ventricular myocytes, I_{to2} was found to be rate independent[1-156]. I_{to2} is sensitive to caffeine[1-148,149,154,157], a compound which inhibits sarcoplasmic reticulum Ca^{++} release, and to Ca^{++}-channel blockers, such as Co^{++}. In rabbit hearts, I_{to2} is depressed by DIDS and SITS[1-148,149], anion transport inhibitors that have frequently been used as Cl^- channel blockers. Substitution of extracellular Cl^- eliminates outward I_{to2}, indicating its Cl^- selectivity[1-149]. Whether I_{to2} can be a target for antiarrhythmic drugs is still unknown. The functional importance of I_{to2} is also unclear, although it has been speculated that I_{to2} may counteract inward Ca^{++} current. In any case, based on the electrophysiologic properties of I_{to2}, it must contribute to the net repolarizing current.

3-4-3. Other Cl^- currents

Swelling-induced Cl^- current ($I_{Clswell}$) This current is induced when the cell swells as a result of differences between intra- and extra-cellular osmolarity[1-248]. $I_{Clswell}$ has also been recorded in canine atrial cells[1-249].

PKC-activated Cl^- current (I_{ClPKC}) I_{ClPKC} activated by intracellular protein kinase C has been found in guinea pig ventricular cells[1-250]. The role of this current is unclear.

ATP-activated Cl^- current ($I_{Clpurinergic}$) This current is activated by extracellular ATP or adenosine binding to a purinergic receptor. This current, like I_{ClcAMP}, shows outward rectification and time independence. It has been recorded only in guinea pig atrial cells[1-251].

Voltage-dependent Cl^- current (I_{Cl}) I_{Cl} is a time-independent, outwardly-rectifying current, and activation of I_{Cl} does not require any involvement of endogenous ligands or receptor. This current has been

observed in rabbit atrial cells[1-252,253].

3-5. Currents carried by Cloned K^+ channels

The first voltage-dependent K^+ channel clone was isolated from experiments with the fruitfly Drosophila by Papazian et al.[1-254] in 1987 and Pongs et al.[1-255] in 1988. The derived protein sequences of the Shaker channels were found to have remarkable similarities to previously cloned Na and dihydropyridine-sensitive Ca^{++} channels. Most K^+ channel proteins contain six transmembrane spanning domains (S1-S6)[1-256,257]. A protein of the fourth segment S4 is positively-charged and believed to be the voltage sensor that controls voltage-dependent gating[1-258]. Based on homology with Shaker K^+ channels, several types of voltage-dependent K^+ channels have now been cloned from rat[1-259,260] and human heart[1-261], including types referred to as Kv1.1, Kv1.2, Kv1.4, and Kv1.5[1-256,257]. Kv1.1 was cloned from rat aorta and brain cDNA[1-259,262]. Kv1.2 was isolated from rat heart and brain cDNA[1-263,264]. Kv1.4 and Kv1.5 have both been cloned from rat[1-265] and human hearts[1-261]. Kv1.4 inactivates rapidly, resembling I_{to1} in native tissues. In contrast, Kv1.1, Kv1.2, and Kv1.5 are all noninactivating or slowly inactivating[1-257]. A depolarization-induced K^+ current found in adult rat atrial cells[1-203] has been thought to represent the physiological counterpart of currents carried by either Kv1.2 or Kv1.5 channels.

Although Kv1.1, Kv1.2, and Kv1.5 are all considered to be delayed rectifiers, their activation kinetics are at least ten times faster than that of the classical cardiac I_K. Another unique type of K^+ channel, structurally different from Shaker-type channels, has also been cloned recently, which may be more closely related to classical I_K. This channel was originally cloned from rat kidney[1-266], and subsequently cloned from hearts of a variety of species[1-267,269-272]. The protein contains only one transmembrane spanning segment, in contrast to Shaker-type K^+ channel proteins. This channel has been called minK because of its small size, or I_{sK} for the slow K^+ current. The current expressed by I_{sK} activates slowly with time without apparent time-dependent inactivation even during a 20-s pulse[1-267]. There is strong evidence that I_{sK} underlies I_{Ks} in native heart[1-267,273].

3-6. Repolarizing currents in human atrial myocytes

Studies on repolarizing currents in human atrial myocytes are sparse. I_{to1} was the first voltage-dependent repolarizing current described in human atrial myocytes by Escande et al. in 1987[1-157], and Shibata and colleagues[1-30] in 1989, respectively. Since then I_{to1} has been commonly believed to be the major repolarizing current in human atrial cells. I_{K1} was also recorded in these studies, but detailed studies of this current were not reported until three years later[1-197,198]. I_K was found in none of these studies, and was believed to be absent in human atrial cells. The plateau K^+ current, as described in guinea pig ventricular cells[1-204] and rat atrial myocytes[1-203], has not been identified in human atrial fibers. I_{KAch} may be the most thoroughly studied K^+ current in human atrial myocytes at both whole-cell[1-209,210] and single channel levels[1-198]. I_{KATP} has been studied only at the single channel level[1-198]. A role for $I_{Na/K}$ in human atrial cells is indicated by some indirect evidence[1-274-276]. The ionic determinants of human atrial repolarization

are still poorly understood. The currents expressed by several K^+ channels (Kv1.4, Kv1.5 and I_{sK}) cloned from human hearts have been more rigorously explored than endogenous currents[1-269-272,279-282].

3-6-1. 4AP-sensitive transient outward K^+ current (I_{to1})

The characteristics of human I_{to1} are quite similar to those in other species, including their voltage-dependency, time dependency, and pharmacologic sensitivity. The major difference between human I_{to1} and that in some other animal species is the recovery of the channels from their inactivation. At room temperature, the reactivation time course of I_{to1} in rabbit heart (τ about 5 sec)[1-120] is of two orders of magnitude slower than that in human atrial cells (τ of 50 msec)[1-30]. One would expect, based on these recovery kinetics, a relative insensitivity of human I_{to1} to changes in stimulation rate, particularly over the physiological range of temperatures. However, Shibata et al.[1-30] observed that the size of I_{to1} decreased dramatically as a function of stimulation frequency between 0.2 and 3.33 Hz with 250-msec pulses to +20 mV from a holding potential of -60 mV at room temperature (21-23°C). They measured recovery time constants of 141 msec at a holding potential of -60 mV, and of 54 msec at -80 mV. One might then ask whether human I_{to1} is also frequency-dependent at physiological temperatures.

Another interesting observation regarding human I_{to1} is that 4-AP-induced inhibition of this current in both multicellular preparations[1-29] and isolated myocytes[1-30] of human atria lead to significant shortening of overall APD, although the early phase (plateau) was prolonged. One explanation offered by Escande et al.[1-29] is that blockade of I_{to1} results in an elevated and prolonged plateau which would favour the activation of I_K, which in turn leads to APD shortening. However, as mentioned above, I_K has not been recorded in human atrium.

3-6-2. 4-AP-resistant transient outward current (I_{to2})

As mentioned above, I_{to2} in the rabbit heart is carried by Cl^-, rather than K^+. I_{to2} has been reported in human atrium in only one study, by Escande and colleagues[1-157]. Although it was electrophysiologically characterized, its ionic nature remains unclear. There are two major differences between human I_{to2} and that in the rabbit: (1) the I-V relationship of I_{to2} from 12 human atrial cells was similar to that of I_{to1}, showing a slight outward rectification between -30 and +10 mV, and a linear relation positive to +10 mV. The bell-shaped I-V curve typical of I_{to2} in other species was seen in only two cells; (2) Activation kinetics of human I_{to2} appeared to be much faster (2-3-fold faster) than that of I_{to1}, which is opposite to what is seen in other species such as rabbit and dog[1-148,149,154], in which the time-dependent activation of I_{to2} lags behind that of I_{to1}. The mean time to peak of human I_{to2} was 5.5 msec, compared to 18 msec for I_{to1}.

3-6-3. Inward rectifier K^+ current (I_{K1})

Human atrial I_{K1} has been characterized at both whole cell[1-30,157,197] and single channel levels[1-198]. It has properties similar to that in other mammals. The strong inward rectification of human I_{K1} renders it tiny in the outward direction. The single channel conductance of I_{K1} was found to be 27 pS with average mean open time of 8.7 msec. Single channel studies confirmed that I_{K1} in human atrial myocytes, like that

in guinea pig atrial cells, is the main basal potassium conductance in the absence of any exogenous hormones or neurotransmitters. The density of I_{K1} channels in human atrium is low, particularly when compared with human ventricle[1-278]. The high input resistance at plateau potentials in human atrial myocytes is a consequence of the strong inward rectification and low channel density of I_{K1}. Whether I_{K1} contributes to the final phase of repolarization of human atrial cells is unclear. Given the small size of I_{K1} outward current, one would not expect a significant role of I_{K1} in repolarizing human atrium.

3-6-4. Ach-induced K⁺ current (I_{KAch})

Both whole cell current[1-209,210] and single channel conductance[1-198] of I_{KAch} have been characterized in human atrial myocytes. Human I_{KAch} has properties similar to that in other species such as guinea pig atrium: (1) Its voltage-dependence shows strong inward rectification; (2) Its time-dependence displays a rapid relaxation; (3) Single I_{KAch} channel activity demonstrates bursting during opening.

3-6-5. ATP-sensitive K⁺ current (I_{KATP})

As in many other species, human atrium has K^+ channels that open when intracellular [ATP] is lowered (I_{KATP}). In human atrial cells, $[ATP]_i$ causing half-maximal inhibition of I_{KATP} was found to be 8 μM[1-198]. Higher concentrations of ATP suppress I_{KATP}. The I-V relation of I_{KATP} shows less inward rectification than I_{K1} and I_{KAch}. The single channel conductance at negative potentials (<0 mV) is about 75 pS[1-198] and at positive potentials is only 30 pS, properties similar to I_{KATP} measured in the hearts of other species or other types of cells.

3-6-6. Na/K pump current

Accurate measurement of the size of Na^+/K^+ pump current, a conceptually straightforward task, has proved to be difficult in practice. Although there is reason to believe that the pump current exists in human atrium[1-274-278], direct recording of this current has not been performed. Evidence for electrogenic Na^+/K^+ pump activity in human atrial cells has come from studies using membrane hyperpolarization or intracellular K^+ activity as an indication of pump activity induced on returning to K^+-containing Tyrode's solution following brief periods of Na^+ loading in K^+-free solution[1-274-278]. Indirect evidence indicates a possible contribution of Na^+-K^+ pump current to human atrial repolarization, particularly at fast heart rates when Na pump activity is supposed to be enhanced: ouabain, a selective pump inhibitor, significantly lengthens the duration of human atrial APs with fast[1-28] but not slow[1-31] pacing.

3-6-7. Currents Expressed by Cloned K⁺ Channels

Two distinct K^+ channel cDNAs, originally designated HK1 and HK2, have been cloned from human ventricle by screening human left ventricular cDNA libraries using rat K^+ channel sequences[1-261]. Under a recently-proposed nomenclature[1-279], these two channels are now referred to as Kv1.4 and Kv1.5, respectively. I_{sK} has also been cloned in both human atrium and ventricle[1-269-272].

3-6-7-1. Current expressed by Kv1.4

Kv1.4 (originally designated as HK1) genes were found to be abundantly expressed in both human

atrium and ventricle[1-261]. Expression of Kv1.4 generates a K^+ current resembling I_{to1}[1-279], as characterized by Escande and co-workers[1-157] and Shibata et al.[1-30], respectively. The voltage-dependent activation and inactivation properties, time-dependent activation and inactivation kinetics, I-V relationships, and pharmacological sensitivity of current carried by Kv1.4 channels are similar to native I_{to1}. Thus, it is believed that channels or subunits derived from Kv1.4 contribute to native human I_{to1}[1-279]. However, the expressed current recovers very slowly from inactivation, with a time constant about two orders slower than native current (3 sec vs. 50 msec)[1-279]. One possibility accounting for this is that some cofactor that modulates inactivation is missing in the expression systems. Another explanation is that native cardiac channels are heterotetramers and consist of different K^+ channel subunits. The latter is supported by a recent elegant experiment using hybrid channels consisting of subunits from different K^+ channel clones ([Kv1.1, Kv1.2, and Kv1.5] and Kv1.4)[1-280]. Results showed that Kv1.4:Kv1.2 heteromultimers resulted in a current with properties including a recovery time constant close to native I_{to1}. This suggests that heteromultimeric assembly of human potassium channels may be the molecular basis of the native transient outward current.

3-6-7-2. Current expressed by Kv1.5

Northern blot analysis with RNA isolated from human skeletal muscle, atrium, ventricle, brain, spleen, kidney, liver and uterus, etc, demonstrated that the Kv1.5 mRNA is predominantly expressed in adult human atrium with little expression elsewhere[1-256,261]. Interestingly, rat Kv1.5 mRNA is equally expressed between rat atrium and ventricle[1-259], while human Kv1.5 transcripts are at least tenfold more abundant in human atrium than in ventricle[1-261]. Current displayed by channels encoded by Kv1.5 genes expressed in a stable mouse L cell line[1-281,282] show characteristics distinct from I_{to1} and classical I_K currents, but many similarities to the plateau current found in adult rat atrial myocytes[1-203]. The physiological counterpart of the human Kv1.5 channel has not yet been identified.

Voltage-dependence Kv1.5 channels show rapid activation upon membrane depolarization, followed by slow and partial inactivation during the pulse and tail currents upon repolarization. The fully activated I-V relationship displays outward rectification in 4 mM external K^+ concentration[1-282]. The voltage threshold of current activation is around -30 mV. The midpoint and slope factor of the activation curve are -14 mV and 5.9 mV, respectively. The voltage-dependence of steady-state inactivation overlaps with that of activation, with a $V_{1/2}$ of -25 mV and k of 3.7 mV.

Time-dependence The activation time course of Kv1.5 is voltage dependent, with time constants declining from 10 msec to <2 msec between 0 and +60 mV. Slow, partial inactivation is observed especially during strong depolarizations (20% after 250 msec at +60 mV), and is incomplete after 5 s at room temperature. This slow inactivation has a biexponential time course with largely voltage independent time constants of approximately 240 and 2,700 msec between -10 and +60 mV[1-281,282].

Pharmacological sensitivity The Kv1.5 channel is highly selective to K^+ (P_{Na}/P_K=0.007), and the dependence of the reversal potential of the expressed current on external K^+ concentration is 55 mV/decade. Kv1.5 channel current is highly sensitive to 4-AP (IC_{50} around 150 μM), compared to Kv1.4 (IC_{50} about 700 μM), but insensitive to external tetraethylamonium and dendrotoxin (which potently blocks Kv1.2)[1-262]. The Kv1.5 channel has also been shown to be blocked by antiarrhythmic drugs, such as quinidine[1-261] (IC_{50}=5 μM), clofilium[1-262] (IC_{50}=1 μM), and verapamil[1-263] (15 μM).

3-6-7-3. Current expressed by I_{sK} or minK

mRNA corresponding to the I_{sK} gene is detectable in both human atrium and ventricle[1-269-272]. Human I_{sK}[1-269-272] has properties identical to guinea pig I_{sK}[1-273]. The expressed current has an threshold of -30 mV, and requires a pulse duration of >300 msec to elicit current at room temperature. It develops slowly during depolarization, and deactivates gradually upon repolarization. The reversal potential is -91 mV in 2 mM external K^+ and shifts to -32 mV when $[K^+]_o$ is elevated to 20 mM, indicating its high K^+ selectivity. Constant ratios of 0.3 for tail current amplitude/step current amplitude for different pulse durations indicate a single population of channels underlying the overall current waveform. Human I_{sK} is sensitive to external TEA (10 mM) and high concentrations of Ba^{++}[1-272]. It is also blocked by several antiarrhythmic agents such as quinidine (30 μM) and clofilium (10 μM), but is unaffected by d,l-sotalol (300 μM)[1-272].

Strong evidence that cloned I_{sK} protein underlies native I_{Ks} of guinea pig ventricular cells has recently been provided by Freeman and Kass[1-273]. They reported that I_{sK} expressed in the HEK 293 cell line demonstrates characteristics similar to those of I_{Ks} recorded from guinea pig heart cells under similar experimental conditions. They also showed that an antibody directed against the I_{sK} channel protein reacts with a surface antigen on adult guinea pig ventricular myocytes and sinoatrial nodal cells, where I_{Ks} is the dominant outward K^+ current. Earlier studies carried out by Folander et al.[1-267] also found that an antisense oligonucleotide, derived from the sequence of the I_{sK} clone from neonatal rat heart, specifically inhibited the expression of the slow outward current observed in cells injected with mRNAs isolated from the parent tissues (i.e., heart, kidney, and uterus), indicating that the cloned gene underlies the major K^+ current expressed from RNA isolated from these tissues.

Like Kv1.5, I_{sK} mRNA has been found in human heart, but the native counterpart has not yet been recorded.

3-7. Summary

ERP is a major determinant of the occurrence of reentrant arrhythmias. APD is the major determinant of ERP, and repolarizing currents are the major determinants of APD. The duration of cardiac action potential is critically determined by a delicate balance between inward and outward currents. Membrane input resistance is very high during the plateau phase, and any small change in current could bring about a substantial shift in membrane potential. Whether the membrane is depolarized or

hyperpolarized depends on whether the net balance of current movement is inward or outward. Therefore, even a current with low amplitude over the plateau potential range could contribute substantially to determining repolarization. Different animal species and tissue types may possess qualitatively different repolarizing currents or quantitatively different contributions of the same repolarizing currents.

Two rules could be applied to the consideration of the contribution of individual ionic currents to repolarization: (1) All currents are independent, having their own intrinsic properties, but they are not functionally unrelated, instead they interact with one another. The current activated first will affect subsequent currents, by changing the membrane potential; (2) The relative importance of individual currents is likely to vary under different conditions, and a change in circumstances may therefore modify the effects of compounds on membrane repolarization or APD.

4. Questions Raised from the Above Overview

The following questions raised from the above overview stimulated the studies included in this thesis.

(1) Cellular electrophysiology has important species specificity and rate dependence. How does repolarization of cells respond to rate and drugs in man compared with other species?

(2) Flecainide is among the most effective drugs currently available to terminate atrial fibrillation. Given its typical Class Ic actions - strong conduction slowing with little effect on APD or ERP, flecainide should favour AF, rather than terminate it. How can this apparent contradiction be resolved?

(3) What are the ionic mechanisms that determine repolarization in the human atrium?

(4) I_{to1} in many species is highly rate-dependent, with minimal contribution to repolarization at rapid heart rates. Does human atrial I_{to1} have similar properties? If so, why does the amplitude of phase 1 remain unchanged at high frequencies, and why does 4-AP, known to be a selective I_{to1} blocker, lengthen APD only at rapid rates?

(5) I_{to1} has been believed to be a major, if not the only, voltage-dependent repolarizing current in human atrial cells. Given the fact that I_{to1} inactivates with a time constant of about 20 msec, while the duration of the action potential is in the order of 300 msec, how can one account for the late phases of repolarization? Are there any other voltage-dependent repolarizing currents in human atrial myocytes?

(6) If I_K is really absent in human atrial cells, how can drugs that specifically block I_K (like d-sotalol and dofetilide) delay repolarization and be effective against supraventricular arrhythmias in patients? I_{sK}, believed to be equivalent to a component of I_K, has been cloned from human heart. If I_{sK} is equivalent to I_{Ks}, why has I_{Ks} not been recorded in man? .

(7) Variation in human atrial action potential morphology and duration is a well-recognized phenomenon, but the underlying ionic mechanisms are still unclear. Is I_{to1} the only current

responsible for this variation? If not, what other currents could be involved?

(8) A K^+ channel cDNA belonging to the Kv1.5 gene subfamily has been cloned from human ventricle, and the corresponding mRNA has been found to be abundant in human atrium. The current expressed in model system has rapid activating and non-inactivating properties. However, the physiological counterpart of the channel has not been identified in native human atrium. Can the current equivalent to the current expressed by Kv1.5 gene be detected in human atrium?

(9) A number of Cl^- channels have been identified in a variety of animal species, and these channels may play a role in regulating membrane potential and repolarization. Are any of these Cl^- currents present in human atrial myocytes?

(10) Can antiarrhythmic drug effects on AF be understood on the basis of actions on ionic currents and electrophysiological properties?

5. Approaches to Address the Above Questions

In order to address the questions raised above, we carried out a series of studies using different techniques at different levels of complexity: mapping techniques (whole animal level), microelectrode techniques (cellular level), and patch-clamp techniques (ionic level).

5-1. Atrial epicardial activation mapping - whole dog experiments

Cardiac mapping is a method utilizing multiple electrodes to detect electrical signals spreading over the surface of the heart, and to produce isochrone maps of activation. It provides a powerful tool for studying electrophysiological properties and mechanisms of arrhythmias. In fact, the reentrant nature of many arrhythmias such as A-V node reentry, atrial flutter, and atrial fibrillation have been clarified with the aid of mapping techniques. This technique would enable us to visualize the overall, as well as the local, activation pattern in either normal or arrhythmic tissue and to localize the sites of origin of arrhythmia. We would expect to obtain data on conduction velocity, ERP and its spatial distribution, and the wavelength for reentry. Therefore, we should be able to get insights into the mechanisms and the determinants of arrhythmia.

5-2. Standard microelectrode techniques - cellular approaches

Standard microelectrode techniques in cardiac research were developed in the 1950s. Since then, they have become a routine approach to study cellular electrophysiology. The cellular mechanisms of some forms of arrhythmias (such as triggered activity induced by EAD or DAD) and actions of antiarrhythmic drugs have been defined by this technique. By using this technique, we would expect to obtain information regarding the modulation of membrane repolarization by heart rate, antiarrhythmic drugs, etc.

5-3. Whole-cell patch-clamp techniques - studies of ion currents

This method has allowed membrane currents which control transmembrane potential of cells to be studied. Intrinsic properties of individual ion currents, including their voltage-dependence, time-dependent

kinetics, frequency-dependence, and ion selectivity, can be revealed by this approach. The relative contribution of various currents to repolarization, the modulation of channels by endogenous or exogenous substances, interactions between different currents, and the potential ionic mechanisms governing arrhythmia occurrence can be addressed with this method. With the aid of this technique, we would be able to characterize repolarizing currents and to explore the possible presence of previously unidentified currents in human atrial myocytes. We could also acquire data on drug effects on repolarizing currents.

REFERENCES

1-1. Rosen MR, Jeck CD, Steinberg SF. Autonomic modulation of cellular repolarization and of the electrocardiographic QT interval. J Cardiovasc Electrophysiol 1992;3:487-499.

1-2. Carmeliet E. Mechanisms and control of repolarization. Eur Heart J 1993;14(suppl H):3-13.

1-3. Noble D. The initiation of heart beat. (2nd ed.) 1978,Oxford, Clarendon.

1-4. Carmeliet E. Repolarization and frequency in cardiac cells. J Physiol (Paris) 1977;73:903-923.

1-5. Carmeliet E. K^+ channels in cardiac cells: mechanisms of activation, inactivation, rectification and K^+ selectivity. Pflügers Arch 1989;414:(Suppl 1):S88-92.

1-6. Kass RS, Tsien RW. Control of action potential duration by calcium ions in cardiac Purkinje fibers. J Gen Phsyiol 1976;67:599-617.

1-7. Siegelbaum SA, Tsien RW. Calcium-activated transient outward current in calf cardiac Purkinje fibers. J Physiol (Lond) 1980;299:485-506.

1-8. Maylie J, Morad M. A transient outward current related to calcium release and development of tension in elephant seal atrial fibers. J Physiol (Lond) 1984;357:267-292.

1-9. Hiraoka M, Kawano S. Calcium-sensitive and insensitive transient outward current in rabbit ventricular myocytes. J Physiol (Lond) 1989;410:187-212.

1-10. Noble D, Tsien RW. Outward membrane currents activated in the plateau range of potentials in cardiac Purkinje fibres. J Physiol (Lond) 1969;200:205-231.

1-11. Sanguinetti MC, Juriewicz NK. Two components of cardiac delayed rectifier K^+ current: different sensitivity to block by class III antiarrhythmic agents. 1990;96:195-215.

1-12. Sanguinetti MC, Jurkiewicz NK. Delayed rectifier outward K^+ current is composed of two currents in guinea pig atrial cells. Am J Physiol 1991;260:H393-399.

1-13. Hume JR, Uehara A. Ionic basis of the different action potential configurations of single guinea pig atrial ventricular myocytes. J Physiol (Lond.) 1985;368:525-544.

1-14. Shimoni Y, Clark RB Giles WR. Role of inwardly rectifying potassium current in rabbit ventricular

action potential. J Physiol (Lond.) 1992;448:709-728.

1-15. Glitsch HG. Electrogenic Na pumping in the heart. Ann Rev Physiol 1982;44:389-400.

1-16. Gadsby DC. The Na/K pump of cardiac cells. Ann Rev Biophys Bioeng 1984a;13:373-398.

1-17. Gadsby DC. The Na/K pump of cardiac moycytes. In: Zipes DP, Jalife J (eds): Cardiac Electrophysiology: from cell to bedside. W.B. Saunders Company, 1990;pp35-51.

1-18. Ackerman MJ, Clapham DE. Cardiac chloride channels. TCM 1993;3:23-28.

1-19. Gross GJ, Auchampach J. Role of ATP-dependent potassium channels in myocardial ischemia. Cardiovasc Res 1992;26:1011-1016.

1-20. Surawicz B. Dispersion of refractoriness in ventricular arrhythmias. In: Zipes DP, Jalife J (eds): Cardiac Electrophysiology: from cell to bedside. W.B. Saunders Company, 1990;pp377-385.

1-21. Nattel S, Zeng FD. Frequency-dependent effects of antiarrhythmic drugs on action potential duration and refractoriness of canine cardiac Purkinje fibers. J Pharmacol Exp Ther 1984;22:283-291.

1-22. Nawrath H. Action potential, membrane currents and force of contraction in mammalian heart muscle fibers treated with quinidine. J Pharmacol Exp Ther 1981;216:176-182.

1-23. Allesie MA, Bonke FIM, Schopman FJG. Circus movement in rabbit atrial muscle as a mechanism of tachycardia. III. The role of nonuniform recovery of excitability in the occurrence of unidirectional block, as studied with multiple microelectrodes. Circ Res 1976;39:168-177.

1-24. Spach MS, Dolber PC, Anderson PAW. Multiple regional differences in cellular properties that regulate repolarization and contraction in the right atrium of adult and newborn dogs. Cric Res 1989;65:1594-1611.

1-25. Spach MS, Dolber PC, Heidlage JF. Interaction of inhomogeneities of repolarization with anisotropic propagation in dog atria: A mechanism for both preventing and initiating reentry. Circ Res 1989;65:1612-1631.

1-26. Olsson SB, Broman H, Hellström C, Talwar KK, Volkmann R. Adaptation of human atrial muscle repolarization after high rate stimulation. Cardiovasc Res 1984;19:7-14.

1-27. Spach MS, Dolber PC, Heidlage JF. Influence of the passive anisotropic properties on directional differences in propagation following modification of the sodium conductance in human atrial muscle: A model of reentry based on anisotropic discontinuous propagation. Circ Res 1988;62:811-832.

1-28. Lauribe P, Escande D, Nottin R, Coraboeuf E. Electrical activity of human atrial fibres at frequencies corresponding to atrial flutter. Cardiovasc Res 1989;23:159-168.

1-29. Escande D, Loisance D, Planche C, Coraboeuf E. Age-related changes of action potential plateau shape in isolated human atrial fibres. Am J Physiol 1985;249:H843-850.

1-30. Shibata EF, Drury T, Refsum H, Aldrete V, Giles W. Contributions of a transient outward current to repolarization in human atrium. Am J Physiol 1989;257:H1773-1781.

1-31. Hordof AJ, Spotnitz A, Mary-Rabine L, Edie RN, Rosen MR. The cellular electrophysiologic effects of digitalis on human atrial fibres. Circulation 1978;57:223-229.

1-32. Gelband H, Rosen MR, Myerburg RJ, Bush HL, Bassett AL, Hoffman BF. Restoration effect of epinephrine on the electrophysiologic properties of depressed human atrial tissue. J Electrocardiol 1977;10:313-320.

1-33. Tuganowski W, Cekanski A. Electrical activity of a single fiber of the human embryonic heart. Pflügers Arch 1971;323:21-26.

1-34. Trautwein W, Kassebaum DG, Nelson RW, Hecht HH. Electrophysiological study of human heart muscle. Circ Res 1962;10:306-312.

1-35. Sleator W, Gubareff TD. Transmembrane action potentials and contractions of human atrial muscle. Am J Pyhsiol 1964;206:1000-1014.

1-36. Fabiato A, Fabiato F. The two components of the human atrial action potential. Circ Res 1971;29:296-305.

1-37. Gelband H, Bush HL, Rosen MR, Myerburg RJ, Hoffman BF. Electrophysiologic properties of isolated preparations of human atrial myocardium. Circ Res 1972;30:293-300.

1-38. Ito S. A comparative study on the electrical and mechanical properties of human and guinea pig atrial muscles in vitro. Jpn Circulation J 1975;39:37-47.

1-39. Hordof AJ, Edie R, Malm JR, Hoffman BF, Rosen MR. Electrophysiologic properties and response of pharmacologic agents of fibres from diseased human atria. Circulation 1976;54:774-779.

1-40. Mary-Rabine L, Hordof AJ, Danilo P, Malm JR, Rosen MR. Mechanisms for impulse initiation in isolated human atrial fibres. Circ Res 1980;47:267-277.

1-41. Le Grand B, Le Heuzey JY, Perier P, peronneau P, Lavergne T, Hatem S, Guize L. Cellular electrophysiological effects of flecainide on human atrial fibres. Cardiovasc Res 1990;24:232-238.

1-42. Prasad K. Transmembrane potential and force of contraction of normal and potassium deficient human atrial tissue in vitro. Can J Physiol Pharmacol 1969;47:1015-1024.

1-43. Gautier P, Escande D, Bertrand JP, Seguin J, Guiraudou P. Electrophysiological effects of penticainide (CM 7857) in isolated human atrial and ventricular fibres. J Cardiovasc Pharmacol 1989;13:328-335.

1-44. Tuganowski W, Tendera M. Components of the action potential of human embryonic auricle. Am J Physiol 1973;224:803-808.

1-45. Sutton MStJ, Morad M. Mechanisms of action of diltiazem in isolated human atrial and ventricular myocardium. J Mol Cell Cardiol 1987;19:497-508.

1-46. Hayward RP, Taggart P. Effects of sotalol on human atrial action potential duration and refractoriness: cycle length dependency of class III activity. Cardiovasc Res. 1986;20:100-107.

1-47. Imainishi S, Arita M. Factors related to the low resting membrane potentials of diseased human

atrial muscles. Jpn J Physiol 1987;37:393-410.

1-48. Hou Z, Lin C, Chiang BN, Cheng K. Electrophysiological effects of low pH in human atrial fibres. J Mol Cell Cardiol 1986;18:109-112.

1-49. Boutjdir M, Le Heuzey JY, Lavergne T, Chauvaud S, Guize L, Carpentier A, Peronneau P. Inhomogeneity of cellular refractoriness in human atrium: factor of arrhythmia? Pace 1986;9:1095-1100.

1-50. Singh BN, Courtney K. On the classification of anti-arrhythmic mechanisms: experimental and clinical correlations. In: Zipes DP, Jalife J (eds): Cardiac Electrophysiology: from cell to bedside. W.B. Saunders Company, 1990;pp882-897.

1-51. Singh BN, Vaughan Williams EM. A third class of antiarrhythmic action: effects on atrial and ventricular intracellular potentials, and other pharmacologic actions on cardiac muscle, of MJ 1999 and AH 3474. Br J Pharmacol 1970;29:675-687.

1-52. Singh BN. Arrhythmia control by prolonging repolarization: the concept and its potential therapeutic impact. Eur Heart J 1993;14(Suppl H):14-23.

1-53. Vaughan Williams EM. A classification of antiarrhythmic actions reassessed after a decade of new drugs. J Clin Pharmacol 1984;24:129-147.

1-54. Colatsky TJ, Follmer CH, Starmer CF. Channel specificity in antiarrhythmic drug action: mechanism of potassium channel block and its role in suppressing and aggravating cardiac arrhythmias. Circulation 1990;82:2235-2241.

1-55. The Sicilian Gambit. Task Force of the working group on arrhythmias of the European Society of Cardiology. A new approach to the classification of antiarrhythmic drugs based on their actions on arrhythmogenic mechanisms. Circulation 1991;84:1831-1851.

1-56. Roden DM. Early after-depolarization and torsade de pointes: implications for the control of cardiac arrhythmias by prolonging repolarization. Eur Heart J 1993;14(Suppl H):56-61.

1-57. Binah O, Rosen MR. Mechanisms of ventricular arrhythmias. Circulation 1992;85(Suppl I):25-31.

1-58. McWilliam JA. Fibrillar contraction of the heart. J Physiol (Lond) 1897;8:296-310.

1-59. Mayer AG. Phythmic pulsation in Scyphomedusae. 1906, Washington DC, Carnegie Institute, Publ No. 47.

1-60. Mines GR. On circulating excitation in heart muscles and their possible relations to tachycardia and fibrillation. 1914; Trans R Soc Can Series 3, Sect IV 8:43-52.

1-61. Garrey WE. Auricular fibrillation. Physiol Rev 1924;4:215-250.

1-62. Lewis T. Observations upon flutter and fibrillation: Part IV. Impulse flutter: Theory of circus movement. Heart 1920;7:293-331.

1-63. Wit AL, Cranefield PF, Hoffman BF. Slow conduction and reentry in the ventricular conducting system. II. Single and sustained circus movement in networks of canine and bovine Purkinje fibers.

Circ Res 1972;30:11-22.

1-64. Moe GK, Mendez C, Han J. Aberrant AV impulse propagation in the dog heart: a study of functional bundle branch block. Circ Res 1965;16:261-286.

1-65. Gallagher JJ, Sealy WC, Wallace AG. Correlation between catheter electrophysiological studies and findings on mapping of ventricular excitation in the WPW syndrome. In Wellens HJJJ, Lie KI, Janse MJ (eds), 1976, Leiden, Stenfert, Kroese. pp388-612.

1-66. Schoels W, Gough WB, Restivo M, El-Sherif N. Circus movement atrial flutter in the canine sterile pericarditis model: Activation patterns during initiation, termination, and sustained reentry in vivo. Circ Res 1990;67:35-50.

1-67. Schmitt FO, Erlanger J. Directional difference in the conduction of the impulse through heart muscle and their possible relation to extrasystolic and fibrillary contractions. Am J Physiol 1928;87:326-347.

1-68. Allesie MA, Bonke FIM, Schopman FJG. Circus movement in rabbit atrial muscle as a mechanism of tachycardia. III. The 'leading circle' concept: A new model of circus movement in cardiac tissue without the involvement of an anatomical obstacle. Circ Res 1977;41:9-18.

1-69. Allessie MA, Lammers WJEP, Bonke FIM, Hollen J. Experimental evaluation of Moe's multiple wavelet hypothesis of atrial fibrillation. In: Zipes DP (ed): Cardiac Electrophysiology and arrhythmias. Orlando, Fla, Grune & Stratton, Inc, 1985,pp265-274.

1-70. Allessie MA, Rensma PL, Brugada J, Smeets JLRM, Penn O, Kirchhof CJHJ. Pathophysiology of atrial fibrillation. In: Zipes DP, Jalife J (eds): Cardiac Electrophysiology. From cell to bedside. Philadelphia, Pa, WB Saunders Co, 1990, pp548-558.

1-71. Waldo AL. Mechanisms of atrial fibrillation, atrial flutter, and ectopic atrial tachycardia: A brief review. Circulation 1987;75(Suppl III):37-39.

1-72. Cox JL, Canavan TE, Schuessler RB, Cain ME, Lindsay BD, Stone C, Smith PK, Corr PB, Boineau JP. The surgical treatment of atrial fibrillation: II. Intraoperative electrophysiologic mapping and description of the electrophysiologic basis of atrial flutter and atrial fibrillation. J Thorac Cardiovasc Surg 1991;101:406-426.

1-73. Garrey WE. The nature of fibrillary contraction of the heart: its relation to tissue mass and form. Am J Physiol 1914;33:397-414.

1-74. Moe GK. On the multiple wavelet hypothesis of atrial fibrillation. Arch Int Pharmacodyn Ther 1962;140:183-188.

1-75. Moe GK, Rheinboldt WC, Abildskov JA. A computer model of atrial fibrillation. Am Heart J 1864;67:200-220.

1-76. Pogwizd SM, Hoyt RH, Saffitz JE, Corr PB, Cox JL, Cain ME. Reentrant and focal mechanisms underlying ventricular tachycardia in human heart. Circulation 1992;86:1872-1877.

1-77. Chen P, Cha Y, Peters BB, Chen LS. Effects of myocardial fiber orientation on the electrical induction of ventricular fibrillation. Am J Physiol 1993;264:H1760-1773.

1-78. Rensma PL, Allessie MA, Lammers WJEP, Bonke FIM, Schalij MJ. Length of excitation wave and susceptibility to reentrant atrial arrhythmias in normal conscious dogs. Circ Res 1988;62:395-410.

1-79. Mines GR. On dynamic equilibrium in the heart. J Physiol (Lond) 1913;46:349-383.

1-80. Lewis T. The mechanism and graphic registration of the heart beat, ed 3. London, Shaw & Sons, 1925, pp265-276.

1-81. Wiener N, Rosenblueth A. The mathematical formulation of the problem of conduction of impulses in a network of connected excitable elements, specifically in cardiac muscle. Arch Inst Cardiol Mex 1946;16:205-265.

1-82. Smeets JLRM, Allessie MA, Lammers WJEP. The wavelength of the cardiac impulse and reentrant arrhythmias in isolated rabbit atrium. Circ Res 1986;58:96-108.

1-83. Ramdat Misier AR, Opthof T, van Hemel NM, Defauw JJAM, de Bakker JMT, Janse MJ, van Capelle FJL. Increased dispersion of "refractoriness" in patients with idiopathic paroxysmal atrial fibrillation. J Am Coll Cardiol 1992;19:1531-1535.

1-84. Luck JC, Engel TR. Dispersion of atrial refractoriness in patients with sinus node dysfunction. Circulation 1979;60:404-408.

1-85. Michelucci A, Padeletti T, Fradella GA. Atrial refractoriness and spontaneous or induced atrial fibrillation. Acta Cardiologica 1982;37:333.

1-86. Cosio FG, Placios J, Vidal JM. Electrophysiologic studies in atrial fibrillation. Slow conduction of premature impulses: A possible manifestation of the background for reentry. Am J Cardiol 1983;51:122.

1-87. Lazzara R. Antiarrhythmic drugs and torsade de pointes. Eur Heart J 1993;14(Suppl H):88-92.

1-88. Singh BN. When is QT prolongation antiarrhythmic and when is it proarrhythmic? Am J Cardiol 1988;63:867-869.

1-89. Fredberg AS, Papp JG, Vaughan Williams EM. The efffect of altered thyroid state on atrial intracellular potentials. J Physiol 1970;207:357-370.

1-90. Johnson PN, Freedberg AS, Marshall JM. Action of thyroid hormone on the transmembrane potentials from sino-atrial node cells and atrial cells in isolated atria of rabbits. Cardiology 1973;58:273-289.

1-91. Singh BN (ed). Control of Cardiac Arrhythmias by Lengthening Repolarization. Mt. Kisco NY, Futura Publishing Co., 1988.

1-92. Allesie M, Lammers W, Smmets J, Bonke F, Hollen J. Total mapping of atrial excitation during acetylcholine-induced atrial flutter and fibrillation in the isolated canine heart. In: Kulbertus HE, Olsson SB, Schlepper M, eds. Molndal, Sweden: AB Hassle, 1982; pp 44-59.

1-93. Guvrilescu S, Cotoi S, Pop T. Monophasic action potential of the right atrium in paroxysmal atrial flutter and fibrillation. Br Heart J 1973;35:585-589.

1-94. Guvrilescu S, Cotoi S. Monophasic action potential of right atrium during atrial flutter and after conversion to sinus rhythm. Br Heart J 1972;34:396-402.

1-95. Guvrilescu S, Cotoi S, Pop T. Monophasic action potential of the right atrium. Cardiology 1972;57:200-207.

1-96. Kumagai K, Akimitsu S Kawahira K, Kawanami F, Yamanouchi Y, Hiroki T, Arakawa K. Electrophysiological properties in chronic lone atrial fibrillation. Circulation 1991;84:1662-1668.

1-97. Henry WL, Morganroth J, Pearlman AS, Clark CE, Redwood DR,Itscoitz SB, Epstein SE. Relation between echocardiographically determined left atrial size and atrial fibrillation. Circulation 1976;53:273-280.

1-98. Olsson SB, Cotoi S, Varnauskas E. Monophasic action potential and sinus rhythm stability after conversion of atrial fibrillation. Acta Med Scand 1971;190:381-387.

1-99. Singh BN, Vaughan Williams EM. A fourth class of anti-disrhythmic action? Effect of verapamil on ouabain toxicity, on atrial and ventricular intracellular potentials, and on other features of cardiac arrest. Cardiovasc Res 1972;6:109-119.

1-100. Nattel S. Antiarrhythmic drug classifications: A critical appraisal of their history, present status, and clinical relevance. Drugs 1991;41:672-701.

1-101. Woosley RL. Antiarrhythmic drugs. Ann Rev Pharmacol Toxicol 1991;31:427-455.

1-102. Lewis T. The value of quinidine in cases of auricular fibrillation and methods of studying the clinical reaction. Am J Med Sci 1922;163:781-794.

1-103. Hondeghem LM, Snyders DJ. Class III antiarrhythmic agents have a lot of potential but a long way to go: Reduced effectiveness and dangers of reverse use dependence. Circulation 1990;81:686-690.

1-104. Kerr CR, Mason MA, Chung DC. Propafenone: An effective drug for prevention of recurrent atrial fibrillation. (abstract) Circulation 1985;72:(suppl III):III-171.

1-105. Chouty F, Coumel P. Oral flecainide for prophylaxis of paroxysmal atrial fibrillation. Am J Cardiol 1988;62:35D-37D.

1-106. Kappengerger LJ, Fromer MA, Chenasa M, Gloor HO. Evaluation of flecainide acetate in rapid atrial fibrillation complicating Wolff-Parkinson-White syndrome. Clin Cardiol 1985;8:321-326.

1-107. Goy JJ, Maendly R, Grbic M, Finci L, Sigwart U. Cardioversion with flecainide in patients with atrial fibrillation of recent onset. Eur J Clin Pharmacol 1985;27:737-738.

1-108. Berns E, Rinkengerger RL, Jeang MK, Dougherty AH, Jenkins M, Naccarelli GV. Efficacy and safety of flecainide acetate for atrial tachycardia or fibrillation. Am J Cardiol 1987;59:1337-1341.

1-109. Crijns HJGM, van Wijk LM, van Gilst WH, Kingma JH, van Gelder IC, Lie KI. Acute conversion of

atrial fibrillation to sinus rhythm: Clinical efficacy of flecainide acetate: Comparison of two regimens. Eur Heart J 1988;9:634-638.

1-110. Goy JJ, Kaufmann U, Kappenberger L, Sigwart U. Restoration of sinus rhythm with flecainide in patients with atrial fibrillation. Am J Cardiol 1988;62:38D-40D.

1-111. Borgeat A, Goy JJ, Maendly R, Kaufmann U, Grbic M, Sigwart U. Flecainide versus quinidine for conversion of atrial fibrillation to sinus rhythm. Am J Cardiol 1986;58:496-498.

1-112. Suttorp MJ, Kingma JH, Lie-A-Huen L, Mast EG. Intravenous flecainide versus verapamil for acute conversion of paroxysmal atrial fibrillation or flutter to sinus rhythm. Am J Cardiol 1989;63:693-696.

1-113. van Gelder I, Crijns HJ, van Gilst WH, Lie KI. Efficacy of flecainide to maintain sinus rhythm after cardioversion of chronic atrial fibrillation and flutter. (abstract) Circulation 1988;78(suppl II):II-626.

1-114. Rasmussen K, Anderson A, Abrahasen AM, Overskeid K, Bathen J. Flecainide versus disopyramide in maintaining sinus rhythm following conversion of chronic atrial fibrillation. (abstract) Eur Heart J 1988;9(suppl I):I-52.

1-115. Clementy J, Dulhoste MN, Laiter C, Denjoy I, Dos Santos P. Flecainide acetate in the prevention of paroxysmal atrial fibrillation: A nine-month follow-up of more than 500 patients. Am J Cardiol 1992;70:44A-49A.

1-116. Kingma JH, Suttorp MJ. Acute pharmacologic conversion of atrial fibrillation and flutter: The role of flecainide, propafenone, and verapamil. Am J Cardiol 1992;70:56A-61A.

1-117. The Cardiac Suppression Trial (CAST) Investigators. Preliminary report. Effect of encainide and flecainide on mortality in a randomized trial of arrhythmia suppression after myocardial infarction. New Engl J Med 1989;321:406-410.

1-118. Cardiac Suppression Trial II Investigators. Ethmozine exerts an adverse effect on mortality in survivors of acute myocardial infarction. New Engl J Med 1991;327:227-233.

1-119. Josephson IR, Sanchez-Chapula J, Brown AM. Early outward current in rat single ventricular cells. Circ Res 1984;54:157-162.

1-120. Clark RB, Giles WR, Imaizumi Y. Properties of the transient outward current in rabbit atrial cells. J Physiol (Lond) 1988;405:147-168.

1-121. Du Brow IW, Fisher EA, Denes P, Hastreister AR. The influence of age on cardiac refractory periods in man. Pediat Res 1976;10:135-139.

1-122. Dubrow IW, Fisher EA, Amat-y-Leon F, Denes P, Wu D, Rosen K, Hastreiter AR. Comparison of cardiac refractory periods in children and adults. Circulation 1975;51:485-491.

1-123. Michelucci A, Padeletti L, Fradella GA, Lova RM, Monizzi D, Giomi A, Fantini F. Ageing and atrial electrophysiologic properties in man. Int J Cardiol 1984;5:75-81.

1-124. Pales de Carvalho A, de Mello WC, Hoffman BF. Electrophysiological evidence for specialized

fibres in rabbit atrium. Am J Physiol 1959;196:483-488.

1-125. Hogan PM, Davis LD. Evidence for specialized fibres in the canine right atrium. Circ Res 1968;23:387-396.

1-126. James TN. The connecting pathways between the sinus node and AV node and between the right and left atrium in the human heart. Am Heart J 1963;66:498-505.

1-127. Wang Z, Fermini B, Nattel S. Repolarization differences between guinea pig atrial endocardium and epicardium: evidence for a role of I_{to}. Am J Physiol 1991;260:H1501-1506.

1-128. Attwell D, Cohen I, Eisner DA. The effects of heart rate on the action potential of guinea pig and human ventricular muscle. J Physiol (Lond) 1981;313:439-461.

1-129. Boyett MR, Fedida D. Changes in the electrical activity of dog cardiac Purkinje fibres at high heart rates. J Physiol (Lond) 1984;350:361-391.

1-130. Litovsky SH, Antzelevitch C. Rate-dependence of action potential duration and refractoriness in canine ventricular endocardium differs from that of epicardium: Role of the transient outward current. J Am Coll Cardiol 1989;14:1053-1066.

1-131. Kukushkin NI, Gainullin RZ, Sosunov EA. Transient outward current and rate dependence of action potential duration in rabbit cardiac ventricular muscle. Pflügers Arch 1983;399:87-92.

1-132. Hiraoka M, Kawano S. Mechanism of increased amplitude and duration of the plateau with sudden shortening of diastolic intervals in rabbit ventricular cells. Circ Res 1987;60:14-26.

1-133. West TC, Amory DW. Single fiber recording of the effects of quinidine at atrial and pacemaker sites in the isolated right atrium of the rabbit. J Pharmacol Exp Ther 1960;130:183-193.

1-134. Ikeda N, Singh BN, Davis LD, Hauswirth O. Effects of flecainide on the electrophysiologic properties of isolated canine and rabbit myocardial fibers. J Am Coll Cardiol 1985;5:303-310.

1-135. Le Grand B, Le Heuzey JY, Périer P, Lavergne T, Chauvaud S, Péronneau P, Guize L. Effects of flecainide on action potential duration of human atrial fibers (abstract). J Am Coll Cardiol 1989;13:140A.

1-136. Samuelsson RG, Harrison DC. Electrophysiologic evaluation of encainide with use of monophasic action potential recording. Am J Cardiol 1981;48:871-876.

1-137. Szabo G, Otero AS. G protein mediated regulation of K^+ channels in heart. Annu Rev Physiol 1990;52:293-305.

1-138. Holmer SR, Homcy CJ. G proteins in the heart: A redundant and diverse transmembrane signalling network. Circulation 1991;84:1891-1902.

1-139. Anumonwo JMB, Freeman LC, Kwok WM, Kass RS. Potassium channels in the heart:electrophysiology and pharmacological regulation. Cardiovasc Drug Rev 1991;9:299-316.

1-140. Kass RS, Freeman LC. Potassium channels in the heart: cellular, molecular, and clinical implications. Trends Cardiovasc Med 1993;3:149-159.

1-141. Escande D, Henry P. Potassium channels as pharmacological targets in cardiovascular medicine. Eur Heart J 1993;14(Suppl B):2-9.

1-142. Hille B. Ionic channels of excitable membrane. Sunderland, Mass, Sinauer Associates Inc, 1984.

1-143. Dudel J, Peper K, Rudel R, Trautwein W. The dynamic chloride component of membrane current in Purkinje fibres. Pflügers Arch 1967,295:197-212.

1-144. Fozzard HA, Hiraoka M. The positive dynamic current and its inactivation properties in cardiac Purkinje fibres. J Physiol 1973;234:569-586.

1-145. Kenyon JL, Gibbons WR. Influence of chloride, potassium, and tetraethylammonium on the early outward current of sheep cardiac Purkinje fibres. J Gen Physiol 1979;73:117-138.

1-146. Kenyon JL, Gibbons WR. 4-Aminopyridine and the early outward current of sheep cardiac Purkinje fibres. J Gen Physiol 1979;73:139-157.

1-147. Siegelbaum SA, Tsien RW. Calcium-activated transient outward current in calf Purkinje fibres J Physiol 1980;299:485-506.

1-148. Zygmunt AC, Gibbons WR. Calcium-activated chloride current in rabbit ventricular myocytes. Circ Res 1991;68:424-437.

1-149. Zygmunt AC, Gibbons WR. Properties of the calcium-activated chloride current in heart. J Gen Physiol 1992;99:391-414.

1-150. Coraboeuf E, Carmeliet E. Existence of two transient outward current in sheep Purkinje fibres. Pflügers Arch 1982;392:352-359.

1-151. Kenyon JL, Sutko JL. Calcium- and voltage-activated plateau currents of cardiac Purkinje fibres. J Gen Physiol 1987;89:921-958.

1-152. Duke ID, Morad M. Analysis of the transient outward current in isolated rat ventricular cells (abstract). Biophys J 1987;51:412a.

1-153. Benndorf K, Markwardt F, Nilius B. Two types of transient outward currents in cardiac ventricular cells of mice. Pflügers Arch 1987;409:641-643.

1-154. Tseng GN, Hoffman BF. Two components of transient outward current in canine ventricular myocytes. Circ Res 1989;64:633-647.

1-155. Giles WR, Imaizumi Y. Comparison of potassium currents in rabbit atrial and ventricular cells. J Physiol (Lond) 1988;405:123-145.

1-156. Hiraoka M, Kawano S. Calcium-sensitive and insensitive transient outward current in rabbit ventricular myocytes. J Physiol (Lond) 1989;410:187-212.

1-157. Escande D Coulombe A, Faivre JF, Deroubaix E, Coraboeuf E. Two types of transient outward currents in adult human atrial cells. Am J Physiol 1987;252:H142-H148.

1-158. Kilborn MJ, Fedida D. A study of the developmental changes in outward currents of rat ventricular myocytes. J Physiol (Lond) 1990;430:37-60.

1-159. Giles WR, van Ginneken ACG. A transient outward current in isolated cells from the crista terminalis of rabbit heart. J Physiol (Lond) 1985;368:243-264.

1-160. Boyett MR: A study of the effects of the rate of stimulation on the transient outward current in sheep cardiac Purkinje fibres. J Physiol (Lond) 1981;319:1-22.

1-161. Boyett MR: Effects of rate-dependent changes in the transient outward current on the action potential in sheep Purkinje fibres. J Physiol (Lond) 1981;319:23-41.

1-162. Imaizumi Y, Giles WR. Quinidine-induced inhibition of transient outward current in cardiac muscle. Am J Physiol 1987;253:H704-708.

1-163. Coraboeuf E, Deroubaix E, Escande D, Coulombe A. Comparative effects of three class I antiarrhythmic agents on plateau and pacemaker currents of sheep Purkinje fibres. Cardiovasc Res 1988;22:375-384.

1-164. Duan DY, Fermini B, Nattel S. Potassium channel blocking properties of propafenone in rabbit atrial myocytes. J Pharmacol Exp Ther 1993;264:1113-1123.

1-165. Dukes ID, Morad M. Tedisamil inactivates transient outward K^+ current in rat ventricular myocytes. Am J Physiol 1989;257:H1746-1749.

1-166. Carmeliet E. Electrophysiologic and voltage clamp analysis of the effects of sotalol on isolated cardiac muscle and Purkinje fibres. J Pharmacol Exp Ther 1985;232:817-825.

1-167. Litovsky SH, Antzelevitch C. Transient outward current prominent in canine ventricular epicardium but not endocardium. Circ Res 1988;62:116-126.

1-168. Litovsky SH, Antzelevitch C. Rate-dependence of action potential duration and refractoriness in canine ventricular endocardium differs from that of epicardium: Role of the transient outward current. J Am Coll Cardiol 1989;14:1053-1066.

1-169. Antzelevitch C, Litovsky SH, Lukas A. Ventricular epicardium vs. endocardium: electrophysiology and pharmacology. In: Zipes D, Jalife J, eds. Cardiac Electrophysiology, From Cell to Beside. New York:WB Saunders, 1989.

1-170. Noble D, Tsien RW. The kinetics and rectifier properties of the slow potassium current in cardiac Purkinje fibres. J Physiol (Lond) 1968;195:185-214.

1-171. Noble D, Tsien RW. Outward membrane currents activated in the plateau range of potentials in cardiac Purkinje fibres. J Physiol (Lond) 1969;200:205-231.

1-172. Bennett PB, Mckinney LC, Kass RS, Begenisich T. Delayed rectification in the calf cardiac Purkinje fiber. Evidence for multistate kinetics. Biophys J 1985;48:553-567.

1-173. Hume JR, Uehara A. Ionic basis of the different action potential configurations of single guinea pig atrial and ventricular myocytes. J Physiol 1985;368:525-544.

1-174. Apkon M, Nerbonne JM. Characterization of two distinct depolarization-activated K^+ currents in adult rat ventricular myocytes. J Gen Physiol 1991;97:973-1011.

1-175. McDonald TF, Trautwein W. The potassium current underlying delayed rectification in cat ventricular muscle. J Physiol 1978;274:217-246.

1-176. Simmons MA, Creazzo T, Hartzell HC. A time-dependent and voltage-sensitive K^+ current in single cells from frog atrium. J Gen Physiol 1986;88:739-755.

1-177. Fermini B, Nattel S. Evidence for a delayed rectifier potassium current, I_K, in rabbit atrial myocytes. Biophys J 1991;59:266A.

1-178. Shrier A, Clay JR. Repolarization currents in embryonic chick atrial heart cell aggregates. Biophys J 1986;50:861-874.

1-179. Shibasaki T. Conductance and kinetics of delayed rectifier potassium channels in nodal cells of the rabbit heart. J Physiol 1987;387:227-250.

1-180. Jurkiewicz NK, Sanguinetti MC. Rate-dependent prolongation of cardiac action potentials by a methanesulfonilide class III antiarrhythmic agent: Specific block of rapidly activating delayed rectifier K^+ current by dofetilide. Circ Res 1993;72:75-83.

1-181. Balser JR, Bennett PB, Hondeghem LM, Roden DM. Suppression of time-dependent outward current in guinea pig ventricular myocytes: Actions of quinidine and amiodarone. Circ Res 1991;69:519-529.

1-182. Sanguinetti MC, Jurkiewicz NK. Lanthanum blocks a specific component of I_K and screens membrane surface charge in cardiac cells. Am J Physiol 1990b;259:H1881-1889.

1-183. Roden DM, Bennett PB, Sbyders DJ, Balser JR, Hondeghem LM. Quinidine delays I_K activation in guinea pig ventricular myocytes. Circ Res 1988;62:1055-1058.

1-184. Follmer CH, Colatsky TJ. Block of the delayed rectifier potassium current I_K by flecainide and E-4031 in cat ventricular myocytes. Circulation 1990;82:289-293.

1-185. Balser JR, Hondeghem LM, Roden DM. Amiodarone reduces time dependent I_K activation (abstract) Circulation 1987;76:IV-151.

1-186. Snyders DJ, Katzung BG. Clofilium reduces the plateau potassium current in isolated cardiac myocytes (abstract). Circulation 1985;72(Suppl III):233.

1-187. Follmer CH, Poczobutt MT, Colatsky TJ. Selective block of delayed rectification (I_K) in feline ventricular myocytes by Wy48,986, a novel class III antiarrhythmic agent (abstract). J Mol Cell Cardiol 1989;21:S185.

1-188. Gwilt M, Dalrymple HW, Burges RA, Blackburn KJ, Arrowsmith JE, Cross PE, Higgins AJ. UK-68,798 is a novel, potent and selective class III antiarrhythmic agent (abstract). J Mol Cell Cardiol 1989;21:S11.

1-189. Dukes ID, Morad M. Tedisamil modulates outward K^+ channels in rat and guinea pig ventricular myocytes (abstract). Circulation 1989;80:(suppl II):517.

1-190. Kass RS, Wiegers SE. The ionic basis of concentration-related effects of noradrenaline on the

action potential of calf cardiac Purkinje fibres J Physiol (Lond) 1982;322:541-558.

1-191. Brown HF, Noble SJ. Effects of adrenaline on membrane currents underlying pacemaker activity in frog atrial muscle. J Physiol (Lond) 1974;238:51-52.

1-192. Walsh KB, Begenisich TB, Kass RS. β-adrenergic modulation in heart: independent regulation of K and Ca channels. Pflügers Arch 1988;411:232-233.

1-193. Arena JP, Kass RS. Block of heart potassium channels by clofilium and its tertiary analogs: Relationship between drug structure and type of channel blocked. Mol Pharmacol 1988;34:60-66.

1-194. Sanguinetti MC. Modulation of potassium channels by antiarrhythmic and antihypertensive drugs. Hypertension 1992;19:228-236.

1-195. Weidmann S. Effect of current flow on the membrane potential of cardiac muscle. J Physiol (Lond) 1951;115:227-236.

1-196. McAllister RE, Noble D. The time and voltage dependence of the slow outward current in cardiac Purkinje fibres. J Physiol (Lond) 1966;186:632-662.

1-197. Thuringer D, Lauribe P, Escande D. A hyperpolarization-activated inward current in human myocardial cells. J Mol Cell Cardiol 1992;24:451-455.

1-198. Heidbüchel H, Vereecke J, Carmeliet E. Three different potassium channels in human atrium: Contribution to the basal potassium conductance. Circ Res 1990;66:1277-1286.

1-199. Kurachi Y. Voltage-dependent activation of the inward-rectifier potassium channel in the ventricular membrane of guinea pig heart. J Physiol (Lond) 1985;366:365-385.

1-200. Hiraoka M, Sawada K, Kawano S. Effects of quinidine on plateau currents of guinea pig ventricular myocytes. J Mol Cell Cardiol 1986;18:1097-1106.

1-201. Sato R, Hisatome I, Singer D. Amiodarone blocks an inward rectifier K^+ channel in guinea pig ventricular myocytes (abstract). Circulation 1987;76:IV-150.

1-202. Arena JP, Kass RS. Block of heart potassium channels by clofilium and its tertiary analogs: Relationship between drug structure and type of channel blocked. Mol Pharmacol 1988;34:60-66.

1-203. Boyle WA, Nerbonne JM. A novel type of depolarization-activated K^+ current in isolated adult rat atrial myocytes. Am J Physiol 1991;260:H1236-H1247.

1-204. Yue DT, Marban E. A novel cardiac potassium channel that is active and conductive at depolarized potentials Pflügers Arch 1988;413:127-133.

1-205. Jeck CD, Boyden PA. Age-related appearance of outward currents may contribute to developmental differences in ventricular repolarization. Circ Res 1992;71:1390-1403.

1-206. Giles W, Noble SJ. Changes in membrane current in bullfrog atrium produced by acetylcholine. J Physiol 1976;261:103-123.

1-207. Inoue D, Hachisu M, Pappano AJ. Acetylcholine increases resting membrane potassium conductance in atrial but not ventricular muscle during inhibition of Ca^{++}-dependent action potentials

in chick heart. Circ Res 1983;53:158-167.

1-208. Iijima T, Irisawa H, Kameyama M. Membrane currents and their modification by acetylcholine in isolated single atrial cells of the guinea pig. J Physiol 1985;359:485-501.

1-209. Heidbuchel H, Vereecke J, Carmeliet E. The electrophysiological effects of acetylcholine in single human atrial cells. J Mol Cell Cardiol 1987;19:1207-1219.

1-210. Sato R, Hisatome I, Wasserstrom JA, Adrentzen CE, Singer DH. Acetylcholine-sensitive potassium channels in human atrial myocytes. Am J Physiol 1990;259:H1730-1735.

1-211. Noma A, Trautwein W. Relaxation of the Ach-induced potassium current in the rabbit sinoatrial node cell. Pflügers Arch 198;377:740-751.

1-212. Sakmann B, Noma A, Trautwein W. Acetylcholine activation of single muscarinic K^+ channels in isolated pacemaker cells of the mammalian heart. Nature 1983;303:250-253.

1-213. Carmeliet E, Mubagwa K. Characterization of the acetylcholine-induced potassium current in rabbit cardiac Purkinje fibres. J Physiol 1986;371:239-255.

1-214. Kurachi Y, Nakajima T, Sugimoto T. Acetylcholine activation of K^+ channels in cell free membrane of atrial cells. Am J Physiol 1986b;251:H681-H684.

1-215. Breitweiser GE, Szabo G. Uncoupling of cardiac muscarinic and ß-adrenergic receptors from ion channels by guanine nucleotide analogue. Nature 1985;317:538-540.

1-216. Inomata N, Ohno T, Ishihara T, Akaike N. Antiarrhythmic agents act differentially on the activation phase of Ach-response in guinea pig atrial myocytes (abstract). Circulation 1992;86:I-695.

1-217. Okabe K, Yatani A, Brown AM. The nature and origin of spontaneous noise in G protein-gated ion channels. J Gen Physiol 1991;97:1279-1293.

1-218. Kaibara M, Nakajima T, Irisawa H. Regulation of spontaneous opening of muscarinic K^+ channels in rabbit atrium. J Physiol (Lond) 1991;433:589-613.

1-219. Irisawa H, Hagiwara N. Ionic current in sinoatrial node cells. J Cardiovasc Electrophysiol 1991;2:531-540.

1-220. Noma A. ATP-regulated K^+ channels in cardiac muscle. Nature 1983;305:147-148.

1-221. Cook DL, Hales CN. Intracellular ATP directly blocks K^+ channels in pancreatic ß-cells. Nature 1984;311:271-273.

1-222. Spruce AE, Standen NB, Stanfield PR. Voltage-dependent ATP-sensitive potassium channels of skeletal muscle membrane. Nature 1985;316:736-738.

1-223. Standen NB, Quayle JM, Davies NW, Brayden JE, Huang Y, Nelson MT. Hyperpolarizing vasodilators activate ATP-sensitive K^+ channels in arterial smooth muscle. Nature 1989;245:177-180.

1-224. Cohen N, Lederer WJ, Nicholas CG. Activation of ATP-sensitive potassium channels underlies contractile failure in single human cardiac myocytes during complete metabolic inhibition. J

Cardiovasc Electrophysiol 1992;3:56-63.

1-225. Wilde AAM, Escande D, Schumacher CA, Thuringer D, Mestre M, Fiolet JWT. Glibenclamide inhibition of ATP-sensitive K^+ channels and ischemia-induced K^+ accumulation in the mammalian heart. Pflügers Arch 1989;414:S176.

1-226. Wu B, Sato Toshiaki, Kiyosue T, Arita M. blockade of 2,4-dinitrophenol induced ATP sensitive potassium current in guinea pig ventricular myocytes by class I antiarrhythmic drugs. Cardiovasc Res 1992;26:1095-1101.

1-227. Arena JP, Kass RS. Enhancement of potassium-sensitive current in heart cells by pinacidil: evidence for modulation of the ATP-sensitive potassium channel. Circ Res 1989;65:436-445.

1-228. Sanguinetti MC, Scott AL, Aingaro GJ, Siegl PKS. BRL 34915 (cromakalim) activates ATP-sensitive K^+ current in cardiac muscle. Proc Natl Acad Sci USA 1988;85:8360-8364.

1-229. Escande D, Thuringer D, Le Guern S, Courteix J, Laville M, Cavero I. Potassium channel openers act through an activation of ATP-sensitive K^+ channels in guinea pig cardiac myocytes. Pflügers Arch 1989;414:669-675.

1-230. Ripoll C, Lederer WJ, Nicols CG. Modulation of ATP-sensitive K^+ channel activity and contractile behaviour in mammalian ventricle by the potassium channel openers cromakalim and RP 49356. J Pharmacol Exp Ther 1990;255:429-435.

1-231. Vassalle M. Electrogenic suppression of automaticity in sheep and dog Purkinje fibres. Circ Res 1970;27:361-377.

1-232. Gadsby DC, Cranefield PF. Effects of electrogenic sodium extrusion on the membrane potential of cardiac Purkinje fibres. In Hoffman BF, Lieberman M, Paes de Carvalho A (eds): Normal and abnormal conduction in the heart. Mt. Kisco, New York, Futura, 1982, pp 225-247.

1-233. Boyett MR, Fedida D. Changes in the electrical activity of dog cardiac Purkinje fibres at high heart rates. J Physiol 1984;339:361-391.

1-234. Cranefield PF, Aronson RS. Cardiac arrhythmias: The role of triggered activity and other mechanisms. Mt. Kisco, New York, Futura, 1988.

1-235. Bean BP. Two kinds of calcium channels in canine atrial cells. J Gen Physiol 1985;385:565-589.

1-236. Kimura J, Miyamae S, Noma A. Identification of sodium-calcium exchange current in single ventricular cells of guinea pig. J Physiol (Lond) 1987;384:199-222.

1-237. Schouten VJA, ter Keurs HEDJ, Quaegebeur JM. Influence of electrogenic Na/Ca exchange on the action potential in human heart muscle. Cardiovasc Res 1990;24:758-767.

1-238. Eisner DA, Lederer WJ. Na-Ca exchange: stoichiometry and electrogenicity. Am J Physiol 1985;248:C189-202.

1-239. Harvey RD, Hume JR. Autonomic regulation of a chloride current in heart. Science 1989;244:983-985.

1-240. Ackerman MJ, Clapham DE. Cardiac chloride channels. Trends Cardiovasc Med 1993;3:23-28.

1-241. Harvey RD, Clark, CD, Hume JR. Chloride current in mammalian cardiac myocytes. J Gen Physiol 1990;95:1077-1102.

1-242. Harvey RD, Hume JR. Histamine activates the chloride current in cardiac ventricular myocytes. J Cardiovasc Electrophysiol 1990;1:309-317.

1-243. Takano M, Noma A. Distribution of the isoprenaline-induced chloride current in rabbit heart. 1992;420:223-226.

1-244. Wolff AA, Levi R. Histamine and cardiac arrhythmias. Circ Res 1986;58:1-16.

1-245. Yamawake N, Hirano Y, Sawanobori T, Hiraoka M. Arrhythmogenic effects of isoproterenol-activated Cl⁻ current in guinea pig ventricular myocytes. J Mol Cell Cardiac 1992;24:1047-1058.

1-246. Maylie J, Morad M: A transient outward current related to calcium release and development of tension in elephant seal atrial fibres. J Physiol (Lond) 1984;357:267-292.

1-247. Siegelbaum SA, Tsien RW, Kass RS. Role of intracellular calcium in the transient outward current of calf Purkinje fibres. Nature (Lond) 1977;269:611-613.

1-248. Tseng GN. Cell swelling increases membrane conductance of canine cardiac cells: evidence for a volume-sensitive Cl channel. Am J Physiol 1992;262:C1056-1068.

1-249. Sorota S. Swelling-induced chloride-sensitive current in canine atrial cells revealed by whole-cell patch-clamp. Circ Res 1992;70:679-687.

1-250. Walsh KB. Activation of a heart chloride current during stimulation of protein kinase C. Mol Pharmacol 1991;40:342-346.

1-251. Matsuura H, Ehara T. Activation of chloride current by purinergic stimulation in guinea pig heart cells. Circ Res 1992;70:851-855.

1-252. Duan D, Fermini B, Nattel S. Sustained outward current observed after I_{to1} inactivation in rabbit atrial myocytes is a novel Cl⁻ current. Am J Physiol 1992;263:H1967-H1971.

1-253. Duan D, Nattel S. Properties of single outwardly rectifying chloride channels in the heart. (submitted to Circ Res).

1-254. Papazian DM, Schwarz TL, Tempel BL, Jan YN, Jan LY. Cloning of genomic and complementary DNA from Shaker, a putative potassium channels gene from Drosophila. Science 1987;237:749-753.

1-255. Pongs O, Kecskemethy N, Muller R. Shaker encodes a family of putative potassium-channel proteins in the nervous system of Drosophila. EMBO J 1988;7:1087-1096.

1-256. Joho RH. Toward a molecular understanding of voltage-gated potassium channels. J Cardiovasc Electrophysiol 1992;3:589-601.

1-257. Roberds SL, Knoth KM, Po S, Blair TA. Bennett PB, Hartshorne RP, Snyders DJ, Tamkun MM. Molecular biology of the voltage-gated potassium channels of the cardiovascular system. J

Cardiovasc Electrophysiol 1993;4:68-80.

1-258. Stumer W, Ruppersberg JP, Schroter KH. Molecular basis of functional diversity of voltage-gated potassium channels in mammalian brain. EMBO J 1989;8:3235-3244.

1-259. Roberds SL, Tamkun MM. Cloning and tissue-specific expression of five voltage-gated potassium channel cDNAs expressed in rat heart. Proc Natl Acad Sci USA 1991;88:1798-1802.

1-260. Roberds SL, Tamkun MM. Developmental expression of cloned cardiac potassium channels. FEBS Lett 1991;284:152-154.

1-261. Tamkun MM, Knoth KM, Walbridge JA, Kroemer H, Roden DM, Glover DM. Molecular cloning and characterization of two voltage-gated K^+ channel cDNAs from human ventricle. FASEB J 1991;5:331-337.

1-262. Christie MJ, Adelman JP, Douglass J. Expression of a cloned rat brain potassium channel in *Xenopus* oocytes, Science 1989;244:221-224.

1-263. Paulmichl M, Nasmith P, Hellmiss R. Cloning and expression of a rat cardiac delayed rectifier potassium channel. Proc Natl Acad Sci USA 1991;88:7892-7895.

1-264. McKinnon D. Isolation of a cDNA clone coding for a putative second potassium channel indicates the existence of a gene family. J Biol Chem 1989;264:8230-8236.

1-265. Tseng-Crank JCL, Tseng GN, Schwartz A. Molecular cloning and functional expression of a potassium channel cDNA isolated from a rat cardiac library. FEBS Lett 1990;268:63-68.

1-266. Takumi T, Ohkubo H, Nakanishi S. Cloning of a membrane protein that induces a slow voltage-gated potassium current. Science 1988;242:1042-1045.

1-267. Folander K, Smith JS, Antanavage J, Bennett C, Stein RB, Swanson R. Cloning and expression of the delayed-rectifier I_{sK} channel from neonatal rat heart and diethylstilbestrol-primed rat uterus. Proc Natl Acad Sci USA 1990;87:2975-2979.

1-268. Forgey R, Giffin K, Huang M, Marino M. Cloning and expression of guinea pig Kv1.5 gene. Biophys J 1992;61:A376.

1-269. Murai T, Kazikuza A, Takumi T, Ohkubo H, Nakanishi S. Molecular cloning and sequence analysis of human genomic DNA encoding a novel membrane protein which exhibits slowly activating potassium channel activity. Biochem Biophys Res Commun 1989;161:176-181.

1-270. Swanson R, Folander K, Bennett C, Antanavage J, Stein RB, Smith JS. Total synthesis, expression and functional assay of a gene encoding a human delayed rectifier potassium channel. Biophys J 1990;57:A211.

1-271. Swanson R, Folander K, Antanavage J, Smith JS. The I_{sK} gene is expressed in human heart. Biophys J 1991;59:A452.

1-272. Krafte DS, Dugrenier N, Dillon K, Volberg WA. Electrophysiological properties of a cloned, human potassium channel expressed in Xenopus oocytes. Biophys J 1992;61:A378.

1-273. Freeman LC, Kass RS. Expression of a minimal K^+ channel protein in mammalian cells and immunolocalization in guinea pig heart. Circ Res 1993;73:968-973.

1-274. Rasmussen HH, Ten Eick RE, McCullough JR, Singer DH. Evidence for electrogenic Na^+ pumping in human atrial myocardium. J Mol Cell Cardiol 1984;16:267-277.

1-275. Rasmussen HH, Singer DH, Ten Eick RE. Characterization of a sodium pump-induced hyperpolarization in isolated human atrium. Am J Physiol 1986;251:H331-339.

1-276. Rasmussen HH, Okita GT, Hartz RS, Ten Eick RE. Inhibition of electrogenic Na^+-pumping in isolated atrial tissue from patients treated with digoxin. J Pharmacol Exp Ther 1990;252:60-64.

1-277. Sako H, Imanishi S, Arita M, Shimada T, Hadama T, Uchida Y. Unaffected electrogenic Na-K pump activity in "diseased" human atrial fibres, as assessed by intracellular K^+ activity. Jpn J Physiol 1989;39:873-890.

1-278. Koumi S, Ten Eick RE, Singer DH, Sakakibara Y, Furukawa T, Eager SL, Arentzen CE, Wasserstrom JA. Inwardly-rectifying K^+ channels in human cardiac myocytes. Circulation 1991;84:I-695.

1-279. Po S, Snyders DJ, Baker R, Tamkun MM, Bennett PB. Functional expression of an inactivating potassium channel cloned from human heart. Circ Res 1992;71:732-736.

1-280. Po S, Roberds S, Snyders DJ, Tamkun MM, Bennett PB. Heteromultimeric assembly of human potassium channels: Molecular basis of a transient outward current? Circ Res 1993;72:1326-1336.

1-281. Snyders DJ, Knoth KM, Roberds SL, Tamkun MM. Time-, voltage-, and state-dependent block by quinidine of a cloned human cardiac potassium channel. J Parmacol Exp Ther 1992;41:322-330.

1-282. Snyders DJ, Tamkun MM, Bennett PB. A rapidly activating and slowly inactivating potassium channel cloned from human heart: Functional analysis after stable mammalian cell culture expression. J Gen Physiol 1993;101:513-543.

1-283. Davies M, Giffin K, Liang CD, Russell MA, Butler A, Salkoff L, Marino M. Verapamil inhibits the human cardiac delayed rectifier (Kv1.5) channel. Biophys J 1992;61:A376.

CHAPTER 2.

FREQUENCY-DEPENDENCE OF REPOLARIZATION AND ARRHYTHMIA

This work originated from question numbers (1) and (2) in Chapter 1, section 5. There could be three possible explanations for the apparent discrepancy between clinical observations about the efficacy of class Ic drugs in AF and basic research on their electrophysiologic characteristics:

(1) Our knowledge about Ic drug action is insufficient;

(2) AF is not a reentrant arrhythmia;

(3) Our understanding of determinants of reentry is incorrect.

We chose to start investigating the first possibility by studying the use-dependent properties of flecainide, a class Ic agent, with microelectrode techniques.

Effects of Flecainide and Quinidine on Human Atrial Action Potentials

Role of Rate-Dependence and Comparison With Guinea Pig, Rabbit, and Dog Tissues

Zhiguo Wang, MSc, L. Conrad Pelletier, MD, Mario Talajic, MD, and Stanley Nattel, MD

Flecainide and other class IC antiarrhythmic drugs are effective in the prevention and termination of atrial fibrillation, but the mechanism of this action is unknown. To gain insights into potential cellular mechanisms, we evaluated the response of human atrial action potentials to equimolar therapeutic concentrations of flecainide and quinidine and compared this response to that of guinea pig, rabbit, and dog atria. Both compounds reduced $\dot{V}_{max}$ more as activation rate increased, but flecainide was more potent than quinidine and had slower kinetics. The rate-dependence of $\dot{V}_{max}$ reduction was similar for all species, but human tissue was more sensitive to the drugs tested. In contrast to changes in $\dot{V}_{max}$, drug-induced alterations in action potential duration showed opposite rate-dependence for the two drugs. Quinidine increased action potential duration to 95% repolarization (APD_{95}) in human atria by 33±7% (mean±SD) at a cycle length of 1,000 msec, but this effect was reduced as cycle length decreased, to 12±4% ($p<0.001$) at a cycle length of 300 msec. Flecainide increased APD_{95} (by 6±3%) much less than quinidine at a cycle length of 1,000 msec, but its effect was increased by faster pacing, to 27±12% at a cycle length of 300 msec and 35±8% ($p<0.001$) at the shortest 1:1 cycle length. The rate-dependent response of APD to drugs was qualitatively similar but quantitatively different among species. Human tissue showed the greatest frequency-dependent drug effects on repolarization, followed by tissue from dogs and rabbits. Guinea pig atria showed the least (and statistically nonsignificant) rate-dependence of drug effect on APD. Drug-induced changes in refractoriness paralleled those in APD. We conclude that: 1) flecainide and quinidine both increase APD in human atrial tissue but with opposite rate-dependence, 2) the effects of flecainide to increase atrial APD and refractoriness are enhanced by the rapid rates typical of atrial fibrillation, and 3) animal tissues may differ importantly from human in both their sensitivity and rate-dependent response to antiarrhythmic drugs. The salutary response of atrial fibrillation to flecainide may be due to enhancement of drug action by the rapid atrial activation rates characteristic of this arrhythmia. (*Circulation* 1990;82:274–283)

Class IC drugs characteristically slow conduction without significantly altering refractory period.[1] Because slow conduction is an important predisposing factor to reentry,[2,3] these properties of IC agents would not be expected to confer beneficial actions against reentrant arrhythmias.

Atrial fibrillation has long been considered a reentrant arrhythmia.[4] The original "multiple wavelet reentry" concept of Moe et al[4] has been confirmed by recent experimental work in both animals[5] and humans.[6] Recently, there has been increasing awareness of the value of class IC drugs in the prevention and termination of atrial fibrillation. Propafenone and flecainide prevent recurrences of paroxysmal atrial fibrillation[7–10]; furthermore, flecainide is effective in cardioverting atrial fibrillation,[11–17] particularly of recent onset.[14–17] The ability of flecainide to stop atrial fibrillation is similar to that of quinidine[16] and greater than that of verapamil.[17] Flecainide reduces the recurrence rate of atrial fibrillation after electrical cardioversion[18] more effectively than disopyramide.[19]

From the Departments of Medicine and Surgery, Montreal Heart Institute, the Departments of Pharmacology and Therapeutics and Medicine, McGill University, and the Departments of Medicine and Surgery, University of Montreal.

Previously published in abstract form as a preliminary report: "Do frequency-dependent effects of flecainide on refractoriness account for its efficacy in atrial fibrillation?" *Circulation* 1989; 80(suppl II):II-137.

Supported by operating grants from the Medical Research Council of Canada, the Quebec Heart Foundation, and the Fonds de Recherche de l'Institut de Cardiologie de Montréal.

Address for correspondence: Stanley Nattel, MD, Montreal Heart Institute, 5000 East, Belanger Street, Montreal, Quebec, H1T 1C8, Canada.

Received December 12, 1989; revision accepted March 6, 1990.

The ability of class IC agents to terminate and prevent atrial fibrillation is difficult to understand in the light of classical determinants of reentry and the typical actions of this class of drugs. Thus, either our concepts of the determinants of reentry are erroneous, or our understanding of the actions of IC agents is inaccurate. Because ideas about reentry are supported by much experimental evidence, we chose to consider in more detail the electrophysiologic actions of class IC compounds. Specifically, we wanted to study in depth the effects of a class IC compound on atrial action potential duration (APD) and refractoriness to assess whether such effects might account for its beneficial actions against atrial fibrillation.

Three variables have not been carefully considered in evaluating IC drug effects on refractoriness: tissue type, species, and heart rate. Most in vitro studies of IC drug action have used ventricular muscle and Purkinje fiber preparations. Very limited data are available regarding IC drug effects on atrial action potentials.[20,21] Because the characteristics of atrial action potentials differ from those of ventricular muscle or Purkinje fibers,[22] ideas based on observations in the latter tissues may not apply to IC effects on atria. Furthermore, it is known that the properties and ionic determinants of APD may differ greatly, even for the same type of tissue, among different animal species.[23–27] To understand the potential mechanisms of IC drug actions on atrial arrhythmias in humans, it is important to know the effects of IC compounds on human atrial tissues, or at least on the tissues of animal atria known to respond similarly to those in humans. Finally, heart rate is known to be an important modulator of drug effects on repolarization.[28–30] It is conceivable that a drug would have little effect on atrial APD and refractoriness at a normal heart rate while substantially increasing these variables at the rapid rates characteristic of atrial fibrillation.

The present experiments were designed to clarify some of these issues. We chose flecainide as the prototype class IC drug for study because it has been the IC agent most extensively evaluated in the treatment of atrial fibrillation.[10–19] Quinidine was chosen as a reference class IA compound because of its widespread and longstanding use in the treatment of atrial fibrillation.[31] We compared the effects of flecainide with those of quinidine on atrial action potentials as a function of activation rate, using tissue from patients undergoing coronary artery bypass surgery, as well as from three animal species (guinea pigs, rabbits, and dogs).

Methods

Preparations

Atrial muscle strips were obtained from guinea pigs, rabbits, dogs, and humans. Adult guinea pigs of either sex weighing about 350 g were killed by decapitation. Their hearts were rapidly removed, washed in cool, oxygenated Tyrode's solution, and the atrial muscle was dissected free. New Zealand rabbits of either sex weighing about 2 kg were anesthetized (sodium pentobarbital, 20 mg/kg i.v.), and their hearts were quickly removed through a subcostal incision. Dog atrial strips were isolated from hearts removed via a right thoracotomy from anesthetized (sodium pentobarbital, 30 mg/kg i.v.) mongrel dogs of either sex weighing 15–20 kg.

Human tissues consisted of small pieces from the apex of the right atrial appendage obtained during coronary artery bypass surgery. The patients (n=12) ranged in age from 45 to 73 (mean, 58) years, and included 11 men and one woman. All patients had normal P waves on electrocardiography, and no patient had a history of supraventricular arrhythmias. No patient had evidence of atrial enlargement or congestive heart failure on chest radiograph, and all but one patient had normal left ventricular function. The patient with abnormal left ventricular function had an ejection fraction of 48% and moderate mitral regurgitation. No other patients had mitral valve disease. The only medications taken by these patients were for the treatment of angina and, in one case, enalapril for hypertension. No patients were taking digitalis or antiarrhythmic drugs. All atrial specimens were grossly normal at the time of excision. Immediately after excision, samples were immersed in oxygenated Tyrode's solution maintained at 10–15° C and brought to the laboratory. The time between excision and the beginning of laboratory processing was about 15 minutes. The dissection procedure was performed in a chamber containing oxygenated Tyrode's solution at room temperature.

Preparations obtained by the above procedures were pinned to the Sylgard-covered bottom of a 20-ml Lucite chamber with the endocardial surface facing upward and were superfused with Tyrode's solution at 8 ml/min. The superfusion solution contained (mM): NaCl 116, $NaHCO_3$ 18, dextrose 10, KCl 4, NaH_2PO_4 0.9, $MgCl_2$ 0.5, and $CaCl_2$ 1. The superfusate was aerated with 95% O_2-5% CO_2, and the bath temperature was maintained at 36° C by a heating element and proportional power supply (Hanna Instruments, Philadelphia, Pennsylvania). One hour was allowed for tissue equilibration before experiments were begun. A total of 17 preparations of guinea pig atrium were studied, compared with 20 for rabbits, 17 for dogs, and 15 obtained from patient samples. Two preparations for study could be obtained from some human atrial samples, allowing us to compare the effects of both drugs in tissues from the same heart.

Microelectrode Techniques

Glass microelectrodes filled with 3 M KCl and with tip resistances of 8–20 MΩ were coupled by a silver–silver chloride junction to a high-impedance microelectrode amplifier (WPI KS-700, World Precision Instruments, New Haven, Connecticut). A bipolar Teflon-coated platinum electrode was used to deliver square-wave pulses of 2-msec duration and

twice late diastolic threshold current to stimulate the preparation. A programmable stimulator and stimulus isolation unit (Bloom Instruments, Flying Hills, Pennsylvania) were used to deliver stimuli with selected stimulation paradigms.

Signals were displayed on a storage oscilloscope (Tektronix 5115, Tektronix Inc., Beaverton, Oregon) and were converted into digital form using a Tekmar 100-kHz A/D converter (Tekmar Co., Cincinnati, Ohio). The differentiated signal was displayed on the oscilloscope, and the maximum amplitude of the signal was transmitted via a peak hold unit into the A/D converter. Custom-made software routines (Bascom Consultants, Montreal, Quebec, Canada) and an IBM PC computer were used to measure action potential characteristics.[28]

Experimental Protocol

Action potential characteristics, including resting potential, action potential amplitude, APD to 50% and 95% repolarization (APD_{50} and APD_{95}, respectively), and maximum rate of voltage rise during phase 0 ($\dot{V}_{max}$), were determined at basic cycle lengths of 1,000, 600, 300, and 150 msec, respectively. In human tissues, 1:1 capture was generally unattainable at a cycle length of 150 msec. The shortest pacing interval attainable averaged 180 msec under control conditions and was increased 34% by flecainide ($p<0.001$) and 24% by quinidine ($p<0.001$). At each cycle length, 5 minutes was allowed for action potential characteristics to reach a steady state before measurements were made. Effective refractory period (ERP) was measured by the extrastimulus technique. A premature stimulus of twice diastolic threshold current was introduced after each train of eight basic beats. Coupling interval was reduced gradually until failure to capture occurred, defining the ERP. Diastolic threshold current was verified at each cycle length, and the stimulus strength was adjusted accordingly. All ERP determinations were performed in duplicate to ensure reproducibility. After measurements were made under control conditions, the test drug was added to the superfusate, and action potential characteristics were monitored over time. The measurements made under control conditions were repeated after 30 minutes of drug superfusion and after 30 minutes of washout. Continuous stable impalement of the same cell under both control and drug conditions was required for all analyzed experiments. In some experiments, when drug effects disappeared completely at washout and the impalement remained stable, the alternative agent was studied in the same preparation. When this was not possible, an attempt was made to study both drugs in tissues from the same animal.

Equimolar concentrations (4.5 μM) of flecainide and quinidine were used in guinea pig, rabbit, and dog, corresponding to 1.8 mg/l flecainide and 1.4 mg/l quinidine. Human tissues were found to be more sensitive to the effects of flecainide than atria from the other species studied, so we reduced the flecainide and quinidine concentrations by 50%, to 2.25 μM, in studies of human atria. The resulting concentrations, 0.9 mg/l of flecainide and 0.7 mg/l of quinidine, are in the therapeutic range of free plasma drug concentration for either compound.[32] Flecainide acetate was obtained from Riker Laboratories, Inc. (St. Paul, Minnesota), and quinidine gluconate was supplied by Rougier-Desbiens, Inc. (Montreal, Canada). Both compounds were dissolved in Tyrode's solution at the molar concentrations noted above, using the formula weight of the salt to calculate the amount of each compound necessary.

Statistical Analysis

Group data are presented as mean±SD. A logarithmic transformation was used for statistical analysis of data that were not normally distributed.[33] The rate-dependence of drug action was evaluated by analysis of variance (ANOVA) with an F test for interaction.[33] Multiple comparisons data were evaluated by ANOVA with Scheffe contrasts.[33] A two-tailed probability of ±5% was taken to indicate statistical significance. Linear regression analysis was performed using the least sum of squares method.[33]

Results

Action Potential Characteristics in Atrial Tissues From Different Species

Representative atrial action potentials recorded from different species under control conditions at a cycle length of 1,000 msec are illustrated in Figure 1, and mean action potential characteristics at the same cycle length are summarized in Table 1. Action potentials of various species differed from each other qualitatively and quantitatively.

Indexes reflecting net phase 0 inward current, such as action potential amplitude, overshoot, and $\dot{V}_{max}$, were smaller in human and rabbit tissues than in guinea pig or dog (Table 1). Initial repolarization was faster in rabbit tissues, as reflected by a short APD_{50}, and in human tissues, causing a consistent "spike and dome morphology" (Figure 1), than in guinea pigs or dogs. Total APD was comparable in rabbits and guinea pigs, was greater in dogs, and was greater still in humans. ERP values generally paralleled those of APD_{95}.

Rate increases did not alter the appearance of canine or guinea pig action potentials but decreased their duration. Rabbit tissues responded to increased rate with the appearance of a distinct plateau, in contrast to the triangular action potentials at a cycle length of 1 second. In human tissue, rapid pacing resulted in a loss of the characteristic spike and dome seen at cycle lengths greater than 500 msec.

Effects of Flecainide and Quinidine on Atrial Action Potential Characteristics

Both drugs significantly increased APD and refractory period while reducing $\dot{V}_{max}$ and action potential amplitude. Drug-induced changes in $\dot{V}_{max}$ were of the

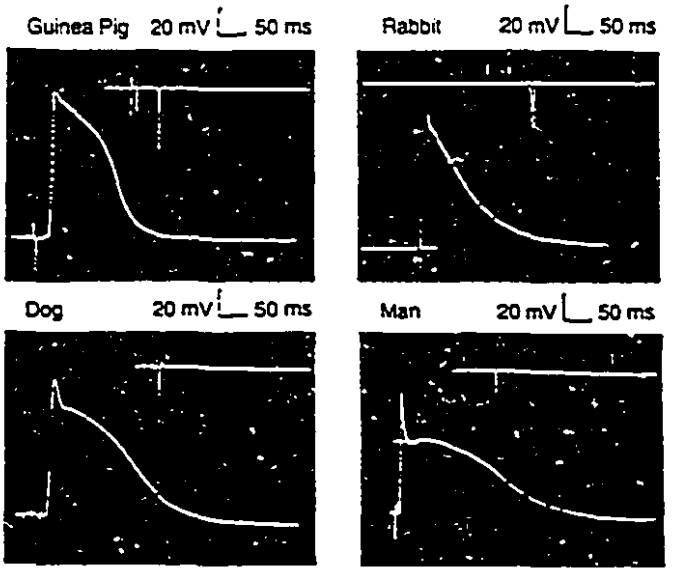

FIGURE 1. *Typical atrial action potentials from the four species studied, at a cycle length of 1,000 msec. Vertical scale represents 20 mV for action potential and 100 V/s for differentiated signal.*

same approximate magnitude in all species tested (Figure 2). Because human tissues were exposed to half the concentration used for other species, however, the sensitivity of human atrium to these compounds was greater than that of the other species tested. The effects of both compounds on $\dot{V}_{max}$ were rate-dependent, with greater depression occurring at shorter cycle lengths.

TABLE 1. Action Potential Characteristics Recorded From Atrial Tissues of Different Species at a Cycle Length of 1,000 msec

	Guinea pig	Rabbit	Dog	Human
RP (mV)	76±4	81±5	76±3	80±3
APA (mV)	113±6	99±9	106±8	98±5
OS (mV)	35±7	20±5	31±4	18±4
APD_{50} (msec)	52±7	20±4	84±10	...§
APD_{95} (msec)	120±13	101±13	205±14	364±59
$\dot{V}_{max}$ (V/sec)	219±35	167±30	206±24	167±26
ERP (msec)	82±7	87±12	180±15	324±59

RP, resting potential; APA, action potential amplitude; OS, overshoot; APD_{50}, APD_{95}, action potential duration to 50% and 95% of repolarization, respectively; $\dot{V}_{max}$, maximum rate of phase 0 voltage rise; ERP, effective refractory period.
Results shown are from 17 preparations for guinea pig, 20 for rabbit, 17 for dog, and 15 for human.
*$p<0.01$, †$p<0.001$, ‡$p<0.0001$ for comparison indicated by analysis of variance with Scheffe's test.
§APD_{50} data not shown for human tissue because action potentials frequently crossed 50% repolarization value twice.

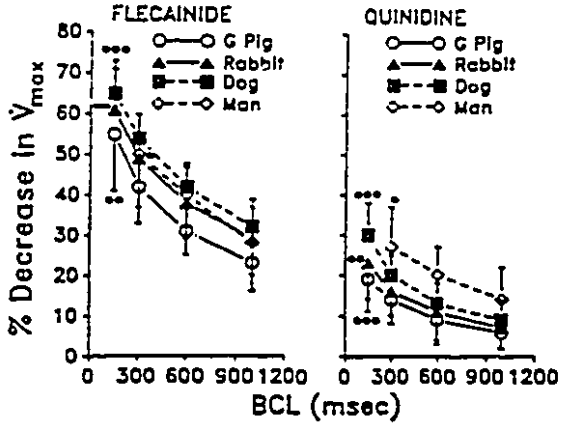

FIGURE 2. *Rate-dependent effects of flecainide and quinidine on $\dot{V}_{max}$ in each species. Changes are shown as percentage decrease relative to corresponding control value in the same cell at the same basic cycle length (BCL). *p<0.05; **p<0.01; ***p<0.001, compared with effect at cycle length of 1,000 msec in the same species.*

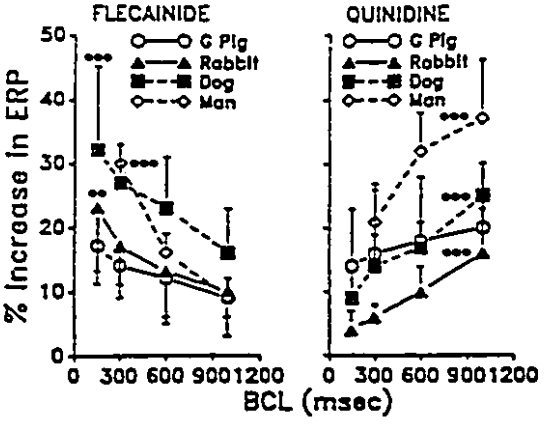

FIGURE 4. *Rate-dependent effects of flecainide and quinidine on effective refractory period (ERP). Values are percentage change from matched control at the same basic cycle length (BCL). **p<0.01; ***p<0.001, compared with effect at the shortest 1:1 cycle length (for quinidine) or 1,000 msec (for flecainide).*

The magnitude and rate-dependence of changes in APD were more variable between species (Figure 3) than those in $\dot{V}_{max}$. Human tissues were the most sensitive to the effects of both compounds. Changes in APD showed significant rate-dependence for both compounds in rabbit, dog, and human atria. No significant rate-dependence was noted for either drug's effect on APD in guinea pigs. There was a striking difference in the direction of rate-dependent effects on APD between compounds. Whereas quinidine's actions were reduced as cycle length decreased, the opposite was true for flecainide: rapid pacing greatly increased the latter's effects on repolarization. These differences were most striking in human tissue. Quinidine increased APD_{95} by 33±7% at a cycle length of 1 second (rate, 60 per minute), a much greater increase than the 6±3% change produced by flecainide at the same rate. On the other hand, at a cycle length of 300 msec (200 per minute), the effect of quinidine was reduced to a 12±4% increase, whereas flecainide increased APD_{95} by 27±12%. These effects were paralleled by changes in ERP (Figure 4). In human tissue, quinidine increased ERP by 37±9% at a rate of 60 per minute compared with an 8±3% increase by flecainide. In contrast, at the fastest pacing rate with 1:1 capture, quinidine increased ERP by 23±4% compared with a 40±6% increase caused by flecainide.

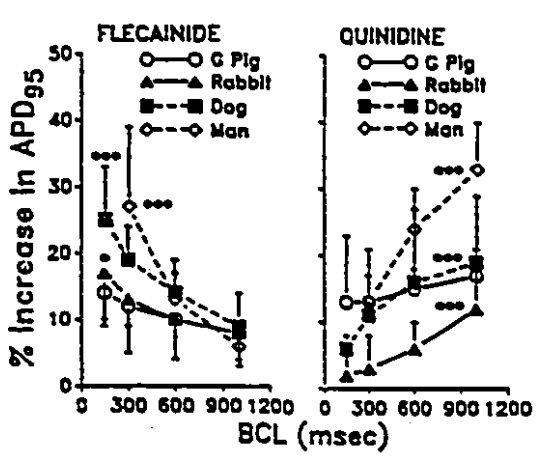

FIGURE 3. *Rate-dependent effects of flecainide and quinidine on action potential duration to 95% repolarization (APD_{95}) in each species. Values shown are percentage change from matched control at the same basic cycle length (BCL) in the same cell. *p<0.05; ***p<0.001, compared with effect at shortest 1:1 cycle length (for quinidine) or 1,000 msec (for flecainide).*

Figure 5 illustrates the effects of both compounds in the same canine preparation. Under control conditions, decreasing the cycle length from 1,000 to 150 msec resulted in substantial shortening of APD. Flecainide attenuated the rate-dependent APD shortening, resulting in a maximal drug-induced APD increase at the shortest cycle length. In the presence of quinidine, however, APD accommodation to changes in frequency was enhanced. This led to maximum changes at long pacing cycle lengths, with effects attenuated by rapid pacing. Drug-induced changes in APD accommodation were even more pronounced in human tissues. Figure 6 shows typical effects of flecainide (top) and quinidine (bottom) in a representative human atrial preparation for each. Under control conditions, decreases in cycle length produce substantial APD reductions (note that the time base is twice as slow as for dog tissue in Figure 5). Flecainide virtually eliminated APD accommodation to rate change in this and all other human atrial preparations, whereas quinidine consistently increased the amount of APD change in response to APD alteration.

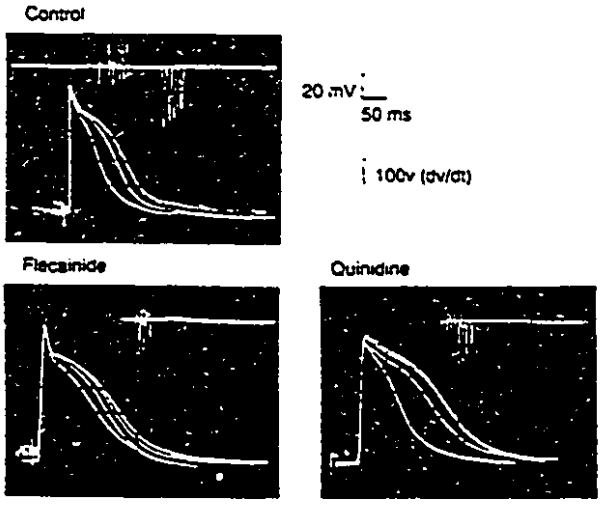

FIGURE 5. *Effects of flecainide and quinidine on action potential characteristics of representative canine atrial preparation. Action potential duration (APD) and $\dot{V}_{max}$ decreased as basic cycle length was reduced from 1,000 to 600, 300, and 150 msec under control conditions* (top left), *and in the presence of flecainide* (bottom left) *and quinidine* (bottom right). *The degree of APD change with changing rate was reduced by flecainide and increased by quinidine. Continuous impalement of the same cell was maintained under control conditions, superfusion of flecainide, washout back to control, and superfusion with quinidine. Vertical scale represents 20 mV for action potential and 100 V/s for differentiated signal.*

Quantitative Analysis of Rate-Dependent Effects of Flecainide and Quinidine

To quantify the rate-dependence of drug effects on $\dot{V}_{max}$ in different species, we used an approach developed theoretically by Starmer.[34] When the inverse of drug-induced blockade (reflected by changes in $\dot{V}_{max}$) is plotted against basic cycle length, a linear relation should result, with a slope proportional to the rate constant of drug action.[34] Figure 7 shows representative results from one experiment in each species with each compound. As predicted, the relations were linear in all experiments. The slopes for each compound were similar across the various species studied, but the slopes for flecainide were consistently less than those for quinidine. Table 2 shows mean rate constants as determined by this approach. There were no significant differences in rate constants for a given drug among different species, but the rate constant for flecainide was consistently less than that for quinidine.

Rate-dependent effects on APD were also analyzed quantitatively. Drug-induced increases in APD were plotted as a function of cycle length in each experiment, and the slope of the resulting relation was calculated. Whereas the absolute value of slopes

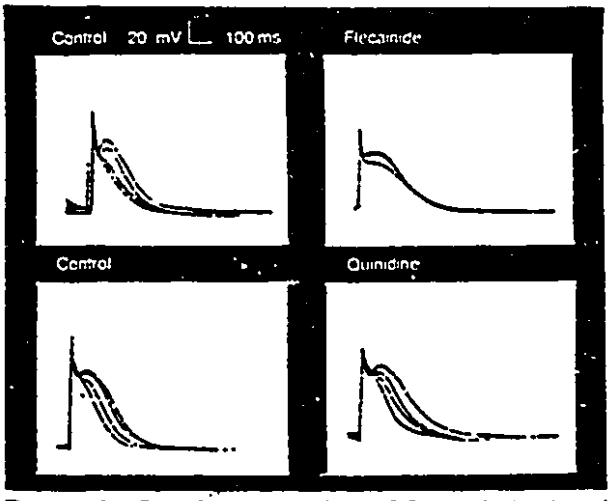

FIGURE 6. *Rate-dependent effects of flecainide* (top) *and quinidine* (bottom) *on action potentials from one representative human atrial preparation for each. Under control condition* (left), *decreasing cycle length from 1,000 to 600, 300, and 220 msec progressively reduced action potential duration (APD). Flecainide* (top) *virtually eliminated APD adaptation to rate change, whereas quinidine* (bottom) *increased APD alteration resulting from rate change.*

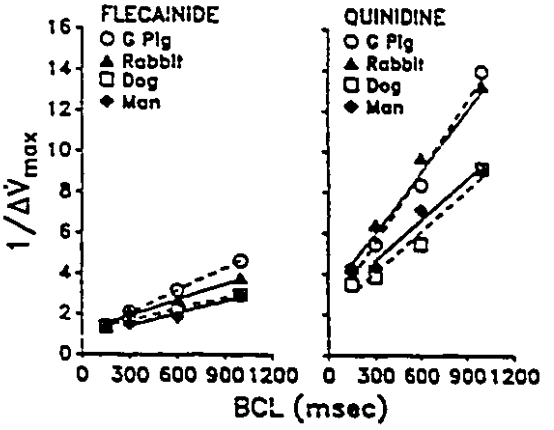

FIGURE 7. *Method used to characterize the kinetics of drug-induced $\dot{V}_{max}$ blockade. According to Starmer,[34] the rate constant for block should be proportional to the slope of a plot of the inverse of blockade at each cycle length versus the basic cycle length (BCL). We therefore plotted the inverse of drug-induced changes in $\dot{V}_{max}$ (calculated as change from control divided by control value) at each BCL vs. BCL in each experiment. The data fell along a straight line, as predicted by Starmer. Slopes of resulting lines were steeper for quinidine than for flecainide, indicating a greater rate constant, and were not significantly affected by species.*

TABLE 2. **Frequency-Dependent Effects of Flecainide and Quinidine: Dependence of $\dot{V}_{max}$ Changes on Cycle Length**

	Rate constant*			
	Guinea pig	Rabbit	Dog	Human
Flecainide	3.6±0.9	2.6±1.7	1.9±0.4	1.9±0.6
Quinidine	16.2±8.2†	10.1±8.4	7.1±3.1‡	7.6±2.9‡

*Rate constant shown is the slope of data plotted as shown in Figure 7, and is proportional to the rate constant for sodium channel blockade.

†$p<0.01$; ‡$p<0.05$ for differences between flecainide and quinidine.

TABLE 3. Frequency-Dependent Effects of Flecainide and Quinidine: Dependence of APD$_{90}$ Changes on Cycle Length

	Slope factor (%/sec)			
	Guinea pig	Rabbit	Dog	Human
Flecainide	−13.2±4.7‡	−15.3±3‡	−20.3±6.4	−23.5±9.0
Quinidine	6.9±19.6*‡	15.6±5.1†‡	15.1±2.9†‡	27.4±4.1†

*$p<0.05$; †$p<0.001$ for difference between flecainide and quinidine; ‡$p<0.05$ compared with slope in human atrium.

were similar for quinidine compared with flecainide, slopes for quinidine were consistently positive (indicating increasing effect with increasing cycle length) and those for flecainide were negative. Consequently, the slopes of APD change were significantly different between drugs in all species (Table 3). The rate-dependence of APD change was greatest in human tissues. The slope of APD change versus cycle length was significantly larger in human atria than in guinea pig and rabbit tissues for flecainide, and greater than in all other species for quinidine.

Discussion

The efficacy of class IC drugs in treating atrial fibrillation is clear, and yet the mechanism of this action has been unexplained. Our results suggest that consideration of the role of atrial activation rate and species-dependent differences in drug response may be important in understanding IC effects in atrial fibrillation.

Role of Rate-Dependent Drug Actions

Both flecainide and quinidine reduced $\dot{V}_{max}$ in a frequency-dependent way. The kinetic rate constant for quinidine was approximately four times as large as that for flecainide, a relation similar to that provided by direct measurements in the literature.[35] There were no significant differences in rate constants for a given drug among species. On the other hand, quinidine and flecainide effects on APD showed opposite rate-dependence, and the rate-dependence of drug action in human tissues was significantly more than in other species. The effects of flecainide on ERP were similarly rate-related. Whereas it would be fair to say that, as is commonly assumed, flecainide has little effect on atrial refractoriness at rates similar to resting sinus rhythm in humans, rapid rates greatly enhance flecainide-induced ERP prolongations. At rates comparable to that of the fibrillating atrium, flecainide had a substantially greater effect on atrial ERP than did quinidine. Moe et al[4] pointed out the critical importance of atrial refractoriness in controlling the occurrence of fibrillation in their computer model. More recently, Feld et al[36,37] have established the importance of changes in atrial refractoriness in determining drug effects in an experimental model of atrial flutter. These results imply that rate-dependent increases in ERP may play a central role in the atrial antifibrillatory actions of flecainide.

Species Specificity of Response

Consistent differences were seen in control atrial action potentials among the species studied. The rapid phase 1 repolarization typical of human and rabbit atria is consistent with the large transient outward current present in these tissues.[24,38–40] The transient outward current activates and inactivates rapidly and then recovers from inactivation with a slower time course.[24,26,38,39] This may result in a "spike and dome" morphology,[26] as we consistently observed in human atria. The rapid activation of this outward current may explain the smaller values for action potential amplitude, $\dot{V}_{max}$, and overshoot in human and rabbit atrial action potentials compared with those from dog.

There have been few comparative studies of the drug response of tissues from various animal species. Our results show that, at least for atrial tissues, there are important species differences in the response to antiarrhythmic drugs. We had to use twice the concentration of flecainide and quinidine in guinea pigs, rabbits, and dogs compared with humans to achieve a pharmacologic response in a similar range. Even at a smaller dose, the effect of quinidine was greater in human tissues than for the other species studied. These results are consistent with previous observations[41–43] of a requirement for larger plasma drug concentrations in dogs to achieve electrophysiologic effects comparable to those of therapeutic concentrations in humans. Furthermore, the rate-dependence of drug-induced repolarization changes also varied among species. The response of guinea pig atrial APD to quinidine and flecainide showed the least rate-dependence, whereas that of human tissue showed the most sensitivity to activation rate. Although the overall pattern of rate-dependent action was similar for all species, its magnitude was not.

Our results bear on both the value and limitations of the pharmacologic response of animal tissues as an indicator of drug effects in humans. Although the responses were qualitatively similar in different species, quantitative differences in sensitivity and in the magnitude of rate-dependence make extrapolation to humans uncertain. The responses of canine atria were most similar to those of humans, and the responses of guinea pig tissues, the least similar, but certainly none were identical.

Mechanisms of Rate- and Species-Dependent Action

Rate-dependent drug effects on $\dot{V}_{max}$ are caused by preferential drug binding to sodium channels in the open or inactivated state, followed by time-dependent unbinding after repolarization.[44,45] We found that the rate-dependence of $\dot{V}_{max}$ blockade by flecainide and quinidine was not substantially affected by species. Previous kinetic studies of $\dot{V}_{max}$ depression by lidocaine in guinea pig papillary muscles[46–49] and canine[50,51] and sheep Purkinje fibers[52] have shown similar time constants. No species dependence of the kinetics of sodium channel

blockade has been found for other drugs tested. Although the kinetics of drug action on $\dot{V}_{max}$ seemed to be species-independent, the magnitude of depression of $\dot{V}_{max}$ differed among the species tested. Human tissue was the most sensitive, with canine intermediate, and rabbit and guinea pig the least sensitive. These differences in sensitivity may have been partially due to differences in APD, which is longest in humans, intermediate in dogs, and shortest in rabbits and guinea pigs. Inactivated state block occurs predominantly during the plateau and is therefore enhanced by longer action potentials.

A variety of mechanisms may play a role in rate-dependent drug effects on APD. The kinetics of activation and inactivation of target plateau currents may be very important. For example, the transient outward current is a major repolarizing current in rabbit[24] and human[38–40] atrial tissue, and is inactivated at rapid rates. Quinidine blocks transient outward current,[24] and this effect would be expected to be most important when the current is large (i.e., slow rates) and least important when the current is small (fast rates). This property would result in APD prolongation by quinidine predominantly at slow rates, as we observed. Flecainide would have to block a current with different kinetics to explain its enhanced action on APD at rapid rates. Alternatively, rate-related drug effects on APD could be due to state-dependent interactions of antiarrhythmic drugs with potassium channels. Roden et al[26] have proposed that quinidine promotes occupancy of a closed state of the delayed rectifier, perhaps by associating preferentially with closed channels. Bradycardia-dependent APD prolongation by quinidine would result from a longer closed-state cycle, whereas tachycardia-dependent APD prolongation (of the type we showed for flecainide) would result from preferential binding to the open state. Definitive identification of the mechanisms underlying rate-dependent APD changes awaits detailed voltage-clamp studies of drug effects on atrial plateau currents.

Relation to Previous Studies in the Literature

The resting potential of our human atrial samples (mean, −80 mV) was in the same range as values obtained by Gelband et al[53] (−86 mV) and Mary-Rabine et al[54] (−78 mV) in normal atrial tissues. Lower values are observed in patients with diseased atria.[54–56] The morphology of our human atrial action potentials had a prominent spike and dome, like the cells termed "atrial specialized fibers" by Gelband et al.[53] Many previous reports of human atrial action potentials are from studies using tissue samples from a pediatric population,[53–55] in which two forms of atrial action potential are seen. The action potential morphology of our human atrial tissues was similar to the morphology uniformly observed in adult atrial fibers by Escande et al,[38,39] who found that the development of the adult action potential morphology coincided with the appearance of a large transient outward current.

Quinidine has been shown to increase APD in guinea pig,[57] rabbit,[24] and canine[58] atrial tissues. We are not aware of in vitro studies of the actions of quinidine on human atrial tissue. West and Amory[58] found, as we did, that increased driving rate reduces the effects of quinidine on canine atrial APD.

Ikeda et al[20] reported that 1 mg/l flecainide increased APD_{90} in rabbit atria by 12.8% at an unspecified frequency. This value is similar to the changes we observed at cycle lengths between 300 and 1,000 msec. Le Grand et al[21] have reported preliminary findings of flecainide-induced increases in human atrial refractoriness in vitro that are enhanced by increased driving rate. They noted rate-dependent increases in APD_{50} but not in APD_{90}. This apparent discrepancy with our findings is difficult to assess because their results are reported only in abstract form. The only other observation of class IC drug effects on atrial tissue that we could find was a study showing that encainide increases atrial monophasic APD in dogs.[59] The role of heart rate as a potential modulator of drug action was not examined.

Potential Limitations

Any study evaluating tissue obtained from patients with heart disease must consider the possibility of abnormalities in the tissue samples. We excluded patients with a history of atrial arrhythmias or electrocardiographic evidence of atrial disease, and all tissue samples appeared grossly normal. The baseline values of atrial ERP that we measured using human tissues in vitro (ERP of 276±38 msec at a cycle length of 600 msec) are in the same range as values previously reported during electrophysiologic study.[60,61]

Significance of These Findings

These findings have implications both for the specific actions of class IC drugs on atrial tissues and for the general approach to understanding the clinical effects of antiarrhythmic drugs. Microelectrode studies of antiarrhythmic drug action on tissues isolated from experimental animals have provided many potential insights into the mechanisms of clinical drug action. On the other hand, we have found that there are important differences between the response of atrial tissues from various animal species. Human tissues appear to be more sensitive to the effects of quinidine and flecainide, a finding compatible with previous in vivo and in vitro observations with other compounds.[41–43] Although the rate-dependence of V_{max} depression was not species-dependent, the dependence of repolarization changes on frequency varied widely among the species studied. Had our experiments been conducted only on guinea pig atria, we would have concluded that quinidine- and flecainide-induced changes in atrial APD are not rate-dependent, a conclusion that would not apply to other species. Extrapolation from observations in other species to humans must therefore be very considered and requires confirmation either by direct observations in isolated human tissue

samples or by evaluation of electrophysiologic properties in the clinical electrophysiology laboratory.

These findings may be relevant for understanding the beneficial actions of flecainide in the treatment of atrial fibrillation. Furthermore, they indicate a potentially desirable antiarrhythmic drug property meriting further investigation. Drugs that increase ERP without altering conduction are the ideal agents with which to treat reentrant arrhythmias. Whereas class III agents have such properties, their use is complicated by the possible occurrence of the acquired long QT syndrome.[62] The potentially lethal ventricular tachyarrhythmias that result are thought to be a consequence of early afterdepolarizations attendant on marked action potential prolongation at slow heart rates.[62] If drugs could be developed that delayed repolarization and prolonged refractoriness selectively at the rapid rates characteristic of clinical tachyarrhythmias, they could prevent the latter without the potential for causing a long QT syndrome. Flecainide appears to have such an action on repolarization, at least on atrial tissues, but its conduction-slowing properties limit its efficacy for reentrant arrhythmias. If other compounds could be developed that preferentially increase refractoriness at rapid rates without altering conduction, a clinically important advance might result.

Acknowledgments

The authors thank Léna Dumais and Lise de Repentigny for typing the manuscript, Nancy Turmel for excellent technical assistance, and the operating room staff of the Montreal Heart Institute for their cooperation in handling human atrial tissue samples. We also thank Riker Canada, Inc., London, Ontario and Rougier-Desbiens, Inc., Montreal, Quebec for providing the drug supplies for our studies.

References

1. Vaughan Williams EM: A classification of antiarrhythmic actions reassessed after a decade of new drugs. *J Clin Pharmacol* 1984;24:129–147
2. Zipes DP: Genesis of cardiac arrhythmias. In Braunwald E (ed): *Heart Disease*, ed 3. Philadelphia, WB Saunders Co, 1988, pp 581–620
3. Bigger JT, Hoffman BF: Antiarrhythmic drugs. In Gilman AG, Goodman LL, Rall TW, Murad F (eds): *The Pharmacological Basis of Therapeutics*, ed 7. New York, Macmillan Publishing Co., 1985, pp 748–783
4. Moe GK, Rheinboldt WC, Abildskov JA: A computer model of atrial fibrillation. *Am Heart J* 1964;67:200–220
5. Allessie MA, Lammers WJEP, Bonke FIM, Hollen J: Experimental evaluation of Moe's multiple wavelet hypothesis of atrial fibrillation. In Zipes DP, Jalife J (eds): *Cardiac Electrophysiology and Arrhythmias*. New York, Grune & Stratton, Inc, 1985, pp 265–276
6. Chen PS, Smith WM, Greer S, Wharton JM, Vidaillet HJ Jr, Ideker RE: Activation patterns during electrically induced atrial fibrillation in humans (abstract). *Circulation* 1986; 74(suppl II):II-483
7. Antman EM, Beamer AD, Cantillon C, McGowan N, Friedman PL: Propafenone for suppression of refractory symptomatic atrial fibrillation (abstract). *Circulation* 1987;76(suppl IV):IV-68
8. Hammill S, Wood D, Sugrue D, Gersh B, Osborn M, Holmes D: Propafenone for chronic treatment of paroxysmal atrial fibrillation (abstract). *Circulation* 1985;72(suppl III):III-171
9. Kerr CR, Mason MA, Chung DC: Propafenone: An effective drug for prevention of recurrent atrial fibrillation (abstract). *Circulation* 1985;72(suppl III):III-171
10. Chouty F, Coumel P: Oral flecainide for prophylaxis of paroxysmal atrial fibrillation. *Am J Cardiol* 1988;62:35D–37D
11. Kappenberger LJ, Fromer MA, Shenasa M, Gloor HO: Evaluation of flecainide acetate in rapid atrial fibrillation complicating Wolff-Parkinson-White syndrome. *Clin Cardiol* 1985; 8:321–326
12. Goy JJ, Maendly R, Grbic M, Finci L, Sigwart U: Cardioversion with flecainide in patients with atrial fibrillation of recent onset. *Eur J Clin Pharmacol* 1985;27:737–738
13. Berns E, Rinkenberger RL, Jeang MK, Dougherty AH, Jenkins M, Naccarelli GV: Efficacy and safety of flecainide acetate for atrial tachycardia or fibrillation. *Am J Cardiol* 1987;59:1337–1341
14. Crijns HJGM, van Wijk LM, van Gilst WH, Kingma JH, van Gelder IC, Lie KI: Acute conversion of atrial fibrillation to sinus rhythm: Clinical efficacy of flecainide acetate. Comparison of two regimens. *Eur Heart J* 1988;9:634–638
15. Goy JJ, Kaufmann U, Kappenberger L, Sigwart U: Restoration of sinus rhythm with flecainide in patients with atrial fibrillation. *Am J Cardiol* 1988;62:38D–40D
16. Borgeat A, Goy JJ, Maendly R, Kaufmann U, Grbic M, Sigwart U: Flecainide versus quinidine for conversion of atrial fibrillation to sinus rhythm. *Am J Cardiol* 1986;58:496–498
17. Suttorp MJ, Kingma JH, Lie-A-Huen L, Mast EG: Intravenous flecainide versus verapamil for acute conversion of paroxysmal atrial fibrillation or flutter to sinus rhythm. *Am J Cardiol* 1989;63:693–696
18. van Gelder I, Crijns HJ, van Gilst WH, Lie KI: Efficacy of flecainide to maintain sinus rhythm after cardioversion of chronic atrial fibrillation and flutter (abstract). *Circulation* 1988;78(suppl II):II-626
19. Rasmussen K, Andersen A, Abrahamsen AM, Overskeid K, Bathen J: Flecainide versus disopyramide in maintaining sinus rhythm following conversion of chronic atrial fibrillation (abstract). *Eur Heart J* 1988;9(suppl I):I-52
20. Ikeda N, Singh BN, Davis LD, Hauswirth O: Effects of flecainide on the electrophysiologic properties of isolated canine and rabbit myocardial fibers. *J Am Coll Cardiol* 1985; 5:303–310
21. Le Grand B, Le Heuzey JY, Périer P, Lavergne T, Chauvaud S, Péronneau P, Guize L: Effects of flecainide on action potential duration of human atrial fibers (abstract). *J Am Coll Cardiol* 1989;13:140A
22. Boyett MR, Jewell BR: Analysis of the effects of changes in rate and rhythm upon electrical activity in the heart. *Prog Biophys Mol Biol* 1980;36:1–52
23. Carmeliet E: Repolarisation and frequency in cardiac cells. *J Physiol* (Paris) 1977;73:903–923
24. Imaizumi Y, Giles WR: Quinidine-induced inhibition of transient outward current in cardiac muscle. *Am J Physiol* 1987; 253:H704–H708
25. Salata JJ, Wasserstrom JA: Effects of quinidine on action potentials and ionic currents in isolated canine ventricular myocytes. *Circ Res* 1988;62:324–337
26. Roden DM, Bennett PB, Snyders DJ, Balser JR, Hondeghem LM: Quinidine delays I_x activation in guinea pig ventricular myocytes. *Circ Res* 1988;62:1055–1058
27. Litovsky SH, Antzelevitch C: Transient outward current prominent in canine ventricular epicardium but not endocardium. *Circ Res* 1988;62:116–126
28. Nattel S, Zeng FD: Frequency-dependent effects of antiarrhythmic drugs on action potential duration and refractoriness of canine cardiac Purkinje fibers. *J Pharmacol Exp Ther* 1984;229:283–291
29. Varro A, Nakaya Y, Elharrar V, Surawicz B: Effect of antiarrhythmic drugs on the cycle length-dependent action potential duration in dog Purkinje and ventricular muscle fibers. *J Cardiovasc Pharmacol* 1986;8:178–185

30. Roden DM, Hoffman BF: Action potential prolongation and induction of abnormal automaticity by low quinidine concentrations in canine Purkinje fibers. *Circ Res* 1985;56:857–867
31. Lewis T: The value of quinidine in cases of auricular fibrillation and methods of studying the clinical reaction. *Am J Med Sci* 1922;163:781–794
32. Gettes LS, Foster JR, Simpson RJ: Clinical use of antiarrhythmic drugs, in Rosen MR, Hoffman RF (eds): *Cardiac Therapy*. New York, Martinus Nijhoff Publishers, 1983, pp 235–298
33. Sachs L: *Applied Statistics*. New York, Springer-Verlag New York, Inc, 1984
34. Starmer CF: Theoretical characterization of ion channel blockade: Ligand binding to periodically accessible receptors. *J Theor Biol* 1986;119:235–249
35. Campbell TJ: Kinetics of onset of rate-dependent effects of Class I antiarrhythmic drugs are important in determining their effects on refractoriness in guinea-pig ventricle, and provide a theoretical basis for their subclassification. *Cardiovasc Res* 1983;17:344–352
36. Feld GK, Venkatesh N, Singh BN: Pharmacologic conversion and suppression of experimental canine atrial flutter: Differing effects of d-sotalol, quinidine, and lidocaine and significance of changes in refractoriness and conduction. *Circulation* 1986; 74:197–204
37. Feld GK, Venkatesh N, Singh BN: Effects of N-acetylprocainamide and recainam in the pharmacologic conversion and suppression of experimental canine atrial flutter: Significance of changes in refractoriness and conduction. *J Cardiovasc Pharmacol* 1988;11:573–580
38. Escande D, Loisance D, Planche C, Coraboeuf E: Age-related changes of action potential plateau shape in isolated human atrial fibers. *Am J Physiol* 1985;249:H843–H850
39. Escande D, Coulombe A, Faivre J, Deroubaix E, Coraboeuf E: Two types of transient outward currents in adult human atrial cells. *Am J Physiol* 1987;252:H142–H148
40. Shibata EF, Refsum H, Aldrete V, Ilnicki T, Giles W: A transient outward current in single cells from human atrial muscle (abstract). *Circulation* 1986;74(suppl II):II-254
41. Nattel S, Keable H, Sasyniuk BI: Experimental amitriptyline intoxication: Electrophysiologic manifestations and management. *J Cardiovasc Pharmacol* 1984;6:83–89
42. Nattel S, Feder-Elituv R, Matthews C, Nayebpour M, Talajic M: Concentration dependence of class III and beta-adrenergic blocking effects of sotalol in anesthetized dogs. *J Am Coll Cardiol* 1989;13:1190–1194
43. Nattel S, Jing W: Rate-dependent changes in intraventricular conduction produced by procainamide in anesthetized dogs: A quantitative analysis based on the relation between phase 0 inward current and conduction velocity. *Circ Res* 1989; 65:1485–1498
44. Hondeghem LM, Katzung BG: Antiarrhythmic agents: The modulated receptor mechanism of action of sodium and calcium channel-blocking drugs. *Annu Rev Pharmacol Toxicol* 1984;24:387–423
45. Starmer CF, Grant AO, Strauss HC: Mechanisms of use-dependent block of sodium channels in excitable membranes by local anesthetics. *Biophys J* 1984;46:15–27
46. Chen CM, Gettes LS, Katzung BG: Effect of lidocaine and quinidine on steady-state characteristics and recovery kinetics of $(dV/dt)_{max}$ in guinea pig ventricular myocardium. *Circ Res* 1975;37:20–29
47. Grant AO, Strauss LJ, Wallace AG, Strauss HC: The influence of pH on the electrophysiological effects of lidocaine in guinea pig ventricular myocardium. *Circ Res* 1980;47:542–550
48. Oshita S, Sada H, Kojima M, Ban T: Effects of tocainide and lidocaine on the transmembrane action potentials as related to external potassium and calcium concentrations in guinea-pig papillary muscles. *Naunyn Schmiedebergs Arch Pharmacol* 1980;314:67–82
49. Courtney KR: Interval-dependent effects of small antiarrhythmic drugs on excitability of guinea-pig myocardium. *J Mol Cell Cardiol* 1980;12:1273–1286
50. Varro A, Elharrar V, Surawicz B: Frequency-dependent effects of several Class I antiarrhythmic drugs on $\dot{V}_{max}$ of action potential upstroke in canine cardiac Purkinje fibers. *J Cardiovasc Pharmacol* 1985;7:482–492
51. Nattel S: Relationship between use-dependent effects of antiarrhythmic drugs on conduction and $\dot{V}_{max}$ in canine cardiac Purkinje fibers. *J Pharmacol Exp Ther* 1987;241:282–288
52. Weld FM, Bigger JT Jr: Effect of lidocaine on the early inward transient current in sheep cardiac Purkinje fibers. *Circ Res* 1975;37:630–639
53. Gelband H, Bush HL, Rosen MR, Myerburg RJ, Hoffman BF: Electrophysiologic properties of isolated preparations of human atrial myocardium. *Circ Res* 1972;30:293–300
54. Mary-Rabine L, Albert A, Pham TD, Hordof A, Fenoglio JJ Jr, Malm JR, Rosen MR: The relationship of human atrial cellular electrophysiology to clinical function and ultrastructure. *Circ Res* 1983;52:188–199
55. Hordof AJ, Edie R, Malm JR, Hoffman BF, Rosen MR: Electrophysiologic properties and response to pharmacologic agents of fibers from diseased human atria. *Circulation* 1976; 54:774–779
56. Ten Eick RE, Singer DH: Electrophysiological properties of diseased human atrium. *Circ Res* 1979;44:545–557
57. Nawrath H: Action potential, membrane currents and force of contraction in mammalian heart muscle fibers treated with quinidine. *J Pharmacol Exp Ther* 1981;216:176–182
58. West TC, Amory DW: Single fiber recording of the effects of quinidine at atrial and pacemaker sites in the isolated right atrium of the rabbit. *J Pharmacol Exp Ther* 1960;130:183–193
59. Samuelsson RG, Harrison DC: Electrophysiologic evaluation of encainide with use of monophasic action potential recording. *Am J Cardiol* 1981;48:871–876
60. Anderson JL, Lutz JR, Allison SB: Electrophysiologic and antiarrhythmic effects of oral flecainide in patients with inducible ventricular tachycardia. *J Am Coll Cardiol* 1983;2:105–114
61. Webb CR, Morganroth J, Senior S, Spielman SR, Greenspan AM, Horowitz LN: Flecainide: Steady state electrophysiologic effects in patients with remote myocardial infarction and inducible sustained ventricular arrhythmia. *J Am Coll Cardiol* 1986;8:214–220
62. Jackman WM, Friday KJ, Anderson JL, Aliot EM, Clark M, Lazzara R: The long QT syndromes: A critical review, new clinical observations and a unifying hypothesis. *Prog Cardiovasc Dis* 1988;31:115–172

KEY WORDS • atrial fibrillation • antiarrhythmic drugs • action potential duration • refractory period • arrhythmias

This study confirmed our hypothesis that our knowledge about class Ic drug action is insufficient. Our results demonstrated that while its effects were minimal at slow rates, just as commonly believed, flecainide produced significant delays in repolarization at rapid activation rates. This finding of use-dependent APD (thereby ERP) prolongation is opposite to the reverse use-dependent action commonly seen with most class III drugs and some class Ia agents. The same year that we proposed the possible role of this use-dependent property in treating arrhythmias, Hondeghem and Snyders[2-1] suggested, in a "Point of View" article, the potential importance of use-dependency and the potential limitations of reverse use-dependent drug action. To test the potential significance of use-dependent repolarization delays in the treatment of arrhythmias and to examine whether our understanding of the determinants of AF is correct, we decided to investigate the efficacy and mechanism of action of flecainide in a dog model of AF by using atrial epicardial activation mapping.

Another finding in this study was that there exist qualitative or quantitative differences in the rate dependence of repolarization rate and action potential morphology among various species. Use-dependent APD shortening was observed in atrial tissues from guinea pig, dog, and man, with the most pronounced repolarization acceleration found in man. In rabbit atrium, the direction of use-dependent change was opposite that in other species: showing prolongation when stimulation frequency was increased from 1 to 3 Hz. Flecainide produced a similar pattern of use-dependent APD change in all species, but the magnitude of this use-dependent APD prolongation was greatest in human tissue. Table 1 summarizes the use-dependence of repolarization expressed as the difference of APD_{95} between the values obtained at a cycle length of 1,000 msec and those measured at 150 msec in the absence of drug, and as the difference of percent APD_{95} prolongation at cycle lengths of 1,000 msec and 150 msec in the presence of drug in various species.

Table 1. Comparison of use-dependent changes of APD_{95} in atrial tissues from various species

	MUDAS (without drug, msec)	MUDAL (with drug, %)
Man	216±29	29±3
Dog	102±4	24±3
Rabbit	12±3	9±2
Guinea Pig	44±5	6±2

MUDAS--magnitude of use-dependent APD shortening=$APD_{95BCL\ 1,000\ msec}$-$APD_{95BCL\ 150\ msec}$;
MUDAL--magnitude of use-dependent APD lengthening=% APD_{95} increase by drug over control at bcl 150 msec-% APD_{95} increase by drug at BCL 1,000 msec;

Reference

2-1. Hondeghem LM, Snyders DJ: Class III antiarrhythmic agents have a lot of potential but a long way to go: Reduced effectiveness and dangers of reverse use dependence. Circulation 1990;81:686-690.

Mechanism of Flecainide's Antiarrhythmic Action in Experimental Atrial Fibrillation

Zhiguo Wang, Pierre Pagé, and Stanley Nattel

Class Ic antiarrhythmic drugs are effective in the treatment of atrial fibrillation, but their mechanism of action is unknown. In previous work, we have found that flecainide causes tachycardia-dependent increases in atrial action potential duration (APD) and effective refractory period (ERP) by reducing APD accommodation to heart rate. The present study was designed to evaluate the efficacy and mechanisms of action of flecainide in an experimental model of sustained atrial fibrillation (AF). AF was produced by a brief burst of atrial pacing in the presence of vagal stimulation and persisted spontaneously until vagal stimulation was stopped. The actions of flecainide at two dose levels were compared with those of isotonic glucose placebo in each dog, with a randomized order of blinded drug administration. Flecainide terminated AF in all 16 dogs, while glucose was effective in none ($p<0.0001$). Flecainide increased atrial ERP and reduced conduction velocity in a tachycardia-dependent manner. Doses of flecainide that converted AF resulted in larger changes in ERP than in conduction velocity, increasing the minimum pathlength capable of supporting reentry (wavelength). In addition, flecainide reduced regional heterogeneity in ERP and wavelength, an action opposite that of vagal stimulation. Atrial epicardial mapping with a 112-electrode atrial array was used to study the mechanism of flecainide action on AF. Under control conditions, multiple small zones of reentry coexisted. Flecainide progressively increased the size of reentry circuits, decreased their number, and slowed the frequency of atrial activation until the arrhythmia finally terminated; all changes were compatible with an increase in wavelength. We conclude that flecainide terminates atrial fibrillation in this experimental model by causing tachycardia-dependent increases in atrial ERP, which increase the wavelength at the rapid rates characteristic of AF to the point that the arrhythmia can no longer sustain itself. (*Circulation Research* 1992;71:271–287)

KEY WORDS • **arrhythmia mechanisms** • **electrocardiography** • **antiarrhythmic drugs** • **action potential duration** • **refractory period** • **heart rate** • **flecainide** • **atrial fibrillation**

Atrial fibrillation (AF) is the most common sustained arrhythmia encountered in clinical practice.[1] Recent studies have shown that the class Ic antiarrhythmic agents propafenone[2–4] and flecainide[5–14] are effective in terminating atrial fibrillation and preventing its recurrence. The availability of class Ic agents has been hailed as a useful addition to the pharmaceutical armamentarium in treating this arrhythmia.[15] On the other hand, the effectiveness of class Ic agents in terminating AF raises questions about the factors determining AF and mechanisms of antiarrhythmic drug action. Class Ic agents are considered to slow cardiac conduction strongly, with little effect on refractoriness.[16,17] Given the classically understood determinants of reentry,[18,19] slowed conduction with no change in refractory period should increase the likelihood of a reentrant arrhythmia like AF.[20–23]

We have shown that flecainide causes tachycardia-dependent increases in atrial action potential duration (APD), apparently by attenuating APD accommodation to heart rate.[24] These effects are paralleled by frequency-dependent increases in atrial refractoriness, which could account for the beneficial effects of flecainide in atrial fibrillation.[24] The latter hypothesis has not, however, been tested.

The purpose of the present work was to evaluate the mechanisms of flecainide's efficacy in an experimental model of atrial fibrillation. Specific goals included 1) the development of an animal model of sustained atrial fibrillation that is reliable and reproducible, 2) the assessment of flecainide's concentration-dependent efficacy in this model using a blinded experimental design to exclude the possibility of investigator bias, 3) an evaluation of the electrophysiological effects of flecainide associated with termination of atrial fibrillation, and 4) an analysis of the mechanism of arrhythmia termination using a computer-based mapping system and epicardial electrode array capable of analyzing data from up to 112 simultaneously recorded electrograms. A

From the Department of Medicine, Montreal Heart Institute, and University of Montreal, the Departments of Pharmacology and Therapeutics, and Medicine, McGill University, and Sacré-Coeur Hospital, Montreal, Canada.

Previously presented in abstract form (*Circulation* 1990;82[suppl III]:III-98).

Supported by the Medical Research Council of Canada, Riker Pharmaceuticals (University-Industry Award), the Quebec Heart Foundation, and the Fonds de Recherche de l'Institut de Cardiologie de Montréal. S.N. is a Nordic-Fonds de Recherche en Santé du Québec Senior Research Scholar.

Address for correspondence: Dr. Stanley Nattel, Montreal Heart Institute, 5000 Belanger Street East, Montreal, Quebec, Canada H1T 1C8.

Received May 22, 1991; accepted March 24, 1992.

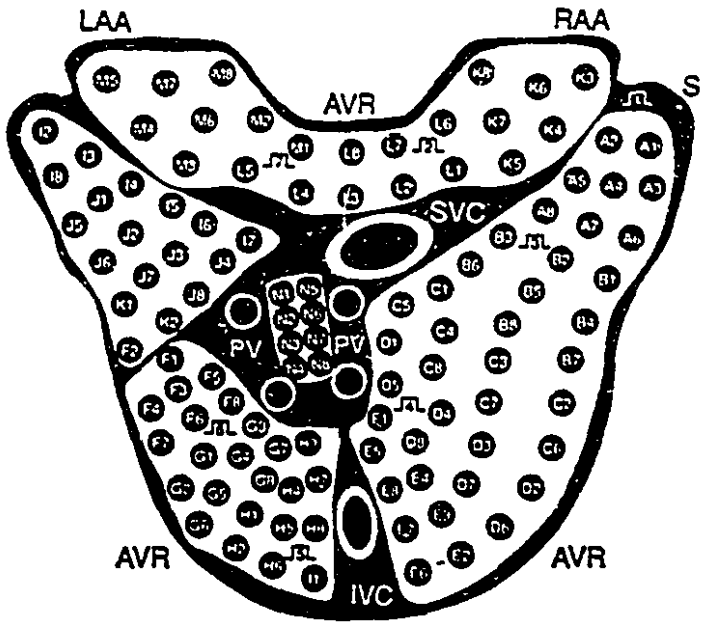

FIGURE 1. *Diagram of atria, electrode arrays (in white), and bipolar electrode sites (filled circles). The sites of various bipolar electrodes used for stimulation to determine regional conduction velocity and effective refractory period are indicated by numbers 1–7. AVR, atrioventricular ring; RAA and LAA, right and left atrial appendage, respectively; IVC and SVC, inferior and superior vena cavae; PV, pulmonary veins; S, site of atrial stimulation for conduction and refractoriness measurement, as well as arrhythmia induction.*

preliminary communication of these results has appeared in abstract form.[25]

Materials and Methods

General Methods

Sixteen mongrel dogs of either sex weighing 18–27 kg were anesthetized with morphine (2 mg/kg i.m.) and α-chloralose (100 mg/kg i.v.) and ventilated by a respirator (NSH 34RH, Harvard Apparatus, South Natick, Mass.) via an endotracheal tube at a rate of 20–25 breaths per minute with a tidal volume obtained from a nomogram. Arterial blood gases were measured to ensure adequate oxygenation (SaO_2 >90%) and physiological pH (7.38–7.45). Catheters were inserted into the left femoral artery and both femoral veins and kept patent with heparinized saline solution (0.9%). A median sternotomy was performed, an incision was made into the pericardium extending from the cranial reflection to the ventricular apex, and a pericardial cradle was created.

A pair of Teflon-coated stainless steel bipolar hook electrodes, one for stimulation and the other for recording atrial electrograms, were inserted intramurally into the tip of the right atrial appendage. The position of the stimulating electrode is indicated by the number "1" in Figure 1. A programmable stimulator and a stimulus isolator (Bloom Assoc., Flying Hills, Pa.) were used to deliver 4-msec square-wave pulses. Another pair of electrodes were fixed in the high right ventricle for stimulating and recording purposes. A demand pacemaker (GBM 5880 Demand Pacemaker, Medtronic, Inc., Minneapolis, Minn.) was used to pace the ventricles when the spontaneous ventricular rate was ≤90/min. Operational amplifiers (Bloom Assoc.) and a Mingograf T-16, 16-channel recorder (Siemens-Elema Ltd., Toronto, Canada) were used to record the six standard surface electrocardiogram leads, arterial pressure, and stimulus artifacts. Electrocardiographic recordings were obtained at a paper speed of 200 mm/sec. To block complicating sympathetic reflex effects, particularly in the presence of varying vagal tone, we administered 0.5 mg/kg i.v. nadolol followed by 0.25 mg/kg every 2 hours. We have previously shown that this regimen produces sustained and stable β-blockade.[26]

Atrial Fibrillation Model

Vagally induced atrial fibrillation was used as a model in this study. Both cervical vagal trunks were isolated and decentralized, and bipolar hook electrodes were inserted via a 21-gauge needle into the middle of each nerve, with the electrode running within and parallel to vagal fibers for several centimeters. Bilateral vagal nerve stimulation (VNS) was delivered by an SD-9F stimulator (Grass Instruments, Inc., Quincy, Mass.), with a pulse width of 0.1 msec and a frequency of 10 Hz. The amplitude of stimulation was between 3 and 10 V, adjusted in each dog to two thirds of the threshold for the production of asystole under control conditions. Five seconds after the initiation of vagal stimulation, a short burst (1–3 seconds) of atrial pacing at a cycle length of 100 msec and with a current amplitude of four times the diastolic threshold for atrial capture was used to induce AF. AF induced in this way persisted spontaneously for over 30 minutes and converted within seconds of the termination of VNS. The presence of AF was determined by the occurrence of a rapid (>500/min under control conditions), irregular spontaneous atrial rhythm with varying atrial electrogram morphology and activation time.

Activation Mapping

An array of 112 bipolar electrodes with 1-mm interpolar and 6-mm interelectrode distance, evenly spaced in five thin plastic sheets, was used (Figure 1). In addition to the recording sites, the sheets also contained six pairs of bipolar electrodes (numbered 2–7 in the figure) for regional stimulation. The sheets covered the entire epicardial surface of both atria and were carefully fixed in position by sewing the edge of the plaques to the atria to assure good electrode contact with the epicar-

dial surface. One sheet was placed under the root of the aorta to cover the anterior aspect of the atrial appendages and Bachman's bundle. Three additional sheets were sewn to the posterior aspects of both atrial appendages and both atrial free walls. The parietal pericardium was gently separated, and a fifth plaque was put in the area between the pulmonary arteries and veins.

Each signal was filtered with 12-bit resolution and a 1-KHz sampling rate and transmitted via duplex fiberoptic cables into a microcomputer (model 286, Compaq Computer, Houston, Tex.). Software routines were used to amplify, display, and analyze each electrogram signal as well as to generate maps showing activation times at each electrode site.[27] Interpolation techniques were used to produce isochrone maps of epicardial activation, but only measured activation times (not interpolated data) were used for quantitative analysis. Each electrogram was analyzed by the use of computer-determined peak-amplitude criteria,[28,29] and was reviewed manually to exclude low-amplitude signals with indiscrete electrograms. The reference point for mapping of each cycle was placed at the chronological midpoint of the cycle. The accuracy of measured activation time was ±0.5 msec. The data were downloaded on high-density diskettes for subsequent off-line analysis. Isochrone maps and activation times for each activation were recorded by the use of an IBM ink jet printer. Hardware and software for the mapping system were obtained from Biomedical Instrumentation, Inc., Markham, Ontario, Canada. To avoid distortion of data by creating artistic renditions or copies, all activation maps are reproduced by directly photographing computer-generated maps from the monitor screen.

Experimental Protocols

Protocol 1: Evaluation of the concentration-dependent efficacy of flecainide in terminating AF. AF was induced under control conditions as described above and its sustained nature over 30 minutes in the presence of vagal stimulation verified. A table of random numbers was used by a third party to determine the order of administration of either flecainide or an isotonic glucose placebo. This third party then prepared syringes containing the appropriate doses of flecainide and identical volumes of isotonic glucose and labeled them "A" and "B" to indicate their order of administration. The experimenters were blinded as to the agent administered until all experiments had been completed. Each agent was given as a loading dose (1 mg/kg flecainide or an equal volume of glucose solution) over 15 minutes, followed by a maintenance dose (1.33 mg/kg per hour flecainide or placebo). If fibrillation terminated during the infusion of drug A, reinitiation of AF was attempted. If reinitiation was successful, VNS was continued for 30 minutes to determine whether AF would convert spontaneously. If reinitiation was prevented, the effects of drug A on vagal bradycardic actions and on atrial conduction and refractoriness were evaluated (according to protocols 2 and 3, below). The maintenance dose was then discontinued, and the reinduction of AF was attempted every 10 minutes thereafter. Sixty minutes after the discontinuation of drug infusion, a time that was always sufficient for the effects of drug A to dissipate, drug B was given. The same procedures were followed as described for drug A above.

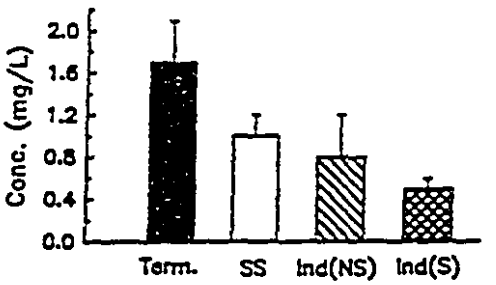

FIGURE 2. *Mean (+SEM) flecainide concentrations at the time of arrhythmia termination (Term.), during maintenance infusion (SS), after the discontinuation of the maintenance infusion when atrial fibrillation was once more inducible but terminated spontaneously [Ind(NS)], and when sustained AF could be induced [Ind(S)].*

If atrial fibrillation persisted for 30 minutes after the onset of drug infusion, the infusion was considered to have failed to terminate AF. Vagal stimulation was then discontinued and AF allowed to terminate spontaneously (which it inevitably did shortly after VNS was stopped). Rate-dependent changes in atrial conduction and refractoriness were then assessed, and a blood sample was obtained for subsequent assay of flecainide plasma concentration by high-performance liquid chromatography.

If the first dose of both A and B were unsuccessful, the same protocols were repeated with doubled loading and maintenance doses of either drug. Blood samples for subsequent drug assay were obtained at the time of conversion of AF to sinus rhythm, at the times of attempted AF induction, and at the end of drug infusion in each dog.

To analyze the mechanism by which flecainide affects vagally induced atrial fibrillation, activation data were obtained for subsequent off-line analysis. Activation data was acquired at the onset of AF and 5 minutes later during sustained AF under control conditions. Data were also acquired at the initiation of AF and 5 minutes later before the administration of each dose of flecainide or placebo, 5 minutes after the onset of drug administration, and at the time of AF termination. The acquisition system samples data continuously and stores it in a memory buffer, so that 8 seconds of data beginning up to 8 seconds before a manual trigger can be obtained. This allowed us to acquire activation data immediately before, and at the time of, AF termination.

Protocol 2: Flecainide effects on the heart rate response to graded vagal nerve stimulation. These experiments were designed to determine whether flecainide in the doses used alter the electrophysiological effects of VNS. Sinus rate was used as index of vagal action. Vagal frequency–response curves (in nine dogs) and intensity–response curves (in three dogs) were first measured under control conditions. Atrial electrograms were recorded at 100 mm/sec for 10 seconds and the total number of complexes counted to determine spontaneous rate. For frequency–response curves, the vagal nerves were stimulated at a fixed amplitude of 10 V with increasing frequency from 2 Hz with 1 Hz increments until a maximum effect was observed. Each frequency was maintained for 30 seconds, with the sinus rate

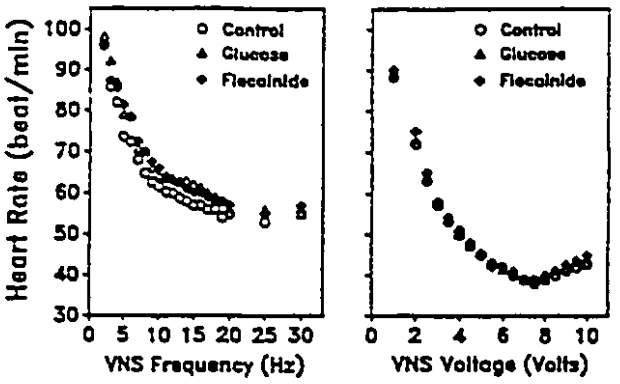

FIGURE 3. *Mean heart rate response to vagal stimulation (VNS) before (control) and after isotonic glucose or flecainide administration.* Left panel, *mean data from nine dogs used to study the vagal frequency–response curve;* right panel, *means from voltage–response studies in three dogs.*

evaluated over the last 10 seconds of stimulation at a given frequency. Intensity–response curves were obtained in a similar fashion, except that VNS frequency was fixed at 10 Hz, the initial stimulation voltage was 2 V, and stimulation intensity was augmented by 0.5-V steps. After each 30-second stimulation period at a given voltage or frequency, VNS was stopped, and the preparation was observed until sinus rate returned to control values.

Protocol 3: Drug effects on atrial refractoriness and conduction. Atrial effective refractory period (ERP) was assessed by the extrastimulus technique, and atrial activation times were determined by isochronal mapping. The direction of rapid propagation was determined from the isochrone maps, and a pair of adjacent bipolar electrode sites in the line of rapid propagation were selected. Conduction velocity was calculated as the distance between the sites divided by the interelectrode conduction time. The activation pattern was assessed for all activations to ensure that changes in conduction time were not caused by rate- or drug-dependent regional block or changes in the direction of impulse propagation.

Results were obtained at basic cycle lengths (BCLs) of 400, 300, 250, 200, and 150 msec. Two minutes were allowed at each BCL before atrial ERP and conduction velocity were measured. For ERP determination, a premature stimulus (S_2) was inserted after every 10 basic (S_1) stimuli while S_1S_2 decreased by 10-msec decrements until failure to capture occurred. The longest S_1S_2 interval that consistently failed to produce a propagated response was defined as the ERP. Measurements of ERP were made in both the presence and absence of VNS. ERP and conduction time were first determined under control conditions after termination of AF and then immediately after drug-induced conversion of AF or during the maintenance dose if the drug failed to convert AF within 30 minutes.

Regional Drug Effects on Wavelength

Vagal stimulation produces nonuniform regional changes in atrial ERP,[30] resulting in nonuniform changes in local wavelength.[31] To determine whether flecainide's effects on wavelength were exerted in a spatially uniform fashion, we studied five additional dogs. Conduction velocity, atrial refractory period, and wavelength were determined during stimulation at a cycle length of 250 msec at each of the seven stimulation sites shown in Figure 1. For the conduction velocity measurement during stimulation at each site, conduction time between two adjacent bipolar electrodes in the direction of rapid impulse propagation was determined, with the proximal bipole in the immediate vicinity of the stimulating electrode. The proximal bipole was used to indicate when regional propagation failed during ERP measurement. Wavelength was calculated from the local conduction velocity and ERP measurement obtained during stimulation at each site under control conditions in both the absence and presence of VNS and then after flecainide administration with and without VNS. To assure that the results of these experiments were relevant to the blinded study described above, an identical protocol was used (in terms of AF induction, drug dose, and assessment of drug efficacy), but flecainide was administered in a nonblinded fashion. ERP and conduction measurements were obtained during drug administration as described above.

Data Analysis

The ability of flecainide to terminate AF was compared with that of an equal volume of glucose by Fisher's exact test.[32] Group data are presented as mean±SEM. Comparison between group means were made by two-way analysis of variance (ANOVA) with Scheffe's test. Student's paired t test was used when only two groups of results were compared. A two-tailed probability of less than 5% defined statistical significance.

Rate-dependent and regional effects of flecainide on atrial ERP, conduction velocity, and wavelength were evaluated by ANOVA with an F test for interaction. Wavelength changes were calculated based on the mathematical formulation of Wiener and Rosenblueth[33] using the relation

$$\lambda = ERP \times CV = ERP \times L/CT$$

where λ is wavelength, CV is conduction velocity, L is length of the conducting pathway (i.e., interelectrode distance), and CT is conduction time.

Results

General Efficacy of Flecainide in AF

A total of 16 dogs were studied using the blinded protocol to determine the efficacy of flecainide in AF, and mapping data were obtained in 14 of these. The mean amplitude of vagal stimulation was 6 V (range, 3–10 V), and sustained AF was readily produced under control conditions in all dogs. Isotonic glucose did not convert AF to sinus rhythm in any dogs (0 of 16, 0% efficacy). In contrast, flecainide converted AF in nine of 16 dogs at the first dose and seven of 16 at the second dose for an overall efficacy of the drug of 100% ($p<0.0001$). The mean time of conversion of AF by flecainide was 13.8 minutes (range, 7–20 minutes). In five dogs used to study regional effects of flecainide, the first dose successfully terminated AF.

The mean concentrations of flecainide associated with arrhythmia termination and various degrees of suppression of arrhythmia induction are shown in Fig-

TABLE 1. Effects of Flecainide on Atrial Effective Refractory Period, Conduction Velocity, and Wavelength

	Effective refractory period (msec)				
BCL (msec)	400	300	250	200	150
Without VNS					
Control	133±3	125±3	115±3	108±4	94±4
Glucose	122±3*	117±4	110±4	106±4	94±4
(*n*=11)	(−7±4%)	(−6±5%)	(−3±5%)	(−1±7%)	(1±6%)
Effective flec	160±5‡	158±4‡	153±5‡	151±6‡	142±2‡
(*n*=11)	(21±3%)	(27±2%)	(34±3%)	(45±6%)	(52±3%)§
Control	132±3	125±3	113±5	106±5	88±6
Ineffective flec	128±5	123±6	118±5	113±2	103±4*
(*n*=6)	(−3±3%)	(−1±3%)	(5±4%)	(8±4%)	(18±4%)§
With VNS					
Control	77±5	75±6	68±5	68±4	63±4
Effective flec	105±8†	118±9†	117±11‡	121±9‡	122±10‡
(*n*=6)	(38±10%)	(68±5%)	(70±9%)	(79±4%)	(92±7%)§

	Atrial Conduction Velocity (cm/sec)				
BCL (msec)	400	300	250	200	150
Without VNS					
Control	119±6	116±6	107±5	99±5	93±5
Glucose	124±6‡	122±5‡	113±5‡	104±5‡	94±8
(*n*=11)	(4±1%)	(5±1%)	(4±1%)	(4±1%)	(0±2%)
Effective flec	105±6‡	98±5‡	88±6‡	79±6‡	69±4‡
(*n*=11)	(−12±2%)	(−16±1%)	(−19±2%)	(−24±3%)	(−29±2%)‖
Control	120±7	116±8	107±7	99±7	93±6
Ineffective flec	114±7†	110±7†	97±7†	92±9*	82±8†
(*n*=6)	(−5±1%)	(−5±1%)	(−9±2%)	(−12±4%)	(−16±3%)
With VNS					
Control	121±4	121±4	117±4	112±3	107±2
Effective flec	105±2†	102±3†	89±3†	81±5‡	72±5‡
(*n*=6)	(−13±3%)	(−16±3%)	(−23±3%)	(−28±3%)	(−33±4%)‖

	Wavelength (cm)				
BCL (msec)	400	300	250	200	150
Without VNS					
Control	15.9±0.9	14.5±1.0	12.4±0.8	10.9±0.8	8.8±0.7
Glucose	15.1±0.8	14.2±0.8	12.4±0.7	10.9±0.5	8.7±0.6
(*n*=11)	(−3.1±4.3%)	(−0.3±5.7%)	(2.1±5.5%)	(4.0±7.1%)	(1.0±6.3%)
Effective flec	17.1±1.5	15.6±1.2*	13.5±1.2*	12.5±1.1*	9.9±0.6†
(*n*=11)	(6.1±4.0%)	(7.5±2.5%)	(8.2±3.6%)	(14.3±4.6%)	(13.5±3.7%)
Control	15.8±1.1	14.4±1.0	12.0±0.9	8.9±1.9	8.2±0.8
Ineffective flec	14.7±1.3*	13.6±1.4	11.5±1.0	10.5±1.1	8.5±0.9
(*n*=6)	(−7.2±2.3%)	(−6.4±3.6%)	(−4.5±3.9%)	(2.7±4.4%)	(4.1±5.4%)
With VNS					
Control	9.2±0.5	9.0±0.5	7.9±0.4	7.6±0.5	6.8±0.5
Effective flec	11.1±0.9	11.2±0.8†	10.4±1.1*	9.8±1.0*	8.8±1.1*
(*n*=6)	(20.8±9.9%)	(23.7±5.4%)	(31.0±10.1%)	(28.5±6.4%)	(28.3±8.9%)

BCL, basic cycle length; VNS, vagal nerve stimulation; flec, flecainide.

*$p<0.05$, †$p<0.01$, ‡$p<0.001$ compared with control in the absence of flecainide at the same cycle length. Results in parentheses are percent change produced by flecainide relative to corresponding control value. §$p<0.001$, ‖$p<0.01$ for rate dependence of drug effects by analysis of variance with *F* test for interaction. Values of percent change are determined relative to corresponding paired control data. All values are mean±SEM in milliseconds.

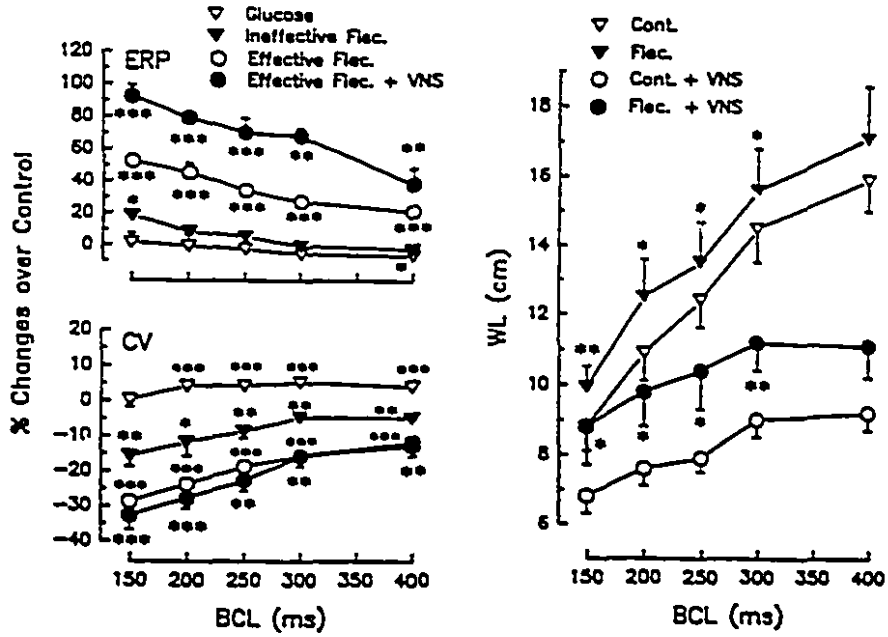

FIGURE 4. *Changes from control in atrial effective refractory period (ERP), atrial conduction velocity (CV), and minimum wavelength for reentry (WL) as a function of basic cycle length (BCL). Results for ERP and CV are presented as a percent change from the corresponding control value, whereas changes in wavelength are shown for effective doses of flecainide only and are absolute values of wavelength. *p<0.05; **p<0.01; ***p<0.001 compared with corresponding control value.*

ure 2. The mean concentration causing arrhythmia termination was 1.7±0.4 mg/l. Atrial fibrillation was not inducible until a mean concentration of 0.8±0.4 mg/l was attained after the drug was stopped, at which point the induced AF terminated spontaneously. When a mean concentration of 0.5±0.1 mg/l was achieved, sustained AF could once more be induced.

Flecainide's Effects on the Response to Vagal Stimulation

Flecainide produced no significant changes in the sinus node response to vagal stimulation. Figure 3 shows mean data from all dogs studied for the vagal frequency–response curves (left) and intensity–response curves (right). In both instances, results in the presence of flecainide were superimposable on results during isotonic glucose administration. These data indicate that flecainide did not exert its actions by generally attenuating the response to vagal stimulation.

Effects of Flecainide on the Electrophysiological Determinants of Reentry

The rate-dependent effects of flecainide on atrial ERP, conduction velocity, and the minimum wavelength for reentry are listed in Table 1 and shown in Figure 4. Minimal differences were seen between values of these variables under control conditions and measurements obtained in the presence of isotonic glucose placebo. Results obtained with dose 1 in the seven dogs whose AF was not converted by this dose are shown by the filled triangles in Figure 4, and results of the dose of flecainide that converted AF in each dog are shown by the open circles. Ineffective doses of flecainide had almost two thirds of the conduction slowing effect of effective doses but produced limited changes in atrial refractoriness and did not alter the wavelength. Effective doses of flecainide, on the other hand, produced substantial rate-related increases in atrial ERP and significantly increased the wavelength.

Vagal stimulation produced substantial decreases in atrial ERP but did not alter atrial conduction velocity (Table 1). Flecainide's effect on atrial ERP in the presence of vagal stimulation (comparing results during VNS in the presence of the drug with those during VNS in its absence) was qualitatively similar to, but quantitatively greater than, its effect without VNS (Figure 4, upper left). The drug's ERP-prolonging action was increased about 2.5-fold in both the presence and absence of VNS over the range of BCLs from 400 to 150 msec. In contrast to its effect on ERP, flecainide's action on conduction velocity was not altered by VNS (Figure 4, lower left). As a consequence, the drug's ability to increase the minimum wavelength for reentry was increased in the presence of VNS.

The changes in atrial conduction produced by flecainide are illustrated in Figure 5. When the right atrial appendix was paced, the site of earliest activation was at the tip of the appendix and latest activation was in the posteroinferior left atrium, as shown in all panels of the figure. When BCL was decreased from 400 msec (top left) to 150 msec (top right) under control conditions, a slight increase in overall atrial conduction time, from 75 msec to 83 msec, occurred. In the presence of flecainide at a BCL of 400 msec (bottom left), the pattern of conduction did not change but the conduction time increased to 88 msec. When the pacing cycle length was decreased to 150 msec in the presence of the drug, conduction slowed uniformly and the conduction time increased to 105 msec.

Effects of Flecainide on Activation During Atrial Fibrillation

During sinus rhythm, earliest activation was consistently found in the right atrium near the superior vena cava (site B_4 in Figure 6). Excitation conducted rapidly throughout the right atrium and then appeared to slow during transseptal propagation. The anterior aspect and appendage were the first regions of the left atrium to be activated, perhaps via specialized conducting pathways,[34]

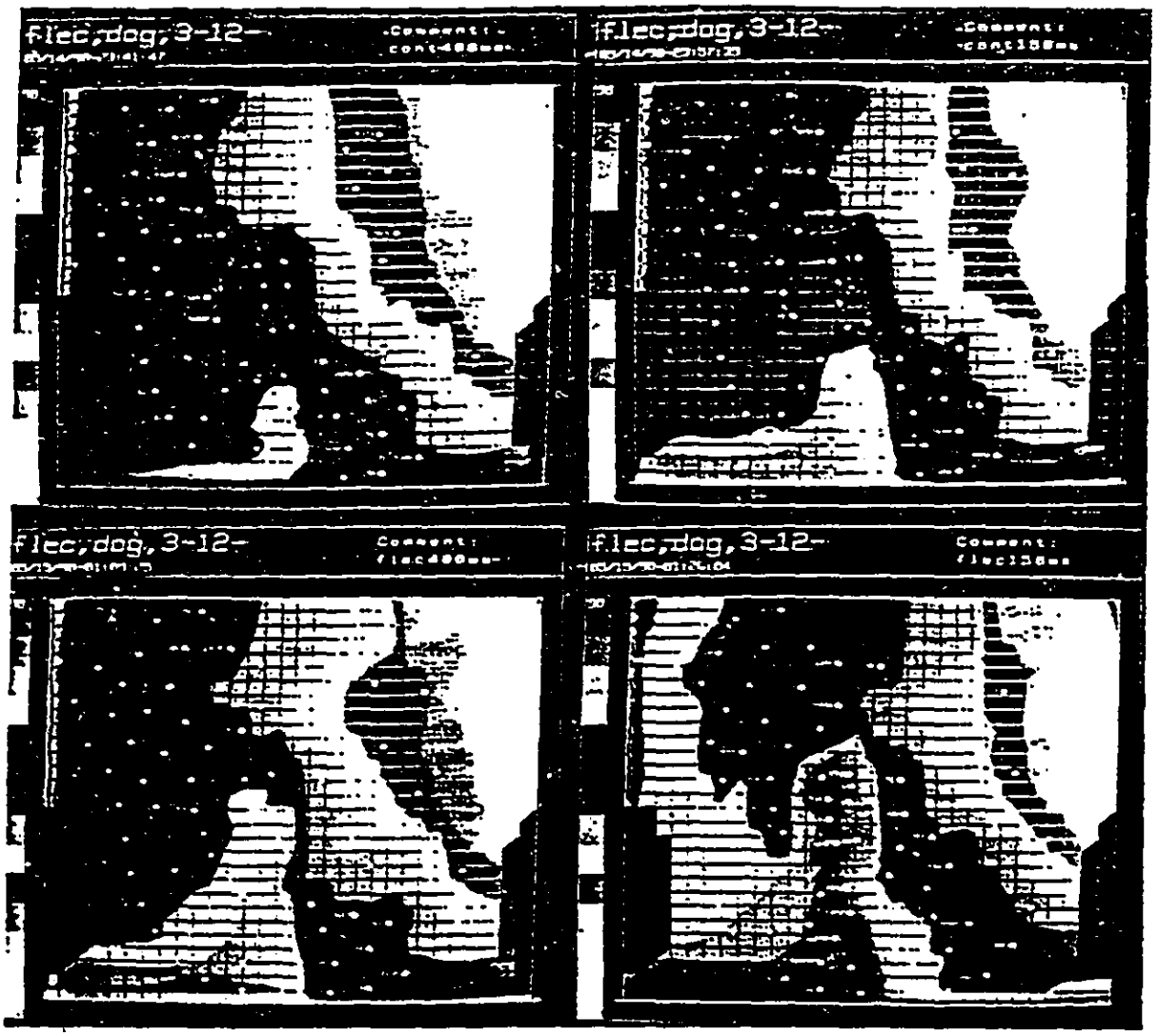

FIGURE 5. *Activation maps at a pacing cycle length of 400 msec* (left) *and 150 msec* (right), *under control conditions* (top), *and after flecainide (flec.,* bottom). *Each color represents a 10-msec isochrone (scale at left of each map). Activation was slowed slightly by rapid pacing under control conditions, but a larger degree of conduction slowing was provoked by tachycardia in the presence of flecainide.*

and the last region to be excited was the posterior left atrium adjacent to the atrioventricular ring.

During atrial fibrillation in the absence of flecainide, rapid atrial activity was observed. Figure 7 (panels A and B) shows electrograms recorded in two sets of eight electrodes from the anterior right atrium (electrodes A_1–A_8, panel A) and left atrium (I_1–I_8, panel B). The left atrial activity was more regular and discrete, so we chose to map atrial activation during one cycle of left atrial activity as shown by the vertical lines in panel B. Because many sites elsewhere were activated twice during this cycle, we created two maps to represent atrial activation during the cycle, the first showing initial activation at each site (panel C), and the second (panel D) incorporating the second time of activation for sites showing two discrete activations during the cycle (as seen in most electrograms in panel A). As shown in panel C, there were three zones of early activation: the superolateral right atrium adjacent to the right atrial appendage (sites A_2, A_3, A_4, and B_4), the mid–left atrium (site K_2), and the posterior aspects of both atria adjacent to the atrioventricular ring (sites E_3, H_3, and H_4). Six islands of late activation are present. In several regions, zones of early and late activation lie close to one another and are separated by narrow isochrones indicating block or very slow conduction. Since conduction during sinus rhythm is rapid and relatively uniform (Figure 6), these zones of slow conduction (represented by the dotted lines in panel C) must represent refractory tissue. Electrical propagation around the zones of refractoriness results in delayed activation at sites close to the first areas to be activated. Subsequent propagation to these sites of early activation (shown by the white arrows in panel D) results in their reexcitation, as shown by the delayed activation in panel D of sites F_3, F_4, and K_3; H_5–H_7 and H_7–H_8; and A_4. Sites K_1, J_7, H_2, and H_4 were activated early and only once in the cycle shown. Propagation from the late-activated sites K_2, H_5, and H_8 (shown by the white arrowheads in panel D) initiated the next cycle in these regions.

Consider the activation of sites A_1–A_8, whose electrograms are shown in panel A. Sites A_1, A_2, A_5, and A_8 are activated at the beginning of the cycle. These correspond to a zone of very early activation in panel C. Site A_7 is activated slightly later and is followed by the activation of sites A_6 and A_4. Site A_3 was activated immediately before the other sites in the cycle, and the propagating wave front returned to activate A_3 just over halfway into the cycle. The impulse then activates A_1, A_2, A_5, and A_8, the first sites activated and therefore the first to recover excitability. This is followed by excitation of sites A_7, A_6, and A_4, activated somewhat later in the primary cycle and therefore also reactivated later.

Some zones were activated only once during the cycle, such as electrodes I_2–I_8 shown in panel B. When such zones were activated early in the cycle and were adjacent to regions reactivated late in the cycle, propagation from the latter areas was able to initiate another cycle. For example, electrodes J_7, K_1, H_2, and H_6 were activated early in the cycle (panel C). Slow conduction resulted in delayed reexcitation of electrodes H_3–H_5 and K_2 (panel D) approximately 70 msec after the initial excitation at electrodes J_7, K_1, H_2, and H_6. Propagation to the latter sites (as shown by the white arrowheads in panel D) initiated the next cycle in these regions.

The cycle illustrated in Figures 7C and 7D suggests several coexistent reentry circuits of relatively small diameter. We observed an average of five such apparent reentry circuits in each cycle of atrial fibrillation mapped under control conditions.

The effect of flecainide on atrial activation during AF is illustrated in Figure 8. The results shown are from the same dog as those in Figure 7. After 5 minutes of flecainide infusion (panel A), atrial activity is more homogeneous and two large macro-reentrant pathways are present. After 12 minutes, flecainide terminated AF. The last two cycles before termination (designated B and C in panels E and F) are shown in panels B and C. In the penultimate cycle (panel B), a single large macro-reentry circuit is present. The next cycle (panel C) begins at a zone similar to the sites of first activation in the penultimate cycle. When the reentering impulse reaches the dark blue zone, block occurs, as shown by failure of activation during cycle C at electrode sites E_1–E_4, and spontaneous atrial activity ceases. This is followed by an atrial activation originating near the sinus node (panel D), whose pattern of activation resembles sinus beats under control conditions (Figure 6). Note that the low-amplitude potentials recorded at sites E_5–E_8 during cycle C are reflections of ventricular activation (corresponding in time to the surface QRS) and are also recorded before and immediately after sinus cycle D. The results of all experiments were similar in the sense that flecainide gradually increased the size and reduced the number of simultaneous reentry circuits, until one or two large circuits remained. No changes in atrial activation were noted after the administration of isotonic glucose.

Activation data adequate for map construction was available at the time of AF termination by flecainide in a total of 15 dogs (12 from the blinded series and three from studies of regional effects). In nine of these, the activation maps before AF termination resembled those shown in Figure 8, with a single macro-reentry circuit encountering refractory tissue. In the remaining six dogs, there were either two separate macro-reentry circuits that terminated independently (three dogs) or a dividing wave front resembling "figure of eight" reentry as previously described in chronically infarcted ventricular preparations.[35,36] Figure 9 shows an example of this form of reentry at the time of AF termination by flecainide. Panels A and B show electrograms from two sets of electrodes at the time of arrhythmia termination, and panels C–F show activation maps of the last three cycles of activation at sites H_3, H_4, and H_5. The first activation at each electrode site during the first cycle analyzed is shown in panel C. There is a large region of early activation in the posterior left atrium, and the impulse conducts toward the right atrium as shown. Functional arcs of block, possibly related to anatomic obstacles (the pulmonary veins to the left of electrodes N_1–N_4 and the inferior vena cava to the right of electrodes H_8 and I_1), cause the impulse to travel through an isthmus of excitable tissue and then divide into two wave fronts propagating back toward the posterior left atrium. The time lag is sufficient for the posterior left atrium to be reexcited during the second half of the same cycle, as shown by the dark blue isochrones in panel D. Propagation back through the functional isthmus as shown by the arrowhead in panel D produces another cycle with a figure of eight pattern as shown in panel E. While the pattern of activation in panel E resembles that in panel C, conduction is more rapid and no subsequent reentrant activity is apparent. Over the last 100 msec of the cycle designated by E, no atrial activation was recorded. The final cycle before restoration of sinus rhythm is shown in panel F. This cycle originates from the region where activity was last noted in panel E but after an interval of over 100 msec. In keeping with the substantial recovery time at all electrode sites, activation propagates rapidly and rather uniformly during cycle F. It is impossible to determine whether the cycle shown in panel F originated from reentry through a zone of very slow conduction that was not detected or as a result of a site of ectopic activity. While the precise mechanism of arrhythmia termination

FIGURE 6. *Activation map during sinus rhythm. Earliest activation (light yellow) was in the right atrium adjacent to the superior vena cava. Latest activation (dark green) was in the posterior left atrium.*

in Figure 9 is unclear. the number of reentry circuits is clearly reduced compared with predrug conditions, making arrhythmia termination more likely.

To quantify the effects of flecainide on atrial activation during AF, we sought an operational definition of a reentry circuit. Since a complete circuit of reexcitation was not always identifiable in an apparent zone of reentry, we defined a reentry region as a zone in which there was a difference of >50 msec in the activation time at adjacent electrode sites, with the earlier site of activation reactivating within 20 msec after the adjacent site of late activation. In the presence of flecainide, cycles of atrial activation were readily identifiable, and 10 consecutive cycles were mapped during each drug infusion after 5 minutes of drug infusion and immediately before arrhythmia termination (when the latter occurred). Under control conditions, as shown in Figure 7, the duration of activation cycles varied among electrode sites. Therefore, we mapped 10 consecutive windows of 80-msec duration. Under control conditions, there was an average of 5.0±0.7 circuits per 80-msec window. The number of circuits was significantly decreased after 5 minutes of flecainide infusion and further decreased immediately before AF termination (Figure 10).

We also determined the mean cycle length of AF under various conditions. The mean cycle length was determined for each study period by determining the number of cycles of activation recorded at each electrode site in a 1-second interval. The results obtained at all sites were averaged to obtain a representative mean cycle length for that study period. Flecainide significantly increased the mean cycle length of AF (Figure 10). Both mean cycle length and number of circuits were calculated for all dogs in which mapping studies were performed during the blinded study. Isotonic glucose did not alter the number of apparent reentrant circuits or the mean cycle length of AF.

Regional Effects of Flecainide and Vagal Nerve Stimulation

During the blinded studies, atrial stimulation was always performed at the single site designated by the number 1 in Figure 1. To evaluate regional changes in refractoriness, conduction, and wavelength, stimulation (BCL, 250 msec) was performed at seven separate sites in five additional dogs. Under control conditions there were small regional differences in refractory period and conduction velocity (Figure 11). Vagal stimulation did not alter conduction but significantly decreased atrial ERP at all sites. The magnitude of vagal action varied at different sites, with average decreases ranging from 10 msec at site 5 to 62 msec at site 2. Flecainide significantly reduced conduction velocity and increased ERP at all sites, in both the presence and absence of vagal stimulation. In the absence of vagal stimulation, flecainide's effect on ERP was relatively uniform throughout the atria. In the presence of vagal stimulation, flecainide's effect was somewhat greater at sites showing the greatest degree of vagally induced ERP abbreviation. Flecainide thus tended to make atrial ERP more uniform in the presence of VNS. Under control conditions, the wavelength (Figure 11, bottom) varied from 13 to 16 cm at the seven sites tested. Vagal stimulation significantly reduced wavelength to between 7.5 and 12 cm at all sites. Flecainide significantly increased wavelength in the presence and absence of VNS, with mean values in the presence of VNS ranging from 12 to 14 cm after flecainide administration.

The effects of flecainide on regional variability in atrial refractoriness are summarized in Figure 12. To quantify the variability in ERP, we calculated the standard deviation of ERP at all seven sites under each experimental condition. Flecainide significantly decreased atrial ERP variability in both the absence and presence of VNS, whereas VNS substantially increased ERP heterogeneity. In the presence of VNS, flecainide returned the standard deviation of atrial ERP toward values measured under control conditions without VNS in the absence of the drug.

Discussion

We have shown that flecainide predictably terminates AF in an experimental dog model and prevents the reinitiation of AF in a concentration-dependent fashion. These actions appear to be caused by tachycardia-related increases in atrial refractoriness produced by the drug, which result in significant increases in the wavelength for atrial reentry.

Relation to Previous Studies of Class I Drug Action in Atrial Fibrillation

Studies of the mechanisms of antiarrhythmic drug action in atrial fibrillation have been quite limited. Rensma et al[31] showed that the wavelength was an accurate predictor of the inducibility of atrial arrhythmias in conscious dogs. Quinidine and *d*-sotalol increased the wavelength and prevented the induction of atrial fibrillation, while the class Ic drug propafenone had little effect on wavelength and apparently did not alter the ability to induce AF.[31] In a subsequent study from the same laboratory, the experimental class Ic compound ORG 7797 was found to reduce the inducibility of AF.[37] This action was associated with a tachycardia-dependent increase in atrial refractory period. The drug limited the minimum wavelength that could be produced by rapid pacing, thus presumably decreasing the number of simultaneous atrial reentry circuits possible and the likelihood of AF.[37]

Our work differs from the above studies in that we have used a model of sustained AF, a blinded design to assess drug action, and epicardial mapping to address antiarrhythmic mechanisms. The results support the mechanisms hypothesized by Kirchhof et al,[37] in that the increase in wavelength produced by flecainide resulted in an increase in the size and a decrease in the number of reentry circuits, until AF was finally terminated. Kirchhof et al found that ORG 7797 attenuated the decreases in atrial refractoriness resulting from increased heart rate, and we noted a similar effect of flecainide. These results parallel our previous direct observations of the effects of flecainide on atrial ADP in vitro,[25] as well as recent studies of the drug's actions on atrial monophasic action potentials in vivo.[38] It is possible that some of the rate-dependent increases in atrial ERP produced by flecainide were due to sodium-channel blockade, but in our previous in vitro[25] and in vivo[38] studies most of the drug's ERP-prolonging action was accounted for by increases in ADP.

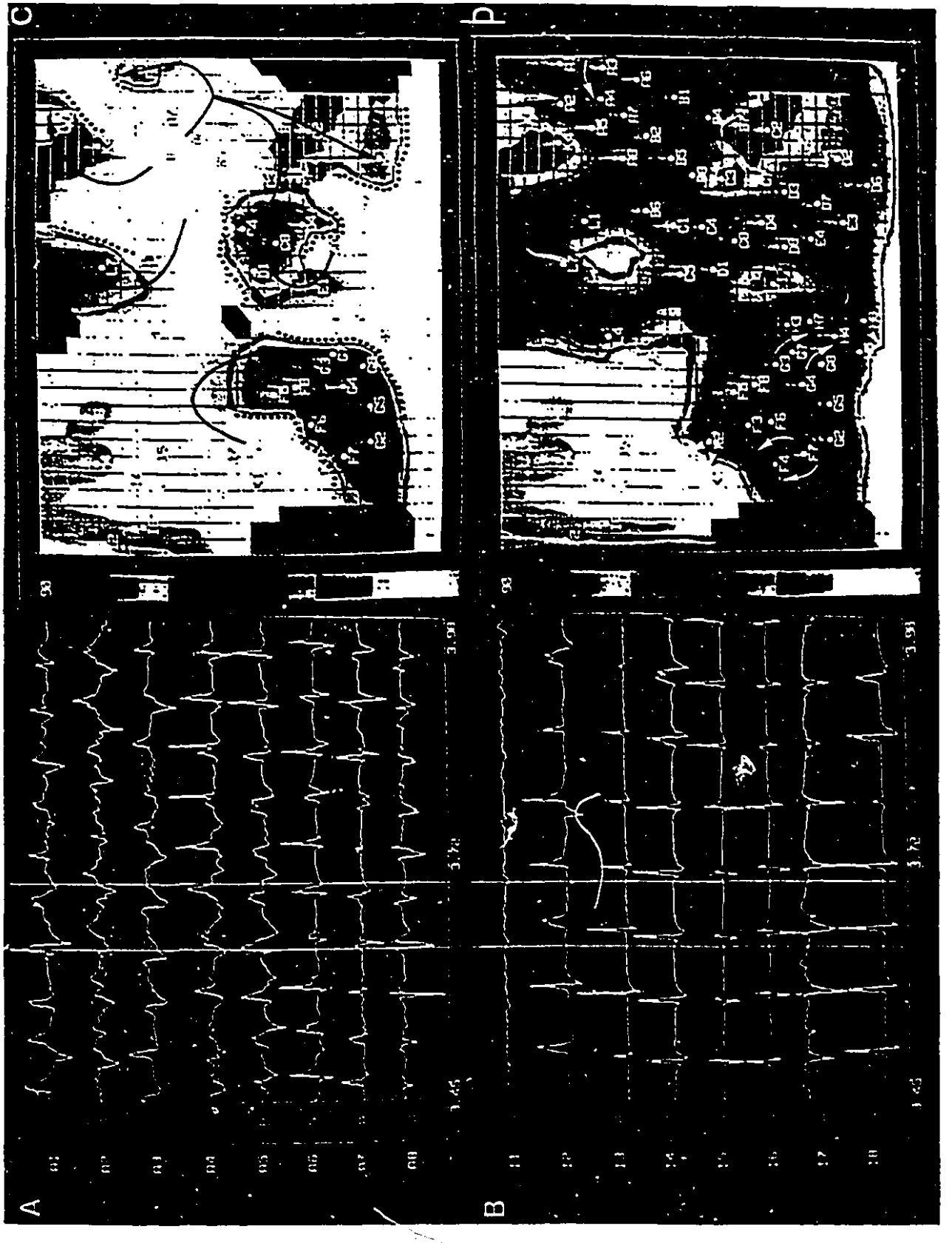

In contrast to the limited information available about mechanisms of drug action in atrial fibrillation, much more work has been done to evaluate drug effects in animal models of atrial flutter.[39–43] Agents that terminate atrial flutter share an ability to increase atrial refractoriness.[39,40,42] On the other hand, the termination of atrial flutter by class I agents appears to be associated with conduction slowing and not with an increased wavelength or decreased excitable gap.[41,43] The mechanism of experimental atrial flutter following atrial inci-

FIGURE 7. Panels A *and* B: *Recordings from 16 electrodes (sites indicated at left, A_1–A_8, I_1–I_8) during sustained AF under control conditions. Time scale (bottom of each panel) is in seconds. One cycle of activation in electrodes I_1–I_8, delimited by the vertical lines, was selected for activation mapping.* Panel C: *Activation map constructed using the time of the first activation at each site during the cycle shown in panels A and B. Each color represents a 10-msec isochrone, with the scale shown at the left. Regions of crowded isochrones (dotted lines) indicate slow conduction and/or block, forcing propagation into pathways designated by the black arrows.* Panel D: *Activation map, constructed using the second activation at each site during the cycle delimited by the vertical lines in panels A and B. White arrows indicate possible directions of impulse propagation from sites activated late in panel C (e.g., F_6, F_7, G_7, G_8, and A_3) to zones previously activated at the beginning of the cycle (F_3, H_3, A_4). White arrowheads indicate propagation from zones activated late in panel D toward zones activated only once during the cycle (e.g., K_1, J_7, H_2, and H_6) that initiates the next cycle. (For detailed discussion, see text.)*

sion involves reentry around a fixed anatomic barrier[44] and is therefore quite different from the functional "multiple wavelet" reentry occurring during atrial fibrillation.[45]

Possible Mechanisms Underlying Flecainide's Actions

Flecainide slowed atrial conduction and increased the refractory period. Whereas both actions were rate dependent, effects on refractoriness predominated, as indicated by drug-induced increases in the wavelength. Conceptually, the wavelength indicates the minimum path length that can support reentry. The relation between wavelength and the occurrence of reentry was first described by Mines.[46] The concept was further developed by Lewis[47] and formulated mathematically by Wiener and Rosenblueth.[33] While Lewis' analysis of the wavelength was based on an anatomically fixed reentry circuit, the wavelength concept was linked to a functionally determined form of reentry by the "leading circle" model of Allessie et al.[48] The latter concept is more directly pertinent to the type of system described in the present study, in which zones of regional refractoriness, rather than anatomic barriers, determine propagation patterns during arrhythmia. In fact, the likelihood of atrial flutter and atrial fibrillation have recently been shown to relate closely to the wavelength in atrial tissue.[31,37] Decreases in atrial wavelength reduce the size of atrial reentry circuits, reduce the revolution time, and facilitate the induction of atrial flutter and fibrillation.[49] Increases in wavelength have the opposite effect.[31,37] In the presence of vagal stimulation, wavelength at a short BCL (150 msec) averaged less than 7 cm (Figure 4), a value below the threshold wavelength for AF of 7.8 cm noted by Rensma et al.[31] As a result of tachycardia-dependent ERP prolongation, flecainide increased the wavelength under the same conditions to about 9 cm, a value similar to control in the absence of vagal stimulation and a value at which AF cannot be sustained. The effects of flecainide that we observed on the size, number, and cycle lengths of atrial reentry circuits are all consistent with the predicted consequences of the increases in wavelength that were produced by the drug. In addition to increasing atrial wavelength, flecainide reduced regional disparities in atrial ERP and wavelength in both the presence and absence of vagal stimulation (Figures 10 and 11). This property could contribute to flecainide's ability to prevent the occurrence of AF by reducing the heterogeneity of atrial refractory properties, particularly in the presence of increased vagal tone.

The probable central mechanism in flecainide's actions on atrial wavelength is its ability to cause tachycardia-dependent increases in atrial APD, resulting in parallel changes in refractoriness.[25,38] The underlying ionic mechanisms remain to be determined. Flecainide blocks the delayed rectifier current (i_k) in cat ventricular myocytes.[50] While i_k is a major repolarizing current in many cardiac tissues,[51] it appears to be of little importance in canine[52] atrial tissue and has been reported to be negligible in humans.[53] The transient outward current (i_{to}) is of greater importance in dog and human atrial cells,[52,53] but flecainide is a relatively weak blocker of this current.[52] Since decreases in atrial APD accommodation to heart rate appear to underlie flecainide's rate-dependent effects on repolarization, studies of the ionic mechanism underlying APD accommodation may provide deeper insights into the drug's ionic properties. We have provided preliminary evidence that at least in canine atrium, flecainide's effect on APD accommodation may be due to reduced sodium entry resulting in a diminution of electrogenic Na^+,K^+-ATPase activity.[54]

Clinical Relevance

While atrial fibrillation remains a common clinical arrhythmia,[1] it is often resistant to drug therapy. The effectiveness of class Ic drugs opens up a new, potentially useful therapeutic option, but one whose mechanism has been uncertain.[15] In the present work, we have shown that tachycardia-dependent atrial ERP prolongation accounts for the efficacy of flecainide in a dog model of AF. Since the rate dependence of flecainide's effects on APD and atrial ERP of isolated human tissue is even greater than its rate dependence on dog atrium,[25] it is likely that similar mechanisms account for the drug's ability to terminate AF in humans. Boahene et al[55] have noted a marked increase in the AA interval produced by propafenone before AF termination. This finding is analogous to the effect of flecainide on AF cycle length that we observed before termination (Figure 10) and suggests an increase in the wavelength after propafenone administration in humans.

The ability of class Ic agents to terminate AF decreases with increasing duration of the arrhythmia.[9,11,56,57] When AF is treated within 48 hours of its onset, class Ic agents terminate the arrhythmia in 70–86% of cases.[9,11,56,57] In our dog model of acute AF, flecainide was uniformly effective if enough of the drug was given. In fact, efficacy in most dogs occurred at a dose (1 mg/kg) equal to the effective dose reported for humans.[7,9–12] A recent clinical study suggests that the persistence of AF may result in structural (and presumably functional) abnormalities of atrial tissue.[58] The reduced efficacy of class Ic agents in chronic AF may be caused by the marked abnormalities in cellular electrophysiology often associated.[59,60] The membrane

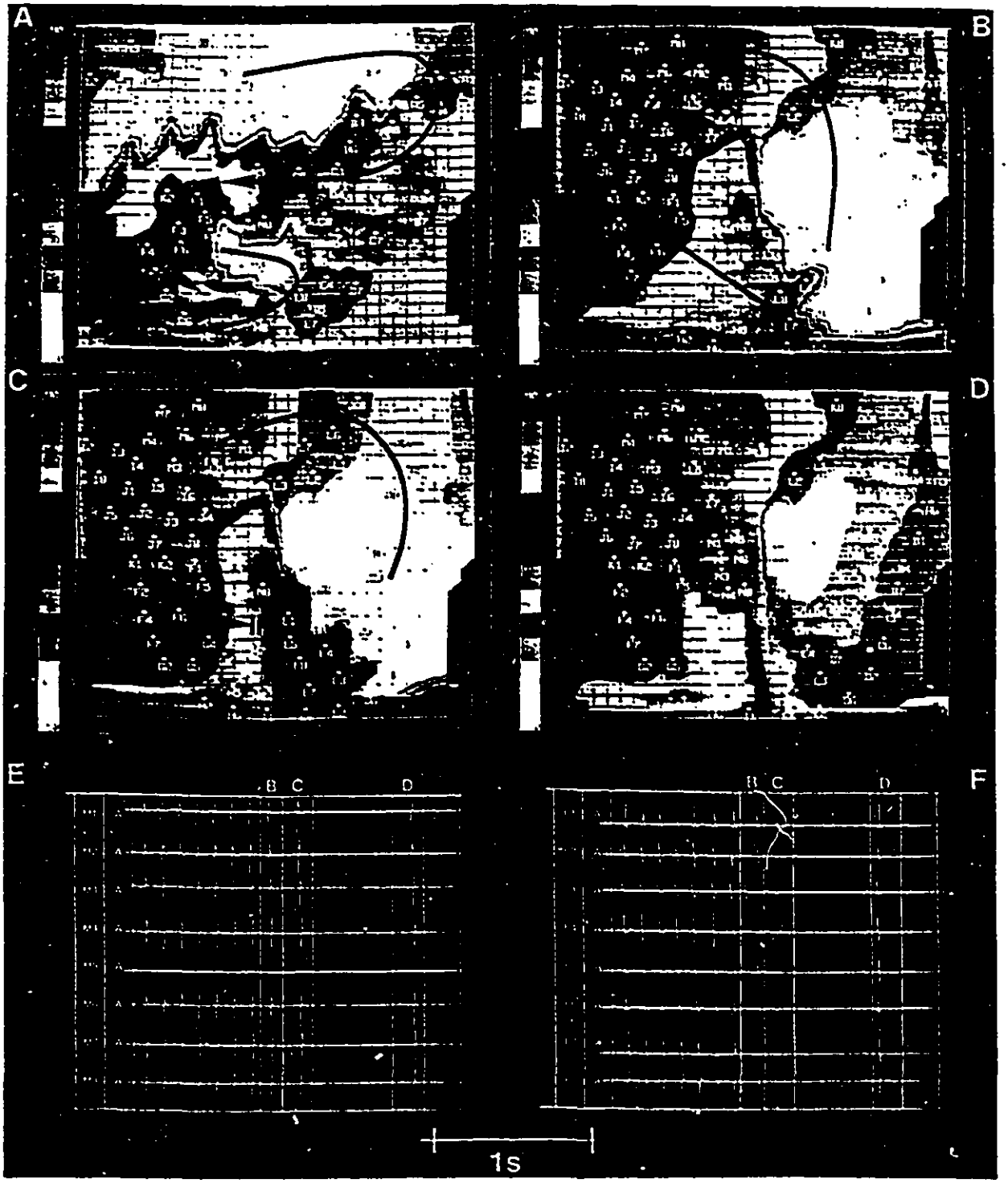

FIGURE 8. *Activation maps after flecainide administration to the same dog whose results under control conditions are shown in Figure 7.* Panel A: *Five minutes after flecainide administration, activation is more homogeneous and there are two large clockwise reentry circuits.* Panel B: *Penultimate cycle of atrial fibrillation (AF) after flecainide administration. A single large counterclockwise reentry pattern is present.* Panel C: *The last cycle of AF in the presence of flecainide. Failure of propagation into the dark blue zone (electrodes E_1–E_8, shown in panel F) results in arrhythmia termination.* Panel D: *The first atrial activation after termination of AF. The activation pattern is very similar to activation during sinus rhythm under control conditions (Figure 6), although propagation is slowed, reflecting the conduction slowing action of flecainide.* Panels E and F: *Electrograms recorded at the time of AF termination by flecainide. The cycles designated B, C, and D are delimited by pairs of vertical lines, and their activation maps are shown in corresponding panels B, C, and D. Similar patterns of activation leading to AF termination after flecainide were seen in eight other dogs. Note that the low-amplitude potentials in electrodes E_1–E_7 in cycle C and after cycle D are reflections of ventricular activation and correspond in time to the QRS on the surface ECG.*

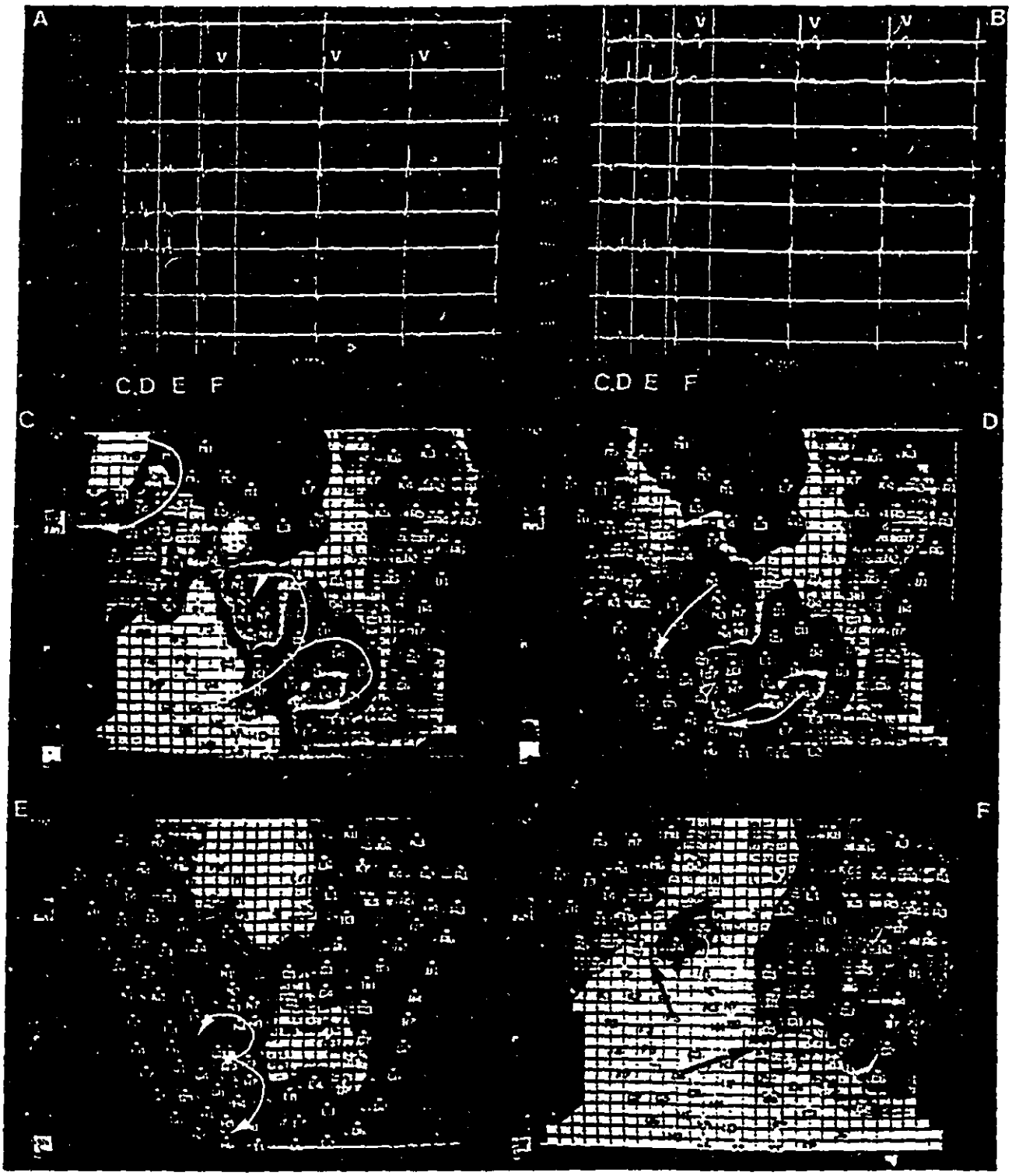

FIGURE 9. *Example of termination of atrial fibrillation (AF) by a mechanism different from that shown in Figure 8.* Panels A *and* B: *Electrograms from 16 sites recorded at the time of termination of AF. The vertical lines designate the last three cycles recorded in electrodes H_3, H_4, and H_5 before the resumption of sinus rhythm. V, electrograms corresponding to ventricular activation.* Panel C: *Isochrone activation map of third to last cycle, using first time of activation at each site.* Panel D: *Activation map of same cycle as shown in panel C but with second activation used to time activation at sites activated twice during the cycle.* Panels E *and* F: *Activation maps of cycles designated by E and F in panels A and B. (For detailed discussion, see text.)*

depolarization, sodium channel inactivation, and severe conduction slowing that occur with chronic atrial disease would decrease the wavelength, making the arrhythmia intrinsically more resistant. Furthermore, they might sensitize the tissue to the sodium-channel blocking and conduction slowing actions of flecainide,

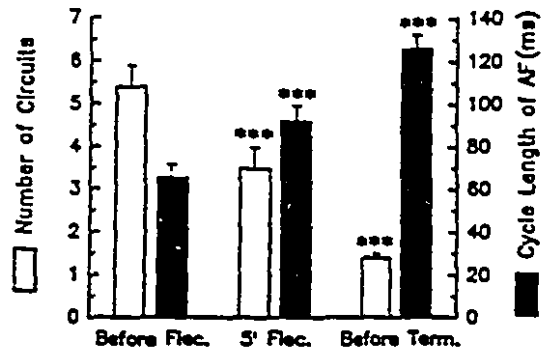

FIGURE 10. *Mean number (+SEM) of simultaneous reentry circuits (open bars) before atrial fibrillation (AF) and 5 minutes after flecainide (Flec.) administration, and mean (+SEM) cycle length (filled bars) of AF. For definitions and description of method of measurement, see text.* ***p<0.001 *compared with control.*

offsetting the increases in refractoriness caused by the drug.

We found that flecainide always regularized AF before terminating the arrhythmia. The regularization resulted from a reduction in the number of simultaneous reentry circuits, an effect consistent with the increase in atrial wavelength caused by the drug. One clinical complication that has been noted with class Ic agents has been the conversion of atrial fibrillation to slow atrial flutter, sometimes causing 1:1 conduction and a rapid ventricular response.[61,62] This observation is compatible with our finding that flecainide decreased the number and increased the size of reentry circuits, often leading to a single macro-reentrant loop, before arrhythmia termination and supports the concept of a class Ic drug-induced increase in atrial wavelength as a mechanism of its clinical action on AF.

An ability to prolong refractoriness without altering conduction would be the ideal property of a drug to treat reentrant arrhythmias. Unfortunately, currently available class 3 drugs increase APD in a bradycardia-dependent way, favoring the occurrence of early afterdepolarizations and torsades de pointes ventricular arrhythmias at slow heart rates.[63] If an agent could be found that selectively increases APD at the rapid rates associated with reentrant arrhythmia, the risk of drug-induced long QT syndromes would be minimized without necessarily limiting drug efficacy.[64] Flecainide's actions on atrial APD and refractoriness appear to possess this desirable tachycardia dependence. Unfortunately, the indications for using flecainide in the treatment of AF remain to be clarified, in view of the Cardiac Arrhythmia Suppression Trial (CAST) results indicating that the drug increases the risk of sudden death among patients with frequent ventricular ectopy after a myocardial infarction.[65] The mechanism of this adverse effect is unclear, but evidence points toward an arrhythmogenic effect of strong sodium-channel blockade in the presence of acute myocardial ischemia.[66-68] If the ionic mechanism of flecainide's rate-dependent APD-prolonging properties were identified and could be dissociated from sodium-channel blockade, molecular modification could result in a compound with improved efficacy against AF with limited adverse effects. The

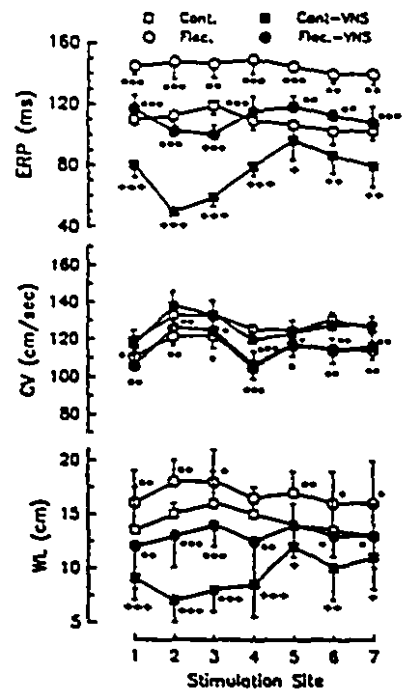

FIGURE 11. *Atrial effective refractory period (ERP), conduction velocity (CV), and wavelength (WL) measured at a cycle length of 250 msec during periods of stimulation at each of the seven sites indicated in Figure 1. Measurements were obtained under control conditions (Cont.), during vagal stimulation in the absence of flecainide (Cont.–VNS), and then in the presence (Flec.–VNS) and absence (Flec.) of vagal stimulation after a dose of flecainide that terminated atrial fibrillation.* *p<0.05, **p<0.01, ***p<0.001 *compared with corresponding drug-free condition;* *p<0.05, **p<0.01, ***p<0.001 *for vagal stimulation (in absence of drug) compared with control.*

relative safety of class Ic compounds compared with alternative therapies for AF remains uncertain. For example, a recent meta-analysis suggests that quinidine therapy may result in a much higher mortality among patients treated for ventricular ectopy than several other drugs, including flecainide.[69]

Limitations of the Present Work

The major potential limitation of the present work is the specific nature of the animal model. It is likely that the properties of atrial fibrillation in the vagotonic dog model are different from arrhythmias in the diseased, dilated atria associated with chronic AF in humans. On the other hand, the dog model may more closely resemble paroxysmal AF, particularly in patients with relatively normal atria. Moreover, the occurrence of AF in some cases of paroxysmal arrhythmia in humans appears to depend on increases in vagal tone.[70] Flecainide therapy was highly effective in a group of 40 patients with drug-resistant AF, 31 of whom had a vagally dependent form of arrhythmia.[5]

The wavelength is rate dependent and likely shorter during the rapid activation characteristic of AF than during sinus rhythm. Conduction velocity and refractory period cannot be measured directly during AF, and the

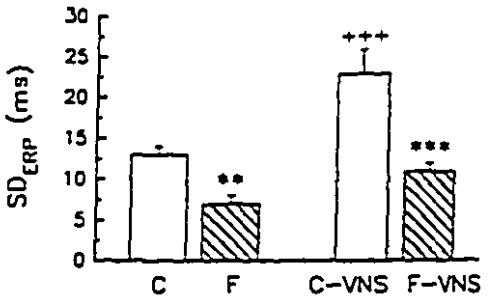

FIGURE 12. *Standard deviation of atrial effective refractory period (SD_{ERP}) at seven sites as measured under control conditions (C), after flecainide (F), drug-free with vagal stimulation (C–VNS), and in the presence of both flecainide and vagal nerve stimulation (F–VNS).* **p<0.012, ***p<0.001 *compared with corresponding drug-free control,* ***p<0.001 *vagal stimulation versus control.*

wavelength cannot be directly calculated. We are therefore forced to draw inferences about flecainide's actions on wavelength from its effects during rapid 1:1 atrial pacing. However, given the slope of the relation between drug effects on atrial ERP and the BCL (Figure 4), it is likely that flecainide's effect on wavelength during AF is larger, if anything, than its effect during rapid atrial pacing.

Activation mapping of reentry is most easily interpreted when applied to single, discrete macro-reentry circuits. There are major limitations, particularly in terms of resolution, when studying nonfixed, multiple wavelet reentry, particularly of the type seen under control conditions in the presence of vagal stimulation. Our goal was not, however, to study in detail the physiological mechanism of AF, which has been well described previously,[22,48,49] with our results being in qualitative agreement. Our goal was rather to evaluate the effects of flecainide on epicardial activation during vagally induced AF and to observe (if possible) the activation changes leading to arrhythmia termination. We found that flecainide qualitatively altered epicardial activation in this model of AF and led to arrhythmia termination in a fashion entirely compatible with its observed effects on wavelength. While procainamide has been shown to stabilize AF by reducing the number of apparent reentry circuits,[71] we are unaware of studies in the literature on the changes in epicardial activation on drug termination of AF.

The basic train used to evaluate ERP consisted of 10 basic (S_1) stimuli, which is much less than the mean onset time constant of about 30 beats for flecainide block of maximal phase 0 upstroke velocity in vitro[72] or conduction slowing in vivo.[73] However, because of the drug's very slow recovery kinetics,[74] the 10-msec decrements in coupling interval of the S_2 extrastimulus should not have had any detectable effect on the level of sodium channel block. Furthermore, since the extrastimulus was consistently inserted after every 10 S_1 stimuli and caused capture until the refractory period had been attained, the activation rate and level of block should have been quite constant until the atrial ERP had been measured. All conduction time measurements were obtained before ERP determination during pacing at the BCL, which had been continued for at least 2 minutes without the introduction of any extrastimuli.

Conclusions

Flecainide causes rate-related increases in atrial ERP and the wavelength for atrial reentry in the dog. It predictably terminates AF (which is otherwise sustained) in the presence of vagal stimulation, with effects on atrial activation during AF consistent with its rate-dependent effects on refractoriness and wavelength. These properties may underlie the beneficial actions of flecainide on atrial fibrillation in humans.

Acknowledgments

The authors thank Christine Villemaire, Nancy Turmel, Emma Deblasio, and Carol Matthews for excellent technical assistance and Lise de Repentigny and Mary Morello for typing the manuscript. We also thank Squibb Pharmaceuticals and Riker-3M Pharmaceuticals for supplying us with the nadolol and flecainide used for these studies.

References

1. Herre JM, Scheinman MM: Supraventricular tachycardia, in Parmley WW, Chatterjee K, Cheitlin MD, Karliner JS, Rapaport E, Scheinman MM (eds): *Cardiology: Physiology, Pharmacology, Diagnosis.* Philadelphia, J.B. Lippincott Co., 1988, pp 1–19
2. Antman EM, Beamer AD, Cantillon C, McGowan N, Friedman PL: Propafenone for suppression of refractory symptomatic atrial fibrillation. (abstract) *Circulation* 1987;76(suppl IV):IV-68
3. Hammill S, Wood D, Sugrue D, Gersh B, Osborn M, Holmes D: Propafenone for chronic treatment of paroxysmal atrial fibrillation. (abstract) *Circulation* 1985;72(suppl III):III-171
4. Kerr CR, Mason MA, Chung DC: Propafenone: An effective drug for prevention of recurrent atrial fibrillation. (abstract) *Circulation* 1985;72(suppl III):III-171
5. Chouty F, Coumel P: Oral flecainide for prophylaxis of paroxysmal atrial fibrillation. *Am J Cardiol* 1988;62:35D–37D
6. Kappenberger LJ, Fromer MA, Shenasa M, Gloor HO: Evaluation of flecainide acetate in rapid atrial fibrillation complicating Wolff-Parkinson-White syndrome. *Clin Cardiol* 1985;8:321–326
7. Goy JJ, Maendly R, Grbic M, Finci L, Sigwart U: Cardioversion with flecainide in patients with atrial fibrillation of recent onset. *Eur J Clin Pharmacol* 1985;27:737–738
8. Berns E, Rinkenberger RL, Jeang MK, Dougherty AH, Jenkins M, Naccarelli GV: Efficacy and safety of flecainide acetate for atrial tachycardia or fibrillation. *Am J Cardiol* 1987;59:1337–1341
9. Crijns HJGM, van Wijk LM, van Gilst WH, Kingma JH, van Gelder IC, Lie KI: Acute conversion of atrial fibrillation to sinus rhythm: Clinical efficacy of flecainide acetate: Comparison of two regimens. *Eur Heart J* 1988;9:634–638
10. Goy JJ, Kaufmann U, Kappenberger L, Sigwart U: Restoration of sinus rhythm with flecainide in patients with atrial fibrillation. *Am J Cardiol* 1988;62:38D–40D
11. Borgeat A, Goy JJ, Maendly R, Kaufmann U, Grbic M, Sigwart U: Flecainide versus quinidine for conversion of atrial fibrillation to sinus rhythm. *Am J Cardiol* 1986;58:496–498
12. Suttorp MJ, Kingma JH, Lie-A-Huen L, Mast EG: Intravenous flecainide versus verapamil for acute conversion of paroxysmal atrial fibrillation or flutter to sinus rhythm. *Am J Cardiol* 1989;63:693–696
13. van Gelder I, Crijns HJ, van Gilst WH, Lie KI: Efficacy of flecainide to maintain sinus rhythm after cardioversion of chronic atrial fibrillation and flutter. (abstract) *Circulation* 1988;78(suppl II):II-626
14. Rasmussen K, Andersen A, Abrahamsen AM, Overskeid K, Bathen J: Flecainide versus disopyramide in maintaining sinus rhythm following conversion of chronic atrial fibrillation. (abstract) *Eur Heart J* 1988;9(suppl I):I-52
15. Marchlinski FE: Propafenone: New therapy for a tough, old arrhythmia. *J Am Coll Cardiol* 1988;12:1012–1014
16. Campbell TJ: Kinetics of onset of rate-dependent effects of Class I antiarrhythmic drugs are important in determining their effects on refractoriness in guinea-pig ventricle, and provide a theoretical basis for their subclassification. *Cardiovasc Res* 1983;17:344–352
17. Harrison DC: Antiarrhythmic drug classification: New science and practical applications. *Am J Cardiol* 1985;56:185–187

18. Zipes DP: Genesis of cardiac arrhythmias, in Braunwald E (ed): *Heart Disease*, ed. 3. Philadelphia, WB Saunders Co, 1988, pp 581–620
19. Bigger JT, Hoffman BF: Antiarrhythmic drugs, in Gilman AG, Goodman LL, Kall TW, Murad F (eds): *The Pharmacological Basis of Therapeutics*, ed. 7. New York, Macmillan Publishing Co., 1985, pp 748–783
20. Moe GK, Rheinboldt WC, Abildskov JA: A computer model of atrial fibrillation. *Am Heart J* 1964;67:200–220
21. Abildskov JA, Millar K, Burgess MJ: Atrial fibrillation. *Am J Cardiol* 1971;28:263–267
22. Allessie MA, Lammers WJEP, Bonke FIM, Hollen J: Experimental evaluation of Moe's multiple wavelet hypothesis of atrial fibrillation, in Zipes DP, Jalife J (eds): *Cardiac Electrophysiology and Arrhythmias*, New York, Grune & Stratton, Inc, 1985, pp 265–276
23. Chen PS, Smith WM, Greer S, Wharton JM, Vidaillet HJ Jr, Ideker RE: Activation patterns during electrically induced atrial fibrillation in humans. (abstract) *Circulation* 1986;74(suppl II):II-483
24. Wang Z, Pelletier LC, Talajic M, Nattel S: Effects of flecainide and quinidine on human atrial action potentials: Role of rate-dependence and comparison with guinea pig, rabbit, and dog tissues. *Circulation* 1990;82:274–283
25. Wang Z, Villemaire C, Pagé P, Nattel S: Mechanism of flecainide's beneficial actions in experimental atrial fibrillation. (abstract) *Circulation* 1990;82(suppl III):III-98
26. Talajic M, Villemaire C, Nattel S: Electrophysiological effects of α-adrenergic stimulation. *PACE* 1990;13:578–582
27. Nattel S, Jing W: Rate-dependent changes in intraventricular conduction produced by procainamide in anesthetized dogs: A quantitative analysis based on the relation between phase 0 inward current and conduction velocity. *Circ Res* 1989;65:1485–1498
28. Gallagher JJ, Kasell JH, Cox JL, Smith WM, Ideker RE, Smith WM: Techniques of intraoperative electrophysiologic mapping. *Am J Cardiol* 1982;49:221–240
29. Gallagher JJ, Kasell J, Sealy WC, Pritchett ELC, Wallace AG: Epicardial mapping in the Wolff-Parkinson-White syndrome. *Circulation* 1978;57:854–866
30. Alessi R, Nusynowitz M, Abildskov JA, Moe GK: Nonuniform distribution of vagal effects on the atrial refractory period. *Am J Physiol* 1958;192:406–410
31. Rensma PL, Allessie MA, Lammers WJEP, Bonke FIM, Schalij MJ: Length of excitation wave and susceptibility to reentrant atrial arrhythmias in normal conscious dogs. *Circ Res* 1988;62:395–410
32. Goldstein A: *Biostatistics—An Introductory Text*. New York, MacMillan Publishers, 1964
33. Wiener N, Rosenblueth A: The mathematical formulation of the problem of conduction of impulses in a network of connected excitable elements, specifically in cardiac muscle. *Arch Inst Cardiol Mex* 1946;16:205–265
34. Goodman D, Van der Steen ABM, Van Dam RT: Endocardial and epicardial activation pathways of the canine right atrium. *Am J Physiol* 1971;220:1–11
35. El-Sherif N, Smith RA, Evans K: Canine ventricular arrhythmias in the late myocardial infarction period: 8. Epicardial mapping of reentrant circuits. *Circ Res* 1981;49:255–265
36. Mehra R, Zeiler RH, Gough WB, El-Sherif N: Reentrant ventricular arrhythmias in the late myocardial infarction period: 9. Electrophysiologic-anatomic correlation of reentrant circuits. *Circulation* 1983;67:11–24
37. Kirchhof C, Wijffels M, Brugada J, Planellas J, Allessie M: Mode of action of a new class 1C drug (ORG 7797) against atrial fibrillation in conscious dogs. *J Cardiovasc Pharmacol* 1991;17:116–124
38. O'Hara G, Talajic M, Villemaire C, Nattel S: Effects of flecainide on atrial refractoriness, atrial repolarization, and atrioventricular nodal conduction in anesthetized dogs. *J Am Coll Cardiol* (in press)
39. Feld GK, Venkatesh N, Singh BN: Pharmacologic conversion and suppression of experimental canine atrial flutter: Differing effects of *d*-sotalol, quinidine, and lidocaine and significance of changes in refractoriness and conduction. *Circulation* 1986;74:197–204
40. Boyden PA: Effects of pharmacologic agents on induced atrial flutter in dogs with right atrial enlargement. *J Cardiovasc Pharmacol* 1986;8:170–177
41. Wu KM, Hoffman BF: Effect of procainamide and N-acetylprocainamide on atrial flutter: Studies in vivo and in vitro. *Circulation* 1987;76:1397–1408
42. Feld GK, Venkatesh N, Singh BN: Effects of N-acetylprocainamide and recainam in the pharmacologic conversion and suppression of experimental canine atrial flutter: Significance of changes in refractoriness and conduction. *J Cardiovasc Pharmacol* 1988;11:573–580
43. Spinelli W, Hoffman BF: Mechanisms of termination of reentrant atrial arrhythmias by class I and class III antiarrhythmic agents. *Circ Res* 1989;65:1565–1579
44. Frame LH, Page RL, Boyden PA, Fenoglio JJ, Hoffman BF: Circus movement in the canine atrium around the tricuspid ring during experimental atrial flutter and during reentry in vitro. *Circulation* 1987;76:1155–1175
45. Allessie MA, Lammers WJEP, Bonke FIM, Hollen J: Experimental evaluation of Moe's multiple wavelet hypothesis of atrial fibrillation, in Zipes DP, Jalife J (eds): *Cardiac Electrophysiology and Arrhythmias*, Orlando, Fla, Grune & Stratton, Inc, 1985, pp 265–276
46. Mines GR: On dynamic equilibrium in the heart. *J Physiol* 1913; 46:349–383
47. Lewis T: *The Mechanism and Graphic Registration of the Heart Beat*, ed 3. London, Shaw & Sons, 1925, pp 319–324
48. Allessie MA, Bonke FIM, Schopman FJG: Circus movement in rabbit atrial muscle as a mechanism of tachycardia: III. The "leading circle" concept: A new model of circus movement in cardiac tissue without the involvement of an anatomical obstacle. *Circ Res* 1977;41:9–18
49. Smeets JLRM, Allessie MA, Lammers WJEP, Bonke FIM, Hollen J: The wavelength of the cardiac impulse and reentrant arrhythmias in isolated rabbit atrium. *Circ Res* 1986;58:96–108
50. Follmer CH, Colatsky TJ: Block of delayed rectifier potassium current, I_K, by flecainide and E-4031 in cat ventricular myocytes. *Circulation* 1990;82:289–293
51. Colatsky TJ, Follmer CH, Starmer CF: Channel specificity in antiarrhythmic drug action: Mechanism of potassium channel block and its role in suppressing and aggravating cardiac arrhythmias. *Circulation* 1990;82:2235–2242
52. Fermini B, Nattel S: Differential effects of flecainide and quinidine on repolarizing currents in dog atrial myocytes. (abstract) *Circulation* 1990;82(suppl III):III-526
53. Shibata EF, Drury T, Refsum H, Aldrete V, Giles W: Contributions of a transient outward current to repolarization in human atrium. *Am J Physiol* 1989;257:H1773–H1781
54. Wang Z, Fermini B, Nattel S: Mechanisms of tachycardia-dependent atrial APD prolongation by flecainide in dogs. (abstract) *Can J Cardiol* 1991;7(suppl A):123A
55. Boahene KA, Klein GJ, Yee R, Sharma AD, Fujimura O: Termination of acute atrial fibrillation in the Wolff-Parkinson-White syndrome by procainamide and propafenone: Importance of atrial fibrillatory cycle length. *J Am Coll Cardiol* 1990;16:1408–1414
56. Wiseman MN, Nathan AW: Intravenous flecainide versus intravenous disopyramide in the reversion of atrial fibrillation. (abstract) *J Am Coll Cardiol* 1989;13:165A
57. Bianconi L, Boccadamo R, Pappalardo A, Gentili C, Pistolese M: Effectiveness of intravenous propafenone for conversion of atrial fibrillation and flutter of recent onset. *Am J Cardiol* 1989;64:335–338
58. Sanfilippo AJ, Abascal VM, Sheehan M, Oertel LB, Harrigan P, Hughes RA, Weyman AE: Atrial enlargement as a consequence of atrial fibrillation. *Circulation* 1990;82:792–797
59. Ten Eick RE, Singer DH: Electrophysiological properties of diseased human atrium: I. Low diastolic potential and altered cellular response to potassium. *Circ Res* 1979;44:545–557
60. Mary-Rabine L, Albert A, Pham TD, Hordof A, Fenoglio JJ Jr, Malm JR, Rosen MR: The relationship of human atrial cellular electrophysiology to clinical function and ultrastructure. *Circ Res* 1983;52:188–199
61. Murdock C, Kyles A, Yeung-Lai-Wah J, Qi A, Kerr CR: Conversion of atrial fibrillation to flutter with propafenone. (abstract) *Clin Invest Med* 1989;12(suppl C):C45
62. Feld GK, Chen PS, Nicod P, Fleck RP, Mezer D: Atrial proarrhythmic effects of class 1C antiarrhythmic drugs. *Am J Cardiol* 1990;66:378–383
63. Jackman WM, Friday KJ, Anderson JL, Aliot EM, Clark M, Lazzara R: The long QT syndromes: A critical review, new clinical observations and a unifying hypothesis. *Prog Cardiovasc Dis* 1988;31:115–172
64. Hondeghem LM, Snyders DJ: Class III antiarrhythmic agents have a lot of potential but a long way to go: Reduced effectiveness and dangers of reverse use dependence. *Circulation* 1990;81:686–690
65. The Cardiac Arrhythmia Suppression Trial (CAST) Investigators: Preliminary report: Effect of encainide and flecainide on mortality in a randomized trial of arrhythmia suppression after myocardial infarction. *N Engl J Med* 1989;321:406–412

66. Nattel S, Pedersen DH, Zipes DP: Alterations in regional myocardial distribution and arrhythmogenic effects of aprindine produced by coronary artery occlusion in the dog. *Cardiovasc Res* 1981;15:80–85
67. Lederman SN, Wenger TL, Bolster DE, Strauss HC: Effects of flecainide on occlusion and reperfusion arrhythmias in dogs. *J Cardiovasc Pharmacol* 1989;13:541–546
68. Nattel S, Waters D: What is an antiarrhythmic drug? From clinical trials to fundamental concepts. *Am J Cardiol* 1990;66:96–100
69. Morganroth J, Goin JE: Quinidine-related mortality in the short-to-medium-term treatment of ventricular arrhythmias: A meta-analysis. *Circulation* 1991;84:1977–1983
70. Coumel P, Leclercq JF, Attuel P, Lavallée JP, Flammang D: Autonomic influences in the genesis of atrial arrhythmias: Atrial flutter and fibrillation of vagal origin. in Narula DS (ed): *Cardiac Arrhythmias—Electrophysiology, Diagnosis and Management.* Baltimore, Md, Williams and Williams, 1979, pp 243–255
71. Pagé PL, Hassanalizadeh, Cardinal René: Transitions among atrial fibrillation, atrial flutter, and sinus rhythm during procainamide infusion and vagal stimulation in dogs with sterile pericarditis. *Can J Physiol Pharmacol* 1991;69:15–24
72. Campbell TJ: Kinetics of onset of rate-dependent effects of class I antiarrhythmic drugs are important in determining their effects on refractoriness in guinea-pig ventricle, and provide a theoretical basis for their subclassification. *Cardiovasc Res* 1983;17:344–352
73. Ranger S, Talajic M, Lemery R, Roy D, Villemaire C, Nattel S: Kinetics of use-dependent ventricular conduction slowing by antiarrhythmic drugs in humans. *Circulation* 1991;83:1987–1994
74. Campbell TJ: Importance of physio-chemical properties in determining the kinetics of the effects of class I antiarrhythmic drugs on maximum rate of depolarization in guinea-pig ventricle. *Br J Pharmacol* 1983;80:33–40

The above study led to three important conclusions:

(1) Use-dependent increase in ERP which resulted in lengthening of WL confers drug efficacy in terminating AF. It appears, therefore, that this property is a clinically desirable drug action;

(2) Our results demonstrated that the persistence of AF is the consequence of 5-6 co-existent reentry circuits in the atria, which is consistent with the "multiple wavelet" hypothesis of AF established by Moe[2-2], and evidenced by later studies[2-3,4].

(3) We provided three lines of evidence indicating that ERP, WL, and CV are the three major determinants of reentry as proposed by previous investigators[2-5]. First, vagal stimulation with sufficient intensity to maintain sustained AF substantially shortened atrial ERP and WL and increased the spatial inhomogeneity of ERP; second, short cycle lengths of AF and multiple micro-reentry circuits during AF were all typical of small values of ERP and WL; third, an intervention which lengthened ERP and WL converted AF to sinus rhythm.

The questions raised from these results were:

(1) Is this use-dependent ERP (and APD) prolongation limited specifically to flecainide or common to other class Ic drugs?

(2) Is use-dependent ERP (and APD) prolongation really favourable over reverse use-dependent drug action against AF?

Our subsequent study was designed to answer these questions.

References

2-2. Moe GK. On the multiple wavelet hypothesis of atrial fibrillation. Arch Int Pharmacodyn Ther 1962;140:183-188.

2-3. Allessie MA, Lammers WJEP, Bonke FIM. Experimental evaluation of Moe's multiple wavelet hypothesis of atrial fibrillation. In: Zipes DP, Jalife J (eds): Cardiac Arrhythmias. New York, Grune & Stratton, 1985,pp265-276.

2-4. Schuessler RB, Grayson TM, Bromberg BI, Cox JL, Boineau JP. Cholinergically mediated tachyarrhythmias induced by a single extrastimulus in the isolated canine right atrium. Circ Res 1992;71:1254-1267.

2-5. Rensma PL, Allessie MA, Lammers WJEP. The length of the excitation wave as an index for the susceptibility to reentrant atrial arrhythmias. Circ Res 1988;62:395-410.

Comparative Mechanisms of Antiarrhythmic Drug Action in Experimental Atrial Fibrillation

Importance of Use-Dependent Effects on Refractoriness

Jinjun Wang, MD; Gerald W. Bourne, MD; Zhiguo Wang, MSc; Christine Villemaire, MScA; Mario Talajic, MD; Stanley Nattel, MD

Background. Antiarrhythmic drugs are considered to terminate atrial fibrillation by prolonging refractoriness, but direct experimental evaluation of this concept has been limited. The atria are activated rapidly during atrial fibrillation, and antiarrhythmic drugs are known to have important rate-dependent actions. The potential role of such properties in determining drug effects during atrial fibrillation has not been evaluated.

Methods and Results. We evaluated the effects of representative class Ia (procainamide), Ic (propafenone), and III (sotalol) antiarrhythmic drugs on sustained cholinergic atrial fibrillation and atrial electrophysiological properties in anesthetized, open-chest dogs. Loading and maintenance doses were used to produce stable plasma concentrations, and computer-based 112-electrode epicardial mapping was used to study atrial conduction and activation during atrial fibrillation. Clinically used doses of procainamide and propafenone terminated atrial fibrillation in 13 of 13 (100%) and 7 of 10 (70%) dogs, respectively, but a dose of sotalol (2 mg/kg IV) in the clinical range terminated atrial fibrillation in only 2 of 8 (25%) dogs (P=.0005 vs procainamide, P=.08 vs propafenone). Procainamide and propafenone prevented atrial fibrillation induction in 13 of 13 (100%) and 7 of 10 (70%) dogs, respectively, compared with none of 8 dogs for 2 mg/kg sotalol (P<.0001 vs procainamide, P=.004 vs propafenone). A larger dose of sotalol (cumulative dose, 8 mg/kg) was uniformly effective in terminating atrial fibrillation and preventing its induction. All drugs significantly increased atrial refractory period, with effects that were use dependent for propafenone but reverse use dependent for sotalol. Effective doses of all drugs significantly increased the wavelength for reentry at rapid atrial rates in the presence of vagal stimulation into the range observed under drug-free conditions in the absence of vagal input. The inefficacy of clinical doses of sotalol was explained by the reverse use dependence of its effects on refractoriness, which resulted in reduced effects on wavelength at rapid rates. The effects of propafenone on refractoriness were significantly increased at rapid rates, contributing to its ability to increase wavelength and terminate atrial fibrillation. Activation mapping showed that drugs terminated atrial fibrillation by reducing the number and increasing the size of reentry circuits, leading to termination by mechanisms related to block in the remaining circuit(s).

Conclusions. We conclude that antiarrhythmic drugs terminate experimental atrial fibrillation by increasing the wavelength for reentry at rapid rates, leading to a reduction in the number of functional reentry circuits and, eventually, failure of reentrant excitation. Use-dependent effects on refractoriness can limit (in the case of the reverse use dependence of sotalol) or contribute (in the case of propafenone) to antiarrhythmic drug efficacy against atrial fibrillation by determining drug-induced changes in wavelength at rapid atrial rates. (*Circulation.* 1993;88:1030-1044.)

KEY WORDS • propafenone • sotalol • procainamide • antiarrhythmia agents

Atrial fibrillation is the most common sustained cardiac arrhythmia in clinical practice[1,2] and is likely to become more common with the aging of the population.[1-3] Antiarrhythmic drugs have been used to convert atrial fibrillation since Thomas Lewis' work with quinidine in 1922.[4] Drugs used to convert atrial fibrillation have included quinidine,[4-6] procainamide,[7,8] propafenone,[9-11] flecainide,[12-20] sotalol,[21] and amiodarone.[20,22]

Experimental studies of antiarrhythmic drug action in atrial fibrillation have been limited. Rensma and colleagues[23] showed that drug effects on the atrial rhythm response to premature stimulation are related to changes in the wavelength for reentry. A subsequent study showed that an experimental class Ic drug reduces the duration of atrial fibrillation induced by burst pacing in awake dogs.[24] We found that clinically used doses of flecainide were highly effective in terminating sustained, vagotonic atrial fibrillation in the dog.[25] The drug's efficacy appeared to be due to tachycardia-dependent increases in atrial effective refractory period, which outweighed conduction changes and increased the

Received January 5, 1993; revision accepted April 7, 1993.

From the Department of Medicine (J.W., G.W.B., C.V., M.T., S.N.), Montreal Heart Institute and University of Montreal, and Departments of Pharmacology and Therapeutics and Medicine (Z.W., S.N.), McGill University, Montreal, Canada.

Correspondence to Dr Stanley Nattel, Montreal Heart Institute, 5000 Belanger St E, Montreal, Quebec, Canada H1T 1C8.

wavelength. These actions are consistent with the ability of flecainide to produce rate-dependent increases in atrial action potential duration in vitro[26] and in vivo.[27]

It remains uncertain whether these properties are peculiar to flecainide or are common to class Ic compounds. Furthermore, the antiarrhythmic mechanisms of other drugs in atrial fibrillation remain poorly understood and have not been tested in experimental sustained atrial fibrillation. We designed the present work to study (1) the efficacy of representative class Ia, Ic, and III drugs in experimental atrial fibrillation; (2) their rate-dependent actions on atrial effective refractory period and conduction; and (3) the mechanisms whereby they terminate atrial fibrillation.

We studied procainamide as a class Ia drug because intravenous procainamide is often used to terminate acute atrial fibrillation in humans and the drug causes less hypotension than quinidine. We chose the class Ic compound propafenone because other than flecainide, it is the only Ic agent widely used to treat clinical atrial fibrillation. To evaluate class III action, we used *d,l*-sotalol. Because our dogs are β-blocked with nadolol, any effects observed with sotalol cannot be mediated by interactions with β-adrenergic receptors.

Methods

Adult mongrel dogs of either sex (weight, 21 to 31 kg) were anesthetized with morphine (2 mg/kg IM) and α-chloralose (100 mg/kg IV) and ventilated with room air supplemented with oxygen. Respiratory parameters were adjusted to maintain physiological arterial blood gases (SaO_2, more than 90%; pH 7.38 to 7.44). Catheters were inserted into the left femoral artery and both femoral veins and kept patent with heparinized saline solution (0.9%). A median sternotomy was performed, and a pericardial cradle was created. Body temperature was maintained at 37 to 39°C with a homeothermic heating blanket. Two bipolar Teflon-coated stainless-steel electrodes were inserted into the right atrial appendage for recording and stimulation. A programmable stimulator (Digital Cardiovascular Instruments, Berkeley, Calif) was used to deliver 4-ms pulses at twice-threshold current. A demand pacemaker (GBM 5880, Medtronic Inc, Minneapolis, Minn) was used to pace the right ventricle when the ventricular rate was less than 90 min^{-1}. A P23 1D transducer (Statham Medical Instruments, Los Angeles, Calif), electrophysiological amplifiers (Bloom Ltd, Flying Hills, Pa), and a paper recorder (Astromed MT-95000, Toronto, Ontario) were used to record six standard surface ECG leads, an atrial electrogram, and stimulus artifacts.

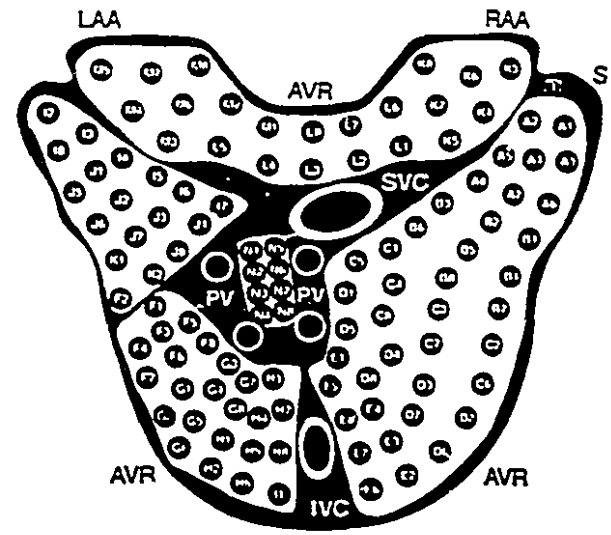

FIG 1. *Diagram of electrode arrays and bipolar electrode stimulation site. LAA indicates left atrial appendage; AVR, atrioventricular ring; RAA, right atrial appendage; and S, stimulation site.*

Nadolol was administered as an initial dose of 0.5 mg/kg IV, followed by 0.25 mg/kg every 2 hours.[28]

Atrial Fibrillation Model

The cervical vagal trunks were isolated and decentralized, and bipolar hook electrodes were inserted via a 21-gauge needle into the middle of each nerve, with the electrode running parallel to vagal fibers for several centimeters.[29] The Teflon insulation was removed from the distal 1 cm of each electrode. Bilateral vagal nerve stimulation was delivered by a DS-9F stimulator (Grass Instruments, Inc, Quincy, Mass) with a pulse width of 0.1 ms and an applied voltage of 5 V. The stimulation frequency was adjusted in each dog to two thirds of the threshold for asystole under control conditions. In the presence of vagal stimulation, a short burst (1 to 3 seconds) of atrial pacing (10 Hz frequency, four times threshold current) induced atrial fibrillation. Atrial fibrillation persisted in the presence of vagal stimulation for more than 30 minutes and terminated within seconds after stopping vagal stimulation. Atrial fibrillation was defined as a rapid (more than 500 min^{-1} under control conditions), irregular atrial rhythm with varying atrial electrogram morphology. To control for time-dependent changes in vagal actions, the vagal frequency-response relation was assessed before each atrial

TABLE 1. Doses of Antiarrhythmic Drugs and Resulting Plasma Concentrations

Drug	Loading dose (mg/kg)*	Maintenance dose ($mg \cdot kg^{-1} \cdot h^{-1}$)	Plasma concentration (mg/L)	
			5 Min MD	40 Min MD
Procainamide	12.5	25	16.7±1.1	19.5±1.9
Propafenone	2	4	3.0±0.6	2.8±0.3
Sotalol (dose 1)	2	1	4.0±0.5	3.0±0.3
Sotalol (dose 2)	6	3	12.3±1.9	9.9±1.6

5 Min MD and 40 Min MD indicate results obtained 5 and 40 minutes after starting the maintenance dose, respectively.

*The loading dose was administered over 15 minutes, and the maintenance infusion was begun immediately after the end of the loading dose.

TABLE 2. Efficacy of Propafenone, Procainamide, and Sotalol in Terminating Atrial Fibrillation and Preventing Atrial Fibrillation Induction

	Termination (%)	Time (min)	Ability to induce AF‡	
			Sustained AF	Nonsustained AF
Propafenone	7/10 (70)	11±5	3/10*	2/7
Procainamide§	13/13† (100)	10±2	0/13†	2/13
Sotalol (2 mg/kg)	2/8 (25)	10±3	8/8	...
Sotalol (6 mg/kg)	8/8* (100)	6±3	0/8†	0/8

*$P<.01$, †$P<.001$ compared with efficacy of 2 mg/kg sotalol.

‡Data shown are for the number of dogs in whom atrial fibrillation could be induced during the maintenance infusion. The denominator for nonsustained atrial fibrillation induction is the number of dogs in whom sustained atrial fibrillation could not be induced, and the numerator is the number of these animals in which nonsustained atrial fibrillation could be induced by bursts of atrial pacing.

§Includes eight dogs studied with the standard protocol, and five dogs in whom vagal stimulation frequency was increased by 80% for atrial fibrillation induction before drug infusion (see Fig 3).

fibrillation induction, and the vagal stimulation frequency was adjusted to produce consistent sinus node slowing. A similar procedure was used to establish vagal stimulation parameters during maintenance drug infusion.

Activation Mapping

Five thin plastic sheets containing 112 bipolar electrodes with 1-mm interpolar and 6-mm interelectrode distances were sewn into position on the atrial epicardial surface (Fig 1). One sheet was placed under the root of the aorta to cover the anterior aspect of the atrial appendages and Bachman's bundle. Three sheets were sewn to the posterior aspects of the atrial appendages and to the free walls. The parietal pericardium was gently separated, and a fifth plaque was placed between the pulmonary arteries and veins.

Each signal was filtered (30 to 400 Hz), digitized with 12-bit resolution and a 1-kHz sampling rate, and transmitted into a microcomputer (model 286, Compaq Computer, Houston, Tex). Software routines were used to amplify, display, and analyze each electrogram signal as well as to generate activation maps.[30] Each electrogram was analyzed with computer-determined peak-amplitude criteria[31,32] and was reviewed manually. The accuracy of activation time measurements was ±0.5 ms. The maps displayed in this manuscript were photographed directly from the monitor screen—artistic renditions and tracings were avoided to prevent distortion of the data.

Assessment of Vagal Frequency-Response Relations

To dissociate direct drug effects on atrial fibrillation from antivagal actions, vagal frequency-response curves were obtained before and after drug administration. Vagal stimulation voltage was kept constant, and the vagus nerves were stimulated for 30 seconds at frequencies ranging from 2 to 10 Hz, with a 30-second rest period between stimulations at each frequency. Heart rate was determined over the last 20 seconds of each stimulation period. Change in heart rate was plotted against vagal stimulation frequency, and stimulation frequency was adjusted during each maintenance infusion to produce the same effect on sinus rate as observed under control conditions.

Experimental Design

Conduction velocity and refractory period were assessed after at least 2 minutes of constant pacing at basic cycle lengths between 150 and 400 ms. The effective refractory period was measured with a train of 15 basic (S_1) stimuli followed by a premature (S_2) stimulus. The effective refractory period was defined as the longest S_1S_2 interval failing to produce a propagated response. Activation maps during steady-state pacing were generated offline after the experiment, and con-

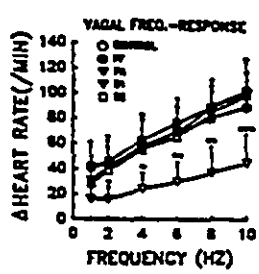

FIG 2. *Plot of vagal frequency-response curve for changes in sinus node rate (Δ heart rate, mean±SEM). Control results were not significantly different from those for propafenone (PF), sotalol dose 1 (S1), or sotalol dose 2 (S2). Procainamide (PA) significantly attenuated the effects of vagal stimulation (*P<.05, **P<.01 vs control at same frequency) (n=10 dogs for propafenone and 8 each for procainamide and each dose of sotalol).*

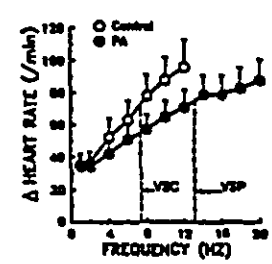

FIG 3. *Plot of vagal frequency-response curves for five experiments in which vagal frequency was increased by 80% during atrial fibrillation before procainamide infusion. Procainamide (PA) attenuated the effects of vagal stimulation, but the vagal frequency used to support atrial fibrillation under control conditions (mean, 7.3 Hz; VSC) resulted in a sinus bradycardic effect similar to the effect in the presence of PA of the vagal frequency used to produce atrial fibrillation immediately before procainamide infusion (12.5 Hz; VSP).*

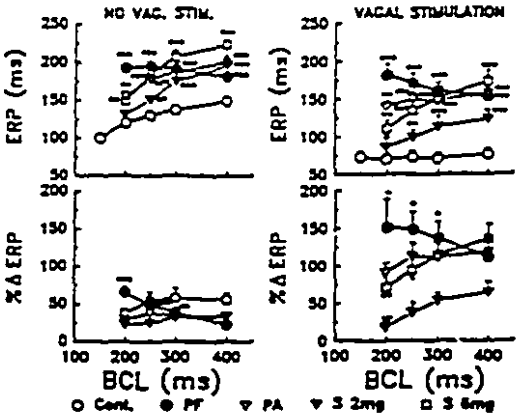

FIG 4. *Plots of effects of antiarrhythmic drugs on atrial effective refractory period (ERP) in the absence (left) and presence (right) of vagal stimulation respectively. Top, Values (mean±SEM) of atrial ERP under control (Cont.) conditions, in the presence of propafenone (PF) and procainamide (PA), and after 2 mg/kg (S 2mg) and 6 mg/kg (S 6mg) doses of sotalol, respectively. Where no error bar is visible, it falls within the symbol for the mean. *P<.05, **P<.01, ***P<.001 compared with control at same cycle length. Bottom, Percent change in ERP compared with control at the same frequency caused by each drug. *P<.05, **P<.01, ***P<.001 compared with the effect of same drug at a cycle length of 400 ms.*

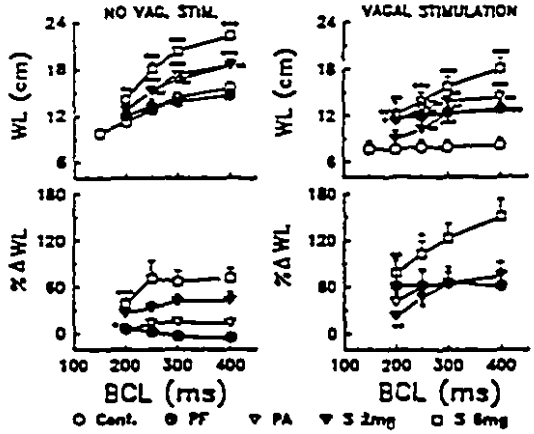

FIG 6. *Plots of effects of antiarrhythmic drugs on wavelength (WL) in the absence (left) and presence (right) of vagal stimulation, respectively. Top, Values (mean±SEM) of WL under control (Cont.) conditions, in the presence of propafenone (PF) and procainamide (PA), and after 2 mg/kg (S 2mg) and 6 mg/kg (S 6mg) doses of sotalol, respectively. *P<.05, **P<.01, ***P<.001 compared with control at same cycle length. Bottom, Percent change in WL compared with control at the same frequency caused by each drug. *P<.05, **P<.01, ***P<.001 compared with the effect of same drug at a cycle length of 400 ms.*

duction time was determined between a site adjacent to the stimulating electrode and another site in the direction of rapid propagation. Interelectrode distance was divided by conduction time to calculate conduction velocity. The same sites were used for conduction velocity measurements during control and drug infusion

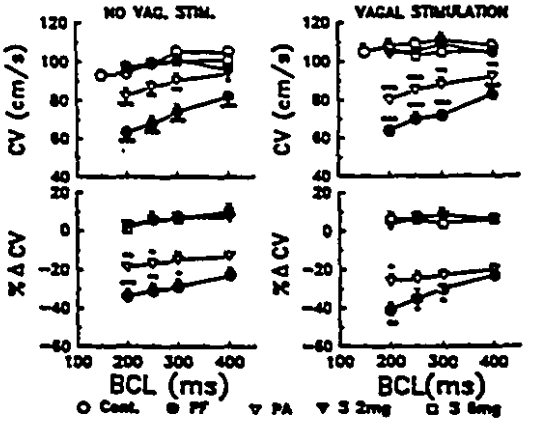

FIG 5. *Plots of effects of antiarrhythmic drugs on conduction velocity (CV) in the absence (left) and presence (right) of vagal stimulation, respectively. Top, Values (mean±SEM) of CV under control (Cont.) conditions, in the presence of propafenone (PF) and procainamide (PA), and after 2 mg/kg (S 2mg) and 6 mg/kg (S 6mg) doses of sotalol, respectively. *P<.05, **P<.01, ***P<.001 compared with control at same cycle length. Bottom, Percent change in CV compared with control at the same frequency caused by each drug. *P<.05, **P<.01, ***P<.001 compared with the effect of same drug at a cycle length of 400 ms.*

periods, after ensuring a constant pattern of impulse propagation.

After conduction velocity and effective refractory period had been measured at all cycle lengths in the absence of vagal stimulation, atrial fibrillation was induced, and an 8-second window of electrogram data was obtained. Vagal stimulation was continued for 30 minutes to verify the stability of atrial fibrillation and then stopped to allow a return to sinus rhythm. Measurements of conduction velocity and effective refractory period then were obtained during vagal stimulation at all cycle lengths.

After the acquisition of baseline data, one of the drugs listed in Table 1 was selected. Vagal stimulation

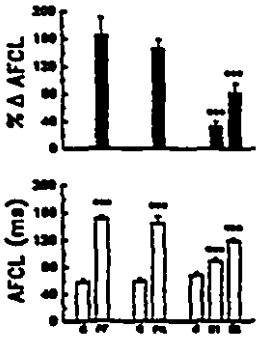

FIG 7. *Bottom, Mean (+SEM) atrial fibrillation cycle length (AFCL) under control conditions (C) and immediately before atrial fibrillation termination by propafenone (PF), procainamide (PA), and the higher dose of sotalol (S2) as well as the value at the end of the loading dose of low-dose sotalol (S1). ***P<.001 vs control. Top, Percent increase in AFCL caused by propafenone, procainamide, and either dose of sotalol relative to control. ***P<.001 vs effect of PF or PA.*

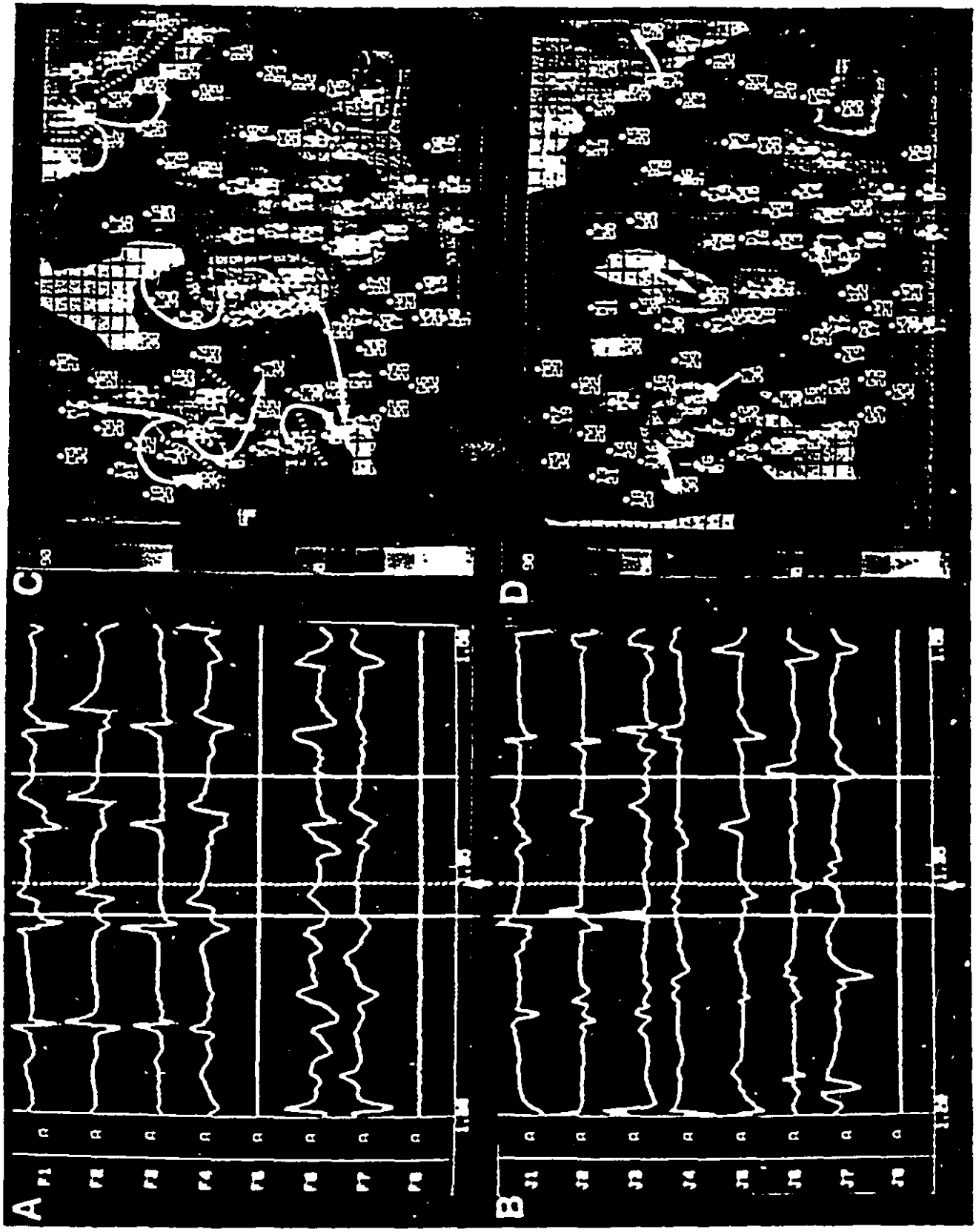

was begun, and atrial fibrillation was initiated. When atrial fibrillation had persisted for 5 minutes, the drug was administered as a loading dose over 15 minutes, followed by the maintenance dose. If atrial fibrillation was terminated, an 8-second window of activation data was acquired, with the trigger for data acquisition set to obtain at least 2 seconds of data before termination. If atrial fibrillation was not terminated within 30 minutes,

FIG 8. *Atrial activation during fibrillation in the presence of vagal stimulation and the absence of antiarrhythmic drugs. A and B, Analog data from 16 electrode sites. Yellow numbers at bottom of each panel indicate time in seconds. Solid vertical lines indicate window being mapped; dotted vertical line is reference time (0). C, Isochrone map of first activation at all sites. D, Map created using second activation for sites reactivated during the window. Scales for isochrones are at the left of each panel. In all maps, each electrode site is indicated by a code corresponding to electrode site codes in Fig 1. The number under the electrode code is the activation time (in ms) relative to the reference. (For discussion, see text.)*

vagal stimulation was stopped to restore sinus rhythm. Atrial fibrillation reinduction then was attempted. Atrial fibrillation was considered nonsustained if it persisted for less than 30 seconds and sustained if it persisted for more than 30 seconds. The measurements of effective refractory period, conduction velocity (with and without vagal stimulation), and response to vagal stimulation were repeated in the presence of the drug. All dogs receiving sotalol had the above procedures performed after an initial dose of 2 mg/kg and again after an additional 6 mg/kg. Plasma drug concentrations were measured by previously described high-performance liquid chromatography approaches.[30,33,34] A total of 10 dogs received propafenone, 13 received procainamide, and 8 received both doses of sotalol.

Data Analysis

Group values are presented as mean±SEM values. Comparisons between groups of data were performed by two-way ANOVA with Scheffe's test, and comparisons between two means only were made by Student's *t* test. A two-tailed $P<.05$ was taken to indicate statistical significance. Rate dependence of effects was evaluated by an *F* test for interaction. Wavelength (λ) was calculated with the formulation of Wiener and Rosenblueth,[35] according to the relation λ=effective refractory period×conduction velocity.

Results

Effects of Antiarrhythmic Drugs to Terminate Atrial Fibrillation and Prevent Its Reinduction

At loading doses similar to clinical doses,[7,9,11] propafenone and procainamide terminated atrial fibrillation in a majority of dogs (70% and 100%, respectively; *P*=NS; Table 2). A loading dose of sotalol (2 mg/kg) similar to the clinical dose (1.5 mg/kg)[36,37] terminated atrial fibrillation in only two dogs (25%), but an additional 6 mg/kg (cumulative dose, 8 mg/kg) terminated atrial fibrillation in all.

Sustained atrial fibrillation could be induced in only 3 of 10 dogs (30%) after propafenone (the dogs in whom propafenone failed to terminate atrial fibrillation) and in no dogs after procainamide or high-dose sotalol. After low-dose sotalol, however, sustained atrial fibrillation could be induced in all dogs (Table 2). The prevention of atrial fibrillation induction could not be due to antivagal actions because vagal frequency was readjusted during each maintenance dose to produce the same bradycardic effect as under control conditions (see "Methods").

Neither propafenone nor sotalol showed significant antivagal actions (Fig 2). Procainamide, on the other hand, significantly reduced the bradycardic effects of vagal stimulation (Fig 2), consistent with its ability to block ganglionic transmission.[38] The termination of atrial fibrillation by procainamide thus could have been due to antivagal actions. To control for antivagal actions, we studied five additional dogs in which vagal stimulation frequency was increased by 80% during atrial fibrillation before procainamide infusion. The adequacy of this adjustment was assessed by comparing the control vagal frequency-response curve to the curve in the presence of procainamide after atrial fibrillation termination (Fig 3) and by showing that the increase in vagal stimulation frequency caused a bradycardic effect in the presence of procainamide similar to the effect under control conditions of the lower vagal frequency. Procainamide terminated atrial fibrillation in all five dogs, despite this compensation for the drug's antivagal actions.

Drug Effects on Effective Refractory Period, Conduction Velocity, and Wavelength

Atrial effective refractory period decreased with decreasing cycle length under control conditions in the absence of vagal stimulation (Fig 4). Propafenone reversed the rate dependence of atrial effective refractory period so that it increased with decreasing cycle length. Consequently, propafenone increased atrial effective refractory period more at faster rates. Sotalol showed an opposite profile of action, with effects being largest at long cycle lengths (slow rates). Vagal stimulation markedly abbreviated atrial effective refractory period, whereas all three drugs increased atrial effective refractory period.

To appreciate better the rate dependence of drug action, we calculated the drug-induced increase in effective refractory period relative to the corresponding control value at each cycle length in each experiment (Fig 4, bottom). Effects at a given cycle length that are significantly different from those at a basic cycle length of 400 ms are shown by the asterisks in the lower panels of Fig 4. A similar approach was taken to the analysis of rate-dependent changes in conduction velocity (Fig 5) and wavelength (Fig 6). The effects of sotalol were dose dependent and increased with increasing cycle length. Propafenone increased effective refractory period most at short cycle lengths, whereas procainamide's actions did not change with cycle length. All drugs increased atrial effective refractory period more in the presence of vagal stimulation (right) than in its absence (left).

Changes in conduction velocity are illustrated in Fig 5. Neither vagal stimulation nor sotalol altered conduction velocity. Sotalol's ability to increase effective refractory period without changing conduction velocity confirms its class III actions in the canine atrium. Propafenone and procainamide slowed atrial conduction, with their effects exaggerated by decreasing basic cycle length. Drug effects on conduction were not altered by vagal stimulation.

Vagal stimulation strongly reduced the wavelength for refractory (Fig 6), decreasing the value at a cycle length of 150 ms from a mean of 11.1±0.4 cm to 7.1±0.4 cm ($P<.001$). Sotalol's effects on wavelength were reduced as cycle length decreased, paralleling its actions on

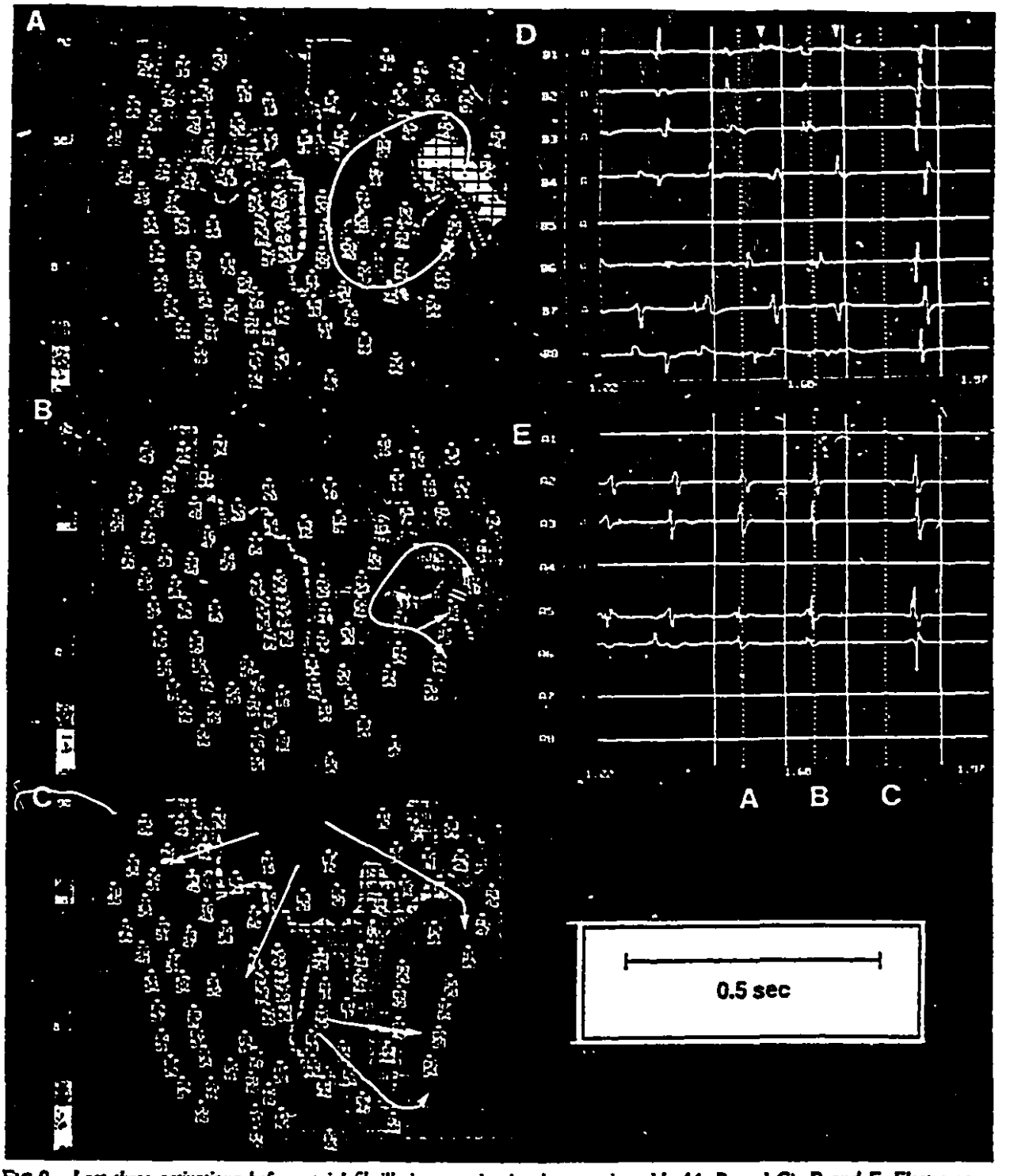

FIG 9. *Last three activations before atrial fibrillation termination by procainamide (A, B, and C). D and E. Electrograms recorded from electrodes B1-B8 and A1-A8. Solid vertical lines delimit cycles corresponding to maps A through C, and dotted vertical lines indicate reference points (time 0). Horizontal scale indicates 0.5 second. (For discussion, see text.)*

effective refractory period. In the presence of vagal stimulation, large changes in effective refractory period resulted in substantial prolongation of wavelength by propafenone. In the absence of vagal stimulation, propafenone had little effect on wavelength, with a greater tendency to increase wavelength at smaller, compared with larger, cycle lengths (Fig 6, bottom left). Procainamide increased wavelength in a rate-independent fashion.

During vagal stimulation, propafenone, procainamide, and high-dose sotalol increased wavelength (basic cycle length, 200 ms) from about 8 cm to 12 cm, similar to control values without vagal stimulation. Because of reverse use-dependent effects on effective

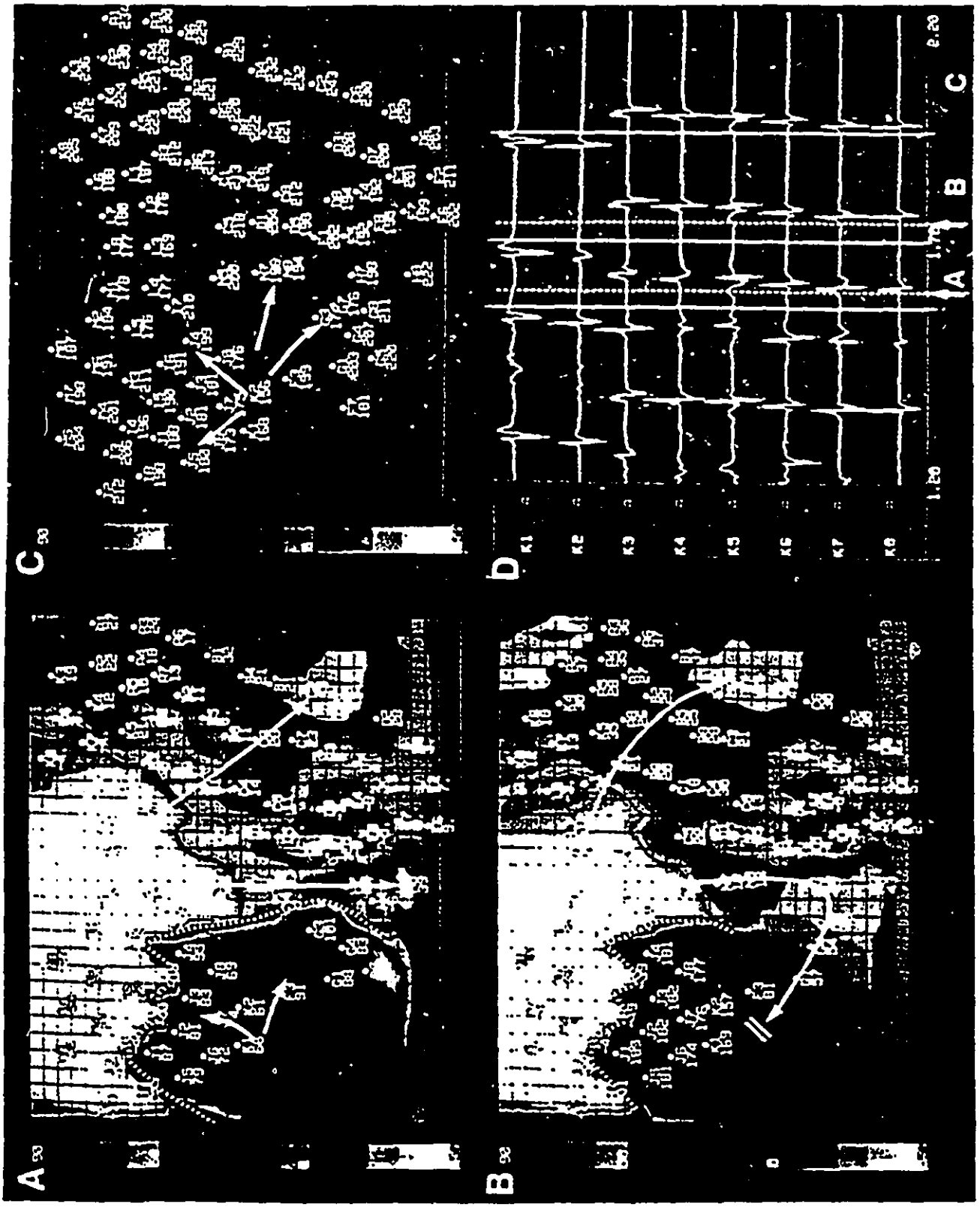

FIG 10. *Maps of last three cycles before atrial fibrillation termination by propafenone. A, B, and C, Maps corresponding to cycles A, B, and C in panel D. Solid vertical lines delimit cycles, whereas dotted vertical lines indicate reference point (time 0) for cycle A (first line) and cycles B and C (second line). Yellow numbers at bottom of panel D indicate time in seconds. (For discussion, see text.)*

refractory period, 2 mg/kg sotalol did not significantly alter wavelength at a basic cycle length of 200 ms during vagal stimulation.

The control data in Figs 4 through 6 are mean values for dogs receiving all drugs. To have shown control results for each individual drug would have so compli-

cated the figures that they would have become indecipherable. Because of small differences in control values among groups of dogs, the percent changes at the bottom of each figure do not correspond exactly to the values expected based on differences from overall control means shown at the top of each figure. Note also that the statistical significance shown at the top of each figure (Figs 4 through 6) is between drug and control values (raw data) at each basic cycle length, whereas the statistical significance at the bottom is for the comparison between percent change produced by a drug at a given basic cycle length and its effects at a basic cycle length of 400 ms.

Drug Effects on Activation During Atrial Fibrillation

All three agents slowed atrial activation during atrial fibrillation. Figure 7 shows the mean cycle length of atrial fibrillation under control conditions and immediately prior to atrial fibrillation termination. The mean atrial fibrillation cycle length was determined, as previously done,[25] by counting the number of cycles over a 1-second period. The cycle length of atrial fibrillation was determined for at least 16 electrode sites widely dispersed over the atria, and the average at all sites was taken to represent the atrial fibrillation cycle length. Although all three agents increased the atrial fibrillation cycle length, the atrial fibrillation slowing effect of sotalol was significantly less than that of the other two drugs.

The mechanism of drug termination of atrial fibrillation was further explored on the basis of activation mapping. Figure 8 shows activation data during atrial fibrillation under control conditions. Analog recordings from selected sites are at the left, and the solid vertical lines delimit the time interval over which the activation maps shown at the right were constructed. The reference point (time 0) for the maps is indicated by the dotted vertical lines. The map at the upper right (panel C) shows the activation map based on the first activation within the time window at each site. Seven zones of early activation (red or orange) are present, along with several zones of late activation (blue). The map at the lower right (D) is based on the second time of activation at each site and shows six zones of latest activation (darker blue). The latter correspond to zones activated early in panel C and likely to have been reactivated as a result of local reentry circuits.

Consider electrograms J1 through J8. J2 and J3 are initially activated just at the onset of the window. The impulse propagates through J6 and J7, passing close to J5 as shown by the low-amplitude potential at that site. Zones of crowded isochrones representing slow conduction or block are indicated by the stippled lines above and below the J2-J3 zone in panel C. The impulse travels superiorly around this region of functional block to activate I4, J1, and then J5. The latter is activated 52 ms after initial activation at J2, and J2 is reactivated 9 ms later, just before reactivation at J3 (panel B). The activation-reactivation interval at J2 is 61 ms, in the range of atrial effective refractory period during vagal stimulation. Similar reentry cycles occur at F2, N5, and K3-K6. The activation-reactivation intervals in each zone are similar to the mean atrial fibrillation cycle lengths at the bottom of Fig 7.

Figure 9 shows the change in activation caused by procainamide immediately before termination of atrial fibrillation in the same dog as Fig 8. Figure 9, A shows activation during the corresponding interval indicated on the electrogram recordings (panels D and E) at the right. A single macroreentry pattern is present, beginning at electrodes B1 and B2 and ending at site B4. A small second deflection at B1 (indicated by the arrow) suggests invasion of adjacent tissue by another wave front. Slow conduction from B4 to B1 initiates the next cycle (panel B), which has a conduction pattern similar to that shown in panel A. There is, however, a subtle difference, with B4 activated slightly earlier in cycle B, before activation at C2. In contrast to cycle A, in which the second deflection at B1 indicated by the arrow precedes activation at B4 by at least 30 ms, a similar deflection in cycle B occurs slightly after activation at B4. Perhaps as a result of this low-amplitude activation, block occurs between B4 and B1, and reentry is terminated. The next cycle is delayed and has initial activation in the sinus node region (D5) and Bachman's bundle (M1, L7), followed by rapid activation of both atria. Comparison between Figs 8 and 9 indicates that procainamide reduced the number of reentry circuits and increased their size until conduction failure in a critical zone led to arrhythmia termination.

Figure 10 shows an example of atrial fibrillation termination by propafenone. Activation begins near Bachman's bundle (sites L2-L4) and proceeds rapidly through both atria toward the atrioventricular ring. A zone of relative refractoriness is present in the posterior left atrium, and activation in this region begins at sites K1 and K2, resulting in rather symmetrical activation in this zone. The mechanism by which the impulse reaches K1 and K2 is unclear, but it may involve conduction from C2 and C3 or H8 via the septum. The next activation (panel B) begins at sites activated early in the preceding cycle (A) adjacent to the zone activated late in cycle A. The posterior left atrium superior to (and including) sites K1 and K2 is activated with a substantial delay, indicating block in the conduction path by which K1 and K2 were previously excited. Because of this delay, the remaining portions of the atria recover excitability and are activated rapidly and symmetrically from the region around K1 and K2. This last activation is illustrated in panel C, in which activation times are referenced to the same time point as in cycle B. As in Fig 9, the drug resulted in a large macroreentry circuit. Block in a critical zone led to recovery of remaining atrial tissue, with consequent rapid, symmetrical activation precluding the possibility of further reentrant cycles.

Figures 11 and 12 illustrate the effects of low- and high-dose sotalol, respectively, on atrial activation during atrial fibrillation. Electrogram recordings from eight sites under control conditions are shown in Fig 11, panel A, and recordings from the same sites after the administration of 2 mg/kg sotalol are shown in panel D. Panels B and C show activation maps of one cycle of control atrial fibrillation, whereas E and F show corresponding maps for a cycle in the presence of sotalol. There are four zones of early activation (yellow) in panel B, with slow conduction around areas of functional block leading to delayed activation (green zones) adjacent to sites of early activity. Subsequent propagation to the early

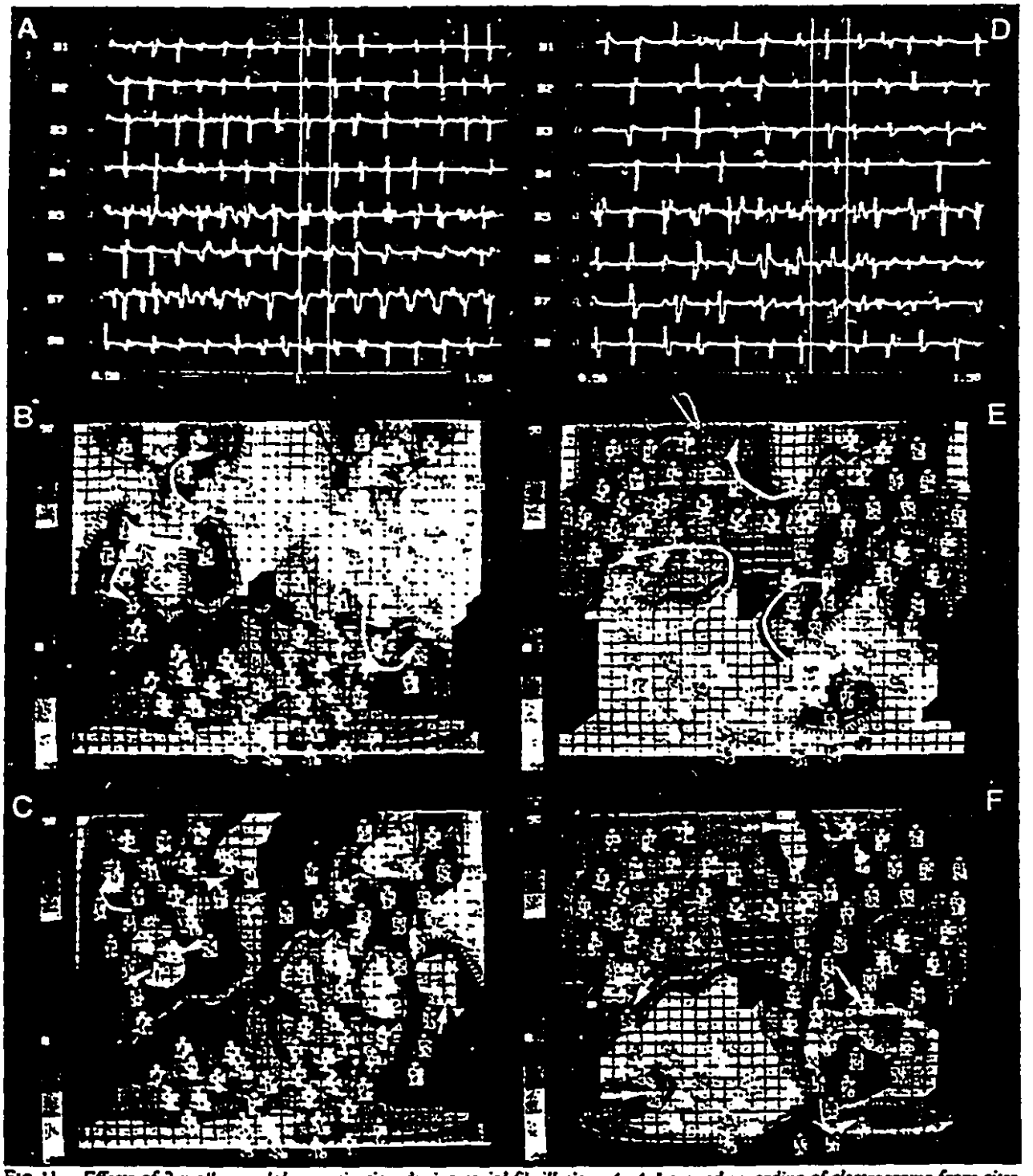

FIG 11. *Effects of 2 mg/kg sotalol on activation during atrial fibrillation. A, A 1-second recording of electrograms from sites B1-B8 during control atrial fibrillation. B, Activation map during a 75-ms cycle of atrial fibrillation under control conditions (shown by vertical lines in A) based on first activation at each electrode site. C, Map of activation during same 75-ms cycle of control atrial fibrillation, showing activation with second time of activation for sites activated twice during the cycle. D, A 1-second recording of electrograms from sites B1-B8 during atrial fibrillation after the administration of sotalol. E, Activation map during a 100-ms cycle of atrial fibrillation (delimited by vertical lines in D) in the presence of sotalol, based on first activation at each electrode site. F, Activation during same cycle as in E, with second activation time shown for sites activating twice during the cycle. The cycles selected for maps B, C, E, and F were defined by a distinct cycle in the anterior left atrium (H electrodes, not shown).*

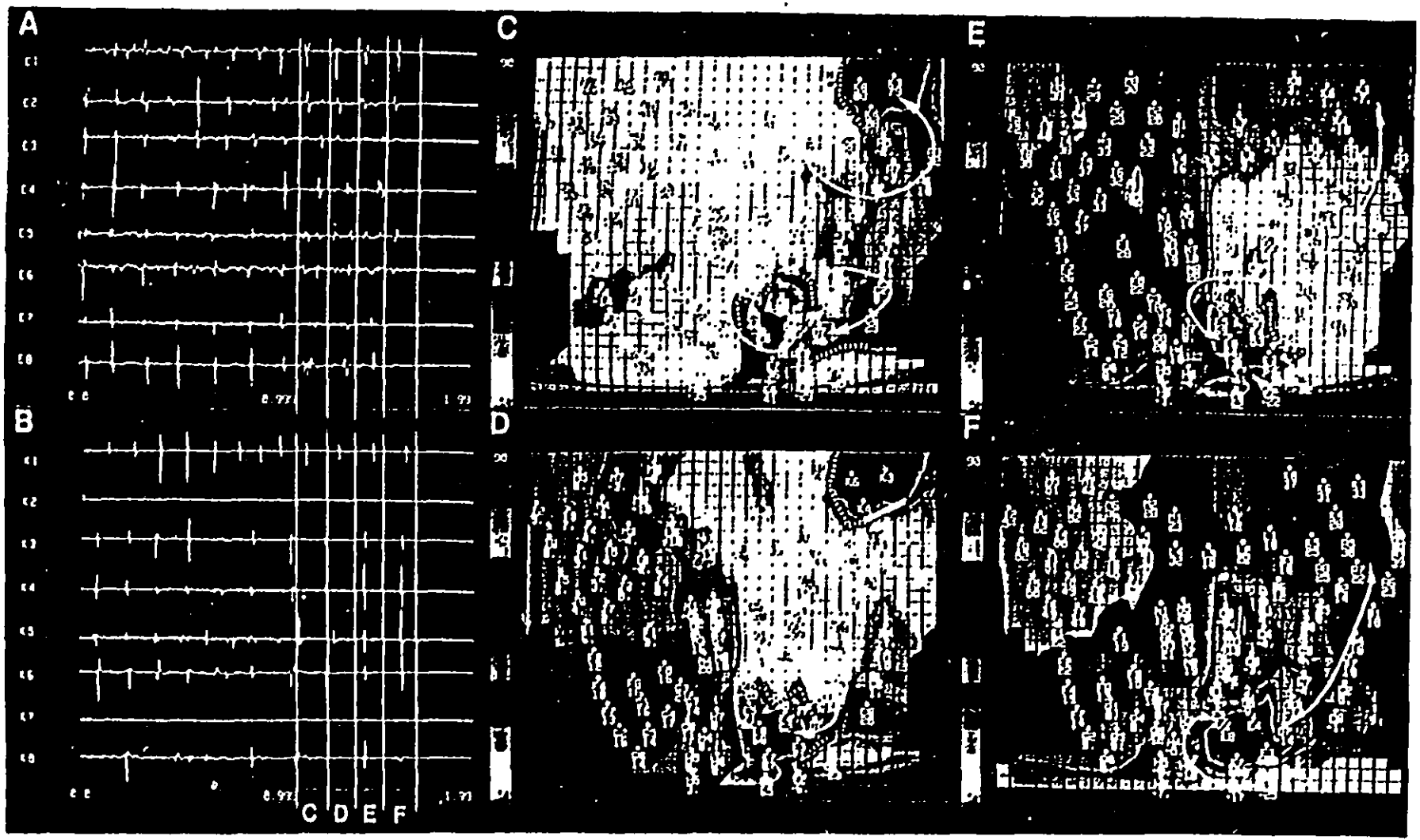

FIG 12. *Termination of atrial fibrillation after the second dose (6 mg/kg) of sotalol. A and B, 2-Second recording of electrograms from sites E1-E8 and K1-K8 at time of atrial fibrillation termination. Cycles mapped in C through F are delimited by vertical lines. C, Cycle of atrial fibrillation, with reentry occurring in the right atrial appendage and the anterior right atrium near the atrioventricular ring. D, Next activation cycle, with reentry in the right atrial appendage terminating by block in sites K3, K4, and K6, but reentry continuing in the anterior right atrium. Reactivation at D8 (indicated by hatched arrows) initiates the next cycle in the anterior right atrium, as illustrated in E. Arrowheads indicate direction of propagation for initiation of next cycle, as shown in F. This cycle terminates because of block at sites E3, E4, E7, and E8.*

activating sites results in their reactivation, as shown (blue areas) in panel C. Sotalol (2 mg/kg) slows activation by about 25% (panel D). Four zones of early activation are present in panel E. Slow conduction around areas of functional block lead to the late reactivation of four atrial zones (panel F). Overall, although the duration of activation-reactivation cycles is slightly larger in the presence of the drug (panels D through F), there is little qualitative change in atrial activation compared with control (panels A through C).

Figure 12 shows an example of atrial fibrillation termination by high-dose sotalol. Electrograms from the right atrium near the atrioventricular ring (E1-E8) are shown in panel A and from the right atrial appendage (K3-K8) in panel B. Activation maps from the last four cycles of atrial fibrillation are illustrated in panels C through F. The cycle prior to that illustrated in C showed a single macroreentry circuit in the right atrial appendage. The same circuit is evident in panel C but is now accompanied by a second, figure-of-eight macroreentry circuit adjacent to the atrioventricular ring. During the next cycle, illustrated in panel D, reentry terminates in the right atrial appendage because of block at K3, K4, and K6 but continues in the lower right atrium. This is followed by two more cycles in the latter zone (panels E and F), with reentry terminating by block at sites E3, E4, E7, and E8. In contrast to atrial activation in the presence of low-dose sotalol (Fig 11), activation in the presence of high-dose sotalol is distinguished by a smaller number of reentry circuits, on which the persistence of atrial fibrillation depends. When reexcitation fails in a critical circuit, atrial fibrillation stops.

The detailed mode of atrial fibrillation termination varied from experiment to experiment for all drugs. However, in each case, the number of circuits immediately prior to termination was one or two, and termination occurred either via failure of reexcitation in a macroreentry circuit (as in Figs 9 and 12) or symmetrical spread from a single region (as in Fig 10). The former mechanism was involved in 6 of 12 terminations mapped for procainamide, 2 of 7 for propafenone, and 4 of 7 for sotalol, whereas variants of the latter mechanism were responsible for the remainder.

Discussion

We have shown that propafenone, procainamide, and sotalol are all capable of terminating atrial fibrillation and preventing its induction in a dog model of sustained atrial fibrillation. Effective doses of all three agents increase the wavelength at short cycle lengths, slow atrial activation during atrial fibrillation, and increase the size of reentry circuits.

Comparison With Previous Experimental Studies of Antiarrhythmic Drug Action During Atrial Fibrillation

Rensma and colleagues[23] evaluated the effects of antiarrhythmic drugs on atrial arrhythmias induced by premature stimulation in dogs. Their study differs from ours in that they studied the inducibility of nonsustained arrhythmias in conscious dogs, mapping techniques were not used, and the details of drug and dose selection were different. Like them, we found that a cumulative dose of 8 mg/kg sotalol suppresses atrial fibrillation induction. In addition, however, we found that a dose of sotalol (2 mg/kg) slightly larger than the standard clinical intravenous dose of 1.5 mg/kg[36,37] has limited ability to terminate atrial fibrillation in our model. This contrasts with the efficacy that we observed for clinical loading doses of procainamide[7] and propafenone.[9,11] Although Rensma and colleagues did not study procainamide, they found that the class Ia drug quinidine suppressed the induction of atrial arrhythmias. Rensma and colleagues did not report efficacy for propafenone, although Kirchhof and colleagues[24] subsequently found another class Ic drug, ORG 7797, to be effective in the same model. Our results resemble those of Rensma and colleagues[23] in that interventions that terminate or prevent atrial fibrillation in both models increase the wavelength for atrial reentry. Our results go beyond those of Rensma and colleagues by evaluating use-dependent drug action and by applying activation mapping to correlate electrophysiological effects with changes in activation during atrial fibrillation.

The effects of propafenone in the present experiments resemble those previously noted with flecainide[25] and suggest a common mechanism of class Ic drug action in atrial fibrillation, with tachycardia-dependent increases in refractoriness counteracting the effects on wavelength of drug-induced conduction slowing. Kirchhof and colleagues also noted use-dependent atrial refractoriness prolongation by ORG 7797.[24] The relative importance of changes in action potential duration[26,27] and sodium channel blockade in the effective refractory period changes caused by Ic drugs remains to be established.

Implications Regarding Mechanisms of Antiarrhythmic Action Against Atrial Fibrillation

Our results support the role of wavelength in mediating antiarrhythmic action in atrial fibrillation. As previously suggested,[23,39,40] increases in wavelength resulted in an increase in the size of functional reentry circuits in our animals. The number of circuits decreased, and the arrhythmia terminated when the remaining circuits failed to sustain themselves. These observations are consistent with the suggested importance of the number of reentrant impulses in sustaining atrial fibrillation.[23,41-44] Termination tended to occur in two general ways—failure of reexcitation at a critical point (Figs 9 and 12) or a delay in activation allowing for recovery of the remaining portions of the atria (Fig 10). In the normal atrium, individual reentrant circuits tend to be unstable, so that in the presence of only one or two circuits functional perturbations readily lead to arrhythmia termination.

Although high-dose sotalol caused similar changes in wavelength (Fig 6) and activation patterns compared with the other two drugs, it caused less slowing in the atrial rate during atrial fibrillation (Fig 7). This is consistent with the smaller increases in atrial effective refractory period produced by sotalol at rapid rates and with the concept that the rate of functional "leading circle" reentry depends on the refractory period,[39] not on conduction velocity or wavelength. Both propafenone and procainamide decrease conduction velocity in addition to prolonging refractoriness. Therefore, they need to cause a larger increase in refractoriness than does sotalol to increase the wavelength sufficiently

to stop atrial fibrillation. Consequently, class 1 agents produce a greater slowing in atrial activation rate before atrial fibrillation termination. The well-known propensity of class 1 agents, particularly 1c compounds, to accelerate the ventricular response rate to atrial fibrillation[45,46] may therefore be due to slowing in atrial activation during atrial fibrillation because of large increases in atrial effective refractory period, rather than to conduction slowing per se, as is commonly assumed.

Relation to Observations of Drug Action in Other Experimental Atrial Arrhythmias

Although there is little published information about antiarrhythmic drug action in experimental atrial fibrillation, many studies have addressed drug actions in atrial flutter.[47-53] Models used have included atrial enlargement due to tricuspid insufficiency,[47] atrial injury by intercaval crush,[48,52] the use of a Y-shaped right atrial incision,[49,50] and sterile pericarditis.[51,53] Efficacy against atrial flutter has been demonstrated for procainamide,[47,49,51] propafenone,[50,52] and sotalol.[48,50] Drug doses and concentrations vary, but they are in the same range as in our study, and changes in refractoriness and conduction are similar.

Several studies examined in detail the mechanism of arrhythmia termination. Spinelli and Hoffman[50] suggested that failure of the lateral boundaries (ie, short-circuiting of reentry) or reflection underlie the efficacy of sotalol, whereas class I agents produce block in the reentrant pathway. Schoels and colleagues[51] suggested that procainamide terminates atrial flutter by suppressing conduction to the point of block in a slowly conducting portion of the reentry circuit. Class I drugs did not eliminate the excitable gap, as would have been expected had they increased wavelength beyond the pathlength available.

The nature of the arrhythmia that we studied was quite different from that of the atrial flutter models. Instead of a single, stable circuit with an anatomic-functional basis, cholinergic atrial fibrillation involves multiple unstable reentry circuits in functionally normal hearts. Atrial activation during atrial fibrillation prior to drug administration reflected this mechanism, as previously observed experimentally[25,43,44] in keeping with Moe's "multiple wavelet hypothesis."[41,42] In contrast to their effects in atrial flutter, class I drugs increased the wavelength in the vagotonic dog, and this increase in wavelength contributed to atrial fibrillation termination by reducing the number of co-existent reentry circuits. On the other hand, it is quite possible that the final extinction of individual macroreentry circuits occurred *via* mechanisms similar to those previously described in atrial flutter models. For example, the small deflections indicated by arrows in Fig 9, D may indicate alternate local activation impinging on site B1, resulting in termination of reentry by failure of the lateral boundary as suggested by Spinelli and Hoffman.[50] Critical depression of conduction by propafenone may have caused the markedly delayed activation at K1 and K2 and arrhythmia termination shown in Fig 10.

Role of Use-Dependent Drug Effects on Refractoriness

We previously found that tachycardia-dependent increases in refractoriness are important in the termination by flecainide of vagal atrial fibrillation[25] and now find that propafenone's efficacy involves similar mechanisms. In contrast, sotalol's ability to terminate atrial fibrillation appeared to be limited by reverse use-dependent actions on effective refractory period. Although 2 mg/kg sotalol increased atrial effective refractory period by about 60% at a basic cycle length of 400 ms during vagal stimulation (Fig 4), its effect was reduced by two thirds at a basic cycle length of 200 ms, resulting in small changes in wavelength and limited ability to terminate atrial fibrillation. The small effect of 2 mg/kg sotalol on wavelength at rapid rates, due to reverse use dependence, accounts for the minor effects of low-dose sotalol on activation patterns during atrial fibrillation (Fig 11).

Limited clinical studies of sotalol in the termination of atrial fibrillation have shown relatively low efficacy,[37] with the exception of postoperative atrial fibrillation,[21] for which β-blockers appear to be particularly effective.[54] It is possible, therefore, that sotalol's reverse use-dependent action limits its ability to terminate a very rapid reentrant arrhythmia like atrial fibrillation. The bradycardia-dependent properties of class III drugs have been recognized for a long time,[55] and their potential clinical importance has recently been emphasized.[56] The limited efficacy of sotalol in terminating cholinergic atrial fibrillation is one of the first experimental demonstrations of the limitation of antiarrhythmic drug efficacy by reverse use-dependent behavior. It should be pointed out that this phenomenon need not limit sotalol's efficacy in preventing atrial fibrillation because atrial fibrillation initiation usually occurs at the slower rates of sinus rhythm.

Study Limitations

Our model has a number of advantages, including the reliability of atrial fibrillation induction, the sustained nature of vagal atrial fibrillation, and the prompt termination of atrial fibrillation when vagal stimulation is stopped. Propafenone and procainamide were effective at doses and concentrations of the same order as those that terminate atrial fibrillation of recent onset in humans.[7,9,11] Enhancement of vagal tone may also play an important role in the clinical occurrence of atrial fibrillation.[57] Our model fails to reproduce the abnormal electrophysiological substrate[58,59] caused by atrial pathology often associated with atrial fibrillation, and may therefore not apply to atrial fibrillation in the setting of structural heart disease. Further observations in experimental atrial fibrillation models involving atrial disease, along with related studies in clinical atrial fibrillation, would be of interest.

The role of vagal tone poses the problem of effects due to antivagal properties. The impact of vagolytic properties was minimized during the assessment of drug effects on effective refractory period, conduction velocity, and atrial fibrillation induction by adjusting vagal stimulation frequency during the maintenance drug infusion to produce the same bradycardic effect as under control conditions. To control for the role of procainamide's vagolytic properties in terminating atrial fibrillation, we increased vagal frequency before procainamide infusion in five dogs, producing a bradycardic action in the presence of drug similar to control conditions. Nonetheless, we cannot completely exclude a contribution to

atrial fibrillation termination of vagolytic actions that may have been incompletely controlled by adjusting vagal stimulation frequency.

The effects of all drugs on atrial effective refractory period were greater in the presence of vagal stimulation (Fig 4). We previously found a similar interaction for flecainide.[25] This interaction between drugs and vagal tone has not, to our knowledge, been reported previously, and its mechanism is unknown. Sodium channel blockade is unlikely to be the sole factor involved because sotalol is devoid of sodium channel–blocking properties at the concentrations studied.[60] Recent work indicates that flecainide, propafenone, and disopyramide can inhibit I_{KACh} in guinea pig atrial myocytes.[61] The potential importance of this mechanism bears further investigation, particularly because I_{KACh} can be activated in the absence of muscarinic agonists by a membrane-bound nucleoside diphosphate kinase.[62]

Conclusions

We have shown that sotalol, propafenone, and procainamide are effective in terminating sustained atrial fibrillation in an experimental dog model. This is, to our knowledge, the first comparative assessment of antiarrhythmic drug mechanisms and efficacy in an experimental model of sustained atrial fibrillation. The results suggest that increases in wavelength are central in arrhythmia termination. Rate-dependent drug effects on atrial refractoriness can contribute to (in the case of propafenone) or limit (in the case of sotalol) drug efficacy, depending on whether drug actions on effective refractory period are enhanced or reduced by the rapid rates characteristic of atrial fibrillation.

Acknowledgments

Supported by the Medical Research Council of Canada, Knoll Pharmaceuticals, the Quebec Heart Foundation, and the Fonds de Recherche de l'Institut de Cardiologie de Montréal. S.N. is a Nordic-Fonds de Recherche en Santé du Québec (FRSQ) Senior Research Scholar. M.T. is a Canadian Heart Foundation Research Scholar. G.W.B. is an FRSQ Research Fellow. Z.W. was supported by a Canadian Heart Foundation studentship. The authors thank Emma De Blasio for expert technical assistance and Mary Morello for typing the manuscript.

References

1. Kannel WB, Wolf PA. Epidemiology of atrial fibrillation. In: Falk RH, Podrid PJ, eds. *Atrial Fibrillation: Mechanisms and Management.* New York, NY: Raven Press, Publishers, 1992:81-92.
2. Pritchett ELC. Management of atrial fibrillation. *N Engl J Med.* 1992;326:1264-1271.
3. Kannel WB, Abbott RD, Savage DD, McNamara PM. Epidemiologic features of chronic atrial fibrillation: the Framingham Study. *N Engl J Med.* 1982;306:1018-1022.
4. Lewis T. The value of quinidine in cases of auricular fibrillation and methods of studying the clinical reaction. *Am J Med Sci.* 1922;163:781-794.
5. Vilko LE, Marvin HM, White PD. A clinical report on the use of quinidin sulphate. *Arch Intern Med.* 1923;31:345-363.
6. Sokolow M, Ball RE. Factors influencing conversion of chronic atrial fibrillation with special reference to serum quinidine concentration. *Circulation.* 1956;14:568-583.
7. Halpern SW, Ellrodt G, Singh BN, Mandel WJ. Efficacy of intravenous procainamide infusion in converting atrial fibrillation to sinus rhythm. *Br Heart J.* 1980;44:589-595.
8. Fenster PE, Comess KA, Marsh R, Katzenberg C, Hager WD. Conversion of atrial fibrillation to sinus rhythm by acute intravenous procainamide infusion. *Am Heart J.* 1983;106:501-504.
9. Bianconi L, Boccadamo R, Pappalardo A, Gentili C, Pistolese M. Effectiveness of intravenous propafenone for conversion of atrial fibrillation and flutter of recent onset. *Am J Cardiol.* 1989;64:335-338.
10. Kondili A, Kastrati A, Popa Y. Comparative evaluation of verapamil, flecainide and propafenone for the acute conversion of atrial fibrillation to sinus rhythm. *Wien Klin Wochenschr.* 1990;102:510-513.
11. Suttorp MJ, Kingma JH, Jessurun ER, Lie-A-Huen L, van Hemel NM, Lie KI. The value of class IC antiarrhythmic drugs for acute conversion of paroxysmal atrial fibrillation or flutter to sinus rhythm. *J Am Coll Cardiol.* 1990;16:1722-1727.
12. Goy JJ, Maendly R, Grbic M, Finci L, Sigwart U. Cardioversion with flecainide in patients with atrial fibrillation of recent onset. *Eur J Clin Pharmacol.* 1985;27:737-738.
13. Kappenberger LJ, Fromer MA, Shenasa M, Gloor HO. Evaluation of flecainide acetate in rapid atrial fibrillation complicating Wolff-Parkinson-White syndrome. *Clin Cardiol.* 1985;8:321-326.
14. Berns E, Rinkenberger RL, Jeang MK, Dougherty AH, Jenkins M, Naccarelli GV. Efficacy and safety of flecainide acetate for atrial tachycardia or fibrillation. *Am J Cardiol.* 1987;59:1337-1341.
15. Goy JJ, Kaufmann U, Kappenberger L, Sigwart U. Restoration of sinus rhythm with flecainide in patients with atrial fibrillation. *Am J Cardiol.* 1988;62:38D-40D.
16. Suttorp MJ, Kingma JH, Lie-A-Huen L, Mast EG. Intravenous flecainide versus verapamil for acute conversion of paroxysmal atrial fibrillation or flutter to sinus rhythm. *Am J Cardiol.* 1989;63:693-696.
17. Wiseman MN, Nathan AW. Intravenous flecainide versus intravenous disopyramide in the reversion of atrial fibrillation. *J Am Coll Cardiol.* 1989;13:165A. Abstract.
18. Crijns HJGM, van Wijk LM, van Gilst WH, Kingma JH, van Gelder IC, Lie KI. Acute conversion of atrial fibrillation to sinus rhythm: clinical efficacy of flecainide acetate: comparison of two regimens. *Eur Heart J.* 1988;9:634-638.
19. Donovan KD, Dobb GJ, Coombs LJ, Lee KY, Weekes JN, Murdock CJ, Clarke GM. Reversion of recent-onset atrial fibrillation to sinus rhythm by intravenous flecainide. *Am J Cardiol.* 1991;67:137-141.
20. Capucci A, Lenzi T, Boriani G, Trisolino G, Binetti N, Cavazza M, Fontana G, Magnani B. Effectiveness of loading oral flecainide for converting recent-onset atrial fibrillation to sinus rhythm in patients without organic heart disease or with only systemic hypertension. *Am J Cardiol.* 1992;70:69-72.
21. Campbell TJ, Gavaghan TP, Morgan JJ. Intravenous sotalol for the treatment of atrial fibrillation and flutter after cardiopulmonary bypass: comparison with disopyramide and digoxin in a randomised trial. *Br Heart J.* 1985;54:86-90.
22. Pilati G, Lenzi T, Trisolino G, Cavazza M, Binetti N, Villecco AS, Fontana G. Amiodarone versus quinidine for conversion of recent onset atrial fibrillation to sinus rhythm. *Curr Ther Res.* 1991;49:140.
23. Rensma PL, Allessie MA, Lammers WIEP, Bonke FIM, Schalij MJ. Length of excitation wave and susceptibility to reentrant atrial arrhythmias in normal conscious dogs. *Circ Res.* 1988;62:395-410.
24. Kirchhof C, Wijffels M, Brugada J, Planellas J, Allessie M. Mode of action of a new class IC drug (ORG 7797) against atrial fibrillation in conscious dogs. *J Cardiovasc Pharmacol.* 1991;17:116-124.
25. Wang Z, Pagé P, Nattel S. The mechanism of flecainide's antiarrhythmic action in experimental atrial fibrillation. *Circ Res.* 1992;71:271-287.
26. Wang Z, Pelletier LC, Talajic M, Nattel S. Effects of flecainide and quinidine on human atrial action potentials: role of rate-dependence and comparison with guinea pig, rabbit and dog tissues. *Circulation.* 1990;82:274-283.
27. O'Hara G, Villemaire C, Talajic M, Nattel S. Effects of flecainide on the rate-dependence of atrial refractoriness, atrial repolarization and atrioventricular node conduction in anesthetized dogs. *J Am Coll Cardiol.* 1992;19:1335-1342.
28. Talajic M, Papadatos D, Villemaire C, Nayebpour M, Nattel S. The antiarrhythmic actions of diltiazem during experimental AV reentrant tachycardias: relationship to use-dependent calcium channel blocking properties. *Circulation.* 1990;81:334-342.
29. Nattel S. Frequency-dependent effects of amitriptyline on ventricular conduction and cardiac rhythm in dogs. *Circulation.* 1985;72:898-906.
30. Nattel S, Jing W. Rate-dependent changes in intraventricular conduction produced by procainamide in anesthetized dogs: a quantitative analysis based on the relation between phase 0 inward current and conduction velocity. *Circ Res.* 1989;65:1485-1498.

31. Gallagher JJ, Kasell JH, Cox JL, Smith WM, Ideker RE, Smith WM. Techniques of intraoperative electrophysiologic mapping. *Am J Cardiol.* 1982;49:221-240.
32. Gallagher JJ, Kasell J, Sealy WC, Pritchett ELC, Wallace AG. Epicardial mapping in the Wolff-Parkinson-White syndrome. *Circulation.* 1978;57:854-866.
33. Nattel S, Feder-Elituv R, Matthews C, Nayebpour M, Talajic M. Concentration dependence of class III and beta-adrenergic blocking effects of sotalol in anesthetized dogs. *J Am Coll Cardiol.* 1989;13:1190-1194.
34. Harapat SR, Kates RE. High performance liquid chromatographic analysis of propafenone in human plasma samples. *J Chromatogr Biomed Appl.* 1982;230:448-453.
35. Wiener N, Rosenblueth A. The mathematical formulation of the problem of conduction of impulses in a network of connected excitable elements, specifically in cardiac muscle. *Arch Inst Cardiol Mex.* 1946;16:205-265.
36. Kopelman HA, Woosley RL, Lee JT, Roden DM, Echt DS. Electrophysiologic effects of intravenous and oral sotalol for sustained ventricular tachycardia secondary to coronary artery disease. *Am J Cardiol.* 1988;61:1006-1011.
37. Singh BN, Nademanee K. Sotalol: a beta blocker with unique antiarrhythmic properties. *Am Heart J.* 1987;121-139.
38. Schmid PG, Nelson LD, Heistad DD, Mark AL, Abboud FM. Vascular effects of procaine amide in the dog. *Circ Res.* 1974;35:948-960.
39. Allessie MA, Bonke IM, Schopman FJG. Circus movement in rabbit atrial muscle as a mechanism of tachycardia: III. the "leading circle" concept: a new model of circus movement in cardiac tissue without the involvement of an anatomical obstacle. *Circ Res.* 1977;41:9-18.
40. Allessie MA, Lammers WJEP, Bonke FIM, Hollen J. Intra-atrial reentry as a mechanism for atrial flutter induced by acetylcholine and rapid pacing in the dog. *Circulation.* 1984;70:123-135.
41. Moe GK. On the multiple wavelet hypothesis of atrial fibrillation. *Arch Int Pharmacodyn Ther.* 1962;140:183-188.
42. Moe GK, Rheinboldt WC, Abildskov JA. A computer model of atrial fibrillation. *Am Heart J.* 1964;67:200-220.
43. Allessie MA, Lammers WJEP, Bonke FIM, Hollen J. Experimental evaluation of Moe's multiple wavelet hypothesis of atrial fibrillation. In: Zipes DP, ed. *Cardiac Electrophysiology and Arrhythmias.* Orlando, Fla: Grune & Stratton, Inc; 1985:265-274.
44. Allessie MA, Rensma PL, Brugada J, Smeets JLRM, Penn O, Kirchhof CJHJ. Pathophysiology of atrial fibrillation. In: Zipes DP, Jalife J, eds. *Cardiac Electrophysiology From Cell to Bedside.* Philadelphia, Pa: WB Saunders Co; 1990:548-558.
45. Murdock C, Kyles A, Yeung-Lai-Wah J, Qi A, Kerr CR. Conversion of atrial fibrillation to flutter with propafenone. *Clin Invest Med.* 1989;12(suppl C):C45. Abstract.
46. Feld GK, Chen PS, Nicod P, Fleck RP, Meyer D. Possible atrial proarrhythmic effects of class 1C antiarrhythmic drugs. *Am J Cardiol.* 1990;66:378-383.
47. Boyden PA. Effects of pharmacologic agents on induced atrial flutter in dogs with right atrial enlargement. *J Cardiovasc Pharmacol.* 1986;8:170-177.
48. Feld GK, Venkatesh N, Singh BN. Pharmacologic conversion and suppression of experimental canine atrial flutter: differing effects of *d*-sotalol, quinidine, and lidocaine and significance of changes in refractoriness and conduction. *Circulation.* 1986;74:197-204.
49. Wu KM, Hoffman BF. Effect of procainamide and *N*-acetylprocainamide on atrial flutter: studies in vivo and in vitro. *Circulation.* 1987;76:1397-1408.
50. Spinelli W, Hoffman BF. Mechanisms of termination of reentrant atrial arrhythmias by class I and class III antiarrhythmic agents. *Circ Res.* 1989;65:1565-1579.
51. Schoels W, Yang H, Gough WB, El-Sherif N. Circus movement atrial flutter in the canine sterile pericarditis model: differential effects of procainamide on the components of the reentrant pathway. *Circ Res.* 1991;68:1117-1126.
52. Inoue H, Yamashita T, Nozaki A, Sugimoto T. Effects of antiarrhythmic drugs on canine atrial flutter due to reentry: role of prolongation of refractory period and depression of conduction to excitable gap. *J Am Coll Cardiol.* 1991;18:1098-1104.
53. Pagé PL, Hassanalizadeh H, Cardinal R. Transitions among atrial fibrillation, atrial flutter, and sinus rhythm during procainamide infusion and vagal stimulation in dogs with sterile pericarditis. *Can J Physiol Pharmacol.* 1991;69:15-24.
54. Fuchs T, Podrid PJ. Pharmacologic therapy for reversion of atrial fibrillation and maintenance of sinus rhythm. In: Falk RH, Podrid PJ, eds. *Atrial Fibrillation: Mechanisms and Management.* New York, NY: Raven Press, Publishers; 1992:233-254.
55. Nattel S, Zeng FD. Frequency-dependent effects of antiarrhythmic drugs on action potential duration and refractoriness of canine cardiac Purkinje fibers. *J Pharmacol Exp Ther.* 1984;229:283-291.
56. Hondeghem LM, Snyders DJ. Class III antiarrhythmic agents have a lot of potential but a long way to go: reduced effectiveness and dangers of reverse use dependence. *Circulation.* 1990;81:686-690.
57. Coumel P, Leclercq JF, Attuel P, Lavallée JP, Flammang D. Autonomic influences in the genesis of atrial arrhythmias: atrial flutter and fibrillation of vagal origin. In: Narula DS, ed. *Cardiac Arrhythmias—Electrophysiology, Diagnosis and Management.* Baltimore, Md: Williams & Wilkins Co; 1979:243-255.
58. Ten Eick RE, Singer DH. Electrophysiological properties of diseased human atrium: I. low diastolic potential and altered cellular response to potassium. *Circ Res.* 1979;44:545-557.
59. Mary-Rabine L, Albert A, Pham TD, Hordof A, Fenoglio JJ Jr, Malm JR, Rosen MR. The relationship of human atrial cellular electrophysiology to clinical function and ultrastructure. *Circ Res.* 1983;52:188-199.
60. Carmeliet E. Electrophysiologic and voltage clamp analysis of sotalol effects in cardiac muscle and Purkinje fibers. *J Pharmacol Exp Ther.* 1985;232:817-824.
61. Inomata N, Ohno T, Ishihara T, Akaike N. Antiarrhythmic agents act differently on the activation phase of ACh-response in guinea-pig atrial myocytes. *Circulation.* 1992;86:1-695. Abstract.
62. Heidbüchel H, Callewaert G, Vereecke J, Carmeliet E. Membrane-bound nucleoside diphosphate kinase activity in atrial cells of frog, guinea pig, and human. *Circ Res.* 1992;71:808-820.

We have demonstrated that propafenone, like flecainide, was effective in terminating and preventing AF by causing use-dependent ERP increases. These results indicate that use-dependent ERP (and APD) prolongation may be a common mechanism of class Ic antiarrhythmic drug action in AF. In contrast, the effectiveness of sotalol, a class III agent, in terminating AF was limited by its reverse use-dependency.

Sustained Atrial Fibrillation in Dogs — Underlying Electrophysiologic Determinants and Mechanism of Antiarrhythmic Action of Flecainide

Zhiguo Wang, MSc; Feng Jianlin; and Stanley Nattel, MD

Short Title: Flecainide and idiopathic AF in dogs

From the Department of Medicine, Montreal Heart Institute and the University of Montreal, and the University of Montreal (SN), and the Departments of Pharmacology and Therapeutics, McGill University (ZW, SN), Montreal, Quebec, Canada.

Supported by the Medical Research Council of Canada, the Quebec Heart Foundation, the Fonds de Recherche de l'Institut de Cardiologie de Montréal. Dr. Wang is the recipient of a studentship award from the Canadian Heart Foundation.

Address for reprints: Dr. Stanley Nattel, Research Center, Montreal Heart Institute, 5000 Belanger Street East, Montreal, Quebec H1T 1C8, Canada.
Tel. #: (514) 376-3330; Fax #: (514) 376-1355.

Abstract

Background. In normal anesthetized dogs (as in man), while atrial fibrillation (AF) can be induced by rapid atrial pacing, it rarely lasts longer than several minutes. Strong vagal tone can increase the duration of AF, but is uncommonly involved in clinical AF. In a small subset of dogs studied over several years, sustained AF (>30 minutes) could be induced reproducibly in the absence of vagal tone and in the presence of β-adrenergic blockade. In previous studies, we have shown that class Ic antiarrhythmic drugs terminate vagotonic AF by causing rate-dependent increases in atrial effective refractory period (AERP). The applicability of such results is uncertain, because they could be due to interactions between the drugs tested and vagal actions. The purpose of the present experiments was to determine the electrophysiologic properties underlying sustained AF in dogs without enhanced vagal tone, and to establish the mechanisms of flecainide action on AF in these animals.

Methods and Results. Five dogs with inducible sustained AF ("AF dogs") were studied before and after flecainide administration, and compared to a concurrent control group of 10 dogs. AF dogs differed from control dogs in displaying greater AERP abbreviation with increased rate, resulting in a significantly smaller AERP and wavelength for reentry at rapid rates, and in showing an increased regional dispersion in AERP. Activation maps during AF showed multiple small co-existent zones of reentry in AF dogs, compatible with short wavelengths for reentry, while in control dogs, activation during self-limited AF was more organized and the number of reentry circuits was significantly smaller. Quantitative analysis of the heterogeneity of atrial activation during AF demonstrated significantly greater inhomogeneity in AF dogs compared to control animals. In AF dogs, flecainide terminated AF and prevented its induction in a concentration-related way. Flecainide terminated sustained AF by increasing the size and reducing the number of reentry circuits, changes compatible with an increased wavelength for reentry, and thereby rendering activation more homogeneous. These effects were due to a tachycardia-dependent increase in AERP, which exceeded drug-induced conduction velocity decreases and caused an increase in the wavelength at short cycle lengths, as well as a drug-induced reduction in the regional dispersion in AERP.

Conclusions. The ability of AF to sustain itself depends on the wavelength at rapid rates, as predicted by leading circle and multiple wavelet reentry concepts, and enhanced rate-dependent shortening in atrial refractoriness can create the conditions for AF in apparently normal animals. Tachycardia-dependent increase in atrial refractoriness, previously demonstrated to be the mechanism by which flecainide terminates AF in dogs with increased vagal tone, also appear to underlie flecainide's ability to terminate experimental AF in the absence of vagal input, suggesting that similar mechanisms may be responsible for the drug's ability to terminate clinical AF in patients with normal levels of vagal tone.

Key Words: antiarrhythmic drugs • sodium channel blockers • atrial arrhythmias • cardiac mapping • ECG • heart

Introduction

Although atrial fibrillation (AF) is one of the most common arrhythmias encountered in clinical practice, the mechanisms and determinants of AF remain incompletely understood. One of the factors limiting our understanding of AF is a lack of readily accessible and appropriate animal models. Investigators have studied repetitive atrial responses and brief episodes of AF induced by programmed electrical stimulation in normal animals,[1,2] but the self-limited and potentially variable nature of these arrhythmias make them difficult to study and render the results of uncertain relevance to sustained arrhythmias. Cholinergic stimulation enhances susceptibility to AF,[3-6] and we have used vagally-mediated sustained AF extensively as a model to study the mechanisms of antiarrhythmic drug action.[7-9] An important limitation of the cholinergic AF model is that interactions between cholinergic and drug effects may occur, making it difficult to determine the extent to which observations in this model can be applied to the clinical setting.

We have previously shown that flecainide terminates AF in the vagotonic AF model by causing tachycardia-dependent increases in atrial refractoriness and wavelength at the rapid rates characteristic of AF.[7] These observations are consistent with on previous observations of flecainide's cellular effects on superfused atrial preparations from multiple species, including dogs and man.[10] However, the changes in refractoriness caused by flecainide were increased in the presence of vagal stimulation, raising questions about the relevance of flecainide's effects in the vagal model to effects on AF in the presence of normal autonomic tone.

Over a 2-year period, approximately 200 dogs have undergone atrial stimulation protocols that included refractory period determinations and pacing at various basic cycle lengths in our laboratory. In five of these dogs, all of whom had bilateral cervical vagotomies as part of the experimental preparation, sustained AF could readily be induced by critically-timed atrial extrastimuli or rapid atrial pacing. The purpose of the present experiments was to evaluate the physiologic substrate of AF and its response to flecainide administration in these dogs. Specific objectives included: 1) to assess atrial electrophysiologic properties associated with the ability to sustain AF; 2) to relate these properties to the mechanisms underlying the ability to manifest sustained AF; and 3) to determine the effects of flecainide on atrial electrophysiology and the ability to sustain AF. A concurrent control group of 10 dogs ("control dogs") was selected in order to compare results in dogs with non-vagal AF with more typical dogs in whom it is impossible to produce sustained AF in the absence of intense vagal nerve stimulation.

Methods

Adult mongrel dogs of either sex (weight, 21 to 31 kg) were anesthetized with morphine (2 mg/kg, i.m.) and α-chloralose (100 mg/kg, i.v.) and ventilated with room air supplemented with oxygen. Respiratory parameters were adjusted to maintain physiological arterial blood gases (SaO_2 >90%; pH 7.38-7.44). Catheters were inserted into the left femoral artery and both femoral veins and kept patent with heparinized saline solution (0.9%). A median sternotomy was performed, and a pericardial cradle was created. Body temperature was maintained at 37°C to 39°C with a homeothermic heating blanket. Two bipolar Teflon-coated stainless steel electrodes were inserted into the right atrial appendage for recording

and stimulation. A programmable stimulator (Digital Cardiovascular Instruments, Berkeley, CA) was used to deliver 4-msec pulses at twice-threshold current. A demand pacemaker (GBM 5880 Demand Pacemaker, Medtronic, Inc, Minneapolis, MN) was used to pace the right ventricle when the ventricular rate was less than 90/min. A P23 1D pressure transducer (Statham Medical Instruments, Los Angeles, CA), electrophysiological amplifiers (Bloom Ltd, Flying Hills, PA) and a paper recorder (Astromed MT-95000, Toronto, Ontario, Canada) were used to record six standard surface ECG leads, an atrial electrogram, and stimulus artifacts. The vagus nerves were isolated in the neck, doubly-ligated and divided. Nadolol was administered at an initial dose of 0.5 mg/kg i.v., followed by 0.25 mg/kg every 2 hours to produce sustained and stable β-blockade.[11]

Atrial Fibrillation Model

The presence of atrial fibrillation was determined by the occurrence of a rapid (>400/min under control conditions), irregular atrial rhythm with varying atrial electrogram morphology and cycle length. AF induction was performed with a brief burst of rapid pacing at a cycle length of 100 msec and four times threshold current. The ability to maintain sustained AF was confirmed by the persistence of AF for >30 minutes on at least two occasions. The five dogs who manifested sustained AF in the absence of vagal stimulation will be referred to as "AF dogs". The 10 control animals will be referred to as "control dogs". In control dogs, AF could be induced by atrial burst pacing, but rarely lasted more than several seconds after induction, and was never sustained for longer than two minutes.

Activation Mapping

An array of 112 bipolar electrodes with 1-mm interpolar and 6-mm interelectrode distance, evenly spaced in five thin plastic sheets was sewn to both atria to cover the entire atrial epicardial surface (Fig 1), as previously described.[7,8] In addition to the recording sites, the sheets also contained six pairs of bipolar electrodes for regional stimulation.

Each signal was filtered with 12-bit resolution and a 1-kHz sampling rate and transmitted via duplex fiber-optic cables into a microcomputer (model 286, Compaq Computer, Houston, TX). Software routines were used to amplify, display and analyze each electrogram as well as to generate maps showing activation times at each electrode site.[12] Interpolation techniques were used to produce isochrone maps of epicardial activation, but only measured activation times (not interpolated data) were used for quantitative analysis. Each electrogram was analyzed by the use of computer-determined peak-amplitude criteria,[13,14] and was reviewed manually to exclude low-amplitude signals with indiscrete electrograms. The reference point for mapping each cycle was placed at the midpoint of the cycle. The accuracy of measured activation times was ±0.5 msec.

Experimental Protocols

Activation data were acquired at the onset of atrial fibrillation and 5 minutes after the onset of drug administration, and again at the time of AF termination. The acquisition system samples data continuously and stores them in a memory buffer, so that 8 sec of data beginning up to 8 sec before a manual trigger can be obtained. This allowed us to acquire activation data immediately before, and at the time of, AF termination.

Atrial refractoriness and conduction properties were assessed under control conditions and then after flecainide administration. Atrial effective refractory period (ERP) was assessed by the extrastimulus technique, and atrial activation times were determined by isochronal mapping. The direction of rapid

propagation was determined from the isochrone maps, and a pair of adjacent bipolar electrode sites in the line of rapid propagation was used to measure conduction velocity. The latter was determined by dividing the distance between the sites by the interelectrode conduction time. The activation pattern was assessed for all activations to ensure that changes in conduction time were not caused by rate- or drug-dependent regional block or changes in the direction of impulse propagation. The wavelength (minimum pathlength that can support reentry) was calculated as the product of conduction velocity and ERP, as described by Wiener and Rosenblueth.[15]

Results were obtained during stimulation at the right atrial appendage (site 1 in Fig 1) at basic cycle lengths (BCL) of 400, 300, 250, 200, and 150 msec. Two minutes were allowed at each BCL before atrial ERP and conduction velocity were measured. For ERP determination, a premature stimulus (S_2) was inserted after every 10 basic (S_1) stimuli, with the S_1S_2 interval decreased by 10-msec decrements until failure to capture occurred. The longest S_1S_2 interval that consistently failed to produce a propagated response was defined as the ERP.

To evaluate the possible role of regional variation in refractoriness and to assess whether flecainide's effects were exerted in a spatially uniform fashion, we determined conduction velocity, atrial refractory period, and wavelength during stimulation at a cycle length of 250 msec at each of the seven stimulation sites shown in Fig 1.

In AF dogs, control measurements were performed and then AF was induced. After AF had persisted for 30 minutes, flecainide was infused as a loading dose of 1 mg/kg over 15 minutes, followed by a maintenance infusion of 1.33 mg/kg h^{-1}. Plasma drug concentrations were measured with previously described HPLC methods.[16] Following the termination of AF, arrhythmia induction was attempted with burst pacing every 10 minutes. For control dogs, atrial ERP, conduction velocity, and wavelength were determined at various basic cycle lengths, and in various regions, as in AF dogs. The cervical vagi were isolated, doubly ligated, and divided in both groups of dogs. Bilateral vagal nerve stimulation was performed in control dogs with 0.1 sec, 10 Hz stimuli at a voltage two thirds of the threshold for inducing 3 sec of asystole, in order to compare electrophysiologic properties of AF dogs with properties in control dogs under conditions (vagal stimulation) permitting the induction of sustained AF in control dogs.

Data Analysis

Group data are presented as mean ± SEM. Comparisons between group means were made by two-way analysis of variance (ANOVA) with Scheffe's test,[17] or Student's *t* test when only two groups of results were compared. Rate-dependent and regionally-determined effects of flecainide on atrial ERP, conduction velocity, and wavelength were evaluated by ANOVA with an F test for interaction.[17] A two-tailed probability of <5% defined statistical significance.

The properties of atrial activation during AF were quantified in two ways, First, the number of apparent atrial reentry circuits was determined as previously described,[7] based on the number of discrete zones in which adjacent electrodes were activated at the beginning and end of a local cycle, with reactivation of the early-activation zone initiating local activity in the next cycle. Second, an index of inhomogeneity of activation was calculated. We reasoned that homogeneous activation should result in orderly successive activation of adjacent electrodes I the line of propagation of the atrial impulse. When activation becomes disorganized, activation times of adjacent sites become less coupled to one another and the differences between activation times of adjacent sites should increase. We therefore calculated

the absolute value of the difference in activation times at adjacent electrode pairs. The mean activation time difference was then divided by the cycle length, to determine the fraction of the overall AF cycle occupied by activation time differences at adjacent electrodes. The latter value was termed the "index of homogeneity". An advantage of this index over an analysis of the number of reentry circuits is that quantitative results are obtained without a need for an interpretation of patterns of reentry, which of necessity introduces a subjective elements.

Results

Electrophysiologic Properties Associated With the Ability to Manifest Sustained AF

There were no gross morphological abnormalities in AF dogs — they had no evidence of heart failure, atrial enlargement, or other pathology. Table 1 compares the results obtained at a cycle length of 150 msec in dogs with AF to results in control animals with and without vagal nerve stimulation (VNS). Atrial conduction velocity was not significantly different among the three groups of dogs. Atrial ERP and wavelength were significantly shorter in AF dogs than in control dogs, and the wavelength in AF dogs was not significantly different from the wavelength in control dogs subjected to vagal stimulation. Spontaneous sinus rate was substantially less, and Wenckebach cycle length was considerably greater, in control dogs during vagal nerve stimulation than in AF dogs or control dogs under basal conditions.

Figure 2 (panels A to C) shows the rate-dependence of electrophysiologic properties in control and AF dogs. The overall pattern of rate-dependence was similar in the two groups. However, ERP showed greater rate-dependent abbreviation in AF dogs, and was significantly less in these animals at the shortest BCL (150 msec) than in control dogs. Correspondingly, the wavelength for reentry showed greater abbreviation with rate in AF dogs, and was significantly shorter than in control dogs at a BCL of 150 msec. In addition to showing greater rate-dependent abbreviation, ERP in AF dogs showed much greater regional variability (Fig 3). While conduction velocity showed less regional variability than ERP, conduction tended to be slower in regions of briefer refractoriness. As a result, there were large regional differences in the wavelength for reentry. The within-dog standard deviation of the ERP (SD_{erp}) was used as an index of regional variation in refractoriness. The SD_{erp} averaged 17±1 msec in AF dogs, and 12±1 msec in control dogs ($P<0.05$). The standard deviation of wavelength averaged 4.3±0.4 cm and 2.6±0.3 cm in the same groups respectively ($P<0.05$).

The increase in regional dispersion of refractoriness in AF dogs appeared to be due to shorter left atrial refractory periods (sites 5 and 7). Fig 4 shows regional values of atrial ERP from four individual AF dogs for which we had complete data and corresponding values in five randomly-selected control dogs. AF dogs (panel B) had consistently shorter refractory periods at left atrial sites (particularly sites 6 and 7) compared to values in the rest of the atria. In contrast, ERP values showed less regional variation in control dogs (panel A). Overall, mean regional variation in ERP was significantly greater in AF dogs than in control dogs (panel C, $P<.05$, two-way ANOVA).

Activation During AF in Control and AF Dogs

Bursts of rapid atrial pacing produced short runs of AF in control dogs. AF induction was attempted 10 times in each control dog, and the mean duration for all control dogs was 12.1±7.2 s. Activation mapping was used to relate the characteristics of AF to underlying electrophysiologic properties and the ability of AF to sustain itself. Fig 5 (left) shows selected electrograms and activation maps from a cycle

of AF in a control dog, and corresponding data from an AF dog (right). In the control dog shown, AF lasted an average of 15 s (range 1 to 50 s). Panel B shows the activation map corresponding to the cycle shown by the vertical lines in A. Panel A shows electrograms from nine electrode sites activated sequentially during one functional reentry circuit during the cycle indicated. The location of these electrodes is indicated by the letters A through I in panel B. Corresponding data from an AF dog are shown in panels C and D. Note that atrial activity is much more heterogenous in the AF dog. Many more isochrones are present, and there is a large number of apparent reentry circuits (arrows).

These differences in activation pattern were seen consistently, as indicated by the quantitative analysis of activation pattern during AF shown in Fig 6. The number of simultaneous reentry circuits during AF in AF dogs averaged 6.3±0.4, and was significantly greater than the number in control dogs (2.8±0.5, $P<.01$ versus AF dogs). The index of inhomogeneity averaged 0.0090±0.0005 during sinus rhythm in AF dogs, and increased to 0.171±0.022 during AF ($P<.01$ versus sinus rhythm). During AF in control dogs, the index of inhomogeneity averaged 0.050±0.016, a value significantly less ($P<.01$) than the index in AF dogs. These quantitative analyses indicate that atrial activation was substantially more heterogenous in AF dogs compared to control dogs, and that the number of simultaneous reentry circuits was considerably greater in AF dogs.

Efficacy of Flecainide in AF

Flecainide converted AF in all five AF dogs, after a mean time of 10 minutes (range, 7 to 14 min), with termination of AF always occurring during the administration of the loading dose. After the termination of AF, electrophysiologic variables were measured during the maintenance infusion, and then the maintenance infusion was stopped. AF reinduction was attempted every 10 minutes after the end of the maintenance infusion, and blood samples were obtained to correlate drug concentrations with the inducibility of AF. Fig 7 shows the plasma concentrations of flecainide at the time of AF termination, during the maintenance infusion, and when AF became reinducible. After AF termination, the arrhythmia could not be induced during drug infusion in any dog. At a mean concentration of 0.6±0.2 mg/L, AF became inducible but failed to sustain itself. Sustained AF could eventually be maintained in all five dogs, at a mean concentration of 0.3±0.1 mg/L. In three dogs, sustained AF began spontaneously, while in the other two it was induced by burst pacing.

Effects of Flecainide on Activation During AF

Flecainide considerably slowed atrial activation during AF. The mean cycle length of AF, determined as reported previously[7], was increased by the drug from 67±7 msec to 123±16 msec prior to AF termination ($P<.001$). Flecainide increased the organization of atrial activation and reduced the number of functional reentry circuits (Fig 6). The mean number of reentry circuits was reduced from over six before flecainide to 1.5±0.3 ($P<.001$) immediately prior to drug-induced termination of the arrhythmia. The index of inhomogeneity was decreased by flecainide from 0.171±0.022 before the drug to 0.053±0.010 ($P<.01$) immediately prior to termination.

The changes in atrial activation associated with flecainide-induced AF termination are illustrated by results from one dog in Fig 8. Panel A shows electrograms from sites corresponding to positions A to J in panels B and C. Panel B and C show activation patterns during the last two cycles of AF during flecainide-induced rhythm reversion. Note that overall activation is more homogeneous than prior to flecainide (compare with results from the same dog in Fig 5D). Activation during the penultimate cycle

panel B) is dominated by a single, figure-of-eight macroreentry circuit. Reactivation from sites I and J to the region of sites A to C initiates the final cycle (panel C). The cycle shown in C terminates because of block in the zone delimited by the heavy line in the lower right atrium adjacent to the AV ring (note the lack of activation at site J during the last cycle in panel A). In all cases, the termination of AF by flecainide was associated with an increase in the homogeneity of atrial activation and a reduced number of reentry circuits, with activation in the final circuits terminating either by block (as in Fig 8) or by collision of wavefronts as previously shown.[8]

Effects of Flecainide on the Electrophysiological Determinants of Reentry

The rate-dependent effects of flecainide on atrial ERP, conduction velocity, and the minimum wavelength for reentry are shown in Fig 2. Flecainide produced substantial rate-dependent reductions in atrial conduction velocity (panel B) and increases in atrial ERP (panel A). Drug-induced changes in ERP exceeded those in conduction velocity, causing important increases in wavelength (panel C). Drug-induced changes in wavelength increased with decreasing cycle length, and at the shortest cycle length (150 msec) the wavelength in the presence of flecainide equalled the value in control dogs. The effects of flecainide on conduction and refractoriness were both significantly rate-dependent (panel D).

Regional Effects of Flecainide on Conduction and Refractoriness

Flecainide increased the ERP and slowed conduction in all regions of the atria (Fig 3). Flecainide increased refractoriness the most in zones that had the shortest refractoriness prior to drug. Consequently, ERP showed much less regional variation after flecainide administration (Fig 3A), with SD_{erp} decreasing from 17±1 msec prior to the drug to 8±2 msec ($P<.01$) after flecainide. As a result of the homogenization in regional ERP, the wavelength became much less variable, and regional wavelength after drug were similar to control values (Fig 3C).

Discussion

We have shown that in a subset of dogs the atria can support sustained AF despite bilateral vagotomy and β-adrenoceptor blockade. The underlying electrophysiologic substrate includes reduced refractoriness and wavelength at rapid rates, and a greater dispersion in atrial refractoriness. These result in increased heterogeneity of activation during AF, associated with a larger number of simultaneous functional reentry circuits. Flecainide terminated AF by causing a tachycardia-dependent increase in atrial ERP, which outweighed conduction slowing and prolonged the wavelength for reentry at rapid rates, reducing the number of increasing the size and reducing the number of reentry circuits and the heterogeneity of atrial activation. sustain itself.

Factors Associated With the Ability to Manifest Sustained AF

The importance of the reentrant pathlength in the physiology of AF was first discussed by Lewis,[18] who agreed with Rothberger and Winterberg[19] that short refractory periods were an important factor in the ability to produce AF. Rensma et al showed that the wavelength was a critical determinant of reentrant atrial arrhythmias.[1] A subsequent study from the same group reported a duration of AF in conscious (autonomically intact) dogs between 4 s and 66 minutes, with a mean of 211 s.[2]

Vagal stimulation results in the ability to sustain AF as long as vagal stimulation continues, and is associated with a reduced wavelength for reentry and an increased regional dispersion in atrial ERP.[7,20-22] In the present experiments, we studied dogs that had the unusual property of supporting sustained AF in

the absence of vagal nerve input. Two electrophysiologic characteristics of these dogs may have contributed to their ability to sustain AF. First, AF dogs manifested greater rate-dependent ERP abbreviation. Consequently, AF dogs had small wavelengths for reentry at short basic cycle lengths, with a wavelength at a cycle length of 150 msec that was substantially smaller than in control dogs (Fig 2C), and in the same range as the wavelength during vagal stimulation in control dogs (Table 1). Activation mapping showed that during AF multiple small zones of reentry coexisted in AF dogs (Fig 5), which requires a short wavelength according to the leading circle hypothesis.[23] Multiple small circuits are essential for the maintenance of reentrant AF, as first proposed in Gordon Moe's "multiple wavelet" hypothesis[24,25] and subsequently demonstrated by Allessie et al.[26]

The second property that may have contributed to AF was an increased dispersion of atrial refractoriness (Fig 3 and 4). Variability in regional refractoriness may have contributed to the greater heterogeneity of activation during sustained AF in AF dogs, which increases the likelihood that recently excited tissue will be located near tissue recovering excitability and thus available for reactivation. Lammers et al have shown that inhomogeneities in conduction are important in the initiation of atrial reentry in isolated rabbit atria.[27,28]

The mechanisms accounting for enhanced rate-dependent atrial ERP abbreviation and dispersion in refractoriness in AF dogs are unclear. AF dogs showed more rate-dependent ERP abbreviation and refractoriness variation than control dogs, but both groups showed the same basic qualitative properties. Thus, AF dogs may present the extreme of a continuum of normal atrial refractory properties.

Mechanism of Flecainide Action in AF

Flecainide has been shown to be effective in the conversion of AF to sinus rhythm,[29-37] in the maintenance of sinus rhythm after cardioversion,[38,39] and in the prevention of AF paroxysms.[39-44] The efficacy of class Ic drugs in AF appears paradoxical, because this class of agents is considered to slow conduction without altering refractoriness,[45,46] changes which would be expected to decrease the wavelength and increase the likelihood of atrial reentry.[1,23] We have shown that flecainide reduces rate-dependent action potential duration (APD) and ERP abbreviation, causing tachycardia-dependent increases in refractoriness.[10,16] The present studies show that flecainide terminates sustained AF in the absence of cardiac vagal input by mechanisms similar to those previously described in the vagotonic model.[7] The drug increased the wavelength by causing tachycardia-dependent increases in atrial ERP, decreasing the number of atrial reentry circuits, as predicted by the leading circle model of functional reentry,[23] and terminating AF in a fashion consistent with the multiple wavelet reentry concept.[24-26] In addition, flecainide reduced the variability of atrial ERP, which may also have contributed to its efficacy.

The potential ionic mechanism of flecainide's actions on atrial tissue are incompletely understood. The drug inhibits the delayed rectifier (I_K)[47] and the transient outward current (I_{to}),[48,49] both of which can play a role in atrial repolarization.[50-52] The rate-dependence of drug action on APD in dog atrium appears to be due to sodium channel blockade, which can reduce tachycardia-dependent cellular sodium loading and Na^+, K^+-ATP'ase stimulation.[48] Rate-dependent sodium channel block could also prolong ERP independently of changes in APD, by depressing atrial excitability.

Novel Aspects and Potential Significance of Our Observations

The present study is the first to show that sustained atrial fibrillation can be induced reproducibly in the absence of vagal tone and β-adrenoceptor stimulation in a subset of dogs, and to study the

electrophysiologic properties which account for their ability to sustained AF. In addition, this study is the first to evaluate the electrophysiologic mechanisms by which flecainide alters atrial activation to terminate AF in a model lacking enhanced vagal tone. Since the latter is unusual in patients with AF, these results are relevant to understanding the drug's ability to terminate AF in Man.

The mechanisms of idiopathic or "lone" AF in man are uncertain. The majority of cases present as paroxysmal AF,[53] and drug-resistant cases may have a variety of associated focal histopathology despite the absence of clinically-detected cardiac disease.[54,55] Patients with lone AF have shorter atrial refractory periods[56,57] and a greater dispersion of atrial refractory periods[57] compared to controls. The ability to sustain AF in man has been associated with evidence of a reduced wavelength.[58] Our AF dogs had a number of features in common with those described in patients with lone AF. They had shorter refractory periods at rapid pacing rates, smaller wavelengths, and greater dispersion in atrial refractory properties than control dogs. The mechanisms permitting AF to be sustained in these animals may thus give insights into the mechanisms of idiopathic AF in man. Activation maps showed multiple small zones of reentry and increased heterogeneity of activation during AF, consistent with small wavelengths at short cycle lengths and accounting for the ability of AF to sustain itself. AF dogs showed similar patterns but greater magnitudes of rate-dependent ERP abbreviation and variability compared to normal dogs. This raises the intriguing possibility that, at least in some patients, idiopathic AF may occur when atrial electrophysiologic properties are at one end of the spectrum of normal, with combinations of regional refractoriness and conduction velocity that allow AF to be sustained.

Limitations of the Model

While the vagus nerves were transected in all our dogs, the cardiac vagal nerve endings could have released acetylcholine and contributed to the electrophysiologic properties of AF dogs. Two pieces of evidence weigh against this possibility. First, while AF dogs had shorter atrial ERP and wavelength values than control dogs, the sinus rate and Wenckebach cycle length in AF dogs were similar to those of control dogs in the absence of vagal stimulation (Table 1), i.e., there was no evidence of enhanced cholinergic action on the sinus and AV nodes. Second, vagal activation results in the shortest ERP values in the right atrium and longest in the left atrium.[7,20-22] In AF dogs (Fig 3), refractory periods were shortest in the left atrium (sites 6 and 7, see Fig 1) and longest at sites in the right atrium (sites 2, 3, and 4).

The ability to manifest sustained AF is unusual in normal dogs, as is the inducibility of sustained AF in patients without organic heart disease. We were therefore limited to a small study group of AF dogs. Although there was no gross cardiac pathology in these animals, the possibility of focal, microscopic heart disease as previously noted clinically in patients with idiopathic AF[54,55] cannot be completely excluded.

The plasma concentration threshold for suppression of AF induction was 0.6 mg/L and for prevention of sustained AF was 0.3 mg/L. Plasma concentrations associated with clinical efficacy against AF average about 0.5 mg/L,[33,35,41] Drug concentrations at the time of AF termination averaged about 1.5 mg/L in our dogs, somewhat higher than values (0.5 mg/L) after flecainide infusions that terminated AF in patients.[33,35] The discrepancy may be due to the fact that Suttorp et al measured concentrations in samples obtained 5 minutes after the end of the drug infusion (rather than at the time of termination), to greater sensitivity of human atrial tissue to flecainide compared to canine atrium,[10] or to undefined pharmacodynamic factors.

Condensed Abstract

In five dogs that manifested inducible sustained atrial fibrillation (AF) despite bilateral cervical vagotomy, we studied the electrophysiological properties that permitted AF to sustain itself and the mechanisms of action of flecainide on AF. Compared to a concurrent control group of 10 dogs, AF dogs showed greater refractoriness abbreviation in response to increased rate and greater regional dispersion in refractoriness. Activation mapping during sustained AF demonstrated an average of 6.3±0.4 (mean±SE) simultaneous regions of reentry, compatible with a reduced wavelength at rapid rates compared to control dogs. Flecainide terminated AF by increasing refractoriness in a tachycardia-dependent way, increasing the wavelength for reentry and reducing the number of reentry circuits until AF could no longer sustain itself. These results show that the ability of AF to sustain itself depends on the wavelength at rapid rates, as predicted by leading circle and multiple wavelet reentry concepts, and that enhanced rate-dependent refractoriness abbreviation can create the conditions necessary for sustained AF in dogs. The ability of flecainide to terminate AF by causing rate-dependent increases in refractoriness, previously shown only in vagotonic dogs, is also demonstrable in dogs with sustained AF in the absence of cardiac vagal nerve input.

Acknowledgments

The authors thank Emma De Blasio and Christine Villemaire for technical assistance, Mary Morello for typing the manuscript, and Riker-3M Pharmaceuticals for providing the flecainide used in these studies.

mm/sustains.8e

References

1. Rensma PL, Allessie MA, Lammers WJEP, Bonke FIM, Schalij MJ. Length of excitation wave and susceptibility to reentrant atrial arrhythmias in normal conscious dogs. *Circ Res.* 1988;62:395-410.
2. Kirchhof C, Wijffels M, Brugada J, Planellas J, Allessie M. Mode of action of a new class 1C drug (ORG 7797) against atrial fibrillation in conscious dogs. *J Cardiovasc Pharmacol.* 1991;17:116-124.
3. Andrus EC, Carter EP. The refractory period of the normally-beating dog's auricle; with a note on the occurence of auricular fibrillation following a single stimulus. *J Exp Med. 1930;*51:357-368.
4. Hoff HE, Geddes LA. Cholinergic factor in auricular fibrillation. *J Appl Physiol.* 1955;8:177-1912
5. Burn JH, Vaughan Williams EM, Walker JM. The effects of acetylcholine in the heart-lung preparation including the production of auricular fibrillation. *J Physiol.* 1955;128:277-293.
6. Allessie MA, Lammers WJEP, Bonke FIM, Hollen J: Intra-atrial reentry as a mechanism for atrial flutter induced by acetylcholine and rapid pacing in the dog. *Circulation.* 1984;70:123-135.
7. Wang Z, Pagé P, Nattel S. Mechanism of flecainide's antiarrhythmic action in experimental atrial fibrillation. *Circ Res.* 1992;71:271-287.
8. Wang J, Bourne GW, Wang Z, Villemaire C, Talajic M, Nattel S. Comparative mechanisms of antiarrhythmic drug action in experimental atrial fibrillation. The importance of use-dependent effects on refractoriness. *Circulation.* 1993;88:1030-1044.
9. Wang J, Feng J, Nattel S. Class III antiarrhythmic drug action in experimental atrial fibrillation: Differences in reverse use-dependence and effectiveness between d-sotalol and the new antiarrhythmic drug ambasilide. *Circulation.* (in revision).
10. Wang Z, Pelletier LC, Talajic M, Nattel S. Effects of flecainide and quinidine on human atrial action potentials: Role of rate-dependence and comparison with guinea pig, rabbit, and dog tissues. *Circulation.* 1990;82:274-283.
11. Talajic M, Villemaire C, Nattel S. Electrophysiological effects of α-adrenergic stimulation. *PACE.* 1990;13:578-582.
12. Nattel S, Jing W. Rate-dependent changes in intraventricular conduction produced by procainamide in anesthetized dogs. A quantitative analysis based on the relation between phase 0 inward current and conduction velocity. *Circ Res.* 1989;65:1485-1498.
13. Gallagher JJ, Kasell JH, Cox JL, Smith WM, Ideker RE, Smith WM: Techniques of intraoperative electrophysiologic mapping. *Am J Cardiol.* 1982;49:221-240.
14. Gallagher JJ, Kasell J, Sealy WC, Pritchett ELC, Wallace AG. Epicardial mapping in the Wolff-Parkinson-White syndrome. *Circulation.* 1978;57:854-866.
15. Weiner N, Rosenblueth A. The mathematical formulation of the problem of conduction of impulses in a network of connected excitable elements, specifically in cardiac muscle. *Arch Inst Cardiol Mex.* 1946;16:205-265.
16. O'Hara G, Villemaire C, Talajic M, Nattel S. Effects of flecainide on the rate dependence of atrial refractoriness, atrial repolarization and atrioventricular node conduction in anesthetized dogs. *J Am Coll Cardiol.* 1992;19:1335-1342.

17. Sachs L. *Applied Statistics.* Springer-Verlag, New York, 1984.
18. Lewis T, Drury AN, Wedd AM, Iliescu CC. Observations upon the action of certain drugs upon fibrillation of the auricles. *Heart.* 1922;9:207-267
19. Rothberger CJ, Winterberg H. Über Vorhofflimmern und Vorhofflattern. *Pflüger Achiv. Ges. Physiologie.* 1915;160:42-90.
20. Zipes DP, Mihalick MJ, Robbins GT. Effects of selective vagal and stellate ganglion stimulation on atrial refractoriness. *Cardiovasc Res.* 1974;8:647-655.
21. Alessi R, Nusynowitz M, Abildskov JA, Moe GK. Nonuniform distribution of vagal effects on the atrial refractory period. *Am J Physiol.*1958;192:406-410.
22. Ninomiya I. Direct evidence of nonuniform distribution of vagal effects on dog atria. *Circ Res.* 1966;19:576-583.
23. Allessie MA, Bonke FIM, Schopman FJG. Circus movement in rabbit atrial muscle as a mechanism of tachycardia. III. The "leading circle" concept: A new model of circus movement in cardiac tissue without the involvement of an anatomical obstacle. *Circ Res.* 1977;41:9-18.
24. Moe GK. On the multiple wavelet hypothesis of atrial fibrillation. *Arch Int Pharmacodyn.* 1962;140:1-2.
25. Moe GK, Rheinboldt WC, Abildskov JA. A computer model of atrial fibrillation. *Am Heart J.* 1964;67:200-220.
26. Allessie MA, Lammers WJEP, Bonke FIM, Hollen H: Experimental evaluation of Moe's multiple wavelet hypothesis of atrial fibrillation, In: Zipes DP & Jalife J, eds. *Cardiac Electrophysiology and Arrhythmias.* New York, Grune & Stratton, Inc, 1985:265-274.
27. Bourne G, Talajic M, Nattel S. Mechanisms of sotalol's antiarrhythmic actions in experimental atrial fibrillation - Role of regional and functional factors (submitted).
28. Kappenberger LJ, Fromer MA, Shenasa M, Gloor HO. Evaluation of flecainide acetate in rapid atrial fibrillation complicating Wolff-Parkinson-White syndrome. *Clin Cardiol.* 1985;8:321-326.
29. Goy JJ, Maendly R, Grbic M, Finci L, Sigwart U. Cardioversion with flecainide in patients with atrial fibrillation of recent onset. *Eur J Clin Pharmacl.* 1985;27:737-738.
30. Borgeat A, Goy JJ, Maendly R, Kaumann U, Grbic M. Sigwart U. Flecainide versus quinidine for conversion of atrial fibrillation to sinus rhythm. *Am J Cardiol.* 1986;58:496-498.
31. Goy JJ, Kaufmann U, Kappenberger L, Sigwart U. Restoration of sinus rhythm with flecainide in patients with atrial fibrillation. *Am J Cardiol.* 1988;62:38D-40D.
32. Crijns HJGM, van Wijk LM, van Gilst WH, Kingma JH, van Gelder IC, Lie KI: Acute conversion of atrial fibrillation to sinus rhythm: Clinical efficacy of flecainide acetate. Comparison of two regimens. *Eur Heart J.* 1988;9:634-638.
33. Suttorp MJ, Kingma JH, Lie-A-Huen L, Mast EG. Intravenous flecainide versus verapamil for acute conversion of paroxysmal atrial fibrillation or flutter to sinus rhythm. *Am J Cardiol.* 1989;63:693-696.
34. Kondili A, Kastrati A, Popa Y. Comparative evaluation of verapamil, flecainide and propafenone for the acute conversion of atrial fibrillation to sinus rhythm. *Wiener klinische Wochenschrift.* 1990;17:510-513.

35. Suttorp MJ, Kingma JH, Jessurun ER, Lie-A-Huen L, van Hemel NM, Lie KI. The value of class IC antiarrhythmic drugs for acute conversion of paroxysmal atrial fibrillation or flutter to sinus rhythm. *J Am Coll Cardiol.* 1990;16:1722-1727.

36. Donovan KD, Dobb GJ, Coombs LJ, Lee KY, Weekes JN, Murdock CJ, Clarke GM. Reversion of recent-onset atrial fibrillation to sinus rhythm by intravenous flecainide. *Am J Cardiol.* 1991;67:137-141.

37. Capucci A, Lenzi T, Boriani G, Trisolino G, Binetti N, Cavazza M, Fontana G, Magnani B. Effectiveness of loading oral flecainide for converting recent-onset atrial fibrillation to sinus rhythm in patients without organic heart disease or with only systemic hypertension. *Am J Cardiol.* 1992;70:69-72.

38. Van Gelder IC, Crijns HJGM, Van Gilst WH, Van Wijk LM, Hamer HPM, Lie KI. Efficacy and safety of flecainide acetate in the maintenance of sinus rhythm after electrical cardioversion of chronic atrial fibrillation flutter. *Am J Cardiol.* 1989;64:1317-1321.

39. Berns E, Rinkenberger RL, Jeang MK, Dougherty AH, Jenkins M, Naccarelli GV. Efficacy and safety of flecainide acetate for atrial tachycardia or fibrillation. *Am J Cardiol.* 1987;59:1337-1341.

40. Chouty F, Coumel P. Oral flecainide for prophylaxis of paroxysmal atrial fibrillation. *Am J Cardiol.* 1988;62:35D-37D.

41. van Wijk LM, den Heijer P, Crijns HJ, van Gilst WH, Lie KI Flecainide versus quinidine in the prevention of paroxysms of atrial fibrillation. *J Cardiovasc Cardiol.* 1989;13:32-36.

42. Anderson JL, Gilbert IM, Alpert BL, Henthorn RW, Waldo AL, Bhandari AK, Hawkinson RW, Pritchett ELC and the Flecainide Supraventricular Tachycardia Study Group. Prevention of symptomatic recurrences of paroxysmal atrial fibrillation in patients initially tolerating antiarrhythmic therapy. A multicenter, double-blind, crossover study of flecainide and placebo with transtelephonic monitoring. *Circulation.* 1989;80:1557-1570.

43. Pritchett ELC, DaTorre SD, Platt ML, McCarville SE, Hougham AJ for the Flecainide Supraventricular Tachycardia Study Group. Flecainide acetate treatment of paroxysmal supraventricular tachycardia and paroxysmal atrial fibrillation: dose-response studies. *J Am Coll Cardiol.* 1991;17:297-303.

44. Lau CP, Leung WH, Wong CK. A randomized double-blind crossover study comparing the efficacy and tolerability of flecainide and quinidine in the control of patients with symptomatic paroxysmal atrial fibrillation. *Am Heart J.* 1992;124:645-650.

45. Campbell TJ. Kinetics of onset of rate-dependent effects of Class I antiarrhythmic drugs are important in determining their effects on refractoriness in guinea-pig ventricle, and provide a theoretical basis for their subclassification. *Cardiovasc Res.* 1983;17:344-352.

46. Harrison DC. Antiarrhythmic drug classification: New science and practical applications. *Am J Cardiol.* 1985;56:185-187.

47. Follmer CH, Colatsky TJ. Block of the delayed rectifier potassium current I_K by flecainide and E-4031 in cat ventricular myocytes. *Circulation.* 1990;82:289-293.

48. Wang Z, Fermini B, Nattel S. Mechanism of flecainide's rate-dependent actions on action potential duration in canine atrial tissue. *J Pharmacol Exp Ther.* 1993;267:575-581.

49. Wang Z, Fermini B, Nattel S: Effects of flecainide, quinidine, and 4-aminopyridine on transient and sustained outward currents in human atrial myocytes. (submitted).
50. Escande D, Coulombe A, Faivre JF, Deroubaix E, Coraboeuf E. Two types of transient outward currents in adult human atrial cells. *Am J Physiol.* 1987;252(Heart Circ Physiol 21):H142-H148.
51. Shibata EF, Drury T, Refsum H, Aldrete V, Giles W. Contributions of a transient outward current to repolarization in human atrium. *Am J Physiol.* 1989;257(Heart Circ Physiol 26):H1773-H1781.
52. Wang Z, Fermini B, Nattel S. Delayed rectifier outward current and repolarization in human atrial myocytes. *Circ Res.* 1993;73:276-285.
53. Davidson E, Rotenberg Z, Weinberger I, Fuchs J, Agmon J. Diagnosis and characteristics of lone atrial fibrillation. *Chest.* 1989;95:1048-1050.
54. Frustaci A, Caldarulo M, Buffon A, Bellocci F, Fenici R, Melina D. Cardiac biopsy in patients with "Primary" atrial fibrillation. Histologic evidnece of occult myocaridal diseases. *Chest.* 1991;100:303-306.
55. Guiraudon CM, Ernst NM, Guiraudon GM, Yee R, Klein GJ. The pathology of drug resistant lone atrial fibrillation in eleven surgically treated patients. In: Kingma JH, van Hemel & Lie KI, eds. *Atrial Fibrillation, a Treatable Disease?* Netherlands, Kluwer Academic Publishers; 1992:41-58.
56. Kumagai K, Akimitsu S, Kawahira K, Kawanami F, Yamanouchi Y, Hiroki T, Arakawa K. Electrophysiological properties in chronic lone atrial fibrillation. *Circulation.* 1991;84:1662-1668.
57. Misier ARR, Opthof T, van Hemel NM, Defauw JJAM, de Bakker JMT, Janse MJ, van Cappelle FJL. Increased dispersion of "refractoriness" in patients with idiopathic paroxysmal atrial fibrillation. *J Am Coll Cardiol.* 1992;19:1531-1535
58. Asano Y, Saito J, Matsumoto K, Kaneko K, Yamamoto T, Uchida M. On the mechanism of termination and perpetuation of atrial fibrillation. *Am J Cardiol.* 1992;69:1033-1038.
59. Attuel P, Childers R, Cauchemez B, Poveda J, Mugica J, Coumel P. Failure in the rate adaptation of the atrial refractory period: its relationship to vulnerability. *Int J Cardiol.* 1982;2:179-197.

Figure Legends

Fig 1. Diagram of the electrode arrays. The position of each recording electrode is shown by a code containing a letter (from A to N) and a number (from 1 to 8). The numbers without letters indicate the positions of stimulating electrodes. (LAA = left atrial appendage, RAA = right atrial appendage, AVR = atrial ventricular ring, PV = pulmonary veins, SVC = superior vena cava, IVC = inferior vena cava, S = site of stimulation used to determine the rate-dependence of conduction and ERP).

Fig 2. Electrophysiologic properties of AF dogs compared to control dogs, and effects of flecainide (Flec.) on properties of AF dogs. A: Dependence of atrial effective refractory period (ERP) on basic cycle length (BCL). B: Dependence of conduction velocity (CV) on BCL. C: Dependence of wavelength (WL) on BCL. D. Percent change in ERP, CV, and WL caused by flecainide in AF dogs as a function of BCL. Statistically-significant cycle-length dependent effects were noted on ERP ($P<.001$) and CV ($P<.01$). $^{*}P<.05$, $^{**}P<.01$, $^{***}P<.001$ for value in presence of flecainide vs pre-drug in AF dog, at each BCL; $\dagger P<.05$, for AF dogs vs control dogs. Results are mean ± SE.

Fig 3. Regional distribution of electrophysiologic properties in control dogs and AF dogs, and in AF dogs after flecainide (Flec.). Data were obtained during stimulation at a cycle length of 250 msec, at each of the sites shown in Fig 1. Results are shown in panel A for refractory period (ERP), panel B for conduction velocity (CV) and panel C for wavelength (WL).

Fig 4. Examples of regional variation in ERP as measured during stimulation at a basic cycle length of 250 msec at each of the seven sites shown in Fig 1. A. Results from five randomly-selected control dogs. B. Results from four AF dogs for whom complete data were available. C. Mean (±SEM) data for control dogs (open circles) and AF dogs (filled circles). Regional variation was significantly greater ($P<.05$, ANOVA) among AF dogs than among control dogs.

Fig 5. Electrical activity during AF in a control dog (left, panels A and B) and an AF dog (right, panels C and D. Recordings from selected electrode sites are shown in A and C, and the activation maps corresponding to the cycles delimited by the vertical dashed lines in A and C are shown in B and D respectively. The arrows in B and D correspond to functional reentry circuits, the lighter lines delimit consecutive 10-ms isochrones, and the heavier lines indicate zones of functional conduction block. The numbers are the activation time range of given isochrones, and letters correspond to the positions of electrodes whose recordings are shown in panel A (for letters on activation map B) or panel C (for letters on map D). Abbreviations are the same as in Fig 1. Isochrones were traced from computer-

derived printouts.

Fig 6. Index of inhomogeneity (open bars, scale at left) during sinus rhythm in AF dogs (Sinus), during AF in control dogs, during AF in AF dogs, and just prior to flecainide-induced termination (Term.) in AF dogs. The mean (+ SE) number of functional reentry circuits during a cycle of AF under each condition is shown by filled bars (scale at right).

Fig 7. Concentration-dependence of flecainide action. Mean (+ SE) drug concentrations are shown at the time of AF termination (Term.), during the maintenance dose (Maint.), and at the times nonsustained AF became inducible [Ind (NS)] and sustained AF became inducible [Ind (S)] following drug discontinuation.

Fig 8. Selected electrograms (panels A) at the time of AF termination by flecainide in the same dog whose control AF is shown in Figs 5D. Panels B and C show activation during the last two cycles of AF, corresponding to the intervals delimited by the vertical lines shown in panels A. The locations of electrodes sites at which the recordings shown in A were obtained are indicated by the cycle shown in B. During the last cycle (C), reentry is terminated by block in the hatched area. (V in panel A designates ventricular electrograms recorded by atrial electrodes). Isochrones were traced from computer-derived printouts.

Table 1. Comparison of Electrophysiologic Properties of AF dogs to Control Dogs, with and Without Vagal Stimulation

	CV (cm/msec)	ERP (msec)	WL (CM)	HR (beat/min)	Wenckebach CL (msec)
AF dogs (n=4)†	90±4	80±7	7.2±0.6	123±5	202±6
Control dogs (n=10)	92±5	95±3*	8.7±0.7*	121±2	198±3
Control dogs, VNS (n=7)	108±4	64±5*	6.9±0.5	74±3**	422±12***

Abbreviations:

CV, conduction velocity; ERP, effective refractory period; WL, wavelength; HR, spontaneous sinus rate; CL, cycle length; VNS, vagal nerve stimulation; AF, atrial fibrillation. *P<.05, **P<.01, ***P<.001 compared to corresponding value in AF dogs.

† Complete results were available only in four AF dogs, because in one dog premature atrial stimuli and rapid atrial pacing readily induced sustained AF.

FIGURE 1

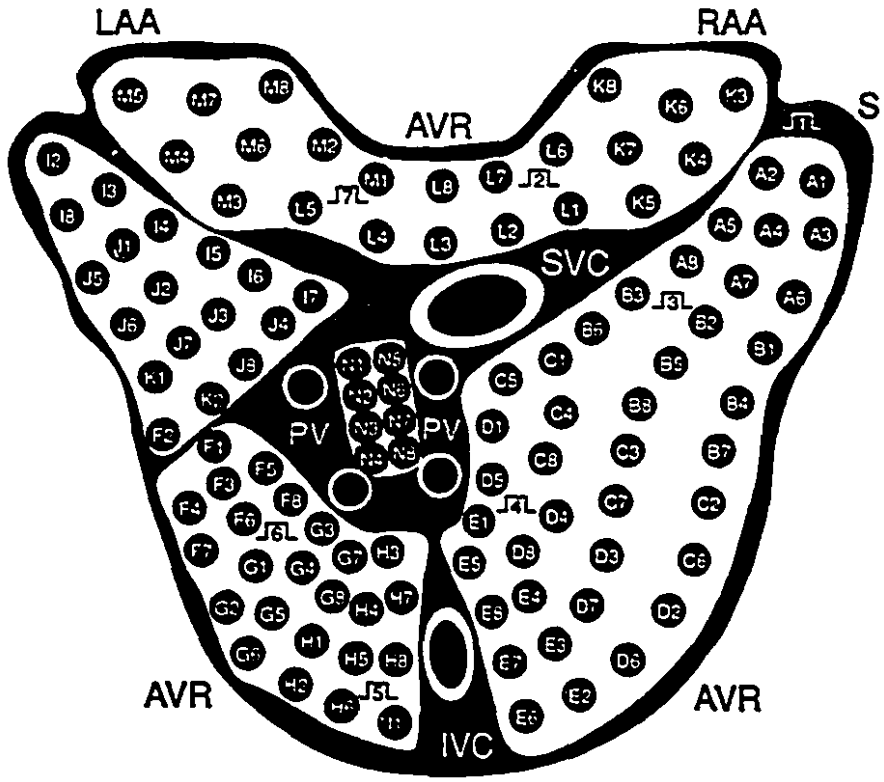

FIGURE 2

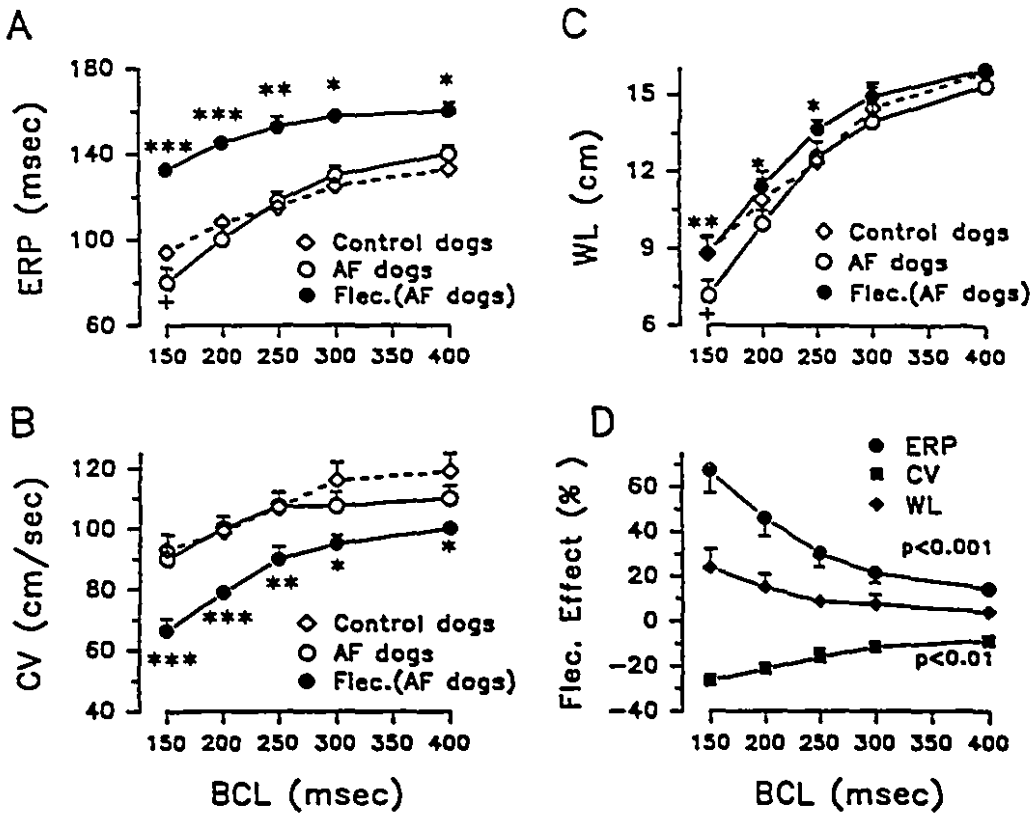
A
ERP (msec)
180
140
100
60
150 200 250 300 350 400
Control dogs
AF dogs
Flec.(AF dogs)
C
WL (cm)
15
12
9
6
150 200 250 300 350 400
Control dogs
AF dogs
Flec.(AF dogs)
B
CV (cm/sec)
120
100
80
60
40
150 200 250 300 350 400
BCL (msec)
Control dogs
AF dogs
Flec.(AF dogs)
D
Flec. Effect (%)
60
40
20
0
−20
−40
ERP
CV
WL
p<0.001
p<0.01
150 200 250 300 350 400
BCL (msec)

FIGURE 3

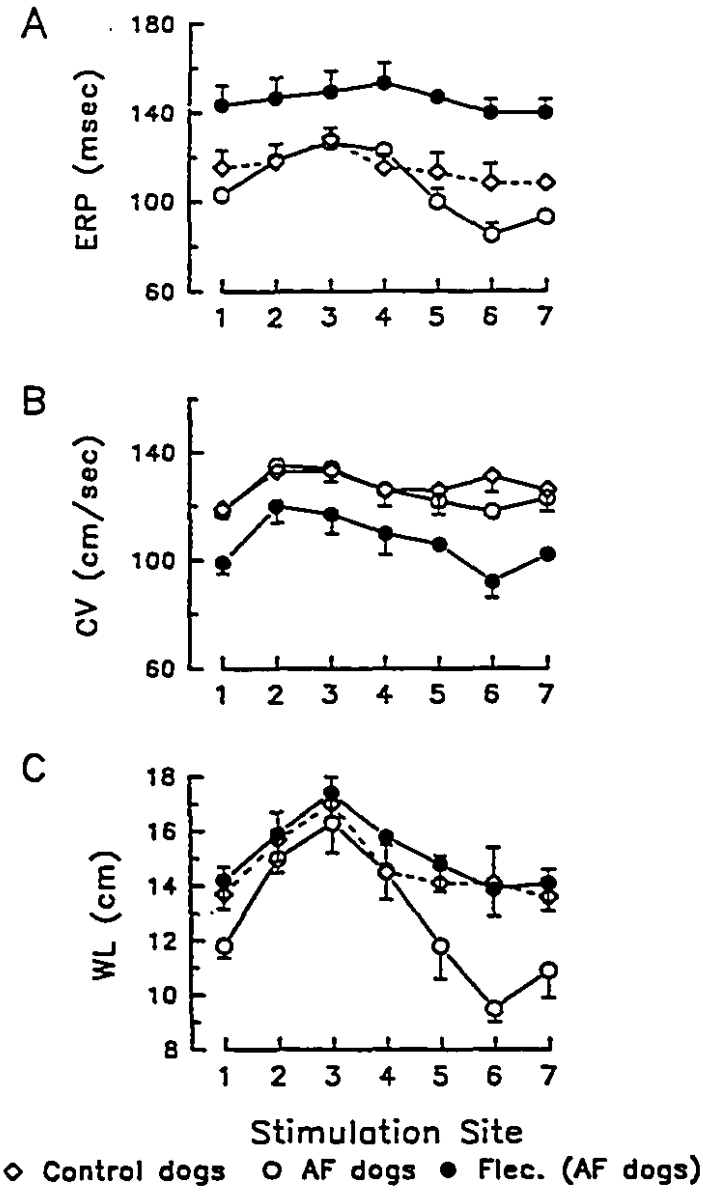
A
ERP (msec)
180
140
100
60
1 2 3 4 5 6 7
B
CV (cm/sec)
140
100
60
1 2 3 4 5 6 7
C
WL (cm)
18
16
14
12
10
8
1 2 3 4 5 6 7
Stimulation Site
◇ Control dogs ○ AF dogs ● Flec. (AF dogs)

FIGURE 4

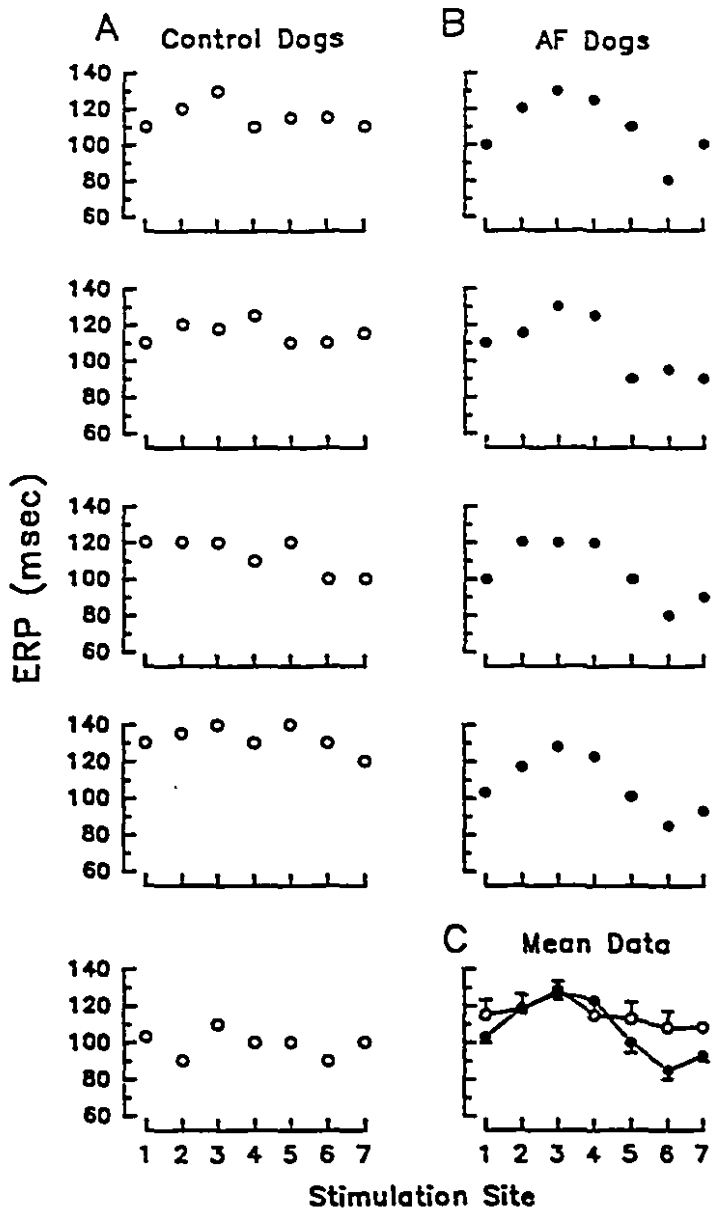
A
Control Dogs
B
AF Dogs
C
Mean Data
ERP (msec)
140
120
100
80
60
1 2 3 4 5 6 7
Stimulation Site

FIGURE 5

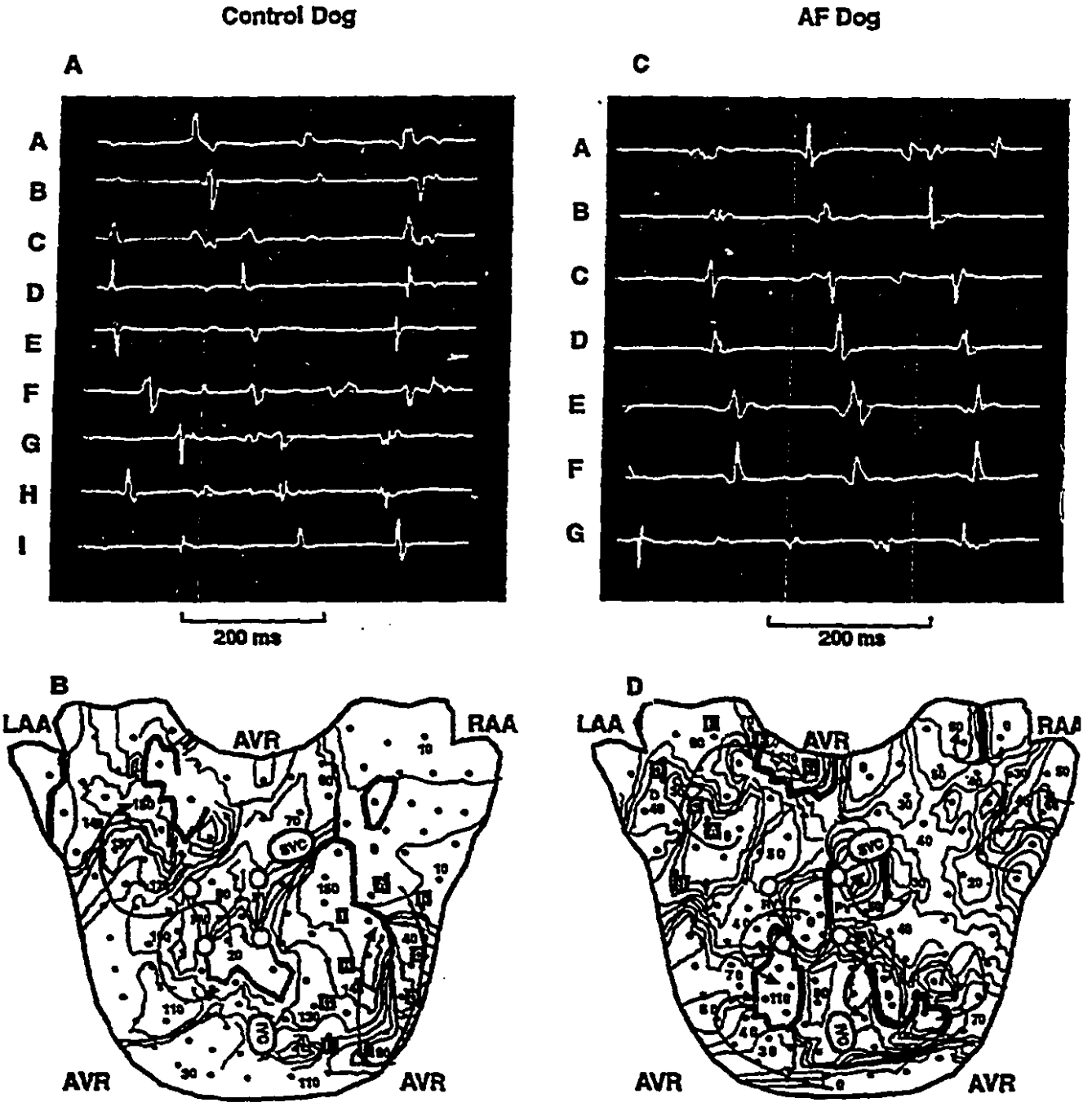
Control Dog
AF Dog
A
C
A
B
C
D
E
F
G
H
I
200 ms
200 ms
B
D
LAA
AVR
RAA
AVR
AVR
SVC
IVC

FIGURE 6

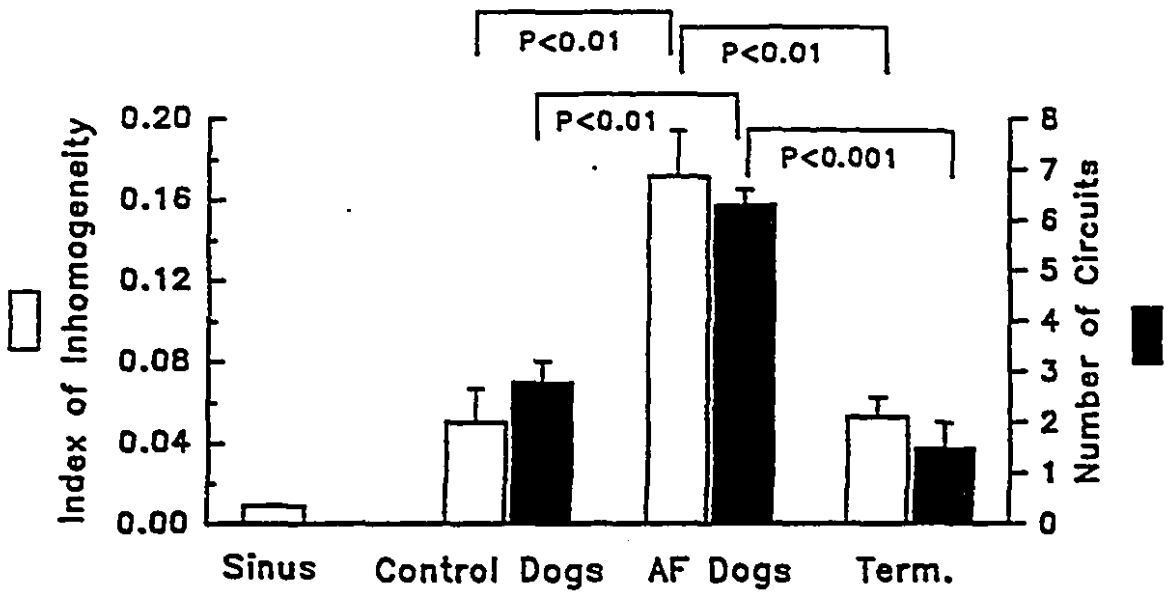
P<0.01
P<0.01
P<0.01
P<0.001
Index of Inhomogeneity
0.20
0.16
0.12
0.08
0.04
0.00
Number of Circuits
8
7
6
5
4
3
2
1
0
Sinus
Control Dogs
AF Dogs
Term.

FIGURE 7

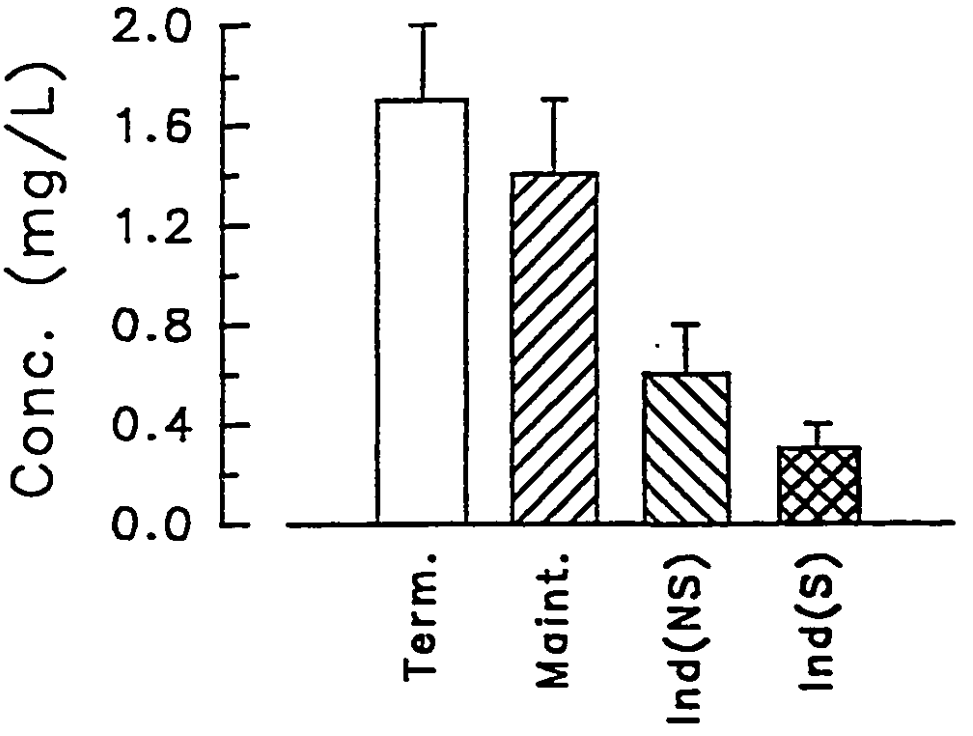

FIGURE 8

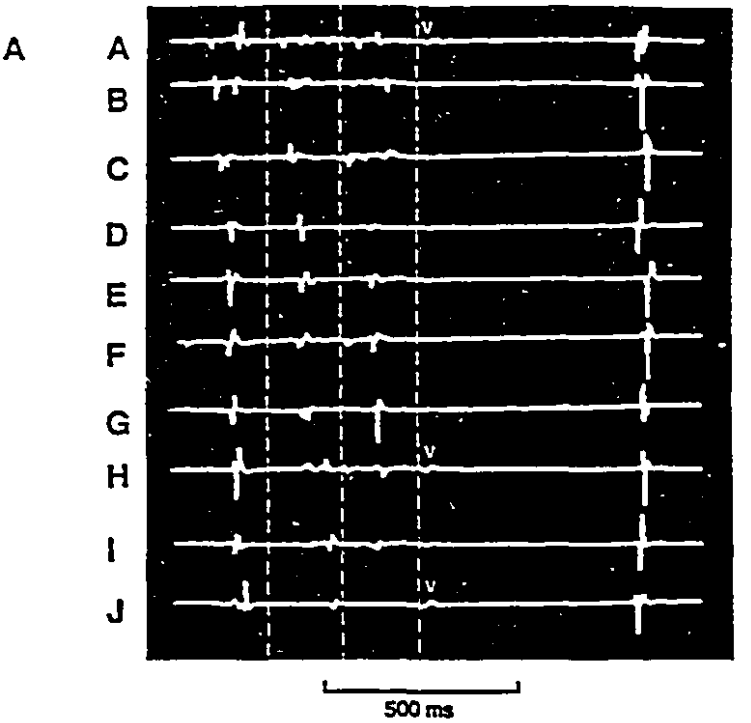
A
A
B
C
D
E
F
G
H
I
J
V
V
V
500 ms

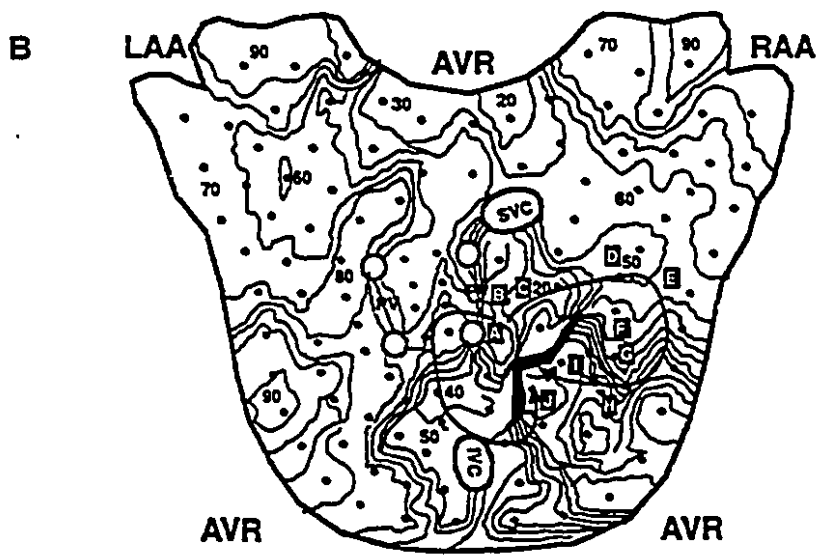
B
LAA
AVR
RAA
SVC
IVC
AVR
AVR

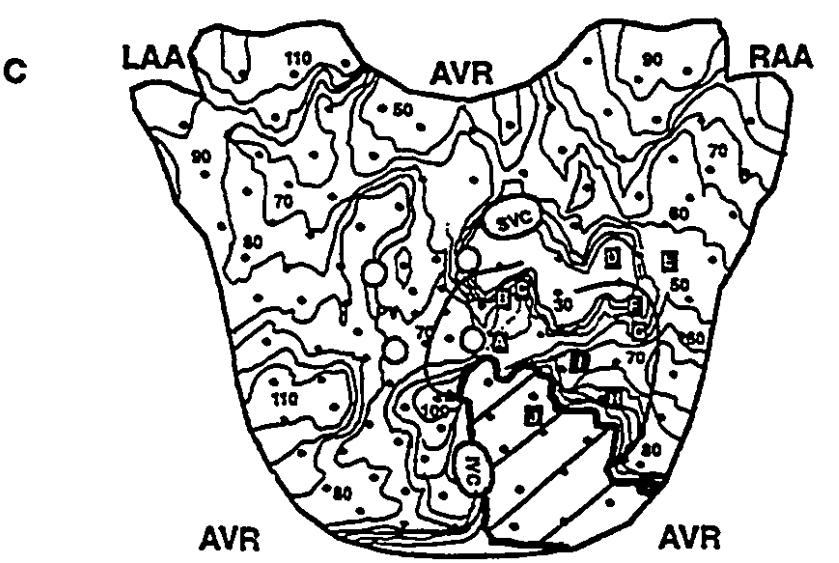
C
LAA
AVR
RAA
SVC
IVC
AVR
AVR

CHAPTER 3

REPOLARIZING CURRENTS IN HUMAN ATRIUM

This study provided further evidence for the importance of ERP and WL in determining AF: in dogs with spontaneous sustained AF, ERP and WL, as well as homogeneity of ERP were markedly decreased. An increase in ERP and WL induced by drugs led to the termination of AF.

So far, we have shown that AF is a reentrant arrhythmia; CV, ERP and WL are the three major determinants of reentry; and use-dependent APD and ERP prolongation may be the common mechanism by which class Ic drugs impose their effectiveness against AF. In fact, this use-dependent property has been recently recognized as a favourable drug action in clinical practice[2-1]. The elucidation of underlying ionic mechanisms would be of great importance. To do so, it is essential to deepen and widen our understanding of the currents governing repolarization. We realized that control of human atrial repolarization remained poorly understood, and many aspects were unexplored. The 4-aminopyridine-sensitive transient outward K^+ current (I_{to1}) was the only voltage-dependent repolarizing current identified[2-6,7], and it was believed since then to be a major, if not the only, repolarizing current in human atrium. Though this current had been characterized, its rate-dependency was incompletely known. I_{to1} is known, based on results from animal studies, to be highly rate-dependent, with minimal contribution to repolarization at fast rates due to its slow recovery from inactivation. This property of I_{to1} causes the rate-dependent APD lengthening seen in rabbit heart. Does human I_{to1} have similar rate-dependency? We have shown substantial rate-dependent APD shortening in human atrium, which was opposite to what happened in rabbits. Possible explanations are that human I_{to1} is rate-independent, or that there are other currents other than I_{to1} contributing to shortening APD with accelerating pacing rates, or both. We started to characterize the rate-dependence of I_{to1} in isolated human atrial myocytes as compared with that in rabbit cells. These results could help us understand the strong rate-dependent APD shortening and class Ic drug-induced rate-dependent APD lengthening in human atrium.

References

2-6. Escande D Coulombe A, Faivre JF, Deroubaix E, Coraboeuf E. Two types of transient outward currents in adult human atrial cells. Am J Physiol 1987;252:H142-H148

2-7. Shibata EF, Drury T, Refsum H, Aldrete V, Giles W. Contributions of a transient outward current to repolarization in human atrium. Am J Physiol 1989;257:H1773-1781.

Differences in rate dependence of transient outward current in rabbit and human atrium

BERNARD FERMINI, ZHIGUO WANG, DAYUE DUAN, AND STANLEY NATTEL
Research Centre, Montreal Heart Institute, Department of Medicine, University of Montreal, Quebec H1T 1C8; and Departments of Pharmacology and Therapeutics and Medicine, McGill University, Montreal, Quebec H3G 1Y6, Canada

Fermini, Bernard, Zhiguo Wang, Dayue Duan, and Stanley Nattel. Differences in rate dependence of transient outward current in rabbit and human atrium. *Am. J. Physiol.* 263 (*Heart Circ. Physiol.* 32): H1747-H1754, 1992.—Both human and rabbit atrial cells possess a large 4-aminopyridine-sensitive transient outward current (I_{to1}). However, the slow reactivation of this current in rabbits suggests that its role may be limited to very slow heart rates. We used whole cell voltage-clamp recordings to evaluate the rate dependency of I_{to1} in rabbit and human atrial myocytes. Our results show that at physiological temperatures in human atrium, I_{to1} is rate independent at rates between 0.1 and 4.0 Hz. Peak I_{to1} at 4.0 Hz in rabbit was 3.4 ± 1.4% (mean ± SE) of current at 0.1 Hz ($P < 0.001$, $n = 8$), whereas in humans, peak I_{to1} at 4.0 Hz averaged 88.8 ± 6.1% of the current at 0.1 Hz ($P > 0.05$, $n = 7$). These differences were due to marked discrepancies in reactivation time course, which was biexponential with time constants that averaged 650 ± 159 ms and 8.4 ± 1.1 s in rabbit ($n = 8$) compared with a single exponential time constant of 33.6 ± 6.8 ms ($n = 8$) in human atrium (both at 30°C). These findings suggest that I_{to1} can contribute importantly to atrial repolarization at all physiological heart rates in humans. Furthermore, these results emphasize that there are important interspecies variations in the rate dependence of I_{to1}, which need to be considered in understanding the physiological and pharmacological regulation of atrial repolarization.

atrial electrophysiology; repolarization; patch clamp

THE PROCESS OF REPOLARIZATION is a major factor in determining the occurrence of a variety of important cardiac arrhythmias. Changes in repolarization alter action potential duration (APD) and consequently refractory period, resulting in considerable changes in the likelihood of reentrant arrhythmias (25). The occurrence of intra-atrial reentrant arrhythmias depends on the balance between conduction velocity and refractory period (25). Furthermore, other cardiac arrhythmia mechanisms, such as early afterdepolarizations, are closely related to alterations in APD and can be precipitated or eliminated by interventions that alter the repolarization process (26).

The factors underlying repolarization are known to be complex and to vary both among species (3, 4) and as a function of heart rate (2, 3). Therefore, when the significance of potential repolarizing currents in a given species is evaluated, their rate dependency must be considered. In human and rabbit atrial cells, the 4-aminopyridine (4-AP)-sensitive transient outward current (I_{to1}) is thought to be the major time-dependent potassium current (9, 12, 13, 28), especially when the interbeat interval is long (15, 22, 27). Because in rabbit atrium this current displays slow reactivation kinetics (12, 13, 22), it can be predicted that its contribution to APD will be determined by stimulation rate. Because of these slow recovery kinetics, its importance to human atrial repolarization at faster rates has been questioned (6).

Whereas detailed studies on the rate dependency of I_{to1} have been reported in diverse animal models, either in tissue (4, 7, 20) or in isolated cell preparations (10, 12, 13, 15, 16, 19), only limited data recorded at room temperature are available for human cardiac preparations (28). In the present work, voltage-clamp techniques and microelectrode recordings were used to study I_{to1} in human and rabbit atrial myocytes. Our results suggest that, contrary to what has been found in rabbit, I_{to1} remains virtually unchanged at rapid rates in human atrium and may therefore contribute importantly to repolarization over a wide range of clinically relevant frequencies.

METHODS

Preparations. The human tissues consisted of small segments of myocardium from the apex of right atrial appendages obtained during coronary arterial bypass surgery. Patients varied in age from 50 to 78 yr with an average of 61 ± 3 yr. All patients had normal P waves on electrocardiography, and no patient had a history of supraventricular arrhythmias. All atrial specimens were grossly normal at the time of excision. Upon excision, the samples were immediately placed in oxygenated Tyrode solution for transport to the laboratory. The time between excision and the beginning of laboratory processing was ~5 min. Tissue was obtained from eight different patients. The procedure for the obtaining of tissue samples and consent was approved by the Ethics Committee of the Montreal Heart Institute.

The samples obtained were quickly immersed in a Ca-free Tyrode solution (100% O_2, 37°C) with the following composition (in mM): 126 NaCl, 5.4 KCl, 1.0 $MgCl_2$, 0.33 NaH_2PO_4, 10 glucose, and 10 *N*-2-hydroxyethylpiperazine-*N*'-2-ethanesulfonic acid (HEPES); pH adjusted to 7.4 with NaOH. The cell isolation procedure was developed based on a technique described by Escande et al. (10). The myocardial specimens were chopped with scissors into cubic chunks and placed in a 25-ml flask containing 10 ml of the Ca-free Tyrode solution previously described. Agitation of the chunks was ensured by continuous bubbling with O_2 and by stirring with a magnetic bar. After 5 min in this solution, the chunks were incubated in a similar solution containing 0.2% collagenase (CLS II, Worthington Biochemical, Freehold, NJ) and 4.0 U/ml protease (Sigma Chemical, St. Louis, MO). The first supernatant was removed after 45 min and discarded. Chunks were then reincubated in a fresh enzyme-containing solution. Microscopic examination of the medium was performed every 15 min to determine the number and quality of the isolated cells. When the cell yield appeared to be maximal, the chunks were suspended in a high K^+ solution containing (in mM) 20 KCl, 10 KH_2PO_4, 10 glucose, 70 glutamic acid, 10 β-hydroxybutyric acid, 10 taurine, 10 ethyleneglycol-bis(β-aminoethyl ether)-*N,N,N',N'*-tetraacetic acid (EGTA), and 1% albumin; pH adjusted to 7.4 with KOH, and gently pipetted.

Rabbit atrial cells were obtained from 1.4- to 2.3-kg rabbits by collagenase dissociation. Rabbits were killed by cervical dislocation, and the heart from each rabbit was rapidly removed.

mounted on a Langendorff apparatus, and perfused with a modified HEPES-buffered Tyrode solution (37°C, 100% O_2, pH adjusted to 7.4 with NaOH) until clear of blood. Perfusion through the coronary system with a Ca-free Tyrode solution was performed until the heart stopped beating, and perfusion was then continued for 15 min with the same solution containing 0.1% collagenase (CLS II, Worthington Biochemical) and 1.0% bovine serum albumin (Sigma Chemicals). The hearts were subsequently washed for a period of 2 min with the calcium-free solution, and then the left or right atrium was removed and placed in the storage solution described previously. The left atrium was used in most experiments to avoid recording from nodal or transitional cells found in the right atrium (1). Cell dissociation was achieved by mechanical agitation using a Pasteur pipette. The isolated cells were stored in the high K^+ solution and left to sediment in 15-ml centrifuge tubes. While all the results presented in this study are from cells stored in high K^+ solutions until use, we now gradually replace the high K^+ solution with normal bath solution (30, 60, and 100% substitution within 60 min), and similar properties are found for I_{to1} in both human and rabbit atrial myocytes.

Microelectrode technique. Details of the procedures and composition of the Tyrode solution as well as electrophysiological recording techniques and data acquisition and analysis for this technique were described in a previous study (30). Briefly, human atrial preparations were pinned to the Sylgard-covered bottom of a 20-ml Lucite chamber with the endocardial surface facing upward and were superfused at 8 ml/min with the following Tyrode solution (in mM): 116 NaCl, 18 $NaHCO_3$, 10 dextrose, 4 KCl, 0.9 NaH_2PO_4, 0.5 $MgCl_2$, and 1.0 $CaCl_2$. The superfusate was aerated with 95% O_2-5% CO_2, and the bath temperature was maintained at 36°C by a heating element and proportional power supply (Hanna Instruments, Philadelphia, PA). The pH of the bathing solution was 7.35–7.4. One hour was allowed for tissue equilibration before experiments were begun.

Glass microelectrodes filled with 3 M KCl and with tip resistances of 8–20 MΩ were coupled by a silver-silver chloride junction to a high-impedance microelectrode amplifier (WPI KS-700, World Precision Instruments, New Haven, CT). A bipolar Teflon-coated platinum electrode was used to deliver square pulses of 2-ms duration and twice diastolic threshold current to stimulate the preparation. A programmable stimulator and stimulus isolation unit (Bloom Instruments, Flying Hills, PA) were used to deliver stimuli with selected stimulation protocols. Signals were displayed on a storage oscilloscope (Tektronix 515, Tektronix, Beaverton, OR) and photographed using a polaroid-type camera (model C59A, Tektronix).

Voltage-clamp technique. A small aliquot of the medium containing the cells was placed in a 1.0-ml chamber mounted on the stage of an inverted microscope. After a brief period to allow cell adhesion to the cover slip at the bottom of the chamber, the cells were superfused at 3 ml/min with a solution containing (in mM) 126 NaCl, 5.4 KCl, 0.8 $MgCl_2$, 1.0 $CaCl_2$, 2.0 $CoCl_2$, 0.33 NaH_2PO_4, 10 HEPES, and 5.5 glucose. The pH of the superfusate was adjusted to 7.4 with NaOH. The bath temperature was monitored by a small thermistor, and temperature was maintained at 30 or 36 ± 1°C with a temperature controller device (N. B. Datyner, Stony Brook, NY).

All current recordings were obtained in the whole cell, voltage-clamp configuration of the patch-clamp technique (14) using 1.0 mm OD borosilicate glass electrodes. While preliminary experiments were performed using electrodes having a tip resistance of 5–10 MΩ, most of the data presented in this study were obtained with electrodes having a tip resistance between 1 and 5 MΩ when filled with (in mM) 130 KCl, 1.0 $MgCl_2$, 10 HEPES, 5.0 EGTA, 5.0 Mg_2ATP, and 5.0 Na_2 creatine phosphate, pH adjusted to 7.4 with KOH. These electrodes were connected to a patch-clamp amplifier (Axopatch 1-D, Axon Instruments, Burlingame, CA). Command pulses were generated with an IBM AT compatible computer interfaced with a digital-analog convertor (Axon Instruments, Burlingame, CA), using pClamp software or by a digital stimulator (Medical Systems, Greenvale, NY). Whole cell currents were filtered at 1 kHz bandwidth. The amplitude of peak I_{to1} was measured as the difference between the peak of the transient outward current and the steady-state current at the end of the pulse. The steady-state component was measured as the difference between the current remaining at the end of the test pulse and the baseline current at the holding potential (HP).

In all of the cells studied, the series resistance was compensated to minimize the duration of the capacitive surge on the current record. The series resistance along the clamp circuit was estimated by dividing the time constant of the capacitive transient (obtained by fitting the decay of the capacitive transient) by the calculated cell membrane capacitance (the time-integral of the capacitive surge measured in response to 5 mV hyperpolarizing steps from a HP of −60 mV). Before series resistance compensation, the decay of the capacity surge in both human and rabbit atrium was expressed by a single exponential having a time constant of 500 ± 60 μs in human (cell capacitance: 78.9 ± 8.4 pF, $n = 10$) and 800 ± 40 μs in rabbit (cell capacitance: 70.3 ± 5.5 pF, $n = 11$), respectively. After compensation these values were reduced to 220 ± 10 μs in human (cell capacitance: 73.7 ± 7.7 pF, $n = 10$) and 280 ± 20 μs in rabbit atrial myocytes (cell capacitance: 65.8 ± 5.3 pF, $n = 11$). The initial series resistance in human atrial cells was calculated to be 6.6 ± 0.7 MΩ and was reduced to 2.9 ± 0.2 MΩ after compensation. In rabbit myocytes, these values were 11.8 ± 0.8 and 4.3 ± 0.4 MΩ before and after compensation, respectively. Depolarizing pulses were applied from a HP of −60 mV. When normalized to the averaged cell capacitance, I_{to1} measured at 0 mV from a HP of −60 mV was 13.5 ± 1.3 pA/pF in rabbit compared with 2.1 pA/pF in human atrial myocytes. In some experiments ($n = 3$), I_{to1} was measured after NaCl was isotonically replaced by choline chloride to minimize interference from inward Na^+ current (I_{Na}). Similar properties and rate dependence were found for I_{to1} under these conditions. Moreover, we, like others (24), have observed that I_{Na} in human atrial cells is almost completely inactivated at HPs positive to −60 mV. Therefore, under our experimental conditions, there was minimal contamination of I_{to1} by I_{Na}. Addition of tetrodotoxin to the bathing medium or zero-sodium solutions were not used on a routine basis, since these procedures have been shown to inhibit I_{to1} (8).

Student's *t* tests and analysis of variance (ANOVA) were used to evaluate the statistical significance of differences between means. Values of $P < 0.05$ were considered to indicate significance. Data are expressed as means ± SE. A nonlinear curve-fitting technique (Marquardt's procedure) was used to fit experimental data to single or double-exponential relations.

RESULTS

Previous studies in human atrium and dog and rabbit atrial and ventricular myocytes (10, 12, 16, 29, 31) have shown that the transient outward current can be resolved into two components. One component, described as a long-lasting 4-AP-sensitive transient outward current (I_{to}), I_{to1}, or I_t, is carried mainly by K^+, has a slow decay, and is inhibited by 4-AP, but not calcium channel blockers such as cobalt (Co^{2+}). The other component, described as a brief caffeine-sensitive transient outward current (I_{to}), I_{to2}, Ca^{2+}-sensitive transient outward current ($I_{K,Ca}$), or Ca^{2+}-activated Cl^- current [$I_{Cl(Ca)}$], is carried mainly by Cl^-, has a shorter rise time and faster decay, and is inhibited by slow inward Ca^{2+} (I_{si}) blockers

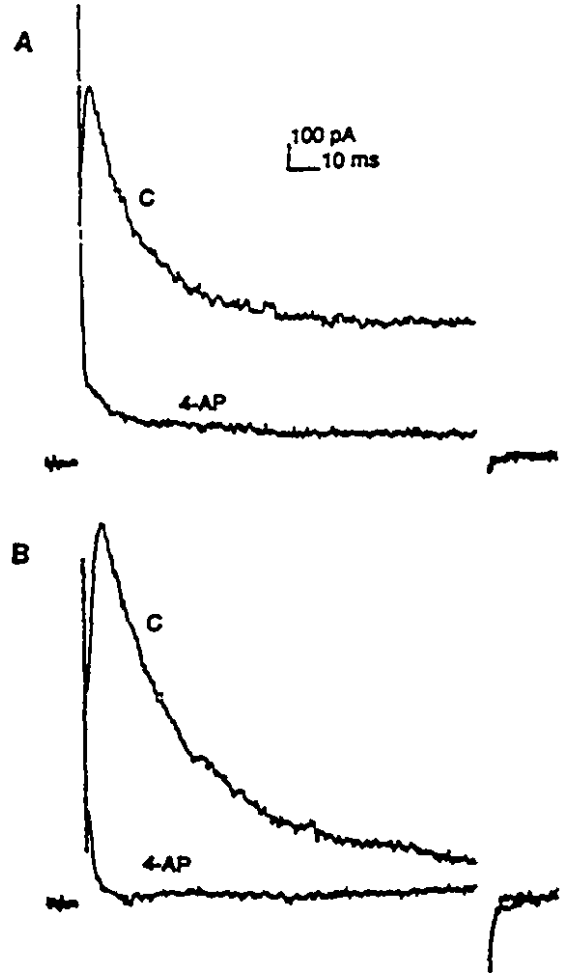

Fig. 1. Effect of 4-aminopyridine (4-AP) on transient outward current (I_{to1}) in human (*A*) and rabbit (*B*) atrial myocytes. Currents were recorded at 0.1 Hz following 80-ms pulses to +20 mV from a holding potential (HP) of −60 mV (*A*) or −50 mV (*B*), before (*line C*) and 5 min after superfusion of 4-AP (2 mM). Cobalt (2 mM) was present in all experiments to inhibit Ca^{2+} current (I_{Ca}) and I_{Na}. Experiments were performed at 36°C.

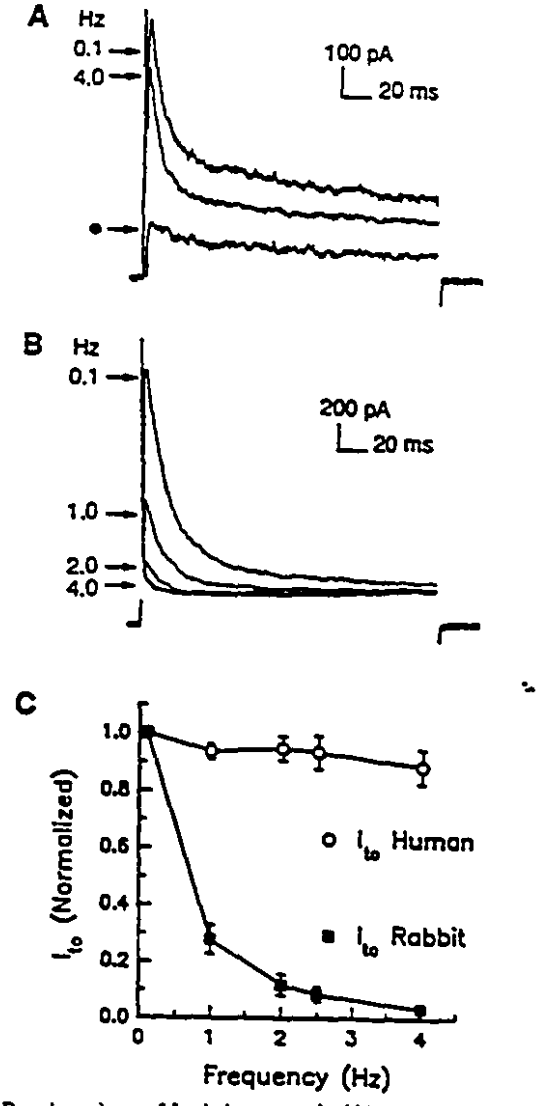

Fig. 2. Rate dependency of I_{to1} in human and rabbit atrial myocytes. *A*: I_{to1} recorded in human atrial myocytes. Depolarizing voltage pulses (200 ms) were applied to 0 mV from a HP of −60 mV. Only traces obtained at 0.1 and 4.0 Hz are shown for sake of clarity. Subtracted current trace (filled circle, 4.0–0.1 Hz) shows that increasing rate of pulses had little effect on peak I_{to1}, while steady-state component of current was reduced. *B*: in contrast, a similar increase in rate produced a significant decrease in size of I_{to1} in rabbit atrium, revealing its strong rate dependency in this structure. *C*: averaged data of normalized peak I_{to1} obtained at different rates from experiments described in *A* and *B*. Current was normalized to peak amplitude at 0.1 Hz. While increasing the rate of stimulation had no effect in human tissue ($P > 0.05$ at all the frequencies studied, $n = 7$), I_{to1} was significantly reduced ($P < 0.001$) at 1.0, 2.0, 2.5, and 4.0 Hz in rabbit atrial myocytes ($n = 8$). Experiments were performed at 36°C.

such as Co^{2+} and by sarcoplasmic reticulum inhibitors such as caffeine. Because 2 mM Co^{2+} was present in the superfusate for voltage-clamp experiments, all of the I_{to} recorded should have consisted of the 4-AP-sensitive current, I_{to1} (10, 12, 16, 29, 31). To confirm this, we studied the effect of 4-AP (2 mM) on I_{to} in rabbit and human atrial myocytes ($n = 10$ of each). As shown in Fig. 1, this current was highly sensitive to 4-AP in both tissues and was strongly inhibited (>80%) at 0.1 Hz. Therefore, in describing the transient outward current in this study, we use the terminology I_{to1}.

Effect of rate on I_{to1}. We examined the effect of increasing the frequency of pulses from 0.1 to 1.0, 2.0, and 4.0 Hz on peak I_{to1} in human and rabbit atrial myocytes. Test pulses to 0 mV from a HP of −60 mV were maintained for 200 ms. The pulse duration was selected to mimic APD in human atrial tissue at rapid rates (30). Figure 2*A* shows an example of I_{to1} recorded in human atrium during test pulses at frequencies of 0.1 and 4.0 Hz (36°C). Increasing the rate of pulses had no significant effect on the amplitude of I_{to1} (as measured from the peak to the steady-state level); however, the steady-state component was decreased. This result is illustrated in Fig. 2*A* (bottom

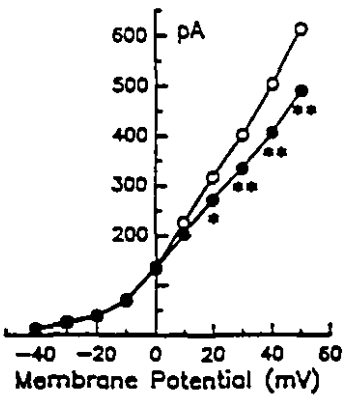

Fig. 3. Effect of rate on steady-state component of I_{to1} in human atrial myocytes. Currents were recorded after 80-ms depolarizing pulses to potentials between −50 and +50 mV from a HP of −60 mV at either 0.1 (open circles) or 2.5 (filled circles) Hz (n = 8). Increasing rate of pulses had no effect on the sustained component of I_{to1} at potentials between −40 and +10 mV. Experiments were performed at 30°C. Error bars are within symbol size. * $P < 0.05$; ** $P < 0.01$.

current trace), which represents the current obtained by subtracting I_{to1} recorded at 4.0 Hz from that obtained at 0.1 Hz. In seven cells studied, the steady-state component decreased by 39.6 ± 5.7% between 0.1 and 4.0 Hz compared with 11.2 ± 6.1% for peak I_{to1}. In contrast, peak I_{to1} recorded in rabbit atrial cells was reduced markedly by a similar increase in rate (Fig. 2*B*), revealing its strong rate dependency in this structure. Figure 2*C* shows averaged data of normalized peak I_{to1} for different rates in human (n = 7) and rabbit (n = 8) atrial myocytes. While peak current was not significantly affected by rate over a range between 0.1 and 4.0 Hz in human tissue (869.8 ± 57.5 pA at 0.1 Hz compared with 823.8 ± 65.2 pA at 4.0 Hz, n = 7, $P > 0.05$), it decreased by 96.6 ± 1.4% in rabbit ($P < 0.001$). The steady-state component of I_{to1} in rabbit decreased by 26.7 ± 4.1% between 0.1 and 4.0 Hz (n = 8). The above results were obtained at 36°C. Similar experiments were performed at 0.1–1.0, 2.0, and 2.5 Hz at 30°C (HP −60 mV, n = 8), and comparable results were obtained in both human and rabbit atrial myocytes. Under these conditions, peak I_{to1} in human atrium was unchanged at all potentials studied (−40 to +60 mV), while the steady-state component was reduced significantly only for potentials positive to +10 mV (Fig. 3). In rabbit atrium, the rate-dependent reduction of peak I_{to1} was independent of voltage over the range −10 to +40 mV. The mean reduction in peak I_{to1} (n = 11 for each potential) was 61.9 ± 5.6, 69.0 ± 4.1, 71.7 ± 3.1, 71.1 ± 2.5, 71.2 ± 2.4, and 71.1 ± 2.3% at −10, 0, +10, +20, +30, and +40 mV, respectively, when the frequency of pulses was changed from 0.1 to 2.5 Hz. In human atrium, peak I_{to1} remained unchanged under these conditions.

The fact that peak I_{to1} appears to be rate independent in human atrium between 0.1 and 4.0 Hz suggests that the reactivation kinetics of this current should be rapid compared with rabbit. This hypothesis was tested using a paired pulse protocol where two identical pulses (P1 and P2) were applied from a HP of −60 mV to +40 mV at 0.1 Hz (30°C) with a variable coupling interval. As shown in Fig. 4*A*, peak I_{to1} elicited by P2 in human atrial cells recovers rapidly to the amplitude of that elicited by P1, and reactivation of peak current is complete within 125 ms. The time course of I_{to1} recovery in human cells was well described by a single exponential relationship with a time constant of 33.6 ± 6.8 ms (Fig. 4*B*, n = 8). In contrast, the time course of recovery from inactivation in rabbit left atrial cells (n = 5) was best described by the

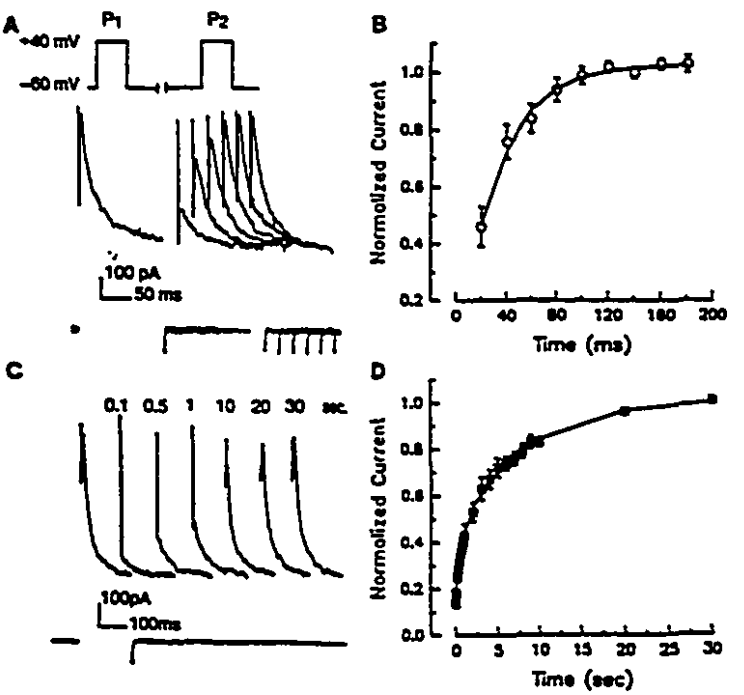

Fig. 4. Time course of recovery from inactivation of transient outward current in human and rabbit atrial myocytes. *A*: typical example of reactivation of I_{to1} in human atrium. Paired pulses (P1 and P2, 150 ms to +40 mV) were applied from a HP of −60 mV with 25-ms increments, and the protocol was repeated every 10 s. Peak current fully recovered within 125 ms. *C*: when a similar protocol was repeated in rabbit atrium (every 30 s), recovery of I_{to1} was found to be significantly slower. Only traces recorded after 0.1, 0.5, 1, 10, 20, and 30 s are shown as indicated. *B* and *D*: average data showing curve fitting of recovery time course from inactivation in human (n = 8) and rabbit (n = 5) atrial myocytes. Recovery in human atrial cells was first order with a time constant of 33.6 ± 6.8 ms. In contrast, time course of recovery in rabbit atrial cells was best described by the sum of 2 exponentials: a fast component with a time constant of 650.6 ± 159.0 ms and a slower component with a time constant of 8.4 ± 1.1 s. Experiments were performed at 30°C.

sum of two exponential components (Fig. 4, *C* and *D*): a fast component with a time constant of 650.6 ± 159.0 ms and a much slower component with a time constant of 8.4 ± 1.1 s. By fitting the reactivation process with an equation of the form

$$Y = A_0 + A_S \exp^{(-t/\tau S)} + A_F \exp^{(-t/\tau F)}$$

where A_S and A_F are the initial amplitudes of the "slow" and "fast" phases of recovery, we found that the mean proportion of the total time-dependent component of reactivation of I_{to1} associated with the fast phase of recovery (i.e., the ratio A_F to $A_F + A_S$) was 0.64 ± 0.06 ($n = 5$), indicating that the contribution of the fast phase to the time course of recovery from inactivation of I_{to1} was ~60%. When studied in right atrial cells ($n = 3$), the recovery from inactivation was well described by a single exponential component with an average time constant of 7.2 ± 2.3 s. In rabbit atrium, full recovery was observed for interpulse intervals longer than 20 s. These results clearly show that the recovery process of I_{to1} in rabbit atrium is significantly slower than in human atrium. When studied at 36°C in humans, the time constant was further reduced to 14 ± 2 ms.

Figure 5 shows typical human atrial action potentials recorded from an atrial strip at 36°C during premature stimulation (Fig. 5*A*) and after an abrupt change in cycle length from 1,000 to 300 ms (Fig. 5*B*). Very early premature activations show an elevated plateau and slowed early repolarization, features that are typical of inhibition of I_{to1} in human atrial tissue (9, 28). However, within an interval of 200 ms, the plateau is lowered and early repolarization becomes very rapid. When cycle length is abruptly changed from 1,000 to 300 ms (Fig. 5*B*), APD gradually decreases over the next 20 beats, but the phase of early repolarization, is unchanged. The rate-dependent differences between human and rabbit atrial action potentials are also illustrated in Fig. 6. The cells were stimulated at 1.0 Hz (30°C) by 2-ms suprathreshold current pulses in current clamp mode after a 1-min rest period. As expected from previous observations of rate-dependent

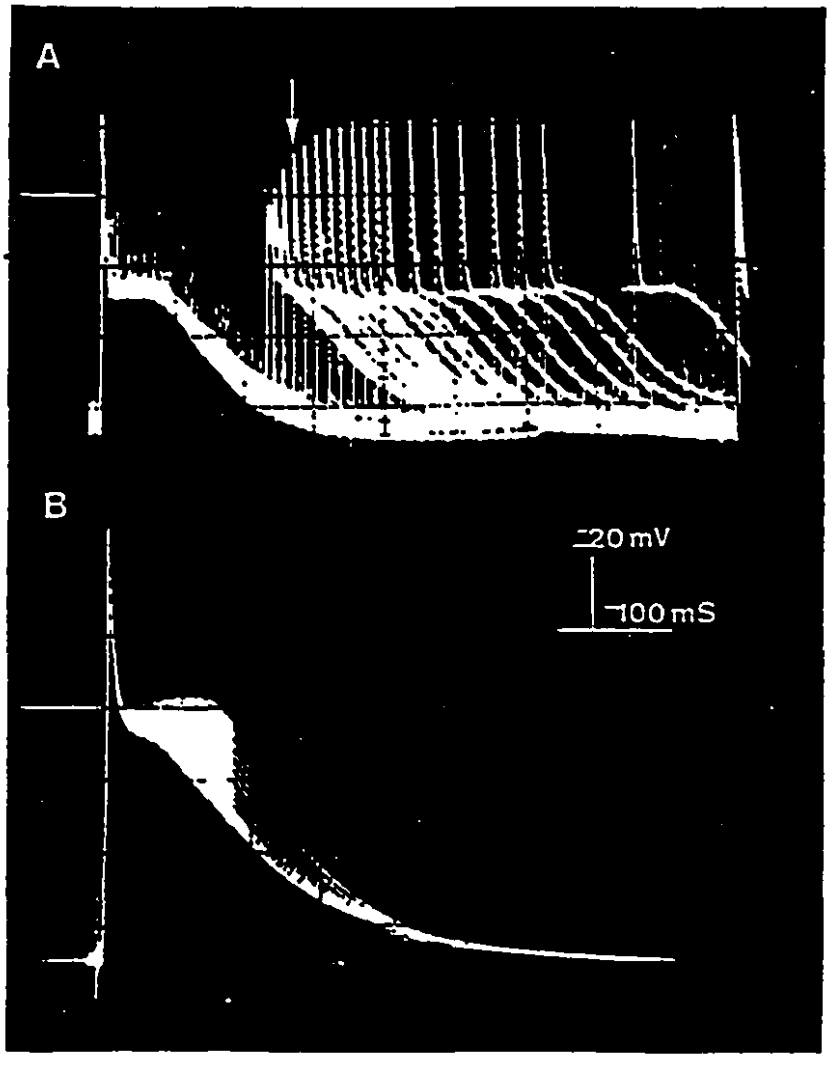

Fig. 5. Effect of premature stimulation and an abrupt change in cycle length on action potential characteristics recorded from a segment of human right atrium at a frequency of 1.0 Hz. *A*: action potentials elicited by early premature activation displayed an elevated plateau and early repolarization. Nonetheless, spike and dome morphology recovered fully within 200 ms, consistent with rapid recovery of I_{to1} from inactivation. *B*: decreasing cycle length abruptly from 1,000 to 300 ms progressively reduced action potential duration; however, *phase 1* repolarization remained unchanged, consistent with the lack of rate dependence of I_{to1}. Experiments were performed at 36°C. Horizontal line on left of each panel indicates zero potential level. Vertical arrow in *A* indicates a 195-ms coupling interval.

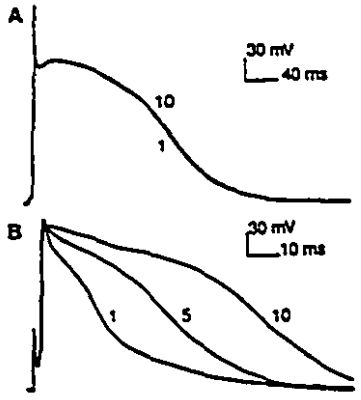

Fig. 6. Rate-dependent differences between human and rabbit atrial action potentials. Action potentials were recorded from cells isolated from human (*A*) and rabbit (*B*) atrium. Panels display the 1st, 5th, and 10th action potential recorded at a driving rate of 1.0 Hz following a 1-min rest period. For sake of clarity, only 1st and 10th action potentials are shown in *A*. In human myocytes, no significant changes were observed in morphology of action potentials between the 1st and 10th stimulus, whereas in rabbit, action potentials displayed rate-dependent prolongation after repetitive activation. These findings are also compatible with rapid recovery of I_{to1} in human atrium. Experiments were performed at 30°C. Co^{2+} (2 mM) was present in *B*. Horizontal line on right of each panel indicates zero potential level.

behavior of rabbit atrium action potentials (12), the duration of the action potential recorded from rabbit myocytes gradually prolonged during repetitive activation. In contrast, no changes were observed in the morphology of the action potentials recorded from human myocytes. These findings are compatible with very rapid recovery of I_{to1} from inactivation in human atrium.

DISCUSSION

Our results show that I_{to1} in human atrium is rate independent at frequencies between 6 and 240 beats/min, and its contribution should therefore remain important at fast heart rates. This finding is consistent with the current's rapid recovery kinetics, with a mean time constant of <40 ms at 30°C and 14 ms at 36°C. In contrast, in rabbit atrium, I_{to1} decreased substantially as frequency was increased from 0.1 Hz, and the current declined steadily by up to 96.6% over the same range of rates. Moreover, the recovery from inactivation of I_{to1} was described by a biexponential process in rabbit atrium with a rapid phase time constant in the order of 700 ms. These results emphasize the possibility of major interspecies differences in the kinetic determinants of otherwise similar ionic currents and the potential danger of extrapolating from one species to another.

Comparison with previous studies in literature. Earlier studies have reported that I_{to1} is very sensitive to activation rate in rabbit atrium (12, 13, 22). Our results in human atrium are, to our knowledge, the first demonstration that this current can display rate-independent properties in an atrial preparation. Rapid reactivation of I_{to1} in human atrial myocytes obtained from adult preparations was also proposed by Escande et al. (9) to explain the rate-dependent differences in APD and morphology recorded from atrial tissue obtained from young and adult patients. Our results support this hypothesis.

A previous study using human atrial myocytes showed that I_{to1} was rate dependent between 0.2 and 3.6 Hz (28). This difference may be partly due to the fact that the voltage-clamp experiments in that study were performed at 23°C, which would have slowed the kinetics of the current. Their results show that I_{to1} decreased by 92.8% over the range of 0.2–3.6 Hz (their Fig. 5). This is consistent with the relatively slower reactivation time constant they obtained (141 ms at HP −60 mV), which should have resulted in the accumulation of substantial inactivation at rates faster than 2.5 Hz with 250-ms depolarizing clamp pulses. However, other factors such as the condition of the atrial tissue upon excision, the isolation procedures, and the nature of the cells obtained may have contributed to some of the differences observed. The same authors found that the steady-state current at the end of the test pulse decreased with increasing rate, with changes in the same order as the decrease that we observed (39.6 ± 5.7%) between 0.1 and 4.0 Hz ($n = 7$). This frequency-dependent change in the steady-state component of I_{to1} is difficult to explain. Although other currents (pump currents, exchange currents) may contribute to this component, it is unlikely that the decrease observed results from a change in amplitude of the inwardly rectifying background current (I_{K1}), since human and rabbit atrium exhibit very little background current of this type, and furthermore this current displays strong inward rectification at the positive test potentials used to study I_{to1} (12, 28). The delayed rectifier current (I_K) could theoretically contribute to the sustained outward current at the end of a pulse, but I_K is not normally inhibited as rate is increased (5) and could not account for the rate dependence of the steady-state component. Moreover, we have experimental evidence (not shown) that in the presence of Ba^{2+} (500 μM to inhibit I_{K1}) and tetraethylammonium (10 mM to inhibit I_K), this sustained component can still be recorded in both human and rabbit atrial myocytes and that it exhibits similar rate-dependent reductions. Finally Fig. 1 shows that, together with peak I_{to1}, the sustained component is highly sensitive to 4-AP, suggesting that it is closely related to I_{to1}. Nonetheless, it is clear that the electrophysiological and pharmacological properties of the sustained component of I_{to1} remains to be investigated.

Potential limitations. The rabbits used in this study were between 8 and 10 wk old (1.4–2.3 kg). A recent study looking at the developmental changes in I_{Ca} and I_{K1} in fetal, neonatal, and adult rabbit ventricular myocytes (17) defined adult rabbits as weighing between 1.5 and 2.5 kg. We therefore assumed that only "adult" rabbits were used in the present study. Saxon and Safronova (27) reported that action potentials recorded from papillary muscle of young rabbits (<1 mo old) showed little change in configuration during repetitive stimulation compared with the action potential changes observed in adult (2 mo old) animals, suggesting maturation of I_{to1} channels during postnatal development in rabbit hearts. Development changes in I_{to1} have also been reported in rat ventricular myocytes (21), but rate dependency was not studied in that report. Escande et al. (9), on the other hand, reported

that the "repriming process rate" of I_{to1} in human atrium was faster in adult and slower in younger tissue, suggesting once again an age-related difference in the reactivation properties of I_{to1}. Therefore, although "adult" tissue from both species was used in this study, we cannot totally exclude the possibility that age differences may have contributed to the observed differences in the reactivation kinetics of I_{to1}.

It is also unlikely that the differences in rate dependency of I_{to1} between human and rabbit atrial myocytes can be accounted for by differences in the voltage dependency of activation or inactivation of this current. Giles and van Ginneken (13) showed that the time course of recovery from inactivation of I_{to1} in rabbit atrium was slowest near the half-inactivation potential ($V_{1/2}$: −30 mV, their Fig. 4) and that the magnitude of changes in the time course of recovery was steepest within a 10- to 20-mV range of $V_{1/2}$. At potentials between −50 and −80 mV, the reactivation time constant (τ_{react}) of I_{to1} was rapid and voltage independent (their Fig. 6). Using a standard double-pulse protocol, we measured the steady-state inactivation characteristics of I_{to1} in both rabbit ($n = 7$) and human ($n = 17$) atrial myocytes, and we found that the average data points were well fitted by a Boltzmann distribution with a $V_{1/2}$ and slope factor of −43.0 ± 4.2 and 15.2 ± 3.1 mV for rabbit and −26.6 ± 1.5 and 5.8 ± 0.3 mV for human cells, respectively. Assuming that our reasoning is correct, one would expect the recovery of I_{to1} at −60 mV to be similar in both rabbit and human tissue. However, our data do not support this hypothesis but rather show that recovery from inactivation was over 20 times faster in human atrium.

Potential significance of our findings. Our findings are important in understanding the physiological role of I_{to1} in human atrial tissue. If one extrapolated directly from results in rabbit atrium to humans, I_{to1} would be expected to be small at 1 Hz and negligible at faster rates. Because, on the contrary, this current remains significant over a wide range of rates in humans, drugs such as quinidine (18) and α-agonists (11), which selectively inhibit I_{to1}, can express this action over the physiological span of frequencies. While a decrease in the sustained component of I_{to1} with increased rates should normally lead to a prolongation of APD in human atrial cells, our results suggest that these changes usually occur at potentials more positive than the plateau level and therefore induce minimal changes in the morphology of the action potential (see Fig. 3).

We do not interpret our results to suggest that in human atrium I_{to1} becomes the major repolarizing current as heart rate is increased, but rather that because of its rate-independent properties, its contribution to repolarization at fast rates in human tissue may be more important than previously recognized, especially compared with rabbit atrium. Because 4-AP produces a significant shortening of APD in human atrium (9, 23, 28), it appears that I_{to1} may influence overall APD by indirectly affecting the properties of other plateau currents. This hypothesis was also proposed by Escande et al. (9) to explain the shortening effect of 4-AP on adult atrial APD. These authors suggested that the increase in plateau level observed after inhibition of I_{to1} by 4-AP would result in greater activation of a repolarizing delayed K^+ current. In support of this hypothesis, we recently identified and characterized a delayed rectifier current showing properties similar to I_K in human atrial myocytes (unpublished observations).

Finally, our results emphasize the potential pitfalls in extrapolating from results in one species to another. Significant differences exist among species in their response to antiarrhythmic agents (6). Better understanding of the properties of ionic currents in human tissue is necessary before the mechanisms of antiarrhythmic drug action in humans can be fully appreciated.

The authors thank Guylaine Nicol for expert technical assistance and Drs. Michel Carrier and Conrad Pelletier for providing the human atrial tissue specimens used in these experiments.

This study was supported by grants from the Quebec Heart and Stroke Foundation, the Medical Research Council of Canada, and the Fonds de Recherche de l'Institut de Cardiologie de Montréal. S. Nattel is a Research Scholar of the Fonds de Recherche en Santé du Québec (FRSQ), and B. Fermini is a Knoll-FRSQ Research Scholar.

Address for reprint requests: B. Fermini, Montreal Heart Institute, 5000 East Belanger St., Montreal, Quebec H1T 1C8, Canada.

Received 6 December 1991; accepted in final form 20 July 1992.

REFERENCES

1. Bleeker, W. K., A. J. C. Mackaay, M. Masson-Pévet, L. N. Bouman, and A. E. Becker. Functional and morphological organization of the rabbit sinus node. *Circ. Res.* 46: 11–22, 1980.
2. Boyett, M. R. A study of the rate of stimulation on the transient outward current in sheep cardiac Purkinje fibres. *J. Physiol. Lond.* 319: 1–22, 1980.
3. Boyett, M. R., and B. R. Jewell. Analysis of the effect of changes in rate and rhythm upon electrical activity in the heart. *Prog. Biophys. Mol. Biol.* 36: 1–52, 1980.
4. Carmeliet, E. Repolarization and frequency in cardiac cells. *J. Physiol. Paris* 73: 902–923, 1977.
5. Cohen, I. S., N. B. Datyner, G. A. Gintant, and R. P. Kline. *The Heart and Cardiovascular System.* New York: Raven, 1986, p. 637–668.
6. Colatsky, T. J., C. H. Follmer, and C. F. Starmer. Channel specificity in antiarrhythmic drug action. *Circulation* 82: 2235–2242, 1990.
7. Coraboeuf, E., and E. Carmeliet. Existence of two transient outward currents in sheep cardiac Purkinje fiber. *Pflugers Arch.* 392: 352–359, 1982.
8. Dukes, I. D., and M. Morad. The transient outward K+ current in rat ventricular myocytes: evaluation of its Ca^{2+} and Na^+ dependence. *J. Physiol. Lond.* 435: 395–420, 1991.
9. Escande, D., A. Coulombe, J. F. Faivre, E. Deroubaix, and E. Coraboeuf. Two types of transient outward currents in adult human atrial cells. *Am. J. Physiol.* 252 (*Heart Circ. Physiol.* 21): H142–H148, 1987.
10. Escande, D., D. Loisance, C. Planche, and E. Coraboeuf. Age-related changes of action potential plateau shape in isolated human atrial fibers. *Am. J. Physiol.* 249 (*Heart Circ. Physiol.* 18): H843–H850, 1985.
11. Fedida, D., Y. Shimoni, and W. R. Giles. A novel effect of norepinephrine on cardiac cells is mediated by α_1-adrenoceptors. *Am. J. Physiol.* 256 (*Heart Circ. Physiol.* 25): H1500–H1504, 1989.
12. Giles, W. R., and Y. Imaizumi. Comparison of potassium currents in rabbit atrial and ventricular cells. *J. Physiol. Lond.* 405: 123–145, 1988.
13. Giles, W. R., and A. C. G. van Ginneken. A transient outward current in isolated cells from the crista terminalis of rabbit heart. *J. Physiol. Lond.* 368: 243–264, 1985.
14. Hamill, O. P., A. Marty, E. Neher, S. Sakmann, and F. J. Sigworth. Improved patch clamp techniques for high resolution current recording from cells and cell-free membrane patches.

Pflugers Arch. 391: 85–100, 1981.
15. Hiraoka, M., and S. Kawano. Mechanism of increased amplitude and duration of the plateau with sudden shortening of diastolic intervals in rabbit ventricular cells. *Circ. Res.* 60: 14–26, 1987.
16. Hiraoka, M., and S. Kawano. Calcium-sensitive and insensitive transient outward current in rabbit ventricular myocytes. *J. Physiol. Lond.* 410: 187–212, 1989.
17. Huynh, T. V., F. Chen, G. T. Wetzel, W. F. Friedman, and T. S. Klitzner. Developmental changes in membrane Ca^{2+} currents in fetal, neonatal, and adult rabbit ventricular myocytes. *Circ. Res.* 70: 508–515, 1992.
18. Imaizumi, Y., and W. R. Giles. Quinidine-induced inhibition of transient outward current in cardiac muscle. *Am. J. Physiol.* 253 (*Heart Circ. Physiol.* 22): H704–H708, 1987.
19. Josephson, I. R., J. Sanchez-Chapula, and A. M. Brown. Early outward current in rat single ventricular cells. *Circ. Res.* 54: 157–162, 1984.
20. Kenyon, J. L., and W. R. Gibbons. Influence of chloride, potassium, and tetraethylammonium on early outward current of sheep cardiac Purkinje fibers. *J. Gen. Physiol.* 73: 117–138, 1979.
21. Kilborn, M. J., and D. Fedida. A study of the development changes in outward currents of rat ventricular myocytes. *J. Physiol. Lond.* 430: 37–60, 1990.
22. Kukushkin, N. I., R. Z. Guinullin, and E. A. Sosunov. Transient outward current and rate dependence of action potential duration in rabbit cardiac ventricular muscle. *Pflugers Arch.* 399: 87–92, 1983.
23. LeGrand, B., J. Y. LeHeuzey, P. Perier, P. Peronneau, T. Lavergne, S. Hatem, and L. Guize. Cellular electrophysiological effects of flecainide on human atrial fibers. *Cardiovasc. Res.* 24: 232–238, 1990.
24. Ouadid, H., J. Seguin, S. Richard, P. A. Chaptal, and J. Nargeot. Properties and modulation of Ca channels in adult human atrial cells. *J. Mol. Cell. Cardiol.* 23: 41–54, 1991.
25. Reneman, P. L., M. A. Allessie, W. J. E. P. Lammens, F. I. Bonke, and M. J. Schalij. Length of excitation wave and susceptibility to reentrant atrial arrhythmias in normal conscious dogs. *Circ. Res.* 62: 395–410, 1988.
26. Roden, M. R., and B. F. Hoffman. Action potential prolongation and induction of abnormal automaticity by low quinidine concentrations in canine Purkinje fibers. *Circ. Res.* 56: 857–867, 1985.
27. Saxon, M. E., and V. G. Safronova. The rate-dependent depression of action potential duration in rabbit myocardium and the possible role of the transient outward current. A pharmacological analysis. *J. Physiol. Paris* 78: 461–466, 1982.
28. Shibata, E. F., T. Drury, H. Refsum, V. Aldrete, and W. R. Giles. Contribution of a transient outward current to repolarization in human atrium. *Am. J. Physiol.* 257 (*Heart Circ. Physiol.* 26): H1773–H1781, 1989.
29. Tseng, G. N., and B. F. Hoffman. Two components of transient outward current in canine ventricular myocytes. *Circ. Res.* 64: 633–647, 1989.
30. Wang, Z., C. Pelletier, M. Talajic, and S. Nattel. Effect of flecainide and quinidine on human atrial action potentials. Role of rate-dependence and comparison with guinea pig, rabbit and dog tissues. *Circulation* 82: 274–283, 1990.
31. Zygmunt, A. C., and W. R. Gibbons. Calcium-activated chloride current in rabbit ventricular myocytes. *Circ. Res.* 68: 424–437, 1991.

A conclusion from this study is that I_{to1} in man, unlike in rabbit, is still important over a physiologic range of heart rates and even at fast rates characteristic of tachycardias, because the size of human I_{to1} is not significantly reduced when stimulation frequency is increased up to 4 Hz. Blockade of this current by drugs, if more at faster rates, may lead to use-dependent APD prolongation, such as that seen with flecainide.

Moreover, two important facts prompted us to continue exploration of other potential currents which may be involved in governing human atrial repolarization. Firstly, the rapid inactivation process of I_{to1} results in complete decay of this current within about 60 msec (inactivation τ=11 msec) at a physiological temperature. Considering that action potential duration of human atrium at 1 Hz is about 350 msec and remains as long as 150 msec even when the activation rate is increased to 3.3 Hz, I_{to1} may be expected to contribute directly to only the early phase of action potential duration. It is not unreasonable, therefore, to speculate that other currents may exist and be responsible for the late phases of repolarization. The delayed rectifier outward K^+ current (I_K) would be a logical candidate, since it has been identified in diverse animal species and tissues. This current has been shown to play an important role in repolarization and in rate-dependent APD shortening. I_K was believed to be absent or have only negligible amplitude in human atrium[2-4,7]. However, it is known that many antiarrhythmic drugs with ability to suppress I_K in animal species, including specific I_K blockers, are effective in treating atrial arrhythmias in patients. How can this paradox be explained?

Delayed Rectifier Outward Current and Repolarization in Human Atrial Myocytes

Zhiguo Wang, Bernard Fermini, Stanley Nattel

Previous work has suggested that the primary time-dependent repolarizing current in human atrium is the transient outward current (I_{to}), but interventions known to alter the magnitude of the delayed rectifier current (I_K) affect atrial electrophysiology and arrhythmias in humans. To explore the potential role of I_K in human atrial tissue, we used the whole-cell configuration of the patch-clamp technique to record action potentials and ionic currents in isolated myocytes from human atrium. A delayed outward current was present in the majority of myocytes, activating with a time constant ranging from 348±61 msec (mean±SEM) at −20 mV to 129±25 msec at +60 mV. The reversal potential of tail currents was linearly related to log $[K^+]_o$ with a slope of 55 mV per decade, and fully activated tail currents showed inward rectification. The potassium selectivity, kinetics, and voltage dependence were similar to those reported for I_K in other cardiac preparations. In cells with both I_{to} and I_K, I_K greatly exceeded both components of I_{to} (I_{to1} and I_{to2}) within 50 msec of a voltage step from −70 to +20 mV. Based on the relative magnitude of I_{to} and I_K, three types of cells could be distinguished: type 1 (58% [73/126] of the cells) displayed a large I_{to} together with a clear I_K, type 2 (13% [17/126] of the cells) displayed only I_K, and type 3 (29% [36/126] of the cells) was characterized by a prominent I_{to} and negligible I_K. Consistent differences in action potential morphology were observed, with type 2 cells having a higher plateau and steeper phase 3 slope and type 3 cells showing a triangular action potential and lesser phase 3 slope compared with type 1 cells. We conclude that I_K is present in a majority of human atrial myocytes and may play a significant role in their repolarization and that previously observed variability in human atrial action potential morphology may be partially due to differences in the relative magnitude of time-dependent outward currents. (*Circulation Research* 1993;73:276-285)

Key Words • electrocardiogram • action potential • atrial arrhythmias • antiarrhythmic drugs • electrophysiology • ion channels • potassium channels

Although the development of the patch-clamp technique has allowed for more detailed characterization of the ionic mechanisms of repolarization of mammalian cardiac tissue, relatively little information is available regarding human cardiac myocytes. The time- and voltage-dependent transient outward current (I_{to}) is considered to be a major repolarizing current in human atrial cells,[1-4] although other currents, like the acetylcholine-activated K^+ current and ATP-sensitive current, may also play a role under certain circumstances.[5-7] The inactivation of I_{to} in human atrial tissue is rapid,[2] especially at physiological temperatures,[4] and since action potential duration in this structure at normal resting rates is in the range of 200–300 msec,[1,3,8-11] I_{to} would be expected to contribute mainly to the very early phases of atrial repolarization in humans.

The delayed rectifier K^+ current (I_K), which is an important repolarizing current in other cardiac tissues and species,[12-18] is believed to contribute, at most, to a minor extent to human atrial repolarization.[2,3] Escande et al[1] suggested that the shortening of the action potential duration observed in human atrial tissue after I_{to} inhibition by 4-aminopyridine (4-AP) could be explained by the activation of a delayed rectifier by the positive shift in plateau levels caused by 4-AP. However, voltage-clamp experiments were not performed in that study. Shibata et al[3] found little evidence for I_K in human atrial myocytes studied at 23°C. While evaluating the kinetics of I_{to} at 37°C,[19] we consistently observed tail currents on returning to the holding potential after depolarizing steps. We designed the present experiments to 1) determine the occurrence and properties of I_K in human atrial myocytes and 2) examine the relative magnitude of I_{to} and I_K as a function of time after depolarization at physiological temperatures. The results suggest that I_K is present in a majority of human atrial myocytes and may play a more important role in repolarizing human atrial tissue than has been previously appreciated.

Received February 25, 1992; accepted March 1, 1993.

From the Department of Medicine, Montreal Heart Institute (Drs Fermini and Nattel), and the Department of Pharmacology, McGill University (Drs Wang and Nattel) (Canada).

Previously presented as a preliminary report in abstract form (*Biophys J* 1993;64:A393).

Correspondence to Montreal Heart Institute, 5000 Belanger Street East, Montreal, Quebec, Canada H1T 1C8 (Dr Fermini).

Materials and Methods

Isolation of Single Atrial Cells

Specimens of human right atrial appendage were obtained from the hearts of 14 patients (59±4 years old) undergoing aortocoronary bypass surgery. The procedure for obtaining the tissue was approved by the Ethics Committee of the Montreal Heart Institute. Samples

were quickly immersed in nominally Ca^{2+}-free Tyrode's solution (100% O_2, 37°C) containing (mM) NaCl 126.0, KCl 5.4, $MgCl_2$ 1.0, NaH_2PO_4 0.33, dextrose 10.0, and HEPES 10.0, pH adjusted to 7.4 with NaOH. The myocardial specimens were chopped with scissors into cubic chunks and placed in a 25-mL flask containing 10 mL Ca^{2+}-free Tyrode's solution. The tissue was gently agitated by continuous bubbling with 100% O_2 and stirring with a magnetic bar. After an initial 5 minutes in this solution, the chunks were reincubated in a similar solution containing 390 U/mL collagenase (CLS II, Worthington Biochemical Corp., Freehold, N.J.) and 4 U/mL protease (type XXIV, Sigma Chemical Co., St. Louis, Mo.). The first supernatant was removed after 45 minutes and discarded. The chunks were then reincubated in a fresh enzyme-containing solution. Microscopic examination of the medium was performed every 15 minutes to determine the number and quality of the isolated cells. When the yield appeared to be maximal, the chunks were suspended in a solution containing (mM) KCl 20, KH_2PO_4 10, glucose 10, glutamic acid 70, β-hydroxybutyric acid 10, taurine 10, and EGTA 10 along with 1% albumin (pH was adjusted to 7.4 with KOH) and gently pipetted.

Only quiescent rod-shaped cells showing clear cross striations were used. The resting membrane potential as measured in 50 cells ranged from −55 to −76 mV with an average of −64±1 mV. A small aliquot of the cell-containing solution was placed in a 1-mL chamber mounted on the stage of an inverted microscope. Five minutes was allowed for cell adhesion to the bottom of the chamber, and then the cells were superfused at 3 mL/min with a solution containing (mM) NaCl 126.0, KCl 5.4, $MgCl_2$ 0.8, $CaCl_2$ 1.0, NaH_2PO_4 0.33, HEPES 10.0, and glucose 5.5; pH was adjusted to 7.4 with NaOH. The bath temperature was maintained at 36°C with a temperature controller device (N.B. Datyner, Stonybrook, N.Y.).

Data Acquisition

The whole-cell patch-clamp technique was used to record ionic currents and action potentials in the voltage- and current-clamp mode, respectively. Borosilicate glass electrodes were filled with (mM) KCl 130.0, $MgCl_2$ 1.0, HEPES 10.0, EGTA 5.0, Mg_2-ATP 5.0, and Na_2-creatine phosphate 5.0 (pH was adjusted to 7.4 with KOH) and connected to a patch-clamp amplifier (Axopatch 1-D, Axon Instruments, Burlingame, Calif.). In selected experiments, electrodes with tip resistances below 4 MΩ were used. However, rundown of I_K was very rapid when low-resistance electrodes were used, with approximately 70% reduction in current amplitude within 10 minutes. Therefore, most of the results were obtained with electrodes having tip resistances from 5 to 10 MΩ. Command pulses were generated by a 12-bit digital-to-analog converter controlled by pCLAMP software (Axon Instruments). Recordings were filtered at 1-kHz bandwidth, and series resistance was compensated. Membrane potentials or currents were stored on VHS tape using an analog-to-digital board (Medical Systems Corp., Greenvale, N.Y.) and simultaneously digitized (model TM 125, Scientific Solutions Inc., Solon, Ohio) and stored on the hard disk of an IBM AT-compatible computer.

Junction potentials (2–14 mV) were zeroed before formation of the membrane-pipette seal in 1 mM Ca^{2+} Tyrode's solution. Mean seal resistance averaged 37.6±2.1 GΩ. Several minutes after seal formation, the membrane was ruptured by gentle suction to establish the whole-cell configuration for voltage clamping. The series resistance (Rs) was electrically compensated to minimize the duration of the capacitive surge on the current recording and the voltage drop produced across the clamped cell membrane. Rs along the clamp circuit was estimated by dividing the time constant obtained by fitting the decay of the capacitive transient by the calculated membrane capacitance (the time integral of the capacitive response to 5-mV hyperpolarizing steps from a holding potential of −60 mV).[20,21] Before Rs compensation, the decay of the capacitive surge was expressed by a single exponential having a time constant of 542±50 μsec (cell capacitance, 83.6±6.4 pF). After compensation the time constant was reduced to 160±10 μsec (cell capacitance, 74.6±0.8 pF). The initial Rs was 6.5±1.2 MΩ, and Rs was reduced to 2.1±0.7 MΩ after compensation. Currents recorded during this study did not exceed 1.4 nA, and the maximum total current at the time of steady-state I_K was <800 pA. Therefore, the voltage drop across Rs never exceeded 3 mV. Cells with significant leak currents were rejected. Residual leak currents were compensated by subtracting a current linearly scaled and opposite in polarity to the current response to a sequence of 5-mV hyperpolarizing pulses.

The length of single cells ranged from 75 to 100 μm (89.8±0.1 μm), and the diameter ranged from 6 to 10 μm (8.9±0.1 μm); the estimated cell surface area was therefore $2.6\pm0.03\times10^{-5}$ cm^2, assuming right cylinder geometry. The input resistance (R_m) was determined from the response to 5-mV hyperpolarizing steps from a holding potential (HP) of −60 mV. Since no time-dependent current was activated with these small steps, the resulting change in current was used to calculate R_m.[22] Mean R_m in 14 cells was 1.51±0.02 GΩ. The resting space constant was calculated based on the following equation: $sc=\sqrt{(r\cdot R_m/2R_i)}$, where sc is the space constant, r is the cell radius, R_m is specific membrane resistance, and R_i is internal resistivity.[22] R_m was estimated from the product of R_{in} and surface area, providing a mean value of 39.4±0.4 kΩ·cm^2, and R_i was assumed to be 100–200 Ω·cm.[14,22–24] The mean resting space constant is 2.95±0.02 mm when R_i=100 Ω·cm and 2.09±0.02 mm when R_i=200 Ω·cm. Both values are over 20 times cell length. To estimate the space constant during maximum current flow (at the time of peak 4-AP–sensitive I_{to} [I_{to1}] conductance), R_{in} was obtained from the slope of the current–voltage relation for peak I_{to1} on depolarization from an HP of −70 mV. The space constant estimated in this fashion is between 540 and 770 μm. Assuming a minimum space constant of 600 μm, the maximum voltage error during peak I_{to} at the end of a cell with a suction pipette at the midpoint would be 7.5%. These estimates of the space constant are, if anything, underestimates, since membrane infolding results in a true surface area larger than that of a right cylinder. In fact, the surface area estimated on the basis of a specific capacitance of 1 μF/cm^2 is approximately twice as large as the value given above, in agreement with histological studies in rabbit atrium.[25]

The 4-AP–sensitive component of the transient outward current (I_{to1}) was inhibited, when needed, by the use of 2 mM 4-AP (Sigma).[2,26,27] In some experiments,

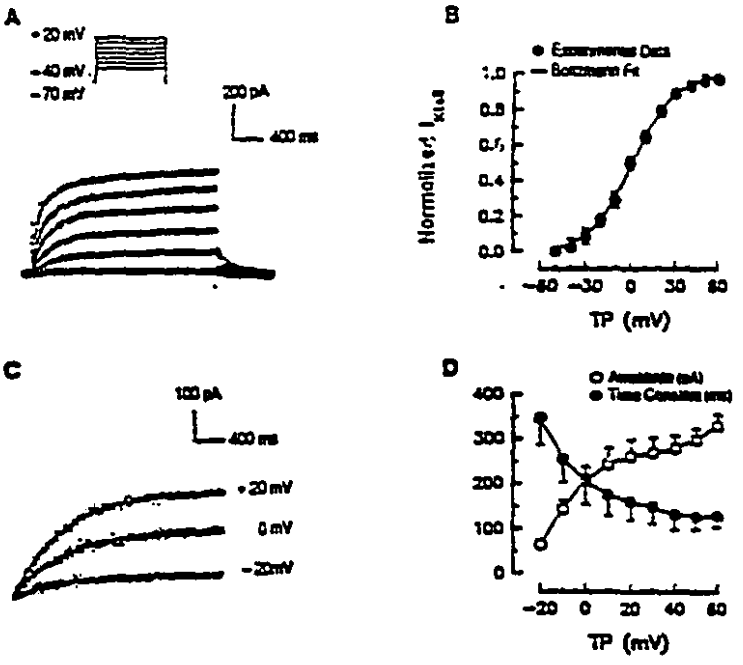

FIG 1. *Electrophysiological properties of the delayed rectifier current (I_K) in human atrial myocytes. $I_{K,tail}$, tail current; TP, test potential. Panel A: Recordings from a representative cell that were obtained using a relatively low-resistance (4-MΩ) electrode. I_K was elicited by 2,000-msec depolarizing pulses at 0.1 Hz to potentials ranging from −50 to +60 mV, from a holding potential of −70 mV. Na^+, Ca^{2+}, and transient outward currents were abolished by replacing NaCl with isotonic choline chloride (126 mM) and adding $CoCl_2$ (2 mM) and 4-aminopyridine (2 mM) to the bath solution. Panel B: Voltage dependence of the activation of I_K, based on analysis of $I_{K,tail}$ after return to the holding potential after a 2-second depolarizing pulse protocol as shown in panel A. Plotted data are mean±SEM (n=12). The continuous line is the best fit to a Boltzmann function, with a half-activation voltage of +1.2 mV and a slope factor of 13.6 mV. Panel C: Analysis of the time course of activation of I_K. Currents were obtained by 2,000-msec depolarizations to −20, 0, and +20 mV from a holding potential of −70 mV. The superimposed continuous line represents the best fit to a monoexponential function. Panel D: Voltage dependence of the activation time constant and amplitude of I_K as recorded with the protocol shown in panel A. The amplitude of I_K was measured as the difference between the initial and final outward current during the depolarizing pulse. Plotted data are mean± SEM for 12 cells.*

10 mM tetraethylammonium chloride (TEA, Sigma) was used to inhibit I_K.[25] $CoCl_2$ (2 mM, Sigma) was added in all experiments (except during action potential recording and experiments studying the brief outward current [I_{to}]), since the presence of Ca^{2+} current (I_{Ca}) can confound the interpretation of time-dependent outward currents.[25] In experiments involving HPs negative to −50 mV, NaCl (126 mM) was isotonically replaced by choline chloride (126 mM, Sigma) to prevent contamination of outward currents by Na^+ current (I_{Na}). The substitution of choline for sodium did not produce any qualitative changes in the currents observed. To exclude direct activation of muscarinic receptors by choline, currents were measured in five cells before and after the addition of atropine (100 nM), and no significant changes were observed.

Data Analysis

Comparisons among groups were performed by analysis of variance with Scheffe contrasts. A nonlinear least-squares curve-fitting program (CLAMPFIT in pCLAMP) was used to fit the inactivation of I_{to} and the activation and deactivation of I_K. Baseline and drug data were compared by Student's *t* test, and a two-tailed probability of ±5% was taken to indicate statistical significance. Group data are presented as mean±SEM.

One disadvantage of working at a physiological temperature is that the rundown of I_K is accelerated. We found that a steady-state decrease in I_K amplitude was achieved approximately 10 minutes after rupture of the membrane, at which time the mean reduction in tail amplitudes relative to initial values was 42±12%. Thereafter, little change occurred, with the reduction in I_K tail currents after 30 minutes averaging 46±5% (relative to initial values after membrane rupture). Therefore, experiments designed to study I_K were begun 5–10 minutes after rupturing the membrane.

Results

Voltage and Time Dependence of I_K in Human Atrium

A total of 126 cells obtained from 14 different preparations were studied, and 86 cells (68%) displayed a delayed outward current with features characteristic of I_K. In Fig 1, panel A shows a typical example of I_K recorded with an electrode having 4-MΩ tip resistance. Currents were elicited by 2,000-msec depolarizing pulses to various test potentials from an HP of −70 mV. I_{Na}, I_{Ca}, and I_{to} were suppressed by isotonic replacement of sodium chloride by choline chloride and by adding $CoCl_2$ (2 mM) and 4-AP (2 mM) to the superfusate. Panel B shows the voltage dependence of I_K activation as determined from analysis of tail currents elicited with the voltage protocol shown in panel A. The curve shown is the best-fit Boltzmann function, given by $1/[1+\exp(V_m-V_{1/2})/k]$, where V_m is membrane voltage, $V_{1/2}$ is half-activation voltage (+1.2 mV), and k is the slope factor (13.6 mV). The activation of I_K was well described by a monoexponential function (panel C: *r* always >0.99), and the time constant of activation of the current decreased from 348±61 msec at −20 mV to 129±25 msec at +60 mV (panel D). The amplitude of the current (measured from the instanta-

neous value after the decay of the capacity transient to the current at the end of the depolarizing pulse) increased with increasing depolarization from 65±4 pA at −20 mV to 331±26 pA at +60 mV (panel D). Deactivation kinetics were also well fitted by a monoexponential function, with a time constant of 162±18 msec at −30 mV (n=9 cells).

Selectivity for Potassium and Rectification Properties

The selectivity of I_K in human atrial myocytes was examined by measuring the reversal potential (E_{rev}) of tail currents in the presence of three external K^+ concentrations. The membrane was depolarized from −60 to +20 mV for 1 second and then repolarized to various test potentials (Fig 2A). In the normal bath solution ($[K^+]_o$=5.4 mM), E_{rev} was −76.4±7.2 mV (n=14) and shifted to −61.2±1.9 mV and −42.7±2.4 mV when $[K^+]_o$ was increased to 10.8 and 21.6 mM, respectively (Fig 2B). The regression line for the E_{rev}–log $[K^+]_o$ relation had a slope of 55 mV per decade shift in $[K^+]_o$.

Fig 2C shows the rectification properties of I_K as obtained from the fully activated current–voltage relation determined with $[K^+]_o$=5.4 mM. The cell was first depolarized to +50 mV for 1,000 msec and then repolarized to various test potentials between −120 and +10 mV. Tail currents were measured as the difference between initial and final values at the test potential and corrected for incomplete deactivation by dividing by $(1-a_{TP}/a_{+50})$, where a_{TP} and a_{+50} are the activation variables (Fig 1B) at the test potential and +50 mV, respectively. The current is linearly related to voltage between −120 and −60 mV but shows considerable inward rectification at more positive test potentials. Nonetheless, because I_K may consist of more than one component (see "Discussion"), the significance of such rectification should be interpreted with caution.

Envelope of Tails

A typical envelope of I_K tails is presented in Fig 3A. Currents were elicited by depolarization from −70 to +50 mV with pulses ranging from 50 to 2,800 msec in duration, and tail currents were recorded on repolarization to −30 mV. Tail current ($I_{K,tail}$) increased more rapidly than the developing current ($I_{K,step}$). The average ratio of $I_{K,tail}/I_{K,step}$ as determined in five cells was 7.40±0.37 after a 50-msec pulse but gradually decreased to a steady-state value (0.46±0.10) as pulse duration increased (Fig 3B).

Repolarizing Currents and Action Potential Morphology

From the 126 cells randomly selected for this study, at least three different cell types could be identified on the basis of outward currents, as illustrated at the left of Fig 4. Action potentials from the same cell as each set of ionic currents are shown in the middle of panels A–C. On depolarization from an HP of −70 mV, some cells displayed a large I_{to} together with a more slowly developing outward current, and they displayed a measurable tail current on return to the HP: these were designated type 1 cells (panel A). Type 2 cells displayed only the slowly activating I_K current (panel B), and type 3 cells had a prominent I_{to} in the apparent absence of I_K (panel C).

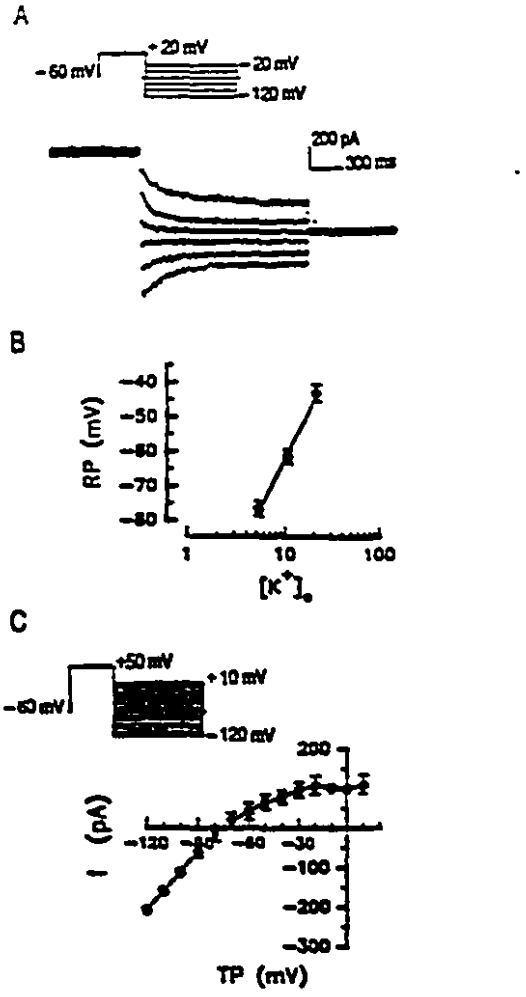

FIG 2. *Reversal potential (RP) measurements for delayed rectifier current (I_K). Panel A: Recordings of RP, which was determined using a double-pulse protocol (frequency, 0.1 Hz). The activating prepulse (1 second) depolarized the cell from a holding potential of −60 to +20 mV, and the test pulse returned the membrane to potentials ranging from −120 to +20 mV. Panel B: Plot of RP for I_K at different values of $[K^+]_o$. The regression line had a slope of 55 mV per 10-fold change in $[K^+]_o$. Results are mean±SEM from 14 cells. Panel C: Fully activated current (I)–voltage relation, as determined with the protocol shown in the inset. I_K was activated by a 1,000-msec pulse to +50 mV, and tail current was measured during subsequent 500-msec repolarizations to test potentials (TPs) between −120 and +10 mV. Tail currents were adjusted for incomplete deactivation, as described in the text. Results are mean±SEM from three cells.*

To quantify these differences in ionic currents among cells, we determined the ratio of I_K/I_{to} on depolarization from −70 to +20 mV for 300 msec. I_K was the activating current measured as the difference between the initial current after the decay of the capacity transient and the current at the end of the test pulse. I_{to} was measured as the difference between the peak of I_{to} and the steady-state current after full inactivation. Since type 1 cells contain both I_K and I_{to}, it is difficult to define the magnitude of each based on the type of current recordings shown at the left of Fig 4A. Therefore, in type 1

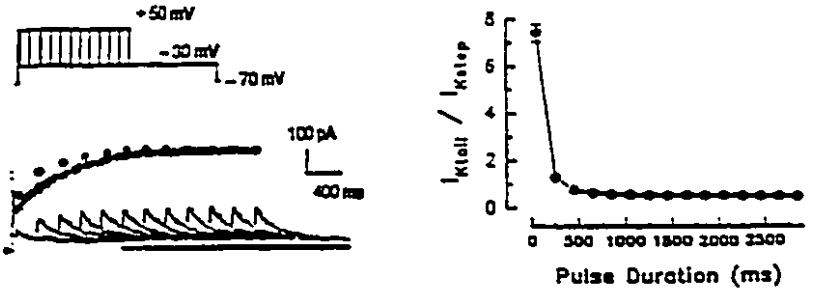

FIG 3. *Envelope-of-tails test for the delayed rectifier current (I_K). Left panel: Scaled tail currents were superimposed onto the activating current with filled circles. The protocol shown in the inset was used to compare the time course of I_K activation with that of I_K tails after varying durations of depolarization to +50 mV. Right panel: Activating current (I_{Ktotp}) was measured as a function of time during the depolarizing pulse; tail current (I_{Ktail}) was measured for each test pulse after repolarization to −30 mV. Plotted data are mean±SEM for five cells.*

cells. I_K was measured before and after the addition of 4-AP (2 mM), and I_{to} was measured before and after the addition of TEA (10 mM). Short (10–15-minute) exposure of cells to TEA was found to block I_K tail current by 82±7% ($p<0.001$) without significantly altering I_{to} (mean change, −3±5%; p=NS). The I_K/I_{to} ratios shown for type 1 cells in Fig 4 are those obtained in the absence of blockers but are in the same range as ratios based on measurements of I_K and I_{to} in the presence of 4-AP and TEA, respectively.

Differences in action potential morphology were also noted among cell types, as shown in the middle of Fig 4. We characterized action potential features by 1) measuring the slope of phase 3 repolarization by fitting a tangent to the steepest portion of phase 3 repolarization (as an index of repolarization rate) and 2) measuring membrane potential 30 msec after the upstroke of the action potential (as an index of plateau height). The rationale for the latter was that phase 1 was completed within 30 msec in all cell types and that the inactivation time constant of I_{to} at +20 mV averaged 10 msec, implying that over 90% of I_{to} (the major ionic current underlying phase 1) was inactivated within 30 msec.

Action potentials showing a spike-and-dome morphology and relatively steep phase 3 repolarization (Fig 4A, middle) were recorded from type 1 cells. The mean I_K/I_{to} ratio in these cells was 0.41±0.09, the plateau voltage averaged −6±1 mV, and the slope of phase 3 repolarization was 1.0±0.08 V/sec (Fig 4A, right). In contrast, type 2 cells (Fig 4B, middle) had a more rectangular morphology, no initial notch, a slightly more positive plateau level (mean, 1±3 mV; p=NS versus type 1 cells), and steep phase 3 repolarization (slope, 1.5±0.07 V/sec; $p<0.01$ versus type 1 cells). The I_K/I_{to} ratio in these cells was >100 (Fig 4B, right). Action potentials of type 3 cells had a small plateau of short duration, a low plateau level (−32±4 mV, $p<0.01$ versus type 1 cells), and slower phase 3 repolarization

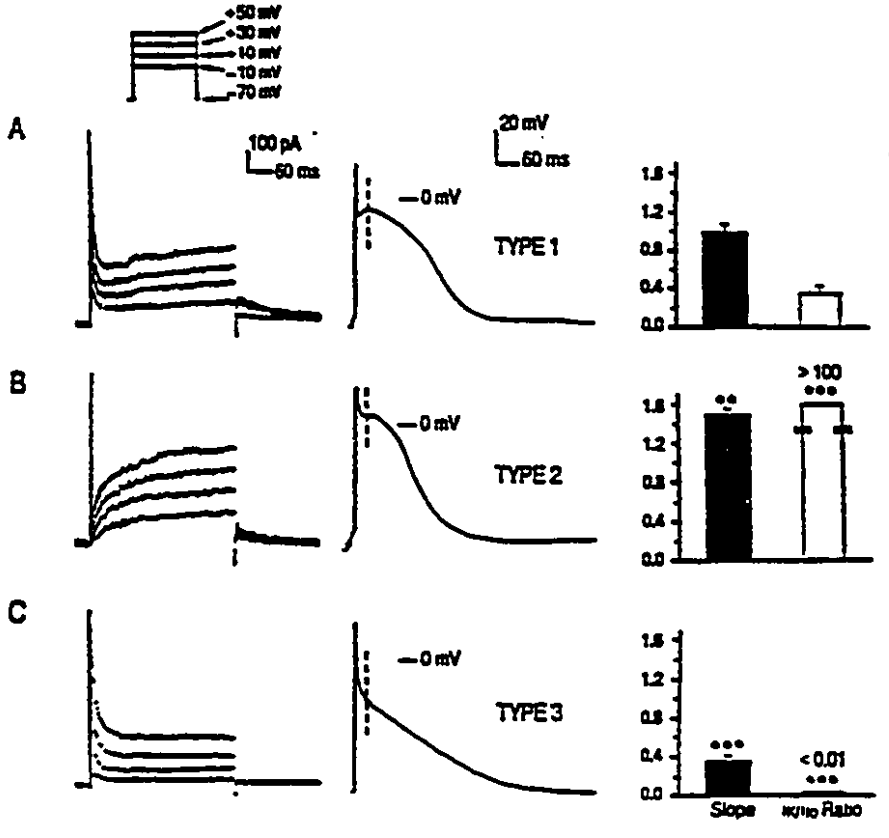

FIG 4. *Characterization of three different outward current patterns (types 1–3) observed in human atrial myocytes. I_K, delayed rectifier current; I_{to}, transient outward current. Shown on the left of each panel are ionic currents elicited by 300-msec depolarizing steps to −10, +10, +30, and +50 mV from a holding potential of −70 mV (choline chloride was isotonically substituted for NaCl). Shown in the middle of each panel are action potentials recorded from the same cells. Shown on the right of each panel are average slopes of phase 3 repolarization and the I_K/I_{to} ratio. Panel A: Type 1 cells (I_{to} and I_K present). Panel B: Type 2 cells (I_K present, I_{to} absent). Panel C: Type 3 cells (I_{to} present, I_K absent; for further details, see text). **p<0.01; ***p<0.001 vs. type 1 cells.*

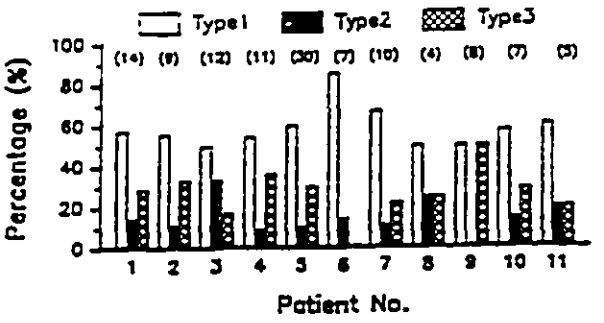

FIG 5. *Bar graph showing individual distribution of the three cell types for the 11 patients from whom at least four cells were studied. Numbers in parentheses indicate the number of atrial cells. Except for patients 6 and 9, all atrial specimens displayed the three different cell types presented in Fig 4. On average, type 1 (58±3%) and type 3 (27±4%) were most frequently encountered.*

(slope, 0.36±0.06 V/sec; $p<0.01$ versus type 1 cells). The I_K/I_{to} ratio in these cells was <0.01. In general, the larger the I_K/I_{to} ratio, the steeper was the phase 3 repolarization and the more positive the plateau voltage. Although the current ratios differed among various cell types, other properties of observed currents were similar. For example, the $V_{1/2}$ for I_K activation in type 1 cells averaged 1.1±0.1 mV, not significantly different from the $V_{1/2}$ of I_K in type 2 cells (1.3±0.1 mV). Similarly, the activation $V_{1/2}$ for I_{to1} averaged 13.4±1.4 mV in type 1 cells and 14.8±0.8 mV in type 3 cells (p=NS). There was no apparent relation between the current ratios or action potential properties and cell size or shape.

Except for one patient in whom no type 3 cells were found (n=7 cells from this preparation) and another two in whom no type 2 cells could be identified (n=8 cells in one patient and n=3 cells in the other), the myocytes studied from the atrial preparations of the remaining 11 patients displayed a similar distribution pattern in their outward currents. Fig 5 shows the distribution of cell types among 11 patients in whom at least four cells were examined (results from three patients with three cells or less are not shown, since the small numbers of cells per patient make the distribution less meaningful). Within the population of cells studied from all 14 patients, 58±3% of the cells in each patient were of type 1 (both I_{to} and I_K present), 13±3% were of type 2 (I_K present, I_{to} absent), and 29±4% (36 of 126 cells overall) were of type 3 (a large I_{to} and no I_K).

Relative Time-Dependent Amplitude of I_K and I_{to} in Cells Displaying Both Currents

To gain further insight into the dynamic contribution of the repolarizing currents of type 1 atrial myocytes, we studied the time and voltage dependence of I_{to} and I_K over a 300-msec pulse duration to mimic the duration of human atrial action potential duration.[13,28-31] Currents were elicited by depolarizing pulses to various potentials from an HP of −70 mV.

Two types of I_{to} have previously been described[27,29-31]: 1) I_{to1}, a longer-lasting outward current carried mainly by K^+ ions, which is suppressed by 4-AP, and 2) I_{to2}, a brief outward current possibly carried by Cl^-,[21,29] which persists in the presence of 4-AP and is inhibited by Ca^{2+} channel blockers such as Co^{2+}. Experiments were performed to determine the potential contribution of both I_{to1} and I_{to2}. Because I_{to2} may depend on intracellular Ca^{2+} concentrations, experiments were performed with (n=5) or without (n=7) EGTA in the pipette, and similar results were obtained. Analog data from one type 3 cell are shown in Fig 6A. In the presence of 2 mM Co^{2+} and the absence of 4-AP, there is no inward current, and a typical I_{to1} current, with rapid activation and slower inactivation,[2,27] is seen. When Co^{2+} is removed and 4-AP is added, an initial inward current is followed by a brief outward current characteristic of I_{to2}.[2,27] The addition of caffeine (10 mM), to block sarcoplasmic reticulum Ca^{2+} release, completely inhibited I_{to2} in this and in all nine other cells studied, leaving only an inward I_{Ca} as previously reported.[2,29] When both 4-AP and Co^{2+} are present, time-dependent outward currents are abolished, and there is virtually no outward current elicited by depolarization from −70 to −20 mV.

Mean data for the time course and maximum amplitude of I_{to1}, I_{to2}, and I_K are shown in Figs 6B and 6C. The results shown for I_{to1} and I_{to2} were obtained in 14 and 12 cells, respectively; I_K was studied in seven cells. I_{to1} was measured in the presence of Co^{2+} (to block I_{Ca} and I_{to2}); I_{to2} was measured in the presence of 4-AP (to block I_{to1}) and in the absence of Co^{2+}. I_K was measured in the presence of Co^{2+} (to block I_{Ca} and I_{to2}) and 4-AP (to block I_{to1}). 4-AP had no effect on I_K, as assessed from the amplitude of tail currents. I_{to1} reached its maximum amplitude within 6.6±1.0 msec at −10 mV and 3.9±0.8 msec at +20 mV and then inactivated very rapidly. The current declined to half of its maximum amplitude after 9 msec and was completely inactivated after 60 msec. Inactivation was well described by a monoexponential function, with time constants of 19.1±2.6 and 10.2±0.6 msec at −10 and +20 mV, respectively. In contrast to I_{to1}, I_K developed more slowly and did not inactivate. During the first 25 msec, I_{to1} was the primary outward current, and I_K was relatively small (Fig 6B). Thereafter, however, I_K exceeded I_{to1}, with an amplitude in the range of 200 pA within 100 msec. These results suggest that, although I_{to1} can contribute substantially to repolarization during the very early phases of the action potential, I_K is likely to be much more important during phase 3 repolarization. When measured at −10 and +20 mV, I_{to2} reached its peak amplitude in 9.1±0.9 and 5.8±0.7 msec, respectively, and was completely inactivated within 30 msec (Fig 6B). In 11 cells studied, the time constant of I_{to2} inactivation was 8.1±0.4 and 5.2±0.5 msec at −10 and +20 mV, respectively. As in previous studies,[29] I_{to2} was difficult, if not impossible, to separate from I_{Ca}, hampering our ability to measure a reliable peak amplitude. Therefore, we chose not to further characterize the properties of this current, which because of its very rapid inactivation can contribute only to very early repolarization.

Discussion

We have shown that I_K is present in approximately two thirds of myocytes from human right atrial appendages. The amplitude and kinetics of this current suggest that it may play a role in repolarizing human atrial tissue and that, when present, it is more likely to participate in phase 3 repolarization than is I_{to}.

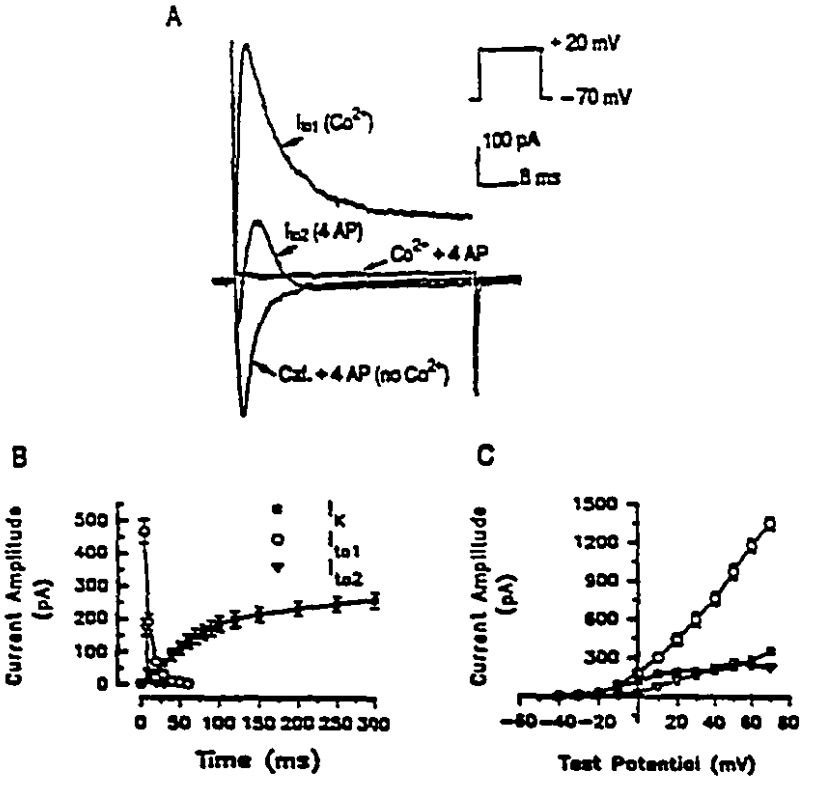

FIG 6. *Time- and voltage-dependent properties of the 4-aminopyridine (4 AP)–sensitive components of the transient outward current (I_{to1}), brief outward current (I_{to2}), and delayed rectifier current (I_K) in human atrial myocytes. Panel A: Recordings showing separation of I_{to1} from I_{to2} in one type 3 atrial myocyte. In the presence of 2 mM Co^{2+}, only I_{to1} is seen. When Co^{2+} is omitted and 2 mM 4 AP is added (frequency, <0.02 Hz to avoid use-dependent unblocking), a brief inward current is followed by a transient outward current, I_{to2}. Caffeine (Caf., 2 mM) eliminates I_{to2}, revealing Ca^{2+} current. When both 4 AP and Co^{2+} are present, outward currents are fully inhibited. Choline was used to replace Na^+ to avoid contamination by Na^+ current. Similar results were obtained in a total of 10 cells. Panel B: Current amplitude plotted as a function of time during a 300-msec depolarizing pulse to +20 mV from a holding potential of −70 mV (choline chloride was used to replace NaCl). I_{to1} was measured in the presence of Co^{2+}, and I_{to2} was measured in the absence of Co^{2+} and the presence of 2 mM 4 AP at <0.02 Hz. I_K was measured in the presence of Co^{2+} and 4 AP. Although both I_{to1} and I_{to2} are fully inactivated after 60 msec, I_K exceeds 100 pA after 60 msec and is in the range of 200 pA within 100 msec. Panel C: Plot showing voltage dependence of maximum amplitude of the three currents studied. Currents were elicited by 300-msec depolarizing pulses from a holding potential of −70 mV, as in panels A and B.*

Comparison With Other Studies of Repolarizing Currents in Human Atrium

Previous studies have not suggested an important role for I_K in human atrial cells.[2,3] However, these studies were all performed at room temperature, and in our experience, the amplitude of I_K is much smaller at room temperature than at 36–37°C. Small I_K tails are present in some recordings (Fig 2) in the article by Escande et al,[2] and one current tracing (fourth from top in Fig 2) of Shibata et al[3] also suggests I_K. Even in our studies, the peak amplitude of I_{to} was substantially greater than that of I_K (Fig 6B), so that unless the appropriate conditions are used (physiological temperature, Ca^{2+} channel blockade), the contribution of I_K can easily be overlooked.

Studies of cDNAs for two voltage-gated K^+ channels in human heart tissue suggest that mRNA coding for a delayed-rectifier type of channel (designated HK-2) is more abundant in human atrium, whereas the mRNA product of a different gene coding for a spontaneously inactivating K^+ channel (HK-1) is slightly more common in human ventricle.[32] Similar K^+ channels have also been cloned from rat hearts,[33,34] and a possible functional equivalent has been identified in rat atrial cells.[35] More recent expression studies of human HK-2 DNA in a mouse cell line indicate that the channel encoded is a delayed rectifier[36] with faster activation kinetics than the I_K we studied. Either the kinetics of the cloned channels are more rapid because of some property of the expression system, or the DNA coding for the I_K that we studied is not HK-2. DNA coding for a structurally distinct I_K channel carrying current more similar to the classical cardiac I_K has been cloned from neonatal rat heart.[37]

Comparison With the Delayed Rectifier in Other Systems

The K^+ selectivity, kinetics, and voltage dependence of I_K in human atrial myocytes resemble those previously reported in other cardiac preparations.[13–18,38–40] We found that I_K in human atrial myocytes fails to satisfy the envelope-of-tails test. Noble and Tsien[38] originally showed that I_K in sheep Purkinje fibers fails to satisfy the envelope-of-tails test and related this observation to two kinetically distinct current components that they designated I_{x1} and I_{x2}. Subsequent workers have suggested that the complex kinetics of I_K could be related to accumulation and depletion of potassium in intracellular clefts[41] or to the existence of multiple closed states of a single channel.[42] Sanguinetti and Jurkiewicz[43,44] have provided evidence to suggest that I_K in guinea pig cardiac myocytes consists of two components, I_{Kr} and I_{Ks}, which can be separated on the basis of

the response to a novel class III drug, E-4031. We have presented preliminary evidence[45] indicating that I_K in human atrium is partially blocked by E-4031 and that the E-4031-sensitive and -resistant currents share similarities in terms of kinetics, voltage dependence, and rectification properties with the currents described by Sanguinetti and Jurkiewicz in guinea pig tissues. Because of the complexities of potential voltage- and time-dependent block by class III drugs, as well as the limitations of inferences drawn from subtracted current recordings, further information is necessary to clarify the mechanisms underlying these aspects of the behavior of I_K in human atrial myocytes.

Relation Between Action Potential Morphology and Repolarizing Currents

The existence of cells with different action potential morphologies in human atrial tissues has long been recognized.[46] Although some of the differences in reported morphologies may be due to age-related changes in ionic currents, variability in action potential morphology remains, even among preparations exclusively from adults.[1,11] Detailed studies have shown important regional differences in action potential morphology in adult canine atrium,[47] with variations observed even in regions in spatial proximity. Differences in superfusate flow, electrotonic interactions, and vagal tone did not account for action potential variability.[47] The most common cell types in our preparations (types 1 and 3) correspond to types described in previous studies of human atrial electrophysiology.[1,11,46]

We were able to subdivide human atrial myocytes into three distinct types based on the relative magnitude of time-dependent repolarizing currents (Fig 4). Consistent differences in action potential morphology were noted among cell types, with significantly more rapid phase 3 repolarization among cells with a more important I_K. Since I_{to} inactivates rapidly and the maximum activation of I_K corresponds temporally to the timing of phase 3, a larger I_K may result in a larger repolarizing current at the end of the plateau.

Potential Significance

Our findings provide potential new insights into the ionic mechanisms of atrial repolarization in humans. I_K, a major repolarizing current in a variety of cell types, has heretofore been considered absent in human atrium. Our results indicate that I_K is present and that it is more likely than I_{to} to play a role in phase 3 repolarization. Action potential duration is a major determinant of the refractory period, which in turn plays a substantial role in governing the likelihood of reentrant arrhythmias.[48] Our observations suggest that I_K blockade could increase atrial action potential duration and prevent reentrant atrial arrhythmias in humans. Indeed, a variety of drugs that selectively block I_K[49–51] are effective in the clinical treatment of reentrant atrial arrhythmias.[52] Autonomic tone is an important regulator of cellular electrophysiology and arrhythmia occurrence.[48] β-Adrenergic receptor stimulation may reduce human atrial action potential duration by enhancing I_K, as in other tissues in which adrenergic stimulation increases I_K[53–55] by activating protein kinases,[56] thus increasing the likelihood of atrial reentry.

Variability in atrial action potential morphology has long interested electrophysiologists and may contribute to atrial arrhythmogenesis by causing dispersion in atrial refractoriness. Our results suggest that some of the differences in action potential morphology and duration among atrial cells may be due to variations in the relative magnitude of time-dependent outward currents. The role of variations in other currents (e.g., inward and background currents) remains to be established, along with that of extrinsic factors determining the expression of various currents in a given cell.

Potential Limitations

Our studies were limited to small samples of right atrial appendages removed at the time of cardiac surgery. Although this is a limitation affecting virtually all studies of human atrial electrophysiology in vitro, it must be recognized that time-dependent outward currents may show some differences in other regions of the human atrium.

In most experiments, I_{Ca} and I_{to2} were blocked with Co^{2+}. The complex effects of divalent cations, both on I_{to}[57] and on I_K,[58] should be kept in mind when interpreting our results. The relative magnitude of I_K and I_{to} could conceivably have been affected by such divalent ion effects.

Rundown of ionic currents is always a potential problem in whole-cell voltage-clamp studies. We minimized time-dependent changes by studying I_K after rundown had reached steady state, 10 minutes after membrane rupture; however, the amplitude of I_K was reduced by approximately 45% relative to initial currents recorded after membrane rupture, so that native I_K is likely approximately 80% larger.

A final limitation is that we have restricted our analysis to the time-dependent outward currents, I_K and I_{to}. Instantaneous outward current "jumps" and residual outward currents after full I_{to} inactivation in cells lacking I_K suggest that there may be an additional type of outward current in these cells. We have made preliminary observations suggesting that this current is carried by potassium ions via background or very rapidly activating K^+ channels.[59,60] The nature of these channels and their potential role in repolarizing human atrial myocytes remain to be elucidated in more extensive studies.

Conclusions

We have shown that human atrial myocytes frequently possess I_K at physiological temperatures. The magnitude and kinetics of this current suggest that it may be important in governing action potential duration. Its role needs to be considered in order to understand the underlying basis of the rate dependence of action potential duration, intercellular variability in action potential morphology, and the pharmacological control of repolarization and arrhythmias in the human atrium.

Acknowledgments

This study was supported by grants from the Medical Research Council of Canada, The Quebec Heart Foundation, and the Fonds de Recherche de l'Institut de Cardiologie de Montréal. Dr Wang is a Canadian Heart Foundation research trainee. Dr Fermini is a Knoll-FRSQ research scholar, and Dr

Nattel is a senior research scholar of the Fonds de Recherche en Santé du Québec. The authors thank Dr Conrad Pelletier and Dr Michel Carrier for providing the human atrial tissue specimens used in these experiments. Guylaine Nicol, BSc, for excellent technical assistance, and Mary Morello and Lise de Repentigny for expert secretarial help.

References

1. Escande D, Loisance D, Planche C, Coraboeuf E. Age-related changes of action potential plateau shape in isolated human atrial fibers. *Am J Physiol.* 1985;249(*Heart Circ Physiol* 18):H843-H850.
2. Escande D, Coulombe A, Faivre JF, Deroubaix E, Coraboeuf E. Two types of transient outward currents in adult human atrial cells. *Am J Physiol.* 1987;252(*Heart Circ Physiol* 21):H142-H148.
3. Shibata EF, Drury T, Refsum H, Aldrete V, Giles W. Contributions of a transient outward current to repolarization in human atrium. *Am J Physiol.* 1989;257(*Heart Circ Physiol* 26):H1773-H1781.
4. Fermini B, Wang Z, Duan DY, Nattel S. Differences in the rate dependence of the transient outward current in rabbit and human atrium. *Am J Physiol.* 1992;263(*Heart Circ Physiol* 32):H1747-H1754.
5. Heidbüchel H, Vereecke J, Carmeliet E. The electrophysiological effects of acetylcholine in single human atrial cells. *J Mol Cell Cardiol.* 1987;19:1207-1219.
6. Sato R, Hisatome I, Wasserstrom JA, Arentzen CE, Singer DH. Acetylcholine-sensitive potassium channels in human atrial myocytes. *Am J Physiol.* 1990;259:H1730-H1735.
7. Heidbüchel H, Vereecke J, Carmeliet E. Three different potassium channels in human atrium. *Circ Res.* 1990;66:1277-1286.
8. Prasad K. Transmembrane potential and force of contraction of the normal and potassium-deficient human atrial tissue in vitro. *Can J Physiol Pharmacol.* 1969;47:1015-1024.
9. Gautier P, Escande D, Bertrand JP, Seguin J, Guiraudou P. Electrophysiological effects of pentacainide (CM 7857) in isolated human atrial and ventricular fibers. *J Cardiovasc Pharmacol.* 1989; 13:328-335.
10. Wang Z, Pelletier LC, Talajic M, Nattel S. Effects of flecainide and quinidine on human atrial action potentials. *Circulation.* 1990;82: 274-283.
11. LeGrand B, Le Heuzey JY, Perier P, Peronneau P, Lavergne T, Hatem S, Guize L. Cellular electrophysiological effects of flecainide on human atrial fibres. *Cardiovasc Res.* 1990;24:232-238.
12. Hume JR, Uehara A. Ionic basis of the different action potential configurations of single guinea-pig atrial and ventricular myocytes. *J Physiol (Lond).* 1985;368:525-544.
13. McDonald TF, Trautwein W. The potassium current underlying delayed rectification in cat ventricular muscle. *J Physiol (Lond).* 1978;274:217-246.
14. Tseng GN, Robinson RB, Hoffman BF. Passive properties and membrane currents of canine ventricular myocytes. *J Gen Physiol.* 1987;90:671-701.
15. Kass RS. Delayed rectification in the cardiac Purkinje fiber is not activated by intracellular calcium. *Biophys J.* 1984;45:837-839.
16. Brown H, DiFrancesco D. Voltage-clamp investigations of membrane currents underlying pace-maker activity in rabbit sino-atrial node. *J Physiol (Lond).* 1980;308:331-351.
17. Gintant GA, Datyner NB, Cohen IS. Gating of delayed rectification in acutely isolated canine cardiac Purkinje myocytes. *Biophys J.* 1985;48:1059-1064.
18. Hume JR, Giles W, Robinson K, Shibata EF, Nathan RD, Kanai K, Rasmusson R. A time- and voltage-dependent K^+ current in single cardiac cells from bullfrog atrium. *J Gen Physiol.* 1986;88: 777-798.
19. Hamill OP, Marty A, Neher E, Sakmann B, Sigworth FJ. Improved patch-clamp techniques for high-resolution current recording from cells and cell-free membrane patches. *Pflugers Arch.* 1981;391:85-100.
20. Sigworth FJ. Electronic design of the patch clamp. In Sakmann B, Neher E, eds. *Single-Channel Recording.* New York, NY: Plenum Publishing Co; 1983:3-35.
21. Zygmunt AC, Gibbons WR. Properties of the calcium-activated chloride current in heart. *J Gen Physiol.* 1992;99:391-414.
22. Giles WR, Van Ginneken ACG. A transient outward current in isolated cells from the crista terminalis of rabbit heart. *J Physiol (Lond).* 1985;368:243-264.
23. Prentler ML. Passive electrical properties of cardiac tissue. In Zipes DP, Jalife J, eds. *Cardiac Electrophysiology: From Cell to Bedside.* Philadelphia, Pa: WB Saunders Co; 1990:108-121.
24. Hume JR, Giles W. Active and passive electrical properties of single bullfrog atrial cells. *J Gen Physiol.* 1981;78:19-42.
25. Masson-Pevet M, Gros D, Besselsen E. The caveolae in rabbit sinus node and atrium. *Cell Tissue Res.* 1980;208:183-196.
26. Apkon M, Nerbonne JM. Characterization of two distinct depolarization-activated K^+ currents in isolated adult rat ventricular myocytes. *J Gen Physiol.* 1991;97:973-1011.
27. Tseng GN, Hoffman BF. Two components of transient outward current in canine ventricular myocytes. *Circ Res.* 1989;64:633-647.
28. Jaeger JM, Gibbons WR. Slow inward current may produce many results attributed to I_{si} in cardiac Purkinje fibers. *Am J Physiol.* 1985;249(*Heart Circ Physiol* 18):H122-H132.
29. Zygmunt AC, Gibbons WR. Calcium-activated chloride current in rabbit ventricular myocytes. *Circ Res.* 1991;68:424-437.
30. Giles WR, Imaizumi Y. Comparison of potassium currents in rabbit atrial and ventricular cells. *J Physiol (Lond).* 1988;405:123-145.
31. Hiraoka M, Kawano S. Calcium-sensitive and insensitive transient outward current in rabbit ventricular myocytes. *J Physiol (Lond).* 1989;410:187-212.
32. Tamkun MM, Knoth KM, Walbridge JA, Kroemer H, Roden DM, Glover DM. Molecular cloning and characterization of two voltage-gated K^+ channel cDNAs from human ventricle. *FASEB J.* 1991;5:331-337.
33. Paulmichl M, Nasmith P, Hellmiss R, Reed K, Boyle WA, Nerbonne JM, Peralta EG, Clapham DE. Cloning and expression of a rat cardiac delayed rectifier potassium channel. *Proc Natl Acad Sci U S A.* 1991;88:7892-7895.
34. Roberds SL, Tamkun MM. Cloning and tissue-specific expression of five voltage-gated potassium channel cDNAs expressed in rat heart. *Proc Natl Acad Sci U S A.* 1991;88:1798-1802.
35. Boyle WA, Nerbonne JM. A novel type of depolarization-activated K^+ current in isolated adult rat atrial myocytes. *Am J Physiol.* 1991;260(*Heart Circ Physiol* 29):H1236-H1247.
36. Snyders DJ, Knoth KM, Roberds SL, Tamkun MM. Time-, voltage-, and state-dependent block by quinidine of a cloned human cardiac potassium channel. *Mol Pharmacol.* 1992;41:322-330.
37. Folander K, Smith JS, Antanavage J, Bennett C, Stein RB, Swanson R. Cloning and expression of the delayed-rectifier I_{sk} channel from neonatal rat heart and diethylstilbestrol-primed rat uterus. *Proc Natl Acad Sci U S A.* 1990;87:2975-2979.
38. Noble D, Tsien RW. Outward membrane currents activated in the plateau range of potentials in cardiac Purkinje fibres. *J Physiol (Lond).* 1969;200:205-231.
39. Matsuura H, Ehara T, Imoto Y. An analysis of the delayed outward current in single ventricular cells of the guinea-pig. *Pflugers Arch.* 1987;410:596-603.
40. DiFrancesco D, Noma A, Trautwein W. Kinetics and magnitude of the time-dependent potassium current in the rabbit sinoatrial node. *Pflugers Arch.* 1979;381:271-279.
41. Attwell D, Cohen I, Eisner D. Membrane potential and ion concentration conditions for a cell with a restricted extracellular space. *Proc R Soc Lond Biol.* 1979;206:145-161.
42. Bennett PB, McKinney LC, Kass RS, Begenisich T. Delayed rectification in the calf cardiac Purkinje fiber: evidence for multiple state kinetics. *Biophys J.* 1985;48:553-567.
43. Sanguinetti MC, Jurkiewicz NK. Two components of cardiac delayed rectifier K^+ current. *J Gen Physiol.* 1990;96:195-215.
44. Sanguinetti MC, Jurkiewicz NK. Delayed rectifier outward K^+ current is composed of two currents in guinea pig atrial cells. *Am J Physiol.* 1991;260(*Heart Circ Physiol* 29):H393-H399.
45. Nattel S, Wang Z, Fermini B. Three types of delayed rectifier potassium currents in human atrial cardiomyocytes. *Biophys J.* 1993;64:A393. Abstract.
46. Gelband H, Bush HL, Rosen MR, Myerburg RJ, Hoffman BF. Electrophysiologic properties of isolated preparations of human atrial myocardium. *Circ Res.* 1972;30:293-300.
47. Spach MS, Dolber PC, Anderson PAW. Multiple regional differences in cellular properties that regulate repolarization and contraction in the right atrium of adult and newborn dogs. *Circ Res.* 1989;65:1594-1611.
48. Zipes DP. Genesis of cardiac arrhythmias: electrophysiological considerations. In Braunwald E, ed. *Heart Disease: A Textbook of Cardiovascular Medicine.* Philadelphia, Pa: WB Saunders Co; 1992: 588-627.
49. Colatsky TJ, Follmer CH, Starmer CF. Channel specificity in antiarrhythmic drug action: mechanism of potassium channel block and its role in suppressing and aggravating cardiac arrhythmias. *Circulation.* 1990;82:2235-2242.
50. Follmer CH, Colatsky TJ. Block of the delayed rectifier potassium current, I_K, by flecainide and E-4031 in cat ventricular myocytes. *Circulation.* 1990;82:289-293.

51. Duan D. Fermini B. Nattel S. Potassium channel blocking properties of propafenone in rabbit atrial myocytes. *J Pharmacol Exp Ther.* 1993;264:1113-1123.
52. Fuchs T. Podrid PJ. Pharmacologic therapy for reversion of atrial fibrillation and maintenance of sinus rhythm. In Falk RH. Podrid PJ. eds. *Atrial Fibrillation: Mechanisms and Management.* New York. NY: Raven Press. Publishers: 1992:253-254.
53. Bennett P. McKinney L. Begenisich T. Kass RS. Adrenergic modulation of the delayed rectifier potassium channel in calf cardiac Purkinje fibers. *Biophys J.* 1986;49:839-848.
54. Bennett PB. Begenisich TB. Catecholamines modulate the delayed rectifying potassium current (I_K) in guinea pig ventricular myocytes. *Pflugers Arch.* 1987;410:217-219.
55. Iijima T. Imagawa JI. Taira N. Differential modulation by beta adrenoceptors of inward calcium and delayed rectifier potassium current in single ventricular cells of guinea pig heart. *J Pharmacol Exp Ther.* 1990;254:142-146.
56. Walsh KB. Kass RS. Regulation of a heart potassium channel by protein kinase A and C. *Science.* 1988;242:67-69.
57. Dukes ID. Morad M. The transient K^+ current in rat ventricular myocytes: evaluation of its Ca^{2+} and Na^+ dependence. *J Physiol (Lond).* 1991;435:395-420.
58. Scamps F. Carmeliet E. Delayed K^+ current and external K^+ in single cardiac Purkinje cells. *Am J Physiol.* 1989;257(*Cell Physiol* 26):C1086-C1092.
59. Wang Z. Duan D. Fermini B. Nattel S. Contrasting ionic mechanisms of sustained outward current in human and rabbit atrial myocytes. *Circulation.* 1992;86(suppl 1):I-697. Abstract.
60. Wang Z. Fermini B. Nattel S. An ultra-rapidly activating delayed rectifier carries sustained outward current in human atrial myocytes. *Biophys J.* 1993;64:A199. Abstract.

Cardiovascular Research 1994;28:1540-1546

Rapid and slow components of delayed rectifier current in human atrial myocytes

Zhiguo Wang, Bernard Fermini, and Stanley Nattel

Objective: Previous studies in guinea pig heart cells have shown pharmacologically and kinetically distinct components of the classical delayed rectifier current (I_K), generally referred to as I_{Kr} (rapid I_K) and I_{Ks} (slow I_K). This study was designed to determine whether the human heart contains corresponding components. **Methods:** The whole cell voltage clamp technique was used to study I_K in single myocytes isolated from human right atrial appendages removed at the time of aortocoronary artery bypass surgery. **Results:** The activation of I_K was best fitted by a biexponential relation, with time constants averaging 204(SEM 20) and 1080(197) ms at +10 mV. I_K was inhibited by the specific I_{Kr} blocker E-4031 (5 μM), with the drug sensitive and drug resistant components having markedly different kinetic properties. The E-4031 sensitive current activated rapidly, while the drug resistant component activated more slowly, and the activation time courses of E-4031 sensitive and resistant currents paralleled the rapid and slow components of I_K between −20 and +50 mV. The E-4031 sensitive component showed strong inward rectification, a half activation voltage ($V_{1/2}$) of −14.0(3.3) mV and a slope factor (k) of 6.5(1.5) mV, while the E-4031 resistant current had a linear current-voltage relationship, and values of +19.9(4.2) mV and 12.7(2.5) mV for $V_{1/2}$ and k respectively. The envelope of tails analysis showed a time dependent change in $I_{K\text{tail}}/I_{K\text{step}}$ under control conditions, and E-4031 strongly reduced the time dependent variation, suggesting that the E-4031 resistant current consisted of one dominant component. **Conclusions:** (1) I_K in human atrium shows kinetically distinguishable rapid and slow components. (2) These components correspond to E-4031 sensitive and resistant currents. (3) The kinetics and voltage dependence of the rapid (E-4031 sensitive) and slow (E-4031 resistant) components correspond to properties previously described in guinea pig myocytes. These findings have important potential implications for understanding the mechanisms of human atrial repolarisation and its regulation by the autonomic nervous system and antiarrhythmic drugs.
Cardiovascular Research 1994;28:1540-1546

Since the first description of the delayed rectifier current (initially referred to as I_x, but now commonly designated I_K) in sheep Purkinje fibres by Noble and Tsien,[1] cardiac I_K has been identified in a variety of animal species and tissue types, including guinea pig ventricle[2] and atrium,[3] rabbit nodal tissues,[4] ventricle,[5] and atrium,[6] canine Purkinje fibre[7] and ventricle,[8] cat ventricle,[9-11] embryonic chick atrial cells,[12] calf Purkinje fibres,[13] and human atrium.[14] The efficacy of many antiarrhythmic drugs, including class III agents and many class I components, has been attributed to their ability to block I_K.[15] In their original description of the delayed rectifier,[1] Noble and Tsien showed that it fails to satisfy the envelope of tails test, and related this observation to kinetically distinct current components which they designated I_{x1} and I_{x2}. Subsequent workers suggested that the complex kinetics of I_K could be related to the accumulation and depletion of potassium in intracellular clefts[16] or to the existence of multiple closed states of a single channel.[17] Sanguinetti and Jurkiewicz have provided evidence to suggest that I_K in guinea pig cardiac cells can be separated into two kinetically distinct components, a more rapid component (I_{Kr}) and a slower component (I_{Ks}), on the basis of the response to a novel class III drug, E-4031.[2,3] I_{Kr}, the E-4031 sensitive component, activates more rapidly and at more negative potentials, and shows strong inward rectification, while I_{Ks} is E-4031 resistant, shows a linear current-voltage (I-V) relation, and is activated slowly and at more positive potentials.[2,3] The voltage dependent properties of I_{Kr} and I_{Ks} in guinea pig cells parallel corresponding kinetic components of the delayed rectifier in sheep cardiac Purkinje fibres[1] and embryonic chick atrial cells,[12] while I_K appears to consist of only one component, similar to I_{Kr} in rabbit heart and in cat ventricle.[4,5,6,9-11]

The specific composition of I_K may have important physiological and pharmacological consequences. Several antiarrhythmic drugs specifically block I_{Kr} with minimal, if any, effects on I_{Ks}.[2,15,18,19] On the other hand, some agents appear to be able to inhibit both components,[19,20] and a compound has been recently described that potently inhibits I_{Ks}.[21] Thus the ability of a given agent to alter repolarisation in a tissue may depend on the presence of a specific component of I_K. Furthermore, there is evidence that I_{Ks} activation may accumulate at greater frequencies of depolarisation, contributing to rate dependent action potential abbreviation.[22] It has been suggested that uninhibited activation of I_{Ks} may contribute to the reverse use dependent effects of I_{Kr} blockers on action potential duration, and that conversely I_{Ks} blockers may be able to increase action potential duration selectively at rapid heart rates.[22] Bradycardia dependent prolongation of action potential duration appears to limit antiarrhythmic drug efficacy[23] and contribute to toxicity,[24-26] while tachycardia dependent prolongation of refractoriness may contribute to drug efficacy.[23,27] Thus whether a given component of I_K is present in a tissue may determine not only whether an

Department of Medicine, Montreal Heart Institute and University of Montreal, 5000 Belanger Street East, Montreal, Quebec H1T 1C3, Canada: B Fermini, S Nattel; Departments of Pharmacology and Medicine, McGill University, Montreal, Canada: Z Wang. Correspondence to Dr Nattel.

antiarrhythmic drug affects the tissue, but also how repolarisation and drug effects on action potential duration are controlled by heart rate.

We have recently demonstrated the presence of delayed rectifier currents in human atrial myocytes.[14] The purpose of the present studies was to assess the properties of I_K in human atrial cells in order to determine whether they suggest the presence of I_{Kr} and/or I_{Ks} as previously described in other systems. In particular, we analysed the kinetic properties of I_K, its response to E-4031, and the kinetic and voltage dependent properties of the E-4031 sensitive and resistant components.

Methods

Isolation of single atrial cells

Specimens of human right atrial appendage were obtained from the hearts of 14 patients (59, SEM 4, years old) undergoing aortocoronary bypass surgery. The procedure for obtaining the tissue was approved by the ethics committee of the Montreal Heart Institute. Specimens were transported to the laboratory in oxygenated Tyrode solution, and single myocytes were isolated as previously described in detail.[14] In brief, cubic chunks of tissue (approximately 1 mm^3) were exposed to collagenase (390 $U \cdot ml^{-1}$, Worthington Biochemical) and proteinase (4 $U \cdot ml^{-1}$, type XXIV, Sigma) and gently agitated with a stirring bar. When cell yield appeared maximal, cells were removed and stored in a solution of the following composition (in $mmol \cdot litre^{-1}$): KCl 20, KH_2PO_4 1.0, glucose 10, glutamic acid 70, β-hydroxybutyric acid 10, taurine 10, and EGTA 10, with albumin 1%; pH adjusted to 7.4 with KOH.

Only quiescent rod shaped cells showing clear cross striations were used. A small aliquot of the solution containing the isolated cells was placed in a 1 ml chamber mounted on the stage of an inverted microscope. Five minutes were allowed for cell adhesion to the bottom of the chamber, and then the cells were superfused at 3 $ml \cdot min^{-1}$ with a solution containing (in $mmol \cdot litre^{-1}$): NaCl 126, KCl 5.4, $MgCl_2$ 0.8, $CaCl_2$ 1.0, NaH_2PO_4 0.33, HEPES 10, and glucose 5.5, with pH adjusted to 7.4 with NaOH. Bath temperature was maintained at 36°C with a thermistor controlled heating unit.

Data acquisition

The whole cell patch clamp technique was employed to record ionic currents. Borosilicate glass electrodes were filled with (composition in $mmol \cdot litre^{-1}$): KCl 130.0, $MgCl_2$ 1.0, HEPES 10.0, EGTA 5.0, Mg_3ATP 5.0, and Na_2-creatine phosphate 5.0 (pH adjusted to 7.4 with KOH), and connected to a patch clamp amplifier. In selected experiments, electrodes with tip resistances below 3 MΩ were used. However, rundown of I_K was very rapid when low resistance electrodes were used, with about 70% reduction in current amplitude within 10 min. Therefore most of the results presented in this manuscript were obtained with electrodes with tip resistances varying from 2 to 10 MΩ. Under these conditions, rundown was reduced and tail currents recorded 10 min after membrane rupture averaged 58(SEM 12)% of the values immediately after membrane rupture, with no significant change over 30 min thereafter. Experiments were begun 10 min after membrane rupture, drug effects were studied after brief (5 min) periods of equilibration, and data from experiments using drugs were only analysed if washout of drug effects was obtained.

Command pulses were generated by a 12 bit digital to analogue converter controlled by pClamp software (Axon Instruments). Recordings were filtered at 1 kHz bandwidth and series resistance was compensated in all experiments. In all of the cells studied, junction potentials (2-14 mV) were zeroed prior to formation of the membrane-pipette seal in 1 mM calcium Tyrode solution. Mean seal resistance averaged 27.7(6.3) GΩ. The series resistance (Rs) after compensation was 2.3(0.9) MΩ. The time constant for capacity decay was 156(45) μs following compensation. The maximum total current at the time of steady state I_K was < 800 pA. The voltage drop across Rs therefore never exceeded 3 mV.

E-4031 (5 μM) was provided as a kind gift by Eisai Ltd, Tokyo, Japan. Nifedipine (Sigma, 1 μM) was added to the superfusate in all experiments to block I_{Ca} and the calcium activated component of the transient outward current. The nifedipine containing solutions were protected from direct light sources to prevent photodegradation. I_{Na} was suppressed by replacing external NaCl (126 mM) by choline chloride (Sigma, 126 mM) or by holding the membrane at –40 mV. To exclude direct activation of muscarinic receptors by choline, atropine (100 nM) was present in the perfusate throughout all experiments, after verifying that this concentration of atropine inhibited $I_{K,ACh}$ but did not alter I_K. In order to block the ultrarapid delayed rectifier current (I_{Kur}) and any possible contribution of transient outward current, 2 mM 4-aminopyridine was included in the superfusate. 4-Aminopyridine (Sigma) was prepared as a 1 molar stock solution in distilled water, with pH adjusted to 7.4 with the addition of HCl.

Data analysis

Comparisons among groups were performed by analysis of variance (ANOVA) with Scheffé contrasts. A non-linear least squares curve fitting program (Clampfit in pClamp or TableCurve, Jandel Scientific) was used to fit the activation of I_K. Baseline and drug data were compared by Student's t test, and a two tailed probability of 5% was taken to indicate statistical significance. Group data are presented as mean(SEM).

Results

Voltage and time dependence of I_K in human atrium

Sixteen cells from 14 preparations were studied. The criteria for cell selection were: (1) the presence of a delayed outward current with features characteristic of I_K, without detectable I_{to} current (type 2 cells as previously defined[14]); (2) tail currents > 50 pA upon repolarisation to –40 mV. Of the total number of cells available for this study, 8.8% fulfilled these criteria. Cells possessing I_{to} were excluded so as to avoid overlapping outward currents early after depolarisation. Figure 1A shows a typical example of I_K recorded from a human atrial myocyte under control conditions. Currents were elicited by 3 s depolarising pulses from a holding potential of –60 mV to various test potentials. Currents recorded from the same cell after the addition of 5 μM E-4031 are shown in fig 1B. The current amplitude measured during depolarising steps was defined as $I_{K,step}$, while the amplitude of the tail current measured upon repolarisation was defined as $I_{K,tail}$. While currents activated during each depolarising step ($I_{K,step}$) were somewhat decreased by E-4031, tail currents observed following repolarisation ($I_{K,tail}$) were reduced to a greater extent. E-4031 sensitive current, obtained by digitally subtracting the current in the presence of E-4031 from the control current, is shown in fig 1C. Three major characteristics of the drug sensitive current were noted. First, the steady state amplitude of the current had a biphasic relation to voltage: it increased at more positive potentials over a certain range, and then decreased with stronger depolarisation. Second, drug sensitive current activated more rapidly than control current, while current in the presence of E-4031 activated perceptibly more slowly than control current. Finally, E-4031 sensitive current showed a time dependent decay during strong depolarisations (positive to +30 mV). Similar results were obtained in five other cells. As shown in fig 1D, the effects of E-4031 were largely reversible upon drug washout. Overall, E-4031 reduced $I_{K,step}$ at 0 mV from 273(SEM 34) pA to 68(30) pA. After 15-20 min of drug washout, $I_{K,step}$ at 0 mV averaged 261(47) pA in the same cells, not significantly different from control values.

Mean data from the current-voltage (I-V) relationship for $I_{K,step}$ (as measured at the end of each pulse) from a holding potential of –60 mV are shown in fig 2A. Qualitatively similar results were obtained with holding potentials of –40 and –70 mV. The control I-V relationship shows a bend in its mid-portion (over the voltage range 0 to +30 mV). E-4031 eliminates this bend, resulting in a smooth I-V relationship and suggesting that the bend is due to a component blocked by E-4031. The E-4031 sensitive current measured at the end of the pulse (filled diamonds) shows strong inward rectification, accounting for the flat portion of the overall I-V curve. When E-4031 sensitive current is measured at the peak current level (empty diamonds), strong inward rectification is still apparent, but absolute current values do not decrease at more positive potentials.

The activation curves of control currents (empty circles), E-4031 resistant currents (filled circles), and E-4031

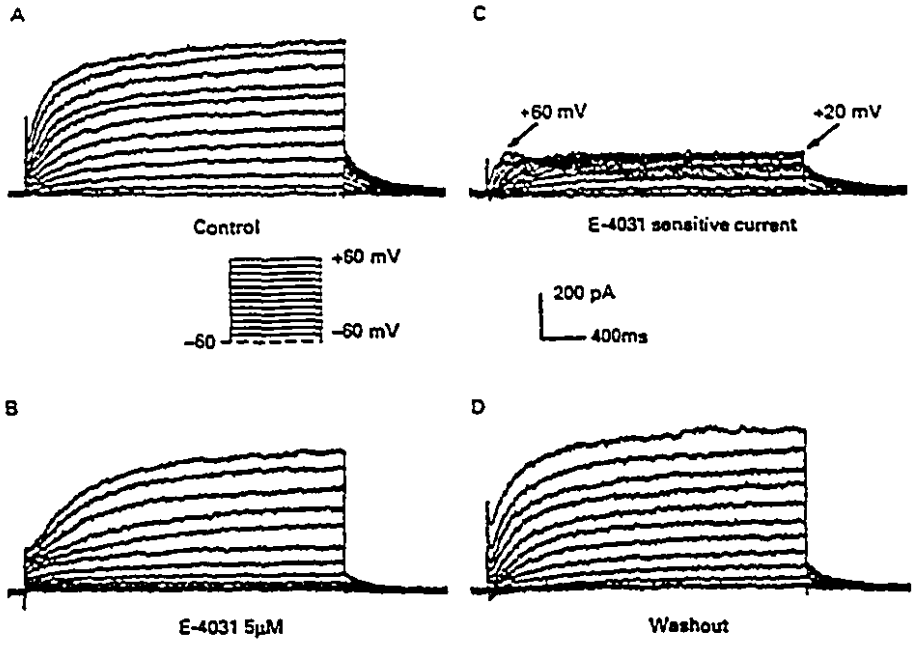

Figure 1 Delayed rectifier currents recorded from a human atrial myocyte. Currents were elicited by 3000 ms depolarising pulses at 0.1 Hz to potentials ranging from –50 to +60 mV, from a holding potential of –60 mV. (A) Currents under control conditions. (B) Currents recorded after exposure to 5 μM E-4031 for 5 min. (C) E-4031 sensitive currents obtained by digital subtraction of currents in panel B from those in panel A. (D) Currents recorded in the same cell after 15 min of drug washout.

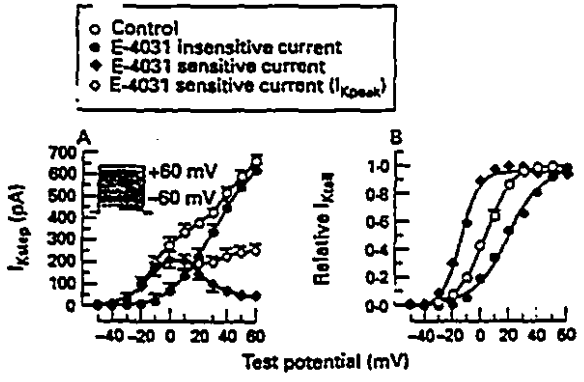

Figure 2 Voltage dependence of I_K current and effects of E-4031. Voltage protocol (inset) was applied at 0.1 Hz. (A) Current-voltage (I-V) relationship for step current, defined as difference between current at the end of a 3 s voltage step and current immediately after decay of the capacitive transient caused by initial depolarisation. Results are shown for control conditions (empty circles), after exposure to 5 μM E-4031 (E-4031 resistant current, filled circles), and the difference current suppressed by E-4031 as measured at the end of the pulse (E-4031 sensitive current, filled diamonds). Note the inflection in the mid-portion of the control I-V curve, the smooth I-V curve in the presence of E-4031, and the strong inward rectification of E-4031 sensitive current. Peak values of E-4031 sensitive current (as obtained by digital subtraction) are shown by empty diamonds. Results are means, error bars = SEM. (B) Activation curve of control, E-4031 resistant, and E-4031 sensitive currents based on analysis of tail currents at –30 mV following a 3 s activating pulse to various test potentials shown. The voltage protocol was as in panel A, but after the depolarising test pulse cells were repolarised to –30 mV to measure tail currents. Results are means of three cells held at –60 mV (same cells as in panel A). Similar results were obtained in three other cells at a holding potential of –40 mV.

sensitive currents (filled diamonds) based on tail current analysis are shown in fig 2B for the same cells whose I-V curves are shown in fig 2A. The continuous curves shown were obtained by fitting experimental data to a Boltzmann distribution function of the form

$$a = 1/(1 + \exp[V_m - V_{1/2}]/k)$$

where a is the activation variable (I_{Ktail} at a test voltage V_m divided by I_{Ktail} at +60 mV), $V_{1/2}$ is the half activation voltage, and k is the slope factor. Under control conditions, $V_{1/2}$ averaged +3.4(0.9) mV, and the slope factor (k) was 9.4(2.4) mV. In the presence of E-4031, $V_{1/2}$ and k were +19.9(4.2) mV and 12.7(2.5) mV respectively, while the $V_{1/2}$ and k of the E-4031 sensitive component were –14.0(3.3) mV and 6.5(1.5) mV.

Activation kinetics

The results presented above are consistent with the concept that I_K in human atrial myocytes is an aggregate of a more rapidly activating component (which is sensitive to blockade by E-4031) and a slower one (which is E-4031 resistant). A detailed analysis of the time course of I_K activation under control conditions supported the concept of two underlying current components. Results from a representative cell under control conditions are presented in fig 3A, with the solid lines representing best fit curves to a single (top) or double (bottom) exponential function. While it was possible to fit current activation as a single exponential function of time (as reported for shorter duration pulses in our previous study[14]), the fit was imperfect and the maximum correlation coefficient that could be obtained for data obtained in this cell at +30 mV was 0.90. A double exponential function provided a perceptibly better fit, with a correlation coefficient of 0.99 and a residual sum of squares reduced by over one third compared to the single exponential. Overall, the residual sum

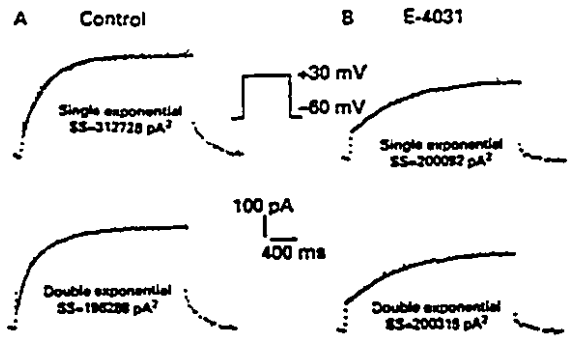

Figure 3 Curve fitting of I_K activation before (A) and after (B) superfusion with 5 μM E-4031. Results shown were obtained by depolarising for 3 s from a holding potential of –60 mV to +30 mV. Best fit curves to activation data are shown for single exponential (top of each panel) and double exponential (bottom of each panel) functions of time, with residual sum of squares (SS) shown. Under control conditions (A), residual sum of squares is reduced by over one third by biexponential fit compared to single exponential, indicating that biexponential is necessary to fit the activation data. In the presence of E-4031 (B), the residual sum of squares is virtually the same for both relations, indicating that a single exponential is adequate to describe current activation.

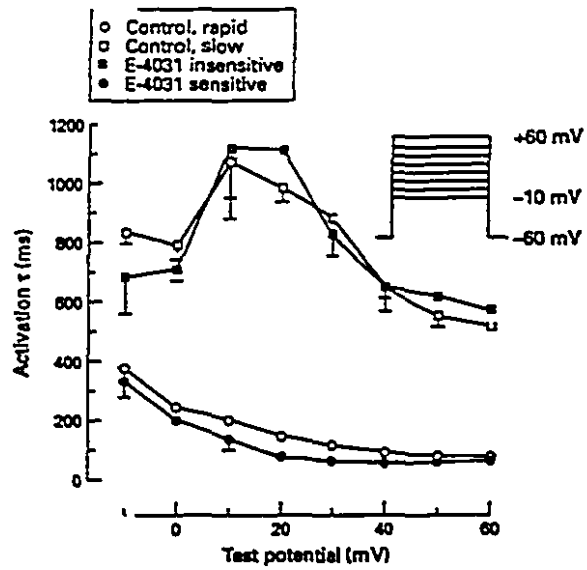

Figure 4 Voltage dependent time constants of I_K activation. Under control conditions (empty symbols), biexponential fits (as in fig 3A) provided a rapid (circle) and slow (square) time constant at test potentials between –10 and +60 mV. In the presence of 5 μM E-4031, only a single exponential was needed to fit activation (as shown in fig 3), and time constants (filled squares) were similar to those of the slow component under control conditions. The activation of E-4031 sensitive current was also well fitted by a single exponential, with time constants (filled circles) similar to those of the rapid component under control conditions. At voltages showing inactivation of E-4031 sensitive current, biexponential curve fitting was used to fit activation and inactivation simultaneously. Results are means, error bars = SEM, for three cells studied at a holding potential of –60 mV (voltage protocol shown in inset); similar data were obtained in three other cells at a holding potential of –40 mV. Where error bars are absent, they fell within symbol for mean.

of squares for single exponential fits of control I_K as measured with a holding potential of –60 mV averaged 248 074(48 747) pA^2, compared to 161 577(30 617) pA^2 for the biexponential ($p<0.05$). In the presence of E-4031 (fig 3B), current activation was slowed, and a single exponential fitted the activation time course well ($r=0.99$), with no obvious improvement from the use of a double exponential. The residual sum of squares for I_K after exposure to E-4031 averaged 161 577(27 101) pA^2 for a single exponential and 161 994(26 921) pA^2 for a double exponential (p=NS). Similar results were obtained in a total of six cells, three with a holding potential of –60 mV and three at –40 mV.

Mean values of activation τ are shown as a function of test potential in fig 4. The rapid kinetic component under control conditions had time constants (empty circles) that decreased at more positive test potentials, while the time course of the slower component (empty squares) reached a maximum at +10 to +20 mV (about the $V_{1/2}$ for activation of the E-4031 resistant component), and declined at more positive or negative potentials. The time constants of current remaining after exposure to E-4031 (filled squares) closely resembled values of the slower component prior to drug superfusion. Similarly, the time constants of currents blocked by E-4031 (filled circles) were quite close to those of the fast component under control conditions. The results shown in fig 4 were obtained with a holding potential of –60 mV, and comparable values for activation τ were obtained at the same test potentials from a holding potential of –40 mV.

We also analysed the kinetics of tail current decay at –40 mV. After a short depolarising pulse to +30 mV, the tail current was well fitted by a single exponential with a mean time constant of 99(22) ms (after a 50 ms pulse). As depolarising pulse duration increased, the deactivation of the tail current became biexponential. For example, tail current deactivation after a 2850 ms depolarising pulse to +20 mV had time constants of 124(24) and 555(125) ms. The E-4031 sensitive tail current had only one exponential component, with a time constant averaging 234(24) ms after the same depolarising pulse voltage and duration. Tail currents in the presence of E-4031 (E-4031 resistant currents) were relatively small, but were as well fitted by a monoexponential relation as a biexponential, and had a mean time constant of 637(211) ms following a 2850 ms pulse to +20 mV.

As described above, the E-4031 sensitive current frequently showed a time dependent decline after achieving a peak at voltages positive to +30 mV. The decay time course was well described by a single exponential function. The time constants of current decay averaged 871(256) ms at +30 mV, 676(121) ms at +40 mV, 513(54) ms at +50 mV, and 430(43) ms at +60 mV, respectively.

Envelope of tails test

To assess further the effects of E-4031 on the composition of I_K, we applied an envelope of tails analysis. Currents were elicited by depolarisation from a HP of –60 mV to +30 mV with pulses ranging in duration from 100 to 2800 ms, and tail currents were recorded upon repolarisation to –40 mV. Results obtained in five cells before and after exposure to E-4031 are shown in fig 5. The ratio of I_{Kmax}/I_{Kstep} averaged 7.40(0.37) after 100 ms under control conditions (filled circles), and gradually decreased to a steady state value of 0.46(0.10) as pulse duration increased. These data suggest that I_K results from the activation of more than a single class of K^+ channels. In the presence of E-4031 (empty diamonds), time dependent changes in the I_{Kmax}/I_{Kstep} ratio were strongly reduced, although they were not eliminated entirely.

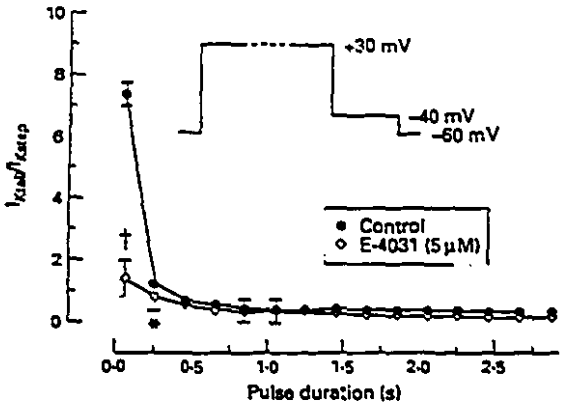

*Figure 5 Ratio of tail current to step current, as measured at −40 mV after depolarising pulses of varying duration from the holding potential (−60 mV) to +30 mV (delivered at 0.2 Hz). Under control conditions (filled circles), the ratio changed substantially over time, indicating more than one current component. In the presence of E-4031 (empty diamonds), time dependent changes in the ratio were substantially reduced. Error bars = SEM, n = 5 cells. *p < 0.05, †p < 0.001 for difference between ratio under control conditions and in the presence of E-4031.*

Discussion

Evidence for two components of I_K in human atrial cells

We have provided several lines of evidence suggesting that the delayed rectifier outward current in human atrial myocytes is comprised of two distinct components, the properties of which correspond to those of I_{Kr} and I_{Ks} as described by Sanguinetti and Jurkiewicz[2,3] and Chinn[28] in guinea pig heart cells. The evidence includes: (1) the biexponential activation time course of aggregate I_K (figs 3 and 4); (2) the ability of E-4031 to inhibit a component of I_K with similar activation kinetics to the rapid component of I_K under control conditions (fig 4); (3) the correspondence between the activation kinetics of residual I_K resistant to E-4031 and those of the slower component under control conditions (fig 4); (4) the elimination by E-4031 of the flattening in the mid-portion of the I-V curve of I_K, by suppressing a current that shows strong inward rectification (fig 2A); and (5) the more positive activation voltage and less steep voltage dependence of I_K tail currents in the presence of E-4031 compared to control, and even more so compared to the E-4031 sensitive component (fig 2B). The presence of both components of I_K has important potential implications regarding the physiological mechanisms of repolarisation and its pharmacological control in the human atrium.

Comparison with previous studies of components of delayed rectifier current

A variety of investigators have described two kinetic components of classical cardiac delayed rectifier current in sheep cardiac Purkinje fibres,[1] calf Purkinje fibres,[13] guinea pig ventricular[2] and atrial[3] myocytes, and chick atrial heart cell aggregates.[12] Analysis of these components has recently been made easier by the demonstration that the potent methanesulphonanilide I_K inhibitor E-4031 is specific for the rapid component I_{Kr}.[2,3,28] The rapid and/or E-4031 sensitive component of I_K displays inward rectification and activates at more negative potentials than the slower E-4031 resistant component, which has a linear I-V relation. Some species appear to display only one component, which can have the properties of I_{Kr} (in the case of the rabbit[4,29] and cat[10,11]) or I_{Ks} (in the frog[30]). The data presented in the present manuscript suggest that both components are present in human atrium, and have similar properties to those previously defined in other species. For example, the E-4031 sensitive I_{Kr} in our studies had a half activation voltage ($V_{1/2}$) of −14.0(3.3) mV and a slope factor (k) of 6.5(1.5) mV, while values for E-4031 resistant I_{Ks} were +19.9(4.2) mV ($V_{1/2}$) and 12.7(2.5) mV (k). The corresponding values reported by Sanguinetti and Jurkiewicz[2,3] for I_{Kr} were −21.5 and −19 mV for $V_{1/2}$ and 7.5 and 5.2 mV for k, and for I_{Ks} were +15.7 and +24 mV for $V_{1/2}$ and 12.7 and 15.7 mV for k. Like Sanguinetti and Jurkiewicz, we found that the E-4031 sensitive current showed strong inward rectification, and that E-4031 substantially reduced the time dependent changes in the tail current/step current ratio (although unlike these workers, we did not find that E-4031 completely eliminated the latter changes).

The strong inward rectification of I_{Kr} could be due to either voltage dependent block of outward current though the channel by an internal ion, such as magnesium, or a rapid voltage gated inactivation process. Our finding that the E-4031 sensitive current showed a time dependent decay during sustained depolarisation may be a reflection of time dependent inactivation. Data suggesting similar time dependent I_{Kr} inactivation at positive potentials have also been obtained in rabbit sinoatrial nodel cells[4] and in cultured AT1 cells derived from transgenic mice.[31] On the other hand, we cannot exclude a role for state dependent and time dependent blocking properties of E-4031 (for example, time dependent unblocking from open channels at positive potentials) in accounting for the decay in drug sensitive current.

Potential significance

Atrial refractoriness governs the occurrence of experimental atrial reentrant arrhythmias and their response to antiarrhythmic drug therapy.[23] Since action potential duration is a major determinant of refractoriness, a detailed understanding of the ionic currents underlying human atrial repolarisation is necessary for improved knowledge of the mechanisms by which various interventions affect the occurrence of such arrhythmias as atrial fibrillation and flutter in man. Our results shed some potentially new light on this issue. For instance, sotalol is known to be effective in treating clinical atrial fibrillation and flutter,[32] and increases human atrial action potential duration and refractory period.[33,34] Since sotalol has been shown to be a specific blocker of I_{Kr},[3] with an action restricted to the rapid component I_{Kr},[2] our results indicating the presence of I_{Kr} in human atrium provide for a probable ionic mechanisms by which sotalol acts to suppress atrial arrhythmias in man. Furthermore, they predict that other I_{Kr} blockers should have similar efficacy. Indeed, a preliminary communication suggests that the specific I_{Kr} blocker defetilide[18] is capable of terminating atrial flutter and fibrillation in man.[35]

On the other hand, our finding of a component with properties of I_{Ks} in human atrium also has potentially important implications. Complementary DNAs, the expression of which results in a potassium current with slow activation kinetics (I_{sK} or MinK), have been cloned from human atrium and ventricle.[36–38] There is good evidence that MinK is responsible for I_{Ks} in the guinea pig heart.[39] Our results indicating the presence of I_{Ks} in the human atrium support the contention that MinK expression plays a role in human atrial repolarisation. It has been shown that isoprenaline increases I_{Ks} but not I_{Kr} in the guinea pig heart.[15,40] We

have obtained evidence suggesting that isoprenaline increases I_K in human atrial cells by adding a slowly activating current with kinetics similar to those of I_{Ks} (unpublished data). The enhancement of I_{Ks} by isoprenaline may contribute to the arrhythmogenic properties of sympathetic activation in some patients with atrial fibrillation.

Finally, the presence of I_{Ks} may indicate the possibility of novel antiarrhythmic approaches. Jurkiewicz and Sanguinetti have provided evidence to suggest that the incomplete interbeat deactivation of I_{Ks} may play a role in rate dependent action potential abbreviation.[21] Blockade of I_{Ks} might result in the attenuation of rate dependent action potential shortening and thereby prolong the action potential selectively during tachycardia, a highly desirable property.[27 41] There is some evidence to suggest that this expectation may have validity.[42 43] NE-10064 is an investigational compound that strongly blocks I_{Ks},[21] although recent studies suggest that it may block I_{Kr}.[44] Selective I_{Ks} blockers are now under active development, and it will be very interesting to study their rate dependent effects on human atrial refractoriness.

Potential limitations

We have previously defined three types of cells in human atrium based on the relative size of time dependent currents.[14] Type 1 cells (58% of the total population) displayed a large I_{to} and a clear I_K, type 2 (13% of cells) displayed only I_K, and type 3 (29% of cells) were characterised by a prominent I_{to} and negligible I_K. To minimise contaminating currents, we elected to study only type 2 cells (with I_K but no I_{to}) in the present series of experiments. We also rejected experiments in which washout of drug effects was not obtained, because they may have been contaminated by current rundown. This limited the number of cells that we could study to less than 10% of the cells available, and it must be understood that our results were therefore based on a subpopulation of cells, selected to allow us to obtain meaningful data. In addition, all tissue samples were obtained from the right atrial appendage, and we have no way of knowing to what extent I_{Kr} and I_{Ks} are expressed in cells from other regions of the human heart.

Our analysis of the components of I_K was partly based on the results of exposure to E-4031. We cannot exclude a possible role of voltage and time dependent drug effects in some of the phenomena observed. The close similarity between the kinetic components of I_K under control conditions and the corresponding E-4031 sensitive and resistant currents (fig 4) argues against important distortions of activation kinetics by time dependent drug action. E-4031 was used as a tool in a similar fashion to isolate the components of I_K in the guinea pig in the studies of Sanguinetti and Jurkiewicz that characterised the components I_{Kr} and I_{Ks}.[2 3]

We have limited our analysis in the present study to the components of I_K that activate with a detectable time course at 36°C. There is an additional potassium current component that activates virtually instantaneously at 36°C, but has detectable activation kinetics at 25°C.[45] Detailed analysis indicates that this current is a novel type of delayed rectifier that activates much more rapidly than I_{Kr}, and we have suggested that it be called an "ultrarapid" delayed rectifier, or I_{Kur}.[45] Since I_{Kur} is not a component of the classical type of I_K studied in this paper, and we have recently presented its properties in detail,[45] we have not included a study of I_{Kur} in the present analysis. To prevent contamination of I_K currents by I_{Kur}, we included 2 mM 4-aminopyridine, which fully blocks I_{Kur},[45] in the superfusate.

Unlike findings by other workers in guinea pig myocytes,[2 3 28] the envelope of tails test was not fully satisfied for I_K in the presence of E-4031. This may be due to species differences. In our cells, the envelope of tails test failed to be satisfied in the presence of E-4031 for very short depolarising pulses (100 ms), shorter than the pulse durations for which values were reported in the other studies.[2 3 28] Very short pulses may elicit some additional, as yet unidentified, current components. Alternatively, it is possible that E-4031 does not fully block I_{Kr} in these cells. Unlike Chinn,[28] we did not observe biexponential tail currents in the presence of E-4031. The reasons for this discrepancy are, at the moment, unclear.

Conclusions

We have shown that I_K in human atrial cells contains both components of I_K previously described in sheep Purkinje fibres, guinea pig atrial and ventricular cells, and chick atrial cell aggregates. Since these components have different kinetic, voltage dependent, and pharmacological properties, our results are important for the appreciation of ionic mechanisms of human atrial repolarisation and it regulation. In addition to adding insights into underlying mechanisms, our work points to the potential value of using more specific I_K blocking drugs in treating human atrial arrhythmias and assessing clinically important basic electrophysiological mechanisms.

The authors thank Dr L Conrad Pelletier, Dr Michel Carrier, and Dr Raymond Cartier for providing human atrial tissue specimens, Guylaine Nicol BSc for excellent technical assistance, Martine Dufort and Lucie Bégin for expert secretarial help. ZW is a Canadian Heart Foundation research trainee, and BF is a Knoll-FRSQ research scholar. Supported by grants for the Medical Research Council of Canada, The Quebec Heart Foundation, and the Fonds de Recherche de l'Institut de Cardiologie de Montréal.

Key terms: repolarisation; potassium channels; antiarrhythmic drugs; ECG; arrhythmias; voltage clamp.

Received 14 April 1994; accepted 29 June 1994. Time for primary review 19 days.

1 Noble D, Tsien RW. Outward membrane currents activated in the plateau range of potentials in cardiac Purkinje fibres. *J Physiol (Lond)* 1969;200:205–31.
2 Sanguinetti MC, Jurkiewicz NK. Two components of cardiac delayed rectifier K^+ current. *J Gen Physiol* 1990;96:195–215.
3 Sanguinetti MC, Jurkiewicz NK. Delayed rectifier outward K^+ current is composed of two currents in guinea pig atrial cells. *Am J Physiol* 1991;260(*Heart Circ Physiol* 29):H393–9.
4 Shibasaki T. Conductance and kinetics of delayed rectifier potassium channels in nodal cells of the rabbit heart. *J Physiol (Lond)* 1987;387:227–50.
5 Carmeliet E. Electrophysiologic and voltage clamp analysis of the effects of sotalol on isolated cardiac muscle and Purkinje fibers. *J Pharmacol Exp Ther* 1985;232:817–25.
6 Duan D, Fermini B, Nattel S. Potassium channel blocking properties of propafenone in rabbit atrial myocytes. *J Pharmacol Exp Ther* 1993;264:1113–23.
7 Gintant GA, Datyner NB, Cohen IS. Gating of delayed rectification in acutely isolated canine cardiac Purkinje myocytes. *Biophys J* 1985;48:1059–64.
8 Gintant GA. Delayed rectifier current (IK) in canine myocardium: two unique conductances (independently modulated) affect repolarization. (Abstract) *Circulation* 1993;88:I–89.
9 McDonald TF, Trautwein W. The potassium current underlying delayed rectification in cat ventricular muscle. *J Physiol (Lond)* 1978;274:217–46.
10 Colatsky TJ, Follmer CH. Delayed rectifier potassium current Ik in cat ventricular myocytes. (Abstract) *Biophys J* 1990;57:506a.
11 Kleiman RB, Houser SR. Outward currents in normal and hypertrophied feline ventricular myocytes. *Am J Physiol* 1989;256:H1450–61.

12 Shrier A, Clay JR. Repolarization currents in embryonic chick atrial heart cell aggregates. *Biophys J* 1986;50:861–75.
13 Bennett P, McKinney L, Begenisich T, Kass RS. Adrenergic modulation of the delayed rectifier potassium channel in calf cardiac Purkinje fibers. *Biophys J* 1986;49:839–48.
14 Wang Z, Fermini B, Nattel S. Delayed rectifier outward current and repolarization in human atrial myocytes. *Circ Res* 1993; 73:276–85.
15 Colatsky TJ, Follmer CH, Starmer CF. Channel specificity in antiarrhythmic drug action. Mechanism of potassium channel block and its role in suppressing and aggravating cardiac arrhythmias. *Circulation* 1990;82:2235–42.
16 Attwell D, Cohen I, Eisner D. Membrane potential and ion concentration conditions for a cell with a restricted extracellular space. *Proc R Soc Lond B Biol Sci* 1979;206:145–61.
17 Bennett PB, McKinney LC, Kass RS, Begenisich T. Delayed rectification in the calf cardiac Purkinje fiber. Evidence for multiple state kinetics. *Biophys J* 1985;48:553–67.
18 Carmeliet E. Voltage- and time-dependent block of the delayed K+ current in cardiac myocytes by dofetilide. *J Pharmacol* 1992;262:809–17.
19 Balser JR, Hondeghem LM, Roden DM. Suppression of time-dependent outward current in guinea pig ventricular myocyter. Actions of quinidine and amiodarone. *Circ Res* 1991;69:519–29.
20 Zhang Z, Follmer CH, Sarma JSM, Chen F, Singh BN. Effect of ambasilide, a new class III agent, on plateau currents in isolated guinea pig ventricular myocytes: block of delayed outward potassium current. *J Pharmacol Exp Ther* 1992;263:40–8.
21 Busch AE, Malloy KJ, Varnum MD, Adelman JP, North RA, Maylie J. A slowly-activating potassium current I_{ks} is the target for the class III antiarrhythmic drug NE-10064. (Abstract) *Circulation* 1993;88(part 2):I-231.
22 Jurkiewicz NK, Sanguinetti MC. Rate-dependent prolongation of cardiac action potentials by a methanesulfonanilide class III antiarrhythmic agent. Specific block of rapidly activating delayed rectifier K+ current by dofetilide. *Circ Res* 1993;72:75–83.
23 Wang J, Bourne GW, Wang Z, Villemaire C, Talajic M, Nattel S. Comparative mechanisms of antiarrhythmic drug action in experimental atrial fibrillation. The importance of use-dependent effects on refractoriness. *Circulation* 1993;88:1030–44.
24 Nattel S, Zeng F-D. Frequency dependent effects of anti-arrhythmic drugs on action potential duration and refractoriness. *J Pharmacol Exp Ther* 1984;229:283–91.
25 Roden DM, Hoffman BF. Action potential prolongation and induction of abnormal automaticity by low quinidine concentrations in canine Purkinje fibers. Relationship to potassium and cycle length. *Circ Res* 1985;56:857–67.
26 Nattel S, Quantz MA. Pharmacological response of quinidine induced early after depolarisations in canine cardiac Purkinje fibres: insights into underlying ionic mechanisms. *Cardiovasc Res* 1988;22:808–17.
27 Wang Z, Pelletier LC, Talajic M, Nattel S. The effects of flecainide and quinidine on human atrial action potentials. *Circulation* 1990;82:274–83.
28 Chinn K. Two delayed rectifiers in guinea pig ventricular myocytes distinguished by tail current kinetics. *J Pharmacol Exp Ther* 1993;264:553–60.
29 Scamps F, Carmeliet E. Delayed rectifier and external K+ in single cardiac Purkinje cells. *Am J Physiol* 1989;257:C1086–92.
30 Hume JR, Giles W, Robinson K, Shibata EF. A time and voltage-dependent K+ current in single cardiac cells from bull frog atrium. *J Gen Physiol* 1986;88:777–98.
31 Yang T, Wathen MS, Field LJ, Tamkun MM, Roden DM, Snyders DJ. I_{Kr}: A major repolarizing current in cultured AT1 cells. (Abstract) *Circulation* 1993;88(part 2):I–88.
32 Ruffy R, Sotalol. *J Cardiovasc Electrophysiol* 1993;4:81–98.
33 Hayward RP, Taggart P. Effect of sotalol on human atrial action potential duration and refractoriness: cycle length dependency of class III activity. *Cardiovasc Res* 1986;20:100–7.
34 Campbell TJ. Cellular electrophysiological effects of D- and DL-sotalol in guinea-pig sinoatrial node, atrium and ventricle and human atrium: differential tissue sensitivity. *Br J Pharmacol* 1987;90:593–9.
35 Singh SN, Falk R, Friedrich T, Singh B. The efficacy and safety of dofetilide in patients with recent onset atrial fibrillation or flutter. (Abstract) *Circulation* 1993;88(part 2):I–65.
36 Murai T, Kakizuka A, Takumi T, Ohkubo H, Nakanishi S. Molecular cloning and sequence analysis of human genomic DNA encoding a novel membrane protein which exhibits a slowly activating potassium channel activity. *Biochem Biophys Res Commun* 1989;161:176–81.
37 Swanson R, Folander K, Bennett C, Antanavage J, Stein RB, Smith JS. Total synthesis, expression and functional assay of a gene encoding a human delayed rectifier potassium channel. (Abstract) *Biophys J* 1990;57:211a.
38 Krafte DS, Dugrenier N, Dillon K, Volberg WA. Electrophysiological properties of a cloned, human potassium channel expressed in xenopus oocytes. (Abstract) *Biophys J* 1992; 61:A378.
39 Freeman LS, Kass RS. Expression of a minimal K+ channel protein in mammalian cells and immunolocalization in guinea pig heart. *Circ Res* 1993;73:968–73.
40 Sanguinetti MC, Jurkiewicz NK, Scott A, Siegl PKS. Isoproterenol antagonizes prolongation of refractory period by the class III antiarrhythmic agent E-4031 in guinea pig myocytes. Mechanism of action. *Circ Res* 1991;68:77–84.
41 Hondeghem LM, Snyders DJ. Class III antiarrhythmic agents have a lot of potential but a long way to go: reduced effectiveness and dangers of reverse use dependence. *Circulation* 1990;81:686–90.
42 Sager PT, Uppal P, Follmer C, Antimisiaris M, Pruitt C, Singh BN. Frequency-dependent electrophysiologic effects of amiodarone in humans. *Circulation* 1993;88:1063–71.
43 Wang J, Feng J, Nattel S. Class III antiarrhythmic drug action in experimental atrial fibrillation: differences in reverse use-dependence and effectiveness between d-sotalol and the new antiarrhythmic drug ambasilide. *Circulation* (in press).
44 Conder ML, Smith MA, Atwal KS, McCullough JR. Effects of NE-10064 on K+ currents in cardiac cells. (Abstract) *Biophys J* 1994;66:A326.
45 Wang Z, Fermini B, Nattel S. Sustained depolarization-induced outward current in human atrial myocytes: evidence for a novel delayed rectifier K+ current similar to KV1.5 cloned channel currents. *Circ Res* 1993;73:1061–76.

We demonstrated the existence of I_K current in human atrial myocytes, and characterized the electrophysiological properties of the two components I_{Kr} and I_{Ks}. We discovered the relation between the relative importance of the time-dependent K^+ currents (I_{to1} and I_K) and the corresponding action potential morphology. Based on this, we grouped cells into three types: type I cells with both I_{to1} and I_K, type II cells with only I_K, and type III cells with only I_{to1}. Moreover, we observed that in type III cells there was always a sustained outward current seen after complete inactivation of I_{to1}. The nature and role of this component are as yet to be determined.

Currents with properties distinct from classical I_K and I_{to1} have been found in several animal species, such as I_{Kp} in guinea pig heart, in rat atrial cells, and in neonatal canine ventricular myocytes. The equivalent current has not be described in human heart. On the other hand, two K^+ channel cDNAs Kv1.4 (HK1) and Kv1.5 (HK2) have been cloned from human heart and found to be expressed abundantly in human atrium. Expression of Kv1.4 results in a current resembling I_{to1}, while current expressed by Kv1.5, with rapid activating and non-inactivating properties, had not been found in native tissue.

Sustained Depolarization-Induced Outward Current in Human Atrial Myocytes

Evidence for a Novel Delayed Rectifier K^+ Current Similar to Kv1.5 Cloned Channel Currents

Zhiguo Wang, Bernard Fermini, Stanley Nattel

Depolarization of human atrial myocytes activates a transient outward current that rapidly inactivates, leaving a sustained outward current after continued depolarization. To evaluate the ionic mechanism underlying this sustained current (I_{ss}), we applied whole-cell voltage-clamp techniques to single myocytes isolated from right atrial specimens obtained from patients undergoing coronary bypass surgery. The magnitude of I_{ss} was constant for up to 10 seconds at +30 mV and was unaffected by 40 mmol/L tetraethylammonium, 100 nmol/L dendrotoxin, 1 mmol/L Ba^{2+}, 0.1 μmol/L atropine, or removal of Cl^- in the superfusate. I_{ss} could be distinguished from the 4-aminopyridine (4AP)–sensitive transient outward current (I_{to1}) by differences in voltage-dependent inactivation (1000-millisecond prepulse to −20 mV reduced I_{to1} by 91.7±0.1% [mean±SEM], $P<.001$, versus 9.4±0.4% reduction of I_{ss}) and 4AP sensitivity (IC_{50} for block of I_{to1}, 1.96 mmol/L; for I_{ss}, 49 μmol/L). I_{ss} activation had a voltage threshold near −30 mV, a half-activation voltage of −4.3 mV, and a slope factor of 8.0 mV. I_{ss} was not inactivated by 1000-millisecond prepulses but was reduced by 16±8% ($P<.05$) at a holding potential of −20 mV relative to values at a holding potential of −80 mV. I_{ss} activated very rapidly, with time constants (τ) at 25°C ranging from 18.2±1.8 to 2.1±0.2 milliseconds at −10 to +50 mV, two orders of magnitude faster than previously described kinetics of the rapid component of the delayed rectifier K^+ current. At 16°C, I_{ss} activation was greatly slowed (τ at +10 mV, 46.7±4.1 milliseconds; τ at 25°C, 7.1±0.8 milliseconds; $P<.01$), and the envelope of tails test was satisfied. The reversal potential of I_{ss} tail currents changed linearly with log $[K^+]_o$ (slope, 55.3±2.9 mV per decade), and the fully activated current-voltage relation showed substantial outward rectification. Selective inhibition of I_{ss} with 50 μmol/L 4AP increased human atrial action potential duration by 66±11% ($P<.01$). In conclusion, I_{ss} in human atrial myocytes is due to a very rapidly activating delayed rectifier K^+ current, which shows limited slow inactivation, is insensitive to tetraethylammonium, Ba^{2+}, and dendrotoxin, and is highly sensitive to 4AP. These properties resemble the characteristics of channels encoded by the Kv1.5 group of cardiac cDNAs and may represent a physiologically significant manifestation of such channels in human atrium. (*Circ Res.* 1993;73:1061-1076.)

KEY WORDS • K^+ currents • repolarization • arrhythmias, cardiac • electrocardiography • action potential

Action potential duration is a major determinant of the refractory period in cardiac tissue.[1,2] The likelihood of reentrant cardiac arrhythmias is greatly influenced by the properties of tissue refractoriness,[1,2] and action potential duration is therefore a major determinant of a number of clinically important arrhythmias. The duration of the cardiac action potential is governed by the balance between a variety of inward and outward currents that flow during the depolarized, and particularly the plateau, phase of the action potential.

Several outward K^+ currents have been identified in human atrial cardiomyocytes. The transient outward current (I_{to}) is prominent in human atrial myocytes.[3-5] I_{to} has two components, a longer-lasting one, which is sensitive to 4-aminopyridine (4AP), and a briefer Ca^{2+}-dependent component, which is blocked by caffeine or Co^{2+}.[3] These components have been identified in other systems and are commonly referred to as I_{to1} and I_{to2}, respectively.[6] Both I_{to1} and I_{to2} inactivate rapidly,[3,6] and both are likely to be fully inactivated before the onset of phase 3 repolarization at physiological temperatures in human atrial cells, which have an action potential duration at 37°C in the order of 300 milliseconds.[7] The inward rectifier current (I_{K1}) and acetylcholine-activated current (I_{KACh}) are present in human atrium, but both show strong inward rectification,[8,9] and basal I_{KACh} activity (in the absence of muscarinic agonists) is small.[9] When intracellular ATP is depleted, a substantial ATP-sensitive current (I_{KATP}) is recorded[9]; however, in the absence of ATP depletion, the open probability of I_{KATP} is low. The classic type of delayed rectifier current (I_K), as originally described by Noble and Tsien,[10] has been

Received January 21, 1993; accepted August 13, 1993.

From the Department of Medicine (B.F., S.N.), Montreal Heart Institute and University of Montreal, and the Department of Pharmacology and Therapeutics (Z.W., S.N.), McGill University, Montreal, Canada.

Correspondence to Dr Stanley Nattel, Montreal Heart Institute, 5000 Belanger Street East, Montreal, Quebec, Canada H1T 1C8.

considered to be minor or absent in human atrial cells. We have recently found, however, that typical delayed rectifier currents, with activation time constants in the range of 100 to 350 milliseconds at 37°C, can be recorded in the majority of human atrial cells.[11]

Several lines of evidence point toward the existence of another, potentially important, repolarizing current in human atrium. Depolarizing pulses positive to +20 mV are always associated with an instantaneous outward current "jump," even in cells that lack I_{to}.[11] After the inactivation of I_{to}, a residual outward current is seen,[3-5,11] even in cells lacking I_K.[11] Similar phenomena are observed in rabbit atrial myocytes, in which they are due to a background Cl^- current.[12] The purpose of the present experiments was to characterize the properties of the sustained depolarization-induced outward current (I_{sus}) in human atrial myocytes. The results suggest that this current is carried by an ultrarapidly activating delayed rectifier, which has many similarities to currents carried by channels identified by cDNA cloning from human[13-17] heart libraries.

Materials and Methods

Isolation of Single Atrial Cells

Specimens of human right atrial appendage were obtained from the hearts of 39 patients with ages ranging from 37 to 74 (61±1 [mean±SEM]) years undergoing aortocoronary bypass surgery. All patients had normal P waves on electrocardiography, and no patient had a history of supraventricular arrhythmias. All atrial specimens were grossly normal at the time of excision. On excision, the samples were immediately placed in oxygenated Tyrode's solution for transport to the laboratory. The time between excision and the beginning of laboratory processing was approximately 5 minutes. The procedure for obtaining the tissue was approved by the Ethics Committee of the Montreal Heart Institute.

The samples obtained were quickly immersed in nominally Ca^{2+}-free Tyrode's solution (100% O_2 at 37°C) of the following composition (mmol/L): NaCl, 126; KCl, 5.4; $MgCl_2$, 1; NaH_2PO_4, 0.33; dextrose, 10; and HEPES (Sigma Chemical Co, St Louis, Mo), 10; pH adjusted to 7.4 with NaOH. The cell isolation procedure was based on a technique described by Escande et al.[3] Myocardial specimens were chopped with scissors into cubic chunks (approximately 1 mm^3) and placed in a 25-mL flask containing 10 mL of the Ca^{2+}-free Tyrode's solution. The tissue was gently agitated by continuous bubbling with 100% O_2 and stirred with a magnetic bar. After an initial 5 minutes in this solution, the chunks were reincubated in a similar solution containing 390 U/mL collagenase (CLS II, Worthington Biochemical Corp, Freehold, NJ) and 4 U/mL protease (type XXIV, Sigma). The first supernatant was removed after 45 minutes and discarded. The chunks were then reincubated in a fresh enzyme-containing solution. Microscopic examination of the medium was performed every 15 minutes to determine the number and quality of the isolated cells. When the yield appeared to be maximal, the chunks were suspended in a solution of the following composition (mmol/L): KCl, 20; KH_2PO_4, 10; glucose, 10; glutamic acid, 70; β-hydroxybutyric acid, 10; taurine, 10; EGTA, 10; and albumin 1%; pH adjusted to 7.4 with KOH. Then the solution was gently pipetted.

Only quiescent rod-shaped cells showing clear cross striations were used. A small aliquot of the solution containing the isolated cells was placed in a 1-mL chamber mounted on the stage of an inverted microscope. Five minutes was allowed for cell adhesion to the bottom of the chamber, and then the cells were superfused at 3 mL/min with a solution containing (mmol/L) NaCl, 126; KCl, 5.4; $MgCl_2$, 0.8; $CaCl_2$, 1; NaH_2PO_4, 0.33; HEPES, 10; and glucose, 5.5; pH adjusted to 7.4 with NaOH. In some experiments, the composition of the Tyrode's solution was modified as specified. Experiments were conducted at room temperature (approximately 25°C), at 16°C, or at 36°C. The higher temperature (36°C) was maintained by a thermostatically controlled heating element (N.B. Datyner, Stony Brook, NY); the lower temperature (16°C) was obtained and maintained with a Pelletier-effect device (N.B. Datyner).

Data Acquisition and Analysis

The whole-cell patch-clamp technique was used to record ionic currents and action potentials in the voltage- and current-clamp mode, respectively. Borosilicate glass electrodes (outer diameter, 1.0 mm) were used, with tip resistances of 2.5 to 4 MΩ (3.1±0.5 MΩ, n=100) when filled with (mM) potassium aspartate, 110; KCl, 20; $MgCl_2$, 1; HEPES, 10; EGTA, 5; Mg_2-ATP, 5; and Na_2-creatine phosphate, 5 (pH adjusted to 7.4 with KOH). The electrodes were connected to a patch-clamp amplifier (Axopatch 1-D, Axon Instruments, Foster City, Calif). The reference electrode was in contact with the bath solution via a 3-mol/L KCl-agar bridge to minimize changes in junction potentials after changing the electrolyte content of bath solutions. Command pulses were generated by a 12-bit digital-to-analog converter controlled by pCLAMP software (Axon Instruments). Recordings were low-pass-filtered at 1 kHz, and data were acquired by analog-to-digital conversion (model TM 125, Scientific Solutions, Solon, Ohio) and stored on the hard disk of an IBM AT-compatible computer. The maximum sampling rate possible was 100 kHz, but because a maximum of 2048 points can be obtained with pCLAMP for each data record, acquisition rates in the present experiments varied from just over 20 kHz (for 100-millisecond data sets) to 0.2 kHz (for 10-second data sets). In some experiments (eg, when current activation was studied), a dual clock option available in pCLAMP was used to allow for sampling of the initial 40 milliseconds of data at 25 kHz, with slower sampling for the remainder of the data set. A nonlinear least-squares curve-fitting program using the Marquardt procedure (CLAMPFIT in pCLAMP) was used to fit current activation and deactivation to single exponential functions.

In all of the cells studied, junction potentials (4 to 17 mV) were zeroed before formation of the membrane-pipette seal in 1 mmol/L Ca^{2+} Tyrode's solution. Mean seal resistance as recorded in 34 cells averaged 44.1±5.7 GΩ, and seals with resistances of <10 GΩ were rejected. Several minutes after seal formation, the membrane was ruptured by gentle suction to establish the whole-cell configuration for voltage clamping. The series resistance was electrically compensated to minimize

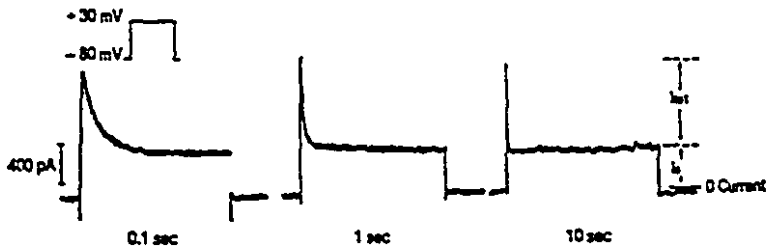

FIG 1. Recordings of depolarization-induced transient outward current (I_{to1}) from a representative myocyte. Currents were elicited by depolarization to +30 mV for 0.1 second (left tracing), 1 second (middle tracing), and 10 seconds (right tracing) from a holding potential of −80 mV at room temperature. A sustained outward current (I_s) remains after complete inactivation of I_{to1}. Note that this current stays constant to the end of the pulse even with prolonged depolarization. The method used to measure I_{to1} and I_s is shown at the right. Similar results were obtained from the eight other cells studied.

the duration of the capacitive surge on the current recording and the voltage drop produced across the clamped cell membrane. Typically, over 60% series resistance compensation was achieved. The series resistance along the clamp circuit was estimated by dividing the time constant obtained by fitting the decay of the capacitive transient by the calculated cell membrane capacitance (the time integral of the capacitive surge measured in response to 5-mV hyperpolarizing steps from a holding potential of −60 mV).[18,19] Before series resistance compensation, the decay of the capacitive surge was expressed by a single exponential having a time constant of 402±50 microseconds (cell capacitance, 74.3±7.6 pF; n=34). After compensation, this value was reduced to 127±7 microseconds (cell capacitance, 66.1±3.3 pF). The initial series resistance was 5.4±1.4 MΩ and was reduced to 1.9±0.5 MΩ after compensation. Currents recorded during this study rarely exceeded 1.5 nA, and maximum total I_{ss} after I_{to} inactivation was <800 pA. The voltage drop across series resistance therefore did not exceed 3 mV. Cells with significant leak currents at −60 mV were rejected. Residual leak currents were compensated when present by subtracting a current linearly scaled and opposite in polarity to the current response to a sequence of 5-mV hyperpolarizing pulses from −60 mV, through the use of software routines incorporated in pCLAMP. To assess the linearity of leakage currents carried by ions other than K^+, we studied 10 cells dialyzed with pipettes containing Cs^+ in place of K^+. In the absence of any compensation, leakage currents were linear and reversed at 0 mV. Although I_{K1} can provide a substantial nonlinear leakage current, we and others have found that I_{K1} is relatively small in human atrial cells, and I_{K1} was suppressed by adding 1 mmol/L $BaCl_2$ to the superfusate in experiments characterizing I_{ss}, after verifying that I_{ss} was not altered by the addition of Ba^{2+} as described below. In addition, in some experiments, leak currents were minimal, and no correction for leakage was performed. Results from these experiments were the same as from those in which leakage correction was applied.

The length of single cells ranged from 60 to 115 μm (88.0±6.1 μm, n=14), and the diameter ranged from 5 to 11 μm (9.2±0.6 μm): the estimated cell surface area was therefore $2.7\pm0.3\times10^{-5}$ cm^2 on the basis of assumed right cylinder geometry. The input resistance was determined by the application of four consecutive 5-mV hyperpolarizing steps from a holding potential (HP) of −60 mV. Since no time-dependent current was activated with these small steps, the resulting change in current was used to calculate input resistance.[21] Mean input resistance as estimated in 10 cells was 1.9±0.1 GΩ. The resting space constant was calculated on the basis of the following equation[20]: $sc=\sqrt{(r\cdot R_m/2R_i)}$, where sc is the space constant, r is the cell radius, R_m is specific membrane resistance, and R_i is internal resistivity. R_m was estimated from the product of input resistance and surface area, providing a mean value of 50.1±4.9 KΩ·cm^2, and R_i was assumed to be 100 to 200 Ω·cm.[20-23] The mean resting sc is 3.4±0.3 mm when R_i is 100 Ω·cm and 2.4±0.2 mm when R_i is 200 Ω·cm. Both values are over 25 times the cell length. During maximum current flow, the corresponding sc estimates become 620 and 880 μm, in the range of 10 times the cell length. These may be underestimates, since membrane infolding results in a true surface area larger than that of a right cylinder. The surface area estimated on the basis of a specific capacitance of 1 μF/cm^2 is about twice as large as the value given above, in agreement with histological studies of the cell surface in rabbit atrium.[24]

The amplitude of peak I_{to1} was measured as the difference between the peak transient outward current and the sustained current level at the end of the pulse (Fig 1). When I_{to1} was present, I_{ss} was measured as the amplitude of the current remaining at the end of the test pulse relative to the zero current level. When I_{ss} was studied in the absence of I_{to1} (through the use of inactivating prepulses or selective inhibition with 4AP), I_{ss} was measured as the maximal outward current level. Concentration-dependent effects of 4AP (Sigma) on both I_{ss} and I_{to1} were evaluated with a series of concentrations of 4AP ranging from 10^{-6} to 10^{-2} mol/L. 4AP was prepared as a 1 mol/L stock solution in distilled water, with pH adjusted to 7.4 with the addition of HCl. Small quantities of the stock solution were added to the superfusate to produce the desired 4AP concentration.

The following chemicals were used to block potential contaminating currents: tetraethylammonium chloride (TEA, 10 mmol/L, Sigma, to inhibit I_K[11,25]), $BaCl_2$ (1 mmol/L, Sigma, to inhibit I_{K1}), and atropine (0.1 μmol/L, Sigma, to inhibit $I_{K,ACh}$ and choline-activated K^+ current[26]). $CoCl_2$ (2 mmol/L, Sigma) was used to block Ca^{2+} current and I_{to2} in all experiments except for those involving action potential recordings. In experiments studying the ionic selectivity of I_{ss}, $[K^+]_o$ was varied, with equivalent and opposite changes in the concentra-

tion of Na^+ or choline to maintain constant osmolarity and ionic strength. 4,4'-Diisothiocyanatostilbene-2,2'-disulfonic acid (DIDS, 150 μmol/L, Sigma) was used to inhibit Cl^- current, and all DIDS-containing solutions were protected from direct light. Dendrotoxin (α-dendrotoxin) was purchased from Alomone Labs, Jerusalem, Israel. Na^+ current was minimized by equimolar replacement of NaCl in the superfusate by choline chloride (126 mmol/L, Sigma) or by an HP positive to −50 mV.

To explore the possible role of I_{ss} in membrane repolarization, action potentials were recorded in the current-clamp mode at 36°C in normal Tyrode's solution free of channel blockers. Action potentials were evoked by clamping the membrane at −80 mV (normal resting potential of human atrial tissue[7]) and then delivering a train of 3-millisecond suprathreshold stimuli at a frequency of 1 Hz. Changes in the time course of repolarization were assessed by measuring the action potential duration to 20%, 50%, and 90% of repolarization.

Statistical Analysis

Comparisons among multiple groups were performed by ANOVA with Scheffé contrasts.[27] Baseline and drug data were compared by Student's *t* test, and two-tailed $P<.05$ was taken to indicate statistical significance. Group data are presented as mean±SEM. For analysis of current kinetics, data points were fitted by CLAMPFIT in pCLAMP. For other curve-fitting procedures, a nonlinear curve-fitting technique (Marquardt's procedure) was performed using TABLECURVE software (Jandel Scientific).

Results

Distinction of I_{ss} From Other Outward Currents

We initially sought to determine whether I_{ss} could be explained by the properties of a variety of known outward currents. The first possibility considered was that a slowly inactivating component of I_{to1} underlies I_{ss}. Fig 1 shows current tracings elicited by voltage steps of various durations to +30 mV from an HP of −80 mV at room temperature. On depolarization, I_{to1} activates rapidly and then decays quickly to a steady-state level. The inactivation of I_{to1} was fit by a single exponential process with a time constant averaging 55±2 milliseconds at 25°C. The average amplitude of I_{ss} was independent of pulse duration, averaging 408±59 pA for 0.1-second pulses, 406±61 pA for 1-second pulses, and 392±58 pA for 10-second pulses (P=NS, n=6). These results indicate that I_{ss} cannot be due to slow inactivation of I_{to1} unless the inactivation time constant is in the order of hundreds of seconds.

A second possibility is that I_{ss} represents an I_{to1} window current. To evaluate this, we determined the voltage dependence of I_{to1} activation and inactivation. Voltage dependence of inactivation was evaluated in 10 myocytes with the two-pulse protocol shown in Fig 2A. Activation was analyzed in two ways: (1) on the basis of tail currents on repolarization to −40 mV after a 5-millisecond pulse to a range of test potentials (six cells, Fig 2B), and (2) on the basis of peak currents at a variety of test potentials, assuming a reversal potential of −80 mV (seven cells). Preliminary experiments showed that no I_{to} was elicited by test pulses to potentials negative to −40 mV. Mean activation and inactivation curves from all experiments are shown in Fig 2C. Crossover between activation and inactivation curves occurs at −20 mV with a value of 0.07, indicating that the maximum I_{to1} window current expected would be ≤7% of fully available I_{to1} at −20 mV, or approximately 2.5 pA. Positive to 0 mV, I_{to1} is fully inactivated, while I_{ss} becomes increasingly larger (see Fig 8). Thus, the substantial sustained current present on maintained depolarization of human atrial myocytes cannot be explained on the basis of a slowly inactivating or window component of I_{to1}.

We then turned our attention to the possible role of the inwardly rectifying currents I_{K1} and I_{KACh}. The addition of 1 mmol/L Ba^{2+} to the superfusate reduced the inward current elicited by hyperpolarization from −80 to −140 mV by 92±13% ($P<.001$, n=3). However, I_{ss} observed on depolarization from −80 to +30 mV was not altered by Ba^{2+} (301±55 pA before and 286±56 pA after Ba^{2+}, n=4, P=NS). Similarly, the addition of 0.1 μmol/L atropine did not affect I_{ss} (361±28 pA before and 358±30 pA after atropine, n=3, P=NS).

To exclude a contribution of the classic type of I_K[10,11] to the I_{ss} under study, we selected cells lacking a slowly activating current and a tail current of >50 pA on return to an HP of −30 mV after ≥1 second at +30 mV. We have previously shown that 10 mmol/L TEA reduces the classic type of I_K activated by a 300-millisecond pulse from −70 to +20 mV by a mean of 76% in human atrial myocytes.[28] Twenty minutes of exposure did not alter I_{ss} at any test voltage, with either 10 mmol/L (mean change at +30 mV, −2.4±0.8%, three cells, P=NS) or 40 mmol/L (−5.6±2.9%, four cells, P=NS) TEA. After showing that I_{ss} is manifest in the absence of I_K, I_{K1}, and I_{KACh}, we elected to add TEA (10 mmol/L), BaCl (1 mmol/L), and atropine (0.1 μmol/L) to all solutions, unless otherwise indicated, to avoid contamination by these currents.

The above experiments indicate that a sustained depolarization-induced outward current exists in human atrial myocytes independent of I_{to1}, I_{K1}, I_{KACh}, and I_K. Since 2 mmol/L Co^{2+} was present in the superfusate for all the above experiments, I_{ss} is manifest under conditions in which I_{to2} is fully suppressed.[3] In rabbit atrium, a depolarization-induced I_{ss} is carried by Cl^- ions and is inhibited by the Cl^- transport blocker DIDS (150 μmol/L) or by substitution of methanesulfonate for extracellular Cl^-.[12] Fig 3 shows the effect of Cl^- substitution and DIDS on I_{ss}. Complete replacement of superfusate Cl^- by methanesulfonate (Fig 3A) did not alter I_{ss} in four cells, with I_{ss} at +30 mV averaging 292±51 pA before and 298±68 pA after Cl^- replacement (P=NS). DIDS (Fig 3B) had a small and variable effect, with I_{ss} decreasing slightly after exposure to 150 μmol/L DIDS in four cells and increasing slightly in three. Overall, I_{ss} at +30 mV averaged 332±69 pA before and 277±61 pA after DIDS (n=7, P=NS), and DIDS did not significantly alter I_{ss} at any test voltage.

These results suggest that I_{ss} is neither a Cl^- current nor one of the well-characterized K^+ currents evaluated above. Two lines of evidence suggested that I_{ss} is a K^+ current. First, we found I_{ss} to be exquisitely sensitive to the K^+ channel blocker 4AP. As shown in Fig 4A, 50 μmol/L 4AP substantially reduced I_{ss} without affecting the inactivating component of I_{to1}. Second, replacement

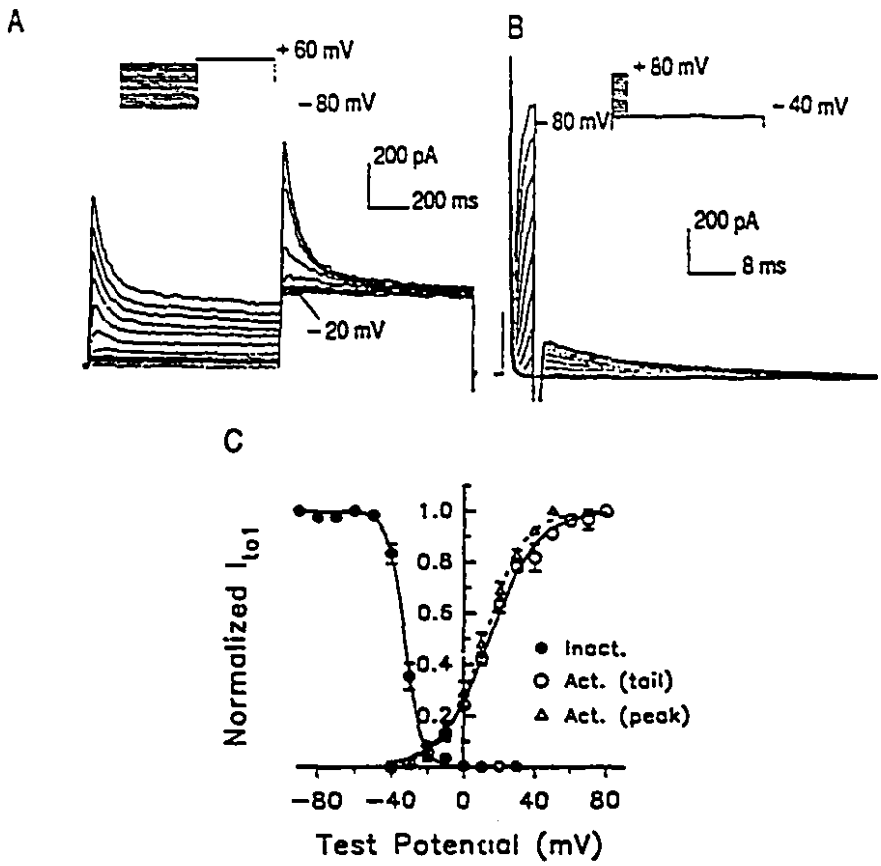

FIG 2. Recordings (A and B) and graph (C) showing voltage-dependent activation and inactivation of transient outward current (I_{to1}). A, Voltage-dependent inactivation was assessed with the use of a two-pulse protocol, with a 1000-millisecond prepulse to voltages between −80 and +40 mV, followed by a 1000-millisecond test pulse to +60 mV. Note that prepulses positive to −20 mV are associated with a very high degree of inactivation. B, Voltage-dependent activation as assessed by the tail current at −40 mV after 5-millisecond depolarizations to a variety of test potentials is shown. C, Mean data for voltage dependence of inactivation (Inact.) and activation (Act.) was assessed in 10 and 6 cells, respectively, using the protocols shown in A (●) and B (○). Results are also shown (△) for voltage dependence of activation as determined from peak current during 1000-millisecond depolarizing pulses from a holding potential of −80 mV to various test potentials, assuming a reversal potential of −80 mV (n=7 cells). The curves shown are fits of mean data to Boltzmann distribution equations (for general form of equation, see text).

of intracellular K^+ by dialysis with Cs^+ eliminated I_{ss}. Fig 4B shows a typical I_{to} decaying to a sustained level elicited by a depolarizing clamp step immediately after membrane rupture with a pipette containing 130 mmol/L Cs^+ (CsCl) in place of K^+. The outward current elicited by depolarization decreased progressively over time, until an identical clamp step 2 minutes after membrane rupture did not elicit any outward current, as shown in Fig 4B. Similar results were obtained in six cells studied with Cs^+-containing pipettes and were never observed in cells studied with standard K^+-containing electrodes. This finding is in marked contrast to our observations in rabbit atrial myocytes, in which a substantial and apparently unaltered I_{ss} is elicited by depolarizations positive to the Cl^- equilibrium potential following the replacement of K^+ by Cs^+ in both the pipette solution and the superfusate.[12]

Sensitivity of I_{ss} and I_{to1} to Block by 4AP

The most important obstacle in discerning the properties of I_{ss} is its separation from I_{to1}. Like the latter current, I_{ss} is carried by K^+ ions, is blocked by 4AP, and is relatively insensitive to the actions of other channel-blocking drugs that we tested. The much greater sensitivity of I_{ss} to blockade by 4AP compared with I_{to1} indicated the possibility of using 4AP as a tool to separate the currents. Fig 5 shows the results of concentration-response analysis of the effects of 4AP on I_{ss} and I_{to1}. Currents were elicited both by 200-millisecond depolarizations (1 Hz) from −80 mV to +30 mV and by a train of ten 200-millisecond pulses (from −80 to +30 mV) followed by a single 2-second test pulse. The latter protocol was used to ensure full inactivation of I_{to1} by the end of the test pulse; the former was used to ensure steady-state effects at a frequency of 1 Hz. Similar results were obtained with either protocol. After baseline measurements had been obtained, 4AP (10^{-4} to 10^{-2} mol/L) was superfused for 5 minutes, and the measurements were repeated. Fig 5A shows recordings from a representative cell. 4AP (50 μmol/L) reduced I_{ss} by approximately 50%, without affecting I_{to1}. When the 4AP concentration was increased to 2 mmol/L, I_{ss} was completely suppressed, and I_{to1} was reduced by approximately 50%. Fig 5B shows mean concentration-response data for 4AP inhibition of I_{ss} and I_{to1} in seven cells. The symbols represent experimental data, and the solid lines are the best-fit curves according to the equation provided in Fig 5B. The dashed vertical lines indicate IC_{50} values for I_{ss} and I_{to1}. Appreciable effects of 4AP on I_{ss} occurred at concentrations as low as 10

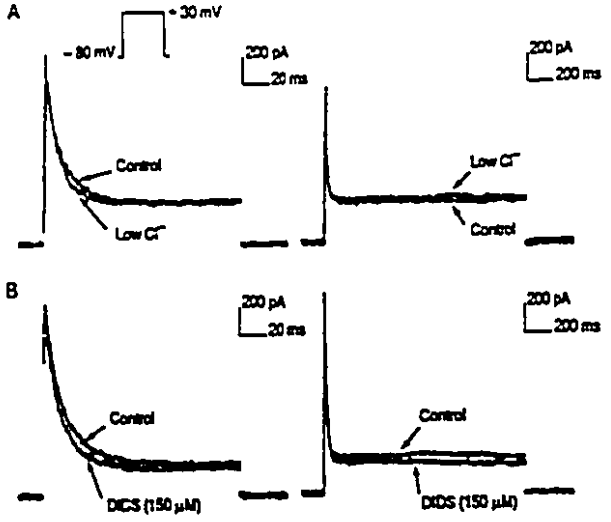

FIG 3. Tracings showing effects of Cl^- replacement and Cl^- transport blockers on sustained outward current elicited by 200-millisecond (left) or 2000-millisecond (right) pulses from −80 to +30 mV in representative cells. A, Results of replacement of Cl^- by methanesulfonate in the perfusate are shown. B, Results of exposure to the organic Cl^- transport blocker 4,4'-diisothiocyanatostilbene-2,2'-disulfonic acid (DIDS, 150 μm) are shown.

μmol/L, and the IC_{50} for I_{ss} was 49 μmol/L, a concentration at which I_{to1} was unaffected. I_{ss} was completely suppressed by 750 μmol/L 4AP, which reduced I_{to1} by only 25%. The IC_{50} for I_{to1} was 1.96 mmol/L, 40-fold higher than that for I_{ss}, and full suppression of I_{to1} was not achieved until a 4AP concentration of 10 mmol/L. Calculated values of the Hill coefficient were 1.45 for I_{ss} and 1.95 for I_{to1}.

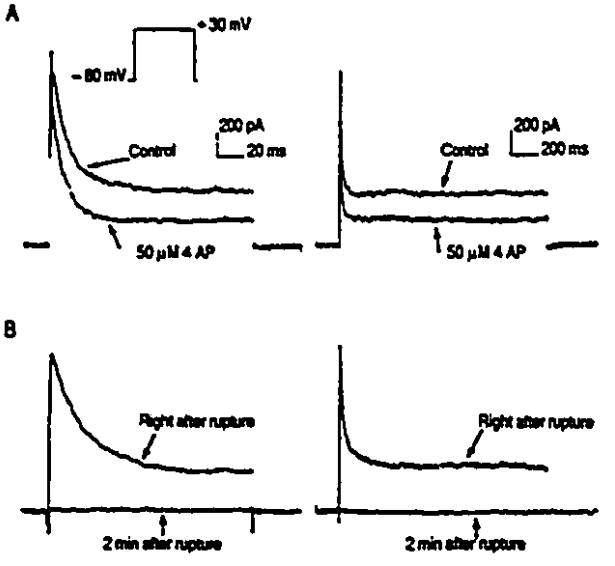

FIG 4. Tracings showing the effects of 4-aminopyridine (4AP) and intracellular dialysis with Cs^+ on sustained outward current elicited by 200-millisecond (left) or 2000-millisecond (right) pulses from −80 to +30 mV in representative cells. A, Results before (control) and after 5-minute exposure to 50 μmol/L 4AP are shown. B, Currents tracings are shown that were recorded immediately on membrane rupture and 2 minutes later, with a micropipette containing 130 mmol/L Cs^+ (CsCl) in place of K^+.

Separation of I_{ss} From I_{to1}

Since 50 μmol/L 4AP blocks I_{ss} by over 50% without affecting I_{to1}, the 50 μmol/L 4AP–sensitive component should consist solely of I_{ss}. Fig 6 shows typical current recordings at 25°C (top) and 36°C (in a different cell, bottom) on depolarization for 100 milliseconds from −50 mV to various test potentials before (left) and after (middle) exposure to 50 μmol/L 4AP. The subtracted current (right) at 25°C reveals a time-dependent current with an activation time constant ranging in the example shown from 13.4 milliseconds at +10 mV to 2.5 milliseconds at +50 mV. At 36°C, the subtracted current appears instantaneous, with small initial fluctuations due to intrinsic variation in early, very large peak I_{to1} currents. Similar results were obtained in five other cells, suggesting that I_{ss} is a very rapidly activating current of the delayed rectifier type.

The use of subtracted currents to analyze I_{ss} presents a number of difficulties, including the possibilities of voltage- and time-dependent block of I_{ss} by 4AP, which could distort the results obtained, and contamination by leakage currents. Therefore, we attempted to exploit the voltage-dependent inactivation properties of I_{to1}[3-6] to suppress I_{to1} under the conditions necessary to record I_{ss}.

Fig 7A shows the effect of 1000-millisecond conditioning pulses to various voltages in 10 cells on the amplitude of I_{to1} elicited by a subsequent test pulse to +40 mV. At a conditioning potential of −20 mV, I_{to1} was 91.7±0.1% inactivated, and full inactivation occurred at +10 mV. I_{ss}, on the other hand, was not significantly altered by depolarizing prepulses. Fig 7B shows the effect of a 200-millisecond prepulse from an HP of −60 to +40 mV on the amplitude of I_{to1} and I_{ss} during an identical test pulse delivered between 1 and 36 milliseconds later (n=5). Although I_{ss} was not significantly affected by the prepulse, I_{to1} of the test pulse at all coupling intervals was <10% of the value during the prepulse. The data shown in Fig 7A and 7B, recorded at room temperature, indicate that I_{to1} is over 90% inactivated at a potential of −20 mV and is fully inactivated by pulses positive to +10 mV and that there is <10% recovery of I_{to1} at −60 mV up to 36 milliseconds after a depolarization to +40 mV. Therefore, we estimated that I_{to1} should be over 99% inactivated when a test pulse from an HP of −20 mV is applied 10 milliseconds after a 200-millisecond prepulse to +40 mV. We were, in fact, unable to detect any transient outward current over the activation voltage range of I_{to1} for test pulses applied under the conditions just described.

Fig 7C shows currents recorded at 25°C when a 40-millisecond test pulse from −20 mV to various potentials is applied 10 milliseconds after a 200-millisecond conditioning pulse to +40 mV. The current activates rapidly, with an activation time constant averaging 2.1±0.2 milliseconds (n=14 cells) at +50 mV. The rate of activation was voltage dependent, with the activation time constant increasing to 18.2±1.8 milliseconds at −10 mV. Results of the same pulse protocol in the same cell at 36°C are shown in Fig 7D. Current amplitudes were not substantially altered by the higher temperature, but activation was

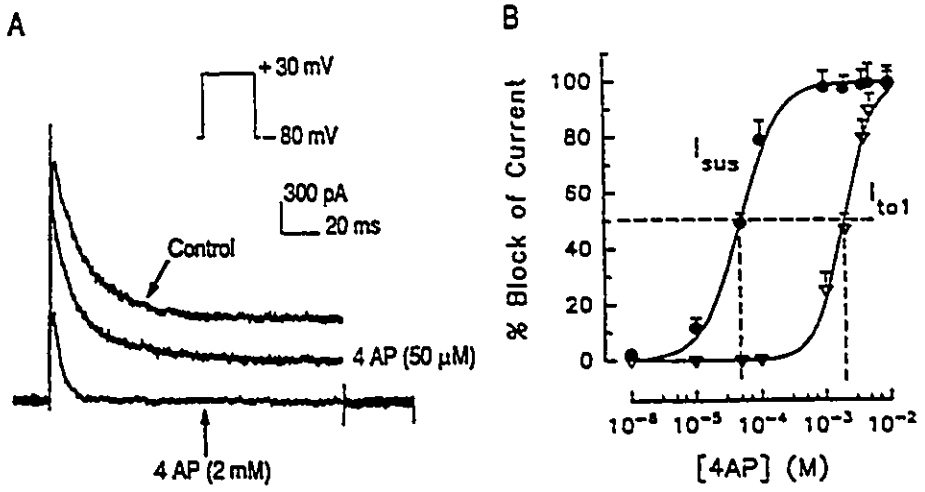

FIG 5. Concentration-dependent effects of 4-aminopyridine (4AP) on sustained outward current (I_{sus}) and 4AP-sensitive transient outward current (I_{to1}). Currents are evoked by 200-millisecond pulses from −30 to +30 mV at 1 Hz. A, Results are shown from a representative experiment. Currents were recorded under control conditions and with 4AP concentrations of 5×10^{-6} mol/L (50 μmol/L) and 2×10^{-3} mol/L (2 mmol/L). B, Dose-response curves are shown. Mean percent reduction in current amplitude from seven cells is plotted as function of logarithm of 4AP concentration. Symbols represent experimental data; solid lines, the best fit to the following equation: $B(\%)=100/[1+(IC_{50}/D)^n]$, where B(%) is the percent current block at a drug concentration D, IC_{50} is the concentration of 4AP that causes 50% block, and n is the Hill coefficient. Dashed lines indicate IC_{50} values for I_{sus} (4.9×10^{-6} mol/L) and I_{to1} (1.9×10^{-3} mol/L).

greatly accelerated and could not be separated from the capacitance decay. Exposure to 50 μmol/L 4AP reduced the currents recorded at 25°C by approximately 50% without appreciatively altering their kinetics (Fig 7E), and 2 mmol/L 4AP completely suppressed the time-dependent current (Fig 7F).

Characterization of I_{sus}: Current-Voltage Relation and Activation Curve

To characterize the current-voltage (I-V) relation and steady-state activation properties of I_{sus}, we used two different protocols. The first is illustrated in Fig 8A and consists of a 1000-millisecond prepulse from an HP

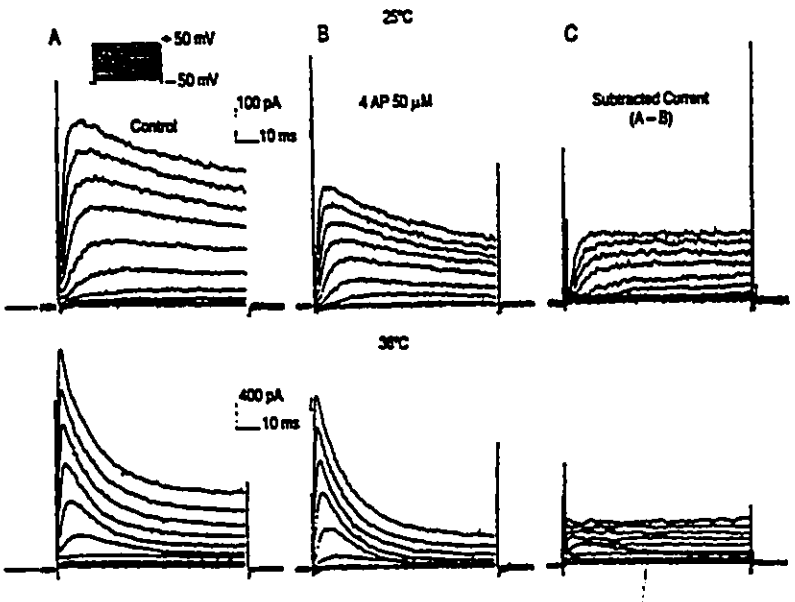

FIG 6. Tracings showing separation of sustained outward current (I_{sus}) from 4-aminopyridine (4AP)–sensitive transient outward current (I_{to1}) with the use of 4AP. Currents were elicited at various test potentials (from −40 to +50 mV) from a holding potential of −50 mV at 1 Hz and room temperature (top) or 36°C (bottom). The zero current level is shown by the horizontal lines at the left. Five minutes of exposure of cells to 50 μmol/L 4AP causes approximately 50% reduction of I_{sus} without altering I_{to1} (B) as compared with baseline currents (A). C shows the current suppressed by 4AP, as obtained by digital subtraction of the current in the presence of 4AP from the current in its absence. Note the initial time-dependent activation of 4AP-sensitive current at room temperature and the lack of detectable time-dependent activation at 36°C.

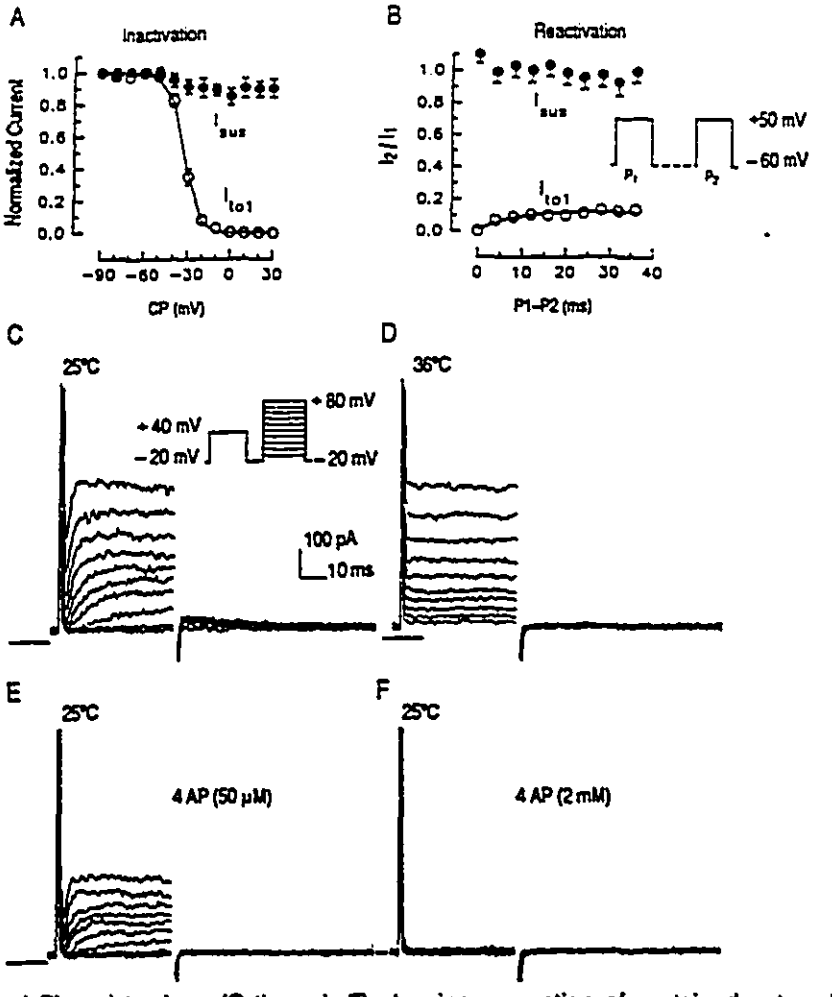

FIG 7. Graphs (A and B) and tracings (C through F) showing separation of sustained outward current (I_{sus}) and 4-aminopyridine (4AP)–sensitive transient outward current (I_{to1}) by voltage protocols. A, Voltage-dependent inactivation of I_{sus} and I_{to1} at room temperature is shown. I_{to1} (○) is measured from the peak current, and I_{sus} (●) is measured from the steady-state current at the end of a 2000-millisecond test pulse at +40 mV preceded by a 1000-millisecond conditioning pulse (CP) at various potentials delivered from a holding potential of −60 mV. Current amplitude is normalized to the maximum value obtained with a conditioning voltage of −90 mV. Over 90% of the I_{to1} is inactivated at voltages positive to −20 mV, whereas I_{sus} is reduced by <10%. B, Reactivation of I_{sus} and I_{to1} at room temperature is shown. The reactivation process was assessed by a paired-pulse protocol consisting of two identical pulses (P1 and P2) from a holding potential of −60 to +40 mV for 200 milliseconds, at a variety of P1-P2 intervals. The ratio of current elicited by P2 to that of P1 (I_2/I_1) is plotted as a function of the P1-P2 interval. Less than 10% of I_{to1} was recovered at a coupling interval up to 36 milliseconds, whereas I_{sus} of P2 was not significantly different from I_{sus} of P1 at any P1-P2 interval. C, A typical example of I_{sus} elicited by depolarizing pulses (1 Hz) to voltages between −10 and +80 mV from a holding potential of −20 mV is shown in the presence of a prepulse to inactivate I_{to1}. The 200-millisecond prepulse to +40 mV preceded the test by 10 milliseconds. The instantaneous current "jump" before time-dependent activation of I_{sus} is likely due to residual I_{sus} activation from the prior conditioning pulse. D, I_{sus} was recorded at 36°C with the same protocol in the same cell as shown in panel C. Activation kinetics cannot be resolved, presumably because of acceleration at the higher temperature, but overall current amplitude is not significantly altered. E and F, 4AP sensitivity of I_{sus} at room temperature is shown. 4AP (50 μmol/L) produces approximately 50% reduction of I_{sus} as recorded (E) in the same cell with the same protocol as in C, and 2 mmol/L 4AP totally suppresses the current (F).

of −50 to +50 mV to inactivate I_{to1}, followed 20 milliseconds later by a 100-millisecond test pulse to a variety of test potentials, followed by a 100-millisecond clamp to −10 mV (to evaluate tail currents). Experiments were conducted at room temperature, and I_{ss} was measured from the maximum current level following activation. The second protocol, illustrated in Fig 8B, consisted of 2000-millisecond depolarizations from an HP of −60 mV to various test potentials between −40 and +50 mV, with I_{ss} measured from the sustained current as indicated in Fig 1.

The I-V relation obtained in six cells studied with the protocol illustrated in Fig 8A is shown in Fig 8C. The current is evident at potentials positive to −30 mV and appears to show outward rectification. Measurement of I_{ss} in a separate group of cells with the

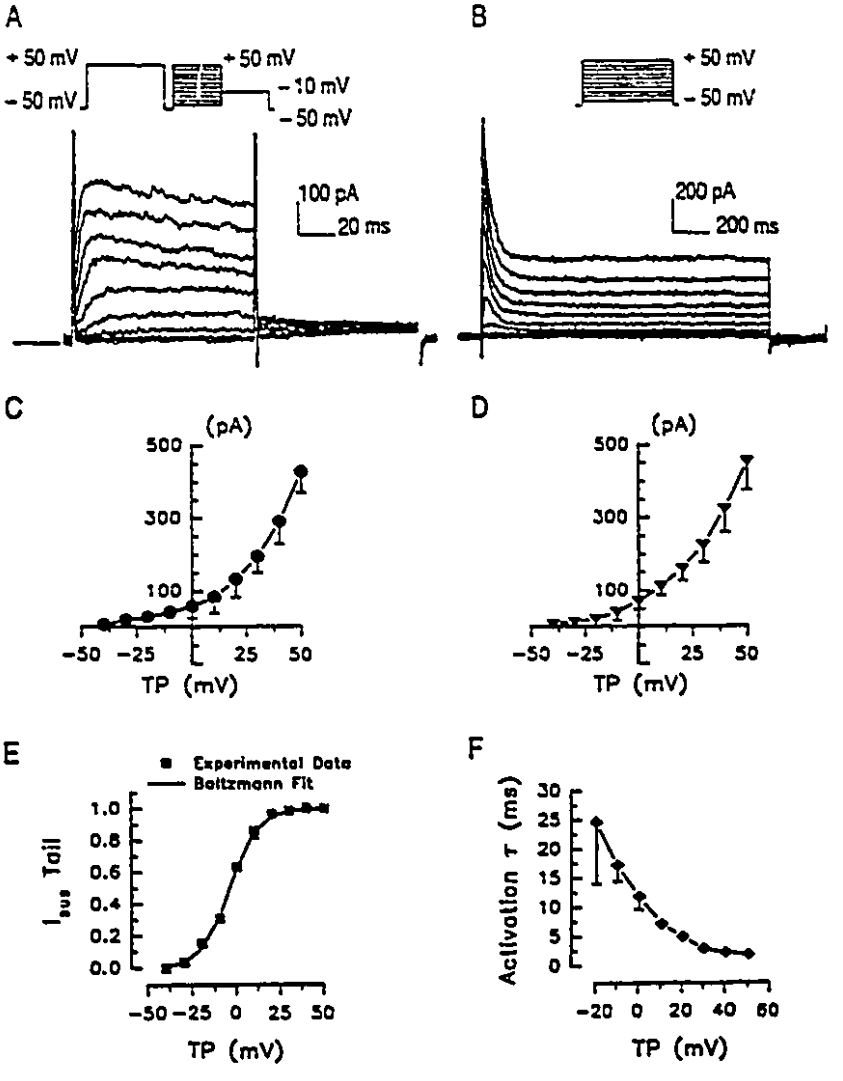

FIG 8. Tracings (A and B) and graphs (C through F) showing the current-voltage relation of sustained outward current (I_{sus}). A, Representative current tracings evoked at room temperature are shown. I_{sus} was obtained by depolarizing the membrane for 100 milliseconds to test potentials (TPs) ranging from −40 to +80 mV from a holding potential of −50 mV, then repolarizing to −10 mV at a frequency of 0.1 Hz. A 1-second prepulse was introduced 20 milliseconds before each test pulse to inactivate the 4-aminopyridine–sensitive transient outward current (I_{to1}). (Horizontal line indicates 0 current.) B, Representative current tracings were elicited by 1000-millisecond depolarizing test pulses at 25°C. Both I_{to1} and I_{sus} were elicited and measured as shown in Fig 1. C, Current-voltage curve of I_{sus} was recorded with the voltage protocol shown in A (mean data from six cells). D, Current-voltage relation for I_{sus} was measured as the current recorded at the end of the 1000-millisecond pulse with the protocol shown in B (mean data from four cells). E, Steady-state activation curve of I_{sus}, as determined from analysis of tail currents at −10 mV, was obtained with the protocol shown in A. Symbols are experimental data normalized to tail current after depolarization to +50 mV, and the line is the best-fit Boltzmann distribution (half-activation voltage, −4.3 mV; slope, 8.0 mV). F, Time course of activation of I_{sus}, as obtained with the voltage protocols shown in A (mean±SEM, n=8). τ indicates the time constant.

protocol shown in Fig 8B resulted in the I-V relation illustrated in Fig 8D (n=4). These data strongly resemble the results (Fig 8C) obtained with the protocol shown in Fig 8A.

The steady-state activation curve of I_{sus} was constructed from data obtained with the protocol in Fig 8A by plotting I_{sus} tail current (normalized to the maximum current) as a function of test potential (Fig 8E). These data were well described by a single Boltzmann distribution: $I(V)=1/\{1+\exp[(V-V_{1/2})/k]\}$, where I(V) is the normalized current as a function of the test potential V, $V_{1/2}$ is the voltage at which 50% of the channels are activated, and k is a slope factor. The best fit (r=.998) to the experimental data was obtained with $V_{1/2}=-4.3$ mV and k=8.0 mV.

Activation and Deactivation Kinetics

The activation kinetics of I_{sus} were determined from the type of data shown in Figs 7C and 8A. Fig 8F shows the activation time constants obtained from nine cells by exponential curve fitting of the activation time course as a function of test potential. The activation time constant is voltage dependent, decreasing from 17.7±2.8 milliseconds at −10 mV to 1.9±0.2 milliseconds at +50 mV. The kinetics of I_{sus} tail currents were determined by repolarizing from a conditioning potential of +60 mV to a variety of test potentials in six cells. Outward tail currents were very small negative to −30 mV, and at potentials positive to −30 mV, there is steady-state activation (Fig 8E), making it impossible to study deactivation kinetics independent of activation changes. At −20 mV, at which there is <20% I_{sus} activation, the time constant of the I_{sus} tail current averaged 13±3 milliseconds.

Inactivation Properties

I_{sus} demonstrated no significant voltage-dependent inactivation during 1000-millisecond conditioning pre-

pulses to between −60 and +40 mV. However, this does not necessarily exclude slow inactivation that fails to develop perceptibly during a 1000-millisecond conditioning pulse. Therefore, we evaluated I_{sus} amplitude in eight cells held at −80, −50, and −20 mV and pulsed to +40 mV at a frequency of 0.2 Hz. I_{sus} averaged 509±72 pA at an HP of −80 mV, 468±68 pA at −50 mV, and 411±59 pA at −20 mV. Holding at −50 mV reduced I_{sus} by 7±5% (P=NS) relative to values at −80 mV, whereas holding at −20 mV reduced I_{sus} by 16±8% (P<.05) relative to values at −80 mV. Thus, I_{sus} showed slight but statistically significant voltage-dependent inactivation over the range from −80 to −20 mV.

Time-dependent inactivation was seen in 33 (46%) of 72 cells during strong depolarizations (positive to +40 mV). In 13 of 27 cells studied with 2-second depolarizing pulses that showed inactivation, I_{sus} was reduced by an average of 19±2% (P<.001) over 2000 milliseconds at +60 mV. The time course of inactivation was very slow, and steady state was not achieved by the end of the pulse.

K^+ Selectivity of I_{sus} and Rectification Properties

Fig 9A shows recordings from an experiment studying the reversal potential of I_{sus} based on tail current measurements. In this experiment, I_{sus} tails reversed between −60 and −80 mV in the presence of 5.4 mmol/L K^+ in the superfusate. At this $[K^+]_o$, the mean I_{sus} reversal potential in seven cells was −75±3 mV, which compares with a value of −83 mV calculated from the Nernst equation for a temperature of 25°C and an assumed $[K^+]_i$ of 130 mmol/L. Increased superfusate K^+ concentration shifted the reversal potential, as illustrated in Fig 10B. The relation between mean I_{sus} reversal potentials and log $[K^+]_o$ was linear, with a correlation coefficient of 0.999 and a slope of 54 mV per decade. Slopes were also calculated from data in each of seven individual experiments and averaged 55.3±2.9 mV.

Rectification properties were studied by analyzing the fully activated I-V relation with the protocol illustrated in Fig 9C. Tail currents were corrected for incomplete deactivation as previously described[11] by dividing the time-dependent (peak minus steady-state) tail current by $(1-a_{TP}/a_{+50})$, where a_{TP} and a_{+50} are the activation variable at the test potential and +50 mV, respectively. The results show substantial outward rectification at potentials positive to −10 mV.

Envelope of Tails Test

Because of the rapid activation of I_{sus} at 25°C, it was difficult to obtain sufficient information for an accurate envelope of tails analysis. Therefore, we studied I_{sus} at 16°C (using prepulses to inactivate I_{to1} according to the protocol illustrated in Fig 10A). The properties of I_{sus} were similar to those observed at 25°C (Fig 8), except that current kinetics were slowed (eg, the activation time constant at 16°C averaged 46.7±4.1 milliseconds at +10 mV versus 7.1±0.8 milliseconds [P<.01] at 25°C and the same potential). The scaled tail currents were superimposed on the activating current tracing (Fig 10A and 10B), indicating that the envelope test was satisfied. Fig 10C shows mean ratios of tail current (I_{Tail}) to step current (I_{Step}) as a function of pulse duration in four cells. There is no significant time dependence of the ratio, consistent with the presence of only one current

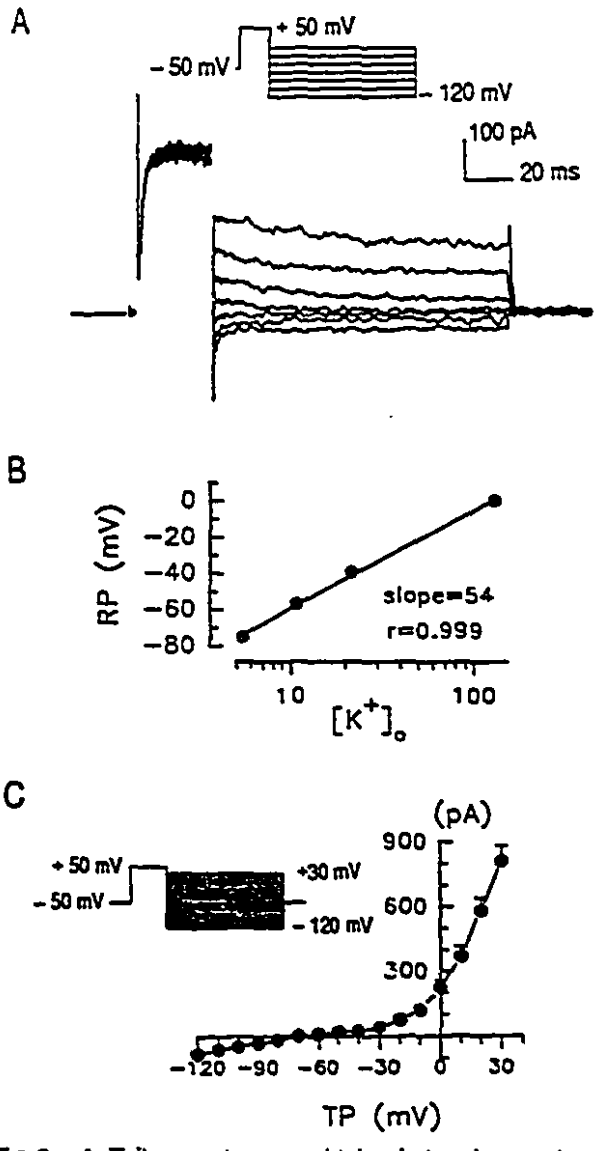

FIG 9. A, Tail currents were obtained at various potentials with the protocol shown, after a 400-millisecond conditioning pulse from −50 to +50 mV to inactivate the 4-aminopyridine–sensitive transient outward current (I_{to1}) (at room temperature). Results at 20-mV test voltage increments are shown. Sustained outward tail current (I_{sus}) reversed between −60 and −80 mV in this cell. B, Graph shows dependence of I_{sus} reversal potential (RP) on logarithm of $[K^+]_o$. Symbols are mean values of the RP from seven cells (standard errors are within the symbols for means), and the line is the best linear fit, with a slope of 54 mV per decade. C, Graph shows fully activated current-voltage relation, as obtained from measurements of tail currents with the protocol shown in the inset (40-millisecond pulse to +50 mV to activate I_{sus} followed by repolarization to various test potentials [TPs]; 400-millisecond prepulse as in A to inactivate I_{to1}). Values plotted are amplitudes of deactivating tail current, adjusted for incomplete deactivation as described in the text.

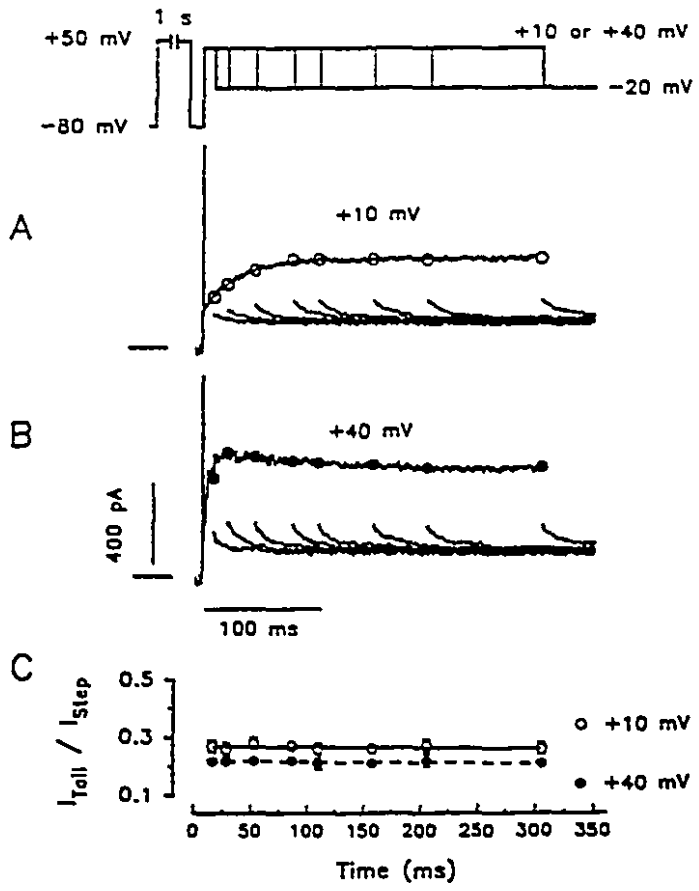

FIG 10. Current activation and envelope of tails test at 16°C. A 1-second conditioning pulse was used to inactivate the 4-aminopyridine-sensitive transient outward current (I_{to1}) and was followed 5 milliseconds later by a depolarizing pulse of varying duration, which ended with repolarization to −20 mV to observe tail currents. A, Step and tail currents were recorded with activating pulses to +10 mV. Open circles are tail currents scaled onto activating current recording. B, Step and tail currents were recorded with activating pulses to +40 mV. Filled circles are scaled tail currents. (Horizontal lines in A and B are zero current levels.) C, Graph shows mean ratio of tail current to step current (I_{Tail}/I_{Step}) with activating pulses to +10 and +40 mV, as a function of activating pulse duration in four cells.

component for I_{sus}. Tail current deactivation was found to be well fit by a single exponential relation, and the deactivation time constant was unrelated to the duration of the activating pulse. For example, time constants of tail deactivation at −20 mV averaged 78±11, 77±11, 77±12, 79±12, and 78±12 milliseconds, respectively, for 10-, 20-, 50-, 100-, and 300-millisecond activating pulses to +10 mV.

Observations in Cells Lacking I_{to1}

In the course of these experiments, we observed 10 cells (out of a total of approximately 100) lacking any current resembling I_{to1} on depolarization from −80 mV to potentials as positive as +60 mV. These cells appeared otherwise normal. Their capacitance (78±8 pF before and 64±5 pF after series resistance and capacitance compensation), capacitive time constant (431±48 microseconds before and 135±11 microseconds after compensation), series resistance (5.5±20 MΩ before and 2.1±0.7 MΩ after compensation), and input resistance (1.6±0.6 GΩ) were not significantly different from those determined in other cells. They averaged 92±6 μm in length and 9.0±0.4 μm in width, similar to other cells.

In these cells, depolarizing pulses at 25°C revealed a current with properties of I_{sus}, as shown in Fig 11A and 11B. The I-V relation and activation kinetics at 25°C of I_{sus} in such cells could be characterized without the use of pharmacologic or voltage protocols otherwise required to separate I_{sus} from I_{to1} and are shown in Fig 11C and 11D. The results are similar to results obtained in cells possessing I_{to1} with the use of depolarizing prepulses to inactivate the latter current.

Effects of Dendrotoxin on I_{sus}

A variety of voltage-gated K^+ channels have been cloned, several of which resemble I_{sus}.[29] Differences in pharmacologic response characterize the various clones in the Kv1 family and may be useful in comparing native currents with specific clones. Pharmacologic probes of interest include 4AP, TEA, and Ba^{2+}. The responses of I_{sus} to 4AP, TEA, and Ba^{2+} were defined in experiments addressing the role of other K^+ currents as described above. To complete the pharmacologic characterization of I_{sus}, we evaluated its response to 1, 10, and 100 nmol/L dendrotoxin in six cells. Dendrotoxin did not significantly alter I_{sus} at any concentration. For example, I_{sus} averaged 149±29 pA at +10 mV and 444±51 pA at +50 mV before dendrotoxin superfusion and 176±39 pA at +10 mV and 444±80 pA at +50 mV after exposure to 100 nmol/L dendrotoxin (n=6).

Effects of Selective Blockade of I_{sus} on the Action Potential

To evaluate the possible role of I_{sus} in mediating repolarization, the effects of 50 μmol/L 4AP were analyzed. At this concentration, 4AP reduced I_{sus} by 50% without affecting I_{to1}. Experiments were carried out at 36°C in normal Tyrode's solution free of channel blockers (to allow for as normal action potentials as possible). Outward currents were evaluated by depolarizing the membrane to various test potentials from an

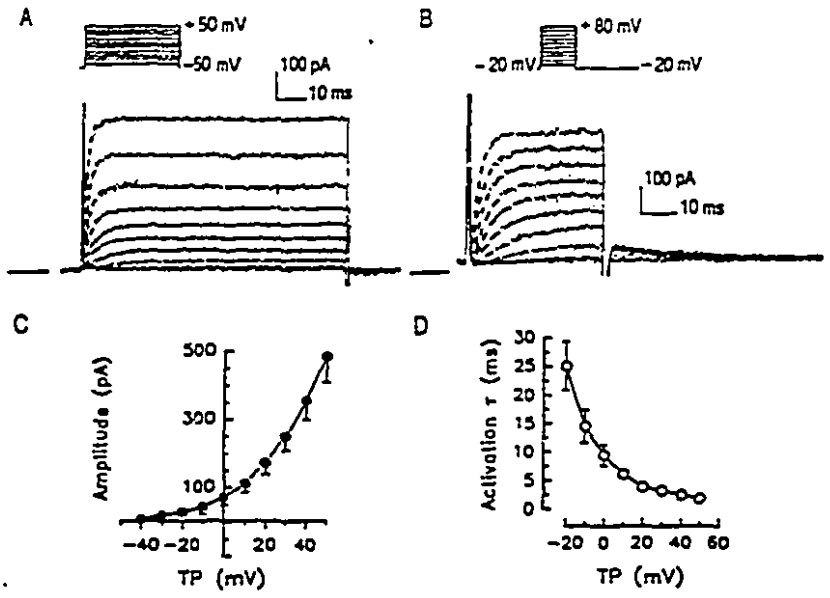

FIG 11. Characteristics of sustained outward current (I_{sus}) in cells lacking 4-aminopyridine–sensitive transient outward current (I_{to1}). A, Currents were elicited by 100-millisecond depolarizing pulses from a holding potential of −50 mV in one cell. B, Currents were elicited by 40-millisecond pulses from a holding potential of −20 mV in a different cell. In both A and B, zero current levels are shown with horizontal lines; dashed lines are exponential curve fits to experimental data. C, Graph shows current-voltage relation for I_{sus} measured by depolarizing pulses in 10 cells lacking I_{to1}. TP indicates test potential. D, Graph shows activation kinetics of I_{sus} in 10 cells lacking I_{to1}, obtained with the use of depolarizing pulses as shown in A. τ indicates the time constant.

HP positive to −50 mV to inactivate the Na^+ current, and action potentials were recorded in the current-clamp mode. After baseline recording of action potentials and outward currents had been obtained under control conditions, cells were superfused with Tyrode's solution containing 4AP at a concentration of 50 μmol/L, and the same measurements were repeated.

The effects of 4AP are illustrated in Fig 12, in which action potentials (A) and current recordings (B) elicited under control conditions and during exposure to 4AP are shown. The action potential is substantially prolonged by 4AP, without any change in overall morphology. Under control conditions, there is a prominent I_{to}, followed by a slowly developing delayed rectifier current. Outward current was reduced by 4AP at all times during the pulse by just over 200 pA, with no effect on time-dependent current components per se. The overall effect of 50 μmol/L 4AP on action potential duration in 10 myocytes is shown in the Table. The drug significantly increased action potential duration at various levels of repolarization, with no significant difference in percent change at each level.

Discussion

We have shown that the depolarization-induced sustained current remaining after I_{to1} inactivation in human atrial myocytes is a K^+ current that can be distinguished from I_{to1} on the basis of differences in voltage-dependent inactivation and sensitivity to block by 4AP. I_{sus} differs from classic I_K in terms of its sensitivity to 4AP, insensitivity to TEA, and extremely rapid activation kinetics. The kinetic properties of I_{sus} are similar to those of a variety of rapidly activating and slowly inactivating K^+ channels encoded by cDNAs from rat[30,31] and human[13-17,29] heart tissue, suggesting that I_{sus} may be a physiological manifestation of this type of channel identified by DNA cloning.

Comparison Between I_{sus} and Similar Currents Carried by Cloned Channels

Tamkun et al[13] described two K^+ channel clones from human heart, one of which (HK2) is much more abundant in human atrium than ventricle. HK2 was transfected into mouse L cells by Snyders et al,[14,16] and the expressed current was found to be highly K^+ selective (55 mV per decade), rapidly activating (the time constant decreased from 10 milliseconds to approximately 2 milliseconds between 0 and +60 mV), and outwardly rectifying. Slow, partial inactivation was seen after strong depolarization, and the single-channel conductance was 15 picosiemens.[14] The current is very sensitive to blockade by 4AP (IC_{50} at +50 mV, 180 μmol/L) and insensitive to inhibition by TEA (10 mmol/L) or dendrotoxin (100 nmol/L).[16]

Philipson et al[32] cloned cDNA (hPCN1) encoding for an islet cell K^+ channel from human pancreatic tissue, with significant homology and functional properties similar to HK2. On expression of this cDNA in *Xenopus* oocytes, the resulting K^+ currents activated rapidly, with time constants in the range of 20 milliseconds at −10 mV and 1 millisecond at +60 mV. Steady-state inactivation was observed at HPs more positive than −50 mV, and the current was fully inactivated at potentials positive to −10 mV. The current was insensitive to TEA but highly sensitive to 4AP, with 30% to 38% block at 50 μmol/L and 54% to 62% block with 100 μmol/L 4AP.

More recently, Fedida et al[17] cloned a cDNA (fHK) from a fetal human heart library. K^+ channels encoded by fHK carry a K^+ current with many similarities to the currents described above. There is substantial sequence homology between fHK and hPCN1 and slightly less homology with HK2. The properties of currents resulting from expression of fHK in a human epithelial kidney cell line include rapid activation (time constants of 11.8 milliseconds at 0 mV and 1.6 milliseconds at +60 mV), K^+ selectivity, and slow inactivation at positive potentials (approximately 40% after 10 seconds at +50 mV). The voltage dependence, pharmacologic response (to TEA and 4AP), and kinetic properties of current carried by fHK strongly resemble the corresponding characteristics of I_{sus}.[17]

A rapidly activating and slowly inactivating delayed rectifier current is carried by channels encoded by a

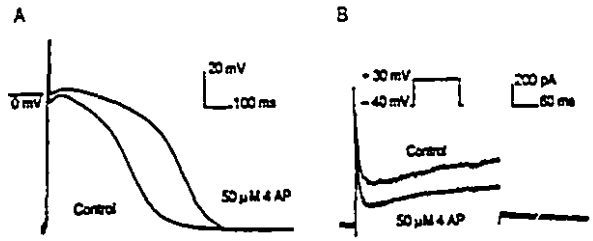

FIG 12. Tracings showing the effects of 4-aminopyridine (4AP, 50 μmol/L) on the action potential of a single atrial myocyte. Experiments were conducted in normal Tyrode's solution, and only cells with a resting potential more negative than −50 mV were used. A, Action potentials were recorded in current-clamp mode by clamping the membrane at −80 mV and then delivering 3-millisecond rectangular pulses at 1 Hz. Action potentials under control conditions and in the presence of 4AP are superimposed. 4AP prolongs action potential duration without substantially changing the morphology. B, Currents in the same cell were elicited by a 350-millisecond pulse to +30 mV from a holding potential of −40 mV. 4AP reduces total depolarization-induced outward current by approximately 50%, without altering transient outward and delayed rectifier current components.

cDNA (designated RAK) cloned from adult rat atrial tissue, as reported by Paulmichl et al.[31] This current also activates rapidly, although somewhat more slowly than HK2 (time constant ranging from 58 milliseconds at −20 mV to 6.4 milliseconds at +60 mV). It is insensitive to TEA and is blocked by 4AP with an IC_{50} of 600 μmol/L.

Cloned K^+ channels are now generally described in terms of a common nomenclature proposed by Chandy[33] in 1991. The activation and inactivation properties of I_{sus} most resemble those of three members of the Kv1 family: Kv1.1, Kv1.2, and Kv1.5.[29] However, Kv1.1 is sensitive to TEA, dendrotoxin, and Ba^{2+}, with IC_{50}s of 2 mmol/L, 12 nmol/L, and 0.8 mmol/L, respectively, and Kv1.2 is exquisitely sensitive to dendrotoxin (IC_{50}, 0.1 nmol/L).[29] Only Kv1.5 has a pharmacologic profile similar to that of I_{sus}, including sensitivity to 4AP (IC_{50} in the order of 100 μmol/L) and insensitivity to TEA and dendrotoxin (to 200 nmol/L).[25] The pharmacologic properties of I_{sus} therefore identify it with the Kv1.5 group of K^+ channel clones, including the clones shown to be present in human heart: HK2,[13-16] hPCN1,[32] and fHK.[17]

Relation of I_{sus} to Previously Described Native Currents

In 1988, Yue and Marban[34] described a novel K^+ channel based on single-channel recordings from guinea pig ventricular myocytes, which they designated I_{K_p}. This channel was observed in approximately 10% of patches, activated rapidly (time constant, <10 milliseconds), and was highly selective for K^+. Depolarization increased open probability, which was 50% of maximum at approximately −10 mV, and no detectable inactivation was noted. Single-channel conductance was 14 picosiemens, a value close to that noted for fHK[17] and HK2.[30] Recently, Backx and Marban[35] have reported the macroscopic current counterpart of I_{K_p} in guinea pig ventricular myocytes. It differs from I_{sus} in that I_{K_p} is strongly inhibited by 1 mmol/L Ba^{2+} and has a relatively linear I-V relation.

Boyle and Nerbonne[36] have described a rapidly activating delayed rectifier current in rat atrial myocytes. The activation time constant of this current ranged from 5.3 to 1.4 milliseconds over the range of −10 to +50 mV. Activation was voltage dependent, with 50% activation at −1.5 mV, similar to I_{sus}. The rat atrial K^+ current was sensitive to 4AP, with an IC_{50} of approximately 1 mmol/L,[36] which is similar to the 4AP sensitivity of the rat atrial delayed rectifier cDNA cloned by Paulmichl et al[31] and about one order of magnitude larger than the IC_{50} for 4AP block of I_{sus}, fHK,[17] HK2,[16] and hPCN1.[32] Finally, the rat atrial K^+ current showed considerable voltage-dependent inactivation and was 50% inactivated at approximately −40 mV.[36] Rat atrial delayed rectifier currents corresponding to both the cloned[31] and native[36] channels are somewhat less sensitive to 4AP than the native human current (I_{sus}) and similar channels encoded by human cDNA clones.[13-16] The rat atrial channel also appears to manifest stronger voltage-dependent inactivation.

Jeck and Boyden[37] have recently observed a very rapidly activating outward current that shows little inactivation in 23% of neonatal puppy cells. The ionic nature of this current was not studied in detail, but it was found to change little or not at all on exposure to 2 mmol/L 4AP. The precise nature of this current and its relation to cloned and other native channels remains to be elucidated.

Relation to Classic Delayed Rectifier Currents and Potential Significance

Delayed rectifier currents in the heart were first described by Noble and Tsien[10] in 1969. Since that time, delayed rectifier K^+ currents have been shown to exist and play a potential role in action potential repolarization of a variety of cardiac cell types and species.[38-45] Recently, it has been suggested that I_K in some species consists of two components, I_{K_r} (or "rapid I_K") and I_{K_s} (or "slow I_K"), which can be distinguished on the basis of different kinetics, voltage dependence, and response to pharmacologic agents.[46,47] A cDNA cloned from neonatal rat heart has been found to encode channels with properties comparable to I_{K_s}.[48]

Classic delayed rectifier currents are present in human atrial myocytes[11] and appear to manifest characteristics[28] comparable to those attributed to I_{K_r} and I_{K_s} in the guinea pig.[46,47] I_{sus}, along with the similar cloned and native current systems discussed above, belongs to a new category of delayed rectifier current, which differs from classic I_K in activating much more rapidly and, in the case of the

Effects of 4-Aminopyridine (50 μmol/L) on Action Potential Duration in 10 Human Atrial Myocytes

	Control	4AP (50 μmol/L)	% Increase
APD_{20}, ms	6±1	9±2*	49±11
APD_{50}, ms	52±7	90±13†	73±8
APD_{90}, ms	207±18	342±32†	66±11

4AP indicates 4-aminopyridine. APD_{20}, APD_{50}, and APD_{90}, action potential duration at 20%, 50%, and 90% repolarization, respectively.

*$P<.05$ and †$P<.01$ vs control.

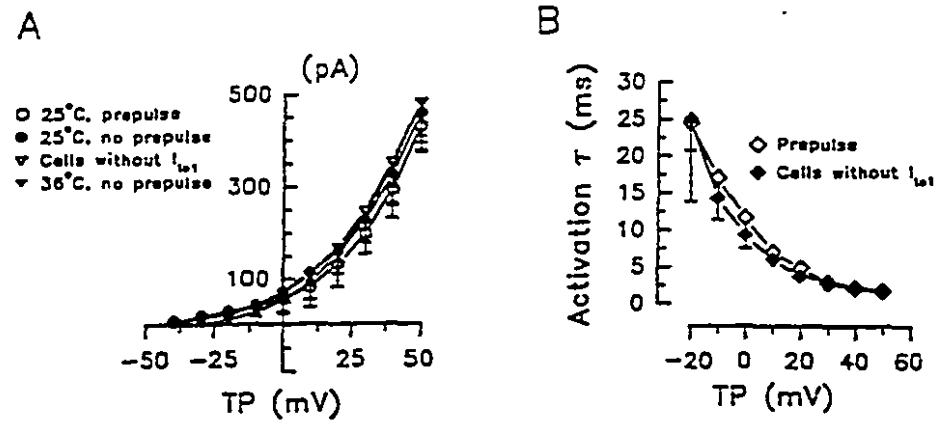

FIG 13. A, Graph shows current-voltage relation for sustained outward current (I_{sus}) obtained with four different protocols: ○, studies at 25°C, with prepulses to *remove* the 4-aminopyridine–sensitive transient outward current (I_{to1}) (as in Fig 8A, n=6); ●, studies at 25°C, without prepulses, with I_{sus} measured from the current at the end of a 2-second pulse (as in Fig 8B, n=4); ▽, studies at 25°C, in cells lacking I_{to1} (as in Fig 11, n=10); and ▼, studies at 36°C, without prepulses and with I_{sus} measured from the current at 2 seconds of a depolarizing pulse (as in Fig 8B, n=8). B, Graph shows activation time constant (τ) for I_{sus} at 25°C, as measured with a prepulse to inactivate I_{to1} (Fig 8A) or in cells lacking I_{to1} (Fig 11). TP indicates test potential.

Kv1.5 clones and corresponding native currents, differing in pharmacologic sensitivity (with markedly greater sensitivity to blockade by 4AP and resistance to TEA). It may be appropriate to term these currents "ultrarapid" delayed rectifiers (I_{Kur}), to distinguish them from the slower delayed rectifiers I_{Kr} and I_{Ks}. Because of their rapidity of activation and limited slow inactivation, these recently described delayed rectifier currents have the capacity to contribute significantly to action potential repolarization. Results of exposure to 50 μmol/L 4AP (Fig 12) are consistent with a role for I_{sus} in repolarizing the human atrial action potential. A deeper understanding of the properties of I_{sus} may allow for a fuller appreciation of the mechanisms of repolarization of human atrial cells, and the development of safe and specific I_{sus} blockers could allow for new approaches to the pharmacologic therapy of atrial arrhythmias.

Potential Limitations

The most important limitation of these studies is the difficulty of separating I_{sus} from other currents, particularly I_{to1}. We have achieved this goal in three ways: (1) by studying current selectively blocked by very low (50 μmol/L) concentrations of 4AP, (2) by using conditioning pulses to inactivate I_{to1}, and (3) by studying cells lacking I_{to1}. All of these methods have potential limitations. Blockers like 4AP are notorious for voltage- and frequency-dependent effects, which could distort the subtracted currents. For this reason, we used the 4AP-sensitive current only for qualitative comparison with results obtained by other methods. One can never be sure that conditioning pulses fully remove a contaminating current, and the short interval between the conditioning and test pulse leaves significant I_{sus} activated at the onset of the test pulse, so that an instantaneous outward component is present at the onset of depolarization (compare Fig 7C, with conditioning pulse method, with Fig 6C, top, using 4AP-sensitive current, to study I_{sus}). Finally, cells lacking I_{to1} may be abnormal or unrepresentative.

On the other hand, the results obtained using all three methods to define I_{sus} are in close agreement. Fig 13A shows the I-V relation for I_{sus} as established with four different sets of protocols in four separate sets of cells: (1) studies at 25°C, with prepulses to remove I_{to1} (same voltage protocol as in Fig 8A, n=6), (2) studies at 25°C, without prepulses, with I_{sus} measured from the current at the end of a 2-second pulse (as in Fig 8B, n=4), (3) studies at 36°C, without prepulses, and I_{sus} measured from the current at 2 seconds of a depolarizing pulse (same voltage protocol as in Fig 8B, n=8), and (4) studies at 25°C, in cells lacking I_{to1} (as in Fig 11, n=10). The results are very similar for all protocols in all sets of cells, making it unlikely that they are an artifact of the method used to study I_{sus}. Similarly, activation kinetics at 25°C (Fig 13B) were not significantly different when assessed with the use of a prepulse to inactivate I_{to1} (as in Fig 8A) or simple voltage steps from the same HP in cells lacking I_{to1} (Fig 11). While recognizing the imperfections of the approaches required to define the properties of I_{sus} in human atrial myocytes, it must be acknowledged that these approaches are the only ones currently available to isolate and describe the native current. Cloned channels may allow one to study in a relatively pure way the properties of a given current but still leave unanswered the role of that specific current in native tissues.

We tested the relative potency of 4AP in blocking I_{sus} and I_{to1} at a frequency of 1 Hz. In preliminary studies, we have found that 4AP block of I_{sus} in human atrium is not rate dependent,[49] whereas 4AP block of I_{to1} shows typical reverse use dependence.[50] Thus, our estimate of the IC_{50} for 4AP block of I_{sus} is rate independent, but the value obtained for 4AP block of I_{to1} applies, strictly speaking, only to a frequency of 1 Hz. This does not limit the validity of the experiments in which we used 50 μmol/L 4AP to selectively block I_{sus}, since the latter were all performed at a frequency of 1 Hz. On the other hand, the relative affinity of 4AP for I_{sus} versus I_{to1} needs to be assessed in light of the state-dependent block of

I_{to1} by 4AP. The K_d of 4AP for the rested state of I_{to1} is likely to be closer to the K_d for I_{sus} than the relative IC_{50}s obtained during pulsing at 1 Hz. Available estimates in the literature suggest that even the resting state I_{to1} affinity for 4AP is probably less than that of I_{sus}.[4,51]

We used Co^{2+} to block Ca^{2+} current and I_{to2}. Since divalent cations can have complex effects on the activation and voltage dependence of outward currents,[52] our results must be interpreted in that light. The use of 2 mmol/L Co^{2+} may have shifted the activation curve in the positive direction, similar to the effect of La^{3+} on cloned Kv1.5.[16] This may be relevant when comparing the position of the activation curve of the human atrial current with cloned Kv1.5 channels that are studied in the absence of divalent cations needed in the present experiments to block Ca^{2+} channels.

Conclusions

We have defined the properties of the current underlying the sustained outward current elicited by depolarization of human atrial myocytes. The properties of this current suggest that it is the native counterpart to Kv1.5 channels cloned from human cardiac tissue. Because of its extremely rapid activation and relative lack of inactivation at physiological temperatures, I_{sus} can contribute to repolarization of the human atrial action potential and to the determination of action potential duration. Consideration of this current may lead to new insights into the physiological and pharmacologic determinants of human atrial repolarization.

Acknowledgments

This study was supported by the Medical Research Council of Canada, Quebec Heart Foundation, and the Fonds de Recherche de l'Institut de Cardiologie de Montréal. Mr Wang is supported by a Canadian Heart and Stroke Foundation Studentship, Dr Fermini is a Knoll–Fonds de Recherche en Santé du Québec (FRSQ) Research Scholar, and Dr Nattel is a Nordic-FRSQ Senior Research Scholar. The authors thank Guylaine Nicol for excellent technical assistance and Mary Morello and Christiane Lussier for typing the manuscript.

References

1. Zipes DP. Genesis of cardiac arrhythmias: electrophysiological considerations. In: Braunwald E, ed. *Heart Disease, A Textbook of Cardiovascular Medicine.* Philadelphia, Pa: WB Saunders Co; 1992: 588-627.
2. Bigger JT, Hoffmann BF. Antiarrhythmic drugs. In: Gilman AG, Goodman LL, Kall TW, Murad F, eds. *The Pharmacological Basis of Therapeutics.* 7th ed. New York, NY: Macmillan Publishing Co; 1985:748-783.
3. Escande D, Coulombe A, Faivre JF, Deroubaix E, Coraboeuf E. Two types of transient outward currents in adult human atrial cells. *Am J Physiol.* 1987;252:H142-H148.
4. Shibata EF, Drury T, Refsum H, Aldrete V, Giles W. Contributions of a transient outward current to repolarization in human atrium. *Am J Physiol.* 1989;257:H1773-H1781.
5. Fermini B, Wang Z, Duan D, Nattel S. Differences in rate dependence of transient outward current in rabbit and human atrium. *Am J Physiol.* 1992;263:H1747-H1754.
6. Tseng GN, Hoffman BF. Two components of transient outward current in canine ventricular myocytes. *Circ Res.* 1989;64:633-647.
7. Wang Z, Pelletier LC, Talajic M, Nattel S. Effects of flecainide and quinidine on human atrial action potentials: role of rate-dependence and comparisons with guinea pig, rabbit, and dog tissues. *Circulation.* 1990;82:274-283.
8. Heidbüchel H, Vereecke J, Carmeliet E. The electrophysiological effects of acetylcholine in single human atrial cells. *J Mol Cell Cardiol.* 1987;19:1207-1219.
9. Heidbüchel H, Vereecke J, Carmeliet E. Three different potassium channels in human atrium: contribution to the basal potassium conductance. *Circ Res.* 1990;66:1277-1286.
10. Noble D, Tsien RW. Outward membrane currents activated in the plateau range of potentials in cardiac Purkinje fibres. *J Physiol (Lond).* 1969;200:205-231.
11. Wang Z, Fermini B, Nattel S. Delayed rectifier outward current and repolarization in human atrial myocytes. *Circ Res.* 1993;73: 276-285.
12. Duan DY, Fermini B, Nattel S. The sustained outward current observed after I_{to} inactivation in rabbit atrial myocytes is a novel Cl^- current. *Am J Physiol.* 1992;263(*Heart Circ Physiol* 32): H1967-H1971.
13. Tamkun MM, Knoth KM, Walbridge JA, Kroemer H, Roden DM, Glover DM. Molecular cloning and characterization of two voltage-gated K^+ channel cDNAs from human ventricle. *FASEB J.* 1991;5:331-337.
14. Snyders DJ, Knoth KM, Roberds SL, Tamkun MM. Stable mammalian expression of a human cardiac K^+ channel. *Circulation.* 1991;84(suppl 2):II-103. Abstract.
15. Snyders DJ, Knoth KM, Roberds SL, Tamkun MM. Time-, voltage-, and state-dependent block by quinidine of a cloned human cardiac potassium channel. *Mol Pharmacol.* 1992;41: 322-330.
16. Snyders DJ, Tamkun MM, Bennett PB. A rapidly activating and slowly inactivating potassium channel cloned from human heart: functional analysis after stable mammalian cell culture expression. *J Gen Physiol.* 1993;101:513-543.
17. Fedida D, Wible B, Wang Z, Fermini B, Faust F, Nattel S, Brown AM. Identity of a novel delayed rectifier current from human heart with a cloned K^+ channel current. *Circ Res.* 1993;73:210-216.
18. Sigworth FJ. Electronic design of the patch clamp. In: Sakmann B, Neher E, eds. *Single-Channel Recording.* New York, NY: Plenum Publishing Corp; 1983:3-35.
19. Zygmunt AC, Gibbons WR. Properties of the calcium-activated chloride current in heart. *J Gen Physiol.* 1992;99:391-414.
20. Giles WR, Van Ginneken ACG. A transient outward current in isolated cells from the crista terminalis of rabbit heart. *J Physiol (Lond).* 1985;368:243-264.
21. Pressler ML. Passive electrical properties of cardiac tissue. In: Zipes DP, Jalife J, eds. *Cardiac Electrophysiology, From Cell to Bedside.* Philadelphia, Pa: WB Saunders Co; 1990:108-121.
22. Hume JR, Giles W. Active and passive electrical properties of single bullfrog atrial cells. *J Gen Physiol.* 1981;78:19-42.
23. Marty A, Neher E. Tight-seal whole-cell recording. In: Sakmann B, Neher E, eds. *Single-Channel Recording.* New York, NY: Plenum Publishing Corp; 1983:107-121.
24. Masson-Pévet M, Gros D, Besselsen E. The caveolae in rabbit sinus node and atrium. *Cell Tissue Res.* 1980;208:183-196.
25. Apkon M, Nerbonne JM. Characterization of two distinct depolarization-activated K^+ currents in isolated adult rat ventricular myocytes. *J Gen Physiol.* 1991;97:973-1011.
26. Fermini B, Nattel S. Choline chloride activates time-dependent and time-independent K^+ currents in dog atrial myocytes. *Am J Physiol.* In press.
27. Sachs L, ed. *Applied Statistics: A Handbook of Techniques,* 2nd ed. New York, NY: Springer-Verlag New York, Inc; 1984:509-512.
28. Nattel S, Wang Z, Fermini B. Three types of delayed rectifier potassium currents in human atrial cardiomyocytes. *Biophys J.* 1993;64:A393. Abstract.
29. Roberds SL, Knoth KM, Po S, Blair TA, Bennett PB, Hartshorne RP, Snyders DJ, Tamkun MM. Molecular biology of the voltage-gated potassium channels of the cardiovascular system. *J Cardiovasc Electrophysiol.* 1993;4:68-80.
30. Roberds SL, Tamkun MM. Cloning and tissue-specific expression of five voltage-gated potassium channel cDNAs expressed in rat heart. *Proc Natl Acad Sci U S A.* 1991;88:1798-1802.
31. Paulmichl M, Nasmith P, Hellmiss R, Reed K, Boyle WA, Nerbonne JM, Peralta EG, Clapham DE. Cloning and expression of a rat cardiac delayed rectifier potassium channel. *Proc Natl Acad Sci U S A.* 1991;88:7892-7895.
32. Philipson LH, Hice RE, Schaefer K, LaMendola J, Bell GI, Nelson DJ, Steiner DF. Sequence and functional expression in Xenopus oocytes of a human insulinoma and islet potassium channel. *Neurobiology.* 1991;88:53-57.
33. Chandy KG. Simplified gene nomenclature. *Nature.* 1991;352:26. Letter.
34. Yue DT, Marban E. A novel cardiac potassium channel that is active and conductive at depolarized potentials. *Pflugers Arch.* 1988;413:127-133.

35. Backx PH, Marban E. Background potassium current active during the plateau of the action potential in guinea pig ventricle myocytes. *Circ Res.* 1993;72:890-900.
36. Boyle WA, Nerbonne JM. A novel type of depolarization-activated K^+ current in isolated adult rat atrial myocytes. *Am J Physiol.* 1991;260(*Heart Circ Physiol* 29):H1236-H1247.
37. Jeck CD, Boyden PA. Age-related appearance of outward currents may contribute to developmental differences in ventricular repolarization. *Circ Res.* 1992;71:1390-1403.
38. McDonald TF, Trautwein W. The potassium current underlying delayed rectification in cat ventricular muscle. *J Physiol (Lond).* 1978;274:217-246.
39. Tseng GN, Robinson RB, Hoffman BF. Passive properties and membrane currents of canine ventricular myocytes. *J Gen Physiol.* 1987;90:671-701.
40. Kass RS. Delayed rectification in the cardiac Purkinje fiber is not activated by intracellular calcium. *Biophys J.* 1984;45:837-839.
41. Brown H, DiFrancesco D. Voltage-clamp investigations of membrane currents underlying pace-maker activity in rabbit sino-atrial node. *J Physiol (Lond).* 1980;308:331-351.
42. Gintant GA, Datyner NB, Cohen IS. Gating of delayed rectification in acutely isolated canine cardiac Purkinje myocytes. *Biophys J.* 1985;48:1059-1064.
43. DiFrancesco D, Noma A, Trautwein W. Kinetics and magnitude of the time-dependent potassium current in the rabbit sinoatrial node. *Pflugers Arch.* 1979;381:271-279.
44. Matsuura H, Ehara T, Imoto Y. An analysis of the delayed outward current in single ventricular cells of the guinea-pig. *Pflugers Arch.* 1987;410:596-603.
45. Hume JR, Uehara A. Ionic basis of the different action potential configurations of single guinea-pig atrial and ventricular myocytes. *J Physiol (Lond).* 1985;368:525-544.
46. Sanguinetti MC, Jurkiewicz NK. Delayed rectifier outward K^+ current is composed of two currents in guinea pig atrial cells. *Am J Physiol.* 1991;260(*Heart Circ Physiol* 29):H393-H399.
47. Sanguinetti MC, Jurkiewicz NK. Two components of cardiac delayed rectifier K^+ current. *J Gen Physiol.* 1990;96:195-215.
48. Folander K, Smith JS, Antanavage J, Bennett C, Stein RB, Swanson R. Cloning and expression of the delayed-rectifier I_{sK} channel from neonatal rat heart and diethylstilbestrol-primed rat uterus. *Proc Natl Acad Sci U S A.* 1990;87:2975-2979.
49. Wang Z, Duan D, Fermini B, Nattel S. Contrasting ionic mechanisms of sustained outward currents in human and atrial myocytes. *Circulation.* 1992;86(suppl 1):I-697. Abstract.
50. Wang Z, Fermini B, Nattel S. State- and voltage-dependent I_{to} block by 4-aminopyridine in human atrial myocytes. *Circulation.* 1992;86(suppl 1):I-696. Abstract.
51. Po S, Snyders DJ, Baker R, Tamkun MM, Bennett PB. Functional expression of an inactivating potassium channel cloned from human heart. *Circ Res.* 1992;71:732-736.
52. Dukes ID, Morad M. The transient K^+ current in rat ventricular myocytes: evaluation of its Ca^{2+} and Na^+ dependence. *J Physiol (Lond).* 1991;435:395-420.

Identity of a Novel Delayed Rectifier Current From Human Heart With a Cloned K^+ Channel Current

D. Fedida, B. Wible, Z. Wang, B. Fermini, F. Faust, S. Nattel, A.M. Brown

In human myocardium, the nature of the K^+ currents mediating repolarization of the action potential is still speculative. Delayed rectifier channels have recently been cloned from human myocardium, but it is unclear whether or not these currents are involved in the termination of the cardiac action potential plateau. In intact human atrial myocytes, we have identified a rapid delayed rectifier K^+ current with properties and kinetics identical to those expressed by a K^+ channel clone (fHK) isolated from human heart and stably incorporated into a human cell line for the first time. The myocyte current amplitude was 3.6±0.2 pA/pF (at +20 mV, n=15) and activated with a time constant of 13.1±2 milliseconds at 0 mV (n=15). The half-activation potential ($V_{0.5}$) was −6±2.5 mV (n=10) with a slope factor (k) of 8.6±2.2 (n=10). The heterologously expressed fHK current amplitude was 136 pA/pF (at +20 mV, n=9) with an activation time constant of 11.8±4.6 milliseconds at 0 mV; $V_{0.5}$ was −4.1±2.4 mV (mean±SEM, n=8); and k was 7.0. The conductance of single fHK channels was 16.9 picosiemens in 5 mM bath K^+. Both native and cloned channel currents inactivated partially during sustained depolarizing pulses. Both currents were blocked by micromolar concentrations of 4-aminopyridine and were relatively insensitive to tetraethylammonium ions and class III antiarrhythmic agents. They had a half blocking concentration ($K_{0.5}$) for block by 4-aminopyridine of ~50 μM but were relatively resistant to clofilium ($K_{0.5}$ was 60±13 μM, n=6 for fHK). The strong correspondence between the properties of the two currents provides the first demonstration that a specific K^+ channel produces a rapid delayed rectifier current in human cardiac tissue. (*Circulation Research* 1993;73:210-216)

KEY WORDS • potassium channels • delayed rectifier currents • human hearts

The first analysis of delayed rectification in heart by Noble and Tsien[1] identified two currents, I_{x1} and I_{x2}, with distinctly different kinetics and voltage dependence. Recent pharmacological[2] and electrophysiological[3-6] data have revealed multiple, often species-specific, cardiac delayed rectifier currents with varying conductances and kinetic properties. Advances in the cloning of ion channels have simplified the study of the complex mixture of ionic currents present during cardiac action potential repolarization. The isolation and expression of individual channel components has led to the description of delayed rectifier channel currents from rat[7-9] and mouse[10] heart and also the description of HK2,[11] a rapidly activating delayed rectifier current from adult human ventricular myocardium. No information exists on repolarizing delayed rectifier currents in human heart myocytes, so the significance of cloned channels has remained unclear. We have cloned a rapidly activating delayed rectifier channel, expressed it in a human cell line, and correlated it with novel currents recently identified in human atrium.[12] The similarities between the cloned channel currents and the native current in atrium are striking and establish the importance of cloned channels in the study of human cardiac repolarization.

Received January 20, 1993; accepted April 16, 1993.

From the Department of Molecular Physiology and Biophysics, Baylor College of Medicine, Houston, Tex (Drs Wible and Brown); the Department of Physiology, Queen's University, Kingston, Canada (Dr Fedida); and the Department of Medicine, University of Montreal, Montreal Heart Institute (Drs Fermini and Nattel), and the Department of Pharmacology and Therapeutics, McGill University (Drs Wang and Nattel), Montreal, Canada.

Correspondence to Department of Molecular Physiology and Biophysics, Baylor College of Medicine, One Baylor Plaza, Houston, TX 77030 (Dr Brown).

Materials and Methods

Detection and Expression of K^+ Channel Clone

A pool of six rat brain K^+ channel cDNAs was random prime-labeled and used to screen a human fetal heart cDNA library (Clontech catalog No. HL1114a). Six positive clones, isolated from 1×10^6 recombinant clones screened, were subcloned into the Bluescript II vector (Stratagene Inc, La Jolla, Calif) and found to encode portions of the K^+ channel clone isolated from human heart (fHK). The longest (1936-bp) cDNA constituted the majority of fHK with the exception of 60 bp of coding sequence at the 5' end of the gene. The missing 60-bp segment was obtained from a 500-bp overlapping clone isolated by screening the library with oligonucleotides from the 5' end of the fHK cDNA. The complete cDNA for fHK was made by attaching synthetic oligonucleotides coding for the first 60 bp (including a consensus sequence for translation initiation) onto the 5' end of the 1936-bp nearly full-length cDNA clone. The entire coding region was then subcloned into

the mammalian expression vector pRC/CMV for transfection into the human embryonic kidney cell line, HEK-293. fHK–pRC/CMV (1 μg) plasmid was linearized with *Sal* I before transfection to facilitate recombination of the plasmid DNA with the HEK chromosomal DNA. The linearized DNA (1 μg) was mixed with 50 μg lipofectin (Bethesda Research Laboratories) and used to transfect 1×10^6 HEK cells. Forty-eight hours after transfection, G418 (0.5 mg/mL) was added to the media to select for resistant clones. Antibiotic-resistant clones were selected after 2 weeks of growth and maintained in minimum essential medium, 10% fetal bovine serum, penicillin-streptomycin-fungizone (Bethesda Research Laboratories), and G418 (0.5 mg/mL).

Electrophysiology

Specimens of atrial appendages were obtained from the hearts of 10 patients undergoing aortocoronary bypass surgery, ranging in age from 48 to 72 years old. All patients had normal P waves on electrocardiography, and no patient had a history of supraventricular arrhythmias. The protocol for tissue procurement was approved by the ethics committee of the Montreal Heart Institute. The cell isolation procedure was according to the method of Fermini et al[13] in 1992, which was based on a technique described by Escande et al.[14] Only quiescent rod-shaped cells showing clear cross striations were used, and they were superfused at 3 mL/min with a Tyrode's solution containing (mM) NaCl, 126; KCl, 5.4; $MgCl_2$, 0.8; $CaCl_2$, 1.0; NaH_2PO_4, 0.33; HEPES, 10, and glucose, 5.5; pH was adjusted to 7.4 with NaOH. The bath temperature was 23° to 25°C for all data presented here. Embryonic kidney cell lines incorporating fHK were maintained at 37°C in a 95% O_2–5% CO_2 incubator in 35-mm Petri dishes on glass coverslips coated with poly-D-lysine. Coverslips were removed from the incubator before the experiments and placed in dishes containing the experimental solution at 23° to 25°C. Whole-cell currents and cell-attached patch-clamp recordings were made using variations of the patch-clamp technique. Electrodes of 1- to 5-MΩ resistance were pulled from Corning 7052 glass (thick wall, Corning Glass Inc, Corning, NY) on a horizontal Flaming-Brown micropipette puller, fire-polished, and filled with a standard internal solution for whole-cell recording that contained (mM) potassium aspartate, 120; KCl, 20; Na_2-ATP, 4.0; HEPES, 5.0; $MgCl_2$, 1.0; and EGTA, 10; pH was adjusted to 7.2 with KOH. For cardiac myocytes, a modified internal solution was used that contained (mM) KCl, 130; $MgCl_2$, 1.0; HEPES, 10; EGTA, 5.0; Mg_2-ATP, 5.0; and Na_2-creatine phosphate, 5.0; pH was adjusted to 7.2 with KOH. An EPC-7 (List Electronic) or an Axopatch 1D (Axon Instruments, Foster City, Calif) amplifier was used for voltage-clamp measurements; data were filtered at 5 to 10 kHz before digitization via a Labmaster DMA interface. The pCLAMP suite of programs was used for data acquisition and analysis. Analog capacity compensation and 50% to 70% series resistance compensation was used during all whole-cell measurements. Isolated single embryonic kidney cells used for electrophysiological analysis had a mean cell capacitance of 21.8±2.9 pF (mean±SEM, n=20). Capacitance was measured by integration of the uncorrected capacity transient. The external solution contained (mM) NaCl, 130; KCl, 5.0; sodium acetate, 2.8; $MgCl_2$, 1.0; HEPES, 10; glucose, 10; and $CaCl_2$, 1.0; pH was adjusted to 7.4 with 1N NaOH. HEK cells possessed a small endogenous delayed rectifier current that rarely exceeded 100 to 200 pA in amplitude at the most positive potentials studied and failed to inactivate during long voltage-clamp depolarizations. The overexpression of fHK at 50 to 100 times the level of endogenous current permitted a clear delineation of fHK current in whole-cell and macropatch measurements (eg, see Fig 3D). For myocytes, special steps were taken to ensure that current recordings were not contaminated by other ionic currents. Recordings were filtered at 1 kHz, series resistance was compensated, and leak current was subtracted. Sodium current was inactivated by holding the membrane potential positive to −50 mV or by isotonic replacement with choline chloride for NaCl. $CoCl_2$ was always present to block Ca^{2+} and Ca^{2+}-activated currents. To minimize contamination from other K^+ currents in myocytes, 10 mM tetraethylammonium (TEA), 1 mM $BaCl_2$, and 100 nM atropine were present in the bathing medium. Chemicals were from Sigma Chemical Co, St Louis, Mo. TEA was included in the external bath solution by equimolar replacement of NaCl. Clofilium was dissolved in dimethyl sulfoxide or Tyrode's solution to make a 0.1-M stock solution and diluted in saline to form final bath concentrations of 1 to 100 μM.

Results

We isolated fHK, a novel clone from human heart, and its amino acid sequence is compared in Fig 1 with other K^+ channels expressed in human heart. fHK differs from hPCN1, originally cloned from a human insulinoma,[15] in only three N-terminal amino acid residues. The nucleotide sequences are identical except for these three codons, but at these codons, fHK is identical to HK2 cloned from human ventricle.[11] This suggests the possibility of cloning errors in the hPCN1 sequence.

Except for two striking differences, fHK is highly homologous to HK2. HK2 lacks a unique stretch of 11 amino acids in the putative extracellular region between domains S1 and S2. Also, fHK has two potential protein kinase A phosphorylation sites in the C terminus, whereas HK2 has only one. Conversely, HK1, also from human ventricle, is quite different from fHK, particularly in the N and C termini. In the standardized nomenclature,[16] fHK, hPCN1, and HK2 might be Kv1.5 a, b, or c, respectively.

fHK is expressed in both the atrium and ventricle of adult human heart (Fig 2). Reverse transcriptase–polymerase chain reaction using total RNA from adult human atrium and ventricle results in the amplification of a 403-bp fHK fragment. Since one of the polymerase chain reaction primers comes from the unique fHK S1-S2 region, this reaction specifically detects fHK message and not HK2. Because the reverse transcriptase–polymerase chain reaction protocol is not strictly quantitative, we cannot compare the level of expression of fHK in atrium and ventricle other than to say that the gene is expressed at easily detectable levels in both tissues. The presence of fHK transcripts in human atrial tissue was confirmed by the Northern blot shown in Fig 2B.

In view of the lack of information regarding delayed rectifiers in human heart, an electrophysiological comparison was made between fHK stably expressed in a

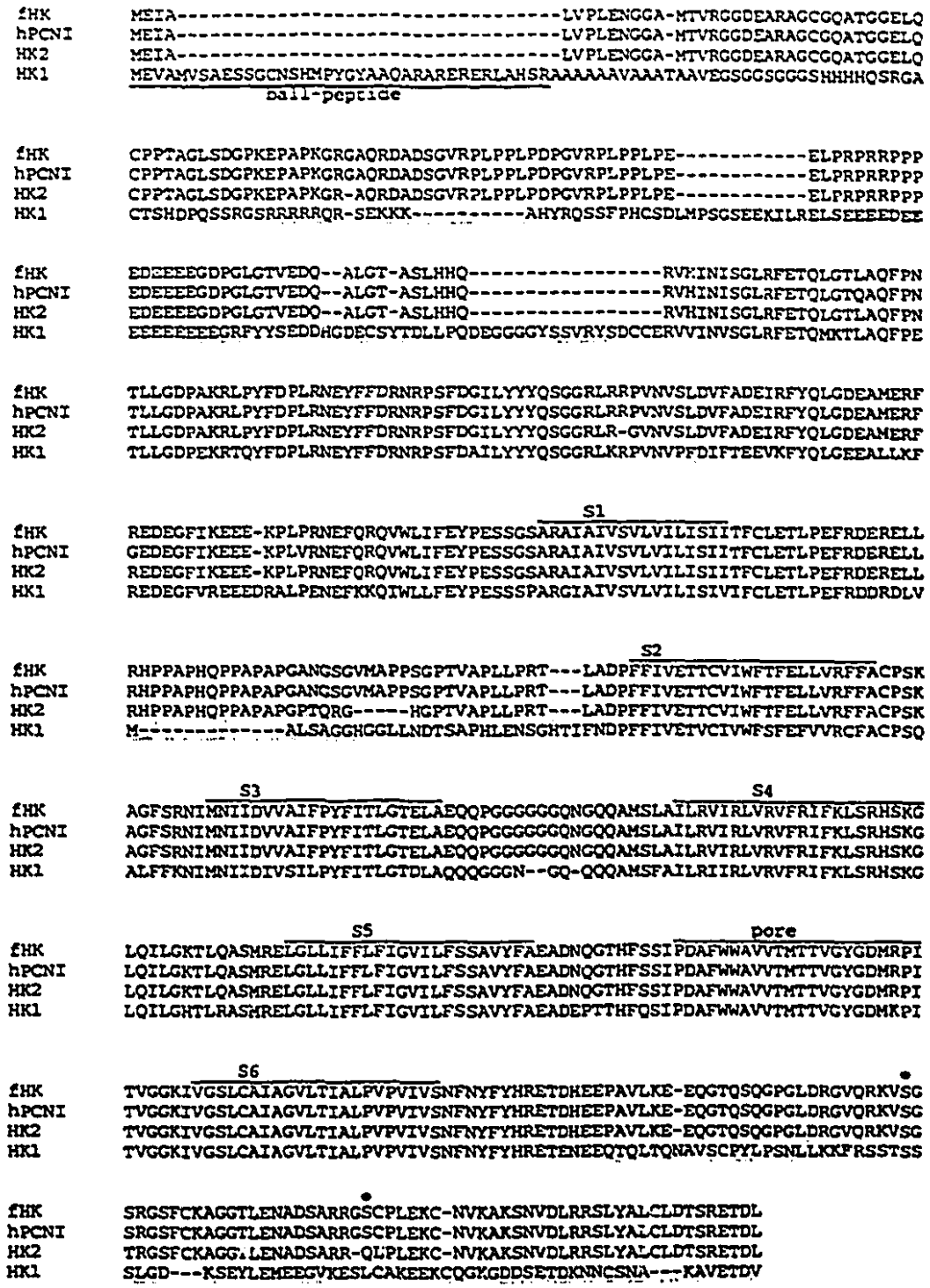

FIG 1. *Peptide sequence alignments of fHK with other cloned human K^+ channels. The deduced amino acid sequence of the novel fetal cardiac clone fHK is compared with a clone from a human insulinoma cell line (hPCN1[13]) and the HK2 and HK1 channels from human heart.[11] The highlighted regions emphasize the differences between fHK and the other channels. The thin bars indicate the six putative transmembrane domains S1-S6 and the ball peptide responsible for N-type inactivation[14,17] in HK1; the thick bar denotes the putative pore region of the subunit. The two filled circles represent the two potential protein kinase A phosphorylation sites in fHK.*

human embryonic kidney cell line, HEK-293, and K^+ currents in myocytes from healthy adult human atrium (Fig 3). Both the atrial current and current from HEK cells expressing fHK showed rapid activation that increased with depolarization. Partial slow inactivation of both currents, especially at more positive potentials, was also noted. The inactivation is not likely to be N type since fHK does not possess the N-terminal ball peptide sequence[14,17] (unlike HK1: compare with Fig 1). The striking similarities between native atrial and heterolo-

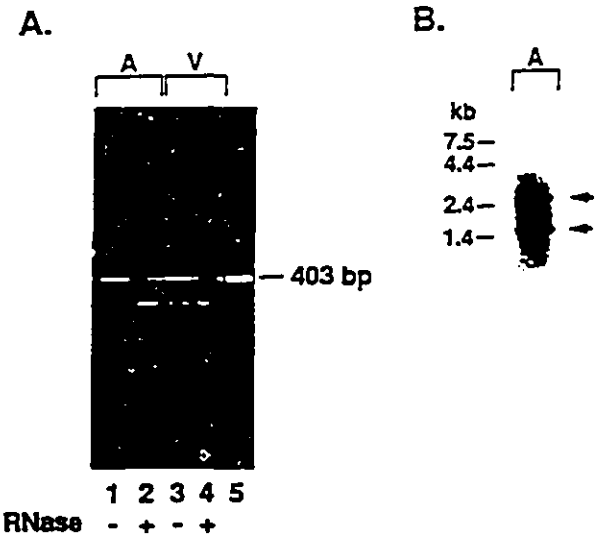

FIG 2. *K⁺ channel clone (fHK) expression in human heart total RNA. Panel A: Reverse transcriptase (RT)–polymerase chain reaction (PCR) detection of fHK sequences in adult human heart total RNA. First-strand cDNA prepared from adult human atrium (A) total RNA (lanes 1 and 2) or adult human ventricle (V) total RNA (lanes 3 and 4) was the template in a PCR using fHK-specific oligonucleotides as primers. Lanes labeled "+RNase" were products of reactions pretreated with RNase to detect the presence of contaminating genomic DNA. Lane 5 shows the expected 403-bp PCR product of this primer pair using cloned fHK cDNA template. Total RNA was prepared from adult human atrium or ventricular muscle (obtained from hypertrophic hearts removed at transplant) with the guanidinium thiocyanate–based RNagents kit (Promega Corp, Madison, Wis). Total RNA (1 μg) (with or without preincubation in the presence of 20 μg/mL DNase-free RNase [Promega] for 30 minutes at 37°C) was used as template in a first-strand cDNA synthesis reaction (RT-PCR kit, The Perkin-Elmer Corp, Norwalk, Conn) primed with random hexamers. The two oligonucleotides that were chosen as PCR primers allowed the specific amplification of fHK and not HK2 sequences. Primer 1 (5' ggggtcatggccccgccctct 3') is from the S1-S2 linker region unique to fHK, and primer 2 (5' gccccagctccctcatggaggc 3') is downstream in the S5 domain and common to both fHK and HK2. The PCR reactions were done after protocols outlined in the RT-PCR kit using 10 pmol of each primer and 35 cycles: 94°C, 30 seconds; 60°C, 30 seconds; and 72°C, 30 seconds. Ten microliters of each PCR was electrophoresed on a 1% agarose gel and visualized with ethidium bromide. In a control reaction with the fHK plasmid as template, this primer pair resulted in the amplification of a 403-bp fragment, which is the expected size based on the cloned sequence. Panel B: Northern blot analysis of fHK expression in human atrium. Human atrial total RNA (10 μg) was fractionated on a 1% agarose-methylmercury gel and transferred to nitrocellulose. The fHK-pRc/CMV plasmid was linearized with* BstEII, *and* ^{32}P*-labeled runoff antisense transcripts corresponding to the 400 bp of coding sequence at the 3' end of the cDNA were made with SP6 polymerase using the MAXIscript RNA synthesis kit (Ambion, Inc, Austin, Tex). Hybridization was performed at 65°C overnight with rapid hybridization buffer (Amersham Corp, Arlington Heights, Ill) at a probe concentration of 10⁶ cpm/mL. The blot was washed twice for 10 minutes in 2× standard saline citrate and 0.1% sodium dodecyl sulfate at room temperature, followed by two 15-minute washes in 1× standard saline citrate and 0.1% sodium dodecyl sulfate at 65°C. Autoradiography was for 20 hours. Two bands are visible, a major one at 2.5 kb and a less intense one at 1.5 kb. This is the same pattern that was observed when human atrial total RNA was probed with HK2.[11] The mobilities of the RNA size markers are noted on the left.*

gously expressed fHK currents are also apparent in the current-voltage relations and activation curves (Figs 3E and 3F). In both cases, outward current activates at approximately −30 mV and increases steeply with potential. Opening probability (Po)–voltage curves for both currents show half-activation potentials between −2 and −8 mV. The channels were selective for K⁺ ions, and the reversal potential was found to be linearly related to $\log[K^+]_o$. For atrial cells, the relation was 56.5 mV per decade (r=0.996), and for fHK, the relation was 57.9 mV per decade for $[K^+]_o$ between 0.5 and 50 mM.

The characteristics of this novel atrial delayed rectifier are different from the slow currents (I_{Ks},[3,19,20] I_{sK},[9,21] minK,[22] and the slowly activating delayed rectifier current in heart $[I_{K_s}]$[2]) and more rapid currents (rapidly activating rectifier current in guinea pig ventricle $[I_{K_r}]$[2]) classically thought to be important in repolarization in heart. I_{sK} is present in human heart but has a completely different peptide sequence to fHK. When expressed in *Xenopus* oocytes, I_{sK} activates very slowly without inactivating.[9] I_{Kr} exhibits inward rectification rather than the prominent outward rectification of the steady-state current-voltage relations noted here.

The pharmacology of this novel atrial current differs from that of I_{Kr} and I_{Ks}/I_{sK}. TEA had virtually no effect on human atrial current (4.8±2.1% reduction at 40 mM, P>.05) or fHK current (15±4.7% reduction at 100 mM, n=7). Both atrial and fHK currents were much more sensitive to 4-aminopyridine (4-AP) than previously described cardiac K⁺ channels. 4-AP at 50 μM blocked atrial K⁺ current by 51.3±3.2% and fHK current by 46.5±5.4% (n=6). In atrial myocytes, 50 μM 4-AP prolonged the action potential by 66±11%.[22] By contrast, I_{Ks} is effectively blocked by 10 mM TEA applied externally,[23,24] is relatively insensitive to 4-AP,[23] and is sensitive to micromolar concentrations of clofilium.[25] Atrial myocyte K⁺ channels were comparatively resistant to clofilium. At +20 mV, 100 μM clofilium reduced current by 41±12% (from 189±21 to 100±16 pA, n=10; holding potential, −80 or −10 mV). fHK current was resistant to clofilium with a half blocking concentration of 60±13 μM (n=6). Interestingly, HK2, which has only limited sequence differences from fHK (Fig 1), has a K_d for block by clofilium of <1.0 μM.[26] I_{Kr} was blocked by sotalol, whereas fHK was not affected by concentrations of 100 μM. The 4-AP sensitivity of the present currents may also be compared with that of the rapidly inactivating transient outward current in human atrium, which required 2 mM 4-AP for 49.7±5.1% blockade.[12] Thus, the pharmacology of the human atrial and fHK currents clearly sets them in a class apart from other native[7] and cloned cardiac delayed rectifier K⁺ channels and from transient outward currents.

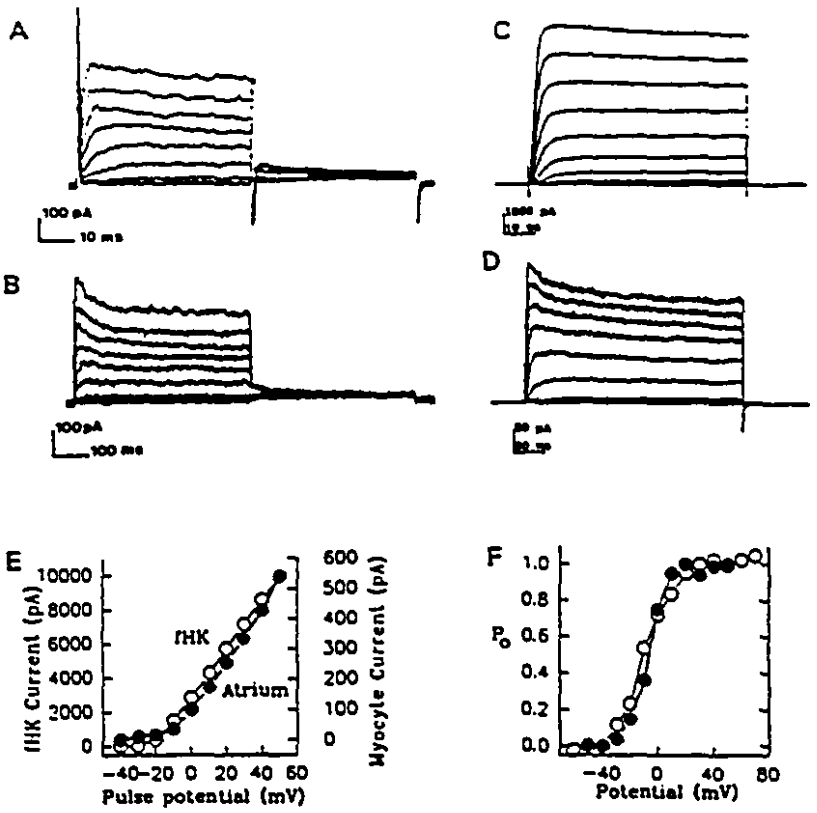

FIG 3. *Basic characteristics of the delayed rectifier current in intact human atrial myocytes and human K^+ channel clone (fHK) expressed in the human embryonic kidney cell line (HEK-293). Panels A and B: Typical examples of currents recorded from a single human atrial cell. Currents were elicited by 50-millisecond (panel A) or 500-millisecond (panel B) voltage-clamp steps from a holding potential of −50 mV to varying test potentials between −40 and +50 mV. Current tails were measured at −10 mV. To inactivate the transient outward current,[13] each test pulse was preceded by a 300-millisecond conditioning pulse to +50 mV, which ended 10 milliseconds before the test pulse. The average current amplitude at +20 mV was 268±12 pA or 3.6±0.2 pA/pF (mean±SEM, n=15). The activation time constants (Fig 3B) ranged from 13.1±2 milliseconds at 0 mV to 1.8 milliseconds at +60 mV (n=15). Panels C and D: Comparable currents recorded from HEK cells expressing the fHK clone. Voltage-clamp steps were from a holding potential of −80 mV to test potentials in the ranging from −50 to +50 mV. In panel C, the pulse duration was 100 milliseconds, and the mode of recording was whole cell. The mean current at +20 mV was 3.0±1.9 nA (n=9, 136 pA/pF). The activation time constants were 11.8±4.6 milliseconds at 0 mV to 1.6±0.2 milliseconds at +60 mV (n=9). In panel D, current was recorded in the cell-attached patch-clamp configuration during 500-millisecond depolarizing pulses. The pipette contained standard bath solution. Panel E: Graph showing typical peak current-voltage relations for atrial K^+ channel (●) and fHK (○). Atrial currents and fHK currents showed increasing currents on depolarization and partial inactivation during pulses. For atrial myocyte K^+ current, this amounted to 24.1±5.3% at +50 mV; the activation time constant was 112.4±46.7 milliseconds in 60% of cells. In HEK cells expressing fHK where the magnitude of inactivation was measured at the end of 10-second depolarizing voltage-clamp pulses, the mean inactivation was 40±8.1% (n=6, at +50 mV). Panel F: Activation curves for human atrial K^+ currents and fHK. Measurements were based on tail current amplitudes on repolarization (at −10 mV for atrial cells and −40 mV for fHK) normalized to tail amplitude on repolarization from +50 mV. The curves were fit to the relation $P_o = 1/\{1+\exp[(V-V_{0.5})/k]\}$, where P_o is the opening probability, $V_{0.5}$ is the voltage at which 50% activation occurred, and k is the slope factor. For atrial cells, $V_{0.5}$ was −6±2.5 mV (n=10). In this cell, $V_{0.5}$ was 6.8 mV, and k was 6.5 (mean±SD, 8.6±2.2; n=10). For fHK, $V_{0.5}$ was −7.1 (mean±SD, −4.1±6.8 mV; n=8), and k was 7.0.*

K^+ channels with single-channel conductances ranging from 5.4 to 16 picosiemens have been suggested to mediate delayed rectification in heart tissue from a number of species, although none were human.[4,27-29] Yue and Marban[4] have described a rapidly activating K^+ channel (14 picosiemens) similar to the macroscopic rectifiers in rat heart.[5,7] Because of the high expression density of fHK channels in HEK cells, it was difficult to obtain single-channel patches. Patches with multiple channels (2 to 10) could be obtained relatively easily, and transition amplitudes similar to those shown in Fig 4 could be seen. Ensemble currents inactivated during step depolarizations of 0.2 to 1 second in duration. Single-channel patches could sometimes be obtained using high-resistance electrodes (<10 MΩ). During 70-mV depolarizations, such single-channel patches (Fig 4A) revealed openings of fHK channels of approximately 1.2 pA in size. Mean slope conductance for patches from four cells was 16.9 picosiemens (Fig 4D). The ensemble average produced a rapid outward current (Fig 4B) that relaxed slightly toward the end of the pulse, consistent with the kinetics of whole-cell currents.

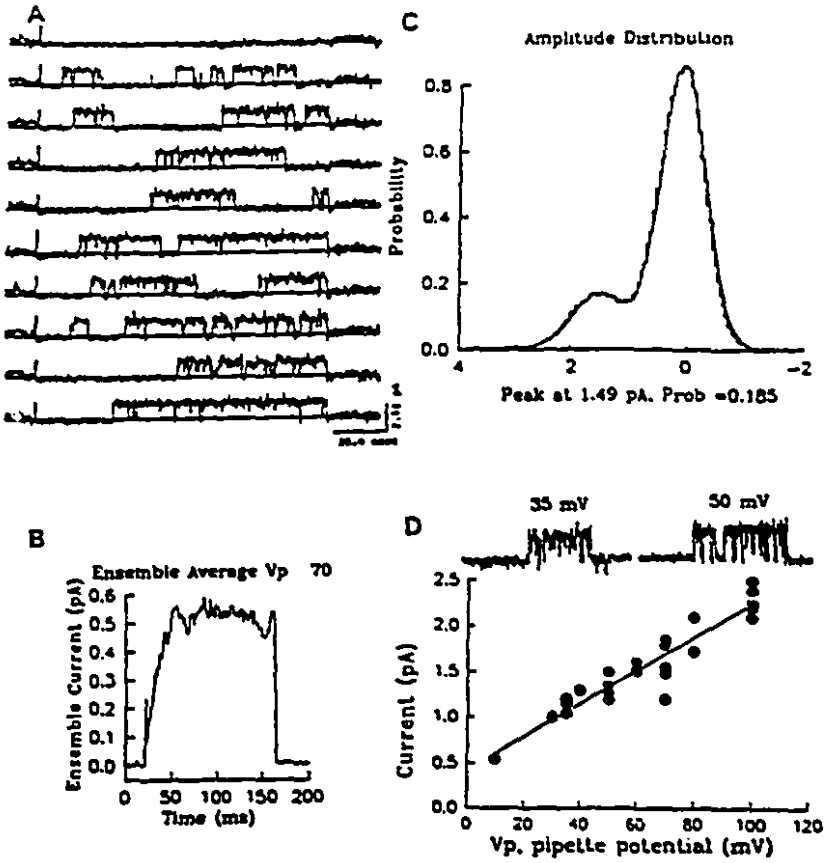

FIG 4. *Cell-attached patch-clamp recordings of human K^+ channel clone (fHK). The bath contained 5 mM K^+, and the same solution was used in the recording pipette. Clone J9, a relatively low expressing cell line, was used in an attempt to make membrane patches that contained only a single K^+ channel. Data were recorded at 4 kHz and digitized at 10 kHz. All recordings in panel A have been leak- and capacity-subtracted and are shown here filtered at 1 kHz. In panel A are sequential sweeps of single-channel activity during 140-millisecond step changes in pipette potential (Vp) from 0 to 70 mV applied 20 milliseconds after the start of each data tracing. Note that the mean resting potential of human embryonic kidney cells expressing fHK was −42 mV so that a Vp of +70 mV correlates with a whole-cell potential of ≈+30 mV. The ensemble current in panel B is the average of 247 sweeps at this pipette potential and shows the macroscopic time course of whole-cell current through these channels. The event amplitude distribution at this potential is shown in panel C for a bin width of 0.05 pA. The peak open probability was ≈0.6 at this test potential, and the channel opening peak occurred at 1.49 pA. The current-voltage diagram for single-channel currents is shown in panel D. Representative recordings of single-channel openings are shown at potentials of +35 and +50 mV with respect to the cell resting potentials. In the graph shown in panel D, single-channel amplitudes have been plotted against the applied pipette potential for data from four patches and have been fitted by a least-squares linear regression method. The resultant mean slope conductance of the single channels in 5 mM bath K^+ was 16.9 pS.*

Discussion

This study constitutes the first demonstration that a delayed rectifier current in native myocytes from human heart has properties identical with current carried by a cloned K^+ channel from human heart and expressed in a human cell line. The atrial current can provide important control of repolarization in human heart, and this K^+ channel must now be considered as a target for antiarrhythmic drug research and therapies. The very rapid activation of this delayed rectifier K^+ current indicates that it is time to reevaluate the mechanisms of termination of human heart action potentials.

Acknowledgments

This study was supported by grants from the National Institutes of Health and Marion Merrell Dow (Dr Brown); the Heart and Stroke Foundation of Ontario (Dr Fedida); and the Medical Research Council of Canada, Quebec Heart Foundation, Fonds de Recherche de l'Institut de Cardiologie de Montreal (Drs Nattel and Fedida).

References

1. Noble D, Tsien RW. Outward membrane currents activated in the plateau range of potentials in cardiac Purkinje fibres. *J Physiol (Lond)*. 1969;200:205-231.
2. Sanguinetti MC, Jurkiewicz NK. Two components of cardiac delayed rectifier K^+ current. *J Gen Physiol*. 1990;96:195-215.
3. Matsuura H, Ehara T, Imoto Y. An analysis of the delayed outward current in single ventricular cells of the guinea-pig. *Pflugers Arch*. 1987;410:596-603.
4. Yue DT, Marban E. A novel cardiac potassium channel that is active and conductive at depolarized potentials. *Pflugers Arch*. 1988;413:127-133.
5. Boyle WA, Nerbonne JM. A novel type of depolarization-activated K^+ current in isolated adult rat atrial myocytes. *Am J Physiol*. 1991;260(*Heart Circ Physiol* 29):H1236-H1247.

6. Wallert MA, Ackerman MJ, Kim D, Clapham DE. Two novel cardiac atrial K^+ channels, I_{KAA} and I_{KPC}. *J Gen Physiol.* 1991;98:921-939.
7. Paulmichl M, Nasmith P, Hellmiss R, Reed K, Boyle WA, Nerbonne JM, Peralta EG, Clapham DE. Cloning and expression of a rat cardiac delayed rectifier potassium channel. *Proc Natl Acad Sci U S A.* 1991;88:7892-7895.
8. Roberds SL, Tamkun MM. Cloning and tissue-specific expression of five voltage-gated potassium channel cDNAs expressed in rat heart. *Proc Natl Acad Sci U S A.* 1991;88:1798-1802.
9. Folander K, Smith JS, Antavanage J, Bennett C, Stein RB, Swanson R. Cloning and expression of the delayed-rectifier I_K channel from neonatal rat heart and diethylstilbestrol-primed rat uterus. *Proc Natl Acad Sci U S A.* 1990;87:2975-2979.
10. Honoré E, Attali B, Romey G, Heurteaux C, Ricard P, Lesage F, Lazdunski M, Barhanin J. Cloning, expression, pharmacology and regulation of a delayed rectifier K^+ channel in mouse heart. *EMBO J.* 1991;10:2805-2811.
11. Tamkun MM, Knoth KM, Walbridge JA, Kroemer H, Roden DM, Glover DH. Molecular cloning and characterization of two voltage-gated K^+ channel cDNAs from human ventricle. *FASEB J.* 1991; 5:331-337.
12. Wang Z, Fermini B, Nattel S. An ultra-rapidly activating delayed rectifier carries sustained outward current in human atrial myocytes. *Biophys J.* 1993;64:A199. Abstract.
13. Fermini B, Wang Z, Duan D, Nattel S. Differences in rate dependence of transient outward current in rabbit and human atrium. *Am J Physiol.* 1992;263:H1747-H1754.
14. Escande D, Coulombe A, Faivre J-F, Deroubaix E, Coraboeuf E. Two types of transient outward current in adult human atrial cells. *Am J Physiol.* 1987;252:H142-H148.
15. Philipson LH, Hice RE, Schaefer K, LaMendola J, Bell GI, Nelson DJ, Steiner DF. Sequence and functional expression in Xenopus oocytes of a human insulinoma and islet potassium channel. *Proc Natl Acad Sci U S A.* 1991;88:53-57.
16. Ruppersberg JP, Frank R, Pongs O, Stocker M. Cloned neuronal I_K(A) channels reopen during recovery from inactivation. *Nature.* 1991;353:657-660.
17. Hoshi T, Zagotta WN, Aldrich RW. Biophysical and molecular mechanisms of Shaker potassium channel inactivation. *Science.* 1990;250:533.
18. Chandy KG. Simplified gene nomenclature. *Nature.* 1991;352:26.
19. McDonald TF, Trautwein W. The potassium current underlying delayed rectification in cat ventricular muscle. *J Physiol (Lond).* 1978;274:217-246.
20. Giles WR, Shibata EF. Voltage clamp of bull-frog cardiac pacemaker cells: a quantitative analysis of potassium currents. *J Physiol (Lond).* 1985;368:265-292.
21. Takumi T, Ohkubo H, Nakanishi S. Cloning of a membrane protein that induces a slow voltage-gated potassium current. *Science.* 1988;242:1042-1045.
22. Blumenthal EM, Kaczmarek LK. Structure and regulation of the MinK potassium channel. *Neurochem Res.* 1992;17:869-876.
23. Kenyon JL, Gibbons WR. Influence of chloride, potassium, and tetraethylammonium on the early outward current of sheep cardiac Purkinje fibers. *J Gen Physiol.* 1979;78:117-138.
24. Kass RS, Scheuer T, Malloy KJ. Blockade of outward currents in cardiac Purkinje fibers by injection of quaternary ammonium compounds. *J Gen Physiol.* 1982;79:1041-1063.
25. Arena JP, Kass RS. Block of heart potassium channels by clofilium and its tertiary analogs: relationship between drug structure and type of channel blocked. *Mol Pharmacol.* 1988;34:60-66.
26. Snyders DJ, Knoth KM, Roberds SL, Tamkun MM. Time-, voltage-, and state-dependent block by quinidine of a cloned human cardiac potassium channel. *Mol Pharmacol.* 1992;41:322-330.
27. Shibasaki T. Conductance and kinetics of delayed rectifier potassium channels in nodal cells of the rabbit heart. *J Physiol (Lond).* 1987;387:227-250.
28. Balser JR, Bennett PB, Roden DM. Time-dependent outward current in guinea pig ventricular myocytes: gating kinetics of the delayed rectifier. *J Gen Physiol.* 1990;96:835-863.
29. Clapham D, Logothetis D. Delayed rectifier K^+ current in embryonic chick heart ventricle. *Am J Physiol.* 1988;254:H192-H197.

Potassium channels are structurally and functionally the most diverse ion channels in the heart. K^+ currents identified in human heart to date are no less than half a dozen, including I_{to1}, I_K, I_{Kur}, I_{K1}, $I_{K,Ach}$ and I_{KATP}. I_{K1} in human atrial cells is known to be responsible for maintaining the resting membrane potential but has less importance in initiating repolarization due to its strong inward rectification property. A contribution of $I_{K,Ach}$ would show up under situations associated with increased vagal tone, while I_{KATP} would be expected to play a role during myocardia ischemia. I_{to1} was found in most human atrial cells, and its large size confers significance as a major repolarizing current, but its rapid kinetics limits its direct contribution to only the early phase of repolarization. I_K exists in a majority of cells, and it develops slowly with time during depolarization. This current may be important in controlling the duration of the plateau and late phases of repolarization. Finally, I_{Kur}, a novel depolarization-induced K^+ current, was seen in almost all human atrial cells, and this current activates rapidly with a time constant in the same range as I_{to1} (or even faster), and about two orders of magnitude faster than classical I_K. The time and rate independent properties of I_{Kur} suggest that it is involved in controlling the duration of the plateau phase of the action potential. These latter three voltage-dependent K^+ currents are the major repolarizing currents in human atrium.

Recently, another category of ion currents, the chloride currents, have been added to the long list of cardiac ion currents, including cAMP-induced Cl^- current, PKC-activated Cl^- current, ATP-activated Cl^- current, Ca^{++}-activated Cl^- current, swelling-induced Cl^- current, and depolarization-induced Cl^- current. These Cl^- currents have the ability to influence membrane potential and repolarization. We were interested in exploring these currents in human atrial cells.

Comparative Mechanisms of 4-Aminopyridine-resistant Transient Outward Current in Human and Rabbit Atrial Myocytes

GUI-RONG LI, JIANLIN FENG, ZHIGUO WANG,
BERNARD FERMINI, AND STANLEY NATTEL
Department of Medicine, Montreal Heart Institute,
University of Montreal (G-RL, JF, BF, SN), and
Department of Pharmacology and Therapeutics, McGill
University (ZW, SN), Montreal, Quebec, H1T 1C8, Canada

Running Head: I_{to} in Human and Rabbit Atrium

Supported by operating grants from the Medical Research Council of Canada, the Quebec Heart Foundation, and the Fonds de recherche de l'Institut de Cardiologie de Montréal (FRICM). Zhiguo Wang was supported by a Canadian Heart Foundation studentship award, and Dr. Bernard Fermini was a Knoll-Fonds de la recherche en santé du Québec (FRSQ) research scholar.

Address for reprint requests: S. Nattel, Montreal Heart Institute, 5000 Belanger Street E., Montreal, Quebec, H1T 1C8, Canada. Telephone: (514) 376-3330; Fax: (514 376-1355.

ABSTRACT

The cardiac transient outward current (I_{to}) has been shown in several species to consist of two components on the basis of the response to 4-aminopyridine (4AP) – a 4AP-sensitive component (I_{to1}) and a 4AP-resistant component (I_{to2}). In rabbits, I_{to2} has been shown to be a Ca^{2+}-dependent Cl^- current ($I_{Cl,Ca}$), and similar mechanisms have been suggested to underlie I_{to2} in human atrium. We used whole-cell patch-clamp techniques to define the mechanism of I_{to2} (defined as the component resistant to 5 mM 4AP) in human atrial myocytes, with parallel experiments performed in rabbit atrial cells. In rabbit atrium, I_{to2} activated more slowly than I_{to1} and had a bell-shaped current-voltage relation. Ryanodine suppressed a component of I_{to} in the rabbit with properties similar to I_{to2}, and a similar component was recorded when the pipette solution contained Cs^+ in the place of K^+. In human cells, a 4AP-resistant I_{to} was recorded at a depolarizing pulse frequency of 1 Hz, but not at 0.1 Hz. As previously reported, I_{to2} in human atrium activated rapidly and inactivated earlier than I_{to1}. The current-voltage relation of I_{to2} was linear and had a similar form to that of I_{to1}. Ryanodine had no effect on human atrial I_{to}, and when K^+-free pipette solutions were used no I_{to} was recorded in 30 human atrial myocytes. Caffeine (10 mM) has previously been reported to suppress human atrial I_{to2}, suggesting a component dependent on sarcoplasmic reticulum Ca^{2+} release and apparently conflicting with the results of our studies with ryanodine. We confirmed that caffeine suppresses human atrial I_{to}, but found that caffeine suppresses I_{to1} (in the presence of 200 μM Cd^{2+} to block I_{Ca} and intracellular dialysis with 5 mM EGTA to buffer $[Ca^{2+}]_i$) in both human and rabbit atrium, indicating an action unrelated to Ca^{2+}-triggered Ca^{2+} release. We conclude that 4AP-resistant I_{to} in human atrium is due to use-dependent 4AP unblocking, a well-described phenomenon, and not $I_{Cl,Ca}$.

Index Terms: Potassium currents - ECG - Arrhythmias, atrial - 4-Aminopyridine - Human atrial cells - Whole cell patch-clamp - Caffeine

INTRODUCTION

The existence of a depolarization-induced transient outward current (I_{to}) in cardiac Purkinje fibers has been recognized since the 1960's (8, 9, 14). Initially believed to be a chloride current (9, 14), I_{to} was subsequently shown in sheep cardiac Purkinje fibers to be due predominantly to an increase in potassium conductance (22). With the advent of whole-cell voltage- clamp techniques, the presence of I_{to} was demonstrated in a wide range of cardiac tissues. These include ventricular cells from the rat (21), rabbit (12, 20, 23), dog (33), ferret (5) and man (2), atrial cells from the rabbit (16, 17), elephant seal (27), dog (34), and man (11, 29), and atrioventricular nodal cells of rabbits (28). Time-dependent recovery of the transient outward current has been implicated in rate-dependent changes of action potential duration and morphology in sheep cardiac Purkinje fibers (3), rabbit ventricle (20, 23), and dog ventricle (24). Important transmural differences in I_{to} density exist in the ventricles of rabbits (12), dogs (1, 25), and cats (15), and may be central in determining the generation of the electrocardiographic T wave, as well as the cellular response to ischemic injury (26). In summary, I_{to} is a repolarizing current of potentially-great physiological importance distributed across a wide range of tissues and species.

Since the seminal report of Kenyon and Gibbons (22), 4-aminopyridine (4AP) has been used widely as a selective inhibitor of transient outward K^+ currents. In the latter report, the authors identified a 4AP-resistant component of I_{to} in sheep cardiac Purkinje fibers that was reduced by Cl^- replacement. A variety of investigators have subsequently reported evidence for distinct 4AP-sensitive and 4AP-resistant components of I_{to} in sheep Purkinje fibers (7), rabbit ventricular (19, 38) and atrial cells (37), dog ventricular cells (33) and human atrial cells (11, 35). The 4AP-sensitive and 4AP-resistant components are often termed "I_{to1}" and "I_{to2}" respectively, after Tseng and Hoffman (33).

Many interventions that impair the increase in cytosolic Ca^{2+} caused by Ca^{2+}-triggered sarcoplasmic reticulum (SR) release of Ca^{2+}, including intracellular dialysis with molar quantities of EGTA, blockade of sarcolemmal voltage-dependent Ca^{2+} channels, the substitution of Sr^{2+} for Ca^{2+} in the extracellular fluid, and the inhibition of SR function with caffeine or ryanodine, suppress I_{to2} (7, 11, 19, 33). Along with observations of predominant Ca^{2+}-dependent transient outward currents in some tissues (27, 30), these results have led to the widespread assumption that I_{to2} is a current resulting from the modulation of membrane conductance by Ca^{2+}-triggered SR Ca^{2+} release. Elegant studies by Zygmunt and Gibbons (37, 38) showed that in rabbit heart I_{to2} results from precisely this type of Ca^{2+}-mediated regulation of membrane permeability to Cl^- ions. It may not be the case, however, that I_{to2} in all tissues results from the same mechanism. Dukes and Morad (10) provided evidence to suggest that in rat ventricle there is only a single component of I_{to} that is modulated by extracellular Ca^{2+}, Na^+, caffeine and ryanodine independently of changes in intracellular free Ca^{2+} concentrations. Furthermore, 4AP block is markedly state-dependent, so that block is relieved at faster depolarization frequencies, and the kinetics of residual I_{to1} are altered by time-dependent blocking and unblocking (6, 31, 36). It has been suggested that the 4AP-resistant component of I_{to} may in some systems be due to 4AP unblocking (4).

The transient outward current is a large and important repolarizing current in the human atrium (11, 29). Escande et al (11) reported the presence of 4AP-sensitive and resistant I_{to} components in human atrial cells. Like Ca^{2+}-dependent I_{to2} in other systems, human atrial I_{to2} was resistant to 2-3 mM 4AP and inhibited by exposure to 10 mM caffeine; however, unlike other types of I_{to2} (7, 27, 33, 37, 38), the 4AP-resistant component in human atrium reached its peak earlier than overall I_{to} and did not generally exhibit a bell-

shaped current-voltage relation. The latter results are compatible with 4AP unblocking as the mechanism of 4AP-resistant I_{to} in human atrial myocytes. The present experiments were designed to determine whether a 4AP-resistant, Ca^{2+}-dependent I_{to2}, possibly carried by Cl^- ions as in rabbit atrium, exists in human atrial cells, or whether human atrial I_{to} can be attributed to a single entity with 4AP unblocking accounting for the drug-resistant moiety. We used rabbit atrial cells as a reference system, since the properties of I_{to2} have been well-characterized in the latter model as a Ca^{2+}-dependent Cl^- current ($I_{Cl,Ca}$).

METHODS

Single Atrial Myocyte Preparation

Atrial cells were isolated from specimens of human right atrial appendage obtained from patients undergoing coronary bypass surgery. The procedure for obtaining the tissue was approved by the Ethics Committee of the Montreal Heart Institute. All atrial specimens were grossly normal at the time of excision. Upon excision, the samples were immediately placed in oxygenated, nominally Ca^{2+}-free Tyrode solution for transport to the laboratory. The time between excision and the beginning of laboratory processing was about 5 min. Atrial myocytes were enzymatically isolated with a technique based on the approach of Escande et al (11). Briefly, the tissue was chopped with scissors into cubic chunks (approximately 1 mm^3) in nominally Ca^{2+}-free Tyrode solution (36°C). The tissue was then placed in a 25-ml flask containing 10 ml of the Ca^{2+}-free Tyrode solution, gently agitated by continuous bubbling with 100% O_2, and stirred with a magnetic bar. After 12 min in this solution, the chunks were reincubated in a similar solution containing 300 U/ml collagenase (CLS II, Worthington Biochemical, Freehold, NJ) and 4.0 U/ml protease (Type XXIV, Sigma Chemicals, St. Louis, MO) for 45 min. The supernatant was then removed and discarded. The chunks were then reincubated in a fresh enzyme solution with 300 U/ml collagenase. Microscopic examination of the medium was performed every 5-10 min to determine the number and quality of the isolated cells. When the yield appeared to be maximal, the chunks were suspended in a hyperkalemic storage medium with the following composition (mM): KCl 20, KH_2PO_4 10, glucose 10, glutamic acid (K salt) 70, β-hydroxybutyric acid 10, taurine 10, EGTA 0.5, albumin 0.5%; pH adjusted to 7.3 with KOH, and gently pipetted. The isolated myocytes were kept in the medium at least 1 hour before the experiment.

Rabbits weighing between 1.4 and 2.3 kg were killed by cervical dislocation, according to procedures approved by the Animal Care Committee of the Montreal Heart Institute. The heart was rapidly removed and mounted on a Langendorff apparatus, and perfused with a HEPES-buffered modified Tyrode solution (37°C, 100% O_2, pH adjusted to 7.4 with NaOH) until clear of blood. The heart was perfused with nominally Ca^{2+}-free Tyrode solution for 10 min, then perfused with Ca^{2+}-free Tyrode solution containing 0.04% collagenase (CLS II, Worthington Biochemical) and 4.0 U/ml protease (Type XXIV, Sigma Chemicals) for 8-10 min, and finally exposed to solution with collagenase alone for 3-5 min. After that, the left atrium was removed and placed in hyperkalemic storage medium. Cells were dispersed by mechanical agitation using a Pasteur pipette. The isolated cells were kept in storage medium at room temperature for subsequent use.

A small aliquot of the solution containing the isolated cells was placed in an open perfusion chamber (1 ml) mounted on the stage of an inverted microscope. Myocytes were allowed to adhere to the bottom of the dish for 5-10 min, and were then superfused at 2-3 ml/min with Tyrode solution. Experiments were

conducted at room temperature (22-24°C). Only quiescent rod-shaped cells showing clear cross-striations were used.

Solutions

Tyrode solution had the following composition (mM): NaCl 126, KCl 5.4, $MgCl_2$ 1.0, $CaCl_2$ 1.8, NaH_2PO_4 0.33, glucose 10 and HEPES 10, pH adjusted to 7.4 with NaOH. For cell dissociation, Ca^{2+} was omitted. A Tyrode solution with reduced Cl^- content was used in some experiments, and contained (mM): Na methanesulfonate 126, KCl 5.4, $MgCl_2$ 1.0, $CaCl_2$ 1.8, NaH_2PO_4 0.33, glucose 10 and HEPES 10, pH adjusted to 7.4 with NaOH. The standard pipette solution contained (mM): KCl 20, K aspartate 110, $MgCl_2$ 1.0, HEPES 10, EGTA 0.025, Na_2ATP (or Mg_2ATP) 5. A K^+-free pipette solution was used in some experiments, and contained (mM): Cs aspartate 110, CsCl 20, $MgCl_2$ 1.0, HEPES 10, EGTA 0.025, Na_2ATP 5 (pH adjusted to 7.2 with CsOH). In some experiments, the pipette solution EGTA concentration was increased to 5 mM, as indicated below.

4-aminopyridine (4AP) was purchased from Sigma Chemicals, and was prepared as a 5 M stock solution, with pH adjusted to 7.0 with hydrochloric acid. Small quantities of the stock solution were added to the superfusate when required, to produce a final concentration of 5 mM. Ryanodine was obtained from Biomol Research Labs (Plymouth Meeting, PA) and prepared as a 20 mM stock solution in distilled water. The effect of ryanodine was determined on the basis of at least 10 min of superfusion with the compound at a 2 μM concentration.

Data Acquisition and Analysis

The whole-cell patch-clamp technique was used to record ionic currents. Borosilicate glass (1.0 mm O.D.) pipettes were prepared with the use of a Brown-Flaming puller (Model P-87), to produce a tip resistance of 2-4 MΩ when filled with the solutions described above. The pipettes were connected to a patch-clamp amplifier (Axopatch 1-D, Axon Instruments, Foster City, CA). Command pulses were generated by a 12-bit digital-to-analog converter controlled by pClamp software (Axon Instruments). Recordings were low-pass filtered at 2 kHz, and data were acquired by analog-to-digital conversion at a maximum rate of 100 kHz (model TM 125, Scientific Solutions, Solon, OH) and stored on the hard disk of an IBM compatible computer. Junction potentials (2-10 mV) were nulled before the pipette touched the cell. A tight seal (>10 GΩ) was produced with gentle suction. After the seal had been established, the cell membrane was ruptured to establish the whole-cell configuration.

The series resistance (R_s) was electronically compensated to minimize the duration of the capacitive transient, while avoiding ringing. R_s along the clamp circuit was estimated by dividing the time constant obtained by fitting the decay of the capacitive transient by the calculated membrane capacitance (the time integral of the capacitive response to a 5-mV hyperpolarization step from a holding potential of -60 mV) (21, 38). Before R_s compensation, decay of the capacitance was expressed by a single exponential having a time constant of 495±80 μs in human (cell capacitance: 79.6±6.7 pF) and 461±36 μs in rabbit (cell capacitance: 74.0±3.6 pF) myocytes respectively. After compensation, these values were reduced to 245±50 μs in human (cell capacitance 74.5±5.7 pF) and 272±19 μs in rabbit (cell capacitance: 63.0±3.1 pF) cells. The initial R_s was 6.2±1.5 MΩ in human and 6.2±0.5 MΩ in rabbit cells, and was reduced to 3.3±1.1 MΩ and 3.2±0.3 MΩ respectively by compensation.

Paired and unpaired Student's *t* tests were used as appropriate to evaluate the statistical significance of differences between means. Values of $P < 0.05$ were considered to indicate significance. Data are expressed as mean ± SE.

RESULTS

Effects of 4AP on I_{to} in Rabbit and Human Atrial Cells

4-aminopyridine inhibited I_{to} in both human and rabbit atrial myocytes. Fig. 1 displays representative traces of I_{to} in a rabbit myocyte before and after 5 mM 4AP. The basic frequency used was 0.1 Hz, because of the strong depressant effect of more rapid pulsing on I_{to1} in rabbit atrium (13, 16, 17). An initial inward I_{Ca} was followed by a transient outward current (Control). The addition of 4AP reduced the amplitude of I_{to}, leaving a 4AP-resistant current (middle of panel A) that activated more slowly than I_{to} in the absence of 4AP. Fig. 1B shows corresponding traces in a human cell under control conditions and after the addition of 4AP with a pulse rate of 1 Hz. The 4AP-resistant current in the human cell (middle of panel B) activates much more rapidly than 4AP-resistant current in the rabbit, and inactivates rapidly.

The current-voltage (I-V) relations for I_{to} before and after 4AP are shown at the bottom of Fig. 1A (for rabbit) and 1B (for human myocytes). All transient outward currents were measured from the peak current to the steady-state level at the end of the pulse. In human myocytes, the I-V relation of control and 4AP-resistant currents have similar general forms, with current continuing to increase at more positive voltages. In contrast, 4AP-resistant current in the rabbit has a bell-shaped I-V relation, with peak current decreasing at voltages positive to -40 mV. On the other hand, 4AP-sensitive current in the rabbit has an I-V relation with a form similar to that of net I_{to} and 4AP-resistant current in human myocytes.

Ryanodine has been used as a tool to demonstrate the dependence of the Ca^{2+}-dependent transient outward current on SR Ca^{2+} release. Fig. 2 shows the effect of exposure to 2 μM ryanodine on I_{to} in rabbit atrial cells. At a frequency of 0.1 Hz, ryanodine inhibits a portion of I_{to} that activates more slowly than the aggregate current, leaving a more rapidly-activating component (Fig. 2A). Similar results were obtained in 5 cells. The addition of 4AP leaves a component similar in appearance to the ryanodine-sensitive current (Fig. 2B), and the subsequent addition of ryanodine eliminates the 4AP-resistant component, leaving only a transient inward current in this cell and five others studied with this protocol.

Fig. 3 shows the effects of ryanodine on I_{to} in a human atrial cell. The current recorded in the presence of ryanodine (filled circles) closely overlapped control (open circles) current. Digital subtraction of current after ryanodine from control current (triangles) showed no appreciable ryanodine-sensitive component. Fig. 4 compares peak I-V relations for I_{to} before (open circles) and after (filled circles) exposure to 2 μM ryanodine in five rabbit (left) and 11 human (right) atrial myocytes. Ryanodine significantly reduced I_{to} in rabbit atrium between 0 and +60 mV, but had no significant effect on I_{to} in human atrium at any voltage. The ryanodine-sensitive current had a bell-shaped I-V relation in rabbit atrium, but the ryanodine-sensitive current was not significantly different from zero at any voltage in human atrial cells.

Calcium-Independence of 4AP-resistant I_{to} in Human Atrium

The lack of change in I_{to} after exposure to ryanodine in human atrial cells argues against a calcium-dependent 4AP-resistant current as reported in other tissues (7, 19, 32, 33). At a depolarization frequency of 1 Hz, we observed a 4AP-resistant component of I_{to} in human atrium (Fig. 1) that kinetically resembles the 4AP-resistant component described by Escande et al (11). At a frequency of 0.1 Hz, however, very

little 4AP-resistant current was observed in human atrial cells, as shown in Fig. 5. Fig. 5A shows currents recorded from a cell with the standard superfusion solution (i.e. no inhibition of Ca^{2+} current). Under control conditions, depolarization for 200 ms from -50 to +30 mV produced a transient outward current (open circle). In the presence of 5 mM 4AP and at a frequency of 1 Hz, a brief outward current is seen (open triangle), decaying rapidly to a steady-state level. In the presence of 5 mM 4AP and at 0.1 Hz, only an inward Ca^{2+} current is seen (filled circle). The amplitude of I_{to} under each condition was measured from the peak to the steady-state current level at the end of the pulse. The mean I-V relation for each condition (6 cells) is shown at the bottom of panel A.

Fig. 5B shows corresponding data obtained in the presence of 200 μM Cd^{2+} to inhibit I_{Ca}. In the absence of Ca^{2+} current, which overlaps with and confounds the analysis of I_{to} in panel A, a clear transient outward current is recorded under control conditions. In the presence of 4AP (5 mM) at 1 Hz, a 4AP-resistant component is evident, peaking slightly earlier and inactivating slightly more rapidly than the control current. At 0.1 Hz, no 4AP-resistant component is seen, and there is crossover between currents at the two frequencies as expected for open-channel unblocking of 4AP (6). The I-V relation for 7 cells is shown at the bottom of panel B. In the absence of Ca^{2+} current, the I-V relation of 4AP-resistant current at 1 Hz resembles that recorded in the presence of Ca^{2+} current (i.e. without Cd^{2+}, Fig. 5A), and in both the presence and absence of I_{Ca}, 4AP-resistant current is suppressed at slow depolarization rates. These results suggest that the presence of 4AP-resistant I_{to} is not dependent on the presence of I_{Ca}, and is likely to be due to use-dependent 4AP unblocking, as previously described (6, 31, 36).

Tseng and Hoffman (33) only recorded clear I_{to2} in dog ventricular cells when I_{Ca} was increased by adding isoproterenol to the bath or by increasing $[Ca^{2+}]_o$. We attempted to elicit 4AP-resistant, Ca^{2+}-dependent I_{to} under such conditions in human atrial cells. Fig. 6A shows currents elicited from one human atrial myocyte. When 1 μM isoproterenol was added in the presence of 4AP and at a frequency of 0.1 Hz (Fig. 6B), I_{Ca} was increased, but no 4AP-resistant transient outward current was seen. When the frequency was increased to 1 Hz, small rapidly-decaying 4AP-resistant currents of the type seen at 1 Hz in the absence of isoproterenol (Fig. 5A) were seen. Similar results were obtained in a total of three cells.

Studies of Cl⁻ Currents Under Conditions Minimizing K^+ Currents

Zygmunt and Gibbons (37) have shown that I_{to2} in rabbit atria is carried by a Ca^{2+}-dependent Cl^- current (I_{ClCa}). It is possible that our inability to detect a Ca^{2+}-dependent component of I_{to} is due to overlapping currents which obscure I_{ClCa}. We therefore replaced K^+ in the pipette solution with equimolar concentrations of Cs^+. Fig. 7 shows illustrative examples of currents recorded upon depolarization from -50 mV to various potentials for 250 ms in a human atrial cell (panel A) and a rabbit atrial cell (panel B). In the rabbit cell, time-dependent outward currents typical of I_{ClCa} are recorded following the inward I_{Ca} transient. In the human cell, only a Ca^{2+} current is recorded, with no evidence of an outward Cl^- component. Results similar to those in panel B were obtained in a total of six rabbit atrial cells. We applied the same techniques to 30 human atrial cells, and always obtained results similar to those in panel A, i.e. no evidence for I_{ClCa} was obtained. Panel C shows the I-V relation for I_{ClCa} in rabbit cells. The I-V relation is bell-shaped, and has a form similar to the I-V relation for 4AP-resistant current (Fig. 1C) and ryanodine-sensitive current (Fig. 4A) in rabbit atrial cells.

Effects of Caffeine on I_{to} in Human and Rabbit Atrial Myocytes

In the initial report of transient outward currents in human atrium, Escande et al (11) showed that the 4AP-resistant component of I_{to} in human atrial cells is suppressed by 10 mM caffeine. Since we did not observe ryanodine sensitivity of I_{to2} in human atrial cells, we considered the possibility that caffeine might suppress I_{to} by a mechanism unrelated to Ca^{2+}-triggered SR Ca^{2+} release. We studied cells under conditions designed to minimize transient increases in free cytosolic Ca^{2+} concentrations, a combination of dialysis with 5 mM EGTA in the pipette solution and the addition of 200 μM Cd^{2+} to the superfusate to block I_{Ca}. Fig. 8A shows mean values for peak I_{to1} from seven rabbit atrial cells exposed to caffeine for 5-10 min, followed by 10 min of washout. Caffeine caused a significant and partially reversible suppression of I_{to} in the absence of I_{Ca} and in the presence of strong buffering of intracellular Ca^{2+} by 5 mM EGTA. In three cells, recordings from one of which are shown in Figs. 8B and C, caffeine completely blocked I_{to1}. Fig. 9A shows the effect of 10 mM caffeine on I_{to} in human atrial cells studied with 5 mM EGTA in the pipette solution and 200 μM Cd^{2+} in the bath. Once again, caffeine significantly and reversibly inhibited I_{to} under conditions that prevented changes in $[Ca^{2+}]_i$ due to Ca^{2+}-triggered Ca^{2+} release from the SR. As in rabbit cells, caffeine was capable of fully suppressing I_{to1}, as shown for one human cell in panels B and C. Finally, we studied the ability of caffeine to suppress I_{to} in human atrial cells under the same conditions used to study ryanodine in human atrial cells (Figs. 3 and 4). As shown in Fig. 10, caffeine strongly suppressed I_{to}, in contrast to the lack of effect of ryanodine shown in Figs. 3 and 4.

DISCUSSION

In the present study, we have obtained evidence which suggests that the 4AP-resistant component of I_{to} in human atrial cells is due to use-dependent drug unblocking rather than I_{ClCa}. Evidence for use-dependent 4AP unblocking underlying 4AP-resistant I_{to} in human cells included the disappearance of this component at low pulse frequencies, and the cross-over between currents recorded at 0.1 Hz and 1 Hz compatible with open-channel unblocking (Fig. 5). In contrast to the rabbit atrium, human atrial cells appear to lack I_{ClCa}, based on the absence of transient outward currents when K^+ is replaced by Cs^+ in the pipette solution and the unchanging amplitude of I_{to} upon exposure to ryanodine. Caffeine inhibits I_{to} in human atrial cells, but this action can be demonstrated under conditions which prevent Ca^{2+}-triggered SR Ca^{2+} release from the sarcoplasmic reticulum, suggesting that this action of caffeine is due to an effect other than suppression of Ca^{2+} release from the SR.

Comparison with Previous Studies of Transient Outward Current

The existence of two distinct components of I_{to} was first reported in sheep cardiac Purkinje fibers by Kenyon and Gibbons (22) and Carmeliet and Coraboeuf (7). Subsequently, two components of I_{to} were reported to exist in rabbit atrium (16, 38), rabbit ventricle (16, 19, 37), canine ventricle (33), and human atrium (11, 35). In seal atrial fibres (27) and calf Purkinje fibres (30), only a single Ca^{2+}-dependent transient outward component was seen. Maylie and Morad (27) showed that the Ca^{2+}-dependent I_{to} had a bell-shaped I-V relation tracking phasic tension development and cellular birefringence (an indicator of SR Ca^{2+} release). The 4AP-resistant component of I_{to} in rabbit atrium (38), rabbit ventricle (19, 37), rabbit Purkinje cells (32), and canine ventricle (33) have characteristic features of a bell-shaped I-V relation, activation slower than that of 4AP-sensitive I_{to}, inhibition by ryanodine and caffeine, and augmentation by

isoproterenol. In rabbit tissues, this component is inhibited by Cl^- replacement and by disulfonic stilbenes (32, 37, 38), indicating that it is a Cl^- current.

In the present study, we were able to demonstrate the typical features of I_{ClCa} characterizing the 4AP-resistant component in rabbit atrium. In contrast, we were unable to demonstrate similar properties in human atrial cells. Escande et al (11) described a second component of I_{to} in human atrial cells that in many ways resembles the 4AP-resistant i_{to2} that we observed and referred to this component as I_{bo} (brief outward current). They found that I_{to2} reached a peak earlier than I_{to1}. The I-V relation that they show for I_{to2} (or I_{bo} in their Fig. 5B) is monotonic, and resembles that of I_{to1} (I_{to} in the same figure) and control current in our Fig. 5. They indicate that in two of 12 cells, a bell-shaped I-V relation was seen, but do not show data for these cells. We have also reported two components of I_{to} in human atrial cells (35), which had properties similar to those described by Escande et al (11). The single feature which I_{to2} in human atrium clearly shares with Ca^{2+}-dependent I_{to} as described in other systems is sensitivity to caffeine. However, we have shown in the present manuscript that caffeine is able to suppress I_{to} in the presence of 200 μM Cd^{2+}, which blocks I_{Ca}, and simultaneous buffering of intracellular Ca^{2+} with 5 mM EGTA. Thus, caffeine is able to inhibit I_{to} independently of Ca^{2+}-triggered SR Ca^{2+} release. In contrast to caffeine, ryanodine had no effect on I_{to} in human atrial cells, in contrast to its clear ability to inhibit I_{to} in rabbit atrium. These results are consistent with previous findings regarding caffeine's ability to inhibit 4AP-sensitive I_{to} in rat myocytes (10). Caffeine has also been found to inhibit directly sodium current in guinea pig ventricular myocytes (18), indicating that this compound may have direct actions on other sarcolemmal ion channels. Such findings urge caution in the use of caffeine as a probe for electrophysiologic consequences of the inhibition of SR Ca^{2+} release.

Potential Limitations

Human atrial cells were obtained from specimens of the right atrial appendage, because this zone is normally incised during cannulation for extracorporeal circulation. We cannot exclude the possibility that I_{ClCa} exists in other portions of the atria. In previous studies, we have not observed qualitative differences between I_{to} in different zones of rabbit atria (13).

We used a low concentration of EGTA (25 μM) in the pipette solution for both the rabbit and human cell studies. Large concentrations of EGTA suppress I_{ClCa} by strongly buffering intracellular Ca^{2+} and preventing the Ca^{2+} transient necessary to activate the Cl^- current (37). We do not believe that the EGTA in our pipette solution was sufficient to explain the absence of Ca^{2+}-dependent I_{to} in our human cell studies for two reasons: 1) the EGTA concentration we used was below the range of concentrations (200-800 μM) used by Zygmunt and Gibbons (37, 38) in their studies of I_{ClCa}, and 2) the same pipette solutions were used to study both rabbit and human atrial cells, and a 4AP-resistant current with properties typical of I_{ClCa} was readily recorded in rabbit cells.

The kinetics and voltage-dependence of 4AP-resistant I_{to} that we recorded from human atrial cells were very similar to those reported by Escande et al. (11). However, the latter investigators were apparently able to record 4AP-resistant current at a pulse frequency of 0.1 Hz, while we were not. This difference may be due to the lower concentrations of 4AP which they used (2-3 mM, compared to 5 mM in our experiments).

Potential Significance of our Findings

The transient outward current is prominent in human atrial cells, and contributes a substantial repolarizing current, particularly during early phases of the action potential. Understanding its physiologic

properties and regulation are important to understanding the factors that control human atrial action potential properties and thereby govern the occurrence of atrial arrhythmias. Our results provide insight into the properties of I_{to} in human atrium by showing that the 4AP-resistant component is due to drug unblocking, rather than to the presence of $I_{Ca,o}$, as in the rabbit. This has important implications for the understanding the interrelations between inward and outward currents during the human atrial action potential, in that there is no direct linkage between inward I_{Ca} and opposing Ca^{2+}-dependent outward Cl^- currents, as exists in the rabbit. Interventions that specifically inhibit $I_{Ca,o}$ would not be expected to suppress transient outward current in human atrium, and this type of action is unlikely to be a favorable target for the development of new antiarrhythmic agents. Finally, these results indicate once more the important potential interspecies differences in ionic current mechanisms, and the risks of extrapolating directly to man results obtained in other species.

tWac2man.SN

Acknowledgments: The authors thank Guylaine Nicol for technical assistance, and Luce Bégin for typing the manuscript.

REFERENCES

1. **Antzelevitch, C., Sicouri, S., Litovsky, S.H., Lukas, A., Krishnan, S.C., Di Diego, J.M., Gintant, G.A., and D.-W. Liu.** Heterogeneity within the ventricular wall. Electrophysiology and pharmacology of epicardial, endocardial, and M cells. *Circ. Res.* 69: 1427-1449, 1991.
2. **Beuckelmann, D.J., Näbauer, M., and E. Erdmann.** Alterations of K^+ currents in isolated human ventricular myocytes from patients with terminal heart failure. *Circ. Res.* 73: 379-385, 1993.
3. **Boyett, M.R.** Effect of rate-dependent changes in the transient outward current on the action potential in sheep Purkinje fibres. *J. Physiol.* 319: 23-41, 1981.
4. **Campbell, D.L., Qu, Y., Rasmusson, R.L., and H.C. Strauss.** Quantitative analysis of closed-state block by 4-aminopyridine of the transient potassium current in ferret ventricular myocytes (Abstract). *Circulation* 84 (suppl II): II-102, 1991.
5. **Campbell, D.L., Rasmusson, R.L., Qu, Y., and H.C. Strauss.** The calcium-independent transient outward potassium current in isolated ferret right ventricular myocytes. I. Basis characterization and kinetic analysis. *J. Gen. Physiol.* 101: 571-601, 1993a.
6. **Campbell, D.L., Qu, Y., Rasmusson, R.L., and H.C. Strauss.** The calcium-independent transient outward potassium current in isolated ferret right ventricular myocytes. II. Closed state reverse use-dependent block by 4-aminopyridine. *J. Gen. Physiol.* 101: 603-626, 1993b.
7. **Coraboeuf, E., and E. Carmeliet.** Existence of two transient outward currents in sheep cardiac Purkinje fibers. *Pflügers Arch.* 392: 352-359, 1982.
8. **Deck, K., and W. Trautwein.** Ionic currents in cardiac excitation. *Pflügers Arch. ges. Physiol.* 280: 63-80, 1964.
9. **Dudel, J., Peper, K., Rüdel, R., and W. Trautwein.** The dynamic chloride component of membrane current in Purkinje fibers. *Pfluegers Arch. Eur. J. Physiol.* 295: 197-212, 1967.
10. **Dukes, I.D., and M. Morad.** The transient K^+ current in rat ventricular myocytes: Evaluation of its Ca^{2+} and Na^+ dependence. *J. Physiol.* 435: 395-420, 1991.
11. **Escande, D., Coulombe, A., Faivre, J.-F., Deroubaix, E., and E. Coraboeuf.** Two types of transient outward currents in adult human atrial cells. *Am. J. Physiol.* 252 (*Heart Circ. Physiol.* 21): H142-H148, 1987.
12. **Fedida, D., and W.R. Giles.** Regional variations in action potentials and transient outward current in myocytes isolated from rabbit left ventricle. *J. Physiol.* 442: 191-209, 1991.
13. **Fermini, B., Wang, Z., Duan, D., and S. Nattel.** Differences in rate dependence of transient outward current in rabbit and human atrium. *Am. J. Physiol.* 263 (*Heart Circ. Physiol.* 32): H1747-H1754, 1992.
14. **Fozzard, H.A., and M. Hiraoka.** The positive dynamic current and its inactivation properties in cardiac Purkinje fibres. *J. Physiol.* 234: 569-586, 1973.
15. **Furukawa, T., Myerburg, R.J., Furukawa, N., Bassett, A.L., and S. Kimura.** Differences in transient outward currents of feline endocardial and epicardial myocytes. *Circ. Res.* 67: 1287-1291, 1990.
16. **Giles, W.R., and Y. Imaizumi.** Comparison of potassium currents in rabbit atrial and ventricular cells. *J. Physiol.* 405: 123-145, 1988.

17. **Giles, W.R., and A.C.G. Van Ginneken.** A transient outward current in isolated cells from the crista terminalis of rabbit heart. *J. Physiol.* 368: 243-264, 1985.
18. **Habuchi, Y., Tanaka, H., Furukawa, T., and Y. Tsujimura.** Caffeine-induced block of Na^+ current in guinea pig single ventricular cells. *Am. J. Physiol.* 261 (*Heart Circ. Physiol.* 30): H1855-H1863, 1991.
19. **Hiraoka, M., and S. Kawano.** Calcium-sensitive and insensitive transient outward current in rabbit ventricular myocytes. *J. Physiol.* 410: 187-212, 1989.
20. **Hiraoka, M., and S. Kawano.** Mechanism of increased amplitude and duration of the plateau with sudden shortening of diastolic intervals in rabbit ventricular cells. *Circ. Res.* 60: 14-26, 1987.
21. **Josephson, I.R., Sanchez-Chapula, J., and A.M. Brown.** Early outward current in rat single ventricular cells. *Circ. Res.* 54: 157-162, 1984.
22. **Kenyon, J.L., and W.R. Gibbons.** 4-aminopyridine and the early outward current of sheep cardiac Purkinje fibers. *J. Gen. Physiol.* 73: 139-157, 1979.
23. **Kukushkin, N.I., Gainullin, R.Z., and E.A. Sosunov.** Transient outward current and rate dependence of action potential duration in rabbit cardiac ventricular muscle. *Pflügers Arch.* 399: 87-92, 1983.
24. **Litovsky, S.H., and C. Antzelevitch.** Rate dependence of action potential duration and refractoriness in canine ventricular endocardium differs from that of epicardium: Role of the transient outward current. *J. Am. Coll. Cardiol.* 14: 1053-1066, 1989.
25. **Litovsky, S.H., and C. Antzelevitch.** Transient outward current prominent in canine ventricular epicardium but not endocardium. *Circ. Res.* 62: 116-126, 1988.
26. **Lukas, A., and C. Antzelevitch.** Differences in the electrophysiological response of canine ventricular epicardium and endocardium to ischemia. Role of the transient outward current. *Circulation* 88: 2903-2915, 1993.
27. **Mayile, J., and M. Morad.** A transient outward current related to calcium release and development of tension in elephant seal atrial fibres. *J. Physiol.* 357: 267-292, 1984.
28. **Nakayama, T., and H. Irisawa.** Transient outward current carried by potassium and sodium in quiescent atrioventricular node cells of rabbits. *Circ. Res.* 57: 65-73, 1985.
29. **Shibata, E.F., Drury, T., Refsum, H., Aldrete, V., and W. Giles.** Contributions of a transient outward current to repolarization in human atrium. *Am. J. Physiol.* 257 (*Heart Circ. Physiol.* 26): H1773-H1781, 1989.
30. **Siegelbaum, S.A., and R.W. Tsien.** Calcium-activated transient outward current in calf cardiac Purkinje fibres. *J. Physiol.* 299: 485-506, 1980.
31. **Simurda, J., Simurdova, M., and G. Christe.** Use-dependent effects of 4-aminopyridine on transient outward current in dog ventricular muscle. *Pflügers Arch.* 415: 244-246, 1989.
32. **Sipido, K.R., Callewaert, G., and E. Carmeliet.** $[Ca^{2+}]_i$ transients and $[Ca^{2+}]_i$-dependent chloride current in single Purkinje cells from rabbit heart. *J. Physiol.* 468: 641-667, 1993.
33. **Tseng, G.-N., and B.F. Hoffman.** Two components of transient outward current in canine ventricular myocytes. *Circ. Res.* 64: 633-647, 1989.
34. **Wang, Z., Fermini, B., and S. Nattel.** Mechanism of flecainide's rate-dependent actions on action potential duration in canine atrial tissue. *J. Pharmacol. Exp. Ther.* 267: 575-581, 1993.

35. **Wang, Z., Fermini, B., and S. Nattel.** Delayed rectifier outward current and repolarization in human atrial myocytes. *Circ. Res.* 73: 276-285, 1993.

36. **Wang, Z., Fermini, B., and S. Nattel.** State- and voltage-dependent I_{to} block by 4-aminopyridine in human atrial myocytes (Abstract). *Circulation* 86 (suppl I): I-696, 1992.

37. **Zygmunt, A.C., and W.R. Gibbons.** Calcium-activated chloride current in rabbit ventricular myocytes. *Circ. Res.* 68: 424-437, 1991.

38. **Zygmunt, A.C., and W.R. Gibbons.** Properties of the calcium-activated chloride current in heart. *J. Gen. Physiol.* 99: 391-414, 1992.

LEGENDS

Figure 1. Effect of 4-aminopyridine (4AP) on I_{to} in rabbit (left) and human (right) atrial cells. **A:** Currents recorded upon 200 ms depolarizing steps from -50 mV to a series of test potentials as shown in the inset. Results are shown before (top panel) and after (middle panel) exposure to 5 mM 4AP, at a frequency of 0.1 Hz. 4AP partially suppressed I_{to}, leaving a component that activated more slowly than under control conditions. Current-voltage relations (mean ± SE) of control (open circles), 4AP-resistant (filled circles), and 4AP-sensitive (diamonds) currents in 6 rabbit atrial cells are shown in the bottom panel. Current amplitude was measured from the peak outward current to the steady-state value at the end of the pulse. Drug-sensitive current was obtained by digital subtraction of current recorded in the presence of the drug from control current. Note that 4AP-sensitive current continually increases as a function of voltage, but that the I-V relation of 4AP-resistant current is bell-shaped. **B:** Currents recorded from a human cell with the same protocol used in the rabbit cell shown in A. Exposure to 4AP (pulse frequency of 1 Hz) resulted in a decrease in I_{to}, leaving a current component that activated and inactivated rapidly. Current-voltage relations for control and 4AP-resistant current in 5 human atrial cells are shown at the bottom. In contrast to the I-V relations in the rabbit, 4AP-resistant current in human cells has an I-V relation with a form similar to that of control current, and both have a form similar to 4AP-sensitive current in the rabbit.

Figure 2. Effects of ryanodine on I_{to} in rabbit atrial cells. **A:** Currents recorded upon depolarization from -50 mV to the voltages indicated under control conditions (open circles) and after at least 10-min exposure to ryanodine (filled squares). The transient current remaining after ryanodine reached a peak more quickly and inactivated more quickly than the current under control conditions. The ryanodine-sensitive current (triangles) activated and inactivated more slowly than the ryanodine-resistant current (filled squares). **B:** Effects of 4AP and ryanodine on I_{to} in rabbit atrial cells. After exposure to 4AP (filled circles), a component of transient outward current remained that activated more slowly than control current (open circles). The addition of ryanodine completely eliminated the remaining transient outward current, leaving only an inward I_{Ca} (triangles). Results similar to those in panel A were obtained in a total of 5 cells, and results similar to those in panel B were obtained in a total of 6 cells.

Figure 3. Effects of ryanodine on I_{to} in a human atrial cell. Currents recorded after the addition of ryanodine (filled circles) did not differ appreciably from currents recorded prior to the addition of ryanodine (open circles). No significant ryanodine-sensitive component was detected by digital subtraction of records in the presence of ryanodine from records in its absence (open triangle).

Figure 4. Current-voltage relations for peak I_{to} (mean ± SE) measured upon depolarization from -50 mV to the potentials indicated under control conditions (open circles) and after exposure to ryanodine (filled circles) in 5 rabbit atrial cells (A) and 11 human cells (B). The I-V relation for ryanodine-sensitive current, as obtained by digital subtraction of records in the presence of ryanodine from control records, is indicated by the open triangles. A bell-

shaped relationship was noted for ryanodine-sensitive current in the rabbit, but ryanodine-sensitive current did not differ significantly from zero in human cells. * $P < 0.05$, ** $P < 0.01$ for current in the presence of ryanodine compared to control current.

Figure 5. Currents recorded from human atrial cells upon depolarization from -50 mV in the absence (A) and presence (B) of 200 μM Cd^{2+}. Results are shown under control conditions (open circles), after exposure to 5 mM 4AP during pulsing at 0.1 Hz (filled circles) and in the presence of 4AP at 1.0 Hz (open triangles). Raw data from one cell studied with each protocol are shown at the top, and I-V relations for peak transient outward current (mean ± SE) measured relative to the current at the end of the voltage pulse are shown at the bottom for 6 cells studied without Cd^{2+} (panel A) and 7 cells studied with Cd^{2+} added to the perfusate (panel B). * $P < 0.05$, ** $P < 0.01$ compared to control; † $P < 0.05$, ‡ $P < 0.01$ compared to results in the presence of 4AP at 1 Hz.

Figure 6. Absence of 4AP-resistant transient outward current at slow pulsing rates in a human atrial cell exposed to isoproterenol. A: Currents recorded upon 200-ms depolarizing steps from -50 mV under control conditions. B: In the presence of 5 mM 4AP and at a pulsing rate of 0.1 Hz, isoproterenol (1 μM) increased inward I_{Ca}, without causing a transient outward current component to appear. C: When the pulsing rate was increased to 1 Hz in the presence of isoproterenol and 4AP, small, rapidly-inactivating transient outward currents were seen. Similar results were obtained in a total of three cells.

Figure 7. Currents recorded from human (A) and rabbit (B) atrial cells with pipettes containing Cs^+ in the place of K^+. Currents were recorded upon 200 ms depolarizing voltage steps from -50 mV with the protocol shown in the inset. In six rabbit cells, substantial transient outward currents were readily recorded despite the replacement of intracellular K^+ by equimolar Cs^+. In 30 human cells studied in the same way, no outward currents were recorded, as illustrated by the results for the cell shown in panel A. C: Current-voltage relation for transient outward current (mean ± SE) recorded in six rabbit atrial cells using pipettes with equimolar replacement of K^+ by Cs^+. Note that the bell-shaped I-V relation is similar in form to that of 4AP-resistant current (Fig. 1C) and ryanodine-sensitive current (Fig. 4A) in rabbit cells.

Figure 8. Effects of caffeine on I_{to1} recorded from rabbit atrial cells in the presence of 200 μM Cd^{2+} in the superfusate and 5 mM EGTA in the pipette. A: Current-voltage relations (mean ± SE) for peak transient outward current recorded under control conditions (open circles), after 5 min of exposure to 10 mM caffeine (filled circles), and after at least 10 min of washout (open triangles) in seven rabbit atrial cells. Currents were recorded upon 200-ms depolarizing pulses from -50 mV to the test potentials shown at a frequency of 0.1 Hz. * $P < 0.05$, ** $P < 0.01$ compared to control; † $P < 0.05$, ‡ $P < 0.01$ compared to corresponding value in the presence of caffeine. B, C: Examples of current recorded under control conditions (open circles), after exposure to caffeine (filled circles) and after washout (open triangles) obtained upon depolarizing steps to the voltages shown in one of three cells in which caffeine completely eliminated I_{to1}.

Figure 9. Effects of caffeine on I_{to1} recorded from human atrial cells in the presence of 200 μM Cd^{2+} in the superfusate and 5 mM EGTA in the pipette. A: Current-voltage relations for peak

transient outward current recorded during 200-ms depolarizing steps from -50 mV at a frequency of 0.1 Hz in eight human atrial cells. * $P < 0.05$, ** $P < 0.01$ for results in the presence of caffeine compared to control; † $P < 0.05$, ‡ $P < 0.01$ for results upon washout compared to results in the presence of caffeine. **B, C:** Current tracings recorded under control conditions (open circles), after the addition of caffeine (filled circles) and upon washout (open triangles) in one of two human cells in which caffeine completely eliminated I_{to1}.

Figure 10. Effects of caffeine on I_{to} in human atrial cells in the absence of Cd^{2+} and with 25 μM EGTA in the pipette. **A, B:** Recordings obtained in one cell upon 200-ms depolarizing pulses from -50 mV to the voltages shown under control conditions (open circles) and after exposure to 10 mM caffeine (filled circles). **C:** Current-voltage relation for peak I_{to} in the absence (open circles) and the presence (filled circles) of 10 mM caffeine in 12 human atrial cells. * $P < 0.05$, ** $P < 0.01$ for results in the presence of caffeine compared to control.

FIGURE 1

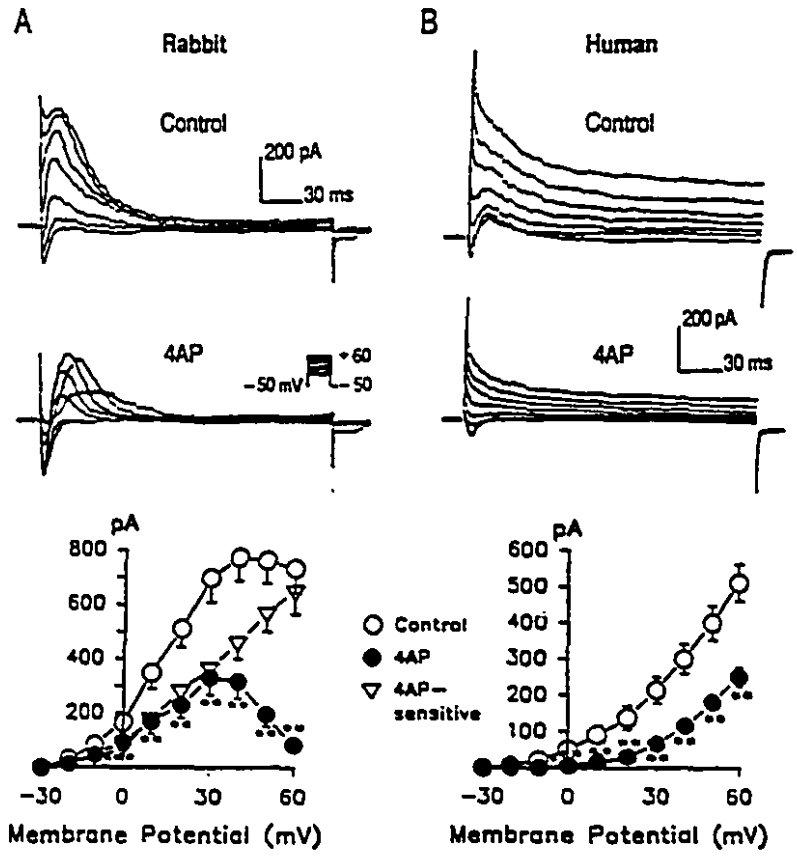
A
Rabbit
Control
200 pA
30 ms
4AP
+60
−50 mV
−50
pA
800
600
400
200
−30
0
30
60
Membrane Potential (mV)
B
Human
Control
200 pA
30 ms
4AP
pA
600
500
400
300
200
100
−30
0
30
60
Membrane Potential (mV)
Control
4AP
4AP−
sensitive

FIGURE 2

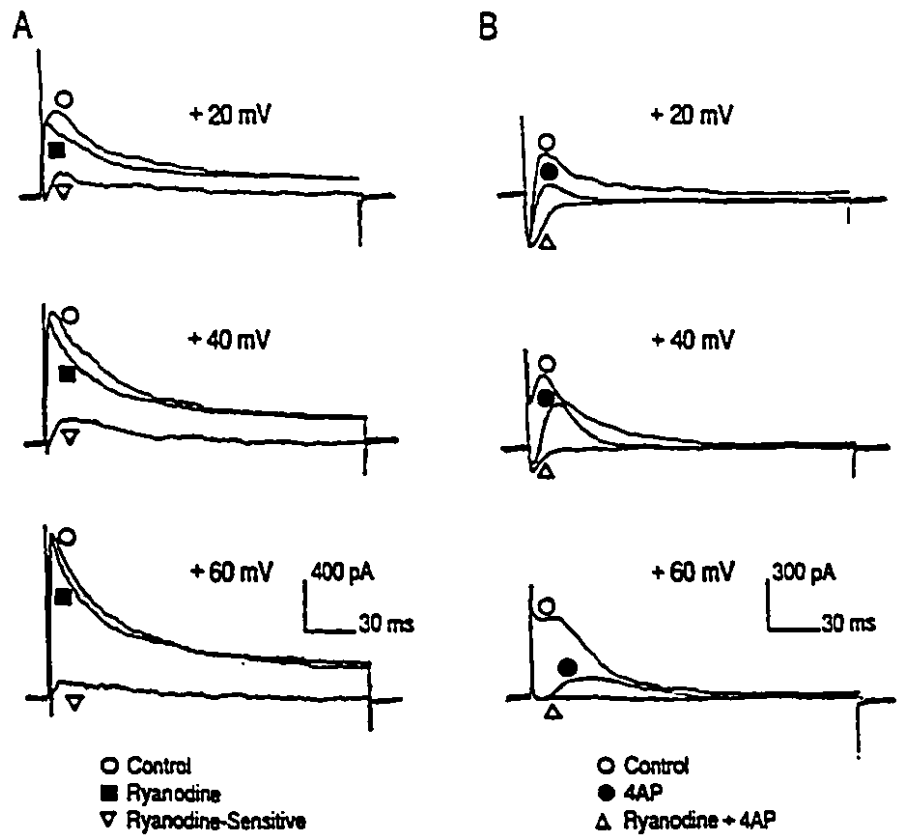
A
B
+ 20 mV
+ 20 mV
+ 40 mV
+ 40 mV
+ 60 mV
400 pA
30 ms
+ 60 mV
300 pA
30 ms
O Control
■ Ryanodine
▽ Ryanodine-Sensitive
O Control
● 4AP
△ Ryanodine + 4AP

FIGURE 3

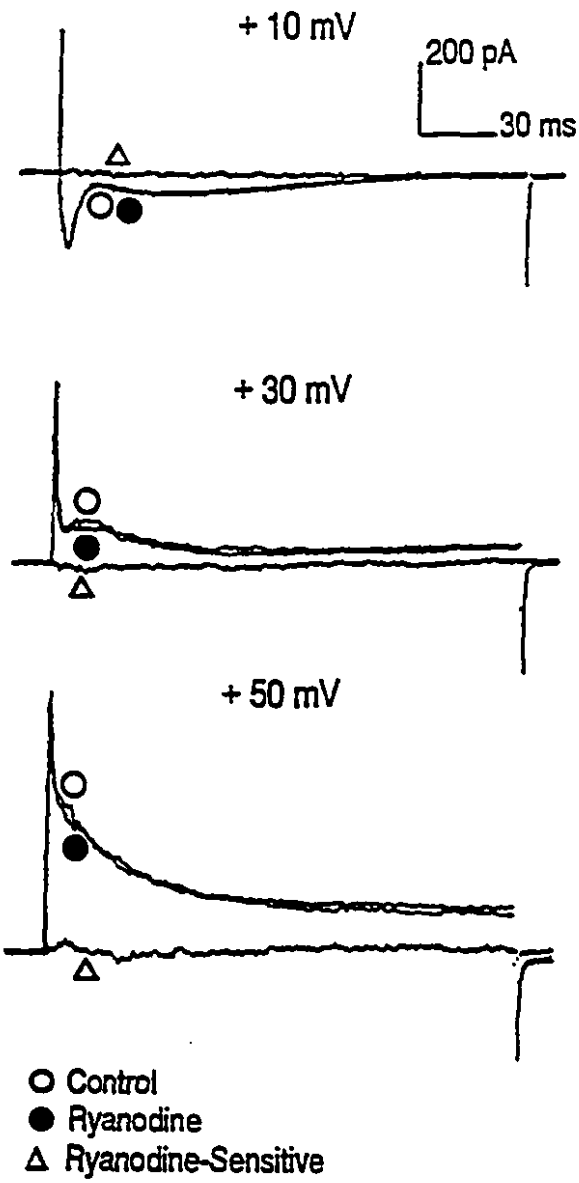
+ 10 mV
200 pA
30 ms
+ 30 mV
+ 50 mV
Control
Ryanodine
Ryanodine-Sensitive

FIGURE 4

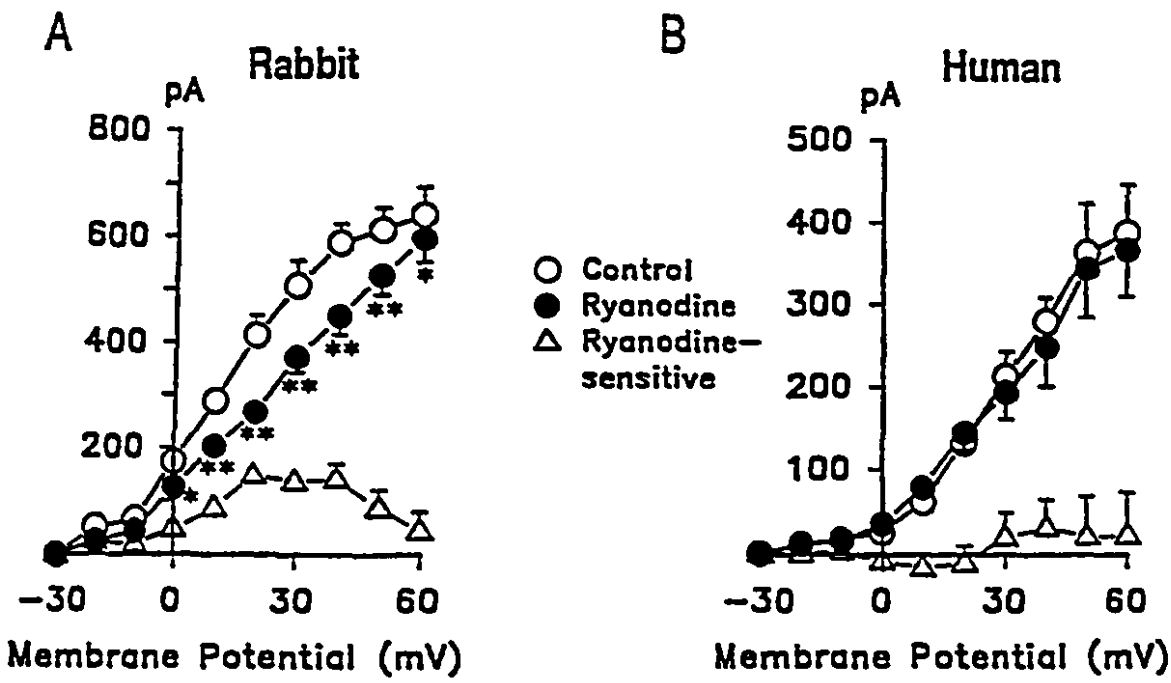
A
Rabbit
pA
800
600
400
200
−30
0
30
60
Membrane Potential (mV)
B
Human
pA
500
400
300
200
100
Control
Ryanodine
Ryanodine–sensitive
−30
0
30
60
Membrane Potential (mV)

FIGURE 5

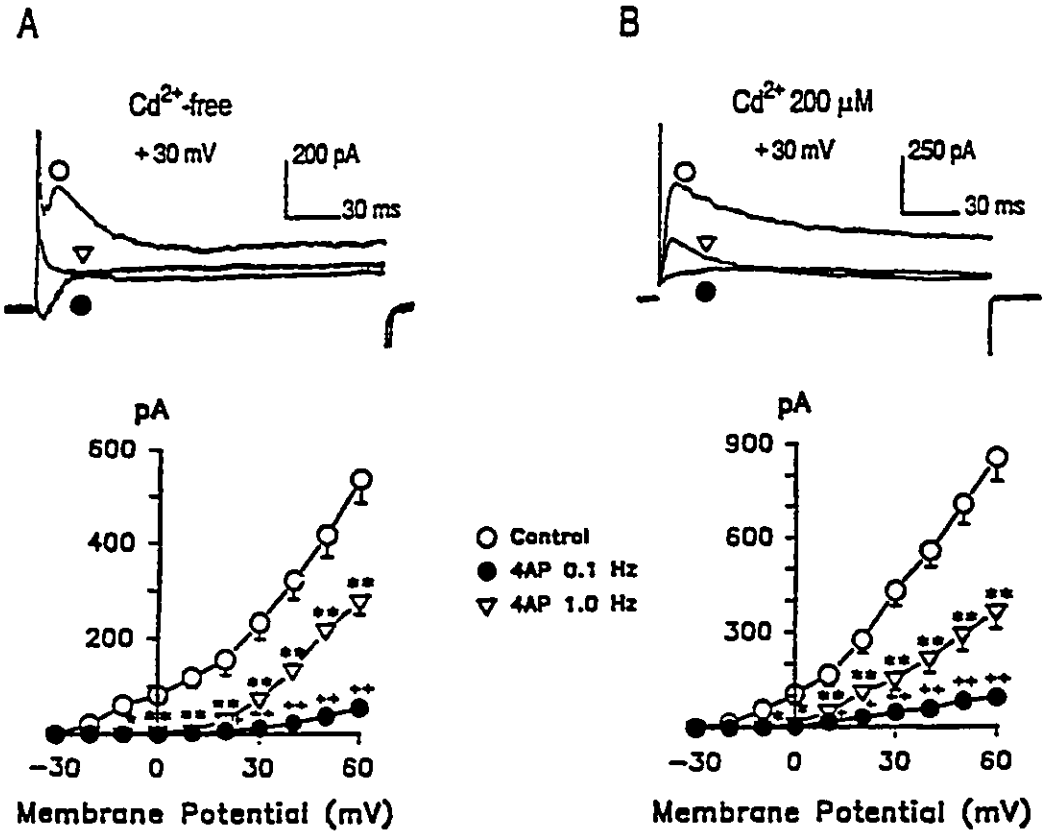
A
B
Cd2+-free
+30 mV
200 pA
30 ms
Cd2+ 200 µM
+30 mV
250 pA
30 ms
pA
600
400
200
900
600
300
Control
4AP 0.1 Hz
4AP 1.0 Hz
−30
0
30
60
Membrane Potential (mV)

FIGURE 6

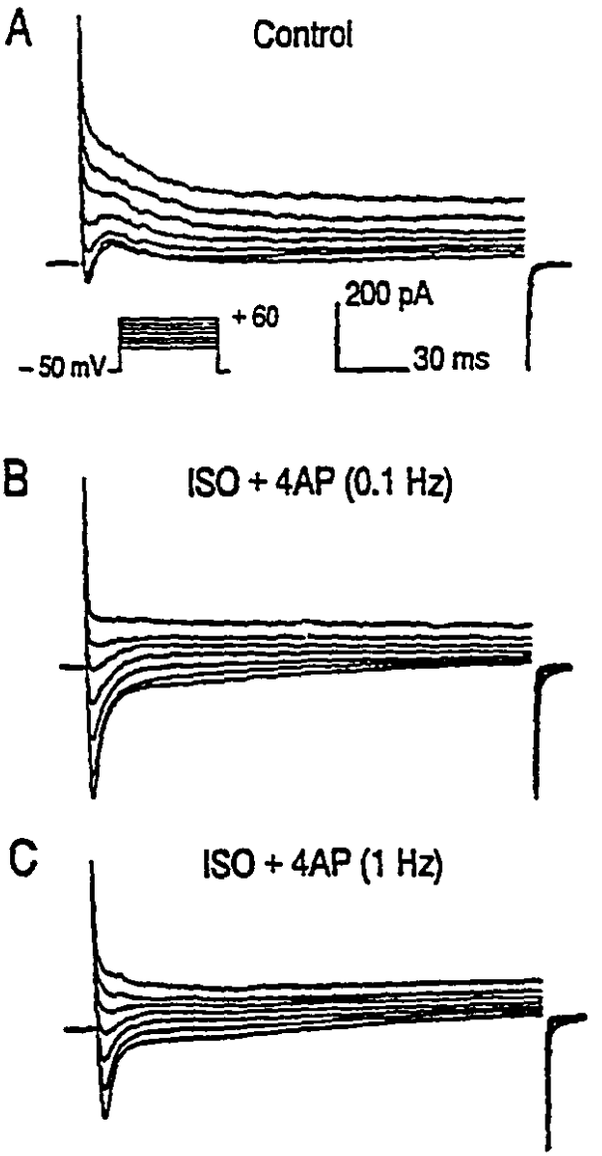

FIGURE 7

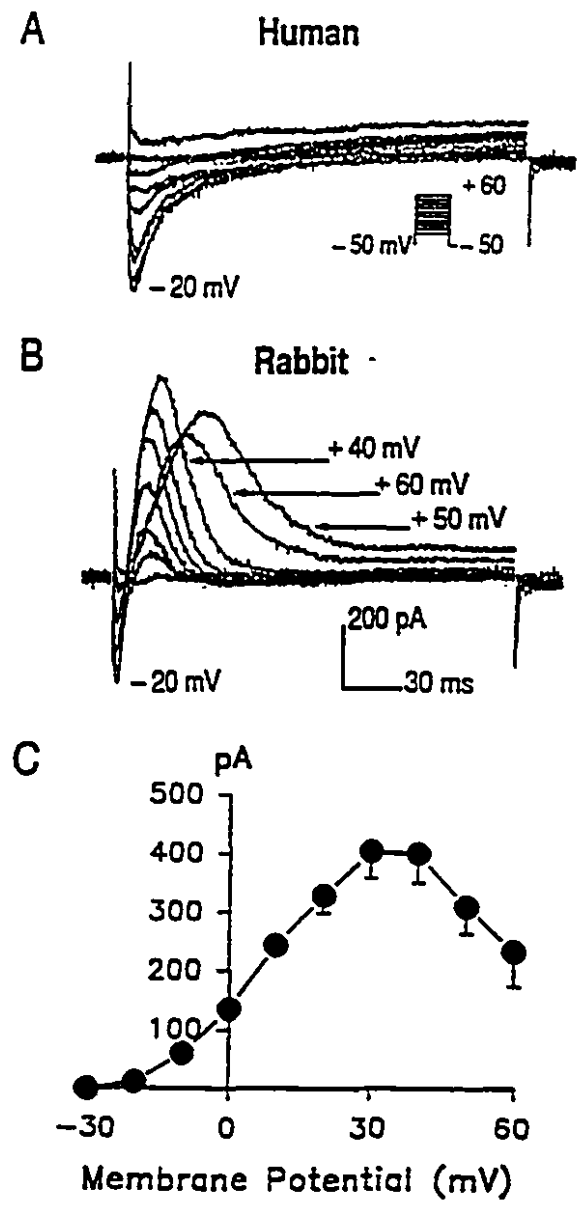
A
Human
+60
−50 mV
−50
−20 mV
B
Rabbit
+40 mV
+60 mV
+50 mV
200 pA
−20 mV
30 ms
C
pA
500
400
300
200
100
−30
0
30
60
Membrane Potential (mV)

FIGURE 8

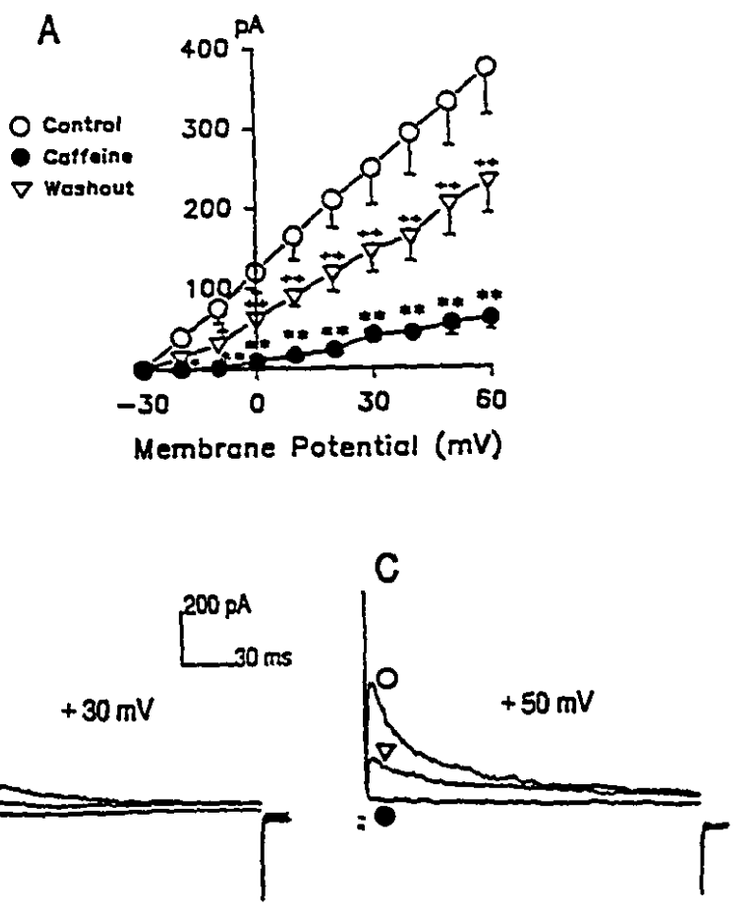
A
pA
400
300
200
100
Control
Caffeine
Washout
−30
0
30
60
Membrane Potential (mV)
B
200 pA
30 ms
+30 mV
C
+50 mV

FIGURE 9

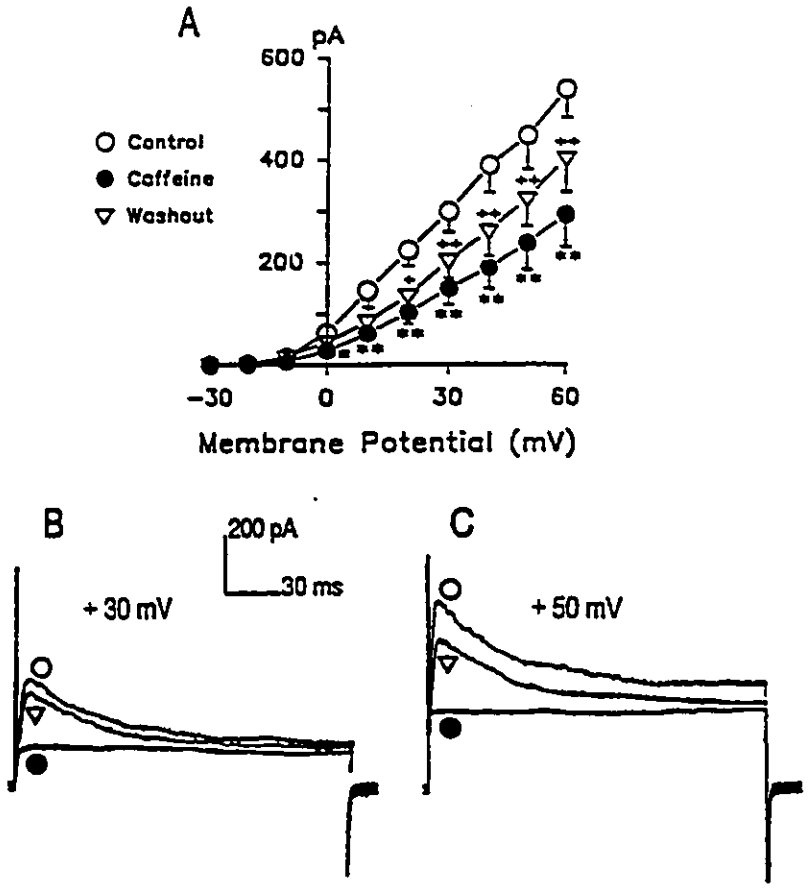
A
pA
600
400
200
Control
Caffeine
Washout
−30
0
30
60
Membrane Potential (mV)
B
200 pA
30 ms
+ 30 mV
C
+ 50 mV

FIGURE 10

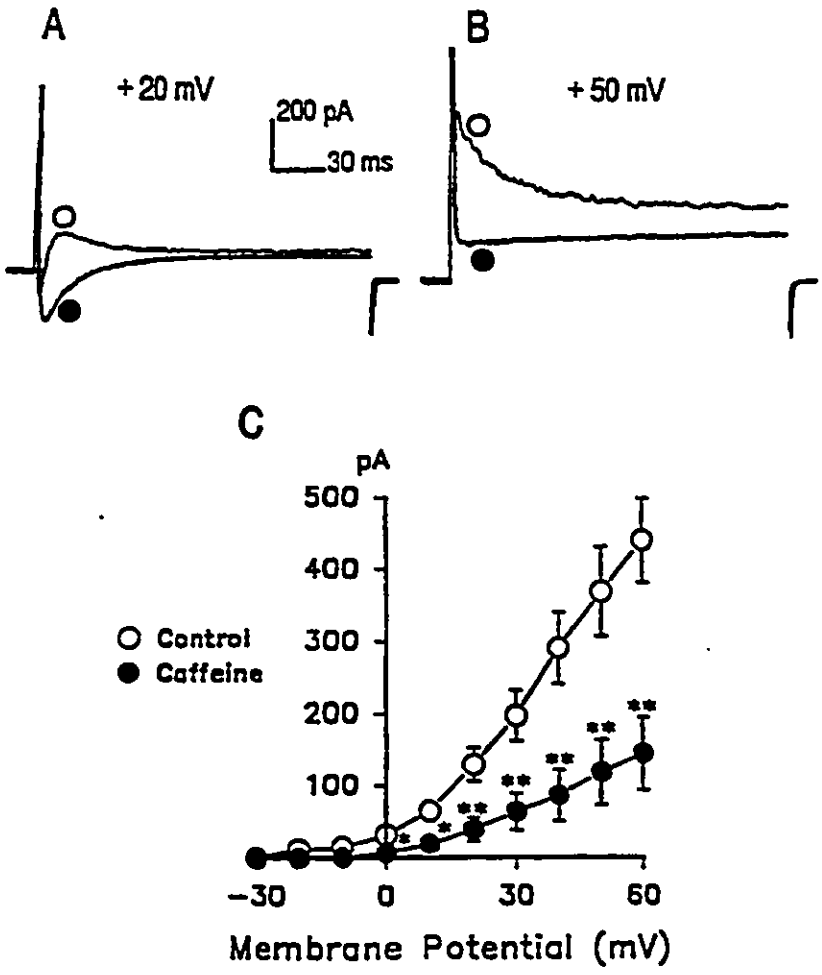
A
+20 mV
200 pA
30 ms
B
+50 mV
C
pA
500
400
300
200
100
Control
Caffeine
−30
0
30
60
Membrane Potential (mV)

Lack of Evidence for Cl^- Conductance in Human Atrial Myocytes

Introduction

Up to date at least six different types of cardiac Cl^- currents have been reported in the literature[1-6]. Among these, I_{ClCa} (Ca^{++}-activated Cl^- current, I_{to2}), I_{ClATP} (extracellular ATP-induced Cl^- current, $I_{Clswell}$ (swelling-induced Cl^- current), and I_{Cl} (depolarization-induced Cl^- current) were described in atrial cells from guinea pig (I_{ClATP}[3]), rabbit (I_{ClCa}[4], I_{Cl}[5]), and dog ($I_{Clswell}$[6]). Except for I_{ClCa}, all other Cl^- currents were found to be time-independent. The physiological functions of these Cl^- currents, including the possible involvement in regulating membrane potential and repolarization process, are *speculative*.

We have presented evidence against the contribution of I_{ClCa} in human atrial myocytes[7], but whether any of the Cl^- currents so far identified in animal species other than I_{ClCa} also exist in man is still unclear. We have previously demonstrated that the sustained outward current seen after complete inactivation of the transient outward K^+ current (I_{to1}) was insensitive to DIDS, an anion transport inhibitor frequently used to block Cl^- channels, indicating a minimal contribution of Cl^- current to human atrial repolarization[7]. However, no studies specifically aimed to clarify this issue and to investigate other Cl^- currents have been reported. We therefore designed this study to further explore the possible role of Cl^- currents by using whole-cell *patch-clamp* techniques in enzymatically isolated human atrial myocytes.

Methods, Results, and Discussion

The methods for isolation of single human atrial cells, and data *acquisition* and analysis have been previously described in details[7-12]. To avoid masking Cl^- currents by other ion currents, internal and external solution were modified. Generally, the constituents of external perfusate were (in mM): Choline Cl, 126; CsCl, 5.4; $MgCl_2$, 0.8; $CaCl_2$, 1; NaH_2PO_4, 0.33; HEPES, 10; and glucose, 5.5; pH adjusted to 7.4 with CsOH. Na ions were replaced with choline to prevent I_{Na}. Glass pipette electrodes were filled with internal solution of (mM): Cesium aspartate, 110; CsCl, 20; $MgCl_2$, 1; HEPES, 10; EGTA, 5; Mg_2ATP, 5; and Na_2-creatine phosphate, 5; pH adjusted to 7.4 with CsOH. Thus, K^+ currents were wholly eliminated because K ions were omitted from both intracellular and extracellular solutions. The ingredients of the solutions favored outward Cl^- currents, if any. The reversal potential would be expected to be around -46 mV, as calculated by the Nernst equation based on the ratio of internal and external Cl^- concentrations. Ca^{++} current was blocked by inclusion of 200 μM Cd^{++} in the external solution throughout the experiments. Experiments were conducted at room temperature (25°C). To acquire reliable data, cells with seal resistance lower than 5 GΩ were discarded.

Two different voltage protocols were employed: (1) step protocol. Step protocol was composed of 21 consecutive 100-msec pulses to various test potentials ranging from -100 to +100 mV with 10-mV increment. Pulses were delivered from a holding potential (HP) of -60 mV at an interpulse interval of 1 sec; (2) Ramp protocol. Ramp protocol was completed by gradually depolarizing the membrane (0.2 V/sec) from -100 mV to +80 mV, then repolarizing back to -100 mV. The holding potential was -40 mV. After membrane rupture, 5 minutes were allowed for a complete dialysis before *measurements* were made.

In about 15% of the cells studied, no ion currents could be detected with either hyperpolarization or depolarization. Small amplitude of non-specific leakage current was observed. To see whether I_{ClcAMP} or I_{ClATP} could be induced, isoproterenol hydrochloride (Iso, 1 μM + 1% ascorbic acid,) or ATP at concentrations ranging from 5 to 500 μM were added to the perfusate. The same protocols used under

control conditions were repeated at 5, 10, and 20 minutes after exposure of cells to the drugs. Data obtained after 20 minutes perfusion of the drugs were used for analysis. 1 μM Iso has been reported to be enough to induce I_{ClcAMP}[1,13-16]. We, however, observed no detectable changes of membrane current in the presence of 1 μM Iso with either step or ramp protocols, as illustrated by the representative recordings before and after drug, shown in Figure 1. Similar results were observed in another 4 cells.

50 μM ATP was used by Matsura and Ehara in their study to activate I_{ClATP} in guinea pig atrial myocytes[4]. No effects were seen, however, in human atrial cells with this concentration of ATP. We then tested a series of concentrations including 5, 25, 50, 250, and 500 μM, but no detectable current was induced with any of these concentrations of ATP. Figure 2 gives a typical example from a total of 4 cells, showing the effects of 0.5 mM ATP on membrane currents. The amplitude of currents elicited by either step protocols or ramp protocols was not affected by ATP at all.

These results do not suggest any possibility of I_{ClcAMP} and I_{ClATP} in human atrial cells under our experimental conditions.

In the majority of cells studied, strong depolarization induced a time-independent outward current. The current-voltage (I-V) relationship of this current displayed strong outward rectification. The voltage threshold for current activation was rather positive, around +10 mV, compared with many other outward currents. The reversal potentials determined from ramp protocol and step protocol were 2.4±0.5 mV (n=41) and 4.5±1.4 mV (n=40), respectively, far more positive than the calculated Cl^- equilibrium potential (-46 mV). To see if this current is sensitive to changes of extracellular Cl^- concentration, choline Cl was substituted with methanesulfonate in the superfusion solution, leaving $[Cl^-]_o$ 7.2 mM. In this set of experiments, 3M KCl bridge was used. The junctional potential ranged from -4 to -12 mV, and this was corrected when reversal potentials were determined. The results of Cl^- substitution on the outwardly rectifying current are illustrated in Figure 3. Panels A and B are analog data obtained with step protocol before and after external Cl^- replacement, respectively. No meaningful alteration of the current was detected. Similar results were obtained with the ramp protocol, as indicated by the superimposed current traces before and after substitution in panel C. The averaged data from a total of 28 cells are shown panel D, as expressed by the I-V curves before (open circles) and after (filled circles) external Cl^- replacement. The mean values of reversal potentials were -3.1±1.3 mV (from step protocol) and -1.6±0.8 mV (from ramp protocol) before, and -3.6±1.7 mV (step) and -2.2±1.1 mV (ramp) after substitution. Evidently, Cl^- substitution with methanesulfonate affects neither the amplitude (both inward and outward) nor the reversal potential of the outwardly rectifying current, suggesting an insensitivity of the current to changes of $[Cl^-]_o$. We then turned to vary the internal Cl^- concentration, while keeping $[Cl^-]_o$ (133 mM) constant, to further test the Cl^- sensitivity of the current. Currents recorded with 21 mM internal Cl^- which favoured outward Cl^- current were compared to those with 133 mM pipette Cl^- that unfavoured inward Cl^- current. The results were shown in Figure 3D: open circles for low pipette Cl^- (control group) vs. open squares for high pipette Cl^-. No significant differences of current amplitude (both outward and inward) were found between the two groups of cells, nor were the reversal potentials changed (-3.1±1.3 mV vs. -2.7±1.1 mV, P>0.05, control n=28, high $[Cl^-]_i$ n=10).

The results presented above exclude the possibility of depolarization-induced Cl^- current (I_{Cl}) in human atrial cells.

We then moved on to test whether this outwardly rectifying current was somehow related to I_{ClcAMP}

or I_{ClATP} by evaluating the effects of external application of 1 μM Iso or 0.5 mM ATP. The results are shown in Figures 4 and 5, respectively, where original current traces are displayed in panel A, B, and C, and the average data (Iso, n=5, ATP, n=6) in panel D. No appreciable differences were found with and without the drugs in either the size or the reversal potentials of the currents. The reversal potentials were -0.6±0.2 mV for control vs. -0.4±0.3 mV for Iso (n=5), and 0.0±0.6 mV for control and 0.1±0.3 mV for ATP (n=6), respectively.

Conclusion

We conclude based on the results from this study that the contribution of Cl^- conductance in human atrial myocytes under physiologic conditions is negligible, if not absent. While the ionic nature of the outwardly rectifying current is still unclear, we speculate that it represents a non-selective cation current which can be carried by cesium ions, similar to the non-specific background current described in rabbit atrial myocytes by Irisawa[17]. The role of this current in repolarizing the membrane would be expected to be minor under physiological conditions based on its small size and 0 mM reversal potential.

References

1. Harvey RD, Hume JR. Autonomic regulation of a chloride current in heart. Science 1989;244:983-985.
2. Walsh KB. Activation of a heart chloride current during stimulation of protein kinase C. Mol Pharmacol 1991;40:342-346.
3. Zygmunt AC, Gibbons WR. Properties of the calcium-activated chloride current in heart. J Gen Physiol 1992;99:391-414.
4. Matsuura H, Ehara T. Activation of chloride current by purinergic stimulation in guinea pig heart cells. Circ Res 1992;70:851-855.
5. Duan D, Fermini B, Nattel S. Sustained outward current observed after I_{to1} inactivation in rabbit atrial myocytes is a novel Cl^- current. Am J Physiol 1992;263:H1967-H1971.
6. Sorota S. Swelling-induced chloride-sensitive current in canine atrial cells revealed by whole-cell patch-clamp. Circ Res 1992;70:679-687.
7. Li G, Feng J, Wang Z, Fermini B, Nattel S. Comparative mechanisms of 4-aminopyridine resistant transient outward current in human and rabbit atrial myocytes. (submitted to AJP)
8. Wang Z, Fermini B, Nattel S: Sustained depolarization-induced outward current in human atrial myocytes: evidence for a novel delayed rectifier potassium current similar to Kv1.5 cloned channel currents Circ Res 1993;73:1061-1076.
9. Fermini B, Wang Z, Duan DY, Nattel S: Differences in the rate dependence of the transient outward current in rabbit atrium. Am J Physiol 263:H1747-H1754, 1992.
10. Wang Z, Fermini B, Nattel S: The delayed outward potassium current (I_K) in human atrial myocytes. Circ Res 73:276-285, 1993.
11. Wang Z, Fermini B, Nattel S: Rapid and slow components of delayed rectifier outward current in human atrial myocytes. (Cardiovasc Res, in revision)
12. Wang Z, Fermini B, Nattel S: Effects of flecainide, quinidine, and 4-aminopyridine on transient and

sustained outward currents in human atrial myocytes. (Submitted to Circ Res)
13. Harvey RD, Hume JR. Isoproterenol activates a chloride current, not the transient outward current, in rabbit ventricular myocytes. Am J Physiol 1989;257:C1177-C1181.
14. Yamawake N, Hirano Y, Sawanobori T, Hiraoka M. Arrhythmogenic effects of isoproterenol-activated Cl^- current in guinea pig ventricular myocytes. J Mol Cell Cardiol 1992;24:1047-1058.
15. Sorota S, Siegal MS, Hoffman BF. The isoproterenol-induced chloride current and cardiac resting potential. J Mol Cell Cardiol 1991;23:1191-1198.
16. Takano M, Noma A. Distribution of the isoprenaline-induced chloride current in rabbit heart. Pflügers Arch 1992;420:223-226.
17. Hagiwara N, Masuda H, Shoda M, Irisawa H. Stretch-activated anion currents of rabbit cardiac myocytes. J Physiol (Lond) 1992;456:285-302.

Figure Legends

Figure 1. No induction of Cl^- currents with isoproterenol (1 μM) in cells without currents. Original recordings with step protocols (see text) in upper panels, and with ramp protocols (see text) in lower panels. No any changes of membrane currents were detected after Iso. Similar results were seen in other 3 cells.

Figure 2. No induction of Cl^- currents with ATP (0.5 mM) in cells without currents. Original recordings with step protocols in upper panels, and with ramp protocols in lower panels. No any changes of membrane currents were detected after ATP. Similar results were seen in other 3 cells.

Figure 3. Lack of effects of varying Cl^- concentration on the time independent outwardly rectifying current. Panel A: Analog data for control obtained by step protocol, $[Cl^-]_o$ 133 mM and $[Cl^-]_i$ 21 mM; Panel B: Analog data after external Cl^- substitution, $[Cl^-]_o$ 7 mM and $[Cl^-]_i$ 21 mM; Panel C: Currents recorded with ramp protocol before and after external Cl^- substitution are superimposed; Panel D: Comparisons of I-V curves before (open circles) and after (filled circles) external Cl^- substitution, and between low $[Cl^-]_i$ group (open circles) and high $[Cl^-]_i$ group (open squares, $[Cl^-]_i$=133 mM).

Figure 4. Lack of effects of isoproterenol 1μM on the time independent outwardly rectifying current. Analog data for control (panel A) and for Iso (panel B) obtained by step protocol. Panel C displays the superimposed current traces before and after Iso recorded with ramp protocol. The averaged data from 5 cells is illustrated in panel D.

Figure 5. Lack of effects of ATP 0.5mM on the time independent outwardly rectifying current. Analog data for control (panel A) and for ATP (panel B) obtained by step protocol. Panel C displays the superimposed current traces before and after ATP recorded with ramp protocol. The averaged data from 6 cells is illustrated in panel D.

FIGURE 1

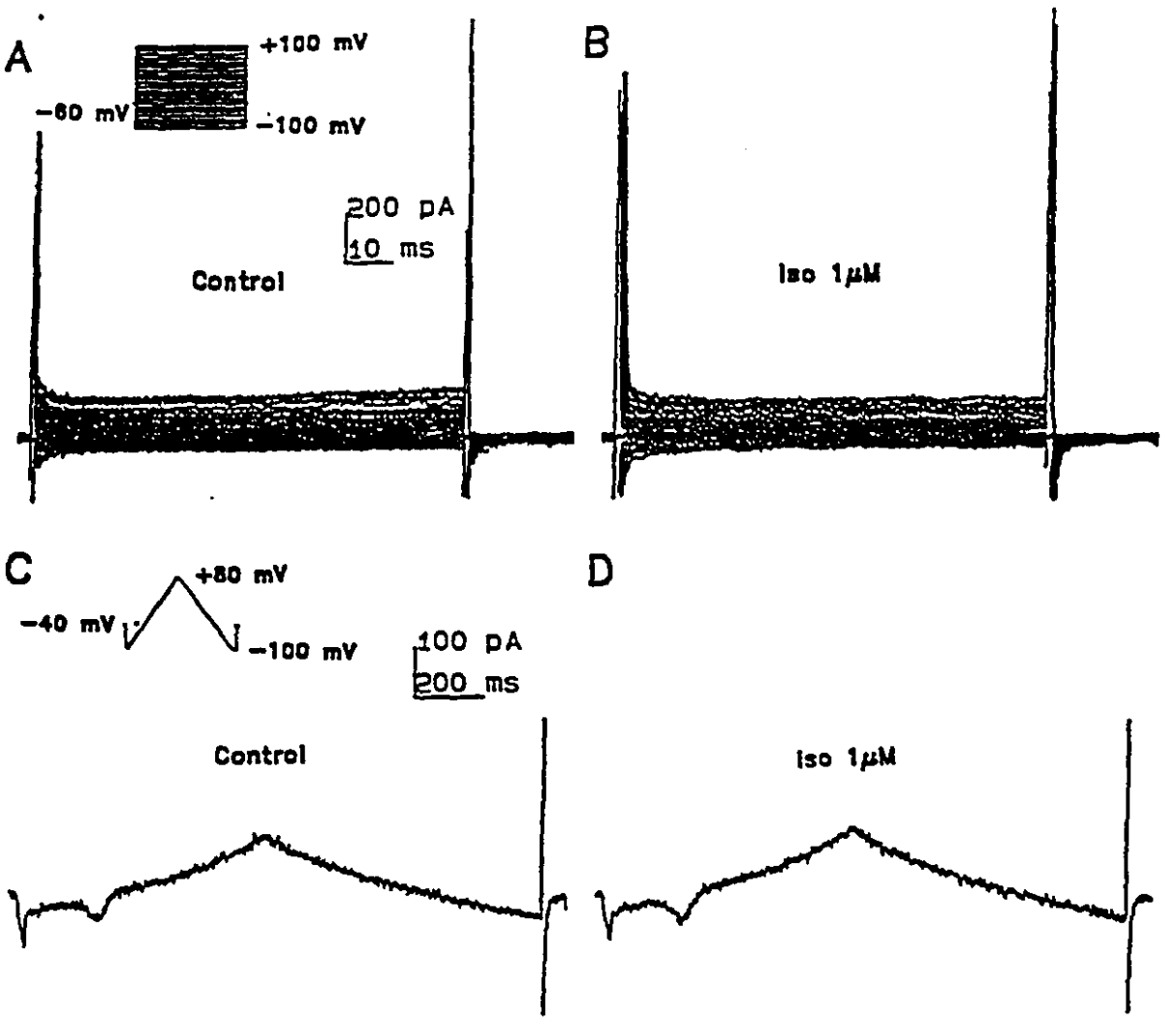
A
+100 mV
−60 mV
−100 mV
200 pA
10 ms
Control
B
Iso 1μM
C
+80 mV
−40 mV
−100 mV
100 pA
200 ms
Control
D
Iso 1μM

FIGURE 2

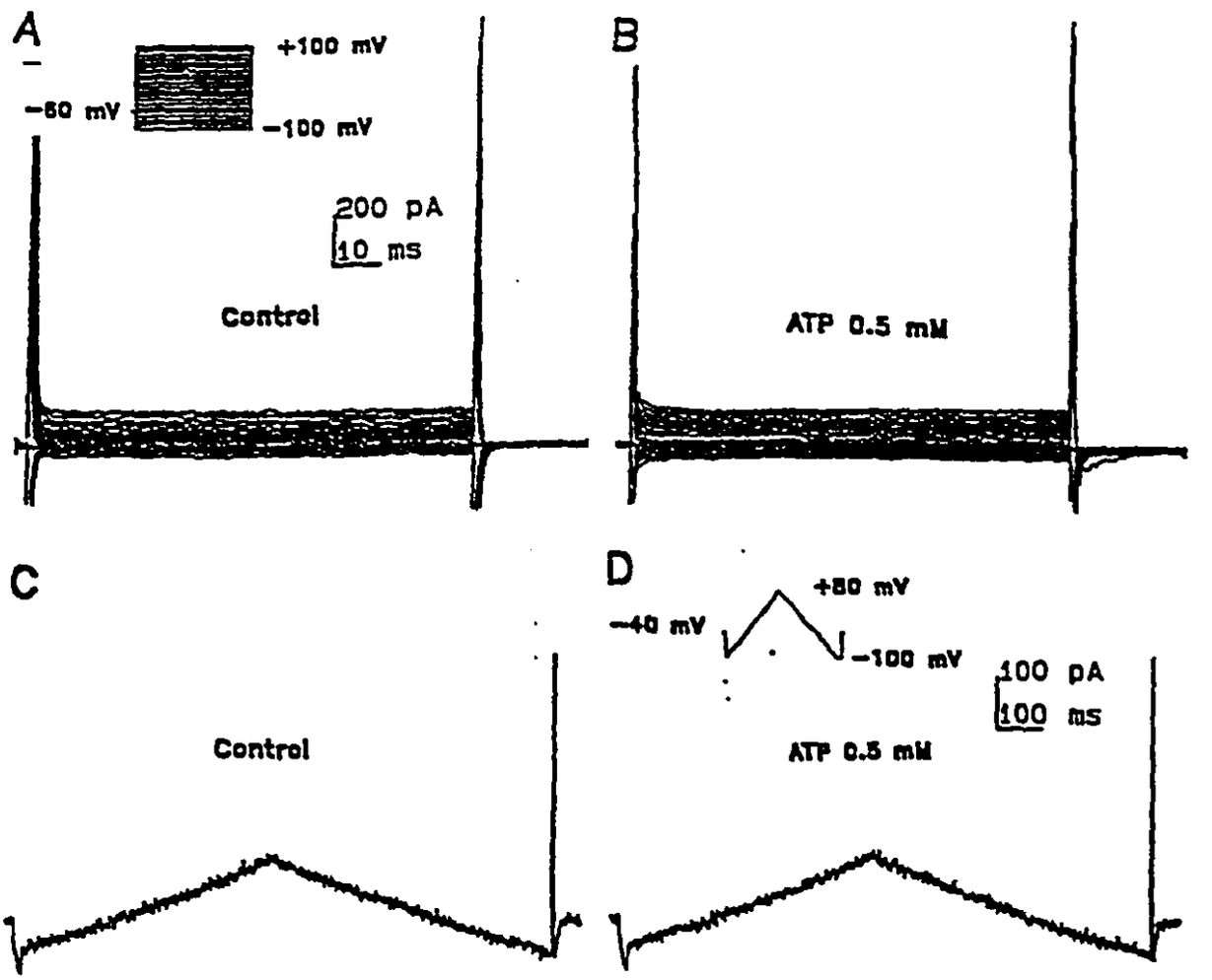
A
+100 mV
−60 mV
−100 mV
200 pA
10 ms
Control
B
ATP 0.5 mM
C
Control
D
+80 mV
−40 mV
−100 mV
100 pA
100 ms
ATP 0.5 mM

FIGURE 3

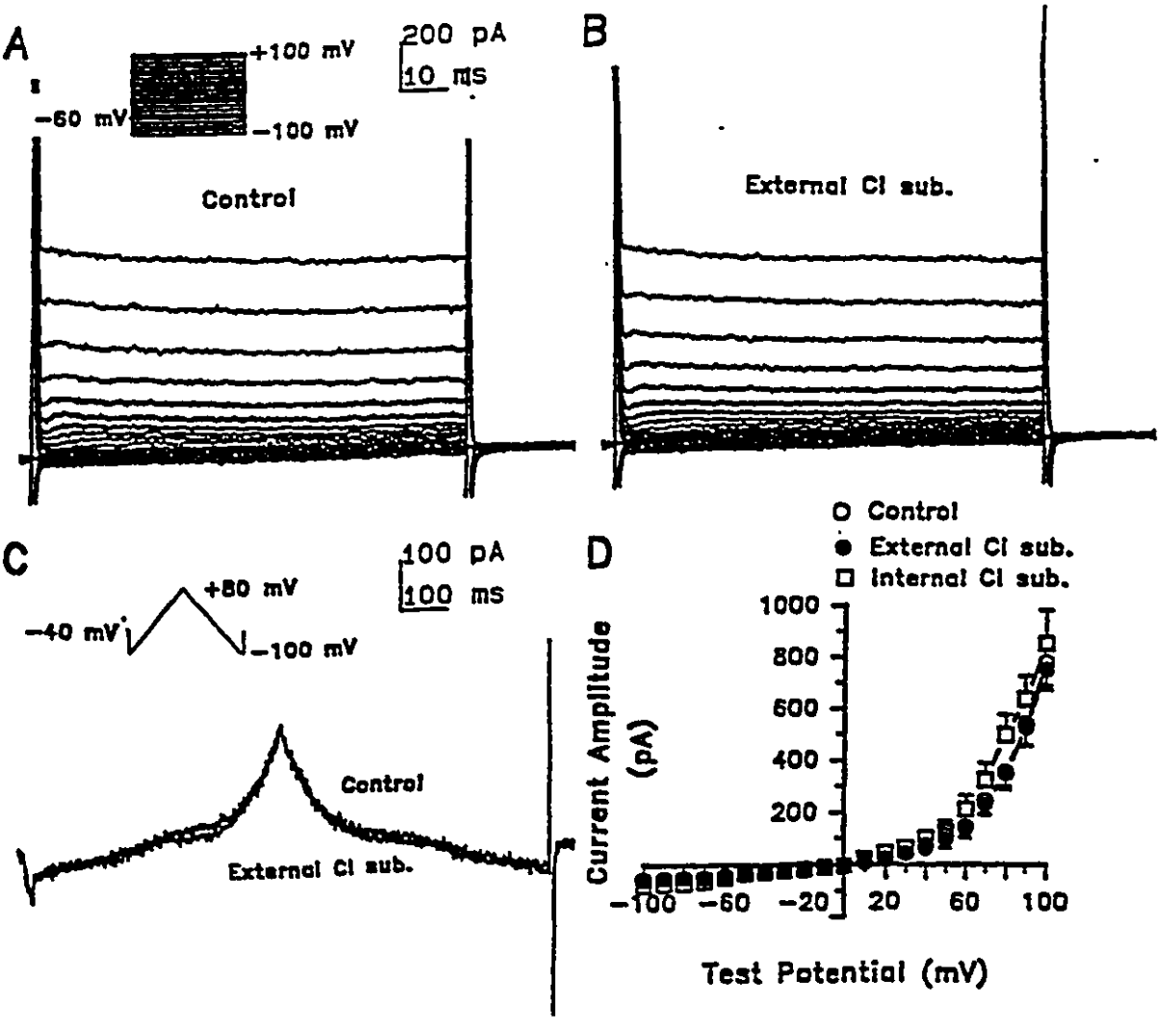
A
+100 mV
200 pA
10 ms
−60 mV
−100 mV
Control
B
External Cl sub.
C
100 pA
100 ms
+80 mV
−40 mV
−100 mV
Control
External Cl sub.
D
Control
External Cl sub.
Internal Cl sub.
Current Amplitude (pA)
1000
800
600
400
200
−100
−60
−20
20
60
100
Test Potential (mV)

FIGURE 4

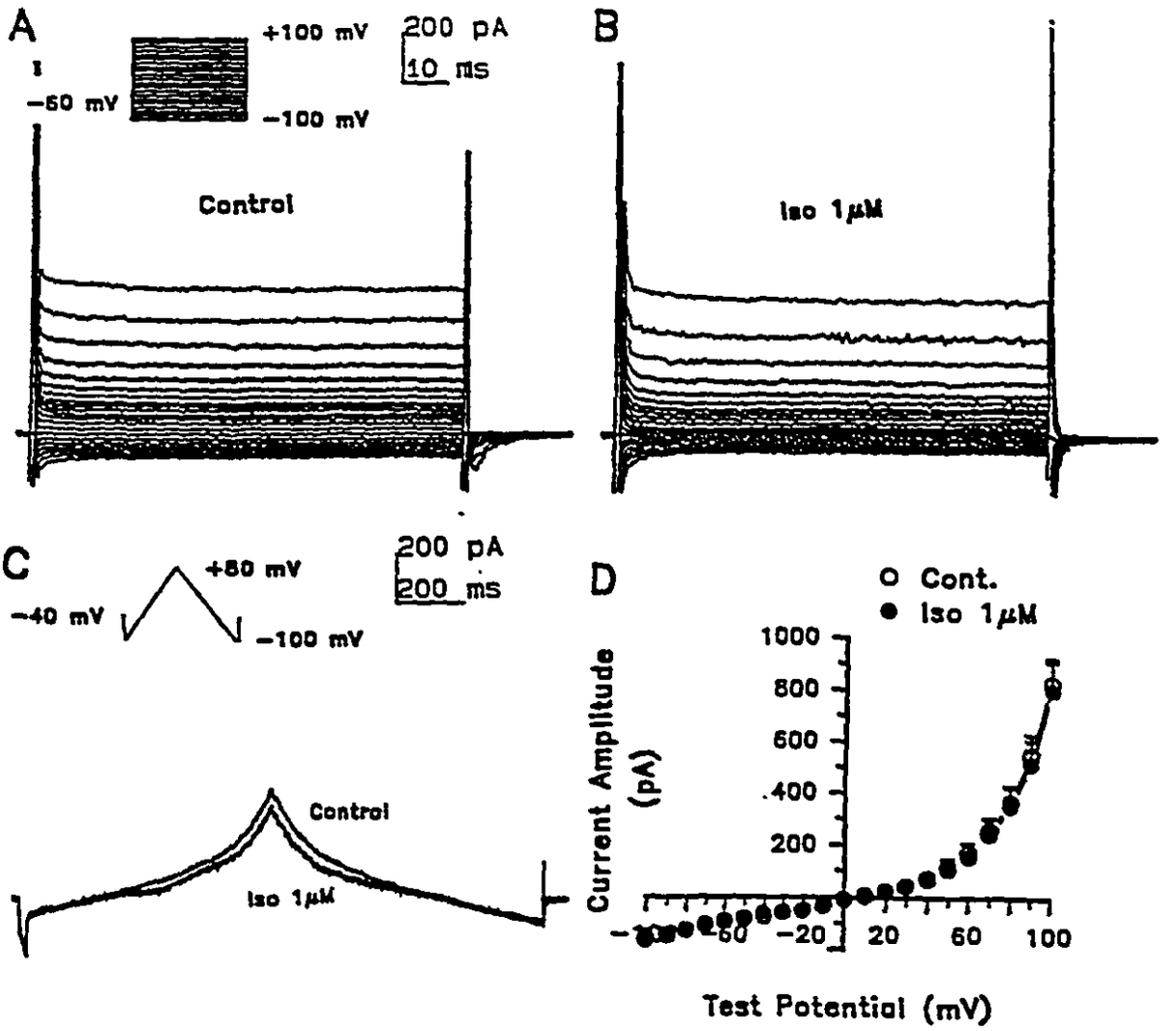
A
+100 mV
200 pA
10 ms
−60 mV
−100 mV
Control
B
Iso 1μM
C
+50 mV
200 pA
200 ms
−40 mV
−100 mV
Control
Iso 1μM
D
Cont.
Iso 1μM
Current Amplitude (pA)
1000
800
600
400
200
−60
−20
20
60
100
Test Potential (mV)

FIGURE 5

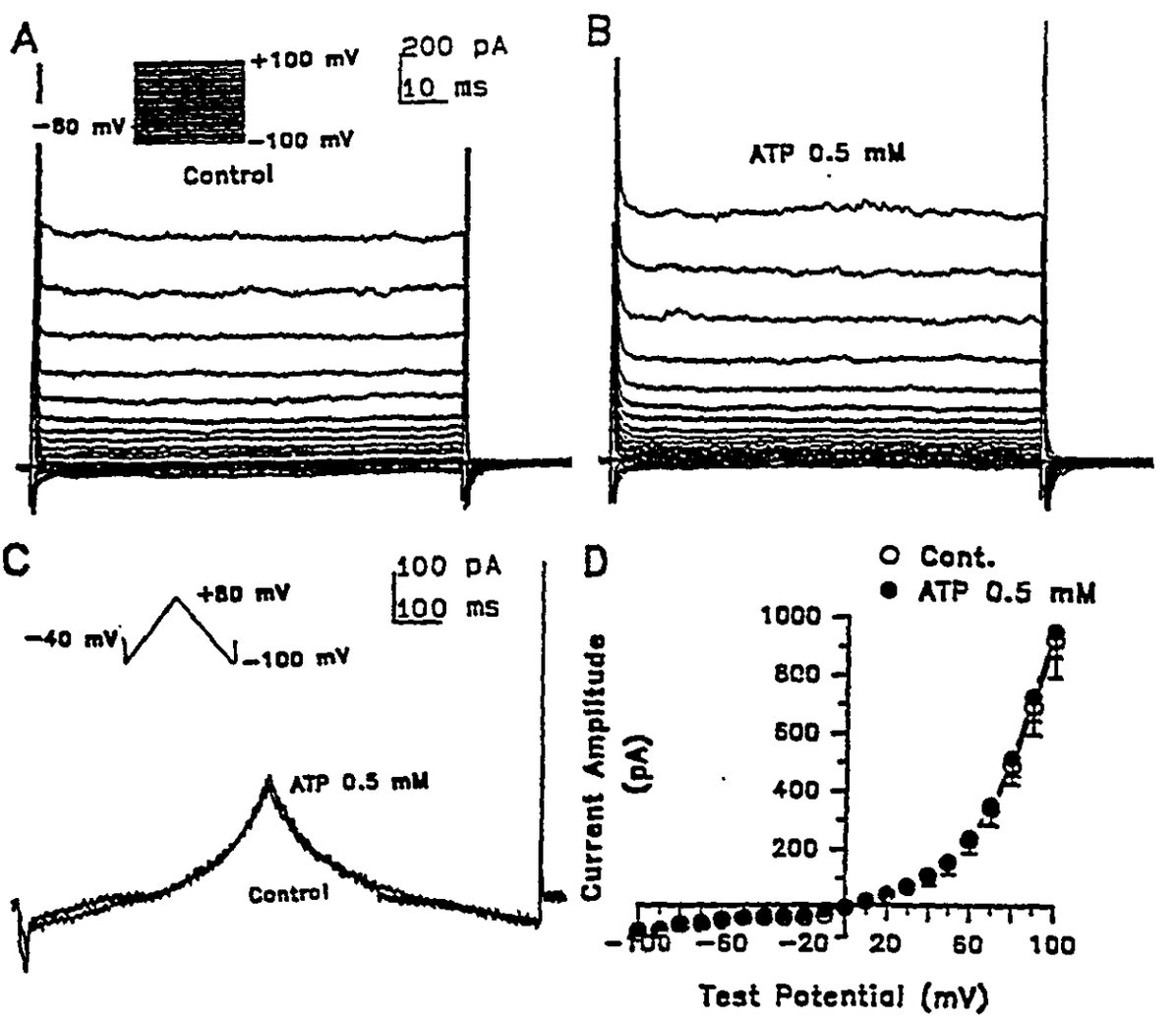
A
+100 mV
200 pA
10 ms
−80 mV
−100 mV
Control
B
ATP 0.5 mM
C
100 pA
100 ms
+80 mV
−40 mV
−100 mV
ATP 0.5 mM
Control
D
Cont.
ATP 0.5 mM
Current Amplitude (pA)
1000
800
600
400
200
−100
−60
−20
20
60
100
Test Potential (mV)

CHAPTER 4

DRUG EFFECTS ON REPOLARIZING CURRENTS IN HUMAN ATRIUM AND MECHANISM OF FREQUENCY DEPENDENCE OF REPOLARIZATION

Our results provide evidence against the existence of a few Cl^- currents including I_{ClCa} (I_{to2}), I_{ClcAMP}, I_{ClATP}, and $I_{Cl,b}$ (background Cl^- current), in normal human atrial myocytes under physiologic conditions. Absence of these Cl^- currents in these experiments rules against their contribution to membrane repolarization. Preliminary results, however, indicate the possibility of swelling-induced Cl^- in human atrial cells.

After detailed characterization of ionic currents in human atrial myocytes, we gained a much clearer picture of the ionic determinants of membrane repolarization. To our best knowledge, voltage-dependent K^+ currents (including I_{to1}, I_K and I_{Kur}) are the major repolarizing currents in human heart. It is also quite possible that these currents constitute the ionic targets for many antiarrhythmic drugs. It is not surprising that modulation of these currents must bring about direct or indirect alteration of the repolarization process, either lengthening or shortening APD and ERP. To investigate whether these currents account for flecainide's rate-dependent APD prolongation, we evaluated the effects of flecainide on I_{to1} and I_{Kur}, as compared to quinidine, a class Ia drug, and 4-AP, an I_{Kur} and I_{to1} blocker.

Effects of Flecainide, Quinidine, and 4-aminopyridine on Transient Outward and Ultra-rapid Delayed Rectifier Currents in Human Atrial Myocytes

ZHIGUO WANG, BERNARD FERMINI, and STANLEY NATTEL

Department of Medicine (B.F., S.N.), Montreal Heart Institute and University of Montreal, and the Departments of Pharmacology and Medicine (Z.W., S.N.), McGill University, Montreal, Canada

[1] Supported by the Medical Research Council of Canada, the Quebec Heart Foundation, and the Fonds de Recherche de l'Institut de Cardiologie de Montréal (FRICM).

Mr. Wang is supported by a Canadian Heart and Stroke Foundation Studentship. Dr. Fermini is a Knoll-Fonds de Recherche en Santé du Québec (FRSQ) Research Scholar.

Antiarrhythmic Drugs and Human Atrial K+ Currents

Send reprint requests to: Dr. Stanley Nattel, Montreal Heart Institute, 5000 Belanger Street East, Montreal, Quebec, Canada H1T 1C8. Tel.: (514) 376-3330. Fax: (514) 376-1355.

ABBREVIATIONS: AF, atrial fibrillation; 4AP, 4-aminopyridine; δ, fractional electrical distance; GΩ, gigohms; HP, holding potential; Hz, hertz (cycles/sec); IC_{50}, concentration for 50% of maximal inhibition; I_{Ca}, calcium current; I_K, delayed rectifier current; I_{K1}, inward rectifier current; $I_{K(ACh)}$, acetylcholine-induced K^+ current; I_{Kur}, ultra-rapid delayed rectifier current; I_{to}, transient outward current; I_{to1}, calcium-independent transient outward current; I_{to2}, calcium-dependent transient outward current; kHz, kilohertz; mg/L, milligrams per litre; min, minute; ml, millilitres; μM, micromoles/litre; mM, millimoles/litre; MΩ, megohms; μs, microseconds; nA, nanoamps; Na^+-K^+ ATP'ase, sodium-potassium ATP'ase; O.D., outside diameter; P_1, first pulse of a paired pulse protocol; P_2, second pulse; PF, picofarads; R_i, interval resistivity; R_{in}, input resistance; R_m, membrane resistance; R_s, series resistance; SC, space constant; S.E.M.. standard error of the mean; τ_c, capacitive time constant; τ_r, recovery time constant; U, unit.

ABSTRACT

Antiarrhythmic drugs prevent atrial reentrant arrhythmias by prolonging atrial action potential duration and refractoriness. The ionic mechanisms by which antiarrhythmic drugs alter human atrial repolarization are poorly understood. The present study was designed to assess the concentration-, voltage-, time-, and frequency-dependent effects of the antiarrhythmic agents quinidine and flecainide, as well as of the K^+ channel blocker 4-aminopyridine, on the calcium-independent transient outward current (I_{to1}) and the ultra-rapid delayed rectifier current (I_{Kur}) in isolated human atrial myocytes. Quinidine and flecainide blocked I_{to1} at clinically-relevant concentrations. Block of I_{to1} by quinidine was use- and frequency-dependent, while block by flecainide was frequency-independent and 4-aminopyridine showed use-dependent unblocking. Depolarizing prepulses enhanced flecainide block and reduced 4-aminopyridine block in a fashion suggesting a preferential interaction with the inactivated state for flecainide and with the resting, closed state for 4-aminopyridine. Quinidine block depended on the potential of a depolarizing test pulse in a fashion suggesting open channel block. All three drugs accelerated channel inactivation during depolarization at 1 Hz, and failed to block I_{to1} during initial current rise, with block appearing with time constants of 6.3 ± 1.2 ms for flecainide, 14.5 ± 4.2 ms for quinidine, and 3.0 ± 0.9 ms for 4-aminopyridine at 16°C, suggesting a role for channel opening in block development. Quinidine blocked I_{Kur} at clinical concentrations, while flecainide had no effect on I_{Kur}. Quinidine block of I_{Kur} was voltage-dependent, with part of the voltage-dependence attributable to open-channel block and the remainder compatible with a blocking site within the voltage field at a position subject to 23% of the total electrical field. These results indicate that flecainide and quinidine block I_{to1}, and quinidine blocks I_{Kur}, in human atrial myocytes in a state-dependent fashion. Since drug effects are manifest at clinically-relevant concentrations, and I_{to1} and I_{Kur} have been shown to be potentially important currents in human atrial repolarization, these findings are relevant to understanding the ionic mechanisms underlying the clinical antiarrhythmic properties of these drugs.

Key Words: Flecainide - quinidine - 4-aminopyridine - potassium channels - arrhythmias, cardiac-antiarrhythmic drugs - cardiac action potential - potassium channel blockers

Atrial fibrillation (AF) is the most common sustained arrhythmia in clinical practice (Kannel and Wolf, 1992). The restoration and maintenance of sinus rhythm would in theory constitute optimal therapy of AF, resulting in improved physical performance (Lipkin *et al.*, 1988) and a reduced risk of thromboembolic events (Cairns and Connolly, 1991). In practice, however, while direct current electrical cardioversion is highly effective in terminating AF and restoring sinus rhythm, relatively few patients remain in sinus rhythm over the subsequent months (Pritchett, 1992). Antiarrhythmic drugs are capable of preventing the recurrence of AF in a significant number of patients, but their efficacy is limited and at least some agents may result in an increased mortality rate in the AF population (Coplen *et al.*, 1990; Feld, 1990; Flaker *et al.*, 1992). The efficacy of antiarrhythmic drugs in AF is related to their ability to prolong atrial refractoriness (Rensma *et al.*, 1988; Kirchhof *et al.*, 1991; Wang *et al.*, 1992; Wang J *et al.*, 1993), generally by prolonging atrial action potential duration (Wang *et al.*, 1990). Currently-used antiarrhythmic drugs that prolong the atrial action potential have features of action, including Na^+-channel blocking properties and bradycardia-dependent effects on repolarization, that limit their efficacy and contribute to their proarrhythmic potential (Nattel, 1991).

In order to develop improved drug therapy for atrial arrhythmias, it is important to understand the mechanisms by which presently available antiarrhythmic drugs alter atrial repolarization in man. There is limited information in the literature about the actions of antiarrhythmic drugs on K^+ currents underlying atrial repolarization. Furthermore, the information that is available is based almost exclusively on results obtained with cells from species other than man. Important differences have been noted between K^+ currents in human atrial cells and those in other species, including discrepancies in kinetic properties (Fermini *et al.*, 1992) and qualitative differences in ionic current mechanisms (Wang *et al.*, 1993b). The present work was designed to evaluate the effects of two antiarrhythmic drugs used to treat atrial fibrillation in man, flecainide (Anderson *et al.*, 1989; Van Gelder *et al.*, 1989) and quinidine (Lewis *et al.*, 1922; Sokolow and Ball, 1956), on K^+ currents in human atrial myocytes. The currents studied were the transient outward current (I_{to}) and the ultra-rapid delayed rectifier (I_{Kur}), both of which may play an important role in human atrial repolarization (Escande *et al.*, 1982; Shibata *et al.*, 1989; Wang *et al.*, 1993b). Specific objectives included an analysis of the concentration-, voltage-, use- and time-dependence of drug action, and an assessment of possible state-selective drug-channel interactions that underlie and account for these properties. The classical K^+ channel blocking drug 4-aminopyridine (4AP) was also studied, in order to compare the mechanisms of channel blockade by this drug in human atrial cardiomyocytes with those already well-characterized in a variety of other cardiac (Castle and Slawsky, 1992; Campbell *et al.*, 1993) and non-cardiac (Thompson, 1982; Wagoner and Oxford, 1990) systems.

Materials and Methods

Isolation of single atrial cells. Specimens of human right atrial appendage were obtained from the hearts of 56 patients (60 ± 2 years old) undergoing aortocoronary bypass surgery. The procedure for obtaining the tissue was approved by the Ethics Committee of the Montreal Heart Institute. Samples obtained were quickly immersed in nominally Ca^{2+}-free Tyrode solution (100% O_2, 37°C) of the following composition (mM): NaCl 126, KCl 5.4, $MgCl_2$ 1.0, NaH_2PO_4 0.33, dextrose 10, N-2-hydroxyethylpiperazine-N'-2-ethanesulfonic acid (HEPES, Sigma Chemicals) 10; pH adjusted to 7.4 with NaOH. The myocardial specimens were chopped with scissors into cubic chunks (approximately 1 mm^3), and placed in a 25-ml flask containing 10 ml of the Ca^{2+}-free Tyrode solution. The tissue was gently agitated by continuous bubbling with 100% O_2 and stirring with a magnetic bar. After 5 min in this solution, the chunks were reincubated in a similar solution containing 390 U/ml collagenase (CLS II, Worthington Biochemical, Freehold, NJ) and 4 U/ml protease (Type XXIV, Sigma Chemicals, St. Louis, MO). The first supernatant was removed after 45 min and discarded. The chunks were then reincubated in a fresh enzyme-containing solution. Microscopic examination of the medium was performed every 15 min to determine the number and quality of the isolated cells. When the yield appeared to be maximal, the chunks were suspended in a solution of the following composition (mM): KCl 20, KH_2PO_4 10, glucose 10, glutamic acid 70, β-hydroxybutyric acid 10, taurine 10, EGTA 10, albumin 1%; pH adjusted to 7.4 with KOH, and gently pipetted. Only quiescent rod-shaped cells showing clear cross-striations were used.

Drugs and solutions. A small aliquot of the solution containing the isolated cells was placed in a 1-ml chamber mounted on the stage of an inverted microscope. Five minutes was allowed for cell adhesion to the bottom of the chamber, and then the cells were superfused at 3 ml/min with a solution containing (mM): choline Cl 126, KCl 5.4, $MgCl_2$ 0.8, $CaCl_2$ 1.0, NaH_2PO_4 0.33, HEPES 10, glucose 5.5; pH adjusted to 7.4 with NaOH. In order to minimize possible contamination from the delayed rectifier (I_K), the inward rectifier (I_{K1}), the acetylcholine-induced K^+ current (I_{KACh}) and choline-activated K^+ current, the following chemicals were used in all of our experiments unless otherwise specified: tetraethylammonium chloride (TEA, Sigma Chemicals, St. Louis, MO, 10 mM, to inhibit I_K) (Apkon and Nerbonne, 1991; Wang *et al.*, 1993a), $BaCl_2$ (Sigma Chemicals, 1 mM, to inhibit I_{K1}) and atropine [Sigma Chemicals, 100 nM, to inhibit I_{KACh} and choline-activated K^+ current (Fermini and Nattel, 1994)]. $CoCl_2$ (2 mM, Sigma Chemicals, St. Louis, MO) was always present to block I_{Ca} and the Ca^{2+}-activated component of transient outward current (I_{to2}). I_{Na} and Na^+ transporter currents such as those carried by the Na^+-K^+ ATPase and Na^+-Ca^{2+} exchange were minimized with the use of choline chloride (Sigma Chemicals, 126 mM) to replace superfusate NaCl (126 mM). In some experiments, the composition of the superfusate was additionally modified as specified below.

4-aminopyridine (4AP) was purchased from Sigma Chemicals, and was prepared as a 1-M stock solution in distilled water, with pH adjusted to 7.4 with hydrochloric acid. Quinidine gluconate was obtained from Rougier-Desbergers, Inc (Montreal, Que), and flecainide acetate was a gift of Riker-3M Pharmaceuticals (London, Ont). The latter agents were added directly to the superfusate reservoir to produce the desired concentrations in the superfusate.

Voltage-clamp technique and data acquisition. The whole-cell patch-clamp technique was employed to record ionic currents in the voltage-clamp mode. Borosilicate glass electrodes (1.0 mm O.D.) were used, with tip resistances of 2-5 MΩ (2.7 ± 0.4 MΩ, mean ± S.E.M., n = 43) when filled with (mM): KCl 130, $MgCl_2$ 1.0, HEPES 10, EGTA 5, Mg_2ATP 5, (pH adjusted to 7.4 with KOH) and connected to a patch-clamp

amplifier (Axopatch 1-D, Axon Instruments, Foster City, CA). Command pulses were generated by a 12-bit digital-to-analog converter controlled by pClamp software (Axon Instruments). Recordings were low-pass filtered at 1 kHz. Currents were digitized (model TM 125, Scientific Solutions, Solon, OH) and stored on the hard disk of an IBM AT compatible computer.

Junction potentials were zeroed prior to formation of the membrane-pipette seal in 1 mM Ca^{2+} Tyrode solution. Mean seal resistance averaged 12.4 ± 3.5 GΩ (n = 30). Several minutes after seal formation, the membrane was ruptured by gentle suction to establish the whole-cell configuration for voltage clamping. Rs along the clamp circuit was estimated by dividing the time constant obtained by fitting the decay of the capacitive transient (τ_c) by the calculated cell membrane capacitance (the time-integral of the capacitive surge measured in response to 5 mV hyperpolarizing steps from a holding potential of -60 mV) (Sigworth, 1983). The series resistance (Rs) was electrically compensated to minimize the duration of the capacitive surge on the current record and voltage drop across the pipette. Before Rs compensation, the decay of the capacitive surge was expressed by a single exponential having a time constant of 425 ± 30 μs (cell capacitance: 79 ± 6 pF, n = 43). Following compensation this value was reduced to 138 ± 12 μs (cell capacitance: 69 ± 4 pF). The initial Rs was calculated to be 5.4 ± 1.0 MΩ, and Rs was reduced to 2.0 ± 0.3 MΩ after compensation. Currents recorded during this study did not exceed 2 nA. The maximum voltage drop across Rs was therefore in the range of 4 mV. Cells with significant leak currents were rejected, and leakage compensation was not routinely used.

The length of single cells ranged from 74 to 116 μm (92.3 ± 5.4 μm, n = 24), and the diameter from 6.3 to 11.2 μm (9.4 ± 0.9 μm): the estimated cell surface area was therefore 3.0 ± 0.4 × 10^{-5} cm^2 based on assumed right cylinder geometry. The input resistance (R_{in}) was determined by the application of four consecutive 5-mV hyperpolarizing steps from a holding potential (HP) of –60 mV. Since no time-dependent current was activated with these small steps, the resulting change in current was used to calculate R_{in} (Giles and Van Ginneken, 1985). Mean R_{in} as estimated in 24 cells was 1.8 ± 0.1 GΩ. The resting space constant was calculated based on the equation: $sc = \sqrt{(r \cdot R_m/2R_i)}$ (Giles and Van Ginneken, 1985), where sc = space constant, r = cell radius, R_m = specific membrane resistance, and R_i = internal resistivity. R_m was estimated from the product of R_{in} and surface area, providing a mean value of 52.8 ± 3.2 kΩ·cm^2, and R_i was assumed to be 100-200 (Hume and Giles, 1981; Marty and Neher, 1983; Giles and Van Ginneken, 1985; Pressler, 1990). The mean space constant is 3.6 ± 0.4 mm if R_i = 100 Ω·cm and 2.5 ± 0.3 mm when R_i = 200 Ω·cm. Both values are over 25 times the cell length. In order to estimate the space constant during maximum current flow (at the time of peak I_{to1} conductance), R_{in} was obtained from the slope of the current-voltage relation for peak I_{to1} as measured upon depolarization from a HP of –70 mV. The space constant estimated in this fashion is between 630 and 890 μm, in the range of eight times the cell length.

Experiments were conducted at 36°C for analysis of I_{to1} (unless otherwise specified), with temperature maintained by a thermistor-controlled device (N.B. Datyner, Wellesley Hills, MA). In some instances, I_{to1} activation was studied at 16°C with the use of a Pelletier effect device (N.B. Datyner) in order to achieve better separation of current activation from the capacitance decay. Because of its very rapid activation, I_{Kur} was studied at room temperature (25°C). We have previously shown that temperature strongly affects the activation kinetics of I_{Kur} without altering its magnitude (Wang *et al.*, 1993b). Ten minutes of drug superfusion were allowed prior to measuring drug effects, after preliminary studies showed that this was ample time for steady-state changes to be achieved with all drugs. Under the experimental conditions

described, both I_{to1} and I_{Kur} were stable over time, with mean changes averaging $-1.2 \pm 2.3\%$ and $-0.9 \pm 1.4\%$ over 45 min of study respectively in the absence of interventions.

Data analysis. The amplitude of peak I_{to1} was measured as the difference between the peak of the transient outward current and the sustained current at the end of the pulse. The sustained current carried by I_{Kur} (Wang *et al.*, 1993b) was measured as the amplitude of the current at the end of the test pulse relative to the zero current level in the absence of voltage protocols to suppress I_{to1}. When depolarizing prepulses were used to inactivate I_{to1} and to study I_{Kur} selectively (Wang *et al.*, 1993b), I_{Kur} was measured as the step current relative to the zero current baseline.

Comparisons among groups were performed by analysis of variance (ANOVA) with Scheffé contrasts (Sachs, 1984). The significance of interactions between variables was evaluated with an F test for interaction. Baseline and drug data were compared by Student's t test, and a two-tailed probability of $\pm 5\%$ was taken to indicate statistical significance. Group data are presented as the mean $\pm$ S.E.M.. Nonlinear curve fitting (Marcquardt's procedure) was performed with the use of *Clampfit* in *pClamp* (Axon Instruments, Foster City, CA) or *Sigmaplot* (Version 5.0, Jandel Scientific Co.) software.

Results

Drug Effects on I_{to1}

Concentration-dependence of I_{to1} Inhibition. Figure 1 shows the concentration-dependent inhibition of I_{to1} by flecainide, quinidine, and 4AP. All three agents significantly inhibited I_{to1}. Results of individual experiments are illustrated in Panel A. While all compounds suppressed peak I_{to1}, they also appeared to accelerate I_{to1} inactivation. In addition, quinidine and 4AP suppressed the sustained current level at the end of the pulse, in contrast to flecainide which left the sustained current unaltered. Mean data for peak I_{to1} inhibition in eight experiments with flecainide, five with quinidine, and six with 4AP are shown in Panel B. Effects of quinidine and flecainide were noted over the clinically-relevant concentration range (1-5 μM), with quinidine inhibiting I_{to1} more potently than flecainide.

Frequency- and Use-Dependence of I_{to1} Inhibition

The actions of many channel-blocking drugs are known to be state-dependent, resulting in effects that depend on the voltage and frequency of depolarization. Figure 2 illustrates the use-dependence of I_{to1} block. Over 10 min after the onset of drug superfusion, the preparation was held at a potential of –50 mV, and then a train of 100 ms depolarizing pulses to +20 mV was delivered at 1 Hz. A similar protocol was applied to study the use-dependence of I_{to1} under control conditions. As shown in Panel A, under control conditions and in the presence of flecainide (5 μM), I_{to1} was not altered by repetitive pulsing. In the presence of quinidine (5 μM), I_{to1} progressively decreased during successive pulses. The opposite was seen in the presence of 4AP (2 mM), with I_{to1} progressively increasing with repeated pulses. Of note, in the presence of 4AP current inactivation was substantially slowed during the first pulse, and accelerated for subsequent pulses. In some experiments with 4AP inactivation of I_{to1} during the first pulse appeared biphasic, with an early rapid phase followed by a greatly slowed terminal phase. Peak I_{to1} was measured during each pulse of the train, and mean values (± S.E.M.) for control and drug conditions are shown in Panel B (a-c). While mean I_{to1} was independent of pulse number under control conditions (open symbols) and in the presence of flecainide (fig. 2B-a), peak current decreased with an exponential time constant of 1.1 ± 0.1 pulses in the presence of quinidine and increased with a time constant of 0.5 ± 0.1 pulses in the presence of 4AP. Of note, quinidine block was absent prior to the first channel opening (pulse 1), in contrast to block by flecainide and 4AP for which first-pulse block was clear. Use-dependence of block was statistically significant for quinidine and 4AP, but not for flecainide (fig. 2B-d). In all instances, peak I_{to1} reached steady-state values within 10 pulses.

To evaluate the steady state frequency dependence of I_{to1} block, we repeated the same voltage protocols as described for figure 2 at 0.1, 1, 2 and 2.5 Hz. Results are shown in figure 3. Consistent with its lack of use-dependent action, flecainide (5 μM) inhibited I_{to1} to the same extent at all frequencies. Quinidine-induced inhibition of I_{to1} was enhanced by more rapid pulsing (e.g., the drug reduced I_{to1} by 33 ± 7% at 0.1 Hz compared to 57 ± 9% at 2.5 Hz, $P < 0.01$). Block by 4AP showed the opposite pattern, averaging 70 ± 5% at 0.1 Hz and 19 ± 5% at 2.5 Hz ($p<0.001$). Qualitatively similar results were obtained at other test potentials ranging from –20 mV to +50 mV.

Kinetics of Pulse-Dependent Blocking and Unblocking

Frequency- and use-dependent drug action during periodic pulsing is due to differential drug interaction with the depolarized and polarized states, along with time-dependent block and unblock. The increase in block by quinidine at faster rates suggests that depolarization enhances the drug's effect on the channel,

and that there is time-dependent recovery following repolarization. Rate-dependent unblock with 4AP suggests the opposite — that depolarization leads to a reduction in the drug-channel interaction, and that block is restored in a time-dependent fashion upon repolarization. We used paired pulses delivered at 0.05 Hz to assess directly time-dependent changes in block at the holding potential following a depolarizing pulse. Two 200-ms pulses (P_1 and P_2) to +40 mV from a HP of –80 mV were separated by a P_1-P_2 coupling interval varying from 5 ms to 1.6 s (flecainide and quinidine) or 16 s (4AP). Figure 4 shows the ratio of peak I_{to1} elicited by P_2 to the value during P_1, plotted as a function of the P_1-P_2 interval. Flecainide did not significantly alter the recovery of I_{to1}, with a recovery time constant (τ_r) that averaged 21 ± 2 ms under control conditions and 27 ± 2 ms in the presence of the drug (Panel A). In contrast, quinidine (Panel B) significantly slowed the recovery of I_{to1}, increasing τ_r from 20 ± 1 ms to 41 ± 2 ms ($P < 0.01$). Panel D shows the degree of drug-induced inhibition of I_{to1} during P_2 relative to control values at the same P_1-P_2 interval. The degree of I_{to1} inhibition by flecainide was not significantly dependent on P_1-P_2 interval ($P > 0.05$, F test for interaction), but that by quinidine was significantly attenuated with increasing P_1-P_2 interval ($P < 0.001$, F test). The dissipation of quinidine block with increasing coupling interval was a monoexponential function of time with a time constant averaging 59 ± 7 ms. 4AP did not alter the reactivation of I_{to1}, as indicated by the superimposition of data recorded for P_1-P_2< 200 ms under control conditions (open diamonds, Panel C) on those in the presence of 4AP (filled diamonds). For P_1-P_2 intervals > 250 ms, however, the current elicited by P_2 in the presence of 4AP diverges increasingly from control values as the coupling interval becomes larger. This process is well described by a single exponential relation with a time constant of 4.2 ± 0.1 s.

Similar results were obtained when reactivation was assessed at other holding potentials. For example, flecainide (5 μM) increased τ_r slightly, but not significantly, from 40 ± 3 ms to 58 ± 7 ms at –50 mV (n = 3), and from 98 ± 9 ms to 124 ± 18 ms at –40 mV (n = 3). Quinidine increased τ_r from 37 ± 4 ms to 91 ± 5 ms at –50 mV ($P < 0.001$, n = 3), and from 98 ± 11 ms to 195 ± 22 ms at –40 mV ($P < 0.01$, n = 3), relative changes quite similar to those produced by the drug at –80 mV. 4AP produced no appreciable change in reactivation of I_{to1} at a HP of either –50 or –40 mV.

The onset of block during a depolarizing pulse was also studied with a paired-pulse protocol, in which a 100-ms test pulse (P_2) from a HP of –60 mV to +30 mV was preceded by a conditioning pulse (P_1) over the same voltage range with a duration that varied from 5 to 180 ms. The P_1-P_2 interval was fixed at 50 ms, selected to be long enough to allow for near-complete recovery of I_{to1} under control conditions, but short enough to observe residual drug-induced block developed during the prepulse. Pairs of pulses were delivered every 10 s. Results are shown in figure 5, with raw data at the left of the figure, and the ratio of current elicited by P_2 to that elicited by P_1 shown as a function of P_1 duration at the right of the figure. Under control conditions, the amplitude of I_{to1} elicited by P_2 was not significantly affected by the presence of a preceding P_1, irrespective of the latter's duration, indicating that the 50-ms interpulse interval was sufficient to allow for near-complete recovery of I_{to1}. In the presence of flecainide, the current elicited by P_2 was not significantly altered by a P_1 of very short duration (5 ms, fig. 5A, right panel). However, as P_1 was progressively prolonged in the presence of the drug, the amplitude of the current elicited by P_2 progressively decreased, reaching a steady state within 40 ms. I_{to1} elicited by the test pulse was a monoexponential function of prepulse duration, with a time constant of 11 ± 3 ms. The presence of a prepulse also significantly reduced the current elicited by the test pulse in the presence of quinidine (fig.

5B), but the onset of additional block was very rapid, reaching steady state for a prepulse duration of 10 ms. The time constant of this process averaged 4.4 ± 1.0 ms. In the case of 4AP, the presence of a prepulse increased the current elicited by the test pulse, with prepulse effects reaching steady state for a prepulse duration of 100 ms. The time constant for the increase in current during P_2 as a function of prepulse duration averaged 42 ± 5 ms.

Voltage-Dependence of I_{to1} Inhibition During a Single Pulse

In order to determine the influence of the fraction of channels opened by a test pulse on drug block during the pulse, we measured I_{to1} during 100-ms pulses from a HP of –50 mV to a variety of test potentials. Figure 6 illustrates drug effects on I_{to1} as a function of pulse potential at a frequency of 0.1 Hz, for which there is minimal residual effect from previous pulses. Current-voltage relations under control conditions and in the presence of each drug (5 μM for quinidine and flecainide, 2 mM for 4AP) are shown in Panels A-C. Panel D shows the reduction in peak I_{to1} caused by each drug as a function of test potential. Quinidine's inhibitory action was strongly voltage-dependent ($P < 0.001$), with very little block at the voltage threshold for I_{to1} activation, and increasing blockade as voltages became more positive (Panel D). In contrast, no statistically-significant voltage-dependence of block by 4AP and flecainide was observed. In order to relate the voltage dependence of quinidine's blocking action to the voltage dependence of I_{to1} activation, we assessed the latter based on the control peak I-V relation, correcting for changes in driving force with an assumed reversal potential of –80 mV. We have previously shown that the activation curve for I_{to1} obtained in this way is very similar to the curve obtained with tail current measurements (Wang *et al.*, 1993b). As shown in Panel E, quinidine-induced I_{to1} blockade was linearly related to fractional channel activation.

The analysis in figure 6 addresses the relationship between voltage-dependent channel activation and block. To assess the relationship between voltage-dependent inactivation and block, we observed the effects of prepulses (600 ms for flecainide and quinidine, 10 s for 4AP) to between –90 and +20 mV on I_{to1} elicited by test pulse depolarization to +50 mV in the absence and presence of blocking drugs. The pulse protocol was delivered at a frequency of 0.05 Hz. Figure 7 (Panels A-C) shows the absolute values of mean currents, while percentage reductions caused by each drug are shown in Panels D-F. The blocking effect of flecainide was significantly voltage-dependent, with stronger inhibition occurring at more positive prepulse potentials. This manifested itself as a hyperpolarizing shift in the I_{to1} inactivation curve, as determined by fitting the peak current following each prepulse to a Boltzmann function of prepulse potential. Flecainide shifted the curve in a hyperpolarizing direction by 1.6 ± 0.3 mV ($n = 8$), 6.4 ± 1.2 mV ($n = 8$), and 8.2 ± 2.1 mV ($n = 8$) at 1, 5, and 10 μM concentrations respectively. Neither quinidine nor 4AP significantly altered the voltage dependence of inactivation. Quinidine's actions were not altered by prepulses to various voltages, while 4AP's blocking actions were weakly reduced by depolarization. In order to further assess the effects of depolarizing prepulses on 4AP's interaction with I_{to1}, we applied the revised voltage protocol shown by the inset in Panel F. A brief period at the holding potential (50 ms) was inserted after the prepulse to allow for recovery from inactivation of drug-free channels. The results, shown by the filled symbols in Panels C and F, indicate that 4AP binding was reduced by depolarization in a voltage-dependent fashion.

The intensity of flecainide blockade of I_{to1} channels was linearly related to the fraction of channels inactivated by the prepulse. In order to test the possibility that flecainide block and 4AP unblock during the

prepulse are related to channel inactivation, fractional inactivation caused by conditioning pulses was determined as a function of prepulse potential from the amplitude of I_{to1} following depolarizing prepulses under control conditions. The linear correlation coefficient between fractional block by flecainide and fractional channel inactivation was 0.98, 0.99, and 0.99 at concentrations of 1, 5, and 10 μM respectively. Block of I_{to1} by 4AP was inversely related to the fraction of channels inactivated by the depolarizing prepulse, with a correlation coefficient of 0.996.

Drug-Induced I_{to1} Blockade and Channel Opening

The above data show that blockade of I_{to1} by quinidine is linearly related to the fraction of channels activated by a test pulse (fig. 6), while block by flecainide is linearly related to the fraction of channels inactivated by a depolarizing prepulse (fig. 7). The former is consistent with open-channel blockade, the latter with preferential inactivated-channel blockade. Depolarizing prepulses enhanced flecainide-induced blockade during a subsequent test pulse with a time constant of 11 ± 3 ms (fig. 5), of the same order as the mean time constant for inactivation (12 ms, see fig. 8), compatible with an interaction with the inactivated state. On the other hand, the effect of prepulses to enhance block by quinidine was fully expressed with much shorter prepulses (fig. 5), compatible with a favoured interaction with the open state. Block by 4AP dissipated in a time-dependent fashion upon depolarization (fig. 5) and re-established itself slowly at a negative holding potential (fig. 4). 4AP unblocking resulted from depolarizing prepulses, with a voltage-dependence that paralleled that of channel inactivation. These observations are consistent with a high affinity of 4AP for the rested closed state of the channel, and a low affinity for the inactivated state.

Despite these apparently different state-dependent interactions with the I_{to1} channel, all three drugs exhibited common features suggesting a blocking reaction that was linked to channel opening. Figure 8 shows the inactivation time constant for I_{to1} as determined upon depolarization from −50 mV to +20 mV at a frequency of 1 Hz in the absence and presence of blocking drugs. Representative experimental tracings are shown in Panels A-C, along with monoexponential fits to current inactivation data. Panel D shows mean inactivation time constants, which were decreased by each drug in a concentration-dependent way.

Acceleration of inactivation can be a result of rapid blocking of open channels (Dukes *et al.*, 1990). Figure 9 shows another line of evidence consistent with this possibility. The time course of I_{to1} current was studied upon depolarization with the same voltage protocol as that used in figure 8. Currents in the absence and presence of flecainide (Panel A), quinidine (Panel B), and 4AP (Panel C) were analyzed at 36°C (left, n = 10, 8, and 11 cells for flecainide, quinidine, and 4AP) or 16°C (right, n = 5, 6, and 4 cells for the same drugs respectively). Experiments were performed at the lower temperature to obtain more complete separation between I_{to1} and the capacitance signal, and to observe the effects of temperature upon the phenomenon studied. Mean I_{to1} data from all experiments are shown in the figure, with open diamonds representing mean currents under control conditions and open circles showing results in the presence of the drug. For each drug, initial current values upon depolarization differed minimally from those under control conditions. With time, however, current in the presence of a blocking drug was reduced compared to control values. When drug-induced block was expressed as a function of time following depolarization (points), it increased in a time-dependent way. The onset of block was well-fitted by an exponential function of time (curve fits shown by solid lines in figure), with a time constant at 36°C of 2.2 ± 0.4 ms for flecainide, 5.5 ± 1.1 ms for quinidine, and 1.1 ± 0.2 ms for 4AP. Results were qualitatively

similar at 16°C, but block onset was slowed about 3-fold, with time constants averaging 6.3 ± 1.2 ms for flecainide, 14.5 ± 4.2 ms for quinidine, and 3.0 ± 0.9 ms for 4AP.

Effects on the Ultra-Rapid Delayed Rectifier (I_{Kur})

As shown in figure 1A, quinidine and 4AP suppressed the sustained outward current observed during a depolarizing pulse after inactivation of I_{to1}. We have previously identified the underlying current (Wang *et al.*, 1993b) as a novel, ultra-rapidly activating delayed rectifier K^+ current (I_{Kur}) whose properties identify it with the Kv1.5 group of cloned K^+ channel currents (Philipson *et al.*, 1991; Snyders *et al.*, 1991; Tamkun *et al.*, 1991; Fedida *et al.*, 1993). We used previously-developed and fully-characterized voltage protocols (Wang *et al.*, 1993b) to study selectively the effects of quinidine, flecainide, and 4AP on I_{Kur}. Figure 10A (top panels, Control) shows typical I_{Kur} recordings elicited by depolarizing pulses from a HP of –50 mV, 10 ms after a 1-s prepulse to +40 mV to inactivate I_{to1}. Experiments were performed at 25°C in order to be able to resolve the very rapid activation kinetics of the current. Flecainide (5 μM) did not alter I_{Kur} (fig. 10A-a, bottom), while the same concentration of quinidine clearly decreased the current (fig. 10A-b). 4AP also substantially reduced I_{Kur} (fig. 10A-c).

Figure 10B provides mean data for the I_{Kur} current-voltage relation before and after drug exposure (n = 9, 11, 15 for flecainide, quinidine, and 4AP respectively) at 5 μM concentrations for flecainide and quinidine, 50 μM and 2 mM for 4AP. While flecainide (fig. 10B-a) did not reduce the current at any test potential, both quinidine (fig. 10B-b) and 4AP (fig. 10B-c) substantially reduced the current elicited over a wide range of voltages. Quinidine's effects were strongly voltage-dependent (filled squares in fig. 10B-d), increasing with stronger depolarization. Similar voltage-dependence was observed at all quinidine concentrations studied. The effect of 4AP was weakly voltage-dependent at a concentration of 50 μM, and voltage-independent at 2 mM.

Figure 11 shows the concentration-dependence of drug action on I_{Kur}. The results shown were obtained at a test potential of +40 mV. At this voltage, both quinidine and 4AP produced concentration-dependent inhibition of I_{Kur}, with an IC_{50} of approximately 5 μM for quinidine and 50 μM for 4AP. Possible rate-dependence of block was analyzed (fig. 12) with a series of ten 100-ms pulses from –50 mV to +40 mV at the frequencies indicated. The tenth pulse was preceded (by 10 ms) by a 500-ms depolarization to +40 mV to inactivate I_{to1}. No frequency dependence of inhibition was observed for any of the drugs at the range of rates studied.

To exclude the possible influence of temperature on drug effects, we also evaluated I_{Kur} by measuring the sustained current at the end of 200-ms pulses (without a prepulse to inactivate I_{to1}), or with the standard prepulse protocol as in figure 12, at a more physiologic temperature of 36°C. Qualitatively similar results to those shown in figure 12 were obtained, in terms of both voltage- and frequency-dependence of drug action.

Discussion

We have shown that flecainide, quinidine, and 4AP cause voltage- and time-dependent block of I_{to1} in human atrial myocytes. The blocking actions of flecainide and quinidine are manifest at clinically relevant concentrations. In addition, quinidine and 4AP inhibit I_{Kur}. These studies are, to our knowledge, the first detailed assessment of the K^+-channel blocking actions of antiarrhythmic drugs in human atrial cells.

Comparison With Previous Studies of State-Dependent I_{to1} Block by Quinidine, Flecainide and 4AP

Imaizumi and Giles were the first to report quinidine's inhibitory action on I_{to} in heart cells from the rabbit (Imaizumi and Giles, 1987). They noted an IC_{50} of 7 μM, of the same order as the value we observed in human atrium (fig. 1). They also observed an acceleration of inactivation and slowed recovery from inactivation, without a shift in the voltage dependence of inactivation, findings which they interpreted as consistent with open-state blocking by the drug (Imaizumi and Giles, 1987). Open-state block was also postulated to account for the properties of quinidine-induced block of transient A-type current in molluscan nerve (Hermann and Gorman, 1984). Liu *et al.* (1991) communicated preliminary data which they interpreted as indicating a lack of voltage- and frequency-dependent block by quinidine of I_{to} in rabbit atrium. However, voltage- and rate-dependence were examined over a limited range, and while statistical analyses are not presented, block appeared to be enhanced at more positive voltages and faster rates, consistent with our findings. It must be noted that the analysis of time- and rate-dependent I_{to} block in rabbit atrial cells is limited by the very slow intrinsic recovery kinetics of I_{to} in this system (Fermini *et al.*, 1992). Yatani *et al.* (1993) studied in detail quinidine block of transient outward K^+ channels encoded by RHK1, a rat heart clone with 98% homology to the human cardiac I_{to}-like channel clone, HK1 (Tamkun *et al.*, 1991; Yatani *et al.*, 1993). While the IC_{50} for quinidine block of RHK1 was in the range of 1 mM, two orders of magnitude larger than values obtained for native currents in our studies or those of Imaizumi and Giles (1987), other aspects of quinidine block were quite similar. Block was enhanced by more positive test voltage, required channel opening to be manifest, and was associated with decreased mean open time of unitary current, all features indicating open-channel block (Yatani *et al.*, 1993). The only study of flecainide block that we could identify was published in abstract form, and indicated that flecainide blocks I_{to} in human ventricular myocytes with an IC_{50} of 2.5 μM while accelerating inactivation (similar to our observations), but without any obvious voltage- or use-dependence (Näbauer and Beuckelmann, 1992). The greater potency of flecainide in the latter study compared to our results (fig. 1) is due (at least in part) to the fact that the IC_{50} calculation in the latter study was based on the time-integral of I_{to}, not peak current (Näbauer M., personal communication). Since flecainide accelerates inactivation, it would have been a much greater effect on the current-time integral than on peak current.

Many investigators have studied the voltage-, time-, and state-dependence of K^+ channel block by 4AP. Three studies of I_{to} block by 4AP in cardiac cells have been published (Simurda *et al.*, 1989; Castle and Slawsky, 1992; Campbell *et al.*, 1993). All three studies found that block is removed by depolarization and restored slowly over time following the return to a more negative holding potential, resulting in use-dependent unblocking and a reverse use-dependent pattern of channel blockade. In a detailed analysis of concentration-, voltage-, and time-dependent 4AP block of I_{to} in rat ventricular myocytes, Castle and Slawsky concluded that the drug has its highest affinity for the resting closed state, and that its affinity progressively decreases through the chain of intermediate closed states between the rested and open state (Castle and Slawsky, 1992). Campbell *et al.* (1993) arrived at similar conclusions, in an elegant study of

4AP block of I_{to1} in ferret ventricular myocytes. A Markov chain model was developed to describe the kinetics of I_{to1}, and state-dependent kinetic terms accounted well for the blocking properties of 4AP. Studies of 4AP block of K^+ currents in non-cardiac systems have produced a variety of findings. Evidence for open-channel block has been obtained in studies of 4AP action on K^+ channels in molluscan neurons (Thompson, 1982), GH_3 pituitary cells (Wagoner and Oxford, 1990), activated murine B lymphocytes (Choquet and Korn, 1992), and cloned Shaker H4 channels expressed in Xenopus oocytes (Hice *et al.*, 1992). Kehl (1990) showed that a model of preferential 4AP binding to the rested state reproduced well the frequency dependence of 4AP block of transient outward current in rat melanotrophs.

Our findings regarding time-, voltage-, and rate-dependent block of I_{to1} in human atrial cells share many features with previous observations in other systems. Like Imaizumi and Giles (1987), Hermann and Gorman (1984), and Yatani *et al.* (1993), we found that the voltage-dependence and kinetics of I_{to1} block by quinidine suggest a favoured interaction with open channels. Time-dependent unblocking on returning to the holding potential slowed the recovery of I_{to1} and caused use- and frequency-dependent inhibition of the current. The enhancement of flecainide block by depolarizing prepulses, its ability to shift the inactivation curve in a hyperpolarizing direction, and the time-dependence of additional block produced by depolarizing prepulses are all compatible with high affinity for the inactivated state. The lack of significant change in I_{to1} reactivation kinetics by flecainide (fig. 4) suggest rapid unblocking upon return to the holding potential, consistent with the lack of use- and frequency-dependence of flecainide block. Our observations regarding 4AP block are in general agreement with previous studies in cardiac tissues (Simurda *et al.*, 1989; Castle and Slawsky, 1992; Campbell *et al.*, 1993). As in these previous studies, we found that 4AP block is reverse use-dependent, decreases upon depolarization, and is restored in a time-dependent fashion upon repolarization. On the other hand, we also observed features suggestive of a role for channel opening in block development, as previously noted in non-cardiac systems (Thompson, 1982; Hice *et al.*, 1992). These features include acceleration of current inactivation (fig. 8) and a time-dependent onset of block following depolarization (fig. 9).

Acceleration of I_{to1} inactivation and time-dependent block upon channel opening were observed for all three drugs (figs. 8 and 9). Similar properties have previously been noted for I_{to} block by tedisamil (Dukes *et al.*, 1990), bupivicaine (Castle, 1990), and propafenone (Duan *et al.*, 1992), and interpreted as indicative of open-channel block. There is an apparent contradiction between this behaviour compatible with open-channel blocking that was present for all three drugs that we studied, and the favoured state for blockade based on other lines of evidence. A simple way to explain these observations is that the initial state-dependent binding of each drug to the channel protein (which may occur preferentially when channels are rested or inactivated) is followed by a final blocking step upon channel activation. Blockade would then rapidly follow channel opening, causing a time-dependent appearance of block and an acceleration in the kinetics of inactivation. This type of behaviour could occur if drug molecules mimicked endogenous N-type inactivation (Hoshi *et al.*, 1991), moving in the voltage field upon depolarization to a cationic binding site and occluding the channel pore. Drug block mimicking intrinsic inactivation was initially postulated by Armstrong to explain tetraethylammonium block of K^+ currents (Armstrong, 1966; Armstrong, 1969; Armstrong, 1971), and has recently been confirmed in studies of gating currents in mutant and wild-type *Shaker* K^+ channels (Perozo *et al.*, 1992). Such a mechanism could also account for kinetic features suggesting open-channel block in the absence of voltage-dependence of block over the voltage range of

current activation, as previously observed for propafenone (Duan *et al.*, 1992). On the other hand, there may be alternative explanations of our findings and the concept proposed above to explain them is, for the moment, purely conjectural. More direct studies, using single-channel recordings and site-directed mutagenesis of channel clones, will be necessary to unravel the precise mechanisms underlying our observations.

Relationship Between Observations Regarding I_{Kur} Block and Previously-Published Findings in Analogous Cloned Channels

We have previously shown that I_{Kur} has properties very similar to those of channels encoded by cDNA present in human heart and belonging to the Kv1.5 subfamily (Philipson *et al.*, 1991; Snyders *et al.*, 1991; Tamkun *et al.*, 1991; Fedida *et al.*, 1993; Roberds *et al.*, 1993; Wang *et al.*, 1993b). Kv1.5 channels are highly sensitive to 4AP, with IC_{50} values of <100 μM (Philipson *et al.*, 1991) and 180 μM (Snyders *et al.*, 1991) reported in two published studies. The sensitivity of I_{Kur} to 4AP observed in the present studies is of the same order as that of Kv1.5 (Philipson *et al.*, 1991; Snyders *et al.*, 1991). Snyders *et al.* (1993) have studied the effect of quinidine on HK2 (one of the Kv1.5 clones) channels expressed in mouse L cells. Quinidine produced open-channel block, with an IC_{50} of about 6 μM at a test potential of +60 mV, and strongly voltage-dependent block over the current activation range. In the present studies, we observed an IC_{50} of about 5 μM for quinidine block of I_{Kur} at +50 mV. As noted by Snyders *et al.* (1991) for HK2, quinidine block was enhanced at more positive test potentials, in parallel with I_{Kur} activation (fig. 10B). Also like Snyders *et al.* (1991), we observed continuing voltage-dependence of block over a range (+20 to +50 mV) at which I_{Kur} activation is virtually maximal. They interpreted this finding as indicating a blocking site within the ion permeation pathway, and calculated a fractional electrical distance (δ) based on the equation $f = D/[D+K_D{}^*\exp(-z\delta FE/RT)]$, where f = current in the presence of drug divided by control current, D = drug concentration, K_D is the estimated dissociation constant at 0 mV, and z, F, R, and T have their usual meanings. Nonlinear curve-fitting of our data to this equation gave values of 7.4 μM for K_D and 0.23 for δ. Snyders *et al.* (1991) used an estimated K_D at 0 mV to calculate the fractional electrical distance (δ), and obtained a value of 0.19 for quinidine in the HK2 channel. Thus, our findings regarding 4AP and quinidine block of I_{Kur} strongly resemble those obtained in studies of Kv1.5 cloned channels. Snyders *et al.* (1993) observed a rapid, time-dependent onset of quinidine block of HK2, resembling the introduction of rapid inactivation, and interpreted this as rapid open-channel block. We failed to observe this phenomenon, perhaps because of the depolarizing prepulse that we required in order to suppress I_{to1} and isolate I_{Kur}. Quinidine association could have occurred during the prepulse, limiting our ability to detect rapid blocking following channel opening during the test pulse. We are not aware of studies of flecainide action on Kv1.5 channels to compare with our results.

Potential Importance of Our Findings

This is, to our knowledge, the first study to examine in detail the pharmacology of K^+ channel blockade by antiarrhythmic drugs in human atrial myocytes. As indicated in the Introduction, action potential duration strongly influences the likelihood of reentrant atrial arrhythmias, such as atrial fibrillation and flutter, by governing tissue refractoriness. Both flecainide and quinidine are effective in the control of atrial fibrillation (Lewis, 1922; Sokolow and Ball, 1956; Anderson *et al.*, 1989; Van Gelder *et al.*, 1989), and both of them increase human atrial action potential duration. An understanding of the ways in which they alter

repolarizing currents in human atrium is important for a more basic appreciation of the mechanisms which mediate and determine their antiarrhythmic properties.

Therapeutic flecainide concentrations are 0.3-0.7 mg/L (0.7-1.7 μM) (Salerno *et al.*, 1986), while those of quinidine are 2-6 mg/L (6-19 μM) (Benet and Williams, 1990). When protein binding is considered (Benet and Williams, 1990), therapeutic free drug concentrations of quinidine become closer to 0.8-2.5 μM. Thus, as shown in figure 1, both flecainide and quinidine block I_{to1} at clinically relevant concentrations. These observations support previous suggestions that block of I_{to} may play a role in mediating the clinical actions of quinidine (Imaizumi and Giles, 1987) and flecainide (Le Grand *et al.*, 1990). Since quinidine was more potent than flecainide at blocking I_{to1}, and therapeutic quinidine concentrations are slightly higher, it appears that I_{to1} blockade is more likely to play a role in the clinical actions of quinidine than those of flecainide. However, the voltage- and use-dependence of drug block need to be considered. As shown in figures 3 and 6, equimolar concentrations of flecainide and quinidine can have very different relative actions depending on activation frequency and voltage.

We found that quinidine blocks I_{Kur} with an IC_{50} in the range of 5 μM, indicating that quinidine is likely to produce significant I_{Kur} block at therapeutic concentrations. Since we have previously shown that selective I_{Kur} inhibition prolongs human atrial action potential duration (Wang *et al.*, 1993b), quinidine's ability to suppress I_{Kur} may be an important contributor to the drug's atrial antiarrhythmic properties. Furthermore, the similarity between quinidine block of I_{Kur} in the present studies and its actions on HK2 channels (Snyders *et al.*, 1993) supports previous observations (Fedida *et al.*, 1993; Wang *et al.*, 1993b) that suggest that I_{Kur} results from the expression of Kv1.5 DNA in the human heart. Since HK2 mRNA is much more plentiful in human atrium than ventricle (Tamkun *et al.*, 1991), the identification of agents that selectively block I_{Kur} may result in the development of drugs that have significant atrial antiarrhythmic actions without a risk of ventricular proarrhythmia.

Our observations of the voltage- and time-dependence of K^+ channel blocking action confirm that the state-dependent mechanisms by which quinidine and 4AP block K^+ currents in human atrial cells are qualitatively similar to those occurring in other systems. However, we have extended previous work by demonstrating the rate-dependence of I_{to1} block by quinidine, by studying the apparent inactivation-linked I_{to1} block by flecainide, and by noting behaviour suggesting a role for channel opening in block development for drugs with apparently widely-differing state-dependent blockade based on other lines of evidence. The latter observation may explain some of the differences in 4AP blocking mechanisms believed to exist among various systems and species (Thompson, 1982; Kehl, 1990; Wagoner and Oxford, 1990; Castle and Slawsky, 1992; Choquet and Korn, 1992; Hice *et al.*, 1992; Campbell *et al.*, 1993).

The physiologic consequences of drug-induced inhibition of I_{to1} and I_{Kur} need further consideration. The degree of inhibition will depend on drug concentration, activation frequency and the voltage-time trajectory of the action potential which determine state-dependent interactions. Furthermore, because inhibition of one current can modify the action potential so as to limit or enhance the activation of other currents, apparently contradictory effects may be observed. For example, inhibition of I_{to} by 4AP can result in action potential abbreviation (Litovsky and Antzelevitch, 1988; Shibata *et al.*, 1989). Since quinidine block of I_{to1} is enhanced at faster rates, it is possible that part of the drug's reverse use-dependent action on human atrial action potential duration (Wang *et al.*, 1990) is paradoxically due to increased inhibition of transient outward current at more rapid rates. 4AP increases human atrial APD at low concentrations that selectively block

I_{Kur} (Wang *et al.*, 1993b), and reduces APD at higher concentrations that strongly affect I_{to1} (Shibata *et al.*, 1989), indicating that the same drug can have opposite effects on APD at different concentrations, with both types of effect caused by blocking an outward K^+ current. Clearly, much more work needs to be done before ionic mechanisms of drug action can be directly linked to changes in the action potential. Such work is essential, however, if rational design of antiarrhythmic drugs is ever to become a reality.

Potential Limitations

Our studies have a number of limitations. First, while we obtained a complete profile of voltage- and time-dependent drug action, as well as substantial information about concentration-, use-, and frequency-dependent properties, such information is insufficient to understand completely drug-receptor interactions. On the other hand, a full comprehension of the interaction of even a single drug with a single channel would require a complex approach combining molecular biology, single channel, and whole-cell voltage-clamp methodologies that go well beyond the scope of a single manuscript. The type of information that we obtained is analogous to that acquired in extensive previous studies of sodium channel blockers, which has been very valuable in defining potential mechanisms of state-dependent drug action (Hondeghem and Katzung, 1977; Grant *et al.*, 1984; Hondeghem and Katzung, 1984; Starmer *et al.*, 1984).

A second limitation is that we examined drug effects on I_{to1} and I_{Kur}, but did not evaluate other currents of potential importance in human atrial repolarization like the classical delayed rectifier, I_K (Wang *et al.*, 1993a), and the calcium-dependent chloride current, I_{ClCa} (Zygmunt and Gibbons, 1991; Zygmunt and Gibbons, 1992). Such studies would be of great interest, particularly in view of the known ability of both flecainide (Follmer and Colatsky, 1990) and quinidine (Roden *et al.*, 1988; Balser *et al.*, 1991) to block I_K, but would require an additional, very extensive series of experiments that go beyond the scope of the present manuscript.

A number of technical factors need to be considered in evaluating our findings. Time-dependent changes in current properties could have influenced our results, but we found that in the absence of interventions the currents studied had very stable properties for at least 45 min. The separation of I_{Kur} from I_{to1} requires the use of depolarizing prepulses, which would be expected to result in residual voltage-dependent drug association with I_{Kur} channels at the onset of the test pulse. While this should have no significant effect on the assessment of steady-state voltage-dependent drug action, it could prevent the observation of rapid changes in drug-induced block that would otherwise occur upon initial depolarization. Finally, the use of divalent cations to block I_{Ca} can affect voltage-dependent phenomena by binding to fixed negative surface charges and modifying channel properties (Hille *et al.*, 1975; Dukes and Morad, 1991). While it is essential to block I_{Ca} in order to eliminate contamination of I_{to1} and I_{Kur}, and organic I_{Ca} blockers are limited by voltage and frequency-dependent blocking properties (Ehara and Kaufmann, 1978; McDonald *et al.*, 1980; Lee and Tsien, 1983), the possible voltage shifts caused by divalent cations need to be considered when comparing our results with studies in which inorganic I_{Ca} blockers are not employed.

Conclusions

We have shown that flecainide and quinidine inhibit I_{to1} in human atrial cells at clinically-relevant concentrations. They appear to block the current with different state-dependence, which manifests as differences in voltage- and use-dependence that need to be considered when evaluating the potential clinical significance of drug effects on I_{to1}. Quinidine, but not flecainide, also inhibits I_{Kur} at therapeutic concentrations, with a concentration-, voltage-, and state-dependence that parallels quinidine block of current carried by Kv1.5 cloned channels. These studies indicate that isolated human atrial cells are an

appropriate model for studying the K^+ blocking actions of antiarrhythmic drugs. Since K^+ currents of human cardiac cells may differ in physiologic properties and pharmacologic responses from K^+ currents in other species, human cells may be a preferred model for the assessment of ionic mechanisms of antiarrhythmic drugs that are pertinent to their clinical actions.

Acknowledgments

The authors thank Guylaine Nicole for technical assistance, Diane Campeau and Luce Bégin for typing the manuscript, Doctors Conrad Pelletier, Raymond Cartier and Michel Carrier for providing atrial tissue samples for cell isolation, and Doctor Vladislav Nesterenko for thoughtful review of the manuscript.

mm/humdrug2.sn

References

ANDERSON, J.L., Gilbert, E.M., Alpert, B.L., Henthorn, R.W., Waldo, A.L., Bhandari, A.K., Hawkinson, R.W., Pritchett, E.L.C. and the Flecainide Supraventricular Tachycardia Study Group: Prevention of symptomatic recurrences of paroxysmal atrial fibrillation in patients initially tolerating antiarrhythmic therapy. Circulation 80: 1557-1570, 1989.

APKON, M. AND NERBONNE, J.M.: Characterization of two distinct depolarization-activated K+ currents in isolated adult rat ventricular myocytes. J. Gen. Physiol. 97: 973-1011, 1991.

ARMSTRONG, C.M.: Inactivation of the potassium conductance and related phenomena caused by quaternary ammonium ion injected in squid axons. J. Gen. Physiol. 54: 553-575, 1969.

ARMSTRONG, C.M.: Interaction of tetraethyl-ammonium ion derivatives with the potassium channels of giant axons. J. Gen. Physiol. 58: 413-437, 1971.

ARMSTRONG, C.M.: Time course of TEA+ -induced anomalous rectification in squid giant axons. J. Gen. Physiol. 50: 491-503, 1966.

BALSER, J.R., BENNETT, P.B., HONDEGHEM, L.M. AND RODEN, D.M.: Suppression of time-dependent outward current in guinea pig ventricular myocytes: Actions of quinidine and amiodarone. Circ. Res. 69: 519-529, 1991.

BENET, L.Z. AND WILLIAMS, R.L.: Design and optimization of dosage regimens: Pharmacokinetic data. in The Pharmacological Basis of Therapeutics, ed. by A. Goodman Gilman, T.W. Rall, A.S. Nies and P. Taylor, pp. 1705-1736, Pergamon Press, New York, 1990.

CAIRNS, J.A. AND CONNOLLY, S.J.: Nonrheumatic atrial fibrillation: Risk of stroke and role of antithrombotic therapy. Circulation 84: 469-481, 1991.

CAMPBELL, D.L., QU, Y., RASMUSSON, R.L. AND STRAUSS, H.C.: The calcium-independent transient outward potassium current in isolated ferret right ventricular myocytes: II. Closed state reverse use-dependent block by 4-aminopyridine. J. Gen. Physiol. 101: 603-626, 1993.

CASTLE, N.A.: Bupivacaine inhibits the transient outward K+ current but not the inward rectifier in rat ventricular myocytes. J. Pharmacol. Exp. Ther. 255: 1038-1046, 1990.

CASTLE, N.A. AND SLAWSKY, M.T.: Characterization of 4-aminopyridine block of the transient outward K+ current in adult rat ventricular myocytes. J. Pharmacol. Exp. Ther. 264: 1450-1459, 1992.

CHOQUET, D. AND KORN, H.: Mechanism of 4-aminopyridine action on voltage-gated potassium channels in lymphocytes. J. Gen. Physiol. 99: 217-240, 1992.

COPLEN, S.E., ANTMANN, E.M., BERLIN, J.A., HEWITT, P. AND CHALMERS, T.C.: Efficacy and safety of quinidine therapy for maintenance of sinus rhythm after cardioversion: A meta-analysis of randomized controlled trials. Circulation 82: 1106-1116, 1990.

DUAN, D., FERMINI, B. AND NATTEL, S.: Potassium channel blocking properties of propafenone in rabbit atrial myocytes. J. Pharmacol. Exp. Ther. 264: 1113-1123, 1992.

DUKES, I.D., CLEEMANN, L. AND MORAD, M.: Tedisamil blocks the transient and delayed rectifier K+ currents in mammalian cardiac and glial cells. J. Pharmacol. Exp. Ther. 254: 560-569, 1990.

DUKES, I.D. AND MORAD, M.: The transient K+ current in rat ventricular myocytes: Evaluation of its Ca^{2+} and Na^{+} dependence. J. Physiol. (London) 435: 395-420, 1991.

EHARA, T. AND KAUFMANN, R.: The voltage- and time-dependent effects of (-l) verapamil on the slow inward current in isolated cat ventricular myocardium. J. Pharmacol. Exp. Ther. **207:** 49-55, 1978.

ESCANDE, D., COULOMBE, A., FAIVRE, J.F., DEROUBAIX, E. AND CORABOEUF, E.: Two types of transient outward currents in adult human atrial cells. Am. J. Physiol. **252:** H142-H148, 1982.

FEDIDA, D., WIBLE, B., WANG, Z., FERMINI, B., FAUST, F., NATTEL, S. AND BROWN, A.M.: Identity of a novel delayed rectifier current from human heart with a cloned K+ channel current. Circ. Res. **73:** 210-216, 1993.

FELD, G.K.: Atrial fibrillation. Is there a safe and highly effective pharmacological treatment? Circulation **82:** 2248-2250, 1990.

FERMINI, B. AND NATTEL, S.: Choline chloride activates time-dependent and time-independent K^+ currents in dog atrial myocytes. Am. J. Physiol. **266:** C42-C51, 1994.

FERMINI, B., WANG, Z., DUAN, D. AND NATTEL, S.: Differences in rate dependence of transient outward current in rabbit and human atrium. Am. J. Physiol. **263:** H1747-H1754, 1992.

FLAKER, G.C., BLACKSHEAR, J.L., MCBRIDE, R., KRONMAL, R.A. AND HALPERIN, J.L.: Antiarrhythmic drug therapy and cardiac mortality in atrial fibrillation. J. Am. Coll. Cardiol. **20:** 527-532, 1992.

FOLLMER, C.H. AND COLATSKY, T.J.: Block of the delayed rectifier potassium current I_K by flecainide and E-4031 in cat ventricular myocytes. Circulation **82:** 289-293, 1990.

GILES, W.R. AND VAN GINNEKEN, A.C.G.: A transient outward current in isolated cells from the crista terminalis of rabbit heart. J. Physiol. **368:** 243-264, 1985.

GRANT, A.O., STARMER, C.F. AND STRAUSS, H.C.: Antiarrhythmic drug action. Blockade of the inward sodium current. Circ. Res. **55:** 427-439, 1984.

HERMANN, A. AND GORMAN, L.F.: Action of quinidine on ionic currents of molluscan pacemaker neurons. J. Gen. Physiol. **83:** 919-940, 1984.

HICE, R.E., SWANSON, R., FOLANDER, K. AND NELSON, D.J.: Aminopyridines alter inactivation rates of transient potassium channels (Abstract). Biophys. J. **61:** A376, 1992.

HILLE, B., WOODHULL, A.M. AND SHAPIRO, B.I.: Negative surface charge near the sodium channels of nerve: Divalent ions, monovalent ions, and pH. Phil. Trans. R. Soc. Lond. [B] **270:** 301-318, 1975.

HONDEGHEM, L.M. AND KATZUNG, B.G.: Antiarrythmic agents: the modulated receptor mechanism of action of sodium and calcium channel-blocking drugs. Ann. Rev. Pharmacol. Toxicol. **24:** 387-423, 1984.

HONDEGHEM, L.M. AND KATZUNG, B.G.: Time-and voltage-dependent interactions of antiarrhythmic drugs with cardiac sodium channels. Biochim. Biophys. Acta **472:** 373-398, 1977.

HOSHI, T., ZAGOTTA, W.N. AND ALDRICH, R.W.: Two types of inactivation in *Shaker* K+ channels: Effects of alterations in the carboxy-terminal region. Neuron **7:** 547-556, 1991.

HUME, J.R. AND GILES, W.: Active and passive electrical properties of single bullfrog atrial cells. J. Gen. Physiol. **78:** 19-42, 1981.

IMAIZUMI, Y. AND GILES, W.R.: Quinidine-induced inhibition of transient outward current in cardiac muscle. Am. J. Physiol. **253:** H704-H708, 1987.

KANNEL, W.B. AND WOLF, P.A.: Epidemiology of atrial fibrillation, in Atrial Fibrillation: Mechanisms and Management, ed. by R.H. Falk and P.J. Podrid, pp. 81-92, Raven Press, New York, 1992.

KEHL, S.J.: 4-aminopyridine causes a voltage-dependent block of the transient outward K+ current in rat melanotrophs. J. Physiol. (London) 431: 515-528, 1990.

KIRCHHOF, C., WIJFFELS, M., BRUGADA, J., PLANELLAS, J. AND ALLESSIE, M.: Mode of action of a new class IC drug (ORG 7797) against atrial fibrillation in conscious dogs. J. Cardiovasc. Pharmacol. 17: 116-124, 1991.

LE GRAND, B., LE HEUZY, J.Y., PERIER, P., PERONNEAU, P., LAVERGNE, T., HATEM, S. AND GUIZE, L.: Cellular electrophysiological effects of flecainide on human atrial fibres. Cardiovasc. Res. 24: 232-238, 1990.

LEE, K.S. AND TSIEN, R.W.: Mechanism of calcium channel blockade by verapamil, D600, diltiazem and nitrendipine in single dialysed heart cells. Nature 302: 790-794, 1983.

LEWIS, T.: The value of quinidine in cases of auricular fibrillation and methods of studying the clinical reaction. Am. J. Med. Sci. 163: 781-794, 1922.

LIPKIN, D.P., FRENNEAUX, M., STEWART, R., JOSHI, J., LOWE, T. AND MCKENNA, W.J.: Delayed improvement in exercise capacity after cardioversion of atrial fibrillation to sinus rhythm. Br. Heart J. 59: 572-577, 1988.

LITOVSKY, S.H. AND ANTZELEVITCH, C.: Transient outward current prominent in canine ventricular epicardium but not endocardium. Circ. Res. 62: 116-126, 1988.

LIU, L., WENDT, D.J., STARMER, C.F. AND GRANT, A.O.: Block of the transient outward current in rabbit atrial myocytes by quinidine: Lack of voltage and frequency dependence (Abstract). Circulation 84 (Suppl II): II-180, 1991.

MARTY, A. AND NEHER, E.: Tight-seal whole-cell recording, in Single-Channel Recording, ed. by B. Sakmann and E. Neher, pp. 107-121, Plenum Publishing Co., New York, 1983.

MCDONALD, T., PELZER, D. AND TRAUTWEIN, W.: On the mechanism of slow calcium channel block in heart. Pfluegers Arch. 385: 175-179, 1980.

NÄBAUER, M. AND BEUCKELMANN, D.J.: Block of transient outward current by class Ic antiarrhythmic agents propafenone and flecainide in human ventricular myocytes (Abstract). Circulation 86 (Suppl I): I-697, 1992.

NATTEL, S.: Antiarrhythmic drug classifications. A critical appraisal of their history, present status, and clinical relevance. Drugs 41: 672-701, 1991.

PEROZO, E., PAPAZIAN, D.M., STEFANI, E. AND BEZANILLA, F.: Gating currents in *Shaker* K+ channels. Implications for activation and inactivation models. Biophys. J. 62: 160-171, 1992.

PHILIPSON, L.H., HICE, R.E., SCHAEFER, K., LAMENDOLA, J., BELL, G.I., NELSON, D.J. AND STEINER, D.F.: Sequence and functional expression in Xenopus oocytes of a human insulinoma and islet potassium channel. Neurobiology 88: 53-57, 1991.

PRESSLER, M.L.: Passive electrical properties of cardiac tissue, in Cardiac Electrophysiology, From Cell to Bedside, ed. by D.P. Zipes and J. Jalife, pp. 108-121, WB Saunders, Philadelphia, 1990.

PRITCHETT, E.L.C.: Management of atrial fibrillation. N. Engl. J. Med. 326: 1264-1271, 1992.

RENSMA, P.L., ALLESSIE, M.A., LAMMERS, W.J.E.P., BONKE, F.I.M. AND SCHALIJ, M.J.: Length of excitation wave and susceptibility to reentrant atrial arrhythmias in normal conscious dogs. Circ. Res. 62: 395-410, 1988.

ROBERDS, S.L., KNOTH, K.M., PO, S., BLAIR, T.A., BENNETT, P.B., HARTSHORNE, R.P., SNYDERS, D.J. AND TAMKUN, M.M.: Molecular biology of the voltage-gated potassium channels of the cardiovascular system. J. Cardiovasc. Electrophysiol. 4: 68-80, 1993.

RODEN, D.M., BENNETT, P.B., SNYDERS, D.J., BALSER, J.R. AND HONDEGHEM, L.M.: Quinidine delays I_k activation in guinea pig ventricular myocytes. Circ. Res. 62: 1055-1058, 1988.

SACHS, L. (ED): Applied Statistics. A Handbook of Techniques. Second Edition, Springer-Verlag, New York, 1984.

SALERNO, D.M., GRANRUD, G., SHARKEY, P., KREJCI, J., LARSON, T., ERLIEN, D., BERRY, D. AND HODGES, M.: Pharmacodynamics and side effects of flecainide acetate. Clin. Pharmacol. Ther. 40: 101-107, 1986.

SHIBATA, E.F., DRURY, T., REFSUM, H., ALDRETE, V. AND GILES, W.: Contributions of a transient outward current to repolarization in human atrium. Am. J. Physiol. 257: H1773-H1781, 1989.

SIGWORTH, F.J.: Electronic design of the patch clamp, in Single-Channel Recording, ed. by B. Sakmann and E. Neher, pp. 3-35, Plenum Publishing Co, New York, 1983.

SIMURDA, J., SIMURDOVA, M. AND CHRISTÉ, G.: Use-dependent effects of 4-aminopyridine on transient outward current in dog ventricular muscle. Plügers Arch. 415: 244-246, 1989.

SNYDERS, D.J., KNOTH, K.M., ROBERDS, S.L. AND TAMKUN, M.M.: Time-, voltage-, and state-dependent block by quinidine of a cloned human cardiac potassium channel. Mol. Pharmacol. 41: 322-330, 1991.

SNYDERS, D.J., TAMKUN, M.M. AND BENNETT, P.B.: A rapidly activating and slowly inactivating potassium channel cloned from human heart: functional analysis after stable mammalian cell culture expression. J. Gen. Physiol. 101: 513-543, 1993.

SOKOLOW, M. AND BALL, R.E.: Factors influencing conversion of chronic atrial fibrillation with special reference to serum quinidine concentration. Circulation 14: 568-583, 1956.

STARMER, C.F., GRANT, A.O. AND STRAUSS, H.C.: Mechanisms of use-dependent block of sodium channels in excitable membranes by local anesthetics. Biophys. J., 46: 15-27, 1984.

TAMKUN, M.M., KNOTH, K.M., WALBRIDGE, J.A., KROEMER, H., RODEN, D.M. AND GLOVER, D.M.: Molecular cloning and characterization of two voltage-gated K^+ channel cDNAs from human ventricle. Faseb J. 5: 331-337, 1991.

THOMPSON, S.: Aminopyridine block of transient potassium current. J. Gen. Physiol. 80: 1-18, 1982.

VAN GELDER, I.C., CRIJNS, H.J.G.M., VAN GILST, W.H., VAN WIJK, L.M., HAMER, H.P.M. AND LIE, K.I.: Efficacy and safety of flecainide acetate in the maintenance of sinus rhythm after electrical cardioversion of chronic atrial fibrillation or atrial flutter. Am. J. Cardiol. 64: 1317-1321, 1989.

WAGONER, P.K. AND OXFORD, G.S.: Aminopyridines block an inactivating potassium current having slow recovery kinetics. Biophys. J. 58: 1481-1489, 1990.

WANG, J., BOURNE, G.W., WANG, Z., VILLEMAIRE, C., TALAJIC, M. AND NATTEL, S.: Comparative mechanisms of antiarrhythmic drug action in experimental atrial fibrillation. Importance of use-dependent effects on refractoriness. Circulation 88: 1030-1044, 1993.

WANG, Z., FERMINI, B. AND NATTEL, S.: Delayed rectifier outward current and repolarization in human atrial myocytes. Circ. Res. 73: 276-285, 1993a.

WANG, Z., FERMINI, B. AND NATTEL, S.: Sustained depolarization-induced outward current in human atrial myocytes: Evidence for a novel delayed rectifier K+ current similar to Kv1.5 cloned channel currents. Circ. Res. 73: 1061-1076, 1993b.

WANG, Z., PAGÉ, P. AND NATTEL, S.: The mechanism of flecainide's antiarrhythmic action in experimental atrial fibrillation. Circ. Res. 71: 271-287, 1992.

WANG, Z., PELLETIER, L.C., TALAJIC, M. AND NATTEL, S.: Effects of flecainide and quinidine on human atrial action potentials: role of rate-dependence and comparison with guinea pig, rabbit and dog tissues. Circulation 82: 274-283, 1990.

YATANI, A., WAKAMORI, M., MIKALAM, G. AND BAHINSKI, A.: Block of transient outward-type cloned cardiac K+ channel currents by quinidine. Circ. Res. 73: 351-359, 1993.

ZYGMUNT, A.C. AND GIBBONS, W.R.: Calcium-activated current in rabbit ventricular myocytes. Circ. Res. 68: 424-437, 1991.

ZYGMUNT, A.C. AND GIBBONS, W.R.: Properties of the calcium-activated chloride current in heart. J. Gen. Physiol. 99: 391-414, 1992.

Figure Legends

Figure 1. Concentration dependence of drug inhibition of I_{to1}. Currents were elicited by 100-ms depolarizing pulses from the holding potential (HP) of -50 mV to +20 mV at 1 Hz. A: Analog traces of I_{to1} before and after various concentrations of flecainide (a), quinidine (b), and 4AP (c). All three compounds produced concentration-dependent inhibition of I_{to1}, with potency in the order of quinidine > flecainide > 4AP. In addition, the apparent inactivation of I_{to1} was accelerated. Note that the steady-state current at the end of the pulse was unaltered by flecainide, reduced by quinidine in a concentration-dependent manner, and completely suppressed by 4AP at concentrations ≥ 2 mM. B: Mean (+S.E.) inhibition of I_{to1} as obtained with voltage protocol shown in A (n=8 for flecainide, 5 for quinidine, and 6 for 4AP). * $P < 0.05$, ** $P < 0.01$, *** $P < 0.001$ vs control.

Figure 2. Use-dependence of drug effects on I_{to1}. Current was elicited by 10 consecutive 100-ms voltage steps at 1Hz from a HP of –50 mV to + 20 mV. A: Representative current traces from the first, second, and tenth pulse after a 10-min period at the HP. Use-dependent changes in I_{to1} were not seen under control conditions (a) or in the presence of 5 μM flecainide (b). A use-dependent onset of block was seen in the presence of 5 μM quinidine (c). In the presence of 2mM 4AP (d), current was strongly reduced during the first pulse and inactivation was slowed, but use-dependent unblocking and an acceleration of inactivation was observed for the second and tenth pulses. B: Mean (± S.E.) peak I_{to1} during each pulse under control conditions (open symbols) and in the presence of the drugs indicated (closed symbols). Only tonic block of I_{to1} was observed in the presence of 5 μM flecainide (a, n=8). Quinidine (5 μM, n=10) produced use-dependent inhibition of I_{to1} (b), with a time constant of 1.1 ± 0.1 pulses (monoexponential curve fit shown). In contrast to quinidine, 4AP (2 mM, n=9) blocked I_{to1} in a reverse use-dependent fashion, with a time constant of 0.5 ± 0.1 pulses. Normalized data for current in the presence of each drug relative to control values in each experiment are shown in d. +++ $P < 0.001$, NS= non-significant, by F test for interaction between pulse number and drug effect.

Figure 3. Steady-state frequency dependence of drug inhibition of I_{to1}. Voltage protocols similar to those shown in Figure 2 were applied at 0.1, 1, 2, and 2.5 Hz. The effects of flecainide (filled circles, n=8) were frequency independent, while those of quinidine (filled squares, n=10) and 4AP (filled diamonds, n=9) were significantly altered by changing frequency. ++ $p<0.01$, +++ $p<0.001$, F test for frequency dependence.

Figure 4. Drug effects on reactivation of I_{to1}. Paired-pulse protocol (inset in panel D) consisted of two identical 200-ms pulses (P_1 and P_2) to +40 mV from a HP of –80 mV, with P_1-P_2 interval varied from 0 to 1.6 sec (for flecainide and quinidine) or 16 sec (for 4AP). Peak I_{to1} elicited by P_2 was normalized to that elicited by the preceding P_1, and the normalized current (P_2/P_1) was plotted as a function of P_1-P_2 interval. Results are mean ± S.E. from

all experiments; where error bars are not visible, they fill within symbol for mean. **A:** No significant change in I_{to1} recovery was seen in the presence of flecainide (5 μM); **B:** Quinidine (5 μM) slowed the reactivation of I_{to1} increasing τ_r from a control value of 20 ± 1 ms to 41 ± 2 ms ($p<0.01$, $n=6$); **C:** I_{to1} recovery curve for control and 4AP (2mM) conditions superimposed ($n=14$) for P_1-P_2 ≤250 ms. For P_1-P_2 >250 ms, the current elicited by P_2 in the presence of 4AP progressively decreases. This process is well described by a single exponential (shown) with a time constant of 4.2 ± 0.1 s. **D:**Percent reduction in I_{to1} relative to control as a function of P_1-P_2 interval. Effects of flecainide (circles) show no significant dependence on diastolic intervals. Suppression of I_{to1} by quinidine (squares) was greater at short P_1-P_2 intervals and gradually relieved as the interval increased. Block of I_{to1} by 4AP (diamonds) was increased by increasing P_1-P_2 intervals.

Figure 5. Influence of the duration of a depolarizing prepulse on drug-induced inhibition of I_{to1}. Double-pulse protocol was applied at 0.1 Hz (inset), with P_1 and P_2 pulses from a HP of -60 mV to +30 mV. Prepulse (P_1) duration was varied from 5 ms to 300 ms, with the P_1-P_2 coupling interval fixed at 50 ms and P_2 duration fixed at 100 ms. **Left:** I_{to1} elicited by P_2 under control (open symbols) and drug (closed symbols) conditions in each cell ($n=10$, 6, and 14 for flecainide, quinidine and 4AP respectively), as a function of P_1 duration. **Right:** I_{to1} elicited by P_2 relative to that of P_1 as a function of P_1 duration. **A:** In the presence of flecainide (5 μM), I_{to1} elicited by P_2 decreased as a function of prepulse duration, with a time constant of 11 ± 3 ms; **B:** In the presence of quinidine, I_{to1} was also reduced by prepulses, but steady-state effects were achieved within 10 ms of the onset of the prepulse; **C:** Effects of 4AP (2mM) were relieved by prepulses, with a time constant of 43 ± 5 ms. Curves in graphs at right are monoexponential fits. + $P < 0.05$; ++ $P < 0.01$, +++ $P < 0.001$ for significance of effect of prepulse duration by F test.

Figure 6. Dependence of drug effects on test pulse potential. Current was elicited by 100-ms pulses (0.1 Hz) from a HP of -50 mV to various test potentials. Results are shown under control conditions (open symbols) and in the presence (closed symbols) in the same cells as under control for flecainide (**A**, $n=13$), quinidine (**B**, $n=13$), and 4AP (**C**, $n=9$). **D:** Percent reduction in I_{to1} relative to control as a function of test potential. +++ $P < 0.001$ for voltage dependence of drug effect. **E:** Relationship between percent reduction in I_{to1} caused by quinidine and fraction of maximum current activated by test pulse, as determined from I-V relation for peak I_{to1} under control conditions, assuming a reversal potential of -80 mV. Line is fit by least-squares regression, and has an r of 0.99.

Figure 7. Voltage-dependent modulation of drug effects on I_{to1} by prepulses to various voltages. Prepulses (600 ms for flecainide and quinidine, 10 sec for 4AP) to potentials ranging from -90 to +20 mV were applied prior to a 200-ms test pulse to +50 mV from a HP of -60 mV. **A-C:** Peak I_{to1} currents (mean ± S.E.) in presence and absence of flecainide ($n=8$), quinidine ($n=9$), and 4AP ($n=12$). Protocol (STD. PROT.) is shown at top. **D-F:**

Concentration-dependent percent reduction of I_{to1} as a function of prepulse potential. In order to dissociate drug-free inactivated from blocked channels in the presence of 4AP, a revised protocol (inset, panel F) was applied in which cells (n=6) were returned to the HP for 50 ms prior to the test pulse. Results obtained with the revised protocol are shown by filled symbols in panels C and F. + $P < 0.05$, ++ $P < 0.01$, +++ $P < 0.001$, F test for voltage-dependence of drug action.

Figure 8. Effects of drugs on the inactivation time course of I_{to1} elicited by 100-ms pulses at 1 Hz from a HP of -50 mV to +20 mV. Analogue records of representative experiments, along with monoexponential curve fits, are shown in the absence and presence of 5 μM flecainide (A), 5 μM quinidine (B), and 2 mM 4AP (C). D: Mean (+ S.E.) inactivation time constants (τ_h) before and after each of three drug concentrations for flecainide (n=8), quinidine (n=5) and 4AP (n=6). * $P < 0.05$, ** $P < 0.01$, *** $P < 0.001$ compared to corresponding control in absence of drug.

Figure 9. Onset of I_{to1} block following depolarization. I_{to1} as a function of time under control conditions (open diamonds) and in the presence (open circles) of 5 μM flecainide (A), 5 μM quinidine (B), or 2 mM 4AP (C) at 36°C (left) or 16°C (right). Results were obtained during 100-ms depolarizing pulses from a HP of -50 mV to +20 mV at 1 Hz, and are means for 10, 8, and 11 cells for flecainide, quinidine and 4AP respectively at 36°C, and 5, 6 and 4 cells for the same drugs at 16°C. Points represent mean fractional block (drug-induced current reduction divided by control current, scale at the right) as a function of time after the onset of depolarization. Block was absent at the onset of depolarization, and appeared as an exponential function of time (curve fits shown).

Figure 10. A. I_{Kur} elicited by 80-ms depolarizing pulses from a HP of -50 mV to various potentials, 10 ms after a 1-s prepulse to + 40 mV to inactivate I_{to1}. Representative recordings are shown before (top, Control) and after (bottom) exposure to flecainide (a), quinidine (b), and 4AP (c). B. Mean (± S.E.) values of I_{Kur} before and after exposure to flecainide (a, n=9), quinidine (b, n=11) and 4AP (c, n=15), as a function of test potential. Percent reduction in I_{Kur} was unrelated to test potential for flecainide and 2 mM 4AP (panel d), but was slightly increased at more positive potentials for 50 μM 4AP. Block by quinidine was strongly voltage-dependent, with most of the voltage dependence attributable to voltage dependence of I_{Kur} activation. The activation curve for I_{Kur} as determined from tail currents is shown by the dashed line (scale at right). Note that voltage-dependent block by quinidine is observed at voltages, positive to + 20 mV, at which I_{Kur} is fully activated. A similar phenomenon has previously been observed for quinidine block of current carried by HK2 channels, and attributed to a blocking site within the voltage field.[57] + $P < 0.05$, +++ $P < 0.001$, for voltage-dependence of quinidine action. Experiments were conducted at room temperature (about 25°C).

Figure 11. Concentration-dependent effects on I_{Kur}. Current was elicited by ten 80-ms pulses from -50 mV to + 40 mV at 1 Hz, with the tenth pulse delivered 10 ms after a 500-ms depolarizing prepulse over the same voltage range to inactivate I_{to1}. Current during the tenth pulse under control conditions is compared to that in the presence of each drug in the same cell, to calculate drug-induced inhibition of I_{Kur}. Results are from 11 cells for flecainide, 7 for quinidine, and 6 for 4AP. Each cell was exposed to all three drug concentrations. * $P < 0.05$, ** $P < 0.01$, *** $P < 0.001$ compared to control.

Figure 12. Inhibition of I_{Kur} as a function of pulse frequency, with a voltage protocol otherwise the same as that used in Figure 11. No frequency dependence of drug action was seen. ** $P < 0.01$, *** $P < 0.001$ for current in presence of drug vs control at same frequency. Results shown are for 11 cells studied with flecainide, 9 with quinidine, and 15 with 4AP.

Index Terms

Flecainide; Quinidine; 4-aminopyridine; Potassium channels; Antiarrhythmic drugs; Potassium channel blockers.

Figure 1

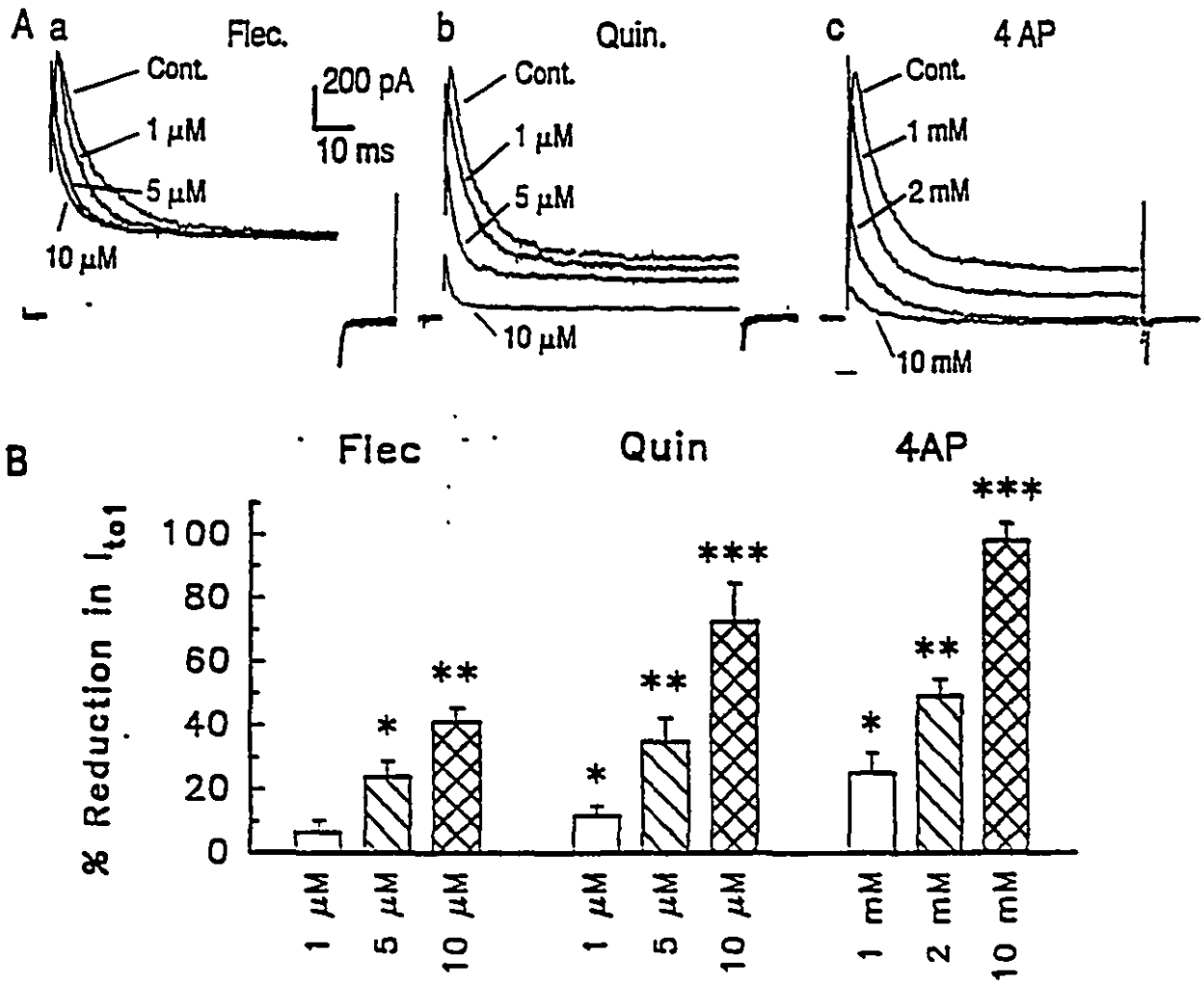
A
a
Flec.
Cont.
1 μM
5 μM
10 μM
200 pA
10 ms
b
Quin.
Cont.
1 μM
5 μM
10 μM
c
4 AP
Cont.
1 mM
2 mM
10 mM
B
Flec
Quin
4AP
% Reduction in I_{to1}
100
80
60
40
20
0
*
**
***
1 μM
5 μM
10 μM
1 μM
5 μM
10 μM
1 mM
2 mM
10 mM

Figure 2

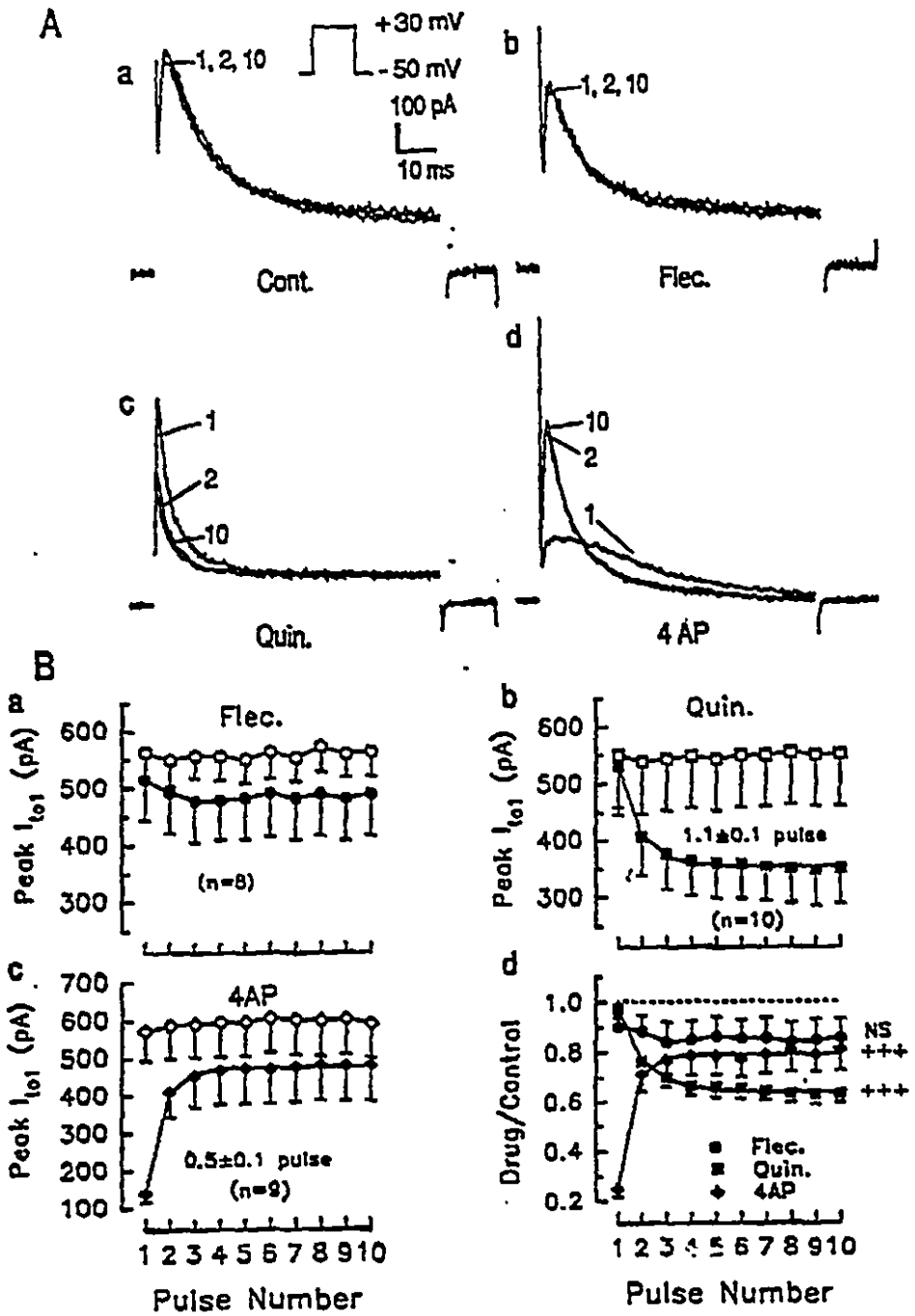
A
a
1, 2, 10
+30 mV
-50 mV
100 pA
10 ms
b
1, 2, 10
Cont.
Flec.
c
1
2
10
d
10
2
1
Quin.
4 AP
B
a
Flec.
Peak I_{to1} (pA)
600
500
400
300
(n=8)
b
Quin.
1.1±0.1 pulse
(n=10)
c
4AP
700
600
500
400
300
200
100
0.5±0.1 pulse
(n=9)
d
Drug/Control
1.0
0.8
0.6
0.4
0.2
NS
+++
+++
Flec.
Quin.
4AP
1 2 3 4 5 6 7 8 9 10
Pulse Number

Figure 3

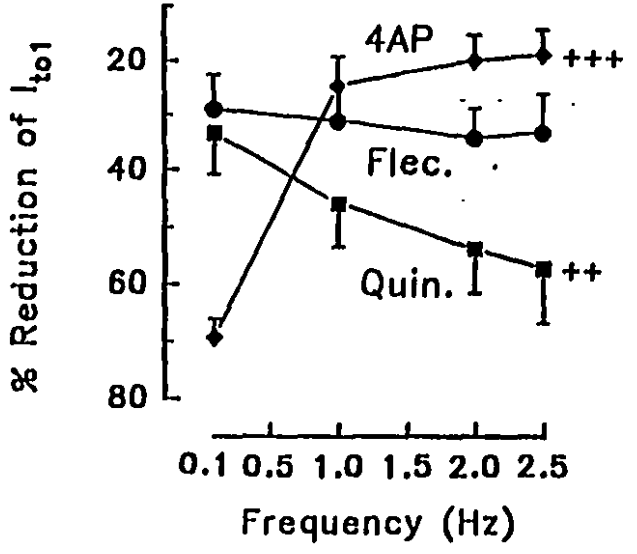
% Reduction of I_{to1}
20
40
60
80
4AP
+++
Flec.
Quin.
++
0.1 0.5 1.0 1.5 2.0 2.5
Frequency (Hz)

Figure 4

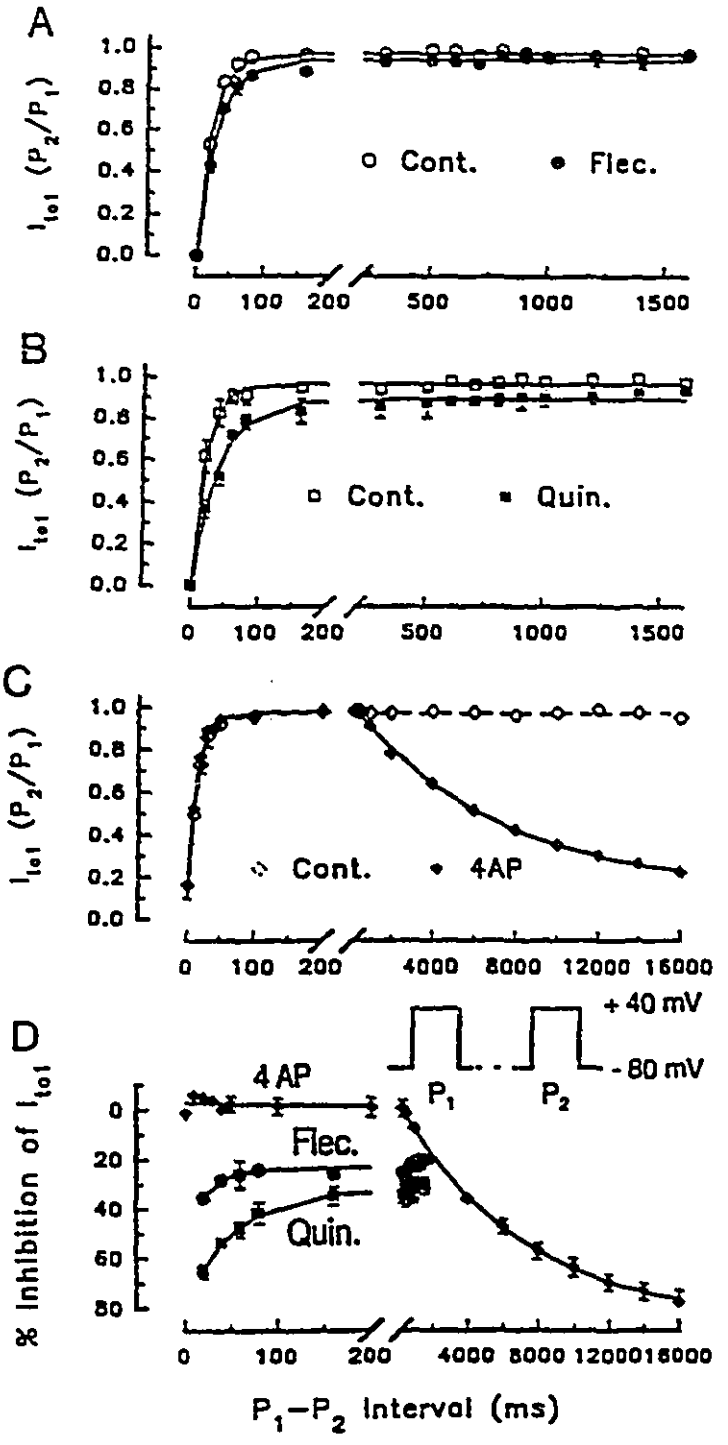
A
B
C
D
I_{tot} (P_2/P_1)
1.0
0.8
0.6
0.4
0.2
0.0
Cont.
Flec.
Quin.
4AP
0
100
200
500
1000
1500
4000
8000
12000
16000
+ 40 mV
- 80 mV
P_1
P_2
4 AP
Flec.
Quin.
% Inhibition of I_{tot}
20
40
60
80
P_1–P_2 Interval (ms)

Figure 6

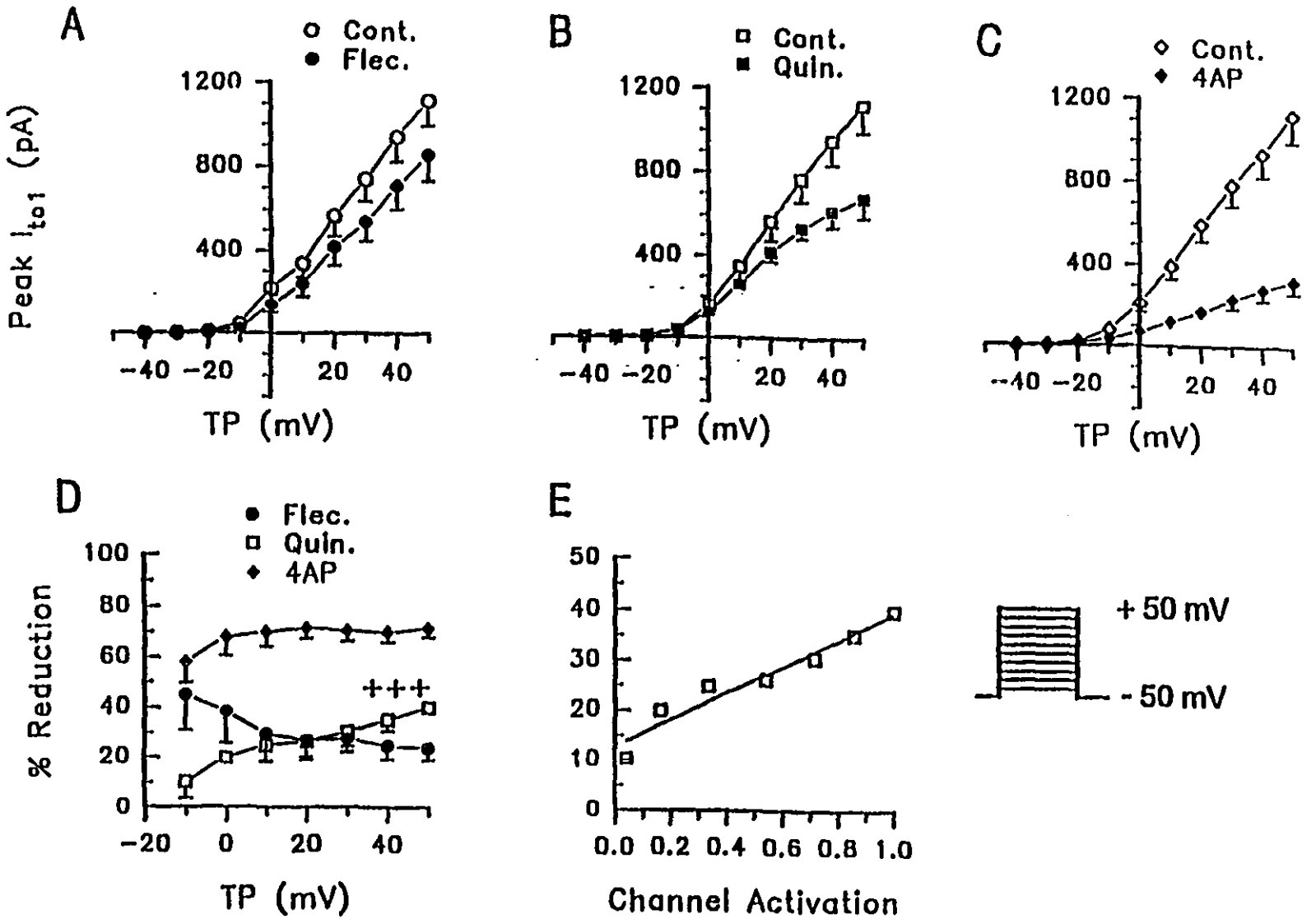
A
Cont.
Flec.
Peak I_{tot} (pA)
1200
800
400
-40 -20 20 40
TP (mV)
B
Cont.
Quin.
1200
800
400
-40 -20 20 40
TP (mV)
C
Cont.
4AP
1200
800
400
-40 -20 20 40
TP (mV)
D
Flec.
Quin.
4AP
% Reduction
100
80
60
40
20
0
+++
-20 0 20 40
TP (mV)
E
50
40
30
20
10
0
0.0 0.2 0.4 0.6 0.8 1.0
Channel Activation
+ 50 mV
- 50 mV

Figure 1

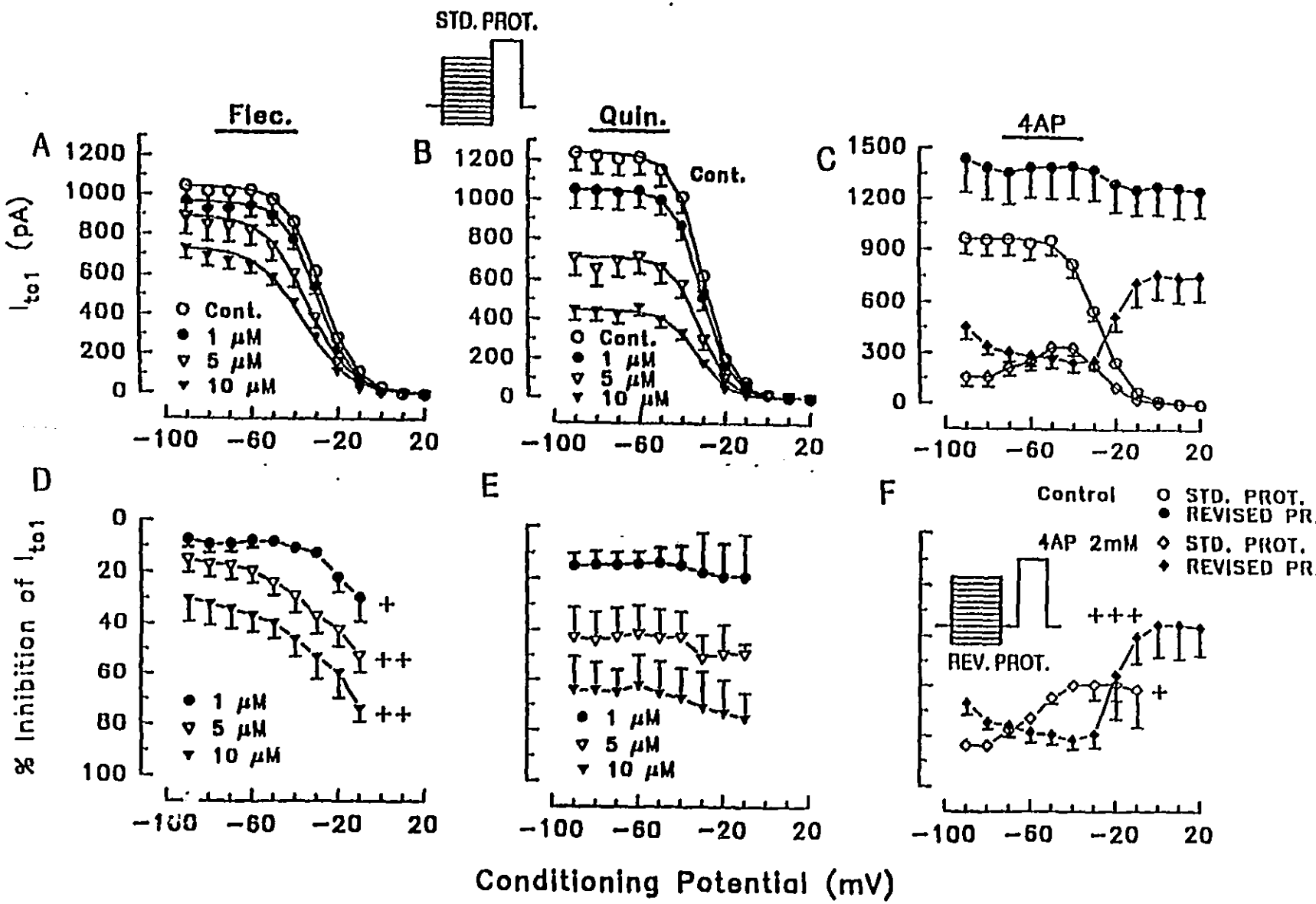
STD. PROT.
A
Flec.
B
Quin.
C
4AP
I_{tol} (pA)
Cont.
1 μM
5 μM
10 μM
D
E
F
% Inhibition of I_{tol}
Control
STD. PROT.
REVISED PR.
4AP 2mM
STD. PROT.
REVISED PR.
REV. PROT.
+
++
+++
Conditioning Potential (mV)

Figure 8

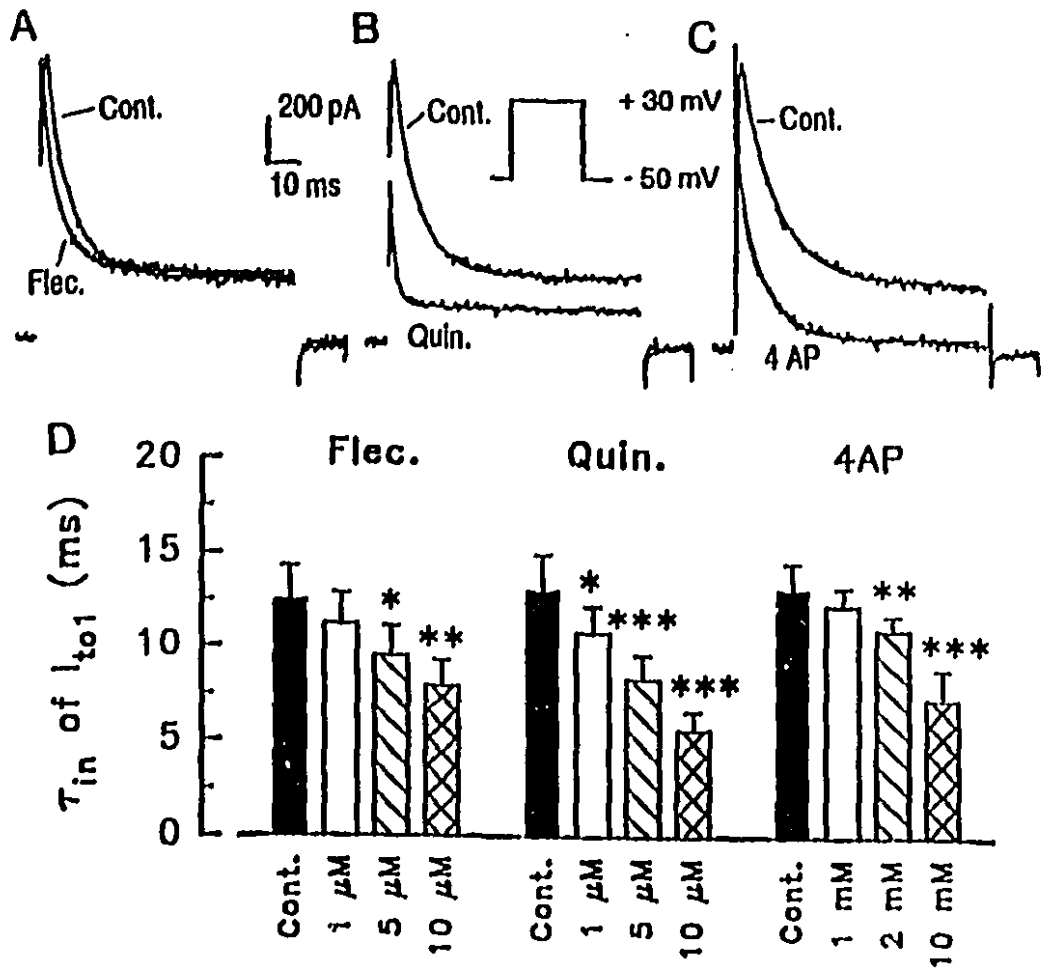
A
B
C
Cont.
200 pA
10 ms
Flec.
Cont.
+ 30 mV
- 50 mV
Quin.
Cont.
4 AP
D
Flec.
Quin.
4AP
τ_{in} of I_{to1} (ms)
20
15
10
5
0
Cont.
1 μM
5 μM
10 μM
Cont.
1 μM
5 μM
10 μM
Cont.
1 mM
2 mM
10 mM

Figure 9

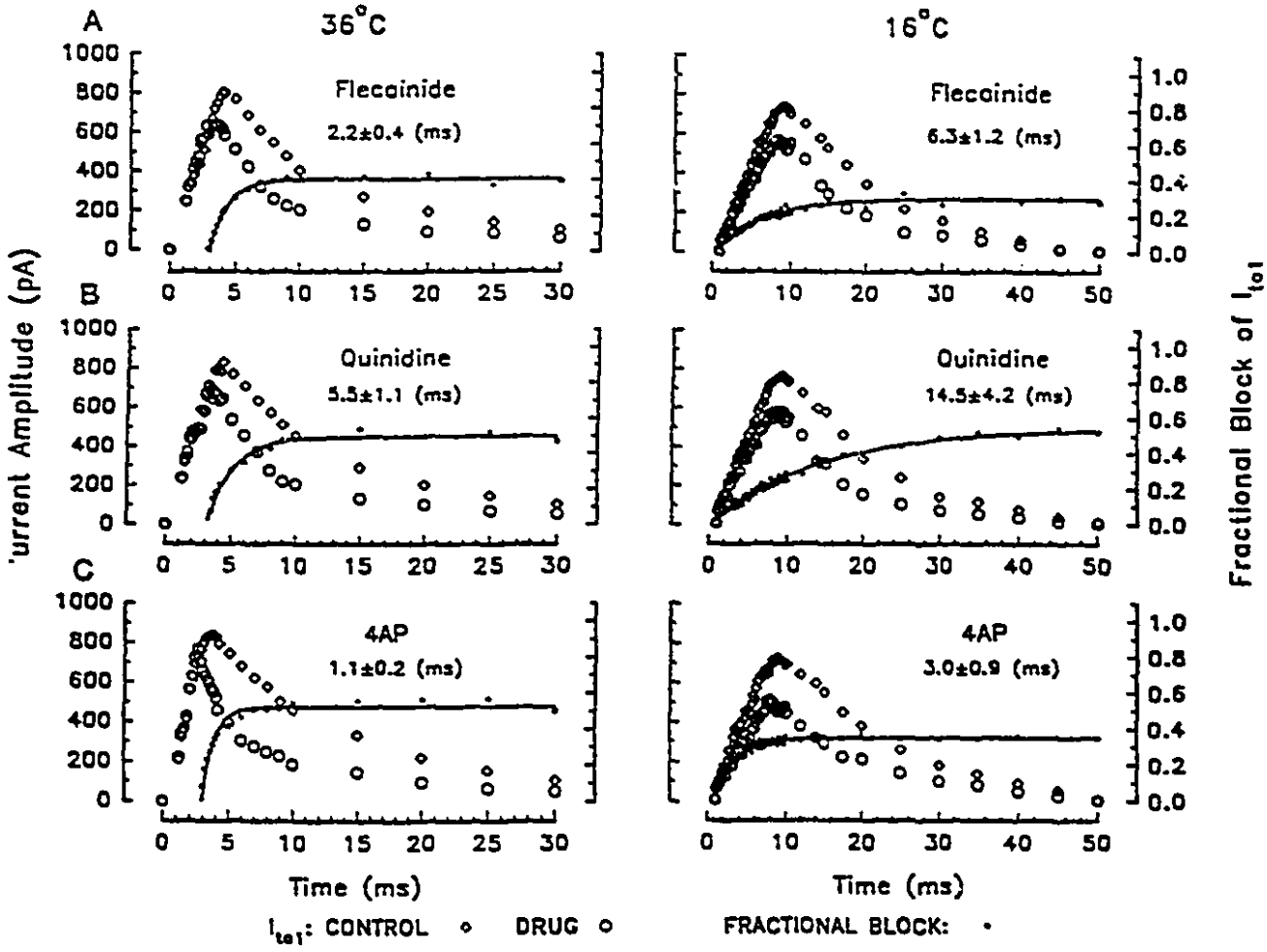
A
36°C
16°C
Flecainide
2.2±0.4 (ms)
Flecainide
6.3±1.2 (ms)
B
Quinidine
5.5±1.1 (ms)
Quinidine
14.5±4.2 (ms)
C
4AP
1.1±0.2 (ms)
4AP
3.0±0.9 (ms)
Current Amplitude (pA)
Fractional Block of I_{to1}
Time (ms)
Time (ms)
I_{to1}: CONTROL ◇ DRUG ○
FRACTIONAL BLOCK: •

Figure 10

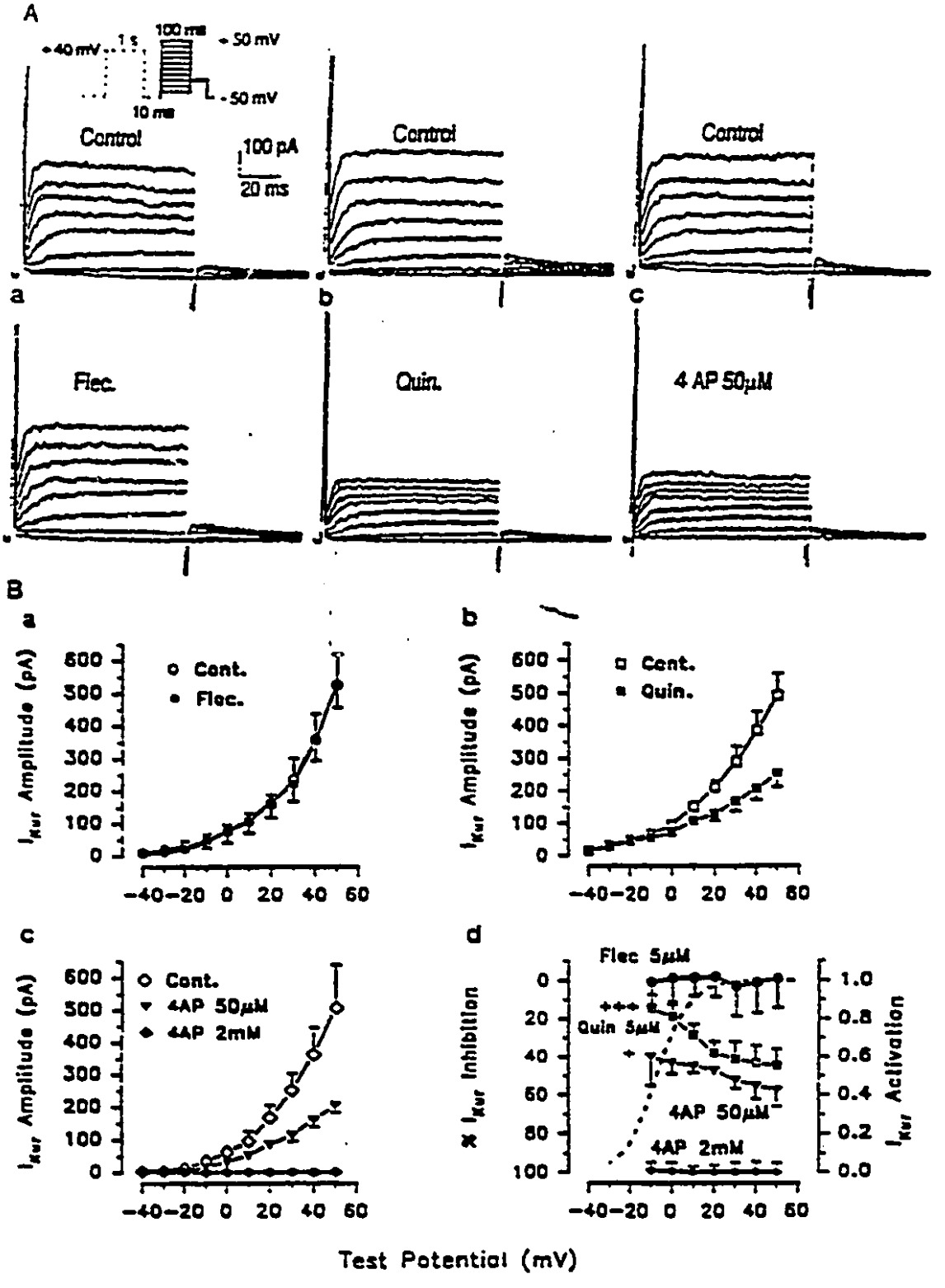
A
+40 mV
1 s
100 ms
+ 50 mV
- 50 mV
10 ms
Control
100 pA
20 ms
Control
Control
a
b
c
Flec.
Quin.
4 AP 50μM
B
a
b
c
d
Cont.
Flec.
Quin.
4AP 50μM
4AP 2mM
Flec 5μM
Quin 5μM
4AP 50μM
4AP 2mM
I_{Kur} Amplitude (pA)
% I_{Kur} Inhibition
I_{Kur} Activation
Test Potential (mV)

Figure 11

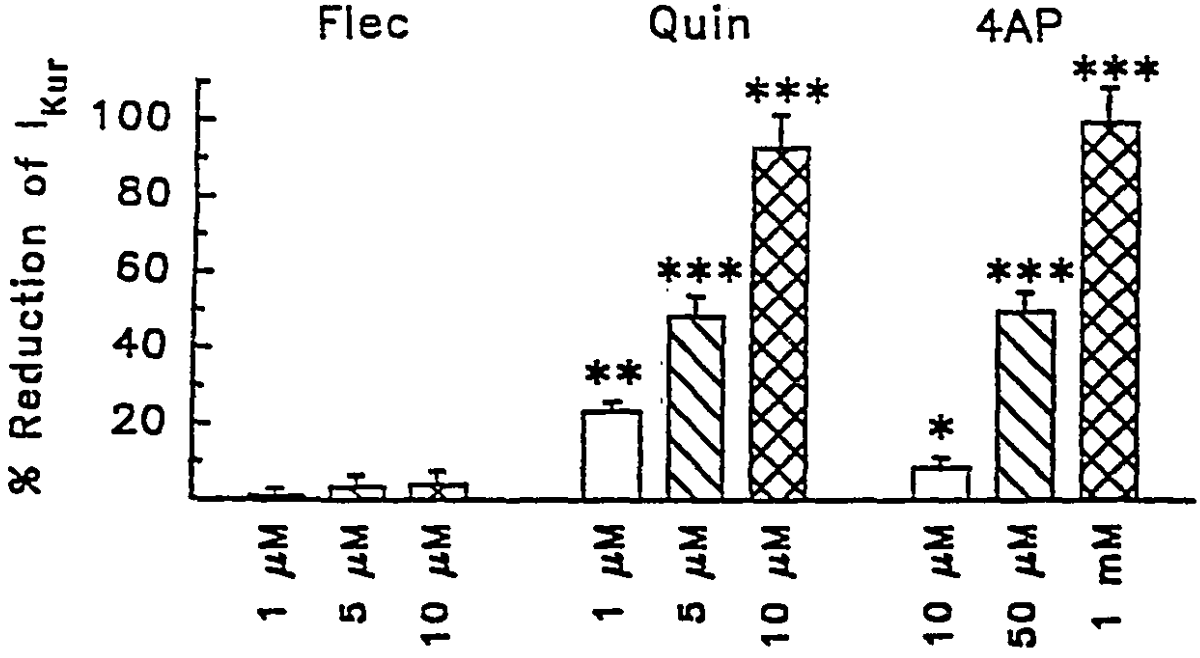
Flec
Quin
4AP
% Reduction of I_{Kur}
100
80
60
40
20
**
***
***
*
***
***
1 μM
5 μM
10 μM
1 μM
5 μM
10 μM
10 μM
50 μM
1 mM

Figure 12

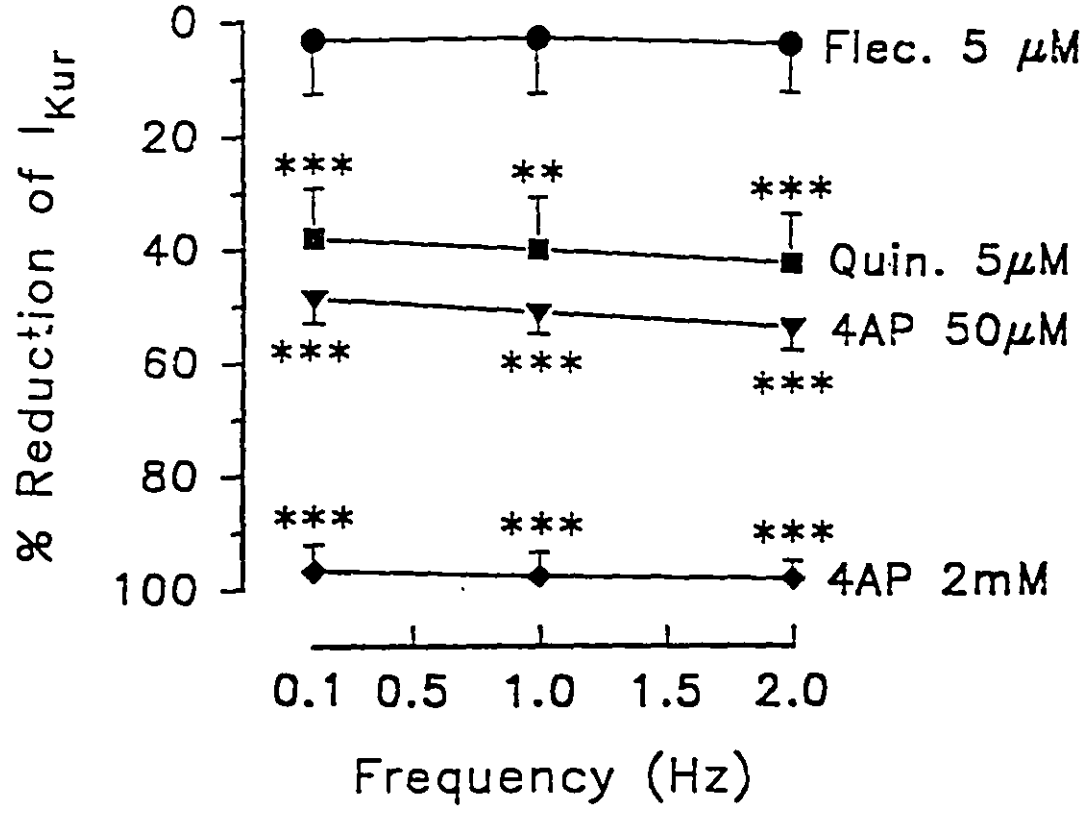
% Reduction of I_{Kur}
0
20
40
60
80
100
Flec. 5 μM
Quin. 5μM
4AP 50μM
4AP 2mM
***
**
***
***
***
***
***
***
***
0.1 0.5 1.0 1.5 2.0
Frequency (Hz)

If I_{to1} or/and I_{Kur} accounted for flecainide's rate-dependent APD prolongation, then rate-dependent blockade of these currents would be expected. Our results, however, demonstrated that flecainide block of I_{to1} was use and frequency independent. Also, no appreciable effect of flecainide on I_{Kur} was observed at concentrations at which flecainide produced significant rate-dependent APD prolongation.

It has been reported that flecainide blocks I_K current in cat ventricular cells, but its use-dependency on this current was not determined. We then turned to assess the use-dependent effects of flecainide on I_K current. Because of the difficulty of preventing I_K from running down in human atrial cells, we decided to carry out the experiments with guinea pig atrial myocytes. Flecainide proved to be a potent blocker of I_K with a IC_{50} of about 2.5 μM, but the blockade of I_K by flecainide was neither use-dependent nor pulse duration-dependent. These results are illustrated in Figure 1. Therefore, although the effects of flecainide on I_{to1} and I_K may contribute to its ability to lengthen APD, none of these currents could sufficiently explain the use-dependent APD prolongation by flecainide. In addition, studies from other groups indicate that flecainide at concentrations below 20 μM does not exert any significant effect on I_{Ca}. It appears, therefore, that there must be another mechanism else responsible for this rate-dependent property of flecainide.

Three important facts led us to propose the Na^+-K^+ ATPase hypothesis to explain rate-dependent APD prolongation by flecainide:

(1) Our results and subsequent studies from other groups demonstrate that the efficacy of class Ic agents in arrhythmias (AF) depends on rate-dependent ERP (APD) prolongation, and we know that a common feature of class Ic drugs is strong rate-dependent blockade of Na^+ channels;

(2) Flecainide produces a similar pattern of rate-dependent APD prolongation in atrial tissues from various species, including guinea pig, rabbit, dog and man. Although different species have different repolarizing currents, their Na^+ channels all have similar properties;

(3) Flecainide produces the same tendency of rate-dependent APD change in different tissue types: atrium, ventricle, and Purkinje fibre[2-8,9]. Although the relative importance of various ion currents are different in different tissue types, the properties of Na^+ channels are similar in these tissues.

It seems likely, therefore, that rate-dependent Na^+ channel block by class Ic drugs might mediate their rate-dependent APD prolongation. But how?

It is known that during the action potential Na^+ enters the cell, initiating depolarization, and K^+ goes out of the cell during phases 2 and 3 to repolarize the membrane. Na^+-K^+ ATPase is crucial in maintaining the normal ionic balance between both side of the membrane by pumping Na^+ back to the outside and K^+ back to the inside. For each turnover, the Na^+-K^+ ATPase pumps $3Na^+$ out and $2K^+$ in, and is thus electrogenic. It generates an outward current, and therefore may contribute to repolarizing the membrane[2-10,11]. Intracellular Na^+ loading is the most efficient stimulus

for Na^+-K^+ pump activity[2-10,11]. With an increased frequency of depolarization, more Na^+ enters into the cell. Therefore, the outward pump current would be expected to be larger at faster activation rates. Preventing intracellular Na^+ loading by blocking Na^+ channels in a frequency-dependent fashion would then result in rate-dependent reduction of the outward current, which in turn may lead to rate-dependent prolongation of APD. Our next study was designed to test this hypothesis[2-12].

References

2-10. Glitsch HG. Electrogenic Na pumping in the heart. Ann Rev Physiol 1982;44:389-400.

2-11. Gadsby DC. The Na/K pump of cardiac cells. Ann Rev Biophys Bioeng 1984a;13:373-398.

2-12. Wang Z, Fermini B, Nattel S: Mechanism of Flecainide's Rate-Dependent Actions on Action Potential Duration in Canine Atrial Tissue. J Pharmacol Exp Ther 1993;267:575-581

0022-3565/93/2671-0573$3.00/0
THE JOURNAL OF PHARMACOLOGY AND EXPERIMENTAL THERAPEUTICS
Copyright © 1993 by The American Society for Pharmacology and Experimental Therapeutics
Vol. 267, No. 2
Printed in U.S.A.

Mechanism of Flecainide's Rate-Dependent Actions on Action Potential Duration in Canine Atrial Tissue[1]

ZHIGUO WANG, BERNARD FERMINI and STANLEY NATTEL

Department of Medicine, Montreal Heart Institute and University of Montreal, and the Department of Pharmacology and Therapeutics, McGill University, Montreal, Canada

Accepted for publication June 24, 1993

ABSTRACT

Increases in action potential duration (APD) caused by most antiarrhythmic drugs are maximal at slow rates and are attenuated during tachycardia, causing decreased action during arrhythmias and maximum effects during sinus rhythm. This property, "reverse use-dependence," limits efficacy and contributes to proarrhythmic potential. We have shown that the class 1c antiarrhythmic drug flecainide increases atrial APD to a greater extent at faster rates and that this property may underlie some of the drug's antiarrhythmic actions. The present studies were designed to evaluate possible underlying ionic mechanisms. Standard whole-cell voltage clamp and microelectrode techniques were used to study ionic currents and action potentials of canine atrial tissue. Flecainide (4.5 μM) increased APD at cycle lengths ranging from 150 to 1000 msec and attenuated the APD shortening that resulted from increased activation rate, resulting in greater APD prolongation at faster rates. The major time-dependent outward current in canine atrial cells, the transient outward current (I_{to}), was reduced by flecainide in a rate-independent fashion. Flecainide's effect on I_{to} was due to inhibition of the 4-aminopyridine-sensitive component (I_{to1}); flecainide did not alter inward calcium current or the calcium-sensitive component of I_{to} (I_{to2}). The specific sodium channel blocker tetrodotoxin (1 μM) and the Na^+, K^+-ATP'ase inhibitor ouabain (1 μM) suppressed rate-dependent APD shortening in a fashion similar to flecainide, and both flecainide and ouabain attenuated postoverdrive membrane hyperpolarization. We conclude that the rate-dependence of flecainide's action on APD is not explained by use-dependent changes in outward currents but may be due to sodium channel blockade resulting in decreased sodium loading and reduced Na^+, K^+-ATP'ase stimulation during tachycardia.

Many drugs exert their antiarrhythmic actions by prolonging APD (Singh and Hauswirth, 1974; Singh and Courtney, 1990). Most drugs that increase APD manifest this effect to a greater extent as activation frequency decreases (Nattel and Zeng, 1984; Roden and Hoffman, 1985; Varro *et al.*, 1986), a phenomenon that has been called reverse use-dependence (Colatsky *et al.*, 1990; Hondeghem and Snyders, 1990). As recently pointed out (Hondeghem and Snyders, 1990), this property limits the efficacy of antiarrhythmic drugs and contributes to their proarrhythmic potential. The reduction of APD-prolonging capacity by tachycardia may limit a drug's effectiveness at the rapid rates characteristic of tachyarrhythmias. Conversely, the enhancement of drug effects on APD by slower rates increases the propensity to produce early after depolarizations (Dangman and Hoffman, 1981; Nattel and Quantz, 1988; Roden and Hoffman, 1985) and to cause Torsades de Pointes ventricular tachyarrhythmias during sinus bradycardia (Jackman *et al.*, 1988; Woosley, 1991). Theoretically, the ideal profile of an APD-prolonging drug would involve positive use-dependence: effects that are maximal at the rapid rates of pathological tachycardias and are minimal during sinus rhythm when APD prolongation can lead to adverse effects (Hondeghem and Snyders, 1990; Wang *et al.*, 1990; Woosley, 1991).

APD is well known to be a function of heart rate (Boyett and Jewell, 1980; Carmeliet, 1977), with APD generally decreasing at faster rates. The reduction of APD in response to an increase in heart rate is often referred to as "APD accommodation." Any drug that increases APD and interferes with APD accommodation would be expected to exert its APD-prolonging action more during tachycardia and therefore to show positive use-dependence. We have previously demonstrated that the class 1c antiarrhythmic agent flecainide possesses such an

Received for publication February 22, 1993.
[1] Supported by the Medical Research Council of Canada, the Quebec Heart Foundation, the Fonds de Recherche en Santé du Québec and the Fonds de Recherche de l'Institut de Cardiologie de Montréal. Dr. Nattel is a Nordic-FRSQ senior research scholar, Dr. Fermini is a Knoll-FRSQ research scholar and Z. Wang is the recipient of a Canadian Heart Foundation Research Studentship.

ABBREVIATIONS: APD, action potential duration; APD_{50}, APD_{90}, action potential duration to 50% and 95% of repolarization, respectively; $\dot{V}_{max}$, maximum rate of voltage rise during phase 0; TTX, tetrodotoxin; I_{to}, transient outward current; 4AP, 4-aminopyridine; I_{to1}, I_{to2}, first and second components of transient outward current; I_{Ca}, calcium current; I_K, delayed rectifier K^+ current; RDAS, rate-dependent APD shortening; MAP, membrane acvation potential; ANOVA, analysis of variance; ms, millisecond; mV, millivolt; V/s, volt/second; R_s, series resistance.

action *in vitro* on atrial tissues from a variety of species, including human (Wang *et al.*, 1990). Similar changes are seen *in vivo* (O'Hara *et al.*, 1992), and they may account for flecainide's beneficial properties in a canine model of atrial fibrillation (Wang *et al.*, 1992). However, the underlying ionic mechanisms remain unknown.

The goal of the present study was to evaluate potential ionic mechanisms of flecainide's tachycardia-dependent APD-prolonging action in canine atrium. Two possibilities were assessed: 1) tachycardia-dependent blockade of an outward current and 2) an action linked to sodium channel blockade. Our results point to the potential importance of the latter, a mechanism dependent on sodium channel blockade.

Materials and Methods

Myocytes and tissues. Atrial tissues were isolated from hearts removed *via* a right thoracotomy from anesthetized (sodium pentobarbital, 30 mg/kg i.v.) mongrel dogs. Specimens of right atrial appendage were immersed in *nominally* Ca^{++}-free Tyrode solution (100% O_2, 37°C) containing (in mM): NaCl 126.0, NaH_2PO_4 0.33, KCl 5.4, $MgCl_2$ 1.0, dextrose 10.0 and HEPES 10.0 (pH adjusted to 7.4 with NaOH). The tissues were chopped into cubic chunks and placed in a 25-ml flask containing 10 ml of Ca^{++}-free Tyrode solution and were gently agitated by stirring with a magnetic bar. Five minutes later, the chunks were incubated in a similar solution containing 390 U/ml collagenase (CLS II, Worthington Biochemical, Freehold, NJ) and 4 U/ml protease (Type XIV, Sigma Chemical Co., St. Louis, MO). The first supernatant was removed after 45 min and replaced with a fresh enzyme-containing solution. When microscopic inspection showed a satisfactory yield, the chunks were suspended in a high K^+ solution containing (in mM): KCl 20, KH_2PO_4 10, glucose 10, glutamic acid 70, β-hydroxybutyric acid 10, taurine 10 and EGTA 10, albumin 1% (pH adjusted to 7.4 with KOH). A small aliquot of isolated cells was placed in a 1-ml chamber on the stage of an inverted microscope. Five minutes was allowed for cell adhesion, and then the cells were superfused at 3 ml/min with a solution containing (in mM): NaCl 126.0, NaH_2PO_4 0.33, KCl 5.4, $CaCl_2$ 1.0, $MgCl_2$ 0.5, dextrose 5.5 and HEPES 10.0 (pH adjusted to 7.4 with KOH). The bath temperature was maintained at 36°C with a temperature controller device (N.B. Datyner, Stony Brook, NY). Only rod-shaped cells with clear cross striations were studied.

Muscle strips of right atrial crista terminalis were used for microelectrode experiments. Preparations were pinned to the bottom of a 20-ml chamber and superfused (12 ml/min) with Tyrode's solution containing (in mM): NaCl 116, $NaHCO_3$ 18, NaH_2PO_4 0.9, KCl 4, $CaCl_2$ 1, $MgCl_2$ 0.5 and dextrose 10. The superfusate was aerated with 95% O_2-5% CO_2, and the bath temperature was maintained at 36°C by a heat controller. One hour was allowed for tissue equilibration before experiments were begun.

Voltage-clamp technique. Borosilicate glass electrodes were used, with tip resistances of 3 to 10 MΩ when filled with (in mM): KCl 130.0, $MgCl_2$ 1.0, HEPES 10.0, EGTA 5.0, ATP 5.0 and Na_2-creatine phosphate 5.0 (pH adjusted to 7.4 with KOH) and were connected to a patch-clamp amplifier (Axopatch 1-D, Axon Instruments, Foster City, CA).

Junction potentials (3–15 mV) were zeroed before formation of the membrane-pipette seal. Several minutes after seal formation (mean resistance measured in 8 cells, 14.4 ± 3.5 GΩ), the membrane was ruptured to establish the whole-cell configuration. R_s was compensated to minimize the duration of the capacitive surge on the current record and to improve voltage control. R_s was estimated by dividing the time constant of the capacitive transient (T_s) by the cell membrane capacitance (the time-integral of the capacitive surge measured in response to 5-mV hyperpolarizing steps from −60 mV). Before R_s compensation, the decay of the capacitive surge as measured in 15 cells had a time constant of 409 ± 73 μs (cell capacitance: 76.6 ± 4.6 pF). After compensation this value was reduced to 141 ± 8 μs (cell capacitance: 59.5 ± 5.8 pF). R_s was reduced from 5.4 ± 0.7 MΩ to 2.5 ± 0.3 MΩ by the compensation procedure. Currents did not exceed 1.5 nA, and the maximum voltage drop across R_s was therefore in the range of 4 mV. Cells with significant leak currents were rejected. Residual leak currents were compensated by subtracting a current linearly scaled and opposite in polarity to the current response to a sequence of 5-mV hyperpolarizing pulses.

Command pulses were generated by a 12-bit digital-to-analog converter controlled by pClamp software (Version 5.5, Axon Instruments, Foster City, CA) on an IBM AT-compatible computer. Recordings were filtered at 1 kHz, digitized at 120 kHz (model TN 125, Scientific Solutions, Solon, OH) and stored on the hard disk of an IBM AT-compatible computer. Current amplitudes were measured by the Clampan routine in pClamp.

Microelectrode techniques. The microelectrode techniques used have been described in detail previously (Nattel, 1987; Wang *et al.*, 1990). Glass microelectrodes filled with 3 M KCl (8–20 MΩ resistance) were coupled to a microelectrode amplifier (WPI KS-700, World Precision Instruments, New Haven, CT). Square-wave pulses (2 msec), two times the late diastolic threshold current, were used to stimulate preparations. Signals were displayed on a storage oscilloscope (Tektronix 5115, Tektronix Inc., Beaverton, OR) and converted into digital form by a Tekmar 100-kHz A/D converter (Tekmar Co., Cincinnati, OH) for analysis with custom-made software routines.

Action potential characteristics, including membrane activation potential (transmembrane potential at the onset of phase 0), action potential amplitude, APD to 50% and 95% repolarization (APD_{50} and APD_{95} respectively) and maximum rate of voltage rise during phase 0 ($\dot{V}_{max}$) were determined at stimulation frequencies of 1.0, 1.7, 3.3 and 6.7 Hz. The magnitude of action potential shortening over the range of rates studied (rate-dependent APD shortening, or RDAS) was determined by subtracting the value of APD_{95} at 6.7 Hz from the value at 1 Hz. After base-line measurements, the test drug was added to the superfusate, and measurements were repeated after 30 min of drug superfusion and after 40 min of washout. Continuous stable impalement of the same cell under both control and drug conditions was required for all analyzed experiments. In some experiments, when drug effects disappeared completely upon washout, an additional agent was studied in the same preparation.

Drugs. Flecainide acetate (Riker Laboratories, Inc., St. Paul, MN) was studied at a concentration of 4.5 μM, which produces effects on canine atrial tissue similar to those caused by therapeutic flecainide concentrations in human atrium (Wang *et al.*, 1990). TTX and ouabain were purchased from Sigma Chemical Co., St. Louis, MO. To prevent cholinergically mediated actions of ouabain, 1 μM atropine (Sigma Chemical Co., St. Louis, MO) was added to ouabain-containing solutions. Action potential characteristics were not altered by the application of 1 μM atropine alone.

Statistical analysis. Group data are presented as the mean ± standard error. The rate-dependence of drug action was evaluated by analysis of variance (ANOVA) with an F test for interaction (Sachs, 1984). Multiple comparisons between repeated-measures data were evaluated by ANOVA with Scheffé contrasts (Sachs, 1984). Student's t test was used for single comparisons between two groups only. A two-tailed probability of ± 5% was taken to indicate statistical significance.

Results

Effects of flecainide on transient outward current (I_{to}). We have reported preliminary data indicating that I_{to} is the predominant time-dependent outward current in canine atrial tissue (Fermini and Nattel, 1990). In the present experiments, these results were confirmed: depolarizing pulses from potentials between −50 and −90 mV revealed a large transient outward current with little or no slowly developing outward current or outward current tails on repolarization (fig. 1). Of 47 cells studied under control conditions, only three had an

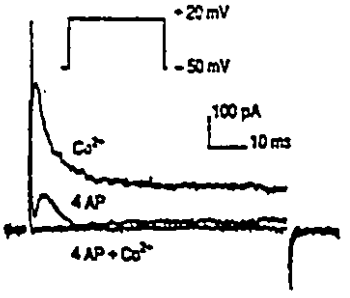

Fig. 1. Examples of transient outward current elicited by the voltage protocol shown in the inset in the presence of 2 mM cobalt (I_{to1}, designated by Co^{++} in the figure) and in the presence of 2 mM 4-aminopyridine (I_{to2}, designated by 4AP in the figure). In the presence of both 4AP and cobalt, no outward current is elicited.

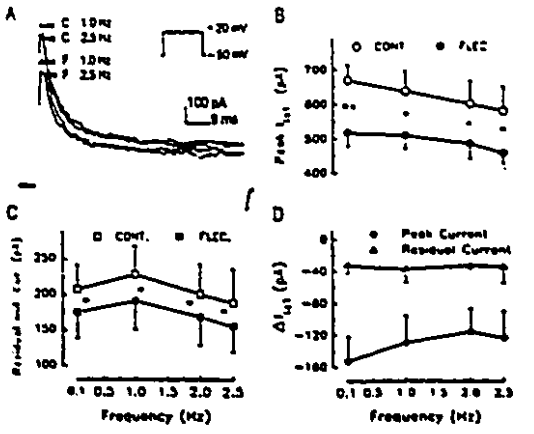

Fig. 2. A) I_{to1} at 1 and 2.5 Hz, in the absence and presence of 4.5 μM flecainide. B) Peak I_{to1} and C) residual outward current, as elicited in four cells by the tenth pulse in a train of ten 100-msec pulses from a holding potential of −50 mV to +20 mV. D) Change in peak I_{to1} and residual outward current produced by flecainide at various frequencies. *P < .05, **P < .01 compared with control.

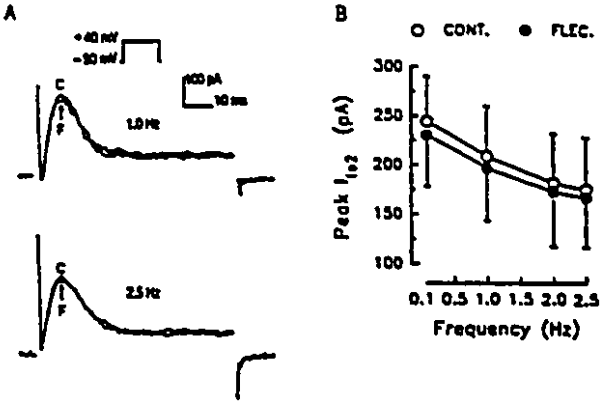

Fig. 3. A) Analog recordings of I_{to2} elicited by 100-msec pulses from a holding potential of −50 mV to +40 mV, under control (C) conditions and in the presence of flecainide (F), at 1.0 or 2.5 Hz. B) Mean (±S.E.) I_{to2} before and after flecainide in three cells.

outward tail current >40 pA upon repolarization after a 100-msec pulse. With longer depolarizing pulses (≥2 sec) to +30 mV, tail currents consistent with a delayed rectifier current (I_K) were seen upon repolarization to −40 mV in 12/47 (25%) of cells. Because I_K was seen in a small minority of cells, particularly with depolarizing pulses of a duration corresponding to the action potential plateau, it was not studied further. The transient outward current consists of two components—a 4AP-sensitive component referred to as I_{to1} or I_{to} (Escande *et al.*, 1987; Tseng and Hoffman, 1989; Furukawa *et al.*, 1990; Colatsky *et al.*, 1990) and a calcium-dependent current, possibly carried by chloride, referred to as I_{to2} or I_{tc} (Escande *et al.*, 1987; Tseng and Hoffman, 1989; Furukawa *et al.*, 1990; Colatsky *et al.*, 1990; Zygmunt and Gibbons, 1991). We used pharmacological tools to separate these components (fig. 1) and to study their modulation by flecainide.

I_{to1}. The membrane was held at −50 mV to inactivate I_{Na}, and 2mM Co^{++} was added to the bath solution to block I_{Ca} and I_{to2}. I_{to1} was elicited by a series of 10 test pulses (100 msec in duration) to +20 mV at 0.1, 1, 2 and 2.5 Hz. Steady-state I_{to1} was achieved within 10 pulses both in the presence and in the absence of flecainide. Peak I_{to1} was defined as the difference between the maximal outward current and the current at the end of the depolarizing pulse. Because the inactivation time constant of I_{to1} was very brief (mean of 15 ± 1 msec, 16 cells), inactivation was complete before the end of the clamp step. The residual current at the end of the pulse (fig. 1) was termed the "residual outward current."

Because the steady-state effects of flecainide were established within 4 min, we evaluated drug effects after 5 min of drug superfusion. A representative experiment is shown in figure 2A. In the absence of flecainide, peak current at 2.5 Hz is slightly decreased compared with that at 1 Hz. Flecainide reduced the peak and residual outward currents to a similar extent at both frequencies. Neither the activation nor the inactivation kinetics of I_{to1} were altered by flecainide. Similar results were observed in a total of nine cells.

The steady-state effects of 4.5 μM flecainide on I_{to1} in four cells are summarized in figures 2B and 2C. Under control conditions, peak I_{to1} amplitude decreased slightly, whereas residual current showed no consistent trend, as the frequency increased from 0.1 to 2.5 Hz. Flecainide produced a downward shift of both current-frequency relations. The magnitude of I_{to1} reduction by flecainide was not significantly altered by stimulation frequency (fig. 2D). To be sure that this apparent lack of frequency-dependent action was not due to inadequate drug concentrations, we studied five additional cells exposed to 15 μM flecainide, which reduced peak I_{to1} by 49 ± 5% ($P < .001$ *vs.* control) at 0.1 Hz, by 51 ± 5% ($P < .01$) at 1 Hz and by 49 ± 6% ($P < .001$) at 2 Hz, and reduced the residual outward current by 27 ± 4%, by 27 ± 4%, and by 26 ± 5% ($P < .01$ *vs.* control for all) at the same rates. For comparison, 4.5 μM flecainide reduced peak I_{to1} by 23 ± 3% ($P = 0.01$ *vs.* control) at 0.1 Hz, by 20 ± 4% ($P < .05$) at 1 Hz and by 19 ± 3% ($P < .05$) at 2 Hz, while reducing the residual outward current by 17 ± 5%, by 17 ± 6% and by 17 ± 3% (all $P < .05$ *vs.* control) at corresponding frequencies.

I_{to2} and I_{Ca}. To study I_{to2}, Co^{++} was omitted and 2 mM 4AP was added to block I_{to1}. I_{to2} was elicited by 100-msec pulses from a holding potential of −50 mV to +40 mV. After an initial inward calcium current of varying amplitude, an outward current typical of I_{to2} was recorded (fig. 3A). Flecainide did not significantly alter I_{to2} at any frequency (fig. 3B).

Attenuation of flecainide's APD-prolonging action at slow

rates could result from blockade of a plateau depolarizing current (such as I_{Ca}) that is manifest preferentially at slow rates. I_{Ca} was studied under the same conditions as I_{sd}, by using a less positive test potential, 0 mV, at which significant I_{Ca} activation occurs in the absence of measurable I_{sd} (fig. 4). The amplitude of I_{Ca} averaged 474 ± 52 pA under control conditions and 458 ± 63 pA in the presence of 4.5 μM flecainide ($P = 0.20$, $n = 3$) at 1.0 Hz; it averaged 451 ± 62 pA for control and 440 ± 67 pA for flecainide at 2.5 Hz ($P = 0.13$, $n = 3$). Thus a calcium-channel blocking action could not account for the rate-dependence of flecainide's effects on APD.

Effects of flecainide and pharmacological probes on APD accommodation. Flecainide failed to produce rate-dependent changes in outward currents or in calcium current that could explain its previously reported actions on APD accommodation (Wang *et al.*, 1990). We therefore sought to evaluate the possible role of sodium channel blockade. We used TTX as a pure sodium channel blocker (Narahashi, 1974) and selected a concentration of TTX that reduced $\dot{V}_{max}$ to the same extent as 4.5 μM flecainide at a rate of 6.7 Hz. In order to inhibit the Na^+K^+-ATP'ase, we used 1 μM ouabain (Isenberg and Trautwein, 1974). All results reported were obtained after 30 min of drug superfusion, at which time the effects of flecainide and TTX had reached steady state, and clear effects were seen with ouabain without delayed afterdepolarizations or triggered arrhythmias.

Figure 5 shows typical recordings of action potentials under control conditions (left) and in the presence of test drugs (right). Superimposed action potentials were recorded at 1.0, 1.7, 3.3 and 6.7 Hz. All three drugs attenuated APD accommodation, as shown by reduced differences in the timing of repolarization at various frequencies compared with control.

To quantify APD accommodation, the difference between APD_{90} at frequencies of 1.0 and 6.7 Hz was used as an index of total RDAS. Figure 6 compares RDAS in the absence and presence of flecainide ($n = 11$ cells), TTX ($n = 8$) and ouabain ($n = 7$). All three drugs decreased RDAS. TTX and flecainide reduced APD accommodation to virtually the same extent.

Overall drug effects on APD are illustrated in figure 7. Flecainide increased APD at all frequencies, and its action became more important as frequency increased. TTX did not alter APD significantly at a frequency of 1.0 Hz, but it tended to increase APD as frequency increased, with this effect becoming statistically significant at 6.7 Hz. Ouabain did not alter APD at 1.0 Hz, but it increased APD progressively as frequency increased. Figure 7D shows drug-induced changes in APD as a function of rate. The effects of all drugs on APD increased significantly with frequency, in a parallel fashion.

Drug effects on MAP, action potential amplitude (APA) and $\dot{V}_{max}$ are summarized in table 1. All three drugs suppressed

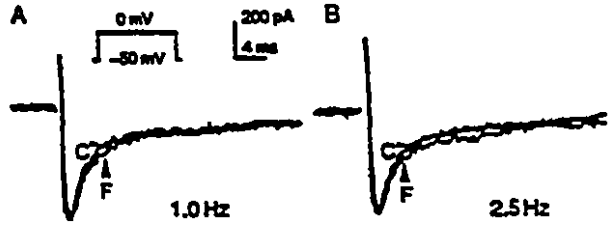

Fig. 4. Representative recordings of I_{Ca} recorded under control (C) conditions and after flecainide (F) at 1.0 and 2.5 Hz. Similar results were obtained in three cells.

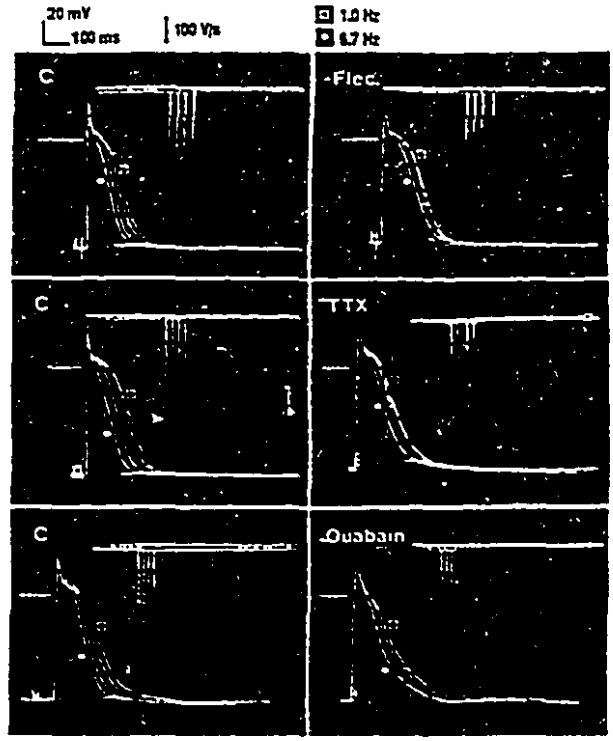

Fig. 5. Action potentials and differentiated signals recorded at frequencies of 1.0, 1.7, 3.3, and 6.7 Hz under control conditions (left) and in the presence (right) of flecainide (top), TTX (middle) and ouabain (bottom). Control and drug recordings are from continuous, stable impalements of the same cell in each case. Differentiated signals are displaced laterally so that results at different frequencies can be distinguished. After flecainide and ouabain, some tracings superimpose so that only three action potential recordings are visible for each. Similar results were obtained in 11 preparations with flecainide, eight with TTX and seven with ouabain.

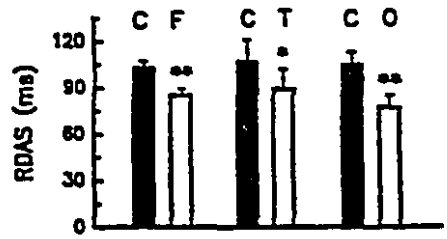

Fig. 6. RDAS under control conditions (C) and in the presence of flecainide (F, $n = 11$), TTX (T, $n = 8$) and ouabain (O, $n = 7$). *$P < .05$; **$P < .01$ compared with control values.

APA and $\dot{V}_{max}$. Flecainide and TTX reduced $\dot{V}_{max}$ to a greater extent than did ouabain, and the degree of $\dot{V}_{max}$ depression at 6.7 Hz was very similar for flecainide and TTX. The tendency to reduce $\dot{V}_{max}$ increased as frequency increased, with flecainide's action showing the greatest rate-dependence. Flecainide did not significantly alter MAP. MAP was decreased slightly in the presence of TTX, with the difference from control achieving statistical significance only at a frequency of 6.7 Hz. Ouabain significantly reduced MAP, to an extent that increased as frequency increased.

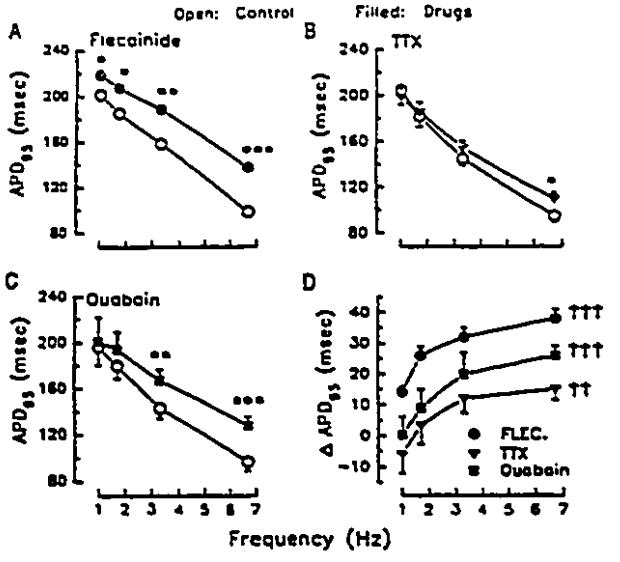

Fig. 7. A-C) Action potential duration as a function of frequency under control conditions (O) and in the presence (filled symbols) of flecainide ($n = 11$), TTX ($n = 8$) and ouabain ($n = 7$). D) Change in APD_{95} (compared with corresponding control values) produced by various drugs at each frequency. *$P < .05$, **$P < .01$, ***$P < .001$ *vs.* control. ††$P < .01$, †††$P < .001$ for rate dependence of drug action.

Effects of flecainide on membrane potential after rapid pacing. To assess the effects of flecainide on electrophysiologic consequences of Na^+, K^+-ATP'ase activity, we studied changes in membrane potential after rapid stimulation. Preparations from five dogs were stimulated for 5 min at 3.3 Hz, and the membrane potential was monitored after the cessation of stimulation. Under control conditions, postoverdrive hyperpolarization was observed in all 18 preparations (fig. 8). Hyperpolarization averaged 6.5 ± 0.8 mV 300 msec after overdrive was stopped, and it disappeared gradually over the following 1 to 2 min. Maximum hyperpolarization occurred within 1 sec and averaged 9.7 ± 0.5 mV. Hyperpolarization was reduced to 2.3 ± 0.6 mV 34 sec after the end of pacing and was no longer statistically significant. Ouabain (studied in 10 cells) and flecainide (studied in 14 cells) substantially attenuated the hyperpolarization after rapid pacing (fig. 8). The effects of flecainide were quantitatively similar to those of ouabain, although they were quantitatively slightly smaller. The maximum hyperpolarization averaged 3.8 ± 0.3 mV in the presence of flecainide and 2.1 ± 0.1 mV in the presence of ouabain (both $P < .001$ *vs.* control). Postoverdrive hyperpolarization was much briefer in the presence of ouabain and flecainide, and it was followed by depolarization. We quantified hyperpolarization at a standard time (300 msec) after the end of overdrive, as measured by computer, and mean results are shown in figure 9. The hyperpolarization after pacing at 3.3 Hz under control and drug conditions was similar whether postoverdrive membrane potentials were compared with the activation potential during rapid pacing (left of figure) or with the MAP before overdrive, at a frequency of 1.0 Hz (right).

Discussion

We found that flecainide significantly inhibited the 4AP-sensitive transient outward current in canine atrial myocytes

TABLE 1
Effects of drugs on MAP, APA and $\dot{V}_{max}$ in canine atrial tissues*

Frequency (Hz)	MVP (mV) 1	12	33	67	APA (mV) 1	17	33	67	$\dot{V}_{max}$ (V/s) 1	17	33	67
Control	78 ± 1	77 ± 1	77 ± 1	77 ± 1	104 ± 2	102 ± 2	98 ± 2	95 ± 1	209 ± 8	206 ± 6	180 ± 5	163 ± 7
Flecainide	77 ± 1	76 ± 1	75 ± 1	74 ± 1	96 ± 2**	95 ± 2***	91 ± 1***	88 ± 1	151 ± 4**	132 ± 4***	99 ± 3***	72 ± 2***
(n = 11)	−0.2 ± 1.2%	−0.3 ± 1.3%	−2.4 ± 1.2%	−3.1 ± 1.7%	−5.7 ± 1.0%	−6.5 ± 1.2%	−8.8 ± 1.4%	−7 ± 1.3%	−27.4 ± 1.8%	−36 ± 1.6%	−45.1 ± 1.6%	−54.8 ± 1.9%
Control	79 ± 1	79 ± 1	78 ± 1	77 ± 1	107 ± 3	103 ± 3	99 ± 2	96 ± 2	199 ± 12	198 ± 12	178 ± 10	150 ± 10
TTX	77 ± 1	75 ± 2	75 ± 2	73 ± 1*	93 ± 2***	91 ± 2***	87 ± 2	83 ± 2***	121 ± 8***	109 ± 9***	84 ± 9***	66 ± 6***
(n = 8)	−2.0 ± 1.2%	−4.3 ± 2.1%	−4.0 ± 1.7%	−5.4 ± 1%	−10.7 ± 0.7%	−11.2 ± 0.9%	−11.5 ± 1.3%	−12.8 ± 1.1%	−40.4 ± 1.6%	−48.5 ± 1.3%	−52.1 ± 3.1%	−54.7 ± 3.2%
Control	79 ± 1	78 ± 1	78 ± 1	77 ± 1	106 ± 2	104 ± 2	100 ± 2	95 ± 2	192 ± 14	193 ± 14	178 ± 11	164 ± 12
Ouabain	78 ± 1	74 ± 1*	73 ± 1*	71 ± 1**	102 ± 2***	100 ± 1***	94 ± 2***	87 ± 1***	171 ± 14	160 ± 13*	142 ± 10**	124 ± 12***
(n = 7)	−3.5 ± 1.1%	−5.3 ± .5%	−6.8 ± .7%	−8.2 ± .8%†	−3.8 ± 0.1%	−4.5 ± 0.4%	−5.7 ± 1%	−7.9 ± 1.5%	−11.3 ± 1.8%	−17.4 ± 1.6%	−20.9 ± 0.9%	−24.8 ± 0.8%

Data are mean ± S.E. *$P < .05$; **$P < .01$; ***$P < .001$, compared with control.
†Values for MAP are absolute values. All measures of MAP were, in fact, the negative of the value shown. ‡$P < .05$; ††$P < .01$; †††$P < .001$, for statistical significance of rate-dependence of drug action by two-way ANOVA with an F test for interaction.

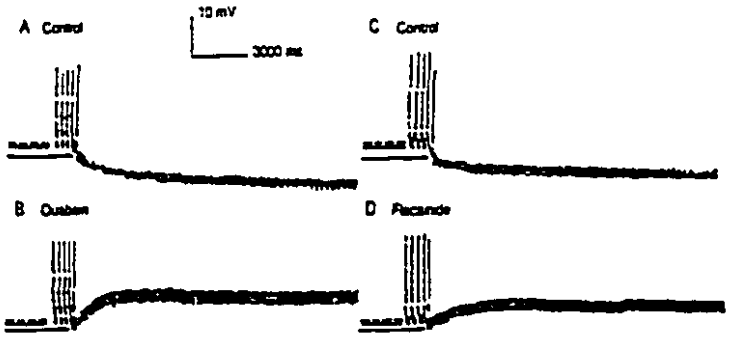

Fig. 8. Postoverdrive hyperpolarization in two cells under control conditions (A and C) and after exposure of the cell in A to ouabain (B) and the cell in C to flecainide (D). Preparations were stimulated for 5 min at 3.3 Hz, and stimulation was abruptly stopped. Under control conditions, the cessation of overdrive is followed by a hyperpolarization that lasts over 30 sec. In the presence of ouabain and flecainide, hyperpolarization is attenuated and evanescent. The solid lines represent the membrane activation potential at 1.0 Hz, whereas the dashed lines represent activation potentials during overdrive (at 3.3 Hz). The vertical arrows indicate the time point (3 msec after overdrive) at which hyperpolarization (value shown by horizontal arrow) at which postoverdrive hyperpolarization was quantified for analysis in figure 9.

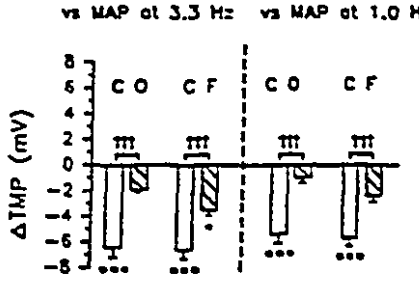

Fig. 9. Postoverdrive hyperpolarization, quantified as the difference in transmembrane potential (ΔTMP) between values 300 msec after the last paced beat at 3.3 Hz and either the membrane activation potential at 3.3 Hz (left) or the membrane activation potential at 1.0 Hz (right); $^{*}P < .05$, $^{***}P < .001$, vs. reference MAP value; $\dagger\dagger\dagger P < .001$, for difference between ΔTMP under control (C) conditions and values in the presence of ouabain (O) or flecainide (F). Results are shown from 14 preparations used in the study of flecainide and 10 used in the study of ouabain.

but that this action was not rate-dependent. The calcium-dependent component of I_{to} and the calcium current were not altered by flecainide. Flecainide reduced APD accommodation to increased rate, an action paralleled by TTX and ouabain. Both ouabain and flecainide attenuated the membrane hyperpolarization that followed the cessation of rapid stimulation.

Possible ionic mechanisms of flecainide's actions on APD. Flecainide significantly increased APD at all cycle lengths (fig. 7). The drug's ability to reduce I_{to1}, the major time-dependent outward current that we observed in canine atrial cells, probably contributed to its APD-prolonging properties. We believe that I_{to} inhibition alone is unlikely to account for the increases in drug effect on APD as frequency increased, because 1) the drug's blocking action on I_{to} was not altered by changes in rate (fig. 2), and 2) the current tended to be larger at slower rates, suggesting that, if anything, flecainide actions related to I_{to} inhibition should be less apparent at rapid rates.

The drug's effects on APD could, however, be explained by a combination of properties, with one action (such as I_{to} blockade) increasing APD at all rates, and another action preventing APD abbreviation when rate is increased (an action shared by ouabain and TTX). The effects of TTX indicate that sodium channel blockade can inhibit APD accommodation. Although TTX did not significantly alter APD at 1.0 Hz, it reduced APD accommodation, resulting in a statistically significant APD increase at a frequency of 6.7 Hz. At concentrations causing equivalent suppression of $\dot{V}_{max}$ at 6.7 Hz (table 1), flecainide and TTX produced equivalent changes in APD accommodation (fig. 6). One way to explain these results is to consider that sodium loading of the cell occurs at rapid rates and activates an electrogenic pump or exchange mechanism that abbreviates APD. Sodium channel blockade attenuates sodium loading by reducing phase 0 sodium entry, thereby decreasing the stimulus to sodium transport and reducing any corresponding component of APD accommodation.

Potential importance of sodium pump current to APD accommodation. The cardiac Na^+K^+-ATP'ase is an electrogenic pump (Akera and Brody, 1982; Gadsby, 1990; Glitsch, 1972). It generates an outward current, tending to repolarize the cell, and it is quite sensitive to intracellular sodium concentration over the physiologic range (Nakao and Gadsby, 1989). Increases in activation rate cause sodium loading and increase the activity of the sodium-potassium pump (Gadsby, 1990). Rate-induced increases in pump current may then decrease APD (Boyett and Fedida, 1984; Gadsby and Cranefield, 1982).

Ouabain significantly attenuated rate-dependent APD abbreviation in canine atrial preparations (fig. 6), suggesting a role for sodium-potassium pump current in mediating APD accommodation. At concentrations that reduced $\dot{V}_{max}$ equipotently at rapid rates, flecainide and TTX inhibited APD accommodation to a very similar extent. It is therefore likely that the observed changes in APD accommodation are due to their common sodium blocking action, which limits cellular sodium loading and Na^+K^+-ATP'ase stimulation at rapid rates.

Potential limitations. Sodium current contributes to maintaining the plateau in cardiac Purkinje fibers (Attwell *et al*, 1979) and ventricular muscle (Kiyosue and Arita, 1989), and it may be directly involved in APD adaptation to rate in canine Purkinje fibers (Elharrar *et al*, 1984). It is unlikely that changes in plateau sodium current account for the effects of TTX in our experiments, because, in contrast to its effects on other tissues (Attwell *et al*, 1979; Elharrar *et al*, 1984), TTX did not significantly decrease canine atrial APD at any frequency, indicating minimal plateau sodium current.

It would be useful to measure directly sodium-potassium pump current as a function of activation rate and to study its response to TTX and flecainide. The pump current is relatively small under physiologic conditions, however, and is difficult to record directly without removing extracellular potassium or increasing sodium concentration by intracellular dialysis (Gadsby, 1990). Our observation that flecainide, like ouabain, diminishes the hyperpolarization after a period of rapid stimulation—a phenomenon believed to be due to Na^+, K^+-ATP'ase activation (Vassalle, 1970)—provides indirect evidence for inhibition by flecainide of rate-induced pump activation.

In some tissues, increased Na^+, K^+-ATP'ase activity causes hyperpolarization at rapid rates (Gadsby, 1990). Canine atrium

tended to depolarize slightly, rather than to hyperpolarize, as rate was increased (table 1). This finding suggests that in canine atrium, the sodium-potassium pump may not be able to compensate fully for changes in extracellular potassium concentration at rapid rates, a phenomenon previously described in other systems (Johnson *et al*, 1980). A role for Na^+, K^+-ATP'ase in preventing rate-induced depolarization is indicated by the enhancement of rate-dependent depolarization by ouabain (table 1). Further evidence for a role of the Na^+, K^+-ATP'ase in maintaining diastolic membrane potential at rapid rates is that the cessation of rapid stimulation is followed by transient hyperpolarization, which is significantly attenuated by ouabain.

Relevance to mechanisms of antiarrhythmic drug action. Positive use-dependence of APD-prolonging action is a highly desirable antiarrhythmic property (Hondeghem and Snyders, 1990); Wang et al., 1990. Flecainide appears to possess such an action on atrial tissue from a variety of species (Wang *et al*, 1990), and this property may account for antiarrhythmic actions in a canine model of atrial fibrillation (Wang *et al*, 1992). The present experiments suggest that, at least in canine atrium, the tachycardia-dependent APD prolongation caused by flecainide is due to sodium channel blockade and decreased Na^+K^+-pump current.

Acknowledgments

The authors thank Lise de Repentigny and Mary Morello for typing the manuscript, and Emma De Blasio and Guylaine Nicole for technical help. They also thank Riker-3M Pharmaceuticals for supplying the flecainide used in these experiments.

References

Akera, T. and Brody, T. M.: Myocardial membranes: Regulation and function of the sodium pump. Annu. Rev. Physiol. 44: 375–388, 1982.

Attwell, D., Cohen, I., Eisner, D., Ohba, M. and Ojeda, C.: The steady state TTX-sensitive ("window") sodium current in cardiac Purkinje fibers. Pflugers Arch. 379: 137–142, 1979.

Boyett, M. R. and Fedida, D.: Changes in the electrical activity of dog canine Purkinje fibres at high heart rates. J. Physiol. (Lond.) 339: 361–391, 1984.

Boyett, M. R. and Jewell, B. R.: Analysis of the effects of changes in rate and rhythm upon electrical activity in the heart. Prog. Biophys. Mol. Biol. 36: 1–52, 1980.

Carmeliet, E.: Repolarization and frequency in cardiac cells. J. Physiol. (Paris) 73: 903–923, 1977.

Colatsky, T. J., Follmer, C. H. and Starmer, C. F.: Channel specificity in antiarrhythmic drug action. Circulation 82: 2235–2242, 1990.

Coraboeuf, E., Deroubaix, E. and Coulombe, A.: Effect of tetrodotoxin on action potentials of the conducting system in the dog heart. Am. J. Physiol. 236 (Heart Circ. Physiol. 5): H561–H567, 1979.

Dangman, K. H. and Hoffman, B. F.: In vivo and in vitro arrhythmogenic effects of N-acetyl procainamide. J. Pharmacol. Exp. Ther. 217: 851–862, 1981.

Elmarrar, V., Atarashi, H. and Surawicz, B.: Cycle length-dependent action potential duration in canine cardiac Purkinje fibers. Am. J. Physiol. 247 (Heart Circ. Physiol. 16): H936–H945, 1984.

Escande, D., Coulombe, A., Faivre, J. F., Deroubaix, E. and Coraboeuf, E.: Two types of transient outward currents in adult human atrial cells. Am. J. Physiol. 249 (Heart Circ. Physiol. 21): H142–H148, 1987.

Fermini, B. and Nattel, S.: Differential effects of flecainide and quinidine on repolarizing currents in dog atrial myocytes (abstract). Circulation 82: suppl. III, III–328, 1990.

Furukawa, T., Myerburg, R. J., Furukawa, N., Bassett, A. L. and Kimura, S.: Differences in transient outward currents of feline endocardial and epicardial myocytes. Circ. Res. 67: 1287–1291, 1990.

Gadsby, D. C.: The Na/K pump of cardiac myocytes. *In* Cardiac Electrophysiology. From Cell to Bedside, ed. by D. P. Zipes and J. Jalife, pp 35–50. W. B. Saunders Company, Philadelphia, 1990.

Gadsby, D. C. and Cranefield, P. F.: Effects of electrogenic sodium extrusion on the membrane potential of cardiac Purkinje fibers. *In* Normal and Abnormal Conduction in the Heart, ed. by B. F. Hoffman, M. Lieberman and A. Paes de Carvalho, pp 225–247. Futura Publishing Company, Inc., Mt. Kisco, New York, 1982.

Gadsby, D. and Nakao, M.: Steady-state current-voltage relationship of the Na/K pump in guinea-pig ventricular myocytes. J. Gen. Physiol. 94: 511–537, 1989.

Glitsch, H. G.: Activation of the electrogenic sodium pump in guinea-pig auricles by internal sodium ions. J. Physiol. (Lond.) 220: 565–582, 1972.

Hondeghem, L. M. and Snyders, D. J.: Class III antiarrhythmic agents have a lot of potential but a long way to go. Circulation 81: 686–690, 1990.

Isenberg, G. and Trautwein, W.: The effect of dihydro-ouabain and lithium ions on the outward current in cardiac Purkinje fibers. Pflugers Arch. 350: 41–54, 1974.

Jackman, W. M., Friday, K. J., Anderson, J. L., Aliot, E. M., Clark, M. and Lazzara, R.: The long QT syndromes: A critical review, new clinical observations and a unifying hypothesis. Prog. Cardiovasc. Dis. 31: 115–172, 1988.

Johnson, E. A., Chapman, J. B. and Kootsey, J. M.: Some electrophysiological consequences of electrogenic sodium and potassium transport in cardiac muscle: A theoretical study. J. Theor. Biol. 87: 737–756, 1980.

Kitosue, T. and Arita, M.: Late sodium current and its contribution to action potential configuration in guinea pig ventricular myocytes. Circ. Res. 64: 389–397, 1989.

Nakao, M. and Gadsby, D. C.: (Na) and (K) dependence of the Na/K pump current-voltage relationship in guinea pig ventricular myocytes. J. Ger. Physiol. 94: 539–565, 1989.

Naramashi, T.: Chemicals as tools in the study of excitable membranes. Physiol. Rev. 54: 813–889, 1974.

Nattel, S.: Relationship between use-dependent effects of antiarrhythmic drugs on conduction and V_{max} in canine cardiac Purkinje fibers. J. Pharmacol. Exp. Ther. 241: 252–258, 1987.

Nattel, S. and Quantz, M. A.: Pharmacological response of quinidine induced early after depolarizations in canine cardiac Purkinje fibres: Insights into underlying ionic mechanisms. Circ. Res. 22: 808–817, 1988.

Nattel, S. and Zeng, F. D.: Frequency-dependent effects of antiarrhythmic drugs on action potential duration and refractoriness of canine cardiac Purkinje fibers. J. Pharmacol. Exp. Ther. 229: 283–291, 1984.

O'Hara, G., Villemaire, C., Talajic, M. and Nattel, S.: Effects of flecainide on atrial refractoriness, atrial repolarization, and atrioventricular nodal conduction in anesthetized dogs. J. Am. Coll. Cardiol. 19: 1335–1342, 1992.

Roden, D. M. and Hoffman, B. F.: Action potential prolongation and induction of abnormal automaticity by low quinidine concentrations in canine Purkinje fibers. Circ. Res. 56: 857–867, 1985.

Sachs, L.: Applied Statistics, Springer Verlag, New York, 1984, pp. 508–512.

Singh, B. N. and Courtney, K. R.: The classification of antiarrhythmic mechanisms of drug action: Experimental and clinical considerations. *In* Cardiac Electrophysiology. From Cell to Bedside, ed. by D. P. Zipes and J. Jalife, pp 882–897. W. B. Saunders Company, Philadelphia, 1990.

Singh, B. N. and Hauswirth, O.: Comparative mechanisms of action on antiarrhythmic drugs. Am. Heart J. 87: 367–382, 1974.

Teeng, G. N. and Hoffman, B. F.: Two components of transient outward current in canine ventricular myocytes. Circ. Res. 64: 633–647, 1989.

Varro, A., Nakaya, Y., Elmarrar, V. and Surawicz, B.: Effect of antiarrhythmic drugs on the cycle length-dependent action potential duration in dog Purkinje and ventricular muscle fibers. J. Cardiovasc. Pharmacol. 8: 178–185, 1986.

Vassalle, M.: Electrogenic suppression of automaticity in sheep and dog Purkinje fibers. Circ. Res. 27: 361–377, 1970.

Wang, Z., Page, P. and Nattel, S.: Mechanism of flecainide's beneficial actions in experimental atrial fibrillation. Circ. Res. 71: 271–287, 1992.

Wang, Z., Pelletier, J. C., Talajic, M. and Nattel, S.: Effects of flecainide and quinidine on human atrial action potentials. Circulation 82: 274–283, 1990.

Woosley, R. L.: Antiarrhythmic drugs. Annu. Rev. Pharmacol. Toxicol. 31: 427–455, 1991.

Zygmunt, A. C. and Gibbons, W. R.: Calcium-activated chloride current in rabbit ventricular myocytes. Circ. Res. 68: 424–437, 1991.

Send reprint requests to: Stanley Nattel, M.D., Montreal Heart Institute, 5000 Belanger Street East, Montreal, Quebec, Canada, H1T 1C8.

CHAPTER 5

GENERAL DISCUSSION

This thesis is constructed based on a series of published articles co-authored by myself and others. Explanation of the results, the potential implication of our findings, and possible limitations of these studies have all been covered in the 'Discussion' session of each paper. To avoid redundancy, this general discussion will focus mainly on the novel findings of our studies and potential future directions of research.

5-1. Summary of novel findings in this thesis

1. Rate-dependent APD prolongation by class Ic drugs;

Although our studies represented the first detailed analysis of use-dependent effects on APD and ERP of class Ic drugs[5-1-4], a few previous reports described similar properties of these compounds. Le Grand et al.[5-5] observed use-dependent lengthening of APD_{50} (but not APD_{90}) in human atrial tissue. Kerr and colleagues[5-6] found that propafenone, another class Ic agent, produced rate-dependent increase in ERP in rabbit atrium. It seems, therefore, that use-dependent APD prolongation may be the common mechanism of class Ic drugs. Our findings have two potential clinical implications: (1) Use-dependent prolongation of APD, and thereby of ERP, induced by class Ic drugs explains the paradox between clinical observations (highly effective against AF in patients) and basic research (strong conduction slowing with little effects on ERP at normal heart rate) for these drugs. (2) It has been shown that flecainide is more effective in AF but less in atrial flutter[5-7]. This can be explained by diminished effects of flecainide on ERP during flutter with reduced activation rate relative to AF. This property of class Ic drugs also provides an alternative explanation for the proarrhythmic[5-8] action of these agents during flutter. (3) Currently available class III agents and some class I drugs (quinidine) produce reverse use-dependent ERP prolongation. This property would limit their therapeutic potential, as pointed out by Hondeghem and Snyders[5-9], by reducing their efficacy in terminating tachycardias due to a diminished ability to prolong repolarization at fast heart rates and by leading to proarrhythmia (Torsade de Pointes) due to a tendency to produce excessive APD prolongation at slow heart rates. Our studies provide evidence in support of this view by showing the role of use-dependent APD prolongation in tachycardias and diminished efficacy in AF of a class III drug (sotalol) characterized with reverse use-dependent ERP increase. Our findings are relevant to the development of new drugs: compounds with a property of use-dependent APD prolongation without slowing conduction would be ideal drugs with maximum effectiveness against tachycardias and minimal possibility of causing reentry and EAD (torsade de pointes).

In fact, this use-dependent property of flecainide is not limited to atrial tissue. Similar use-dependent APD lengthening has also been reported by Varro and colleagues[5-10] and by Antzelevitch[5-11] in isolated canine ventricular muscles. In dog Purkinje fibres, although flecainide was found to shorten APD[5-10,12], a similar tendency of use-dependency was consistently revealed with flecainide; that is, APD was shortened to a lesser extent at faster pacing rates. Furthermore, Varro et al. observed that prolongation

of the duration of premature action potentials by flecainide was accentuated with decreasing diastolic interval[5-13]. It appears, therefore, that the use-dependency of flecainide is an electrophysiologic property common to different tissue types. A possible ionic mechanism underlying this similar use-dependency is interference with electrogenic Na^+-K^+ pump activity as described in Chapter 4-flecainide causes use-dependent blockade of Na^+ channels so as to prevent intracellular Na^+ loading, which in turn weakens electrogenic Na^+-K^+ pump activity, thereby reducing outward current at rapid activation rates[5-14]. Different effects of flecainide on APD in different type of tissues (prolongation in atrium, little change in ventricle, and shortening in Purkinje fiber) can be explained by the different contribution of various currents. For example, if TTX-sensitive Na^+ current plays a more important role in maintaining plateau duration in Purkinje fiber relative to ventricle and atrium, then blockade of this current shortens APD. On the other hand, if outward currents such as I_{to} and I_K are more important in atrium, then the lengthening effect of flecainide on APD due to blockade of these outward currents[5-15] would outweigh the shortening due to the blockade of TTX-sensitive Na^+ window current, and lead to a net increase in APD. This may also be the explanation for the fact that class Ic drugs are highly effective in AF but potentially proarrhythmic in the ventricle.

Our findings also revealed some pitfalls of the current classification system of antiarrhythmic drugs[5-16]. While drug actions are importantly determined by heart rate, tissue type, and species, the current classification system is constructed mainly based on experimental results obtained from normal ventricular preparations driven at slow rates (1-2 Hz). According to this system, class Ic drugs are characterized by strong suppression of V_{max} with little change in APD and ERP. It is true that flecainide exerts minor effects on APD in the ventricle and even shortens APD in Purkinje fibers, but results from our studies and the literature demonstrate that flecainide prolongs APD in the atrium. It is also true that flecainide has little effects on APD at physiologic heart rates even in the atrium, but it significantly lengthens APD at the rapid heart rates manifested with arrhythmias. In addition, although flecainide increases APD with a similar rate-dependent pattern in atrial tissues from various species, the magnitude of prolongation and the degree of rate-dependency are significantly different among different species, with human atrium most sensitive to the drug. Obviously, arbitrary extrapolation of results from one species to another, or from resting heart rates to heart rates characteristic of arrhythmias, or from one type tissue to another , could be seriously erroneous. Therefore, all these factors modulating drug effects should be taken into account in the classification of antiarrhythmic drugs.

2. Development of an animal model of atrial fibrillation and mechanisms of drug termination of atrial fibrillation

We have developed a vagotonic dog model of AF to assess the efficacy and mechanism of drug termination of this arrhythmia. To our best knowledge, this represents the first experimental study on AF termination by antiarrhythmic drugs. Although a variety of animal models of atrial flutter has been available[5-

[17-20], and AF was also witnessed in these models, the poor stability and reproducibility of AF limit the validity of these models to flutter. Thus, experimental studies on drug efficacy and mechanisms against AF have been sparse, due to the difficulty of obtaining reliable animal models of AF. The vagotonic dog model of AF we established has the reliability required for drug studies, including its sustained nature, stability and reproducibility[5-2,4]. However, one potential limitation of this model is that it does not directly mimic the diseased, dilated atria often associated with chronic AF in humans, and the other limitation is that the model is suitable only to drugs without vagolytic actions. Another animal model used to investigate drug actions in AF in previous studies is AF induced by rapid pacing in dogs with normal hearts. For example, Platou et al.[5-21] evaluated efficacy of class III drugs in converting AF to sinus rhythm. Kirchhof et al.[5-22] tested the ability of a class Ic agent to prevent induction of AF and to shorten the duration of AF. In our own experience, pacing-induced AF rarely persisted longer than 2 minutes in dogs with normal hearts without enhanced vagal tone[5-23]. The short duration and poor stability of this model make it uncertain when used to evaluate drug efficacy in terminating AF. It is more practical to use this model to examine drug effects on AF initiation and persistence.

Although it is commonly believed that efficacy of drug termination of AF depends on a drug's ability to increase ERP, our experiments were the first demonstration of this hypothesis. We found that the common mechanism for drug termination of AF is ERP prolongation, which results in lengthening of WL, and that the common property of class Ic drugs' action was rate-dependent ERP prolongation. Reverse rate-dependent effects of class III agents limited their efficacy against AF.

3. Identification and characterization of I_K in human atrium

We identified and characterized I_K current in human atrial myocytes[5-24] where this current had been claimed to be absent or minimal. We found that I_K in human cells was an aggregate of two kinetically and pharmacologically different components I_{Kr} and I_{Ks}[5-25,26], similar to those firstly described in sheep Purkinje fibres by Noble and Tsien[5-27], in chick atrial cells by Shrier and Clay[5-28], and recently established in guinea pig heart by Sanguinetti[5-29,30]. Similar data regarding I_K current in human atrial myocytes was also recently presented by Crumb and Brown[5-31]. Discovery of I_K in human heart helps to understand many well-recognized but unexplained facts.

The finding of I_K in man explains why drugs known to block I_K in animal species are effective in patients. For example, sotalol is known to be effective in suppressing some supraventricular arrhythmias[5-32] by prolonging APD and ERP[5-33-35]. It has been shown to be a potent and highly selective I_K blocker in animal species[5-36,37]. Our data (unpublished observations) showed that sotalol at concentrations up to 15 μM exerted no effects on I_{to1} and I_{Kur} in human atrial cells. Were there no I_K in human heart, sotalol's action in arrhythmias could not be understood. The other example is E-4031, which has been demonstrated to be a specific I_{Kr} blocker devoid of any other actions such as conduction slowing, ß-blocking etc in cardiac

tissues[5-29,30,38]. Experimental studies showed that E-4031 suppresses reentrant tachyarrhythmias due to prolongation of ERP, such as tachycardias in rabbit right atrium[5-39] and canine atrial flutter[5-40,41]. More importantly, Isomoto et al. found that E-4031 significantly increased atrial ERP in patients with superaventricular tachyarrhythmias[5-42]. Since it does not alter sodium current and calcium current, it is impossible that ERP prolongation by E-4031 is due to delaying of recovery of excitability or to lengthening of the APD by increasing inward currents. Evidently, APD prolongation due to K^+ channel blockade is the mechanism by which E-4031 increases ERP. Were there no I_{Kr} in human atrium, the ERP prolonging effect of E-4031 would be unexplainable. Another example comes from the effects of almokalant, a selective class III agent devoid of class I and II activity, on repolarization and refractoriness of human heart[5-43,44]. This drug has been shown to be a selective I_K blocker[5-45]. Almokalant significantly increases monophasic atrial APD and ERP, as well as ventricular APD and ERP[5-46,47]. In addition, Escande et al. reported prolongation of human atrial APD by external superfusion of 10 mM TEA[5-48]. Although they ascribed this effect to TEA block of I_{K1}, lack of effects of TEA on resting potential argues against this explanation. TEA is known to be a selective I_K blocker[5-24,49]. It is quite possible that the APD-prolonging action of TEA in human atrium was the consequence of I_K blockade.

Because of the different deactivation kinetics of I_{Kr} and I_{Ks}, the relative contribution of I_{Kr} and I_{Ks} to net repolarizing current changes with decreasing pacing intervals, which result in incomplete deactivation and accumulation of I_{Ks}. In multicellular tissues, an increase in I_{Ks} due to its incomplete deactivation at fast activation rate will be accompanied by an increase in I_{K1} due to extracellular K^+ accumulation, and the combined increase in outward currents would diminish the impact of I_{Kr} blockade by class III antiarrhythmic agents during rapid heart rates[5-50]. It has been reported that all specific I_{Kr} blockers, the methanesulfonanilide class III agents such as E-4031[5-50], d-sotalol[5-51], dofetilide[5-52], UK-66,914[5-53], and Way-123,398[5-54] cause reverse rate-dependent APD prolongation due to the diminished contribution of I_{Kr} to net repolarizing current during rapid pacing. We have also shown that reverse rate-dependency limited the efficacy of sotalol to terminate AF. It is quite plausible, therefore, that a specific I_{Ks} blocker would produce rate-dependent APD prolongation, because of the increased contribution of I_{Ks} to net repolarizing current at rapid rates. The development of specific I_{Ks} blockers could result in the availability of improved antiarrhythmic drugs with properties of rate-dependent APD lengthening and devoid of conduction slowing effects, as proposed in Chapter 2. The finding of I_{Kr} and I_{Ks} in human atrial myocytes indicates the potential practical importance of I_{Ks} blockers.

Variation of action potential morphology has been a well-recognized phenomenon in human atrium. Action potentials could be roughly divided into three different types based on their morphology described in the literatures: (1) low plateau "spike and dome" configuration, (2) high plateau rectangular shape, and (3) triangular contour.

The variation of action potential morphology with age was attributed by Escande et al. to more

prominent I_{to1} in adult atrial cells than in young ones. Our results showed that differences in I_{to1} did not fully account for the variation of action potential morphology. We proposed the ratio of I_K over I_{to1} as an explanation for action potential alteration. In this regard, we grouped human atrial cells into three types with different relative quantities of I_{to1} and I_K. Our findings provide potential insight into the ionic mechanisms underlying action potential variation. This may be important, because drugs acting on different K^+ currents would preferentially change different types of action potentials. For example, flecainide is more potent in blocking I_K[5-55] than in blocking I_{to1}[5-15]. Thus it would produce the most pronounced prolongation of APD in type II cells with only I_K and with the shortest duration, less effect in type I cells with both I_K and I_{to1} and with medium duration, and least in type III cells with only I_{to1} and with the longest APD. In doing so, one would expect to see homogenization of APD and ERP. This is exactly what we found in our mapping study (see Chapter 2). We can therefore propose that the mechanism by which antiarrhythmics homogenize ERP, and thereby suppress arrhythmias in patients is, at least partially, their differential actions on different types of cells because of their relative potency in blocking different K^+ currents. It should, however, be emphasized that use of I_K/I_{to1} ratio could be an over simplified consideration. It is well-known that slow Ca^{++} current is important in maintaining plateau duration, and the properties of Ca^{++} current may also play an important role.

Finally, the finding that I_{Kr} and I_{Ks} in human atrial cells have many similarities with those in guinea pig atrial cells indicates the relevance of results obtained in this lower species.

4. **Identification of a novel delayed rectifier (I_{Kur}) equivalent to the currents expressed by cloned K^+ channel cDNAs of Kv1.5 subfamily**

The HK2 channel was cloned from human heart in 1988[5-56]. Although The mRNA was found to be abundant in human atrium, the physiological counterpart was not identified and its physiologic role was uncertain until we discovered I_{Kur} in 1993[5-57]. It has recently been demonstrated that heteromultimeric K^+ channels are formed by coinjection of cloned mRNAs synthesized from different K^+ channel cDNAs and that the properties of the expressed channels are distinct from those of their homopolymeric counterparts[5-58-61]. It is possible that I_{Kur} in human atrial myocytes reflect the presence of heteromultimeric K^+ channels comprised of the protein products of several different K^+ channel genes.

Based on the activation voltage range of I_{Kur}, its non-inactivating property and its rate independence, one would expect a contribution of I_{Kur} to repolarizing current. This was confirmed by the APD-prolonging effects of specific I_{Kur} blockade by 50 μM 4-AP[5-57]. Our finding indicated the potential physiologic role of Kv1.5 in native tissue, which had not been previously defined. Lauribe et al. also reported 4-AP prolongation of APD at a cycle length of about 220 msec[5-62]. They considered this to be the result of I_{to1} block by 4-AP. This is, however, unlikely, because many studies have shown that 4-AP unblocks from I_{to1} channels during rapid activation[5-63-66]. The effects of 4-AP on I_{to1} at a cycle length of 220

msec would be minimal. In fact, the prolongation of APD by 4-AP could well be explained by the blockade of I_{Kur}.

Another important implication of this discovery is that I_{Kur} may prove to be a target for antiarrhythmic drugs. We have evaluated the effects of several antiarrhythmic drugs on I_{Kur}. Quinidine, a class Ia agent, inhibits I_{Kur} with a potency slightly higher than for I_{to1}. Similar effects of quinidine on current expressed by Kv1.5 K^+ channels (HK2) was reported by Snyders et al[5-67]. Results from our preliminary experiments showed that ambasilide, a new class III drug, is a potent I_{Kur} blocker with an IC_{50} of 2.5 μM. The effects of quinidine seem to be voltage-dependent, but those of ambasilide are not. Sotalol was found to act on neither I_{Kur} nor I_{to1}. Clofilium, another class III agent, did not affect I_{Kur}[5-68], although it reduced I_K[5-69]. Flecainide blocks I_{to1} without altering I_{Kur}[5-15]. In addition, we have also shown that perhexiline, an antianginal drug with antiarrhythmic effects in man, suppressed the K^+ current expressed by fHK cloned from human heart as well as I_{Kur} in human atrial myocytes. One might therefore expect antiarrhythmic effectiveness of drugs that inhibit I_{Kur} which results in prolongation of APD and thereby ERP. It would be intriguing to develop new compounds that specifically block I_{Kur}, and to assess their antiarrhythmic profile. It is likely that this may become one direction of new drug development.

Currents resembling the expressed channels of Kv1.5 subfamily have also found in adult rat atrial myocytes, guinea pig ventricular cells, and neonatal puppy cells. They all possess properties similar to I_{Kur} in many aspects. It is possible that they are all equivalent currents in different species and represent the natural expression of I_{K1}.5 genes in corresponding native cells. However, some differences, such as in their pharmacologic sensitivity, exist among them. These differences could be due to different conditions with which these currents were recorded, but it is also possible that some intrinsic differences exist in critical amino acids to explain their different response to drugs.

5. Drug block of K^+ channels (I_{to1}): drug mimicking of inactivation gate of channels

We have used human I_{to1} as model to explore the drug-channel interaction. One of our most important finding was that channel opening was required for the final block of channels by drug molecules, regardless of different preferential affinity of different drugs for different states of channels. For example, as shown in Chapter 4, Page 2-43, although 4-AP had high affinity to the closed state, quinidine preferentially bound to the open state, and flecainide tended to associate with the inactivated state, channel opening was necessary for drug blockade of channels. Ambasilide was also found to block open channels of I_{to1} in human atrial cells. In addition, propafenone block of I_{to1} in rabbit atrial myocytes[5-70] and block by tedisamil in rat cells[5-71] all happen after channel opening. All these results indicate that drug molecules may mimic the intrinsic inactivation gates of channels, occluding channels upon opening. This concept may help us to understand the nature of the drug molecule-channel protein interaction, and thereby the mechanisms of drug blockade of channels.

6. **Contribution of electrogenic Na^+-K^+ pump to rate-dependent shortening of APD**

We have carried out studies (see Chapter 4, Pages 2-43) designed to reveal the possible contribution of electrogenic Na^+-K^+ pump to rate-dependent acceleration of repolarization. Although the study was undertaken in canine atrium, the conclusion might be validly applied to man. Lauribe et al. showed that ouabain significantly prolonged APD, with concomitant reduction of membrane potential in human atrial fibres at frequencies corresponding to atrial flutter[5-62]. Other groups observed abbreviation of APD by ouabain at physiological heart rate[5-72]. These results indicate that pump inhibition produces rate-dependent APD prolongation in human atrial cells. Existence of electrogenic Na/K pump activity in human atrium has been provided by several studies[5-73-76]. Rasmussen and colleagues[5-74] studied in detail the characteristics of a sodium pump-induced hyperpolarization in isolated human atrium, and they came to the conclusion that this hyperpolarization resembles that described for cardiac tissue from other mammalian species. It should be emphasized that rate-dependent APD shortening is the consequence of a net increase in outward current, and other currents besides pump currents including I_{Ks}, I_{K1}, I_{to1}, and I_{Kur} could all contribute to net repolarizing currents during rapid activation. The relative importance of these different currents in rate-dependent APD shortening is yet to be determined.

5-2. Direction of future research

With increased knowledge from recently-developed patch-clamp and molecular biology techniques, we have achieved a better understanding of the determinants of atrial repolarization and arrhythmias. Yet many issues remain unexplored.

We have answered most of the questions raised in Chapter 1, but new questions have been raised in the process.

1. **Identity of I_{Kur} and Kv1.5**

Powerful technologies of molecular biology have discovered many new genes encoding receptors or channels, which are yet to be identified in the native tissues. HK2, cloned from human heart, is an example. Although we have obtained evidence suggesting that I_{Kur} is the natural expression in the native human heart of Kv1.5 genes, we are still one step away from a conclusive answers. The establishment of a linkage between I_{Kur} and currents expressed by Kv1.5 genes is of great theoretical and practical importance, in order to define the physiological role of Kv1.5 K^+ channels in the heart.

One way of testing the relation between I_{Kur} and current expressed by Kv1.5 genes is to characterize I_{Kur} at the single channel level in both cell-attached and excised membrane patches. Comparison of single channel conductance, channel gating properties, and modulation of single channel activity (see below) of I_{Kur} with those of currents expressed by Kv1.5 genes would shed more light on the relation between I_{Kur} and Kv1.5.

Another way of examining whether I_{Kur} is the physiological counterpart of current expressed by Kv1.5 is to employ an antisense oligonucleotide of Kv1.5 gene in a cell culture system. The rationale for this is that antisense should prevent expression of Kv1.5 genes. Thus when this antisense is introduced into the cell culture system, the cells will eventually lose the ability to express Kv1.5 channel proteins. If the association between I_{Kur} and Kv1.5 is real, then I_{Kur} will not be recorded in cells cultured with the antisense, whereas in cells without antisense persistent expression of I_{Kur} is expected. To do this, the first step is the synthesis of antisense oligonucleotide based on the nucleotide sequence of Kv1.5 gene. The second step would be to co-inject this antisense and mRNA of the Kv1.5 gene into cell lines which can express Kv1.5, such as Xenopus oocytes or human kidney cell line. The third step is to culture isolated human atrial cells, and to compare I_{Kur} in cell group with and without incubation with antisense.

Another method is to develop a specific antibody directed against Kv1.5 channel proteins. Animal antibody will be generated against a fusion protein that includes the entire amino acid sequence of human Kv1.5 channel protein. A cell culture system would be employed. If I_{Kur} is recorded in control cells but not in cells incubated with the anti-Kv1.5 antiserum, then there is little doubt that I_{Kur} is a current equivalent to current expressed by Kv1.5. Alternatively, immunofluoresent labelling of isolated human atrial myocytes with the antibody directed against Kv1.5 could be used to explore further the relation between Kv1.5 and native cardiac I_{Kur}[5-77].

2. Autonomic, hormonal, and pharmacologic modulation of I_{Kur}

One of most important aspects of channel activity is the modulation of channels by endogenous hormones, neurotransmitters, and exogenous compounds, etc. We have evaluated the effects of several antiarrhythmic drugs on I_{Kur}, including the class Ia drug quinidine, the class Ic drug flecainide, and the class III drugs sotalol, ambasalide, and clofilium. Both quinidine and ambasalide proved potent I_{Kur} blockers with IC_{50} of 5 μM and 2.5 μM, respectively, and they appear to act on the open state of the channels. Neither flecainide nor sotalol and clofilium were found to exert any significant action on I_{Kur}. The future work on drug modulation of I_{Kur} should be: (1) to include more antiarrhythmics in study; (2) to correlate the drugs' ability to inhibit I_{Kur} with their clinical ability to delay repolarization and their efficacy in arrhythmias; (3) to get insight into the mode of drug-channel interaction.

We have conducted some preliminary experiments aimed to investigate the adrenergic modulation of I_{Kur} (unpublished data). We found that the β-receptor agonist isoproterenol (1 μM) enhanced I_{Kur} by approximately 30%, and that its effects were abolished by β-blocker propranolol. On the other hand, the α-receptor agonist phenylephrine caused concentration-dependent reduction of I_{Kur}. More work should be done to clarify further the subtypes of α-receptors responsible for the response of I_{Kur} to α-stimulation.

It has been shown that some hormones such as angiotensin II[5-78], thyroid hormone[5-79], insulin[5-80], 5-HT[5-81], and atrial natriuretic peptide[5-82,83] can modulate cardiac repolarization. For instance, thyroid

hormone simultaneously increased I_{Ca} and I_K, resulting in net shortening of APD in guinea pig ventricular myocytes[5-79]. 5-HT was found to increase L-type I_{Ca} in human atrial myocytes via the newly described 5-HT_4 receptors, which explains the positive inotropic effect of 5-HT[5-81]. The increase of I_{Ca} involves an elevation of intracellular cAMP likely to promote a phosphorylation of Ca^{++} channel. Interestingly, this action of 5-HT was not observed in atrial cells from other animal species such as rat, rabbit, guinea pig and frog. Lately, a study by Le Grand et al. indicated that in human atrial cells when the intracellular solution contained GTP, 10 nM ANF reduced I_{Ca} and I_{to1}, whereas in the absence of intracellular GTP, ANF increased I_{Ca} but still depressed I_{to1}[5-82,83]. More recently, ANF was reported to block L-type I_{Ca} and increase I_K in fetal chick ventricular cells and cells from human fetuses[5-82,83]. Whether these endocrine compounds also affect I_{Kur} is still unknown. It would be interesting to pursue studies in this field.

It is known that the regulation of ion channels by neurotransmitters and hormones is fulfilled via G-proteins coupled to receptors and channels, directly or indirectly[5-84,85]. Phosphorylation of channel proteins by either PKA (protein kinase A) or PKC (protein kinase C) is the most common way of altering channel activity. It would be important to determine which types of G-proteins are involved and how they mediate the autonomic and hormonal modulation of I_{Kur}.

3. Development of novel and specific blockers of I_{Ks} and I_{Kur}

The final goal of characterizing ion channels is to help in developing novel compounds that are of therapeutic value. It is known that most of, if not all, I_{Kr} blockers produce reverse use-dependent effects on repolarization, which limits these drugs' efficacy in tachyarrhythmias and renders them arrhythmogenic at slow activation rates. In contrast, I_{Ks} blockers are expected to have an opposite profile. I_{Ks}, with its slowly activating and deactivating properties, is commonly believed to be the major current determining rate-dependent APD shortening (APD accommodation or adaptation) because this current tends to increase at rapid rates due to its incomplete deactivation at short diastolic intervals. Blockade of this current would oppose APD accommodation, or in other words, result in rate-dependent APD prolongation, a property which would maximize drug effects on repolarization at rapid activation rates and minimize drug actions at resting heart rates. Therefore, specific I_{Ks} blockers are one of the directions for new drug development.

I_{Kur} is a novel current which may play an important role in repolarizing human atrial cells, and may therefore be an important factor in determining the likelihood of arrhythmias in man. Specific blockers of I_{Kur}, however, have not yet been developed, although we have found that some currently available antiarrhythmic agents inhibit this current. A specific I_{Kur} blocker devoid of effects on other currents would be expected to delay all phases of human atrial repolarization due to the rapid activating and non-inactivating properties of I_{Kur}.

4. **Direct recording of Na^+-K^+ pump current to explore its importance in controlling rate-dependent shortening of APD**

To conclude that Na^+-K^+ pump current contributes to rate-dependent APD shortening as suggested by our experimental data (see Chapter 4), direct recording of Na^+-K^+ pump current in human atrial cells would be necessary. Na^+-K^+ pump activity has been indicated by the membrane hyperpolarization induced by changing $[K^+]_o$ and temperature[5-73-78] or by intracellular K^+ activity, but direct recording of this current has not been performed in human cells. To record the pump current, modification of superfusion solutions and alteration of experimental conditions is needed. Changes of Na^+-K^+ pump current with changed pacing rate should be assessed to see whether the size of the current increases at higher frequencies, and action potential duration should be determined in the same cells in which current is recorded.

5. **Clarification of mechanisms of state-dependent block**

Based on the mode of action of various drugs on human I_{to1}, we proposed a hypothesis that drug blockade of K^+ channels is actually a process of drug acting like the endogenous inactivation "ball" mimicking N-type inactivation of channels[5-86]. To clarify this issue, single channel recording of I_{to1} would be required to get deeper insight into the interaction between drug molecules and channel gating. Furthermore, computer simulation of drug-channel interaction is also necessary.

6. **Characterization of other currents that determine human atrial repolarization, AP model accounting for drug effects.**

Although we have improved our understanding of the determinants of human atrial repolarization, much still needs to be done. For example, preliminary results from our laboratory (Guirong Li, personal communication) indicates the existence of swelling-induced Cl^- current in human atrium. This could be an important finding, considering pathological conditions which might enhance this current, such as atrial enlargement which is common in patients with atrial fibrillation. Characterization of this current and the development of blockers might provide a new way of handling clinical AF. In addition, our studies demonstrate that when intracellular K^+ was replaced by Cs+, a strongly outward-directed rectifying current was recorded in human atrial myocytes which activated from +20 mV with a reversal potential between -10 mV and 0 mV. The nature of this current is still unclear, but evidence points to a non-specific cation current similar to that seen in rabbit atrial cells by Irisawa et al[5-87].

Membrane repolarization is a complex process, with all ion currents (including inward and outward, channel current, pump current, and exchange current) involved. All currents interact directly or indirectly. The rate of repolarization is determined by the balance of inward and outward currents. The isolation of a current is necessary to obtain a clear picture of the current interest, but this manipulation makes us miss information about the interaction among currents. It is extremely difficult, if not impossible, to obtain accurate data without separation of currents. One way of solving this problem is to employ computer

simulation to integrate the experimentally-obtained information for different ion currents. The expression generated by simulation will be able to predict the overall changes of membrane currents and potentials due to alteration of one or more currents, the consequence of these changes on repolarization, and the influence of one current on others.

REFERENCES

5-1. Wang Z, Pelletier LC, Talajic M, Nattel S. Effects of flecainide and quinidine on human atrial action potentials: role of rate-dependence and comparison with guinea pig, rabbit and dog tissues. Circulation. 1990;82:274-283.

5-2. Wang Z, Pagé P, Nattel S. Mechanism of flecainide's antiarrhythmic action in experimental atrial fibrillation. Circ Res. 1992;71:271-287.

5-3. O'Hara G, Villemaire C, Talajic M, Nattel S. Effects of flecainide on the rate-dependence of atrial refractoriness, atrial repolarization and atrioventricular node conduction in anaesthetized dogs. J Am Coll Cardiol. 1992;19:1335-1342.

5-4. Wang J, Bourne GW, Wang Z, Villemaire C, Talajic M, Nattel S. Comparative mechanisms of antiarrhythmic drug action in experimental atrial fibrillation: Importance of use-dependent effects on refractoriness. Circulation. 1993;88:1030-1044.

5-5. Le Grand B, Le Heuzey JY, Périer P, Lavergne T, Chauvaud S, Péronneau P, Guize L. Effects of flecainide on action potential duration of human atrial fibres (abstract). J Am Coll Cardiol 1989;13:140A.

5-6. Kerr CR, Mason MA, Chung DC. Propafenone: An effective drug for prevention of recurrent atrial fibrillation. (abstract) Circulation 1985;72:(suppl III):III-171.

5-7. Kingma JH, Suttorp MJ. Acute pharmacologic conversion of atrial fibrillation and flutter: The role of flecainide, propafenone, and verapamil. Am J Cardiol 1992;70:56A-61A.

5-8. Feld GK, Chen P, Nicod P, Fleck RP, Meyer D. Possible atrial proarrhythmic effects of class Ic antiarrhythmic drugs. Am J Cardiol 1990;66:378-383.

5-9. Hondeghem LM, Snyders DJ: Class III antiarrhythmic agents have a lot of potential but a long way to go: Reduced effectiveness and dangers of reverse use dependence. Circulation 1990;81:686-690.

5-10. Varro A, Nakaya Y, Elharrar V, Surawicz B. Effect of antiarrhythmic drugs on the cycle length-dependent action potential duration in dog Purkinje and ventricular muscle fibres. J Cardiovasc Pharmacol. 1986;8:178-185.

5-11. Krishnan SC, Antzelevitch C. Flecainide-induced arrhythmia in canine ventricular epicardium: Phase 2 reentry? Circulation 1993;87:562-572.

5-12. Ranger S, Sheldon R, Fermini B, Nattel S. Modulation of flecainide's cardiac sodium channel blocking actions by extracellular sodium: A possible cellular mechanism for the action of sodium salts in flecainide's cardiotoxicity. J Pharmacol Exp Ther 1993;264:1160-1167.

5-13. Varro A, Nakaya Y, Surawicz B. Effect of antiarrhythmic drugs on the premature action potential duration in canine cardiac Purkinje fibers. J Pharmacol Exp Ther 1985;233:304-311.

5-14. Wang Z, Fermini B, Nattel S. Mechanism of flecainide's rate-dependent actions on action potential duration in canine atrial tissue. J Pharmacol Exp Ther. 1993;267:575-581.

5-15. Wang Z, Fermini B, Nattel S. Effects of flecainide, quinidine, and 4-aminopyridine on transient and sustained outward currents in human atrial myocytes. (submitted to J Pharmacol Exp Ther)

5-16. Vaughan Williams EM. A classification of antiarrhythmic actions reassessed after a decade of new drugs. J Clin Pharmacol 1984;24:129-147.

5-17. Boyden PA. Effects of pharmacologic agents on induced atrial flutter in dogs with right atrial enlargement. J Cardiovasc Pharmacol. 1986;8:170-177.

5-18. Spinelli W, Hoffman BF. mechanisms of termination of reentrant atrial arrhythmias by class I and class III antiarrhythmic agents. Circ Res. 1989;65:1565-1597.

5-19. Schoels W, Yang H, Gough WB, El-Sherif N. Circus movement atrial flutter in canine sterile pericarditis model: differential effects of procainamide on the components of the reentrant pathway. Circ Res. 1991;68:1117-1126.

5-20. Feld GK, Venkatesh N, Singh BN. Pharmacologic conversion and suppression of experimental canine atrial flutter: differing effects of d-sotalol, quinidine, and lidocaine and significance of changes in refractoriness and conduction. Circulation. 1986;74:197-204.

5-21. Platou ES, Refsum H. Class III antiarrhythmic action in experimental atrial fibrillation and flutter in dogs. J Cardiovasc Pharmacol 1982;4:839-846.

5-22. Kirchhof C, Wijffels M, Brugada J, Planellas J, Allessie M. Mode of action of a new class Ic drug (ORG 7797) against atrial fibrillation in conscious dogs. J Cardiovasc Pharmacol 1991;17:116-124.

5-23. Wang Z, Feng J, Nattel S. Sustained atrial fibrillation in dogs-underlying electrophysiologic determinants and mechanism of antiarrhythmic action of flecainide. (submitted to Circulation, in revision).

5-24. Wang Z, Fermini B, Nattel S. Delayed rectifier outward current and repolarization in human atrial myocytes. Circ Res 1993;73:276-285.

5-25. Nattel S, Wang Z, Fermini B. Three Types of Delayed Rectifier Potassium Currents in Human Atrial Cardiomyocytes. Biophysical J (abstract) 1993;64:A393.

5-26. Wang Z, Fermini B, Nattel S. Rapid and slow components of delayed rectifier outward current in human atrial myocytes. (submitted to Cardiovasc Res)

5-27. Noble D, Tsien RW. Outward membrane currents activated in the plateau range of potentials in

cardiac Purkinje fibres. J Physiol (Lond) 1969;200:205-231.

5-28. Shrier A, Clay JR. Repolarization currents in embryonic chick atrial heart cell aggregates. Biophys J 1986;50:861-874.

5-29. Sanguinetti MC, Juriewicz NK. Two components of cardiac delayed rectifier K^+ current: different sensitivity to block by class III antiarrhythmic agents. 1990;96:195-215.

5-30. Sanguinetti MC, Jurkiewicz NK. Delayed rectifier outward K^+ current is composed of two currents in guinea pig atrial cells. AM J Physiol 1991;260:H393-399.

5-31. Crumb WJ, Brown AM. Terfenadine blockade of a potassium current in human atrial myocytes. Circulation (abstract) 1993;I-230

5-32. Daubert C, Mabo P, Gras D, Leclercq C. Clinical role of d-sotalol and dJ-sotalol in supraventricular arrhythmias, including pre-excitation. Eur Heart J 1993;14(suppl H):67-73.

5-33. Echt DS, Berte LE, Clusin WT, Samuelsson RG, Harrison DC, Mason JW. Prolongation of the human cardiac monophasic action potential by sotalol. AM J Cardiol 1982;50:1082-1086.

5-34. Hayward RP, Taggart P. Effects of sotalol on human atrial action potential duration and refractoriness: cycle length dependency of class III activity. Cardiaovasc Res 1986;20:100-107.

5-35. Edvardsson N, Hirsch L, Emmanuelsson H, Poten J, Olsson SB. Sotalol-induced delayed ventricular repolarization in man. Eur Heart J 1980;1:335-340.

5-36. Carmeliet E. Electrophysiologic and voltage clamp analysis of the effects of sotalol on isolated cardiac muscle and Purkinje fibres. J Pharmacol Exp Ther 1985;232:817-825.

5-37. Berger F, Borchard U, Hafner D. Effects of (+)- and (±)-sotalol on repolarizing currents and pacemaker current in sheep cardiac Purkinje fibres. Naunyn Schmiedeberg's Arch Pharmacol 1989;340:696-704.

5-38. Chinn K. Two delayed rectifier in guinea pig ventricular myocytes distinguished by tail current kinetics. J Pharmaol and Exp Ther 1993;264:553-560.

5-39. Adaniya H, Hiraoka M. Effects of a novel class III antiarrhythmic agent, E-4031, on reentrant tachycardias in rabbit right atrium. J Cardiovasc Pharmacol 1990;15:976-982.

5-40. Inoue H, Yamashita T, Usui M, Nozaki A, Saihara S, Sugimoto T. Effects of pentisomide and E-4031 on canine atrial flutter due to reentry: a comparative study with disopyramide and propafenone. J Cardiovasc Pharmacol 1991;18:137-143.

5-41. Shimizu A, Kaibara M, Centurion OA, Kapuku G, Hirata T, Fukatani M, Yano K. Electrophysiologic effects of a new class III antiarrhythmic agent, E-4031 on the atrial flutter, atrial refractoriness and conduction delay in a canine sterile pericarditis model. J Cardiovasc Pharmacol 1993;

5-42. Isomoto S, Shimizu A, Konoe A, Kaibara M, Centurion OA, Fukatani M, Yano K. Electrophysiologic effects of E-4031, a new class III antiarrhythmic agent, in patients with supraventricular tachyarrhythmias. Am J Cardiol 1993;71:1464-1467.

5-43. Darpö B, Vallin H, Bergstrand R, Almgren O, Fager G, Haglund E, Edvardsson N. The selective I_K-blocker almokalant exhibits class III-specific effects on repolarization and refractoriness of the human heart. Circulation 1992;86:I-264.

5-44. Darpö B, Almgren O, Bergstrand R, Gottfridsson C, Sandstedt B, Edvardsson N. Class III mode of action of H 234/09-a double-blind, cross-over, study using transesophageal atrial stimulation in healthy volunteers. Cardiovasc Drugs Ther 1991;5(suppl III):364.

5-45. Carmeliet E. Block of the delayed K^+ current by Hässle 234/09 in rabbit cardiac myocytes. J Mol Cell Cardiol 1991;23:(suppl V):S79.

5-46. Lundberg C, Abrahamsson C, Carlsson L, Duker G. Effects of the novel class III antiarrhythmic agent H 234/09 on inotropy and action potential duration in human ventricular muscle. Eur Heart J 1990;11(suppl):P2357.

5-47. Carlsson L, Abrahamsson C, Almgren O, Lundberg C, Duker G. Prolonged action potential duration and positive inotropy induced by the novel class III antiarrhythmic agent H 234/09 (almokalant) in isolated human ventricular muscle. J Cardiovasc Pharmacol 1991;18:882-887.

5-48. Escande D, Loisance D, Planche C, Coraboeuf E. Age-related changes of action potential plateau shape in isolated human atrial fibres. Am J Physiol 1985;249:H843-850.

5-49. Apkon M, Nerbonne JM. Characterization of two distinct depolarization-activated K^+ currents in adult rat ventricular myocytes. J Gen Physiol 1991;97:973-1011.

5-50. Sanguinetti MC, Jurkiewicz NK, Scott A, Siegl PKS. Isoproterenol antagonizes prolongation of refractory period by the class III antiarrhythmic agent E-4031 in guinea pig myocytes. Mechanism of action. Circ Res 1991;68:77-84.

5-51. Sawada K, Nomoto K, Hiraoka M. Effects of a novel class III antiarrhythmic agent, E-4031, on ventricular arrhythmias (abstract). Jpn Circ J 1988;52:919.

5-52. Varro A, Nakaya Y, Elharrar V, Surawicz B. Effect of antiarrhythmic drugs on the cycle length-dependent action potential duration in dog Purkinje and ventricular muscle fibres. J Cardiovasc Pharmacol 1986;8:178-185.

5-53. Jurkiewicz NK, Sanguinetti MC. Rate-dependent prolongation of cardiac action potentials by a methanesulfonanilide class III antiarrhythmic agent: Specific block of rapidly activating delayed rectifier K^+ current by dofetilide. Circ Res 1993;72:75-83.

5-54. Spinelli W, Moubarak IF, Parsons RW, Colatsky TJ. Cellular electrophysiology of WAY-123,398, a new class III antiarrhythmic agent: specificity of I_K block and lack of reverse use dependence in cat ventricular myocytes.

5-55. Follmer CH, Colatsky TJ. Block of the delayed rectifier potassium current I_K by flecainide and E-4031 in cat ventricular myocytes. Circulation 1990;82:289-293.

5-56. Tamkun MM, Knoth KM, Walbridge JA, Kroemer H, Roden DM, Glover DM. Molecular cloning and

characterization of two voltage-gated K^+ channel cDNAs from human ventricle. FASEB J 1991;5:331-337.

5-57. Wang Z, Fermini B, Nattel S. Sustained Depolarization-induced Outward Current in Human Atrial Myocytes: Evidence for a Novel Delayed Rectifier Potassium Current Similar to Kv1.5 Cloned Channel Currents. Circ Res 1993;73:1061-1076.

5-58. Christie MJ, North RA, Osborne PB, Douglass J, Adelman JP. Heteropolymeric potassium channels expressed in Xenopus oocytes from cloned subunits. Neuron 1990;2:495-411.

5-59. Isacoff EY, Jan YN, Jan LY. Evidence for the formation of heteromultimeric potassium channels in Xenopus oocytes. Nature (Lond) 1990;345:530-534.

5-60. Ruppersberg JP, Schöter KH, Sakmann B, Stocker M, Sewing S, Pongs O. Heteromultimeric channels formed by rat brain potassium channel proteins. Nature (Lond) 1990;345:535-537.

5-61. Po S, Roberds S, Snyders DJ, Tamkun MM, Bennett PB. Heteromultimeric assembly of human potassium channels: Molecular basis of a transient outward current? Circ Res 1993;72:1326-1336.

5-62. Lauribe P, Escande D, Nottin R, Coraboeuf E. Electrical activity of human atrial fibres at frequencies corresponding to atrial flutter. Cardiovasc Res 1989;23:159-168.

5-63. Wang Z, Fermini B, Nattel S: State- and voltage-dependent actions of 4-aminopyridine on the transient outward potassium current in human atrial myocytes. Circulation (abstract) 86:I-696,1992.

5-64. Simurda J, Simurdovà M, Christé G. Use-dependent effects of 4-aminopyridine on transient outward current in dog ventricular muscle. Pflügers Arch 1989;415:244-246.

5-65. Castle NA, Slawsky MT. Characterization of 4-aminopyridine block of the transient outward K^+ current in adult rat ventricular myocytes. J Pharmacol Exp Ther 1992;264:1450-1459.

5-66. Campbell DL, Qu Y, Rasmusson RL, Strauss HC. The calcium-independent transient outward potassium current in isolated ferret right ventricular myocytes: II. Closed state reverse use-dependent block by 4-aminopyridine. J Gen Physiol 1993;101:603-626.

5-67. Snyders DJ, Knoth KM, Roberds SL, Tamkun MM. Time-, voltage-, and state-dependent block by quinidine of a cloned human cardiac potassium channel. J Parmacol Exp Ther 1992;41:322-330.

5-68. Fedida D, Wible B, Wang Z, Fermini B, Faust F, Nattel S, Brown AM. Identity of a novel delayed rectifier current from human heart with a cloned K^+ channel current. Circ Res 1993;73:210-216.

5-69. Arena JP, Kass RS. Block of heart potassium channels by clofilium and its tertiary analogs: Relationship between drug structure and type of channel blocked. Mol Pharmacol 1988;34:60-66.

5-70. Duan DY, Fermini B, Nattel S. Potassium channel blocking properties of propafenone in rabbit atrial myocytes. J Pharmacol Exp Ther 1993;264:1113-1123.

5-71. Dukes ID, Morad M. Tedisamil inactivates transient outward K^+ current in rat ventricular myocytes. Am J Physiol 1989;257:H1746-1749.

5-72. Hordof AJ, Spotnitz A, Mary-Rabine L, Edie RN, Rosen MR. The cellular electrophysiologic effects

of digitalis on human atrial fibres. Circulation 1978;57:223-229.

5-73. Rasmussen HH, Ten Eick RE, McCullough JR, Singer DH. Evidence for electrogenic Na^+ pumping in human atrial myocardium. J Mol Cell Cardiol 1984;16:267-277.

5-74. Rasmussen HH, Singer DH, Ten Eick RE. Characterization of a sodium pump-induced hyperpolarization in isolated human atrium. Am J Physiol 1986;251:H331-339.

5-75. Rasmussen HH, Okita GT, Hartz RS, Ten Eick RE. Inhibition of electrogenic Na^+-pumping in isolated atrial tissue from patients treated with digoxin. J Pharmacol Exp Ther 1990;252:60-64.

5-76. Sako H, Imanishi S, Arita M, Shimada T, Hadama T, Uchida Y. Unaffected electrogenic Na-K pump activity in "diseased" human atrial fibres, as assessed by intracellular K^+ activity. Jpn J Physiol 1989;39:873-890.

5-77. Freeman LC, Kass RS. Expression of a minimal K^+ channel protein in mammalian cells and immunolocalization in guinea pig heart. Circ Res 1993;73:968-973.

5-78. Hermsmeyer K. Angiotensin II increases electrical coupling in mammalian ventricular myocardium. Circ Res 1980;47:524-529.

5-79. Rubinstein I, Binah O. Thyroids hormone modulates membrane currents in guinea pig ventricular myocytes. Naubyn-Schmiedeberg's Arch Pharmacol 1989;340:705-711.

5-80. Magyar J, Rusznàk, Szentesi P, Szucs G, Kovacs L. Action potential and potassium currents in rat ventricular muscle during experimental diabetes. J Mol Cell Cardiol 1992;24:841-853.

5-81. Ouadid H, Seguin J, Dumuis A, Bockaert J, Nargeot J. Serotonin increases calcium current in human atrial myocytes via the newly described 5-hydroxytryptamine receptors. Mol Pharmacol 1992;41:346-351.

5-82. Bkaily G, Perron N, Wang S, Sculptoreanu, Jacques D, Ménard D. Atrial natriuretic factor blocks the high-threshold Ca^{++} current and increases K^+ current in fetal single ventricular cells. J Mol Cell Cardiol 1993;25:1305-1316.

5-83. Le Grand, Couétil DE, Coraboeuf E. Effects of atrionatriuretic factor on Ca^{++} current and Ca-independent transient outward K^+ current in human atrial cells. Pflügers Arch 1992;421:486-491.

5-84. Brown AM, Birnbaumer L. Direct G protein gating of ion channels. Am J Physiol 1988;254:H401-410.

5-85. Szabo G, Otero AS. G protein mediated regulation of K^+ channels in heart. Annu Rev Physiol 1990;52:293-305.

5-86. Armstrong CM, Bezanilla F. Inactivation of the sodium channel. J Gen Physiol 1977;70:567-590.

5-87. Hagiwara N, Masuda H, Shoda M, Irisawa H. Stretch-activated anion currents of rabbit cardiac myocytes. J Physiol (Lond) 1992;456:285-302.